

### UNIVERSIDADE DE LISBOA INSTITUTO SUPERIOR TÉCNICO

# A Taste Of The Flavour Puzzle: Is Symmetry The Missing Ingredient?

#### Miguel Pissarra Levy

Supervisor: Doutor Ivo de Medeiros Varzielas

Thesis approved in public session to obtain the PhD Degree in  ${\bf Physics}$ 

Jury final classification: Pass with Distinction and Honour



### UNIVERSIDADE DE LISBOA INSTITUTO SUPERIOR TÉCNICO

## A Taste Of The Flavour Puzzle: Is Symmetry The Missing Ingredient?

#### Miguel Pissarra Levy

Supervisor: Doutor Ivo de Medeiros Varzielas

Thesis approved in public session to obtain the PhD Degree in

#### **Physics**

Jury final classification: Pass with Distinction and Honour

#### Jury

#### Chairperson:

Doctor Mário João Martins Pimenta, Instituto Superior Técnico, Universidade de Lisboa;

#### Members of the committee:

Doctor Maria Margarida Nesbitt Rebelo da Silva, Instituto Superior Técnico, Universidade de Lisboa;

Doctor Ricardo Jorge Gonzalez Felipe, Instituto Superior de Engenharia de Lisboa, Instituto Politécnico de Lisboa;

Doctor Dipankar Das, Department of Physics, Indian Institute of Technology Indore, India; Doctor Ivo de Medeiros Varzielas, Instituto Superior Técnico, Universidade de Lisboa

Funding Institution: Fundação para a Ciência e Tecnologia (FCT)

Dedicado à avó Teresa

#### Acknowledgments

No PhD is an island, so thanks are in order.

First and foremost, I would like to thank my supervisor, Ivo, for all the guidance, patience, and trust in me. His relaxed demeanour was able to always keep me from spiralling, and I am grateful for all his encouraging. It goes without saying that none of this would be possible without his help. Second, I would also like to thank all my collaborators, who had a major part in my growth as a physicist. In particular, I thank Dipankar for all he taught me, and for his patience in doing so. I would also like to thank Igor, Steve King, and Petcov, for their sunny disposition and their patience for all my doubts and mistakes. My gratitude also goes to Gustavo, Palash, Ye-Ling, Luís Ventura and João Rosa, for being there and believing in me in the beginning. Last but not least, I thank João Penedo and Sílvia for all the moments shared, physics-wise and otherwise.

I also thank Fundação para a Ciência e Tecnologia (FCT) and IDPASC for the grant that supported my doctorate degree, as well as Centro de Física Teórica de Partículas (CFTP) for both the financial support for conferences, and for providing a good environment for discussions. Sandra Oliveira and Gui have my eternal gratitude for all the help with bureaucracies.

Agradeço também à minha mãe e à minha irmã, tal como ao resto da minha família, por me terem apoiado incondicionalmente desde o início ao fim. Em segundo, tenho de agradecer ao Manel e ao Bernardo por estarem sempre presentes. Um obrigado também às pessoas todas que me manteviram são de uma forma ou doutra por este processo todo: um abraço ao Zé, pela companhia e encorajamento; obrigado ao André e ao Naruto por todas as conversas de treta; um brinde ao Mira e ao Ved, pela boa disposição; ao Braz e ao Miguel, pelos fonões trocados entre canecos; ao Zé Gui e ao Duarte, por todo o carinho ao longo dos tempos. Aos meus colegas e amigos do CFTP, obrigado por todas as conversas entre canecas.

This work was supported by FCT, Portugal, through the grant No. PD/BD/150488/2019, in the framework of the Doctoral Programme IDPASC-PT and the projects CERN/FIS-PAR/0002/2021, CERN/FIS-PAR/0019/2021, CFTP-FCT Unit UIDB/00777/2020 and UIDP/00777/2020, which are partially funded through POCTI (FEDER), COMPETE, QREN and EU.

#### Resumo

A misteriosa réplica dos fermiões permanece um dos mais intrigantes quebra-cabeças da física de partículas. A descrição da física elementar através de simetrias de gauge permite uma descrição económica dessas interacções. Por outro lado, a existência de múltiplas gerações está no cerne da maioria dos parâmetros livres do modelo padrão. Desta forma, é natural questionar-nos se é possível recuperar o princípio de gauge para o sector de sabor. É esta a origem das simetrias de sabor: impôr uma simetria no espaço de sabor, visando a redução do número de parâmetros livres.

Nesta tese estudamos diferentes propostas para o problema do sabor. Começamos por investigar modelos com três dobletos escalares e simetrias Abelianas. Vemos como a conservação natural de sabor e a simetria custodial podem ser usadas para proteger contra contribuições perigosas a processos bem medidos, e estudamos as implicações fenomenológicas deste modelo. Seguidamente, estudamos modelos com simetrias não-Abelianas, fazendo o primeiro passo para classificar as diferentes direcções em que os termos que quebram a simetria suavemente podem impactar as teorias, apresentando depois um modelo que se foca em como propriedades fermiónicas podem ter origem na dinâmica escalar, e não na arbitrariedade do sector de sabor. Posteriormente, estudamos a forma como sectores de gauge estendidos podem estar na origem de simetrias de sabor. Por último, estudamos simetrias modulares aplicadas ao sector de sabor. Aqui, estudamos os estabilisadores das simetrias, e apresentamos um modelo com várias simetrias modulares que apresenta um sector dos neutrinos extremamente preditivo, estendendo-o para uma teoria de grande unificação em SU(5), de forma a explicar as hierarquias dos quarks. Por último, fazemos um estudo exaustivo de modelos de  $\Gamma'_4$  para verificar se é possível obter modelos preditivos onde as hierarquias dos quarks resultam da proximidade a  $\tau = \omega$ .

Palavras-chave: Física além do Modelo Padrão, massas e misturas fermiónicas, simetrias de sabor, simetrias modulares, puzzle do sabor

#### Abstract

The threefold replication of fermions remains one of the most intriguing puzzle of particle physics. The gauge description of elementary physics allows for an economical description of gauge interactions. Conversely, the existence of multiple generations is at the heart of most free parameters of the Standard Model. So it is natural to wonder if this economical principle can be recovered in the flavour sector. This is the origin of flavour symmetries: impose a symmetry on the flavour space, such that the number of free parameters are reduced.

Here, we study different approaches to the flavour puzzle. We first investigate three Higgs doublet models with Abelian flavour symmetries. We see how natural flavour conservation, and the custodial symmetry, can be employed to safeguard against dangerous contributions to well measured processes, and study its phenomenological implications. Afterwards, we study models with non-Abelian symmetries, and make the first step to classify the different directions in which soft-breaking terms can impact the theories, later presenting a model which highlights how the fermionic masses and mixings can be a feature of the scalar dynamics, rather than be fully determined by the arbitrariness of the flavour sector. We then study a model of two Higgs doublet models with approximate flavour symmetries, showcasing how extended gaugse sectors can be the source of the flavour symmetries. Afterwards, we study the modular approach to flavour. Here, we study the stabilisers of these symmetries, and present a model based on multiple modular symmetries to provide a very predictive model for neutrino mixing, as well as extend it to an SU(5) grand unification theory, explaining the quark hierarchies. Lastly, we do a comprehensive study of  $\Gamma'_4$  modular symmetric models to see if a predictive scenario where the quark hierarchies are naturally explained from the proximity to  $\tau = \omega$  can be obtained.

**Keywords:** Beyond the standard model physics, fermion masses and mixings, flavour symmetries, modular symmetries, flavour puzzle

## Contents

	Ack	nowledg	gments	iii				
	Resumo							
	Abs	Abstract						
	List	of Abb	previations	xiii				
	Pref	ace .		1				
1	Intr	oduct	ion	3				
	1.1	Yang-	Mills Theories and the Standard Model	4				
		1.1.1	Yang-Mills Theories	4				
		1.1.2	Spontaneous Symmetry Breaking: from Goldstone to Higgs	10				
		1.1.3	The Standard Model	15				
	1.2	Going	Beyond the Standard Model	20				
		1.2.1	Multi-Higgs Models	20				
		1.2.2	Neutrino Masses	27				
	1.3	The F	Flavour Puzzle and Flavour Symmetries	32				
	1.4	Modu	lar Symmetries	41				
		1.4.1	Modular Invariant Theories	43				
		1.4.2	Multiple Modular Symmetries	46				
		1.4.3	Hierarchies and the Proximity to Enhanced Symmetry Points	48				
2	Der	nocrat	cic 3HDMs	55				
	2.1	Custo	dial Symmetry	57				
		2.1.1	SM Recap	57				
		2.1.2	Generalisation to nHDMs	60				
		2.1.3	Validation of the Custodial Limit by Explicit Calculation	62				
		2.1.4	Examples of the Custodial Limit: the 2HDM and Democratic 3HDMs	63				
	2.2	Prosp	ects for Light Charged-Scalars in Democratic 3HDMs	66				
		2.2.1	Scalar Sector	67				
		2.2.2	Quark Yukawa Sector	68				
		2.2.3	Constraints from Flavour Data	70				
	2.3	Wrong	g Sign Yukawa	74				

	2.4	Discus	ssion	79
3	Soft	ly-Bro	oken nHDMs with Large Discrete Symmetry Groups	81
	3.1	$\Sigma(36)$	-Symmetric 3HDM	83
		3.1.1	The Scalar Potential and its Minima	83
		3.1.2	The Physical Higgs Bosons	85
		3.1.3	The Scalar Sector of $\Sigma(36)$ 3HDM: a Summary	86
	3.2	Align	ment Preserving Soft-Breaking	86
		3.2.1	How to Preserve the vev Alignment	87
		3.2.2	An Example	88
		3.2.3	Physical Scalars in the Softly-Broken $\Sigma(36)$ 3HDM	90
		3.2.4	Global vs. Local Minimum	91
		3.2.5	Decoupling Limits	93
		3.2.6	Decays of Non-Standard Higgses	94
	3.3	Discus	ssion	95
4	Dilu	ıting (	Quark Hierarchies with $D_4$	97
5	Cro	$\mathbf{ssed} \; 2$	m HDMs	107
	5.1	Yukaw	va Sector of 2HDMs: Some Generalities and Reducible Yukawa Couplings	108
		5.1.1	Quark Masses, Mixings and Couplings	109
		5.1.2	Reducible Yukawa Couplings	110
		5.1.3	Notational Digression	111
	5.2	Crosse	ed 2HDMs	112
		5.2.1	Retrieving Type-I and Type-II 2HDMs	113
		5.2.2	First Example of Crossed 2HDM: Connection with Left-Right Symmetry $\ \ . \ \ . \ \ .$	114
		5.2.3	One Other Example of a Crossed 2HDM	116
	5.3	Some	Specificities on the x2HDMs	117
	5.4	Pheno	omenology of x2HDMs	118
	5.5	Discus	ssion	120
6	Mo	dular S	Symmetries and Stabilisers	123
	6.1	Doma	in, Fixed Points, and Residual Symmetries	124
	6.2	Fixed	Points of Finite Modular Groups	126
		6.2.1	$\Gamma_2$	128
		6.2.2	$\Gamma_3$	130
		6.2.3	$\Gamma_4$	131
		6.2.4	$\Gamma_5$	134
	6.3	Discus	ssion	135

7	Litt	lest M	fodular Seesaw and its $SU(5)$ Extension	139				
	7.1	The L	ittlest Modular Seesaw	. 140				
		7.1.1	Symmetries and Stabilisers	. 141				
		7.1.2	Charged-Leptons	. 143				
		7.1.3	Neutrinos	. 144				
		7.1.4	Analytical Results	. 145				
		7.1.5	Numerical Results	. 148				
		7.1.6	Weighton Models	. 150				
	7.2	SU(5)	Extension	. 152				
		7.2.1	SU(5) Details	. 153				
		7.2.2	The Model	. 154				
	7.3	Discus	sion	. 162				
8	Qua	arks at	the $S_4$ Modular Cusp	163				
	8.1	Frame	work	. 165				
		8.1.1	Quark Mass Matrices	. 166				
		8.1.2	Assignments, Transposition, and gCP	. 170				
	8.2	Analy	tical Results for the Mass Matrices	. 171				
	8.3	3.3 Numerical Results for the Mass Matrices						
		8.3.1	Fits without $\delta_{\mathrm{CP}}$ in the Presence of gCP	. 177				
		8.3.2	Fits with $\delta_{\mathrm{CP}}$ in the Presence of gCP	. 178				
		8.3.3	Fits with 11 Parameters	. 179				
		8.3.4	12-Parameter Fits without gCP	. 179				
		8.3.5	Fits with Two Moduli in the Presence of gCP	. 180				
	8.4	A Clos	ser Look at Natural Hierarchies	. 181				
		8.4.1	Hierarchical Parameters	. 183				
		8.4.2	The Role of $ \epsilon $ and Possible Cancellations	. 184				
	8.5	Discus	ssion	. 185				
9	Con	clusio	ns	187				
$\mathbf{A}$	Den	nocrat	ic 3HDMs: Custodial Symmetry and Flavour Observables	191				
	A.1	Brief I	Note on $SU(2)$ Triplets	. 191				
	A.2	A.2 Custodially Invariant Scalar Potential						
	A.3	Flavou	ır Observables in Democratic 3HDMs	. 193				
		A.3.1	Computing $b \to s \gamma$	. 193				
		A.3.2	Neutral Meson Mixing: $\Delta M_{Bq}$					
В	$\Sigma(36$	6) <b>and</b>	Alignment Preserving Soft-Breaking Terms	199				
	B.1	$\Sigma(36)$	vs. $\Delta(54)$ 3HDM	. 199				
	B.2	Alignr	nent Preserving Soft-Breaking Terms for all the Minima	. 200				

$\mathbf{C}$	$S_4$ (	Group Theory and the Littlest Modular Seesaw	205
	C.1	Group Theory of $S_4$	205
	C.2	Stabilizers and Residual Symmetry	206
	C.3	$S_4$ : Another Basis and Modular Forms at $\tau = \omega$	208
	C.4	Possible Corrections to the $\ensuremath{\mathrm{CSD}}(n)$ Structure	210
	C.5	Driving Superpotential for the Weighton Fields	212
D	Mod	dular $S_4'$ and Hierarchies at the Cusp	215
	D.1	Group Theory	215
	D.2	Modular Forms	215
Bi	bliog	graphy	221

## List of Abbreviations

$\mathbf{SM}$	Standard Model
$\mathbf{QFT}$	Quantum Field Theory
$\operatorname{QCD}$	Quantum Chromodynamics
$\mathbf{E}\mathbf{W}$	Electroweak
$\mathbf{CP}$	Charge-Parity
$\mathbf{L}\mathbf{H}$	Left-handed
$\mathbf{R}\mathbf{H}$	Right-handed
SSB	Spontaneous Symmetry Breaking
vev	vacuum expectation value
$\mathbf{EWSB}$	Electroweak Symmetry Breaking
$\mathbf{C}\mathbf{K}\mathbf{M}$	Cabibbo-Kobayashi-Maskawa
$\mathbf{CPV}$	Charge-Parity Violating
PMNS	Pontecorvo-Maki-Nakawaga-Sakata
$\mathbf{B}\mathbf{A}\mathbf{U}$	Baryon Asymmetry of the Universe
$\mathbf{D}\mathbf{M}$	Dark Matter
NP	New Physics
$\mathbf{BSM}$	Beyond the Standard Model
nHDMs	n-Higgs Doublet Models
2HDM	Two-Higgs Doublet Model
FCNCs	Flavour-Changing Neutral Currents
$_{ m LHC}$	Large Hadron Collider
$\mathbf{U}\mathbf{V}$	Ultraviolet
$\mathbf{GIM}$	Glashow–Iliopoulos–Maiani
NFC	Natural Flavour Conservation
3HDM	Three-Higgs Doublet Model
$\mathbf{F}\mathbf{N}$	Froggatt-Nielsen
TBM	Tri-Bimaximal
gCP	generalised Charge-Parity
$\mathbf{SUSY}$	Supersymmetric
MSSM	Minimal Supersymmetric Standard Model
$\mathbf{CS}$	Custodial Symmetry
HL-LHC	High-Luminosity Large Hadron Collider
$\mathbf{CL}$	Confidence Level
BR	Branching Ratio
$\operatorname{BGL}$	Branco-Grimus-Lavoura
LRSM	Left-Right Symmetric Model
x2HDM	Crossed Two-Higgs Doublet Model

**RHN** Right-Handed Neutrino

 ${f SD}$  Sequential Dominance

**2RHN** Two Right-Handed Neutrino

 $\mathbf{CSD} \quad \text{Constrained Sequential Dominance}$ 

 $\mathbf{TM} \quad \mathrm{Tri\text{-}Maximal}$ 

 $\mathbf{GUT} \quad \mathbf{Grand} \ \mathbf{Unified} \ \mathbf{Theory}$ 

**LMS** Littlest Modular Seesaw

 ${f SK}$  Super Kamiokande

**BG** Barbieri-Giudice

## **Preface**

In this thesis, we address the Flavour puzzle with specific emphasis on the symmetry approach to it. The work presented here is organised as follows. The first chapter is dedicated to explaining all the necessary ingredients to follow the remaining chapters, including the basics of Yang-Mills theories, and of spontaneous symmetry breaking, to arrive at the Standard Model (SM) of Particle Physics. Afterwards, we dedicate ourselves to presenting the relevant SM extensions for the remainder of the work, as well as focus on their properties. This sets the stage to introduce the Flavour puzzle, and different symmetry approaches to tackle it, with particular emphasis on Natural Flavour Conservation (NFC), the Froggatt-Nielsen (FN) mechanism, and non-Abelian symmetries. A section is dedicated to the modular symmetry approach, where the basics and workings of modular-invariant theories are underlined. The second chapter is dedicated to the study of some properties of democratic 3HDMs, which are a particular case of NFC models. Here, we discuss the custodial limit for nHDMs, as well as look into the phenomenology of these models, in particular when compared to the type-II 2HDMs. Finally, we discuss the possibility to accommodate the wrong-sign Yukawa limits. These topics are based on the publications:

- Manimala Chkraborti, Dipankar Das, Miguel Levy, Samadrita Mukherjee, Ipsita Saha, Prospects
  of light charged scalars in a three Higgs doublet model with Z<sub>3</sub> symmetry, Phys.Rev.D 104 (2021)
  7, 075033, arXiv: 2104.08146 [hep-ph],
- Dipankar Das, Miguel Levy, Palash B. Pal, Anugrah M. Prasad, Ipsita Saha, Democratic three-Higgs-doublet models: The custodial limit and wrong-sign Yukawa couplings, Phys.Rev.D 107 (2023) 5, 055035, arXiv: 2301.00231 [hep-ph].

Chapter three deals with the study of softly-broken 3HDMs with large symmetry groups, namely  $\Sigma(36)$ . It lays down the groundwork to analysing the different directions in soft-breaking space in which these models can be broken. Namely, it analyses the consequences that some soft-breaking directions have on the scalar sector of the theory, following the work

• Ivo De Medeiros Varzielas, Igor P. Ivanov, Miguel Levy, Exploring multi-Higgs models with softly broken large discrete symmetry groups, Eur.Phys.J.C 81 (2021) 10, 918, arXiv: 2107.08227 [hep-ph].

The fourth chapter is dedicated to a 4HDM which leverages a  $D_4$  symmetry to relate the quark masses and mixings via the scalar sector. It shows an interesting possibility where the Wolfenstein parametrization follows automatically from the necessary hierarchies of the scalars to get the correct quark masses, following

 Ayushi Srivastava, Miguel Levy, Dipankar Das, Diluting quark flavor hierarchies using dihedral symmetry, Eur.Phys.J.C 82 (2022) 3, 205, arXiv: 2107.03756 [hep-ph].

The fifth chapter is dedicated to presenting types of 2HDMs in which the flavour symmetries do not commute with the gauge symmetries. The resulting models have an interesting feature of having the flavour-changing neutral currents (FCNCs) dictated entirely by the quark masses and both Left-Handed (LH) and Right-Handed (RH) mixings. Although the RH mixing is unphysical in 2HDMs, the fact that the flavour symmetry does not respect the gauge symmetries points towards a possible Ultraviolet realisation of these models, as is the case for one of them. This chapter is based on the work

 Gustavo C. Branco, Dipankar Das, Miguel Levy, Palash B. Pal, Crossed two Higgs-doublet models: reduction of Yukawa parameters in the low-scale limit of left-right symmetry and other avatars, Phys.Rev.D 102 (2020) 3, 035007.

The sixth chapter is the first dedicated to modular-invariant theories, and lists the stabilisers for the smallest five modular symmetries, as well as the elements which each point preserves, and is based on

 Ivo De Medeiros Varzielas, Miguel Levy, Ye-Ling Zhou, Symmetries and stabilisers in modular invariant flavour models, JHEP 11 (2020) 085.

Chapter seven is dedicated to presenting the modular version of the Littlest seesaw, which is a very predictive scenario for neutrino mixing, which shows a quite good agreement with experiment. It includes possible extensions of the model to justify the charged-lepton mass hierarchies from a FN-style mechanism. A GUT-inspired model is also shown which is able to preserve the successes of the Littlest Modular Seesaw, while introducing the FN-style mechanism to explain the quark hierarchies, both in the masses and the mixings. A relevant point is the use of lower and upper-triangular forms for the Mass matrices of the charged-leptons and the down quarks, to have sizeable contributions to the quark mixing, while suppressing the contributions to the neutrino mixing. This connection is brought forth due to the SU(5) unification framework which relates the charged-leptons to the down quarks. This chapter closely follows the works

- Ivo De Medeiros Varzielas, Steve F. King, Miguel Levy, *Littlest Modular Seesaw*, JHEP 02 (2023) 143, arXiv: 2211.00654 [hep-ph],
- Ivo De Medeiros Varzielas, Steve F. King, Miguel Levy, A Modular SU(5) Littlest Seesaw, JHEP 05 (2024) 203, arXiv: 2211.00654 [hep-ph].

Finally, chapter eight comprises an extensive study on the possibility of having the main driver behind the quark hierarchies being the closeness of the modulus to the cusp in  $S'_4$  modular-invariant theories. After an *ad hoc* albeit valid choice of modular form normalisations, we list all possible scenarios which can lead to hierarchical quark masses while not having an over-abundance of parameters. We then analyse numerically the results and present our conclusions, following the work

Ivo De Medeiros Varzielas, Miguel Levy, João Penedo, Serguey Petcov, Quarks at the modular S<sub>4</sub>
 cusp, JHEP 09 (2023) 196, arxiv: 2307.14410 [hep-ph].

In the ninth and final chapter, we present our conclusions.

1

## Introduction

The importance of symmetries in modern physics cannot be understated. From Noether's theorem to gauge theories, symmetries are fundamental to our present understanding of Particle Physics. The Standard Model (SM) of particle physics [1–3] remains hitherto the most consensual description of particles and their interactions at a fundamental level. It is a Quantum Field Theory (QFT) based on a Yang-Mills theory [4] locally-symmetric under the gauge group

$$SU(3)_c \times SU(2)_L \times U(1)_Y, \tag{1.1}$$

where  $SU(3)_c$  is the group responsible for Quantum Chromodynamics (QCD), i.e., the strong interactions between coloured particles, and  $SU(2)_L \times U(1)_Y$  is the electroweak (EW) gauge group. The information about the particles and their interactions of the SM are encoded in the Lagrangian,  $\mathcal{L}_{SM}$ , which is determined by the field content of the theory, as well as the gauge group (that is to say, the transformation properties of the fields under the gauge group). In this way, the Lagrangian is the cornerstone of any model, which contains information about physical and mensurable processes, which can be used to test the theory's prediction against experimental confirmations.

In this introduction, we start by doing a brief (and necessarily incomplete) review of the ideas and frameworks upon which the SM is built, in a general way. We then take this knowledge to present the SM, by specifying the language to the gauge group and field content which make up the theory. Despite its numerous successes, the SM is widely regarded as an effective theory, and not the ultimate theory of nature. For this reason, we then introduce the Beyond the SM scenarios most relevant for the remainder of our work. Lastly, we present the central topic of this thesis: the flavour puzzle. On this topic, we introduce the idea of flavour symmetries as a solution to this puzzle, but also dedicate a separate section to a more recent proposal based on modular invariance.

The remainder of the thesis is organised based on the properties of the groups acting as flavour symmetries. As such, we dedicate the next chapter (Chapter 2) to the study of models with Abelian symmetries. This chapter will be dedicated to a specific realisation of a model with three Higgs doublets, in which the Abelian flavour symmetry is employed such that tree-level flavour-changing neutral currents are absent at the tree-level. The following two chapters concern non-Abelian symmetries. In the first (Chapter 3), we perform a study of the scalar sector of a model with three Higgs doublets, when the non-Abelian symmetry is softly-broken. Expanding this study could chart out the phenomenological implications of different directions in parameter space, which could be a helpful tool for model-building. In the second (Chapter 4), we present a model which makes use of a non-Abelian symmetry and four Higgs doublets such that the quark hierarchies are a result of the scalar sector of the theory, rather than relying on the inherent arbitrariness of the Yukawa sector. Next, Chapter 5 is dedicated to uncovering models in which the flavour symmetry does not commute with the gauge symmetry, a scenario which has not received much attention in the literature. The following three chapters are dedicated to modular-invariant theories. First, we dedicate Chapter 6 to the study of the points of different modular symmetries which preserve residual symmetries. Next, Chapter 7 is dedicated to a model which takes advantage of modular symmetries (and their residual symmetries) to arrive at predictive scenarios for the neutrino mixing. Lastly, in Chapter 8 we perform a study to see if the quark hierarchies can be explained in a natural way using properties of the modular symmetries. Finally, Chapter 9 is where we give our conclusions.

#### 1.1 Yang-Mills Theories and the Standard Model

#### 1.1.1 Yang-Mills Theories

Before presenting the full Lagrangian for the SM, let us do a brief review of Yang-Mills theories. For simplicity, let us take a theory composed by a single (complex) scalar transforming as the fundamental representation of the SU(N) gauge group. That is, the scalar field  $\phi(x) = \left(\varphi_1(x), \varphi_2(x), \dots, \varphi_N(x)\right)$  is an N-component complex scalar field, which transforms under the group action of SU(N) as  $\phi \to U\phi$ , where U is a group element of SU(N). If we require global invariance under SU(N), we can write down the usual scalar Lagrangian

$$\mathcal{L} = (\partial_{\mu}\phi)^{\dagger} (\partial_{\mu}\phi) - V(\phi^{\dagger}\phi). \tag{1.2}$$

This is obviously invariant since  $\phi^{\dagger}\phi \to \phi^{\dagger}\phi$ , and  $(\partial_{\mu}\phi)^{\dagger}(\partial_{\mu}\phi) \to (\partial_{\mu}\phi)^{\dagger}(\partial_{\mu}\phi)$ , given that a global transformation does not depend on the spacetime coordinates:  $\partial_{\mu}U = 0$ . On the other hand, if we now require the theory to be invariant under local transformations  $(U \equiv U(x))$ , we have  $\partial_{\mu}U(x) \neq 0$  and  $\partial_{\mu}\phi \to U\partial_{\mu}\phi$  no longer holds. To regain invariance, we need to need to introduce some connection such that the ordinary derivative  $\partial_{\mu}$  is generalised to a covariant derivative  $D_{\mu}$ :

$$D_{\mu} = \partial_{\mu} - i g A_{\mu}(x), \qquad (1.3)$$

which includes a coefficient g as well as some spacetime vector  $A_{\mu}(x)$ , transforming in such a way that  $D_{\mu}\phi \to UD_{\mu}\phi$  under the group action (if  $D_{\mu}\phi$  transforms as  $\partial_{\mu}\phi$  transformed in the global case, then invariance is automatically restored). It is easy to show that the ensuing transformation properties for

 $A_{\mu}$  are

$$A_{\mu} \to U A_{\mu} U^{\dagger} - \frac{i}{q} \left( \partial_{\mu} U \right) U^{\dagger} \,.$$
 (1.4)

The action of SU(N) can be described by  $U(x) = e^{i\varepsilon^a T^a}$ , where  $\varepsilon(x)^a$  are generic parameters in which the spacetime dependence of U(x) is encoded, and  $T^a$  are the generators of SU(N). If we go to the limit of infinitesimal transformations,  $U(x) \simeq \mathbb{1} + i\epsilon^a T^a$ , the transformation of  $A_\mu$  can be recast as

$$A_{\mu} \to A_{\mu} + i\varepsilon^a \left[ T^a, A_{\mu} \right] + \frac{1}{q} \partial_{\mu} \varepsilon^a T^a \,.$$
 (1.5)

Since  $A_{\mu}$  can be taken to be both hermitian and traceless,<sup>1</sup> then we are free to decompose the vector into component fields as  $A_{\mu} = A_{\mu}^{a}T^{a}$ , since the generators of SU(N) span a basis of hermitian and traceless  $N \times N$  matrices. It follows that we have a component fields for  $A_{\mu}$ , one per generator, and we can further simplify the transformation of  $A_{\mu}$ , using

$$\left[T^a, T^b\right] = if^{abc} T^c, \tag{1.6}$$

where  $f^{abc}$  are the group structure constants, from which we get (using the anti-symmetry of  $f^{abc}$ )

$$A^a_\mu \to A^a_\mu - f^{abc} \varepsilon^b A^c_\mu + \frac{1}{g} \partial_\mu \varepsilon^a \,, \tag{1.7}$$

which we can identify as the (global) transformation properties for the adjoint representation of the group G. In this way, we see that Yang-Mills theories posit the existence of vector bosons (one for each generator of the gauge group) which transform as the adjoint representation of the gauge group [5].

We have re-established invariance under local SU(N) transformations for our scalar Lagrangian. Nonetheless, this does not entail that

$$\mathcal{L} = (D_{\mu}\phi)^{\dagger} (D_{\mu}\phi) - V (\phi^{\dagger}\phi)$$
(1.8)

is the most general SU(N) invariant Lagrangian we can write. Indeed, we have seen that  $A_{\mu}$  transform as the adjoint representation, which is always self-conjugate. As such, we are necessarily missing all  $A_{\mu}$  self-interactions (in other words, we have yet introduced any dynamics for the vector bosons). To that end, we can introduce a p-form as

$$H = \frac{1}{p!} H_{\mu_1 \,\mu_2 \,\dots \,\mu_p} dx^{\mu_1} dx^{\mu_2} \,\dots dx^{\mu_p} \,, \tag{1.9}$$

and a differential operator d which acts on a p-form as

$$dH = \frac{1}{p!} \partial_{\nu} H_{\mu_1 \, \mu_2 \, \dots \, \mu_p} dx^{\nu} dx^{\mu_1} dx^{\mu_2} \dots dx^{\mu_p} \,, \tag{1.10}$$

<sup>&</sup>lt;sup>1</sup>We can see that both the trace of  $A_{\mu}$ , as well as the hermiticity condition  $A_{\mu} - A_{\mu}^{\dagger} = 0$  are preserved by the gauge transformations, for any group such as SU(N) whose generators are traceless. Thus, taking  $A_{\mu}$  to be traceless and hermitian is enough to restore the invariance of the theory.

where the differentials  $dx^{\mu}$  are Grassmann variables: dxdy = -dydx. Since the vector bosons carry a spacetime index, a self-interaction term should be (at least) a two-indices tensor, and so our goal is to construct a 2-form  $F = (1/2)F_{\mu\nu}dx^{\mu}dx^{\nu}$ . We start with the 1-form  $A = A_{\mu}dx^{\nu}$ , which from Eq. (1.4) we already know transforms under the action of U as

$$A \to UAU^{\dagger} + \frac{i}{g}UdU^{\dagger}$$
. (1.11)

To build the 2-form using only A, there are only two possibilities:  $A^2$  and dA, and so it follows that F must be some combination of the two. From Eq. (1.11), we can figure out the transformation of both  $A^2$  and dA as

$$A^2 \rightarrow UA^2U^{\dagger} + \frac{i}{g}UAdU^{\dagger} - \frac{i}{g}dUAU^{\dagger} + \frac{1}{g^2}dUdU^{\dagger},$$
 (1.12a)

$$dA \rightarrow UdAU^{\dagger} + dUAU^{\dagger} - UAdU^{\dagger} + \frac{i}{g}dUdU^{\dagger},$$
 (1.12b)

where we used  $UU^{\dagger} = \mathbb{1} \Rightarrow UdU^{\dagger} = -dUU^{\dagger}$ . The minus sign  $UAdU^{\dagger}$  comes from the Grassmann nature of the differentials, since we need to anti-commute the d with the 1-form A. Finally, the term  $Ud^2U^{\dagger}$  is absent since  $d^2 = \partial_{\mu}\partial_{\nu}dx^{\mu}dx^{\nu}$  is identically zero due to fact that the derivatives are symmetric under the exchange of indices, whereas the differentials are anti-symmetric. Interestingly, we see that there is a combination which, although it is not invariant under the action of the gauge symmetry, transforms in a simple fashion:

$$F = dA - igA^2$$
, such that  $F \to UFU^{\dagger}$ . (1.13)

Unfolding the notation to write down the indices explicitly again, we can recast F as

$$F = (\partial_{\mu}A_{\nu} - igA_{\mu}A_{\nu}) dx^{\mu}dx^{\nu} = \frac{1}{2} (\partial_{\mu}A_{\nu} - \partial_{\nu}A_{\mu} - ig[A_{\mu}, A_{\nu}]) dx^{\mu}dx^{\nu}, \qquad (1.14)$$

using, once again,  $dx^{\mu}dx^{\nu} = (1/2)(dx^{\mu}dx^{\nu} - dx^{\nu}dx^{\mu})$ . From  $F = (1/2)F_{\mu\nu}dx^{\mu}dx^{\nu}$ , we can extract the gauge field strength tensor:

$$F_{\mu\nu} = \partial_{\mu}A_{\nu} - \partial_{\nu}A_{\mu} - ig [A_{\mu}, A_{\nu}] \Leftrightarrow F_{\mu\nu}^{a} = \partial_{\mu}A_{\nu}^{a} - \partial_{\nu}A_{\mu}^{a} + gf^{abc}A_{\mu}^{b}A_{\nu}^{c}.$$
 (1.15)

We have already seen that the field strength tensor  $F_{\mu\nu}$  is not invariant under the group action U. However, we can trace out over SU(N), to obtain an invariant quantity:<sup>2</sup>

$$\mathcal{L}_{YM} = -\frac{1}{4} F^{a}_{\mu\nu} F^{a,\,\mu\nu} \,, \tag{1.16}$$

which encodes the  $A_{\mu}$  self-interactions and kinetic terms (note that for a U(1) theory,  $f^{abc}=0$  and we

 $<sup>^2\</sup>mathcal{L}_{\text{YM}}$  is not the only gauge invariant term which can be written. Indeed, the  $\theta$ -term,  $\theta \epsilon^{\mu\nu\lambda\rho} F^a_{\mu\nu} F^a_{\lambda\rho}$ , is not only gauge invariant, but in the origin of the so-called Strong CP problem [6–8], despite being a total derivative. We will ignore this term by taking  $\theta \to 0$ , since we will not address this issue.

recover the QED Lagrangian with the photon propagator and no photon self-interactions).

In this discussion, we assumed the scalar field  $\phi$  to be N-dimensional, and in particular, to transform under the gauge group SU(N) as the fundamental representation. Obviously, the prescription to regain invariance under local transformations does not depend on this, otherwise the scope of Yang-Mills theories would be very limited.<sup>3</sup> Indeed, for a field (which we can now take to be a fermion,  $\psi$ ) in any representation  $\mathbf{r}$  of the gauge group G, we need only to specify in the covariant derivative that the generators  $T^a$  are to be taken in the representation  $\mathbf{r}$ :

$$D_{\mu} = \partial_{\mu} - i g A_{\mu}^{a} T_{\mathbf{r}}^{a}, \qquad (1.17)$$

such that both the scalar Lagrangian, as well as the interacting fermionic theory given by (with  $\gamma^{\mu}$  being the Dirac gamma matrices and  $\overline{\psi}$  the Dirac adjoint:  $\overline{\psi} \equiv \psi^{\dagger} \gamma^{0}$ )

$$\mathcal{L} = \overline{\psi} \left( i \gamma^{\mu} D_{\mu} - m \right) \psi \tag{1.18}$$

are invariant under local transformations of G.

Now that we have seen how the Lagrangian accommodates scalars, fermions, and the vector bosons emerging from the gauge group G, let us introduce more particularities. First, since our ultimate goal in this section is to introduce the SM, we introduce chirality. Established from the start in the SM, there is a different treatment of left-handed (LH) and right-handed (RH) particles. Indeed, the gauge group includes interactions which distinguish chirality: the  $SU(2)_L$ , where L stands for "Left". As such, we introduce the projection operators

$$P_L = \frac{1 - \gamma^5}{2}$$
, and  $P_R = \frac{1 + \gamma^5}{2}$ , (1.19)

where  $\gamma^5 = i\gamma^0\gamma^1\gamma^2\gamma^3$ . A 4-component Dirac spinor  $\psi$  is decomposed into left- and right-handed components as  $\psi_{L,R} = P_{L,R}\psi$ . A direct consequence is that a fermionic mass term cannot arise from a single chirality, as  $m\overline{\psi_L}\psi_L = 0$ . In this sense, we see that the usual Dirac Lagrangian cannot include the term proportional to m, unless we have two fields,  $\psi_L$  and  $\psi_R$ , which transform identically under G. For this reason, we will separate the fermionic Lagrangian into the Dirac  $\overline{\psi_{L,R}}i\rlap/\!\!\!D\psi_{L,R}$ , and mass  $m\overline{\psi_L}\psi_R$  terms, where we introduced the Dirac slash notation,  $\rlap/\!\!\!D = \gamma^\mu D_\mu$ . Through the projection operators, it is easy to see that the kinetic part must couple the same chiralities, whereas the mass terms couple LH to RH fields.

As a first step to see how this generalises to a collection of fields, lets take a collection of n chiral fermionic fields,  $\psi_{L,R}^i$ , where  $i=1,\ldots,n$ . We have already seen that the only non-zero terms are

$$\mathcal{L} = \sum_{i,j} K_{ij}^L \overline{\psi_L^i} i \not \!\! D \psi_L^j + K_{ij}^R \overline{\psi_R^i} i \not \!\! D \psi_R^j + \left( M_{ij} \overline{\psi_L^i} \psi_R^j + \text{h.c.} \right) , \qquad (1.20)$$

where h.c. refers to the hermitian conjugate, and we use  $K^{L,R}$  to denote a matrix for the kinetic terms.

<sup>&</sup>lt;sup>3</sup>The importance of Yang-Mills theories was cemented after these theories were shown to be renormalizable [9].

We have seen that  $D_{\mu}$  was designed to transform as  $D_{\mu}\psi \to UD_{\mu}\psi$ , and thus gauge-invariance requires  $\overline{\psi_L^i}i\not\!\!D\psi_L^j$  and  $(L\to R)$  to vanish if  $\psi_L^i$  and  $\psi_L^j$  transform differently under G. For the mass term, on the other hand, we see that if  $\psi_L^i \to U_L^i\psi_L^i$  and  $\psi_R^j \to U_R^j\psi_R^j$  under the action of G, the term can only be present if  $U_L^i = U_R^j$ . In other words, the (fully symmetric) theory can only have massive fermions if it includes  $\psi_L$  and  $\psi_R$  transforming identically (i.e., as the same representation) under G.

If we now denote the representation of the fields by  $\psi_{\mathbf{r}}$ , since we have seen different representations cannot interact via the Dirac Lagrangian, it decomposes into a sum over the different collections of  $n_{\mathbf{r}}^L$  left-handed and  $n_{\mathbf{r}}^R$  right-handed fields for each  $\mathbf{r}$ :

$$\mathcal{L} = \sum_{\mathbf{r}} \sum_{i,j}^{n_{\mathbf{r}}^L} \sum_{i',j'}^{n_{\mathbf{r}}^R} \left\{ K_{\mathbf{r},ij}^L \overline{\psi_{\mathbf{r},L}^i} i \not \!\!D \psi_{\mathbf{r},L}^j + K_{\mathbf{r},i'j'}^R \overline{\psi_{\mathbf{r},R}^{i'}} i \not \!\!D \psi_{\mathbf{r},R}^{j'} + \left( M_{\mathbf{r},ij'} \overline{\psi_{\mathbf{r},L}^i} \psi_{\mathbf{r},R}^{j'} + \text{h.c.} \right) \right\}.$$
(1.21)

It is clear that the theory does not distinguish between fields with the same quantum numbers (that is to say, which transform identically under G or, equivalently, that have the same representation). We have labelled these fields which an index i, j, i', and j', which is called a flavour index. We can define a flavour space, which acts on the space of the collection of fields with the same representation, chirality and spin (that are indistinguishable from the gauge point of view), that is, on the spaces of  $n_{\mathbf{r}}^L$  and  $n_{\mathbf{r}}^R$  (separately).

The matrix entries of  $K_{\mathbf{r}}^{L,R}$  are not constrained by the gauge structure of the theory and are then general. Since the terms of Eq. (1.21) will (also) be responsible for the propagator of the  $\psi^i$  fields, it becomes clear that we have off-diagonal terms connecting  $\overline{\psi^i} i \not\!\!D \psi^j$ . As such, a field  $\psi^i$  freely-propagating can change its flavour to  $\psi^j$ . Nonetheless, we are free to perform a (non-unitary) transformation on the flavour space of the fields<sup>4</sup>

$$\psi_{L,R}^i \to \psi_{L,R}^{\prime i} = T_{L,R}^{ij} \psi_{L,R}^j,$$
 (1.22)

with  $T_{L,R}$  chosen in such a way that  $T_{L,R}^{\dagger}K^{L,R}T_{L,R} = 1$ , since  $K^{L,R}$  must be hermitian. After this transformation, the Lagrangian becomes

$$\mathcal{L} = \overline{\psi_L^i} \, i \not\!\!D \, \psi_L^i + \overline{\psi_R^i} \, i \not\!\!D \, \psi_R^i + \left( M_{ij} \overline{\psi_L^i} \psi_R^j + \text{h.c.} \right) \,, \tag{1.23}$$

where we redefined  $M = T_L^{\dagger} M T_R$ , since both matrices are completely general from the start, and we see that the kinetic terms are now diagonal. Interestingly, this does not completely fix the basis on the flavour space. Indeed, we see that if we now do a unitary rotation on the fields

$$\psi_{L,R}^i \to U_{L,R}^{ij} \psi_{L,R}^j$$
, (1.24)

the kinetic term remains unchanged, since the Kronecker delta is invariant under unitary transformations.<sup>5</sup>

<sup>&</sup>lt;sup>4</sup>We drop the subscript  $\mathbf{r}$ , since it can be either thought of as left understood, with an implicit summation of all different representations present in the theory, or we can define the space of all fields where the matrix structure is block-diagonal, with the *i*-th block corresponding to the collection of fields with representation  $\mathbf{r}_i$ .

 $<sup>^5\</sup>mathrm{A}$  similar procedure can be applied to the Scalar Lagrangian.

A direct consequence of this is that we can now perform a unitary transformation which diagonalises M, leading to a Lagrangian fully diagonal in flavour. In practice, and for the remainder of the thesis, we refer to flavour (also known as generations or families) as the space where the unitary transformations act, after the canonical diagonalisation of the kinetic terms.

Now that we have seen the Dirac Lagrangian, let us go back to the scalar sector. Previously, we have (surreptitiously) introduced a generic function  $V(\phi^{\dagger}\phi)$  which is manifestly invariant under G, given it is only a function of  $\phi^{\dagger}\phi$ . While appropriate when we are dealing with a single scalar multiplet, we should comment on the generalisation to include an arbitrary number of scalars in arbitrary representations (this has no influence on the discussion above, apart from the necessary specification of the representation in the covariant derivative, already alluded to in Eq. (1.17)). Up to this point, we have been dealing with bilinears, such that it is easy to understand that invariance requires  $\psi^i$  and  $\psi^j$  to transform in the same way.<sup>6</sup> This is justified for the case of fermions, since the mass dimension of 3/2 forbids any (renormalisable) terms which include more than 2 fermionic fields. On the other hand, scalar fields have mass dimension 1, and thus it is possible (i.e., renormalizable) to write polinomial terms up to order 4 in the scalar fields. This is encoded in the Scalar potential,  $V(\Phi)$ , where we use  $\Phi$  to denote the collection of all scalar fields in the theory. Note that we cannot define the scalar potential as a function of  $\Phi^{\dagger}\Phi$ , since this is not the most general gauge-invariant scalar potential for a general theory. Indeed, we have already seen examples of trilinear couplings during our brief review of the gauge sector. The gauge Lagrangian

$$\mathcal{L} = -\frac{1}{4} F^{a}_{\mu\nu} F^{a,\mu\nu} , \quad \text{with} \quad F^{a}_{\mu\nu} = \partial_{\mu} A^{a}_{\nu} - \partial_{\nu} A^{a}_{\mu} + g f^{abc} A^{b}_{\mu} A^{c}_{\nu} , \quad (1.25)$$

already includes terms which are cubic in the (bosonic) fields,  $f^{abc}A^{b,\mu}A^{c,\nu}$  ( $\partial_{\mu}A^{a}_{\nu} - \partial_{\nu}A^{a}_{\mu}$ ), as well as quartic terms. An easy takeaway is that by including a scalar in the adjoint representation, the scalar potential should include the invariant  $\alpha\phi\phi\phi$ , with  $\alpha$  having mass dimension 1. The scalar potential itself can only be constructed after specifying the scalar content of the theory, so for now it suffices to define it as a manifestly invariant combination of scalars, which we write concisely as

$$V\left(\Phi\right) = M_{ij}^{2} \left(\Phi_{i} \otimes \Phi_{j}\right)_{\mathbf{1}} + \alpha_{ijk} \left(\Phi_{i} \otimes \Phi_{j} \otimes \Phi_{k}\right)_{\mathbf{1}} + \lambda_{ijkl} \left(\Phi_{i} \otimes \Phi_{j} \otimes \Phi_{k} \otimes \Phi_{l}\right)_{\mathbf{1}}, \tag{1.26}$$

where  $(...)_1$  denotes the singlet combination(s) of the group tensor product.

In this way, we have generalised the Lagrangians responsible for the Dirac and Klein-Gordon equations to a Yang-Mills theory. However, in practice we gauged a fermionic and a scalar theory separately. In this way, we have effectively ignored the possibility of a fermion-scalar interaction: the Yukawa Lagrangian. Simply by dimensional analysis, it is clear that we can include these interactions via

$$\mathcal{L} \supset Y_{ijk} \overline{\psi_L^i} \psi_R^j \Phi_k + \text{h.c.}, \qquad (1.27)$$

with  $Y_{ijk}$  a dimensionless parameter, which will be non-zero if a gauge-invariant combination of the product  $\overline{\psi_L^i} \otimes \psi_R^j \otimes \Phi_k$  exists.

<sup>&</sup>lt;sup>6</sup>Note that for a field transforming under G as  $\mathbf{r}$ , its hermitian conjugate transforms as  $\overline{\mathbf{r}}$ , such that  $\overline{\psi_{\mathbf{r}}} \otimes \psi_{\mathbf{r}}$  includes a combination which transforms trivially under G.

Summing up all the different pieces we have introduced, we can write a general Lagrangian for a Yang-Mills theories including scalars and fermions as

$$\mathcal{L} = \mathcal{L}_{kin} + \mathcal{L}_{M} + \mathcal{L}_{Yuk} - V(\phi) + \mathcal{L}_{YM}, \qquad (1.28a)$$

$$\mathcal{L}_{kin} = (D_{\mu}\phi^{i})^{\dagger} (D_{\mu}\phi^{i}) + \overline{\psi_{L}^{i}} i \mathcal{D} \psi_{L}^{i} + \overline{\psi_{R}^{i}} i \mathcal{D} \psi_{R}^{i}, \qquad (1.28b)$$

$$\mathcal{L}_M = M_{ij}\overline{\psi_L^i}\psi_R^j + \text{h.c.}, \qquad (1.28c)$$

$$\mathcal{L}_{\text{Yuk}} = Y_{ijk} \overline{\psi_L^i} \psi_R^j \phi_k + \text{h.c.}, \qquad (1.28d)$$

$$V\left(\Phi\right) = M_{ij}^{2} \left(\Phi_{i} \otimes \Phi_{j}\right)_{\mathbf{1}} + \alpha_{ijk} \left(\Phi_{i} \otimes \Phi_{j} \otimes \Phi_{k}\right)_{\mathbf{1}} + \lambda_{ijkl} \left(\Phi_{i} \otimes \Phi_{j} \otimes \Phi_{k} \otimes \Phi_{l}\right)_{\mathbf{1}}, \qquad (1.28e)$$

$$\mathcal{L}_{YM} = -\frac{1}{4} F^{a}_{\mu\nu} F^{a,\mu\nu} \,. \tag{1.28f}$$

#### 1.1.2 Spontaneous Symmetry Breaking: from Goldstone to Higgs

A downside of Yang-Mills theories is that they predict the vector bosons to be massless. This is a direct consequence of the transformation properties of  $A_{\mu}$  seen in Eq. (1.11), which show that mass terms for the gauge bosons  $(A_{\mu}A^{\mu})$  violate local invariance under G. It becomes clear that if we want to construct theories that represent Nature, we need to introduce terms that are not gauge-invariant, at least due to the need for massive force carriers. The interesting possibility is not to include terms which are manifestly not invariant under the gauge symmetry (explicit symmetry breaking), but rather allow the system itself to break the symmetry. The idea behind this is that even if the theory is invariant under the action of G, its solutions (vacuum) may not exhibit the same level of symmetry. This is denoted as spontaneous symmetry breaking (SSB).

To understand the consequences of SSB, we need to go through Goldstone's theorem. We start by denoting a general scalar  $\phi$  as an n-dimensional vector of real fields:  $\phi = (\phi_1, \phi_2, \dots, \phi_n)$ . Note that even if  $\phi$  is taken to be complex, we can just double the dimension of the vector space such that  $\phi$  can be written as a vector of real fields, taken that we change the group generators appropriately. Then, a general scalar Lagrangian can be written as

$$\mathcal{L} = \frac{1}{2} (\partial_{\mu} \phi)^{\dagger} (\partial^{\mu} \phi) - V(\phi) , \qquad (1.29)$$

where  $V(\phi)$  encodes the scalar self-interactions, and the derivatives are the kinetic terms. Note that we are not imposing local invariance (gauging the symmetry) since the Goldstone theorem is relevant regardless of the locality of the symmetry. The kinetic terms and the scalar potential are, by construction, invariant under the action of G, such that under infinitesimal transformations we have

$$\delta V = \frac{\partial V}{\partial \phi_i} \delta \phi_i = \frac{\partial V}{\partial \phi_i} \left( i \varepsilon^a \left( T^a \right)_{ij} \phi_j \right) = 0.$$
 (1.30)

Since this condition must hold for arbitrary transformations, the solution cannot depend on  $\varepsilon^a$ , and we are left with a (the number of generators of G) independent equations, which we can differentiate with

respect to  $\phi_k$ :

$$\frac{\partial}{\partial \phi_k} \left( \frac{\partial V}{\partial \phi_i} (T^a)_{ij} \phi_j \right) = \frac{\partial^2 V}{\partial \phi_k \partial \phi_i} (T^a)_{ij} \phi_j + \frac{\partial V}{\partial \phi_i} (T^a)_{ij} \frac{\partial \phi_j}{\partial \phi_k} = 0.$$
 (1.31)

Now, our goal is to evaluate the vacuum state, which is defined by  $\langle \phi \rangle$  such that  $V(\phi)$  is at a minimum:

$$\left. \frac{\partial V}{\partial \phi_i} \right|_{\phi = \langle \phi \rangle} = 0. \tag{1.32}$$

Together with  $\partial \phi_i / \partial \phi_k = \delta_{ik}$ , we find

$$\frac{\partial^2 V}{\partial \phi_k \partial \phi_i} \bigg|_{\phi = \langle \phi \rangle} (T^a)_{ij} \langle \phi_j \rangle = 0.$$
(1.33)

The missing part of the puzzle is to recognize that the second order derivatives of  $V(\phi)$  computed at the minimum of the potential are nothing more than the mass terms for the scalar fields. Indeed, we can decompose the fields into  $\phi_i(x) = \langle \phi_i \rangle + \varphi_i(x)$ , where we separate the fields from the groundstate. Then, the second order derivatives of  $\varphi$  analysed at the vacuum correspond to the bilinear terms of the  $\varphi$  fields, that is, their mass-squared terms. Thus, we can rewrite the invariance condition as

$$M_{ki}^{2}(T^{a})_{ij}\langle\phi_{j}\rangle=0, \qquad a=1,\ldots,n_{G},$$
 (1.34)

where  $n_G$  is the number of generators of G. Inspecting this condition, we see that there are two possible solutions: Either  $T^a \langle \phi \rangle = 0$ , or  $M_k^2 = 0$ . The conclusion is straightforward: for each generator of G that does not leave the vacuum state invariant (i.e.,  $T^a \langle \phi \rangle \neq 0$ ) there must exist an associated massless scalar. On the other hand, if the vacuum is left invariant under the action of  $n_H$  generators of G, then the theory is still unbroken for the subgroup H these generators form, and the scalar masses are unrestricted. Thus, Goldstone's theorem states that if the vacuum state breaks the full group of the theory onto a subgroup  $G \supset H$ , there are  $n_G - n_H$  massless scalar particles (Nambu-Goldstone bosons), where  $n_G$  and  $n_H$  are the number of generators of G and its subgroup G, respectively. Interestingly, we can quickly take two lessons from the theorem. First, if a field is a singlet under G, it cannot be responsible for SSB, since G and break G via a non-zero vacuum state is G. Second, the number of generators which are broken by a scalar is restricted by the number of degrees of freedom of the scalar itself. That is, since we require one massless particle for each broken generator, the number of fields in G cannot be lower than the number of broken generators.

We have just seen that scalars with non-zero vevs lead to a number of massless scalars corresponding to the number of broken generators of the symmetry. If the symmetry is local, we had seen that, to restore invariance, we need to introduce vector bosons which will be massless. How these two points interact is called the Higgs mechanism [10–14]. To understand this, we now impose the requirement of local-invariance under G, and introduce the Yang-Mills fields. It is more convenient to work with real

fields, and so we double the space for the case of non-real  $\phi$ . The transformation properties are

$$\phi_i \to (\mathbb{1} + i\varepsilon^a T^a)_{ij} \,\phi_j \,, \tag{1.35}$$

and since the fields are real, we can find a basis where the representation matrices  $T^a$  are pure imaginary and anti-symmetric.<sup>7</sup> The covariant derivative for a generic scalar field  $\phi$  is then given by

$$D_{\mu}\phi = \left(\partial_{\mu} - igA_{\mu}^{a}T^{a}\right)\phi, \tag{1.36}$$

leading to its kinetic term

$$(D^{\mu}\phi)^{\dagger}(D_{\mu}\phi) = (\partial^{\mu}\phi)^{T}(\partial_{\mu}\phi) - 2ig(\partial^{\mu}\phi)^{T}(T^{a}\phi)A_{\mu}^{a} + g^{2}A^{\mu,a}(\phi^{T}T^{a}T^{b}\phi)A_{\mu}^{b},$$
(1.37)

where we used the anti-symmetry of the generators, and the fact that we are working in a real basis. Now, let us admit some non-zero groundstate for  $\phi$ , which we denote by  $\phi = \langle \phi \rangle + \varphi$ . At the same time, we specify an index which runs through the broken generators  $(\alpha, \beta = n_H + 1, \dots, n_G)$  where H is the residual symmetry group), while we keep the original indices to run over all generators  $(a, b = 1, \dots, n_G)$ . Then, the expression reads

$$(D^{\mu}\phi)^{\dagger}(D_{\mu}\phi) = (\partial^{\mu}\varphi)^{T}(\partial_{\mu}\varphi) - 2ig(\partial^{\mu}\varphi)^{T}(T^{a}\varphi)A^{a}_{\mu} + g^{2}A^{\mu,a}(\varphi^{T}T^{a}T^{b}\varphi)A^{b}_{\mu}$$
$$-2ig(\partial^{\mu}\varphi)^{T}(T^{\alpha}\langle\phi\rangle)A^{\alpha}_{\mu} + g^{2}A^{\mu,\alpha}\left(\langle\phi\rangle^{T}T^{\alpha}T^{\beta}\langle\phi\rangle\right)A^{\beta}_{\mu}$$
$$+g^{2}A^{\mu,\alpha}\left(\langle\phi\rangle^{T}T^{\alpha}T^{b}\varphi\right)A^{b}_{\mu} + g^{2}A^{\mu,a}\left(\varphi^{T}T^{a}T^{\beta}\langle\phi\rangle\right)A^{\beta}_{\mu}, \tag{1.38}$$

where we used the fact that some generators are unbroken:  $T^a \langle \phi \rangle A^a_\mu = T^\alpha \langle \phi \rangle A^\alpha_\mu$ . This Lagrangian encodes the trilinear and quartic interactions between the gauge bosons and the scalar fields, but here we are interested in the terms which couple only two fields. Before separating the field from a vacuum, the only bilinear present was  $(\partial^\mu \phi)^T (\partial_\mu \phi)$ , responsible for the dynamics of the scalar fields. However, now we have

$$(D^{\mu}\phi)^{\dagger}(D_{\mu}\phi) \supset (\partial^{\mu}\varphi)^{T}(\partial_{\mu}\varphi) - 2ig(\partial^{\mu}\varphi)^{T}(T^{\alpha}\langle\phi\rangle)A^{\alpha}_{\mu} + g^{2}A^{\mu,\alpha}\left(\langle\phi\rangle^{T}T^{\alpha}T^{\beta}\langle\phi\rangle\right)A^{\beta}_{\mu}. \tag{1.39}$$

Here, a few notes are in order. First, we see that now we have mass terms for the gauge fields whose generators were broken (the last term in Eq. (1.39) runs only for  $A^{\alpha}_{\mu}A^{\mu,\beta}$ , with  $T^{\alpha}\langle\phi\rangle\neq0$ ). In this way, we have one massive vector field for each generator which is not left invariant by the vacuum. On the other hand, we also see that there are terms mixing exactly these vector fields with the scalar fields:  $(\partial^{\mu}\varphi)^{T}(T^{\alpha}\langle\phi\rangle)A^{\alpha}_{\mu}$ . This makes the identification of a propagator more complicated. The fact that this is true for not all, but only the subset of  $A^{\alpha}_{\mu}$ , which is exactly the number of massless Goldstone bosons

<sup>&</sup>lt;sup>7</sup>This can be easily understood by noting that the generators of SO(N) can be taken to be purely imaginary and anti-symmetric, and that SU(N) is a subgroup of SO(2N).

is not coincidental. Indeed, this is solved by the gauge-fixing Lagrangian, which in the  $R_\xi$  gauge reads

$$\mathcal{L}_{gf} = \frac{1}{\xi} G^{a\dagger} G^a, \quad \text{with} \quad G^a = \partial^{\mu} A^a_{\mu} - \xi i g \left( \varphi^T T^a \left\langle \phi \right\rangle \right), \qquad (1.40)$$

$$= \frac{1}{\xi} \left( \partial^{\mu} A^{a}_{\mu} \right) \left( \partial^{\nu} A^{a}_{\nu} \right) + 2 i g \left( \partial^{\mu} \varphi \right)^{T} \left( T^{\alpha} \left\langle \phi \right\rangle \right) A^{\alpha}_{\mu} + \xi g^{2} \varphi^{T} \left( T^{\alpha} \left\langle \phi \right\rangle \left\langle \phi \right\rangle^{T} T^{\alpha} \right) \varphi \,. \tag{1.41}$$

It is clear that the gauge-fixing eliminates the bilinear terms which were mixing the Goldstone bosons with the vector bosons.

This may be best seen through the Unitary Gauge [15, 16] and by the Kibble decomposition [13, 17]. The general idea is to perform a gauge transformation on our collection of fields  $\phi$ , such that the new fields are independent of the Goldstone bosons. Once more, we assume there is a non-zero vacuum expectation value (vev) of the scalars fields which breaks the group G onto a subgroup H. Let us divide the notation for the broken and unbroken generators, for clarity. In the following, we take  $T^a$  to run over all generators of G,  $T^i$  to run over the generators of H, and  $T^\alpha$  to run over the generators of G which are not generators of G (the broken generators). We can freely define a new set of fields  $\widetilde{\phi}$  which are related by a general transformation of G,  $\gamma(x)$ , as

$$\widetilde{\phi}(x) = \gamma(x)\phi(x). \tag{1.42}$$

We now wish to impose that  $\widetilde{\phi}(x)$  has no dependence on the Goldstone bosons. Goldstone's theorem tells us that the eigenvectors which must have a zero eigenvalue are given by  $T^{\alpha}\langle\phi\rangle\neq0$ . Then, the condition

$$\widetilde{\phi}^T T^a \langle \phi \rangle = 0 \quad \Leftrightarrow \quad \widetilde{\phi}^T T^\alpha \langle \phi \rangle = 0, \qquad (1.43)$$

effectively guarantees that  $\widetilde{\phi}$  is independent of the Goldstone bosons, since it states that the space spanned by the Goldstone bosons  $(T^{\alpha}\langle\phi\rangle)$  and the space spanned by  $\widetilde{\phi}$  must be orthogonal. Looking at the condition of Eq. (1.43), we effectively decreased the degrees of freedom we had in  $\phi$  by  $n_G - n_H$  (we have one independent condition for each  $\alpha$ , which are the number of broken generators, and thus massless modes). Obviously, these degrees of freedom must reappear elsewhere, and in short, the dependence on the Goldstone fields is transferred onto  $\gamma(x)$ . This can be seen by explicitly taking a decomposition of the generators (and thus of the group elements) as

$$g = \exp\left(i\epsilon^{a}(x)T^{a}\right) = \exp\left(i\zeta^{\alpha}(x)T^{\alpha} + i\theta^{i}(x)T^{i}\right) = \exp\left(i\zeta^{\alpha}(x)T^{\alpha}\right)\exp\left(i\theta^{i}(x)T^{i}\right). \tag{1.44}$$

From the invariance of  $\mathcal{L}$ , up to the necessary transformations of  $A_{\mu}$ , the theory is invariant under the transformation  $\phi \to g\phi$ , as it must. However, we have that  $h \langle \phi \rangle = \langle \phi \rangle$  for  $h = \exp(i\theta^i(x)t^i) \in H$ , that is, there is a residual subgroup which leaves the vacuum invariant (even if trivial). Then, the transformation  $\gamma(x)$ , or in other words the condition of Eq. (1.43), is not uniquely defined, and leads to redundant conditions when acted with h on the right (i.e., live on the coset space of G/H [13, 18]).<sup>8</sup> Then, we can

<sup>&</sup>lt;sup>8</sup>For clarity, we could define  $\phi' = h\phi$  and the condition  $\widetilde{\phi}^T T^{\alpha} \langle \phi \rangle = 0$  would be the same.

define the transformation as

$$\gamma(x) = \exp\left(i\zeta^{\alpha}(x)T^{\alpha}\right). \tag{1.45}$$

Lo and behold, the number of degrees of freedom we need to fully specify  $\gamma(x)$  such that  $\widetilde{\phi}(x)$  is independent of the Goldstone bosons exactly matches their number. As we predicted, the missing degrees of freedom of  $\widetilde{\phi}$  are shifted to  $\gamma(x)$ .

Lastly, we just need to understand how this redefinition affects our Lagrangian. Realising that  $\gamma(x)$  is just an element of G, lets define  $\gamma(x)^{-1} \equiv U$ , such that

$$\phi(x) = U(x)\widetilde{\phi}(x). \tag{1.46}$$

This is nothing more than a gauge transformation, and we already know that the theory will be invariant under U(x), such that the Goldstones disappear from the Lagrangian. Namely,

$$D_{\mu}\phi = \left(\partial_{\mu} - igA'_{\mu}\right)U\widetilde{\phi} = \left(U\partial_{\mu} - igA'_{\mu}U + (\partial_{\mu}U)\right)\phi = U\left(\partial_{\mu} - igA_{\mu}\right)\widetilde{\phi}.$$
 (1.47)

Finally, if we now shift the fields  $\widetilde{\phi} = \langle \phi \rangle + \varphi$ , and keep the bilinear terms, we find

$$(D^{\mu}\phi)^{\dagger} (D_{\mu}\phi) \supset (\partial^{\mu}\varphi)^{\dagger} (\partial_{\mu}\varphi) + g^{2} A^{\mu,\alpha} \left( \langle \phi \rangle^{T} T^{\alpha} T^{\beta} \langle \phi \rangle \right) A^{\beta}_{\mu}, \tag{1.48}$$

where the term that mixed the Gauge and scalar fields which was present in Eq. (1.39) vanishes due to the condition of Eq. (1.43). In this way, the Goldstones effectively decouple from the theory, and the Gauge bosons are now massive. In practice, we should not worry about the missing degrees of freedom, since the gauge transformations of Eq. (1.11) effectively means we have reabsorbed these fields onto the vector fields:

$$A_{\mu} \to U A_{\mu} U^{\dagger} + \frac{i}{g} U \left( \partial_{\mu} U^{\dagger} \right) ,$$
 (1.49)

where

$$U = \exp\left(i\zeta^{\alpha}(x)T^{\alpha}\right)\,,\tag{1.50}$$

and  $\zeta^{\alpha}$  are the Goldstone modes. In this way, our vector fields have now three degrees of freedom, rather than the original two. This turns out to be instrumental, since massive vector fields require a longitudinal polarization (and thus three degrees of freedom). In the end, we end up with a theory which has one massive gauge boson for each of the broken generators, with each ensuing Goldstone boson being absorbed into the definition of the gauge bosons themselves. Thus, from a theory with massless vector bosons and phenomenologically-troublesome massless scalars, we arrive at a theory with short-range forces.

Interestingly, a second consequence of a non-zero vacuum state comes from the Yukawa interaction terms. We had seen that mass terms for the fermions require a vector-like nature for the fermions, since

we needed to construct an invariant combination,  $M_{ij}\overline{\psi_L^i}\psi_R^j$ . Now, we see that we can generate effective mass terms for the fermions arising from the  $Y_{ijk}\overline{\psi_L^i}\psi_R^j\phi_k$  terms.

#### 1.1.3 The Standard Model

After the above recap of Yang-Mills theories, we are in a position to describe the Standard Model of Particle Physics. The gauge group is  $SU(3)_c \times SU(2)_L \times U(1)_Y$ , where the SU(3) group is responsible for QCD, and  $SU(2)_L \times U(1)_Y$  is the electroweak sector of the theory. We will not address QCD here, and thus focus on the EW theory. As we have seen previously, for the theory to be gauge-invariant, we need to define the covariant derivative:

$$D_{\mu} = \partial_{\mu} - ig W_{\mu}^{a} T_{\mathbf{r}}^{a} + ig' Y B_{\mu}, \qquad a = 1, 2, 3,$$
 (1.51)

where  $T_{\mathbf{r}}^a$  are the SU(2) representation matrices for  $\mathbf{r}$ , Y is the field's hypercharge, g and g' are the gauge couplings associated with the  $SU(2)_L$  and  $U(1)_Y$  symmetries, with  $W_{\mu}^a$  and  $B_{\mu}$  their respective gauge bosons. The associated gauge field strengths are defined by the group alone, and are given by

$$W_{\mu\nu}^a = \partial_{\mu}W_{\nu}^a - \partial_{\nu}W_{\mu}^a - g\epsilon^{abc}W_{\mu}^bW_{\nu}^c, \qquad (1.52a)$$

$$B_{\mu\nu} = \partial_{\mu}B_{\nu} - \partial_{\nu}B_{\mu} \,, \tag{1.52b}$$

where  $\epsilon^{abc}$  is the 3-dimensional Levi-Civita symbol (the group structure constants for SU(2)), and we note the absence of the third term for  $B_{\mu\nu}$  since the U(1) group structure constants are zero (the group is Abelian).

Next, we need to define the field content of the model and their transformation properties under the SM gauge group:

$$Q_{iL} \sim \left(\mathbf{3}, \mathbf{2}, \frac{1}{6}\right) \quad , \qquad u_{iR} \sim \left(\mathbf{3}, \mathbf{1}, \frac{2}{3}\right), \qquad d_{iR} \sim \left(\mathbf{3}, \mathbf{1}, -\frac{1}{3}\right),$$

$$L_{iL} \sim \left(\mathbf{1}, \mathbf{2}, -\frac{1}{2}\right) \quad , \qquad e_{iR} \sim \left(\mathbf{1}, \mathbf{1}, -1\right),$$

$$\phi \sim \left(\mathbf{1}, \mathbf{2}, \frac{1}{2}\right) \quad , \tag{1.53}$$

where i = 1, 2, 3 is a flavour index, meaning there are three fields with the same quantum numbers both for the quarks (coloured fermions), as well as for the leptons (uncoloured fermions).

We see that we only have doublet and singlet representations under SU(2). Thus, we can specify normalised the Pauli matrices  $(T_2^a = \tau^a/2)$  as the representation matrices for an SU(2) doublet in Eq. (1.51). The Lagrangian reads

$$\mathcal{L}_{kin} = (D_{\mu}\phi)^{\dagger} (D_{\mu}\phi) + \overline{\psi_{iL}} i \not D \psi_{iL} + \overline{\psi_{iR}} i \not D \psi_{iR}, \quad \text{with} \begin{cases} \psi_{iL} = Q_{iL}, L_{iL} \\ \psi_{iR} = u_{iR}, d_{iR}, e_{iR} \end{cases}$$
(1.54a)

$$\mathcal{L}_{YM} = -\frac{1}{4} W^a_{\mu\nu} W^{\mu\nu,a} - \frac{1}{4} B_{\mu\nu} B^{\mu\nu} , \qquad (1.54b)$$

$$\mathcal{L}_{\text{Yuk}} = Y_u \, \overline{Q_L} \, \widetilde{\phi} \, u_R + Y_d \, \overline{Q_L} \, \phi \, d_R + Y_\ell \, \overline{L_L} \, \phi \, e_R + \text{h.c.} \,, \tag{1.54c}$$

$$V(\phi) = \mu^2 \left(\phi^{\dagger}\phi\right) + \lambda \left(\phi^{\dagger}\phi\right)^2, \tag{1.54d}$$

where we introduced the notation  $\psi_{L,R} = \begin{pmatrix} \psi_{1L,R}, & \psi_{2L,R}, & \psi_{3L,R} \end{pmatrix}^T$ , such that  $Y_{u,d,\ell}$  are  $3 \times 3$  matrices in flavour space. Additionally, we introduced the conjugate Higgs doublet  $\widetilde{\phi}$  which is defined as

$$\widetilde{\phi} = i\tau_2 \phi^* \,, \tag{1.55}$$

which also transforms as a doublet under SU(2), but with opposite hypercharge to  $\phi$ .

We can parametrise the scalar field, including a non-zero vev, as

$$\phi = \frac{1}{\sqrt{2}} \begin{pmatrix} \sqrt{2}\phi^+ \\ v + h + iz \end{pmatrix} , \qquad (1.56)$$

where  $\phi^+$  is a complex field (with  $\phi^-$  as its conjugate), h and z are real fields, and v denotes the vev. The choice of allocating the vev to the real component of  $\phi$  is a convenient basis choice. Minimizing the scalar potential, we find a non-zero vev as long as  $\mu^2 < 0$  and  $\lambda > 0$ , and we find three Goldstone bosons,  $\phi^{\pm}$  and z, and a physical scalar h. Thus, there are three broken generators, leading to a preserved U(1) group which corresponds to the electric charge generator (the  $\phi$  field is a singlet under  $SU(3)_c$ , and thus is unable to break any of the colour generators, and the h field is electrically neutral, and thus electromagnetism remains unbroken):

$$SU(3)_c \times SU(2)_L \times U(1)_Y \to SU(3)_c \times U(1)_Q$$
, with  $Q = T^3 + Y$ . (1.57)

As expected for a locally-invariant theory, the three Goldstone bosons will be absorbed into the definitions of the massless gauge bosons, and three bosons associated with the electroweak group will become massive. Since the unbroken generator is a linear combination of  $T^3$  and Y, the massless gauge boson will also be a linear combination of the original fields. This can be easily seen by computing the mass terms for the gauge bosons and noticing there are mixed terms between  $B_{\mu}$  and  $W_{\mu}^3$ . Thus, we can write the physical (mass eigenstates) gauge bosons as

$$A_{\mu} = -s_{\mathbf{w}}W_{\mu}^{3} + c_{\mathbf{w}}B_{\mu}, \qquad (1.58)$$

$$Z_{\mu} = c_{\mathbf{w}} W_{\mu}^{3} + s_{\mathbf{w}} B_{\mu} , \qquad (1.59)$$

where  $s_{\rm w}$  and  $c_{\rm w}$  are the usual shorthand notation for  $\cos \theta_{\rm w}$  and  $\sin \theta_{\rm w}$ , respectively, and the weak mixing angle,  $\theta_{\rm w}$  is defined by

$$\tan \theta_{\rm w} = \frac{g'}{g} \,. \tag{1.60}$$

The gauge bosons  $W^{1,2}_{\mu}$  are already mass eigenstates, but have no definite electric charge. Since this generator is still unbroken, the electric charge is preserved by all processes within the SM, and thus it is

helpful to define the charge eigenstate gauge bosons:

$$W^{\pm} = \frac{1}{\sqrt{2}} \left( W_{\mu}^{1} \mp i W_{\mu}^{2} \right) . \tag{1.61}$$

The (tree-level) masses of the gauge bosons are given by

$$M_{W^{\pm}} = \frac{1}{2}gv, \qquad M_Z = \frac{1}{2}\sqrt{g^2 + g'^2}v, \qquad M_A = 0.$$
 (1.62)

The massless gauge boson is identified with the unbroken  $U(1)_Q$  symmetry, which describes the electromagnetic interaction. The relation between the  $W^{\pm}$  and Z vector bosons is protected by an accidental (approximate) symmetry called the custodial symmetry, and reads

$$\frac{M_{W^{\pm}}}{M_Z} = \cos \theta_{\rm w} \,, \tag{1.63}$$

and will be further explored in Chapter 2.

We see that there are no bare mass terms for the fermions, since the different chiralities cannot combine into a SM-singlet combination. As such, the mass terms for the fermions comes from the Yukawa terms after the electroweak symmetry breaking (EWSB), that is, after  $\phi$  acquires a non-zero vev. Parametrizing the SU(2) doublets as

$$Q_{iL} = \begin{pmatrix} u \\ d \end{pmatrix}_{iL}, \qquad L_{iL} = \begin{pmatrix} \nu \\ \ell \end{pmatrix}_{iL}, \qquad (1.64)$$

we can expand the Yukawa terms around the vev and obtain the mass terms for the fermions:

$$\mathcal{L}_{\text{yuk}} = Y_u \overline{Q_L} \widetilde{\phi} u_R + Y_d \overline{Q_L} \phi d_R + Y_u \overline{L_L} \phi e_R + \text{ h.c.}$$

$$\supset \frac{v}{\sqrt{2}} Y_u \overline{u_L} u_R + \frac{v}{\sqrt{2}} Y_d \overline{d_L} d_R + \frac{v}{\sqrt{2}} Y_\ell \overline{\ell_L} e_R + \text{ h.c.}, \qquad (1.65)$$

leading to  $3 \times 3$  mass matrices for the up- and down-type quarks, as well as for the charged-leptons:

$$M_u = \frac{v}{\sqrt{2}} Y_u , \qquad M_d = \frac{v}{\sqrt{2}} Y_d , \qquad M_\ell = \frac{v}{\sqrt{2}} Y_\ell .$$
 (1.66)

Since the quantum numbers across a family are identical, that is, there is no way to distinguish  $Q_{1L}$  from  $Q_{2L}$ , for example, we are free to perform any unitary  $3 \times 3$  rotations across the different generations without changing the overall physics (recall that the kinetic terms will be invariant under these rotations). Thus, we are free to perform the field redefinitions

$$Q_L = U_u Q'_L, \qquad u_R = V_u u'_R, \qquad L_L = U_\ell L'_L, \qquad e_R \to V_\ell e'_R,$$
 (1.67)

such that the matrices

$$D_u = U_u^{\dagger} Y_u V_u , \qquad D_{\ell} = U_{\ell}^{\dagger} Y_{\ell} V_{\ell} , \qquad (1.68)$$

are diagonal with positive eigenvalues. These rotations allow us to find a basis where the charged-leptons and the up-type quarks are mass eigenstates. Since  $Y_d$  was a general complex matrix, the new matrix,  $U_u^{\dagger}Y_d$ , remains a general complex matrix. The necessary rotation to send it to a diagonal form would require both a right- and left-handed rotation:

$$d_L = U_d d'_L, \qquad d_R = V_d d'_R.$$
 (1.69)

Nonetheless, since the  $u_L$  and  $d_L$  fields are components of the same SU(2) doublet, we cannot redefine these two separately without off-diagonal terms appearing somewhere else in the theory. Indeed, in a basis where both  $D_u$  and  $D_d$  are diagonal, we see that the gauge interactions that connect the up- and down-type quarks are modified as

$$\mathcal{L}_{kin} \supset \overline{Q_L} i \not \!\! D Q_L$$

$$\supset \frac{g}{\sqrt{2}} \overline{u_{iL}} \gamma^{\mu} d_{iL} W_{\mu}^{+} + h.c.$$

$$= \frac{g}{\sqrt{2}} \overline{u'_{iL}} \gamma^{\mu} \left( U_{u}^{\dagger} U_{d} \right)_{ij} d'_{jL} W_{\mu}^{+} + h.c.,$$
(1.70)

such that the charged-current interactions, which were diagonal in the flavour basis, now have off-diagonal terms when written in terms of the quark mass eigenstates. This mixing matrix is the Cabibbo-Kobayashi-Maskawa (CKM) matrix [19, 20]:

$$V_{\rm CKM} = U_n^{\dagger} U_d \,. \tag{1.71}$$

The CKM matrix is a complex unitary  $3 \times 3$  matrix, and thus has 9 real parameters: 3 mixing angles and 6 phases. Nonetheless, we can reabsorb 5 of these phases onto the definition of the left-handed upand down-type quarks fields. Although we have 6 quarks, the final phase cannot be reabsorbed this way as it merely becomes a global redefinition of the phases (and the theory is already U(1) invariant). Thus, the final count of parameters in the CKM matrix is 3 mixing angles ( $\theta_{12}$ ,  $\theta_{13}$ ,  $\theta_{23}$ ), and a CP-violating (CPV) phase ( $\delta$ ). The standard parametrization following the PDG is [21]:

$$V_{\text{CKM}} = \begin{pmatrix} 1 & 0 & 0 \\ 0 & c_{23} & s_{23} \\ 0 & -s_{23} & c_{23} \end{pmatrix} \begin{pmatrix} c_{13} & 0 & s_{13}e^{-i\delta} \\ 0 & 1 & 0 \\ -s_{13}e^{i\delta} & 0 & c_{13} \end{pmatrix} \begin{pmatrix} c_{12} & s_{12} & 0 \\ -s_{12} & c_{12} & 0 \\ 0 & 0 & 1 \end{pmatrix}$$

$$= \begin{pmatrix} c_{12}c_{13} & s_{12}c_{13} & s_{13}e^{-i\delta} \\ -s_{12}c_{23} - c_{12}s_{23}s_{13}e^{i\delta} & c_{12}c_{23} - s_{12}s_{23}s_{13}e^{i\delta} & s_{23}c_{13} \\ s_{12}s_{23} - c_{12}c_{23}s_{13}e^{i\delta} & -c_{12}s_{23} - s_{12}c_{23}s_{13}e^{i\delta} & c_{23}c_{13} \end{pmatrix}, \qquad (1.72)$$

where the quark mixing angles and CPV phase can be extracted from experiments involving quarks.

A clear distinction between the quark and lepton sector comes from the fact that the RH fields are present for both types of quarks, but there are no RH counterparts to the LH neutrino fields in  $L_L$ . In this way, as we have seen previously, there is no mass matrix for the neutrinos, and we are free to redefine

the  $\nu_L$  fields as we see fit, since they are degenerate (and massless) and thus indistinguishable. As a consequence, we can always choose  $U_{\nu}$  to compensate  $U_{\ell}$  such that the charged-current interactions of the leptons remain diagonal.

The discovery of neutrino oscillations is a clear sign that the SM as described breaks down. The reason is that neutrino oscillations imply that (at least two) neutrinos are massive (and non-degenerate) [22–25], and so we need to include some neutrino mass generation mechanism in the theory. There are different possibilities on how to actually include this, but we are not interested in specific realisations for now. Instead, we just assume there is some way to obtain a  $3 \times 3$  mass matrix for the neutrinos,  $M_{\nu}$ , such that the field redefinitions needed for both  $M_{\ell}$  and  $M_{\nu}$  to be diagonal do not match in general. Thus, the leptonic equivalent to the CKM matrix, the Pontecorvo-Maki-Nakawaga-Sakata (PMNS) matrix, arises in the charged-current interactions in the leptonic sector [22, 26].

We do note a peculiarity which may give rise to a significant difference between the quark and lepton sectors, such that the CKM and the PMNS may not be exact analogues. Although it was not imposed from the start, there are lingering accidental symmetries in the SM. In particular, the difference between the number of baryons and leptons in any given process is a conserved charge. In some of the neutrino mass generation mechanisms, the leptonic number is violated through some processes, meaning the low-energy neutrinos (after EWSB) are not charged under any unbroken symmetry. Thus, it is possible to build the 4-dimensional Dirac fermion spinor from a single 2-dimensional Weyl spinor [28], such that we can build Majorana mass terms of the form

$$\mathcal{L}_{\text{Weinberg}} = \frac{1}{2} \overline{\nu_L^c} M_\nu \nu_L + \text{h.c.}, \qquad (1.73)$$

where  $\psi^c$  is the charge-conjugated field of  $\psi$ . We will go into detail about these terms later, and for now we just note that  $\nu$  and  $\overline{\nu^c}$  transform identically under phase redefinitions. Since these terms are not invariant under global phase redefinitions, the neutrino fields cannot be rephased, and we find two additional CPV phases in the PMNS matrix:

$$V_{\text{PMNS}} = \begin{pmatrix} c_{12}c_{13} & s_{12}c_{13} & s_{13}e^{-i\delta} \\ -s_{12}c_{23} - c_{12}s_{23}s_{13}e^{i\delta} & c_{12}c_{23} - s_{12}s_{23}s_{13}e^{i\delta} & s_{23}c_{13} \\ s_{12}s_{23} - c_{12}c_{23}s_{13}e^{i\delta} & -c_{12}s_{23} - s_{12}c_{23}s_{13}e^{i\delta} & c_{23}c_{13} \end{pmatrix} \begin{pmatrix} e^{i\eta_{1}} & 0 & 0 \\ 0 & e^{i\eta_{2}} & 0 \\ 0 & 0 & 1 \end{pmatrix}.$$
 (1.74)

The PMNS parameters can be extracted from neutrino oscillation experiments [29–31], although they are insensitive to the Majorana phases [32, 33]. These phases can only be extracted from Lepton number violating processes, such as neutrinoless double beta decay [34].

<sup>&</sup>lt;sup>9</sup>The B and L numbers are separately conserved, but there are non-perturbative effects (instantons/sphalerons) which violate B + L, leaving B - L as a conserved charge [27].

# 1.2 Going Beyond the Standard Model

The SM continues to successfully accommodate the increasingly precise experimental measurements. This does not entail, however, that it can be the ultimate theory of Nature. The paradigmatic problem of the SM lies with neutrino masses. Within the SM as originally proposed, there is a striking left-right asymmetry in the field content, as neutrinos do not have their RH counterpart. This was intended to forbid massive neutrinos in the theory. Originally well motivated, the discovery of neutrino oscillations requires at least two neutrinos to be massive, requiring physics beyond the SM. Moreover, several experimental observations suggest the existence of dark matter (DM) [36–39], and since the SM cannot provide a suitable candidate for DM, it is another evidence for the need for SM extensions. Finally, other cosmological considerations, such as the baryon asymmetry of the Universe (BAU) [40] and inflation [41, 42] also suggest New Physics (NP) must be present.

These are just a few of the myriad of reasons why beyond the SM (BSM) physics remains such an active area of research. Among the many paths to BSM theories, one attribute that seems to be consistently present is a larger scalar sector. Indeed, the SM relies a minimal scalar sector, which in turn leads to several properties being a feature of the SM, but no longer guaranteed when the scalar sector is extended. For this reason, we focus now on extensions to the scalar sector of the theory.

# 1.2.1 Multi-Higgs Models

The extension of the SM's scalar sector is one of the best motivated paths to BSM. Indeed, scalars are necessary for the spontaneous breaking of symmetries, such that any gauge extension of the SM must rely on an extended scalar sector from the low-energy perspective. Global symmetries, such as the Peccei-Quinn symmetry which was proposed as a solution to the strong CP problem [43–45], also rely on new scalars.

However, not all scalar extensions are on equal footing. The scalar sector is intrinsically connected to the gauge sector via the Higgs mechanism, such that the inclusion of arbitrary representations can lead to different contributions to the gauge boson masses. This is encompassed in the  $\rho$ -parameter, which can be cast as [46–48]:

$$\rho = \frac{M_W^2}{M_Z^2 \cos^2 \theta_W} = \frac{\sum_i \left[ T_i (T_i + 1) - Y_i^2 \right] v_i}{2 \sum_i Y_i^2 v_i}, \tag{1.75}$$

in the convention where the electric charge operator is given by  $Q_i = T_i^{(3)} + Y_i$ , with  $T_i^{(3)}$  being the third component of the weak isospin, and where the vev is  $v_i/\sqrt{2}$  for complex fields, and  $v_i$  for real scalars. Experimentally, this value is found to be very close to one [21], which can effectively constrain the vev of the representations which can drive  $\rho$  away from unity. While it is possible to construct models with large multiplets which respect  $\rho = 1$  at the tree-level [48], a simple observation is that we can include any number of SM-like doublets  $(T_i = 1/2, Y_i = \pm 1/2)$  or SU(2) singlets  $(T_i = 0)$ , since they cannot drive  $\rho$  away from one.<sup>11</sup> This motivates the study of n-Higgs doublet models (nHDMs). Indeed, the introduction

<sup>&</sup>lt;sup>10</sup>Perhaps the most striking, but which we do not address, is that it cannot account for gravitational interactions [35].

<sup>&</sup>lt;sup>11</sup>This applies at the tree-level. To be safeguarded against loop contributions, it is useful to introduce a custodial

of additional Higgs doublets has been one of the most popular choices for new physics extensions beyond the SM. A minimal choice, the two Higgs doublet model (2HDM) [49] has been discussed widely in the literature from both theoretical and phenomenological points of view (see [47] and references within). Here, our goal is not to do a comprehensive review of nHDMs, but rather to draw the attention to a number of defining characteristics of these models.

#### The Scalar Potential

The scalar sector of the SM is exceptionally simple, including only two real parameters. The inclusion of additional SM-like doublets will lead to a more complicated scalar potential, which can be cast as [50]

$$V = \mu_{ij} \left( \phi_i^{\dagger} \phi_j \right) + \lambda_{ij,kl} \left( \phi_i^{\dagger} \phi_j \right) \left( \phi_k^{\dagger} \phi_l \right) , \qquad (1.76)$$

where the indices run from 1 to n, and the condition of hermicity mandates

$$\mu_{ij} = \mu_{ji}^*$$
, and  $\lambda_{ij,kl} = \lambda_{kl,ij} = \lambda_{ji,lk}^* = \lambda_{lk,ji}^*$ . (1.77)

We can see that for n doublets, the scalar potential will have  $n^2 + n^2(n^2 + 1)/2$  real parameters [51]. As it must, if we set n = 1, then we recover the SM case with two real parameters. A relevant remark is that given the invariance under  $SU(2)_L$ , we have a freedom to rotate the SU(2) basis of the fields in the theory as a whole. As such, if we assign non-zero vevs to all four components of  $\phi$ , we still have the freedom to perform a unitary  $2 \times 2$  SU(2) transformation such that only one of the components has a non-zero vev. In this sense, we can understand two remarkable features of the SM: the vacuum state cannot break the  $U(1)_Q$  symmetry (in other words, the EWSB always leads to a massless photon), nor the CP symmetry in the scalar sector (the vev can always be rephased to be real). On the other hand, this is a consequence of having only one scalar doublet. By including additional doublets, the rotations need to render each doublet with neutral vacua only are generally not the same for each doublet. As such, it is possible for some configurations of nHDMs to lead to charge-breaking vacua [52]. Not surprisingly, the possibility of having complex vacua for the doublets (i.e., CP violation in the scalar sector) also becomes a possibility (note that the existence of complex parameters in the potential does not necessarily entail CPV) [53].

Unremarkably, one difference between having a minimal scalar sector and extending the number of Higgs representations, is the number of physical spin-0 particles. Each SM-like doublet includes 4 fields, which can be divided into two neutral scalars ( $H_i$  and  $A_i$ ) and two charged-Higgs ( $H_i^{\pm}$ ). In the SM, the pseudoscalar and the charged-Higgs are Goldstone bosons, and we are left with a single CP-even scalar (the SM-Higgs). On the other hand, in an nHDM framework, apart from the Goldstones, the models will feature 2n-1 neutral scalars, and n-1 physical charged-Higgs. If CP is conserved, we can further divide the neutral particles into n CP-even and n-1 CP-odd scalars. Due to the existence of these particles, the models have a much richer phenomenology. The nonstandard particles can allow for signals impossible within the SM, such as new resonances and decay channels, DM candidates, deviations from the SM-Higgs couplings, modifications of the phase transitions of the early Universe, and flavour-changing neutral symmetry on the scalar sector. A detailed discussion is deferred to Chapter 2.

currents (FCNCs), to name a few, besides also providing a suitable low-energy framework for some BSM extensions.

The richer phenomenology comes at the expense of a more complicated scalar potential. This also obfuscates the conditions for the theoretical considerations such as boundedness from below and perturbative unitarity, but these must still be kept in check [54, 55]. Additionally, the parameters must be such that the vacuum is neutral, otherwise the photon becomes massive. This can be imposed by following a SSB procedure similar to the SM, and attributing

$$\langle \phi_1 \rangle = \frac{1}{\sqrt{2}} \begin{pmatrix} v^{\pm} \\ v_1 \end{pmatrix}, \qquad \langle \phi_i \rangle = \frac{1}{\sqrt{2}} \begin{pmatrix} 0 \\ v_i \end{pmatrix}, \qquad i = 2, \dots, n$$
 (1.78)

where  $v^{\pm}$  is the charge-breaking vacuum, whereas  $v_i$  can be complex. It is interesting to note that the imposition that  $v^{\pm}=0$  (such that  $U(1)_Q$  is unbroken) does not amount to fine-tuning (in the sense that it does not require small parameters or cancellations) but rather selects a subset of the parametric space. Namely, selecting a neutral vacuum only requires the parameters that govern  $(\phi_i^{\dagger}\phi_i)(\phi_j^{\dagger}\phi_j) - (\phi_i^{\dagger}\phi_j)(\phi_j^{\dagger}\phi_i)$  to be positive [51]. Finally, the vevs of each individual doublets are not constrained, but cannot be arbitrarily large. Since all the doublets have the same quantum numbers, they couple to the gauge bosons in the same way, and thus contribute equally to their masses, which will be governed by a single quantity,  $v^2 = \sum_i |v_i|^2$ , which must match the observed value of  $(246 \text{ GeV})^2$ .

#### Yukawa Sector and FCNCs

Extending the scalar sector with arbitrary representations will not generally lead to additional couplings with the SM fermions. On the other hand, as already alluded to in Eq. (1.28), including copies of the SM doublet (extending the concept of generations to the scalar sector) will, in fact, introduce a large multiplicity of Yukawa couplings. In general, for an nHDM, we can write

$$\mathcal{L}_{\text{Yuk}} = -\overline{L_L}\Pi_i e_R \phi_i - \overline{Q_L}\Gamma_i d_R \phi_i + \overline{Q_L}\Delta_i u_R \widetilde{\phi}_i + \text{h.c.}, \quad i = 1, \dots, n,$$
(1.79)

where we suppress the flavour indices and introduce a notation widely used in the context of 2HDMs for the Yukawa matrices among the different sectors. In the most general case, all Yukawa matrices can be complex (albeit not all coefficients are physical), further worsening the proliferation of free parameters in nHDMs.

After the EWSB, the fermion masses and mixings follow in a manner similar to the SM, with

$$M_{\ell} = \frac{1}{\sqrt{2}} \sum_{i} \Pi_{i} v_{i}, \qquad M_{d} = \frac{1}{\sqrt{2}} \sum_{i} \Gamma_{i} v_{i}, \qquad M_{u} = \frac{1}{\sqrt{2}} \sum_{i} \Delta_{i} v_{i}^{*}.$$
 (1.80)

One key difference lies in the fact that with  $n \geq 2$ , the diagonalisation of the mass matrices no longer implies the individual Yukawa matrices are diagonal. As a consequence, there can be non-diagonal couplings between the fermions and neutral scalars, something that is absent in the SM.

The simplest way to see this is by performing a rotation on the generation space of the scalars to the

Higgs basis [56–58], where only one doublet has a non-zero vev. This merely amounts to a basis choice, since it is brought by a unitary transformation of the scalar doublets:

$$\phi_j^H = X_{jk}\phi_k$$
, with  $X_{1k} = \frac{1}{v}v_k^*$ , (1.81)

where we introduce the superscript H to identify the fields in the Higgs basis. It is easy to see that the first Higgs,  $\phi_1^H$  will get the entirety of the vev, whereas the remaining will be vevless, due to the unitary nature of the transformation.

In this basis, the mass matrices simplify to

$$M_{\ell} = \frac{1}{\sqrt{2}} \Pi v , \qquad M_d = \frac{1}{\sqrt{2}} \Gamma v , \qquad M_u = \frac{1}{\sqrt{2}} \Delta v , \qquad (1.82)$$

with

$$Y = X_{i1}Y_i$$
, with  $Y = \Pi, \Gamma, \Delta$ , (1.83)

although that is not relevant in this scenario, since these matrices are arbitrary from the start, and remain arbitrary after this transformation. More importantly, we can rewrite the Yukawa Lagrangian in this basis as

$$-\mathcal{L}_{\text{Yuk}} = \frac{\sqrt{2}}{v} \left( \overline{L_L} M_{\ell} e_R \phi_1^H + \overline{Q_L} M_d d_R \phi_1^H + \overline{Q_L} M_u u_R (\phi_1^H)^* \right)$$

$$+ \overline{L_L} \Pi_i e_R \phi_i^H + \overline{Q_L} \Gamma_i d_R \phi_i^H + \overline{Q_L} \Delta_i u_R (\phi_i^H)^* + \text{h.c.},$$

$$(1.84)$$

where i = 2, ..., n, and we redefined the  $\Pi_i, \Gamma_i, \Delta_i$  matrices accordingly  $(Y_i = X_{ij}Y_i \text{ with } Y_i = \Pi_i, \Gamma_i, \Delta_i)$ . We label the scalar component fields in the Higgs basis as

$$\phi_1^H = \frac{1}{\sqrt{2}} \begin{pmatrix} \sqrt{2}G^+ \\ H + iG^0 \end{pmatrix}, \qquad \phi_{i+1}^H = \frac{1}{\sqrt{2}} \begin{pmatrix} \sqrt{2}H_i^+ \\ R_i + iI_i \end{pmatrix}, \quad i = 1, \dots, n-1,$$
 (1.85)

where  $G^{\pm}$  and  $G^0$  are the Goldstone bosons (a consequence of the Higgs basis). Expanding the SU(2) contractions, the Yukawa Lagrangian becomes

$$-\mathcal{L}_{\text{Yuk}} = \frac{R_{i} + iI_{i}}{\sqrt{2}} \left( \overline{e_{L}} \Pi_{i} e_{R} + \overline{d_{L}} \Gamma_{i} d_{R} - \overline{u_{L}} \Delta_{i}^{\dagger} u_{R} \right) + H_{i}^{+} \left( \overline{\nu_{L}} \Pi_{i} e_{R} + \overline{u_{L}} \Gamma_{i} d_{R} - \overline{u_{R}} \Delta_{i}^{\dagger} d_{L} \right)$$

$$+ \frac{R_{i} - iI_{i}}{\sqrt{2}} \left( \overline{e_{R}} \Pi_{i}^{\dagger} e_{L} + \overline{d_{R}} \Gamma_{i}^{\dagger} d_{L} - \overline{u_{R}} \Delta_{i} u_{L} \right) + H_{i}^{-} \left( \overline{e_{R}} \Pi_{i}^{\dagger} \nu_{L} + \overline{d_{R}} \Gamma_{i}^{\dagger} u_{L} - \overline{d_{L}} \Delta_{i} u_{R} \right)$$

$$+ \sqrt{2} \frac{H}{v} \left( \overline{e_{L}} M_{\ell} e_{R} + \overline{u_{L}} M_{u} u_{R} + \overline{d_{L}} M_{d} d_{R} + \text{h.c.} \right).$$

$$(1.86)$$

To get a better grasp on the implications, it is useful to write the Lagrangian in terms of the fermions' mass eigenstates:

$$-\mathcal{L}_{\text{Yuk}} = \frac{R_i + iI_i}{\sqrt{2}} \left( \overline{e} N_{\ell}^i P_R e + \overline{d} N_d^i P_R d - \overline{u} N_u^i P_R u \right)$$

$$+ \frac{R_{i} - iI_{i}}{\sqrt{2}} \left( \overline{e} N_{\ell}^{i\dagger} P_{L} e + \overline{d} N_{d}^{i\dagger} P_{L} d - \overline{u} N_{u}^{i} P_{L} u_{L} \right)$$

$$+ H_{i}^{+} \left( \overline{\nu} U_{\nu}^{\dagger} U_{\ell} N_{\ell}^{i} P_{R} e + \overline{u} U_{u}^{\dagger} U_{d} N_{d}^{i} P_{R} d - \overline{u} N_{u}^{i\dagger} U_{u}^{\dagger} U_{d} P_{L} d \right)$$

$$+ H_{i}^{-} \left( \overline{e} N_{\ell}^{i} i^{\dagger} U_{\ell} U_{\nu}^{\dagger} P_{L} \nu + \overline{d} N_{d}^{i\dagger} U_{d}^{\dagger} U_{u} P_{L} u - \overline{d} U_{d} U_{u}^{\dagger} N_{u}^{i} P_{R} u \right)$$

$$+ \sqrt{2} \frac{H}{v} \left( \overline{e} D_{\ell} e + \overline{u} D_{u} u + \overline{d} D_{d} d \right) , \qquad (1.87)$$

where we made use of the chiral projectors, and defined the matrices which control the FCNCs [59]:

$$N_{\ell}^{i} = U_{\ell}^{\dagger} \Pi_{i} V_{e} , \qquad N_{d}^{i} = U_{d}^{\dagger} \Gamma_{i} V_{d} , \qquad N_{u} = U_{u}^{\dagger} \Delta_{i} V_{u} , \qquad (1.88)$$

under the convention

$$D_f = U_f^{\dagger} M_f V_f \,. \tag{1.89}$$

Finally, we can rewrite the Yukawa Lagrangian as

$$-\mathcal{L}_{\text{Yuk}} = \sqrt{2} \frac{H}{v} \left[ \overline{e} D_{\ell} e + \overline{u} D_{u} u + \overline{d} D_{d} d \right]$$

$$+ R_{i} \left[ \overline{e} \left( N_{\ell}^{i} P_{R} + N_{\ell}^{i\dagger} P_{L} \right) e + \overline{d} \left( N_{d}^{i} P_{R} + N_{d}^{i\dagger} P_{L} \right) d - \overline{u} \left( N_{u}^{i} P_{R} + N_{u}^{i\dagger} P_{L} \right) u \right]$$

$$+ i I_{i} \left[ \overline{e} \left( N_{\ell}^{i} P_{R} - N_{\ell}^{i\dagger} P_{L} \right) e + \overline{d} \left( N_{d}^{i} P_{R} - N_{d}^{i\dagger} P_{L} \right) d - \overline{u} \left( N_{u}^{i} P_{R} - N_{u}^{i\dagger} P_{L} \right) u \right]$$

$$+ H_{i}^{+} \left[ \overline{\nu} V_{\text{PMNS}} N_{\ell}^{i} P_{R} e + \overline{u} \left( V_{\text{CKM}} N_{d}^{i} P_{R} - N_{u}^{i\dagger} V_{\text{CKM}} P_{L} \right) d \right] + \text{h.c.}.$$

$$(1.90)$$

The fact that the diagonalisation of  $M_f$  no longer mandates each Yukawa matrix to be diagonal implies that, in a general nHDM, the matrices  $N_{u,d}^i$  will be general and, most importantly, non-diagonal. As such, we can have a neutral particle  $(R_i \text{ or } I_i)$  mediating interactions (say,  $b \to s$ ) which change the flavours of the quarks (the so-called FCNCs) at the tree-level. Experimentally, these processes are found to be very suppressed, and compliance with flavour data requires mechanisms to keep these in control.

# The Alignment Limit and Unitarity

The existence of nonstandard scalars and their rich phenomenology in nHDMs may run into conflict with experiments. With the continuing agreement between the experimental data and the SM predictions, it is useful to find ways to be safeguarded against dangerous contributions which lead to large deviations between the model's predictions and those of the SM. One possibility is to go to the decoupling limit, where the nonstandard masses are much heavier than the EW scale, such that the deviations are suppressed by  $(\Lambda_{\rm EW}/\Lambda_{NP})^2$  [60–63]. However, there is a possibility which encompasses the decoupling limit, but which does not necessarily require such a degree of decoupling: the alignment limit [64–66].

Experimentally, the magnitudes of the couplings between the observed Higgs at the LHC and the vector bosons (W and Z) as well as the fermions are well-measured via, for instance, Higgs decays. Given their good agreement with the SM values, it is desirable to have a way to keep these values in check when extending the framework to nHDMs. If we recall our discussion on the Higgs basis, we see it has two

important characteristics: the whole EW vev is in a single Higgs doublet, and that same scalar couples to fermions in a SM-like fashion (that is, flavour-conserving and proportional to their mass,  $m_f/v$ ). Expanding the covariant derivative  $(D^{\mu}\phi_i)^{\dagger}(D_{\mu}\phi_i)$ , it is clear that all trilinear couplings  $H_iVV$  vanish if  $H_i$  is vevless, such that the only surviving (trilinear) gauge-gauge-scalar coupling in the Higgs basis is HVV, whose magnitude will be controlled by the EW vev, v. In other words, in the Higgs basis, the field with non-zero vev H couples to two gauge bosons exactly as in the SM. Additionally, since it also couples to fermions identically to the SM, fermionic Higgs decays cannot disentangle the H scalar from the SM's sole scalar particle.

However, the rotation to the Higgs basis does not imply that H is a mass eigenstate, and thus, a physical particle which can be observed at particle colliders. On the other hand, if the model has one mass eigenstate which coincides with H, then the mass and Higgs bases are aligned, and there exists a physical scalar (whose mass must match the 125 GeV to be identified with the observed scalar) whose couplings identically match those of the SM Higgs, such that we automatically comply with the Higgs coupling modifiers.<sup>12</sup> This is called the alignment limit [63–71].

The conditions for the alignment limit are easy to see for an nHDM. If the Higgs basis is given by

$$\phi^H = X\phi_k \,, \quad \text{with} \quad X_{1k} = \frac{1}{v}v_k^* \,,$$
 (1.91)

and the mass basis is generically

$$\phi' = \mathcal{O}_{\alpha}\phi \quad , \tag{1.92}$$

meaning the two bases are related by

$$\phi' = (\mathcal{O}_{\alpha} X^{\dagger}) \phi^H \,, \tag{1.93}$$

where the condition  $(\mathcal{O}_{\alpha}X^{\dagger})_{11} = 1$  is enough to describe the alignment limit. For clarity, we specify for the case of a CP-conserving scenario. We can parametrise the vevs as

$$v_{1} = v \cos \beta_{1} \cos \beta_{2} \dots \cos \beta_{n-1},$$

$$v_{2} = v \sin \beta_{1} \cos \beta_{2} \dots \cos \beta_{n-1},$$

$$\dots$$

$$v_{k} = v \left( \prod_{i=2}^{k} \sin \beta_{k-1} \right) \left( \prod_{i=k}^{n-1} \cos \beta_{k} \right),$$

$$\dots$$

$$v_{n} = v \sin \beta_{n-1},$$

$$(1.94)$$

with  $\sum_i v_i^2 = v^2 = (246 \text{ GeV})^2$ . This fixes the first line of X following the usual prescription. Now, we need to define a basis for  $\mathcal{O}_{\alpha}$ . We note that we can define a  $n \times n$  rotation matrix similar to the standard

<sup>&</sup>lt;sup>12</sup>The Higgs basis (see Eq. (1.81)) is not unique, since it only fixes one line of the SO(n) rotation matrix, leaving us with a SO(n-1) rotation freedom between the vevless doublets.

parametrization for the fermion mixing matrices (without phases) through

$$(R^{ij})_{k,l} = \left(\delta_k^i \delta_l^i + \delta_k^j \delta_l^j\right) (\cos \alpha_{ij} - 1) + \delta_i^k + \left(\delta_k^j \delta_l^i - \delta_k^i \delta_l^j\right) \sin \alpha_{ij},$$
 (1.95a)

$$\mathcal{O}_{\alpha}^{T} = \prod_{i=1}^{n} \prod_{j=i+1}^{n} R^{ij} \tag{1.95b}$$

with i = 1, ..., n-1 and j > i. Note that the parametrisations for  $\mathcal{O}_{\alpha}$  and  $v_k$  were judiciously chosen to have

$$v_k = O_{\alpha}^T \begin{pmatrix} v \\ 0 \\ \vdots \\ 0 \end{pmatrix}, \quad \text{if} \quad \alpha_{1j} = \beta_{j-1}. \tag{1.96}$$

In other words, the condition  $(O_{\alpha}X^{T})_{11}=1$  translates to

$$\alpha_{1i} = \beta_{i-1}, \quad i = 2, \dots, n.$$
 (1.97)

It is important to state that, as noted in [67], this prescription differs from the usual notation for the 2HDM.

As a final remark, we note that the experimental data is mostly sensitive to the magnitude of the Higgs couplings, such that, for example, wrong-sign limits (where the couplings of the observed scalar have the same magnitude than those of the SM, but with an opposite sign) can still be allowed. However, since this constitutes a deviation from the alignment limit, it implies that unitarity is violated at some scale, mandating the existence of New Physics below that energy. More accurately, if the couplings of the observed Higgs are not SM-like, we can compute the scale at which unitarity breaks down, for example from the  $\overline{f}f \to VV$  processes, as [72]:

$$\Lambda_{\rm UV} = \frac{8\pi v^2}{m_f} \frac{1}{1 - \kappa_f^h \kappa_V^h} \,, \quad V = W, Z \,, \tag{1.98}$$

where we introduced a notation where [73, 74]

$$\kappa_X^h = \frac{g_{hXX}}{g_{hXX}^{\text{SM}}}. (1.99)$$

In the alignment limit, we have  $\kappa_f^h = \kappa_W^h = \kappa_Z^h = 1$ , such that  $\Lambda_{\rm UV} \to \infty$ . Therefore, the alignment limit not only helps circumventing the stringent constraints from experiments, but also allows for the theory to be valid at all scales, from the unitarity point of view. If the alignment between the mass and Higgs basis is not perfect, then the masses of the nonstandard scalars must be below  $\Lambda_{\rm UV}$  to restore unitarity, such that Eq. (1.98) gets modified to

$$\Lambda_{\text{UV}} = \frac{8\pi v^2}{m_f} \frac{1}{1 - \kappa_f^h \kappa_V^h - \sum_{k=1}^{n-1} \kappa_f^{H_k} \kappa_V^{H_k}}, \quad V = W, Z,$$
(1.100)

restoring unitarity up to arbitrary scales. 13

## 1.2.2 Neutrino Masses

The discovery of neutrino oscillations is a clear sign of the need for physics beyond the Standard Model. The reason being that neutrino oscillations mean that (at least two) neutrinos must be massive. This is in stark contrast with the SM, where neutrinos come out naturally massless. Here, we will understand why it is so, and go through a simple extension which allows for neutrino masses.

In a four-dimensional spacetime, the Lorentz group is isomorphic to  $SU(2)_L \times SU(2)_R$ , generated by  $\vec{J} \pm i\vec{K}$  respectively, where  $\vec{J}$  are the generators of the angular momentum and  $\vec{K}$  are the boosts [17, 76]. These are connected by complex conjugation, as well as parity. As such, when we refer to a (2-component) spinor, these can have representations under the first and/or second SU(2) groups. Spin 1/2 representations under the first (second) SU(2) are left-handed (right-handed). Since conjugation transforms  $SU(2)_L$  onto  $SU(2)_R$ , the conjugate of a left-handed field is right-handed. So, if we define a LH and a RH field:

$$\psi_L \sim (\mathbf{2}, \mathbf{1}), \qquad \psi_R \sim (\mathbf{1}, \mathbf{2}),$$
 (1.101)

under  $SU(2)_L \times SU(2)_R$ , the Lorentz transformation is given by

$$\psi_{L,R} \to \Lambda_{L,R} \psi_{L,R} = e^{\frac{i}{2}\vec{\sigma} \cdot (\vec{\omega} \mp i\vec{\nu})} \psi_{L,R} , \qquad (1.102)$$

where  $\vec{\sigma}$  are the Pauli matrices, and  $\vec{\omega}$  and  $\vec{\nu}$  are the real rotation and boost angles. For infinitesimal transformations, we can expand in powers and keep the first term as

$$\psi_{L,R} \to \left[ 1 + \frac{i}{2} \left( \sigma_1(\omega_1 \mp i\nu_1) + \sigma_2(\omega_2 \mp i\nu_2) + \sigma_3(\omega_3 \mp i\nu_3) \right) \right] \psi_{L,R} \,.$$
 (1.103)

It can easily be seen that complex conjugation will not produce a spinor which transforms simply under the Lorentz group. However, we can indeed find combinations which allow us to construct LH spinors from RH conjugated spinors:

$$\overline{\psi_L} \equiv \pm \sigma_2 \psi_R^* \sim (\mathbf{2}, \mathbf{1}) \;, \qquad \overline{\psi_R} \equiv \pm \sigma_2 \psi_L^* \sim (\mathbf{1}, \mathbf{2}) \;.$$
 (1.104)

Since a parity transformation leaves  $\vec{J}$  invariant, but changes  $\vec{K} \to -\vec{K}$ , it is easy to see that, under the parity operator, we have  $\psi_L \to \psi_R$  and  $\psi_R \to \psi_L$ . Later, we will see that we can also define a charge-conjugation operator, which in the Weyl basis can be written as (the superscript W is used to avoid confusion)

$$C = i\gamma_2^W \gamma_0^W = \begin{pmatrix} i\sigma_2 & 0\\ 0 & -i\sigma_2 \end{pmatrix}, \qquad (1.105)$$

<sup>&</sup>lt;sup>13</sup>The alignment limit restores unitarity up to arbitrary scales from the  $VV \to VV$  and  $f\overline{f} \to VV$  processes. However, unitarity can still be compromised for an unreasonably large number of multiplets [75].

such that, in this basis, the charge conjugation relates

$$\psi_L \to i\sigma_2 \psi_R^*, \qquad \psi_R \to -i\sigma_2 \psi_L^*.$$
 (1.106)

However, it is more consensual to work with Dirac spinors, which we present below.

If we go back to the Dirac Lagrangian:

$$\mathcal{L}_{\text{Dirac}} = i\overline{\Psi}\gamma^{\mu}\partial_{\mu}\Psi - m\overline{\Psi}\Psi, \qquad (1.107)$$

and expand it in terms of the 2-component spinors that compose  $\Psi$ :

$$\Psi = \begin{pmatrix} \chi \\ \xi^{\dagger} \end{pmatrix}, \qquad \Psi^{\dagger} = \begin{pmatrix} \chi^{\dagger} & \xi \end{pmatrix} \tag{1.108}$$

we find

$$\mathcal{L}_{\text{Dirac}} = i\chi^{\dagger} \overline{\sigma}^{\mu} \partial_{\mu} \chi + i\xi^{\dagger} \overline{\sigma}^{\mu} \partial_{\mu} \xi - m(\chi \xi + \chi^{\dagger} \xi^{\dagger}), \qquad (1.109)$$

where we used the Weyl basis for the gamma matrices ( $\mu = 0, \dots, 3$  and k = 1, 2, 3)

$$\gamma^{\mu} \equiv \begin{pmatrix} 0 & \sigma^{\mu} \\ \overline{\sigma}^{\mu} & 0 \end{pmatrix}, \quad \text{with} \quad \begin{cases} \sigma^{\mu} = (\mathbb{1}_{2}, \sigma^{k}) \\ \overline{\sigma}^{\mu} = (\mathbb{1}_{2}, -\sigma^{k}) \end{cases}$$
 (1.110)

One interesting point of showing explicitly the Dirac Lagrangian with respect to the 2-component spinors is that the symmetry  $\chi \leftrightarrow \xi$  symmetry is evident. However, we note that while  $\chi$  and  $\xi$  obviously have the same chirality (transformation properties under the Lorentz group), one comes from  $\Psi$  and the other from  $\Psi^{\dagger}$ . As such, they must have opposite additive quantum numbers (in other words, opposite charges). We can then define the charge conjugation operator  $\mathcal C$  as something which is able to perform the transformation:

$$\Psi = \begin{pmatrix} \chi \\ \xi^{\dagger} \end{pmatrix} \xrightarrow{\text{Charge Conjugation}} \Psi^c \equiv \begin{pmatrix} \xi \\ \chi^{\dagger} \end{pmatrix} . \tag{1.111}$$

The particles will obey the Dirac equation

$$(i\partial - qA - m)\psi = 0, \qquad (1.112)$$

and our goal is to find the field which obeys the same equation, but with opposite charge:

$$(i\partial + qA - m)\psi^c = 0. (1.113)$$

Using  $(\gamma^{\mu})^{\dagger} = \gamma^0 \gamma^{\mu} \gamma^0$ , we can do the hermitian conjugate and multiply on the right by  $\gamma^0$  to find the

equation for the adjoint:

$$\overline{\psi}(-i\partial \!\!\!/ - qA - m) = 0. \tag{1.114}$$

Transposing, and writing  $-\gamma_{\mu}^{T} = \mathcal{C}^{-1}\gamma_{\mu}\mathcal{C}$ , we find

$$(i\mathcal{C}^{-1}\gamma^{\mu}\partial_{\mu}\mathcal{C} + q\mathcal{C}^{-1}\gamma^{\mu}A_{\mu}\mathcal{C} - m)\overline{\psi}^{T} = 0.$$
(1.115)

Finally, multiplying by C on the right, the equation reduces to

$$(i\partial + qA - m)C\overline{\psi}^T = 0, \qquad (1.116)$$

such that the charge-conjugated spinor,  $\Psi^c$  can be defined by

$$\Psi^c = \mathcal{C}\overline{\Psi}^T, \tag{1.117}$$

where C must obey a few conditions (most notably  $C^{-1}\gamma^{\mu}C = -(\gamma^{\mu})^{T}$ ), but is not independent of the matrix representation chosen for the gamma matrices. In both the Dirac and Weyl bases, it can be written as  $C = i\gamma_2\gamma_0$ .

Let us now investigate the possible mass terms we can write with two Weyl spinors,  $\psi_1$  and  $\psi_2$ :

$$\mathcal{L}_{\text{mass}} = \frac{1}{2} \begin{pmatrix} \overline{\psi_1^c} & \overline{\psi_2^c} \end{pmatrix} \begin{pmatrix} m_L & m_D \\ m_D & m_R \end{pmatrix} \begin{pmatrix} \psi_1 \\ \psi_2 \end{pmatrix} + \text{h.c.}.$$
 (1.118)

Since they have well-defined chiralities, let us make the judicious choice

$$\psi_1 = \psi_L^c \to \overline{\psi_1^c} = \overline{\psi_L} \qquad \psi_2 = \psi_R \to \overline{\psi_2^c} = \overline{\psi_R^c},$$
(1.119)

where we used  $C^TC = 1$ . This helps us understand why the matrix is symmetric. Indeed, the off-diagonal elements can be recast as:

$$\overline{\psi_2^c} \, \psi_1 = \overline{\psi_R^c} \, \psi_L^c = \psi_R^T \, \mathcal{C}^2 \, \overline{\psi_L}^T = -\psi_R^T \, \overline{\psi_L}^T = -\psi \, P_R \, \overline{\psi}^T \,, \tag{1.120}$$

using the property  $C^2 = -1$ . If we now evaluate  $-\psi^T \overline{\psi}^T$ , we find (using  $\gamma^0 = \text{diag}(\mathbb{1}_2, -\mathbb{1}_2)$  in the Dirac Basis)

$$-\begin{pmatrix} \psi_L & \psi_R \end{pmatrix} \gamma^0 \begin{pmatrix} \psi_L^{\dagger} \\ \psi_R^{\dagger} \end{pmatrix} = -(\psi_L \psi_L^{\dagger} - \psi_R \psi_R^{\dagger}) = +(\psi_L^{\dagger} \psi_L - \psi_R^{\dagger} \psi_R) = \overline{\psi} \psi, \qquad (1.121)$$

since the fermionic fields are anti-commuting. Thus,

$$\overline{\psi_2^c} \, \psi_1 = \overline{\psi_R^c} \, \psi_L^c = \overline{\psi_L} \, \psi_R = \overline{\psi_1^c} \, \psi_2 \,, \tag{1.122}$$

and the matrix must be symmetric. If we include more generations, this is simply generalised to

$$\mathcal{L}_{\text{mass}} = \frac{1}{2} \begin{pmatrix} \overline{\psi_1^c} & \overline{\psi_2^c} \end{pmatrix} \begin{pmatrix} m_L & m_D \\ m_D^T & m_R \end{pmatrix} \begin{pmatrix} \psi_1 \\ \psi_2 \end{pmatrix} + \text{h.c.}.$$
 (1.123)

As such, the off-diagonal terms are nothing other than the usual Dirac mass terms, which lead to a degeneracy between the LH and RH fields, if the diagonal entries are absent. This is the exactly what we had seen before for the SM fermions.

In the SM, the neutrinos are purely left-handed (and the anti-neutrinos right-handed), consequence of  $\nu_R$  being absent. Therefore, the Dirac mass term cannot be built, and we said that was enough to justify their masslessness. Now we see that we could have written a mass term of the type  $\overline{\nu_L}m_L\nu_L^c+h.c.$ , which could lead to massive neutrinos even without their RH counterpart. However, it is important to recall that  $\overline{\psi_L}$  and  $\psi_L^c$  have the same charges, and thus the term  $m_L\overline{\psi_L}\psi_L^c$  violates any additive quantum numbers by two units. As such, for any fermion with a non-zero electric charge, this mass term would imply a non-neutral electroweak vacuum, and thus the remnant  $U(1)_Q$  symmetry of the SM forbids this term at all orders. Nevertheless, neutrinos are neutral particles, and  $U(1)_Q$  cannot forbid this combination. Indeed, this is the origin for the Weinberg operator already introduced in Eq. (1.73). In the Standard Model, the Weinberg term is forbidden due to the accidental Lepton number conserved symmetry. Even though the  $U(1)_L$  symmetry is anomalous, the mass term also violates B-L such that the operator would need to be extended to also violate B by two units. Furthermore, it is also not invariant under the relative lepton numbers  $L_e - L_\mu$  and  $L_e - L_\tau$ , which are exactly conserved in the SM, and thus the neutrinos are exactly massless [17].

Below, we discuss the extension of the SM with RH counterparts to the SM, given not only its simplicity, as the relevance for one of the later chapters.

# Dirac Neutrinos and the Type-I Seesaw

One possibility to generate neutrino masses is to mimic the mass generation mechanism of all other fermions in the SM, to the case of neutrinos. To do so, we need to introduce fermion degrees of freedom to act as the RH counterpart to  $\nu_L$ , which we denote  $N_R$ . It is a straightforward exercise to see that if we want to include Yukawa couplings of the type  $\overline{\nu_L}\widetilde{\phi}N_R$ , then gauge invariance implies that  $N_R$  are gauge singlets:  $N_R \sim (1,0)$  under the EW group. By doing so, the EWSB is able to provide massive neutrinos and their mixing through an identical manner as for the quarks. More specifically, the Yukawa terms

$$\mathcal{L}_{\text{Yuk}} = Y_D \overline{L} \widetilde{\phi} N_R + \text{h.c.}$$
 (1.124)

provide a mass matrix of the type

$$m_D \overline{\nu} \nu \,, \quad \nu = \nu_L + N_R \tag{1.125}$$

exactly as for charged-fermions. After the EWSB, the mismatch between the charged-lepton and neutrino mass basis will provide a CKM-like mixing:

$$U_{\rm PMNS} = U_{\nu}^{\dagger} U_{\ell} \,. \tag{1.126}$$

Two remarks are in order. Although this extension is perfectly viable, it implies very small couplings in  $Y_D$ , given the smallness of neutrino masses. This is something which accentuates the hierarchies in the flavour sector. Furthermore, for this to be the whole story, the Lepton number symmetry must be promoted from an accidental to a global symmetry. The reason lies in the fact that  $N_R$  are gauge singlets, and thus electrically neutral. As such, we can write a bare mass term for the RH neutrinos as

$$M_R \overline{N_R^c} N_R \,, \tag{1.127}$$

similarly to what we had seen in Eq. (1.123). Once again, this term violates any additive quantum numbers, but given that these are gauge singlets, they have none, and there is no symmetry in the SM to forbid such terms. As such, Lepton number conservation no longer holds automatically (accidentally), and if we insist on forbidding the bare mass terms, lepton number conservation must be imposed. Otherwise, the bare mass terms are present, and unbounded by the EW scale (they do not follow from the EWSB). Indeed, since these terms do not rely on the EWSB to generate a mass term, a second mass scale is introduced in the theory, which can lie anywhere (below the Planck scale). Interestingly, we recall that the reason why neutrinos are massless in the SM is due to the conservation of the lepton number, which no longer verifies. As such, the presence of the  $M_R \overline{N_R^c} N_R$  must necessarily imply that  $m_L \overline{\nu_L^c} \nu_L$  is also present, even if only at the non-renormalizable level. Looking at Eq. (1.123) after EWSB for this case, we find

$$M = \begin{pmatrix} 0 & vY_D \\ vY_D^T & M_R \end{pmatrix} . \tag{1.128}$$

Now, since  $vY_D$  is limited to the EW scale, whereas  $M_R$  is not bounded by perturbativity and thus can be at any scale, we can take the interesting limit that  $M_R \gg vY_D$ . In this case, we can approximate the Majorana mass matrix as (defining the ratio of the scales  $\epsilon \sim vY_D/M_R$ ) [17]

$$M = \mathcal{V}^T D \mathcal{V}$$
, with  $\mathcal{V} = \begin{pmatrix} U_{11} & \epsilon U_{12} \\ \epsilon U_{21} & U_{22} \end{pmatrix}$ , and  $D = M_R \begin{pmatrix} \epsilon^2 D_{\nu} & 0 \\ 0 & D_R \end{pmatrix}$ , (1.129)

where the entries are taken to be matrices. Interestingly, this automatically leads to 3 light mass states due to the  $\epsilon$  suppression with respect to the EW scale, and 3 heavy neutrinos around the  $M_R$  scale (we factor out the  $M_R$  scale such that  $D_{\nu}$  and  $D_R$  are dimensionless). The unitarity of  $\mathcal{V}$  together with the smallness of  $\epsilon$  further means that both  $U_{11}$  and  $U_{22}$  are almost unitary. Therefore, if  $M_R \gg v Y_D$ , we can justifiably use the approximation where the light and heavy states are decoupled, and take the heavy states to be (almost) purely RH, and the light eigenstates to be given by (a more strict reasoning can be

found in ref. [77])

$$m_{\nu} \approx m_D \cdot M_R^{-1} \cdot m_D^T \tag{1.130}$$

whose diagonalisation gives the neutrino contribution to the PMNS:

$$U_{\nu}^{T} m_{\nu} U_{\nu} = D_{\nu} \quad \rightarrow \quad U_{\text{PMNS}} = U_{\nu}^{\dagger} U_{\ell} \,.$$
 (1.131)

We see that in this case, contrary to the case of Dirac neutrinos, there is a natural suppression of the light neutrino masses with the scale of the heavy states. For this reason, this mechanism is called the Type-I seesaw mechanism [78–82].

Lastly, we comment on the difference in the mixing of Majorana and Dirac type neutrino masses. Usually, we have the freedom to absorb phases of the mixing matrices onto the LH and RH fields, such that 3 generations give rise to a single CPV phase. On the other hand, if  $m_{\nu}$  is non-zero, any rephasing performed on the LH neutrinos will reappear in  $m_{\nu}$ , such that these phases are no longer unphysical. As such, in the presence of Majorana mass terms, the PMNS matrix is complemented by two Majorana phases, as we had written in Eq. (1.74).

# 1.3 The Flavour Puzzle and Flavour Symmetries

The mysterious threefold replication of the fermion generations is one important open issue of the Standard Model at the heart of the flavour puzzle. Ignoring the fact that all the particles predicted by the SM have already been experimentally observed, it seems that the inclusion of multiple generations serves the sole purpose of complicating our lives. Nevertheless, it is interesting to note that the existence of six quarks was proposed when only three had been observed. Indeed, the existence of the charm quark was proposed as a way to justify the suppression of strangeness-changing neutral currents [83], which had been confirmed by the Gargamelle Neutrino Collaboration [84]. Even more impressive, the observation of CPV in Kaon oscillations led to the proposal of the bottom and top quarks, even before the charm had been observed [20]. In this way, we see that the inclusion of multiple flavours was an interplay between experimental and theoretical advances, rather than just a mere inclusion of new particles which were observed.

The flavour sector is responsible for most of the free parameters of the SM. While the gauge sector features only one coupling constant for each symmetry (plus the QCD vacuum), and the scalar sector can be fully determined by measuring the Higgs mass and its vev, overall, one counts 20 (22) low-energy independent parameters contained in the Yukawa sector of the SM extended with three massive Dirac (Majorana) neutrinos. These are six quark masses, three charged-lepton masses, three neutrino masses, as well as three quark and three lepton flavour mixing angles, together with one CPV phase in the CKM and one (or three) CPV phases in the PMNS matrix. All of these, either independently or relating to each other, lead to pieces of the flavour puzzle. For starters, all of the masses of the (charged) fermions originate from the same mechanism, and yet one observes a large hierarchy between

the masses of different particles. This hierarchy is present not only between different sectors of the theory (the charged-fermion masses span six orders of magnitude), but also in each sector ( $m_u \ll m_c \ll m_t$ , and similarly for the down-quarks and charged-leptons). Even worse, another six orders of magnitude separate the neutrinos from the lightest of the charged-fermions (this has prompted the question about the nature of the neutrino mass generation mechanism, to justify the smallness of their masses, as already alluded to in the discussion around the seesaw mechanism). Additionally, the mixing observed in the quark and lepton sectors also poses interesting questions. The CKM is approximately diagonal, where only the Cabibbo angle is sizeable. While in some BSM theories this smallness is associated with the hierarchies in the quark masses, in the SM these are completely uncorrelated and the mixing could have any value, regardless of the hierarchies found in the masses of the associated particles. On the other hand, the PMNS is far from diagonal, but somewhat close to patterns which would easily emerge from theories with additional symmetries. Again, the hierarchies (or possible lack thereof in the case of neutrinos) cannot be used to justify this observation, as they are not related in the SM. Finally, there is the question of CP violation. Three generations is the minimum we can have to introduce CPV in the Yukawa sector. This is one of the Sakharov conditions to produce the BAU [85]. However, it seems that the amount of CPV present in the SM is not enough for the BAU not to be washed-out [86, 87]. In the SM, the origin of CPV must come from CP not being a symmetry of the Lagrangian. On the other hand, if the SM is extended, CPV can originate from the spontaneous (or geometrical) breaking of a CP symmetry. It is the sum of these mysteries – this lack of guiding principle for the Yukawa coefficients, the hierarchical nature of the fermion masses, the observed pattern of fermionic mixing, etc. - which constitutes the flavour puzzle.

In sum, in an era of increasing experimental precision, the flavour puzzle stands as an enigma that hints at new physics beyond the SM. The observed hierarchies among the masses of the three generations of up quarks, down quarks and charged leptons suggest the action of a mechanism which is not yet understood. The peculiar and seemingly unrelated mixing patterns in the quark and lepton sectors add to the mystery. The quest for a principle, akin to the gauge principle, which economically describes this plethora of parameters is enticing and has led to the development of the discrete symmetry approach to flavour [88], largely focused on the leptonic sector [89–93]. Recent reviews include [93–95].

In this section, we will briefly present the governing principles of the applications of flavour symmetries which are more appropriate for the remainder of the thesis.

# **Natural Flavour Conservation**

The study of nHDMs leads to a rich phenomenology, as well as a sharp increase of the number of parameters, due to the addition of a SM-like Yukawa structure for each doublet, in general. As already mentioned in the previous section, one important consequence is that the diagonalization of the mass matrices will not lead to the simultaneous diagonalization of all the associated Yukawa matrices, which will bring in FCNCs at the tree-level. These are processes in which a neutral mediator is able to change the flavour of a given fermion (more accurately, a process in which the initial and final states have the same electrical charge, but different flavours), and experimental data suggest that FCNCs are highly

suppressed [96]. As such, it would be ideal to find a way to suppress these processes.

The requirement of invariance under a larger symmetry will unavoidably lead to correlations between parameters and, most notably, can forbid certain couplings which would otherwise be allowed (and general). Then, flavour symmetries are also a prime candidate to justify why some processes are so rare in Nature. An appealing possibility is to apply flavour symmetries to keep the FCNCs under control: in the SM, the GIM mechanism is responsible for this suppression [83], but the same does not happen in general for BSM theories. This led to the idea of natural flavour conservation (NFC), which are a class of models (nHDMs) in which FCNCs are absent at the tree-level [97, 98] (other possibilities include having some mechanism not to eliminate but control the FCNCs [59, 99–103]). In models with (flavour-universal) NFC, each type of RH fermion is coupled to a single scalar doublet, ensuring the simultaneous diagonalization of the Yukawa and Mass matrices, leading to the absence of FCNCs at tree-level.<sup>14</sup>

Within the framework of 2HDMs, there are four known types of models featuring NFC, which amount to the distinct possibilities of coupling each scalar to the fermions (notice that interchanging the labelling  $\phi_1 \leftrightarrow \phi_2$  does not lead to physically distinct models, and thus we use the notation where  $\phi_1$  always couples to the RH up-type quarks). These four types can be enforced by including a  $Z_2$  flavour symmetry, where the assignments of the different fields will give rise to different types:

• In the Type-I 2HDM, all fermions couple to the same scalar doublet, and we just need to decouple  $\phi_2$  from fermionic interactions. This can be easily realised by setting  $\phi_2$  to be the only field transforming non trivially under the  $Z_2$  flavour symmetry:

$$\phi_2 \to -\phi_2 \,. \tag{1.132}$$

This ensures that any Yukawa interaction involving  $\phi_2$  is non-invariant,  $\overline{\psi_i}\phi_2\psi_j \rightarrow -\overline{\psi_i}\phi_2\psi_j$ , whereas in the terms  $\overline{\psi_i}\phi_1\psi_j$  all fields transform trivially, and thus the term is invariant.

• For the case of the Type-II 2HDM, one possibility is to take the RH charged-leptons and down-type Yukawas to also transform non-trivially,

$$\phi_2 \to -\phi_2$$
,  $\ell_R \to -\ell_R$ ,  $d_R \to -d_R$ . (1.133)

Following the above reasoning, the up quarks have the same Yukawa terms as the type-I, but now the down quarks and charged-leptons can only couple to  $\phi_2$ , to cancel the sign-flip.

• The Type-X (also called lepton-specific) and the Type-Y (sometimes referred to as flipped) are similar in implementation, and follows easily from the Type-II. If only the charged-leptons transform non-trivially, we arrive at the Type-X:

$$\phi_2 \to -\phi_2$$
,  $\ell_R \to -\ell_R$ . (1.134)

If, on the other hand, we exchange the charged-leptons with the down quarks in the type-X, we

<sup>&</sup>lt;sup>14</sup>Versions without the requirement of flavour-universality exist, as long as the diagonalisation of the mass matrices implies diagonal individual Yukawa couplings [104–106]. In all that follows, we implicitly refer to flavour-universal NFC.

fermion	Type-I	Type-II	Type-X	Type-Y	Democratic
$\overline{u}$	$\phi_1$	$\phi_1$	$\phi_1$	$\phi_1$	$\phi_1$
d	$\phi_1$	$\phi_2$	$\phi_1$	$\phi_2$	$\phi_2$
$\ell$	$\phi_1$	$\phi_2$	$\phi_2$	$\phi_1$	$\phi_3$

**Table 1.1:** All nonequivalent possibilities for models featuring NFC. The first four types can be realized within 2HDMs, while the last requires at least a 3HDM.

find the Type-Y:

$$\phi_2 \to -\phi_2$$
,  $d_R \to -d_R$ . (1.135)

Enlarging the framework to a 3HDM only adds one more nonequivalent possibility which ensures NFC. Here, we can have different realisations of the democratic Yukawa structure, which can lead to different scalar sectors. The different types of models, characterized by their Yukawa structures, are shown in Table 1.1.

Nevertheless, these models rely on having some scalar doublets transforming non-trivially under the flavour symmetry, such that not all bilinears are invariant. Moreover, if these doublets acquire a non-zero vacuum state, then they contribute to the EWSB, and thus their vev cannot be arbitrarily large without affecting the successful SM predictions. Thus, the upper bound on the vev, together with the absence of the most general set of bilinears will provide an upper bound for the masses of the new scalar particles, such that tension with collider experiments may arise. Often, to escape this problem, soft symmetry breaking is assumed, introducing non-invariant bilinears, to provide a new mass scale to the theory, such that a larger decoupling of the new scalar masses is possible.

# Froggatt-Nielsen Mechanism

To better understand the flavour puzzle, and the flavour symmetry approach, let us take a step back and look at the SM. The existence of three generations of fermions means that the gauge Lagrangian is invariant under unitary transformations between the members of the generations. In other words, there is a  $U(3)^5$  global symmetry, with each U(3) factor associated with mixing of the families of fermions with the same quantum numbers  $(Q_{Li}, u_{Ri}, d_{Ri}, L_{Li}, e_{Ri})$ . Furthermore, the scalar Lagrangian is invariant under rephasings, leading to an additional  $U(1)_H$  symmetry. Then, the full symmetry under which the SM Lagrangian without the Yukawa interactions is invariant is  $G = U(3)^5 \times U(1)_H$  (this is extended to  $U(3)^6 \times U(1)_H$  if three copies of RH neutrinos are introduced for a neutrino mass source), which includes the hypercharge global transformations [93]. Obviously, since the fermions have non-degenerate masses, this large symmetry group is explicitly broken by the Yukawa interactions. Curiously, not only the fermions are non-degenerate, but they turn out to be very hierarchical in their masses. The Froggatt-Nielsen proposal is that the two aspects are related: the explicit breaking of the flavour group  $G = U(3)^5 \times U(1)_H$  by the Yukawa interactions may have its origin from a spontaneous symmetry breaking of a flavour group  $G_f$  which can be as large as  $G = U(3)^5 \times U(1)_H$  for the SM [107]. If the

group  $G_f$  is Abelian, we have  $G_f = U(1)_{FN}$ , and we can analyse all of the quark dimensionless parameters (mass ratios and mixings angles) as powers of some amount of symmetry breaking of  $G_f$ .<sup>15</sup> It is useful to introduce the Wolfenstein parametrization of the CKM matrix [108]:

$$V \approx \begin{pmatrix} 1 - \lambda^2/2 & -\lambda & \mathcal{O}(\lambda^3) \\ \lambda & 1 - \lambda^2/2 & \mathcal{O}(\lambda^2) \\ \mathcal{O}(\lambda^3) & \mathcal{O}(\lambda^2) & 1 \end{pmatrix}, \tag{1.136}$$

with  $\lambda \sim 0.22$ , the order of the Cabibbo angle. If we express the quark dimensionless observables in terms of  $\lambda$ , we find (at the low-energy scale)

$$\frac{m_u}{m_t} \sim \lambda^{7.5} \,, \quad \frac{m_c}{m_t} \sim \lambda^{3.3} \,, \quad \frac{m_d}{m_b} \sim \lambda^{4.5} \,, \quad \frac{m_s}{m_b} \sim \lambda^{2.5} \,, 
|V_{ud}| \sim 1 \,, \qquad |V_{us}| \sim \lambda \,, \qquad |V_{cb}| \sim \lambda^2 \,, \qquad |V_{ub}| \sim \lambda^3 \,.$$
(1.137)

Then, we can envision a scenario where we assign different charges to the various fields such that the Yukawa terms are forbidden and we recover the invariance under the full  $G = U(3)^5 \times U(1)$  (or at least a subgroup if some Yukawas survive). This can be simply put by describing the charges of the quarks under  $U(1)_{\text{FN}}$  by  $q_i^{\psi}$  for i = 1, 2, 3 and  $\psi = Q_L, u_R, d_R$ . Then, the transformation properties of a field  $\psi$  under  $U(1)_{\text{FN}}$  in flavour space can be represented as  $\psi \to F_{\psi} \psi$ , with

$$F_{\psi} = \begin{pmatrix} e^{i\alpha q_1^{\psi}} & 0 & 0\\ 0 & e^{i\alpha q_2^{\psi}} & 0\\ 0 & 0 & e^{i\alpha q_3^{\psi}} \end{pmatrix}, \qquad (1.138)$$

where  $\alpha$  is just the infinitesimal parameter independent of the spacetime coordinates ( $U(1)_{\rm FN}$  is a global symmetry). It follows that the transformation properties of the Yukawa interactions are (assuming, without loss of generality, that the Higgs doublet transforms trivially under the FN symmetry)

$$Y_u \to F_Q^* \cdot Y_u \cdot F_u , \qquad Y_d \to F_Q^* \cdot Y_d \cdot F_d ,$$
 (1.139)

such that if  $q_i^Q \neq q_j^u$ , then the Yukawa interaction  $\overline{Q_{L_i}} \phi u_{R_j}$  is forbidden by  $U(1)_{FN}$  (and similarly for  $d_R$ ), such that we recover the invariance under G.

Up to this point, we merely succeeded in forbidding mass terms for the fermions, making the theory phenomenologically not viable. The final ingredient is to assume there is a scalar field,  $\varphi$ , which is usually taken to be a singlet under the gauge group, but which transforms non-trivially under  $U(1)_{\rm FN}$ . By acquiring a non-zero vev, this field spontaneously breaks the global symmetry (these fields are called 'flavons'). Then, from a non-renormalizable point of view, we can transmit this  $U(1)_{\rm FN}$  breaking onto the Yukawa sector, and generate the fermion masses. Denoting the FN charge of  $\varphi$  as  $q_{\varphi}$ , we can write

<sup>&</sup>lt;sup>15</sup>The original proposal focused on the quark sector, and thus so will we for the sake of the introductory character of this section. Nonetheless, the framework can be extended to the leptonic sector.

the term

$$v Y_{ij}^{u} \left(\frac{\varphi}{\Lambda}\right)^{n} \overline{Q_{L_{i}}} u_{R_{j}}, \quad \text{or} \quad v Y_{ij}^{u} \left(\frac{\varphi^{\dagger}}{\Lambda}\right)^{n} \overline{Q_{L_{i}}} u_{R_{j}},$$
 (1.140)

which will be invariant under the FN symmetry if  $nq^{\varphi} = q_i^Q - q_j^u$  (left) or  $nq^{\varphi} = -(q_i^Q - q_j^u)$  (right), where  $\Lambda$  is the suppression scale due to the term being non-renormalizable, and  $Y_{ij}^u$  are undetermined coefficients. After the SSB of the FN symmetry, we can define an expansion parameter

$$\epsilon = \langle \varphi \rangle / \Lambda < 1,$$
 (1.141)

such that Yukawa interactions are generated at higher orders as (taking  $q^{\varphi} = -1$  without loss of generality, since it amounts to a rescaling of the other charges)

$$Y^{u} = \begin{pmatrix} \epsilon^{q_{1}^{Q} - q_{1}^{u}} & \epsilon^{q_{1}^{Q} - q_{2}^{u}} & \epsilon^{q_{1}^{Q} - q_{3}^{u}} \\ \epsilon^{q_{2}^{Q} - q_{1}^{u}} & \epsilon^{q_{2}^{Q} - q_{2}^{u}} & \epsilon^{q_{2}^{Q} - q_{3}^{u}} \\ \epsilon^{q_{3}^{Q} - q_{1}^{u}} & \epsilon^{q_{3}^{Q} - q_{2}^{u}} & \epsilon^{q_{3}^{Q} - q_{3}^{u}} \end{pmatrix} = \begin{pmatrix} \epsilon^{n_{11}^{u}} & \epsilon^{n_{12}^{u}} & \epsilon^{n_{13}^{u}} \\ \epsilon^{n_{21}^{u}} & \epsilon^{n_{22}^{u}} & \epsilon^{n_{23}^{u}} \\ \epsilon^{n_{31}^{u}} & \epsilon^{n_{32}^{u}} & \epsilon^{n_{33}^{u}} \end{pmatrix}, \quad (u \to d)$$

$$(1.142)$$

where an undetermined coefficient is assumed in each entry. If we assume these coefficients are all  $\mathcal{O}(1)$ , then we find it is the non-universal treatment of the different families under the symmetry which gives rise to the hierarchical patterns. Interestingly, if we assume that the charges are such that the matrices are hierarchical  $(q_1^Q < q_2^Q < q_3^Q)$ , there are some predictions which are independent of the specific choices of the FN charges [93]

$$V_{ud} \approx V_{cs} \approx V_{tb} \approx \mathcal{O}(1)$$
,  $V_{ub} \approx V_{td} \approx V_{us} V_{cb}$ . (1.143)

For intelligent choices of the FN charges, and taking  $\epsilon \approx \lambda$ , it is possible to successfully recover the correct quark mass ratios and mixings [109–115].

We should remark that this mechanism is simple from a low-energy point of view, by taking the Yukawa terms to come from non-renormalizable operators. If one wanted to extend the theory to provide an Ultraviolet (UV) completion which may generate these terms, one possible way is to include additional fermions, with the same quantum numbers as the RH SM fields, together with their chiral partners, such that they can acquire bare mass terms. The FN charges of these fields can be read from the relevant diagrams such that, after the SSB of the  $U(1)_{\text{FN}}$  symmetry, we can integrate out these fermions, giving rise to the desired operators. Specific examples of these diagrams in the context of modular symmetries are given in Appendix C, applied to a specific realisation of the FN mechanism in the context of modular symmetries within an SU(5) theory.

<sup>&</sup>lt;sup>16</sup>Note that realistic implementations can follow from string models, where we can dispense with the heavy fermion fields and instead write operators suppressed by the string scale. Interestingly, the expansion factor can be computed in specific models, where it is close to the order of the Cabibbo angle [114, 116].

### Non-Abelian Symmetries: the Discrete Symmetry Approach

For both the cases of natural flavour conservation as well as the Froggatt-Nielsen mechanism, the flavour symmetry is Abelian. However, the observation that the neutrino mixing pattern is quite different from that of the quarks suggests a different venue for flavour symmetries. Namely, the fact that neutrino mixing is substantially large points towards non-Abelian flavour symmetries. This symmetry is posited to exist at some high-energy scale, and to be broken spontaneously at lower energies. In the case where this discrete symmetry is not fully broken in all sectors, then some residual symmetries survive (which may differ from sector to sector). Since this approach has mostly been applied to the leptonic mixing, here we will focus on this sector. However, discrete symmetries also have their applications for the quark sector (see, for example, Chapter 4). Furthermore, here we focus exclusively on the case where the flavour group commutes with the gauge symmetry (for cases where this does not verify, see Chapter 5 and, for example, refs. [117–119]). Lastly, we will also assume that the flavour symmetry commutes with the Poincaré group (relaxing this condition leads to generalised CP transformations [90, 92, 93, 120–123]).

For non-Abelian groups, the representations do not need to be one-dimensional. Given that we have observed three generations in Nature, groups with a three-dimensional irrep present an enticing choice. In this way, the threefold replication of flavours would not be an  $ad\ hoc$  assumption, but rather follow directly from the flavour symmetry. For this reason, discrete groups such as  $A_4$ ,  $A_5$ , among others have been popular choices [88].

Since the flavour symmetry  $G_f$  commutes with the gauge sector, the LH charged-fields and the neutrinos must transform identically under the action of the flavour symmetry (in other words, the flavour symmetry acts on the  $SU(2)_L$  lepton doublet field), but the RH charged-lepton fields can transform independently:

$$L_{L_i} \to \rho_{\mathbf{r}}(g)_{ij} L_{L_j}, \qquad e_{R_i} \to \rho_{\mathbf{r}'}(g)_{ij} e_{R_j}, \qquad g \in G_f.$$
 (1.144)

where  $\mathbf{r}$  and  $\mathbf{r}'$  are the representations of  $L_L$  and  $e_R$  under  $G_f$ . At low-energy, the flavour symmetry  $G_f$  must be broken (the only exact symmetry which can survive is either a  $Z_2$  if Majorana masses are allowed, or a  $U(1)_L$  if neutrinos are Dirac in nature [93]). If we take  $G_f$  to be some discrete group under which the lepton doublets are assigned to some representation  $\mathbf{r}$  which is not one-dimensional, then it is easy to understand that an unbroken symmetry would require degenerate charged-leptons and neutrinos. The breaking of  $G_f$  can be realised by scalar flavon fields, similarly to the FN mechanism, but extended to non-Abelian groups (and larger-dimensional representations). These flavons acquire non-zero vevs, such that  $G_f$  is broken down to some residual subgroup if the vev does not break all of the symmetry's generators. If we envision a number of different flavons, whose vevs follow different alignments (leave different subgroups unbroken), then it becomes clear that different residual symmetries can be left unbroken in different sectors of the theory, depending on which flavons act in each of the sectors. More specifically, the charged-lepton and neutrino sectors can have different residual symmetries,  $G_\ell \in G_f$  and

 $G_{\nu} \in G_f$  respectively, which will in turn be symmetries of the respective mass matrices:

$$M_{\ell} = \rho_{\mathbf{r}}^{\dagger}(g_{\ell}) M_{\ell} \rho_{\mathbf{r}'}(g_{\ell}), \qquad m_{\nu} = \rho_{\mathbf{r}}(g_{\nu})^{T} m_{\nu} \rho_{\mathbf{r}}(g_{\nu}).$$

$$(1.145)$$

If we now look at the relevant hermitian combinations, this implies

$$M_{\ell}M_{\ell}^{\dagger} = \rho_{\mathbf{r}}(g_{\ell})^{\dagger}M_{\ell}M_{\ell}^{\dagger}\rho_{\mathbf{r}}(g_{\ell}), \qquad g_{\ell} \in G_{\ell}, \qquad (1.146a)$$

$$M_{\nu}^{\dagger} M_{\nu} = \rho_{\mathbf{r}}(g_{\nu})^{\dagger} M_{\nu}^{\dagger} M_{\nu} \rho_{\mathbf{r}}(g_{\nu}), \qquad g_{\nu} \in G_{\nu}. \tag{1.146b}$$

As a consequence, the hermitian matrices commute with the representation matrices, and thus the hermitian matrices and their respective representation matrices are diagonalised by the same matrix:

$$U_{\ell}^{\dagger} \rho_{\mathbf{r}}(g_{\ell}) U_{\ell} = \rho_{\mathbf{r}}^{\mathrm{diag}}(g_{\ell}), \quad \text{and} \quad U_{\ell}^{\dagger} M_{\ell} M_{\ell}^{\dagger} U_{\ell} = \mathrm{diag}$$
 (1.147a)

$$U_{\nu}^{\dagger} \rho_{\mathbf{r}}(g_{\nu}) U_{\nu} = \rho_{\mathbf{r}}^{\text{diag}}(g_{\ell}), \quad \text{and} \quad U_{\nu}^{\dagger} M_{\nu}^{\dagger} M_{\nu} U_{\nu} = \text{diag}.$$
 (1.147b)

For a given choice of subgroups and representations, the matrices  $U_{\ell}$  and  $U_{\nu}$ , which diagonalise the hermitian mass matrices, may be constrained (obviously if no residual symmetries survive, then both  $G_{\ell}$  and  $G_{\nu}$  are the trivial subgroup, and the rotation matrices are left completely unconstrained). Then, the mixing matrix follows as (without accounting for the Majorana phases)

$$U_{\rm PMNS} = U_{\ell}^{\dagger} U_{\nu} \,, \tag{1.148}$$

and is constrained by the residual subgroups  $G_{\ell}$  and  $G_{\nu}$ . The choices of the flavour group  $G_f$ , as well as its residual symmetries  $G_{\ell}$  and  $G_{\nu}$  are preponderant in shaping the mixing matrix. As such, it is important to further discuss the possible choices of these groups.

We start by noting that the largest possible symmetry of the charged-lepton sector is  $U(1)\times U(1)\times U(1)$  (the individual lepton numbers) given their non-degenerate nature. On the other hand, the neutrino sector can have either a  $Z_2\times Z_2\times Z_2$  or a  $U(1)\times U(1)\times U(1)$  symmetry, depending whether the neutrinos are Majorana or Dirac particles. If we follow the widely taken assumption that  $G_f$  is a subgroup of SU(3), the residual symmetries  $G_\ell$  and  $G_\nu$  must be subgroups of  $U(1)\times U(1)$  and  $Z_2\times Z_2$  ( $U(1)\times U(1)$ ), respectively for  $G_\ell$  and  $G_\nu$  with Majorana (Dirac) neutrinos.

Due to its relevance (historical and present) for model building, we showcase here the case for Tri-Bimaximal (TBM) mixing, and its origin from  $G_f = S_4$ . Although this mixing structure is no longer phenomenologically viable, it is instructive to understand the above reasoning. The group  $S_4$  is a discrete group generated by two elements, S and T. Often times, it is helpful to describe the group with three generators, S, T, and U, with presentation [88]

$$S^{2} = T^{3} = (ST)^{3} = U^{2} = (TU)^{2} = (SU)^{2} = (STU)^{4} = 1,$$
(1.149)

with 1 the identity element. In the basis of ref. [124], the representation matrices of the 3 representation

can be written as

$$S = \frac{1}{3} \begin{pmatrix} -1 & 2 & 2 \\ 2 & -1 & 2 \\ 2 & 2 & -1 \end{pmatrix}, \quad T = \begin{pmatrix} 1 & 0 & 0 \\ 0 & \omega^2 & 0 \\ 0 & 0 & \omega \end{pmatrix}, \quad U = -\begin{pmatrix} 1 & 0 & 0 \\ 0 & 0 & 1 \\ 0 & 1 & 0 \end{pmatrix}, \tag{1.150}$$

where  $\omega = e^{2\pi i/3}$ . If the residual subgroups are such that (see, e.g., ref. [125])

$$G_{\ell} = Z_3^T = 1, T, T^2, \quad \text{and} \quad G_{\nu} = Z_2^S \times Z_2^U = 1, S, U, SU,$$
 (1.151)

we find that  $\rho_3(g_\ell) = T$ , such that the diagonalising matrix must be an unphysical diagonal phase matrix. Finally, since S and U commute, we need to find the matrix which simultaneously diagonalises  $\rho_3(g_\nu) = S$  and  $\rho_3(g_\nu) = U$ , which turns out to be

$$U_{\nu} = U_{\text{TBM}} = \begin{pmatrix} \sqrt{\frac{2}{3}} & \frac{1}{\sqrt{3}} & 0\\ -\frac{1}{\sqrt{6}} & \frac{1}{\sqrt{3}} & -\frac{1}{\sqrt{2}}\\ -\frac{1}{\sqrt{6}} & \frac{1}{\sqrt{3}} & \frac{1}{\sqrt{2}} \end{pmatrix} . \tag{1.152}$$

and the final neutrino mixing matrix comes out to be exactly  $U_{\text{PMNS}} = U_{\text{TBM}}$  (up to a diagonal phase matrix on the right), completely determined by the choices of subgroups, independently of the specific values of the Yukawa coefficients.

Of course, current neutrino data excludes  $\theta_{13} = 0$ , which is predicted by the TBM mixing. Nonetheless, it is possible to arrange for models where these predictions are softened, and become compatible with current experimental data. A simple example is to take  $G_f = A_4$ , which follows the same presentation as  $S_4$ , without the U generator. If we now take the residual subgroups to be (see, for example, ref. [126])

$$G_{\ell} = Z_3^T = 1, T, T^2, \quad \text{and} \quad G_{\nu} = Z_2^S = 1, S,$$
 (1.153)

there arises a very specific difference between the models. Indeed, the diagonalisation of S is non-unique, due to the degeneracy of the first and third eigenvalues. This was constrained to be unique by the requirement of diagonalisation of U for the case of  $S_4$ :

$$U_{\text{TBM}}^{\dagger} \rho_{\mathbf{3}}(S) U_{\text{TBM}} = \text{diag}(-1, 1, -1), \qquad U_{\text{TBM}}^{\dagger} \rho_{\mathbf{3}}(U) U_{\text{TBM}} = \text{diag}(1, 1, -1).$$
 (1.154)

However, if now we do not need to simultaneously diagonalise S and U, it follows from the eigenvalue degeneracy that

$$U_{\nu} = U_{\text{TBM}} \cdot \begin{pmatrix} \cos \theta_{13}^{\nu} & 0 & \sin \theta_{13}^{\nu} e^{i\alpha} \\ 0 & 1 & 0 \\ -\sin \theta_{13}^{\nu} e^{-i\alpha} & 0 & \cos \theta_{13}^{\nu} \end{pmatrix}$$
(1.155)

also diagonalises  $\rho_3(S)$ , where  $\theta_{13}^{\nu}$  and  $\alpha$  are arbitrary (determined by the specific values of the Yukawa

coefficients in the actual mass matrices). The PMNS matrix then becomes (again, up to a diagonal phase matrix on the right)

$$U_{\text{PMNS}} = \begin{pmatrix} \sqrt{\frac{2}{3}}c_{13} & \sqrt{\frac{1}{3}} & \sqrt{\frac{2}{3}}se^{i\alpha} \\ -\frac{c}{\sqrt{6}} + \frac{s}{\sqrt{2}}e^{-i\alpha} & \sqrt{\frac{1}{3}} & -\frac{c}{\sqrt{2}} - \frac{s}{\sqrt{6}}e^{i\alpha} \\ -\frac{c}{\sqrt{6}} - \frac{s}{\sqrt{2}}e^{-i\alpha} & \sqrt{\frac{1}{3}} & \frac{c}{\sqrt{2}} - \frac{s}{\sqrt{6}}e^{i\alpha} \end{pmatrix},$$
(1.156)

where we see that we are no longer predicting  $\theta_{13} = 0$ .

Other examples and mixing schemes can be found in the literature, and more detailed accounts can be seen in [88, 89, 92–94, 115, 127, 128] and references therein.

#### 1.4 Modular Symmetries

In the past years, a new avenue in model building has been opened by the proposal of using modular invariance [129, 130] as a flavour symmetry [131] (see [132] for a recent review). <sup>17</sup> In this supersymmetric (SUSY) framework, the components of Yukawa and mass matrices may be obtained from modular forms of level N as well as from a set of coupling constants in the superpotential. It is the holomorphicity of the latter which allows for a predictive setup. In the simplest case, these forms are functions of a single complex scalar field, the modulus  $\tau$ . The theory is assumed to be invariant under the whole modular group  $\Gamma \equiv SL(2,\mathbb{Z})$ . Matter fields, however, transform in representations of a finite inhomogeneous (homogeneous) modular group  $\Gamma_N^{(\prime)}$ , which plays the role of a flavour symmetry. The finite groups  $\Gamma_N$ , for small N, are isomorphic to the permutation groups  $S_3$ ,  $A_4$ ,  $S_4$  and  $A_5$  [136] typically used in model building, while the groups  $\Gamma_N'$  are isomorphic to the corresponding "double covers". This idea was generalised to multiple modular symmetries with moduli fields [137], and extended to half-integer modular forms [138].

No flavons are required in modular flavour models, since the vacuum expectation value of  $\tau$  may be the only source of symmetry breaking, fixing the values of the modular forms and, consequently, the flavour structure of fermion mass matrices. Moreover, the vev of  $\tau$  may also be the only source of breaking of a generalised CP (gCP) symmetry, which can be consistently combined with the modular symmetry [139] (see also [140]). Note that any vev for  $\tau$  breaks the full modular symmetry. A remnant symmetry may still be preserved, but only at one of three fixed points,  $\tau_{\rm sym} = i, \, \omega, \, i\infty$  [141], with  $\omega \equiv \exp(2\pi i/3)$ — the (left) cusp. 18 For each of these cases, a residual  $\mathbb{Z}_2^S$ ,  $\mathbb{Z}_3^{ST}$ , or  $\mathbb{Z}_N^T$  symmetry, respectively, is left  $unbroken.^{19}$ 

Modular symmetries can further be exploited to explain the mass hierarchy of the fermions by use of an extra field referred to as a weighton [143, 144]. While similar to the Froggatt-Nielsen mechanism, the weighton explicitly relies on modular invariance and does not require the extra Abelian symmetry.

We can define the modular group  $\Gamma$  as special linear group of  $2 \times 2$  matrices of integer coefficients and

 $<sup>\</sup>overline{^{17}\text{Modular}}$  invariance may also play a role in solving the strong CP problem [133–135].

<sup>&</sup>lt;sup>18</sup> If multiple modular symmetries are considered, then more fixed points can be considered. <sup>19</sup> In the case of the finite groups  $\Gamma'_N$ , an extra residual  $\mathbb{Z}_2^R$  is preserved [142].

unit determinant  $SL(2, \mathbb{Z})$ :

$$\Gamma \equiv SL(2, \mathbb{Z}) \equiv \left\{ \begin{pmatrix} a & b \\ c & d \end{pmatrix}, \quad a, b, c, d \in \mathbb{Z}, ad - bc = 1 \right\}.$$
(1.157)

The group has a set of three generators, which must obey the group relations (we use 1 to denote the identity element of  $\Gamma$ ) [131, 142]

$$S^2 = R$$
,  $(ST)^3 = 1$ ,  $R^2 = 1$ ,  $RT = TR$ . (1.158)

We can take these generators to be

$$S = \begin{pmatrix} 0 & 1 \\ -1 & 0 \end{pmatrix}, \qquad T = \begin{pmatrix} 1 & 1 \\ 0 & 1 \end{pmatrix}, \qquad R = \begin{pmatrix} -1 & 0 \\ 0 & -1 \end{pmatrix}, \tag{1.159}$$

which are group elements that obey the appropriate relations.

The modular transformation acts on the upper-half complex plane via fractional linear transformations. Then, we posit the existence of a complex modulus  $\tau$  which is restricted to the upper-half complex plane (Im( $\tau$ ) > 0), which will be the object on which the modular group acts. As a consequence, the action of an element  $\gamma$  of the modular group is described by fractional linear transformations as

$$\gamma = \begin{pmatrix} a & b \\ c & d \end{pmatrix} \in \Gamma : \tau \to \gamma \tau = \frac{a\tau + b}{c\tau + d}. \tag{1.160}$$

The generators of Eq. (1.159) then act on  $\tau$  as

$$S: \tau \to -\frac{1}{\tau}, \qquad T: \tau \to \tau + 1, \qquad R: \tau \to \tau.$$
 (1.161)

We will comment later on the invariance of  $\tau$  under R.

Furthermore, we need to define infinite normal subgroups of  $\Gamma$ , defined by

$$\Gamma(N) = \left\{ \begin{pmatrix} a & b \\ c & d \end{pmatrix} \in SL(2, \mathbb{Z}), \begin{pmatrix} a & b \\ c & d \end{pmatrix} = \begin{pmatrix} 1 & 0 \\ 0 & 1 \end{pmatrix} \pmod{N} \right\}, \tag{1.162}$$

where N=1,2,3,... is the *level*. For N=1, we see that  $\Gamma(1)=\Gamma$ , and  $\Gamma(N\geq 2)$  are the principal congruence groups, and are infinite. We need to further define the quotient group  $\Gamma'_N$ :

$$\Gamma_N' \equiv \Gamma/\Gamma(N) \simeq SL(2, \mathbb{Z}_N),$$
(1.163)

which is the finite modular group. For  $N \leq 5$ , these finite modular groups are isomorphic to permutation groups (and their respective double covers), which are widely used as flavour symmetries. In particular, we have  $\Gamma_2' \equiv \Gamma_2 \simeq S_3$ ,  $\Gamma_3' \simeq A_4' \equiv T'$ ,  $\Gamma_3 \simeq A_4$ ,  $\Gamma_4' \simeq S_4'$ ,  $\Gamma_4 \simeq S_4$ ,  $\Gamma_5' \simeq A_5'$ , and  $\Gamma_5 \simeq A_5$ .

If we assume that the matter superfields transform trivially (up to a possible multiplicative factor)

when restricted to some  $\Gamma(N)$ , then they transform under  $\Gamma$  as [129]

$$\varphi_i \xrightarrow{\gamma} (c\tau + d)^{-k} \rho_{ij}(\gamma) \varphi_j$$
 (1.164)

where  $\psi$  is a matter superfield,  $\gamma \in \Gamma$ ,  $(c\tau + d)^{-k}$  is called an automorphy factor, and k is the modular weight. Finally,  $\rho$  is a unitary representation of  $\Gamma'_N$ .

Note that, if we take the weights of all the matter superfields of the theory to be zero, the automorphy factor (and thus the  $\tau$  dependency on the field transformations) plays no role in the field transformations. Additionally, if this also eliminates the role of  $\tau$  in the other aspects of the theory connected to the flavour puzzle, then the theory effectively becomes a traditional flavour symmetric (SUSY) model, based on one of the  $\Gamma_N$  permutation groups. We will see later that this is indeed the case, and in that sense, the modular symmetry formalism provides a generalisation for a (subset) of solutions to the flavour puzzle.

# 1.4.1 Modular Invariant Theories

Now that we have introduced the concept of modular symmetries, we can delve deeper onto how to build modular-invariant theories. We start with the Lagrangian for  $\mathcal{N}=1$  global supersymmetric theories:

$$\mathcal{L} = \int d^2\theta \, d^2\overline{\theta} \, K(\Phi, \overline{\Phi}) + \left( \int d^2\theta \, W(\Phi) + \text{h.c.} \right) \,, \tag{1.165}$$

where K is the Kähler potential, W is the superpotential,  $\theta$  and  $\overline{\theta}$  are Grassmann variables, and  $\Phi$  denotes the entirety of the chiral superfields of the theory. The imposition of modular invariance of the Lagrangian requires the invariance of the superpotential, as well as the invariance of the Kähler potential up to a Kähler transformation:<sup>20</sup>

$$\begin{cases} W(\Phi) \xrightarrow{\gamma} W(\Phi), \\ K(\Phi, \overline{\Phi}) \xrightarrow{\gamma} K(\Phi, \overline{\Phi}) + f(\Phi) + f(\overline{\Phi}) \end{cases}$$
 (1.167)

The requirement of invariance of the Kähler potential can be easily satisfied by taking its minimal form:  $^{21}$ 

$$K(\Phi, \overline{\Phi}) = -h\log(-i\tau + i\overline{\tau}) + \sum_{I} (-i\tau + i\overline{\tau})^{-k_I} |\varphi^{(I)}|^2, \qquad (1.168)$$

where h is a positive constant, and I separates different sectors of the theory, according to their trans-

$$\begin{cases} W(\Phi) \xrightarrow{\gamma} (c\tau + d)^{-h} W(\Phi) \\ K(\Phi, \overline{\Phi}) \xrightarrow{\gamma} K(\Phi, \overline{\Phi}) + f(\Phi) + f(\overline{\Phi}) \end{cases}$$
 (1.166)

 $<sup>^{20}</sup>$ This is true for the case of global supersymmetry. In the case of local supersymmetry, the transformations of  $K(\Phi, \overline{\Phi})$  can be compensated by appropriate transformation of the superpotential, which must then transform as a singlet of non-trivial weight, *i.e.*,

up to a phase rotation. An increasingly studied case in the literature are the eclectic models [145–153], where h=1.

 $<sup>^{21}</sup>$ Deviating from the minimal form of the Kähler potential for a more general form could lead to loss of predictivity of modular-symmetric models [154–156].

formation properties under  $\Gamma$ . For ease of notation, we do not explicitly write down the index of the superfields of each sector, although (in general) each  $\varphi^{(I)}$  will denote a collection of superfields. This gives rise to kinetic terms of the form

$$\frac{h}{\langle -i\tau + i\overline{\tau} \rangle^2} \partial_{\mu} \overline{\tau} \partial^{\mu} \tau + \sum_{I} \frac{\partial_{\mu} \overline{\varphi}^{(I)} \partial^{\mu} \varphi^{(I)}}{\langle -i\tau + i\overline{\tau} \rangle^{k_I}}.$$
 (1.169)

Foreshadowing later results, this will, in turn, have some consequences when figuring out the concepts of naturalness and fine-tuning in modular-invariant theories. The reasoning is that the kinetic terms of the form of Eq. (1.169) are not canonically normalised, such that a field rescaling is necessary:

$$\varphi^{(I)} \to \sqrt{(2\mathrm{Im}\tau)^{k_I}}\varphi^{(I)}$$
. (1.170)

As we have seen, the Kähler potential will be responsible for the kinetic terms for our fields. On the other hand, the application of modular-invariance for the flavour puzzle relies on the restriction it applies to the superpotential, which will be in the origin of the Yukawa terms. The superpotential can be written as

$$W(\Phi) = \sum_{n} Y_{I_1 \dots I_n}(\tau) \varphi^{I_1} \dots \varphi^{I_n} , \qquad (1.171)$$

where n is the order of the superpotential term, and, contrary to traditional flavour-symmetric theories, we now allow the Yukawa coefficients to be some function of  $\tau$ . If we now require the invariance of  $W(\Phi)$ under the modular action, we find that the functions  $Y_{I_1 \dots I_n}(\tau)$  must be modular forms. Modular forms are holomorphic functions of  $\tau$  with well-defined transformation properties under the group  $\Gamma(N)$ :

$$f(\gamma \tau) = (c\tau + d)^k f(\tau), \qquad \gamma = \begin{pmatrix} a & b \\ c & d \end{pmatrix} \in \Gamma(N)$$
 (1.172)

where  $k \geq 0$  is the weight of the modular form. It can be shown that these modular forms transform trivially (up to automorphy factors) under  $\Gamma(N)$ , but are non-trivial under the quotient group  $\Gamma'_N$  [131]. Thus, we can describe the transformation of the modular forms as

$$f_i(\gamma \tau) = (c\tau + d)^k \rho_{ij}(\gamma) f_j(\tau), \qquad \gamma \in \Gamma'_N.$$
 (1.173)

These functions allow for a Fourier expansion (q-expansion) of the form

$$f(\tau) = \sum_{i=0}^{\infty} a_n q_N^n, \qquad q_N = e^{i2\pi\tau/N},$$
 (1.174)

which automatically satisfies  $f(\tau) = f(\tau + N)$ , as demanded by  $\Gamma(N)$ .

Referring back to a general term in the superpotential,

$$Y_{I_1 \dots I_n}(\tau) \varphi^{I_1} \dots \varphi^{I_n} , \qquad (1.175)$$

the imposition of modular invariance requires  $Y_{I_1...I_n}$  to be a modular form of weight  $k_Y$ . Two more requirements follow, one which is responsible for the cancellation of the automorphy factors (this cancellation depends only on the weights of the superfields), and one which is responsible for a singlet combination to exist given the representations of each superfield and of the modular form:

$$Y_{I_1 \dots I_n}(\tau) \xrightarrow{\gamma} Y_{I_1 \dots I_n}(\gamma \tau) = (c\tau + d)^{k_Y} \rho_Y(\gamma) Y_{I_1 \dots I_n}(\tau), \qquad (1.176a)$$

$$k_Y = k_{I_1} + \dots + k_{I_n}$$
, (1.176b)

$$\rho_Y \otimes \rho_{I_1} \otimes \cdots \otimes \rho_{I_n} \supset \mathbf{1}. \tag{1.176c}$$

The result that the Yukawa coefficients must be modular forms is in the genesis of the restrictions that the modular group provides for a theory, especially given that there are few modular forms of a given weight [131]. Indeed, at least in particular for  $\Gamma'_N$  with  $N \leq 5$ , we need only to define the unique modular form of weight 1, and we can find the modular forms of higher weights for each level by carrying out successive tensor products under  $\Gamma'_N$ :

$$Y^{(k)}(\tau) = \bigotimes_{i=1}^{k} Y^{(1)}(\tau), \qquad (1.177)$$

where  $\otimes$  is to be read as the tensor product of the relevant level. If we now take into account that the entries of the weight 1 modular form are particular functions of  $\tau$  subject to constraints, such that it transforms appropriately as a modular form, we realise that not all of the combinations of the tensor products will lead to non-vanishing and independent modular forms. In that sense, we can understand that modular-invariant theories are restrictive (especially if using low weights) due to the small dimensionality of the sets of independent modular forms of a certain weight. Furthermore, all of the modular forms (*i.e.*, Yukawas) of the theory will be functions of (and thus fixed by) the same set of variables: the modulus  $\tau$ . A last property of the modular forms is that there are no modular forms of negative weight, while the only possible modular form of weight 0 is trivial (a constant). As such, we now see that if all the weights of a modular-invariant theory are zero, the Yukawa modular forms become trivial, and the requirement of invariance under the modular group simply reproduces a usual traditional flavour-symmetric SUSY theory. Hence our previous statement that modular-invariant theories generalise a (subset) of solutions to the flavour problem.

As a final remark, we note that we have throughout this section always referred to the double covers  $\Gamma'_N$ . The reason for this lies in the fact that the formalism for the double covers is more general, and envelops the case of  $\Gamma_N$ . Indeed, a  $\Gamma_N$ -invariant theory belongs to the more general set of  $\Gamma'_N$ -invariant theories, where all representations of the theory transform trivially under the R generator. Since modular forms are functions of  $\tau$ , and the linear fractional transformations are not sensitive to the sign of  $\gamma$ , they must transform trivially under R. On the other hand, we see that the transformations of Eq. (1.173) do indeed distinguish between  $\gamma$  and  $-\gamma$  due to an extra factor of  $(-1)^k$  in the automorphy factor. For odd-weighted representations (this factor trivially disappears for even weights), the extra factor must be cancelled by  $\rho_Y$ . This selects representations with  $\rho_Y(R) = -1$  for odd-weighted Yukawa

modular forms (hatted representations) [142, 157, 158]. In practice, if a theory does not assign any hatted representations to the matter fields, then the requirement of  $\rho_Y \otimes \rho_{I_1} \otimes \cdots \otimes \rho_{I_n} \supset \mathbf{1}$  will select only unhatted representations for the Yukawa modular forms. An ensuing consequence is that only even-weighted Yukawa modular forms are permitted.

# 1.4.2 Multiple Modular Symmetries

The framework of modular-invariant theories described above relies on invariance under a single modular symmetry. In principle, the framework can be extended to include multiple modular symmetries. Here, we address this extension, based on the work of ref. [137]. We will adopt a general notation, allowing the inclusion of M modular symmetries. However, it should be noted that the origin of the modular symmetries is tied to string theories, where the modulus is related to the radius of compactification of 2 extra dimensions. The bridging of the gap between bottom-up and top-down constructions has been addressed in, for example, the eclectic constructions [145–148].

In this section, for ease of notation, we will omit the prime in  $\Gamma'_N$ , and always assume we are referring to the double covers, since it is the most general framework. Extending this to the unprimed groups is trivial, and explained in the previous section.

We define a set of modular symmetries,  $\Gamma^i$ , each with a corresponding modulus  $\tau_i$ . Our goal is to extend the single modular symmetry framework to one where we have multiple commutative modular symmetries. In other words, we want to extend the symmetry from  $\Gamma$  to  $\Gamma^1 \times \cdots \times \Gamma^M$ . Due to the commutative nature of the different modular symmetries, the modulus  $\tau_i$  must transform trivially under any modular action  $\gamma_j$  with  $j \neq i$ . Then, the modular symmetry  $\Gamma^i$  acts on  $\tau_i$  as usual as

$$\gamma_i = \begin{pmatrix} a & b \\ c & d \end{pmatrix} \in \Gamma^i : \tau_i \to \gamma_i \tau_i = \frac{a\tau_i + b}{c\tau_i + d}. \tag{1.178}$$

The generalisation is straightforward:

1. The automorphy factor becomes a product of different automorphy factors for each symmetry. The elements  $\gamma_i$  are, in general, different, and thus are not able to cancel among themselves.

$$(c\tau + d)^{-k} \to \prod_{i=1,\dots,M} (c_i \tau_i + d_i)^{-k_i}$$
 (1.179)

2. The transformations of the fields under the  $\Gamma_N$  symmetry now need to account for multiple symmetries, as would be the case for a  $G \times \cdots \times G'$  traditional flavour-symmetric model:

$$\rho(\gamma) \to \bigotimes_{i=1,\dots,M} \rho_i(\gamma_i). \tag{1.180}$$

Once again, the limiting case where all the fields transform trivially under  $\Gamma^i$  with i > 1 corresponds to the case described in the previous section.

Under the same assumptions as the previous section, a superfield will now transform as

$$\varphi_{\alpha} \to \left[ \prod_{i=1,\dots,M} (c_i \tau_i + d_i)^{-k_i} \right] \left[ \bigotimes_{i=1,\dots,M} \rho_i(\gamma_i)_{\alpha\beta} \right] \varphi_{\beta}.$$
(1.181)

The Kähler potential will generate the kinetic terms for the fields (after the moduli acquire vevs) as

$$\sum_{i=1,\dots,M} \frac{h_i}{\prod_{i=1,\dots,M} \langle -i\tau_i + i\overline{\tau}_i \rangle^2} \partial_{\mu} \overline{\tau}_i \partial^{\mu} \tau_i + \sum_{I} \frac{\partial_{\mu} \overline{\varphi}^{(I)} \partial^{\mu} \varphi^{(I)}}{\prod_{i=1,\dots,M} \langle -i\tau_i + i\overline{\tau}_i \rangle^{k_i}}.$$
 (1.182)

Finally, the superpotential can be written as

$$W(\Phi) = \sum_{n} \left[ \prod_{i=1,\dots,M} Y_{I_{1}\dots I_{n}}^{k_{i}}(\tau_{i}) \right] \varphi^{I_{1}} \dots \varphi^{I_{n}}, \qquad (1.183)$$

where  $k_i$  is the weight of the Yukawa modular form for the  $\Gamma^i$  symmetry such that the automorphy factor cancels. The invariance conditions are:

• The automorphy factors need to cancel separately for each symmetry:

$$\vec{k_Y} = \vec{k_{I_1}} + \dots + \vec{k_{I_n}},\tag{1.184}$$

where we define the vector of weights  $\vec{k} = (k_1, \ldots, k_M)$ .

• There must be an invariant combination under all  $\Gamma_i$  symmetries:

$$\rho_Y^i(\gamma_i) \otimes \rho_{I_1}^i(\gamma_i) \otimes \cdots \otimes \rho_{I_n}^i(\gamma_i) \supset \mathbf{1}, \quad \forall i = 1, \dots, M,$$
(1.185)

where we use  $\rho^i$  to denote the unitary representation matrix under  $\Gamma_N^i$ .

The study and understanding of the framework of multiple modular symmetries is still in its infancy. In general, if fields of the same sector (*i.e.*, LH and RH quarks) transform as higher-dimensional (irreducible) representations of different modular symmetries, we must either rely on non-trivial Higgs representations (adding more scalars to the underlying MSSM framework), or the necessary independent parameters to have 3 massive eigenstates quickly renders the theory non-predictive. Nonetheless, it is possible to use this framework to disentangle the quark and leptonic sectors, effectively having one modulus for each sector, instead of relying on a universal modulus, otherwise mimicking the usual single modular-invariant theories.

The hitherto most common avenue for multiple modular symmetries is to introduce some (gauge-singlet) scalar fields, which transform non-trivially under multiple modular symmetries. Assuming they acquire a vev at a high scale, it is possible to break the  $\bigotimes \Gamma_N^i$  symmetry to an effective single  $\Gamma_N$  symmetry, but allowing the moduli of different invariant combinations to differ.

This will be the focus of Chapters 6 and 7.

#### Hierarchies and the Proximity to Enhanced Symmetry Points 1.4.3

A new proposal was set forth in ref. [158] which quickly gained a lot of attention in the literature. This new avenue sought to connect the fermion hierarchies to the proximity of the modulus  $\tau$  to certain points (called either stabilisers, fixed points, or symmetric points) in which a residual symmetry is preserved. Here, we will review the framework following [158], which will set the stage for Chapter 8.

The modular symmetry is broken when the modulus field acquires a vev. While there are no values of  $\tau$  which preserve the (full) modular symmetry, there are certain points which preserve a subgroup of the original symmetry. Let us assume throughout this section that there are no flavons which further break the modular symmetry.<sup>22</sup> Then, we can restrict ourselves to the fundamental domain  $\mathcal{D}$  [141], where we can find a total of 3 (non-equivalent) fixed points, regardless of the level of the modular symmetry.<sup>23</sup> Recalling Eq. (1.161), we can clearly see that all points of  $\tau$  leave R unbroken. As a consequence, all points of  $\tau$  will preserve a  $\mathbb{Z}_2^R$  symmetry. Furthermore, we can identify:

- $\tau = i\infty$ : This point is obviously symmetric under T since  $i\infty \to i\infty + 1 = i\infty$ . As a consequence, this point preserves a  $Z_N^T \times Z_2^R$  symmetry, where N is the level of the modular symmetry.
- $\tau = i$ : This point is invariant under S, given that its action sends  $\tau$  to itself,  $i \to -1/i = i$ . As such, a  $\mathbb{Z}_4^S$  symmetry is preserved.<sup>24</sup>
- $\tau = \omega \equiv e^{2\pi i/3}$ : also called the (left) cusp, this point is invariant under the action of ST. This can be seen explicitly by successively acting with the generators on the point:

$$T: \omega \to \omega + 1 = -\omega^2,$$
  
 $ST: \omega \to \frac{-1}{\omega + 1} = \frac{-1}{-\omega^2} = \frac{1}{e^{-2\pi i/3}} = e^{2\pi i/3} \equiv \omega.$  (1.186)

Evidently, the cusp  $\tau = \omega$  preserves a  $Z_3^{ST} \times Z_2^R$  residual symmetry, since  $(ST)^3 = \mathbb{1}$  (conference) Eq. (1.158)).

Now that we have seen that there are points which preserve a residual symmetry, we need to understand how the weighted representations of the modular symmetry transform under the preserved residual group. The preserved subgroups belong to the class of  $Z_N$  (or  $Z_N \times Z_2$ ) symmetries, which are characterised solely by N 1-dimensional (irreducible) representations. As such, all weighted representations of  $\Gamma'_N$  will necessary decompose into a sum of 1-dimensional irreps, which transform under the group as n-th roots of unity:

$$\mathbf{1}_k: \quad \rho(a) = e^{2\pi i k/n} \,. \tag{1.187}$$

We will not go through the process of obtaining the results, since it can become quite tedious. Nonetheless, we will outline here the process.

 $<sup>^{22} \</sup>overline{\text{Including}}$  additional sources of symmetry breaking would require a dedicated study.

<sup>&</sup>lt;sup>23</sup>In Chapter 6, we will see why there are only 3 non-equivalent stabilisers in the fundamental domain.  $^{24}$ Since  $S^2=R$ , the preserved  $Z_2^R$  symmetry is already included in the  $Z_4^S$  residual symmetry of  $\tau=i$ .

For each of the symmetry points, there is an element which is preserved  $(T, S, \text{ and } ST \text{ for } \tau = i\infty, i, \omega, \text{ respectively})$ . The results become clear and intuitive working in the respective diagonal basis for each point  $(i.e., \text{ for } \tau = i\infty, \text{ we want to be working in the basis where the representation matrices } \rho_{\mathbf{r}}(T) \text{ of } \Gamma'_{N}$  are diagonal). In this basis, the matter fields of a general weighted representation  $(\mathbf{r}, k)$  will transform under the modular symmetry as

$$\varphi_{i} \to (c\tau + d)^{-k} \rho_{\mathbf{r}}(g)_{ij} \varphi_{j} = \begin{cases} (1)^{-k} \rho_{\mathbf{r}}(T)_{ij} \varphi_{j} = e^{2\pi i k_{i}/N} \varphi_{i}, & \text{for } \tau = i\infty \\ (-i)^{-k} \rho_{\mathbf{r}}(S)_{ij} \varphi_{j} = (i)^{k} e^{2\pi i k_{i}/4} \varphi_{i}, & \text{for } \tau = i \end{cases}, \quad (1.188)$$

$$(-\omega - 1)^{-k} \rho_{\mathbf{r}}(ST)_{ij} \varphi_{j} = \omega^{k} e^{2\pi i k_{i}/3} \varphi_{i}, & \text{for } \tau = \omega$$

with g = T, S, ST (which determines the automorphy factor), and where we assumed we were in the appropriate diagonal basis for each case, and thus there is no implied summation of i. Since the representations  $(\mathbf{r}, k)$  must decompose into representations of the residual group, we can take any diagonal generator  $\rho_{\mathbf{r}}(g)$  to have entries  $e^{2\pi i k_i/N}$ , where  $k_i = 1, ..., N$ , since otherwise  $\mathbf{r}$  would decompose into a representation outside of those present in the residual subgroup. The specific values of  $k_i$  for each representation require the actual computation.

As we have already seen previously, the modular-symmetric (renormalizable) superpotential includes Yukawa terms of the type

$$W(\varphi) \supset Y_{\mathbf{r}}^{(k_Y)}(\tau)\varphi_i\varphi_j^c H,$$
 (1.189)

where  $H \equiv H_{u,d}$  depending on the hypercharges of  $\varphi$  and  $\varphi^c$ . After the EWSB, these terms generate mass terms for the fields as

$$\varphi_i M(\tau)_{ij} \varphi_i^c \,. \tag{1.190}$$

For the superpotential to be invariant, each component of  $M(\tau)_{ij}$  must be a modular form of level N and weight  $k_Y = k + k^c$ . Moreover, the requirement of modular invariance imposes

$$M(\tau) \xrightarrow{\gamma} M(\gamma \tau) = (c\tau + d)^{k_Y} \rho(\gamma)^* M(\tau) \rho^c(\gamma)^{\dagger},$$
 (1.191)

where we defined

$$\varphi \to (c\tau + d)^{-k}\rho(\gamma)\varphi$$
, (1.192a)

$$\varphi^c \rightarrow (c\tau + d)^{-k^c} \rho^c(\gamma) \varphi^c,$$
 (1.192b)

and it is useful to remind ourselves that  $\varphi$  and  $\varphi^c$  are independent. Finally, for each of the symmetry points, we can set  $\gamma$  to the residual symmetry generator, and we can use the transformation rule for  $M(\tau)$  to uncover the leading contributions for each component of the mass matrix.

# Vicinity of $\tau = i\infty$

The symmetry point  $\tau = i\infty$  leaves the T generator unbroken, and so we set  $\gamma = T$ . This automatically cancels the automorphy factor, since c = 0 and d = 1 (recall Eq. (1.159)). Since we can always find a basis where this generator is diagonal, we denote  $\rho_i = \rho_{ii}$ . In this way, we find

$$M_{ij}(T\tau) = (\rho_i \rho_i^c)^* M_{ij}(\tau).$$
 (1.193)

For our goals, it is useful to work with the quantity  $q = \exp(2\pi i \tau/N)$  instead of merely  $\tau$ , and we note that the mass matrices are analytical functions of q, since the modular forms admit q-expansions of the form of Eq. (1.174). Furthermore, it is clear to see that the action of  $\gamma = T$  on q is described by  $q \xrightarrow{T} \zeta q$ , with  $\zeta = \exp(2\pi i/N)$ . If we do a power series expansion of  $M(\tau)$  and  $M(T\tau) \equiv M(\zeta q)$ , these matrices can be written as

$$M_{ij}(\tau) = \sum_{n} \frac{M_{ij}^{(n)}(q_0)}{n!} (q - q_0)^n,$$
 (1.194a)

$$M_{ij}(T\tau) = \sum_{n} \frac{M_{ij}^{(n)}(\zeta q_0)}{n!} (\zeta q - \zeta q_0)^n,$$
 (1.194b)

where  $M_{ij}^{(n)}(q_0)$  are the *n*-th derivatives of  $M_{ij}(q)$  at  $q=q_0$ .

If we now take into account that  $q_0 = 0$ , the condition of Eq. (1.193) becomes

$$\zeta^n M_{ij}^{(n)}(0) = (\rho_i \rho_j^c)^* M_{ij}^{(n)}(0), \qquad (1.195)$$

which can only be satisfied if either  $M_{ij}^{(n)} = 0$ , or  $(\rho_i \rho_j^c)^* = \zeta^n$ . As such, we see that if  $(\rho_i \rho_j^c) = \zeta^l$  (with  $l \mod N$ ), then, in the vicinity of the symmetry point, by virtue of  $\zeta^N = 1$ ,

$$M_{ij}(q) = a_0 q^l + a_1 q^{N+l} + a_2 q^{2N+l} + \dots$$
(1.196)

Amazingly, we see that by identifying the residual group decomposition of  $\rho$  and  $\rho^c$ , we can immediately get the power structure in terms of  $\epsilon$  of  $M(\tau)$ . Notably, we also see that since T cancels the automorphy factor regardless of the weights, the power structure of the mass matrices is independent of the modular weights.

As an example, we can take the case of  $\varphi \sim \mathbf{3}$  and  $\varphi^c \sim \mathbf{3}'$  for the case of  $\Gamma_4'$ . The residual group decompositions under  $Z_4^T$  (we can safely ignore  $Z_2^R$  since  $M(\tau)$  is R-even) are  $\varphi \rightsquigarrow \mathbf{1}_1 \oplus \mathbf{1}_2 \oplus \mathbf{1}_3$  and  $\varphi^c \rightsquigarrow \mathbf{1}_0 \oplus \mathbf{1}_1 \oplus \mathbf{1}_3$ . Using Eq. (1.187), we can define (note that  $\zeta = e^{2\pi i/4} = i$ )

$$\rho = \begin{pmatrix} i, & -1, & -i \end{pmatrix}, \qquad \rho^c = \begin{pmatrix} 1, & i, & -i \end{pmatrix},$$
(1.197)

where the fact that  $\mathbf{1}_{0,2}$  are real (self-conjugate) whereas  $\mathbf{1}_{1,3}$  are complex becomes obvious. In the case

of  $\tau = i\infty$ , it is convenient to define the quantity

$$\epsilon = e^{-2\pi \text{Im}\tau/N} \tag{1.198}$$

which will effectively act as a spurion which parametrises the breaking of the  $Z_N$  residual symmetry. Then, we can find the power structure of  $M(\tau)$  through

$$M(\tau) \sim (\rho^T \rho^c)^* \sim \begin{pmatrix} \epsilon^3 & \epsilon^2 & 1 \\ \epsilon^2 & \epsilon & \epsilon^3 \\ \epsilon & 1 & \epsilon^2 \end{pmatrix} \quad \text{with} \quad \epsilon = e^{-2\pi \text{Im}\tau/4} \,.$$
 (1.199)

# Vicinity of $\tau = i$

In this case, we are close the symmetry point preserving  $Z_4^S$ , and thus we want  $\gamma = S$ . In an S-diagonal basis,  $\rho(S) = \text{diag}(\rho_i)$ , from Eq. (1.188), we see that

$$M_{ij}(S\tau) = (-i\tau)^{k_Y} (\widetilde{\rho}_i \widetilde{\rho}_j^c)^* M_{ij}(\tau), \qquad (1.200)$$

where we used Eq. (1.188) to define  $\tilde{\rho} = i^k \rho$ , which determines the actual residual subgroup decomposition under  $Z_4^S$ .<sup>25</sup> We define a convenient parameter as

$$s = \frac{\tau - i}{\tau + i},\tag{1.201}$$

and note that, similarly to q, the entries of  $M(\tau)$  will be analytical functions of s, such that a power series is justified. Furthermore, this parameter is also convenient to parametrise the deviation from the symmetric point of  $\tau = i$ , with  $\epsilon = |s|$ . Using  $s \xrightarrow{S} -s$ , we can manipulate Eq. (1.200) into

$$M_{ij}(S\tau) = M_{ij}(-s) = \left(-\frac{s+1}{s-1}\right)^{k_Y} (\widetilde{\rho}_i \widetilde{\rho}_j^c)^* M_{ij}(s).$$
 (1.202)

If we now introduce  $\widetilde{M}_{ij}(s) = (1-s)^{-k_Y} M_{ij}(s)$ , we get

$$\widetilde{M}_{ij}(-s) = (\widetilde{\rho}_i \widetilde{\rho}_j^c)^* \widetilde{M}_{ij}(s), \qquad (1.203)$$

and the procedure of the previous case holds, with (in this case, since  $s \xrightarrow{S} -s$ , we have  $\zeta = -1$ )

$$(-1)^n \widetilde{M}_{ij}^{(n)}(0) = (\widetilde{\rho}_i \widetilde{\rho}_j^c)^* \widetilde{M}_{ij}^{(n)}(0).$$
(1.204)

As an example, we can take the same case of  $\varphi \sim 3$  and  $\varphi^c \sim 3'$  for the case of  $\Gamma'_4$ . Under  $Z_4^S$ , we have  $\varphi \leadsto \mathbf{1}_{k+2} \oplus \mathbf{1}_k \oplus \mathbf{1}_k$  and  $\varphi^c \leadsto \mathbf{1}_{k+2} \oplus \mathbf{1}_{k+2} \oplus \mathbf{1}_k$ . The power structure can be found through

$$\widetilde{\rho} = (i^{k+2}, i^k, i^k), \qquad \rho^c = (i^{k^c+2}, i^{k^c+2}, i^{k^c}),$$
(1.205)

<sup>&</sup>lt;sup>25</sup>Here, we can see the explicit dependency of the weights for the residual subgroup decomposition, which is absent for the case of  $\tau = i\infty$ 

where now the power structure requires a specific assignment of the modular weights.

### Vicinity of $\tau = \omega$

Finally, for the case of  $\tau = \omega$ , where the ST element is preserved, we can follow the above procedure, with

$$\widetilde{\rho}_i = w^k \rho_i, \qquad (1.206a)$$

$$u = \frac{\tau - \omega}{\tau - \omega^2}, \quad \epsilon = |u| \tag{1.206b}$$

$$u = \frac{\tau - \omega}{\tau - \omega^2}, \quad \epsilon = |u|$$
 (1.206b)  
 $\widetilde{M}_{ij}(u) = (1 - u)^{-k_Y} M_{ij}(u),$  (1.206c)

leading to

$$\omega^{2n}\widetilde{M}_{ij}^{(n)}(0) = \left(\widetilde{\rho}_i\widetilde{\rho}_j^c\right)^* \widetilde{M}_{ij}^{(n)}(0). \tag{1.207}$$

#### Masses and Mixing from the Residual Symmetry

After we find the residual group decomposition, and the power structure of  $M(\tau)$ , we can translate this into the expected hierarchical patterns which arise in the fermion masses and mixings. It should be noted that the power structure is not necessarily present in a specific model. As a matter of fact, the residual group decomposition gives us the maximal power of  $\epsilon$  allowed by the residual symmetry. However, the number of linearly independent modular forms for a certain weight is fixed, and this may result in some entries to vanish. In the same vein, the results for the expected mass hierarchies give us the maximally allowed structure for the masses, but specific models may predict vanishing masses, due to either the absence of modular forms for a certain weight, or due to proportionality between columns (or lines) of the mass matrices.

Following refs [158, 159], we can leverage the relations

$$\sum_{i_1 < \dots < i_p} m_{i_1}^2 \dots m_{i_p}^2 = \sum |\det M_{p \times p}|^2 , \qquad (1.208)$$

with p = 1, ..., n, for a  $n \times n$  complex matrix M.  $m_i$  are the eigenvalues of M, and the summation refers to all possible  $p \times p$  submatrices of M.

For the particular case of n=3, we can order  $m_i$  in descending order in powers of  $\epsilon$ , such that

$$m_3^2 \sim \sum_{i,j} |M_{ij}|^2 \Rightarrow m_3^2 \sim \text{Tr} M^{\dagger} M,$$
 (1.209a)

$$m_2^2 m_3^2 \sim \sum |\det M_{2\times 2}|^2 \Rightarrow m_2^2 \sim \frac{\sum |\det M_{2\times 2}|^2}{\operatorname{Tr} M^{\dagger} M},$$
 (1.209b)

$$m_2^2 m_3^2 \sim \sum |\det M_{2\times 2}|^2 \Rightarrow m_2^2 \sim \frac{\sum |\det M_{2\times 2}|^2}{\operatorname{Tr} M^{\dagger} M},$$
 (1.209b)  
 $m_1^2 m_2^2 m_3^2 = |\det M|^2 \Rightarrow m_1^2 \sim \frac{|\det M|^2}{\sum |\det M_{2\times 2}|^2},$  (1.209c)

where the approximate symbol denotes a power counting approximation. Following this procedure, we are able to determine the expected hierarchical pattern of mass hierarchies in the vicinity of symmetry points.

We can go one step further, and use the power structure of  $M(\tau)$  and the residual group decomposition to understand the expected ensuing hierarchies in the mixing. Indeed, we can exploit the residual group decomposition to understand the allowed mixing in the symmetric limit [158, 160]. If more than one flavour of fermion decompose into the same representation under the residual symmetry, their allowed mixing is expected to be  $\mathcal{O}(1)$ . This should be reflected in the power structure of the mass matrices themselves. In that sense, the limit  $\epsilon \to 0$  could also provide an insight on (some of) the mixing angles. For example, in cases where there is a single vanishing mass in  $Y_u$  and  $Y_d$ , we can easily see if  $|V_{tb}|$  is predicted to be  $\sim 1$  or  $\ll 1$ . Other estimates can be found by dividing the (3×3) mass matrices into 2×2 sub-blocks, and comparing relative sizes of the diagonal and off-diagonal entries, somewhat similarly to the Froggatt-Nielsen estimates.

In Chapter 8, we perform a comprehensive study which attempts to leverage this behaviour to explain the hierarchies in the quark sector.

# Democratic 3HDMs

The complexity behind the flavour Puzzle does not allow for a single avenue to stand out as unquestionably more fruitful than others. In this way, it becomes necessary to follow along different paths to understand their strengths and downfalls. Amongst the most common approaches, the inclusion of Abelian groups as flavour symmetries in the 2HDM led the community's efforts for a large period of time. These efforts are now diversifying to apply Abelian groups (either one or multiple  $Z_N$  symmetries) to nHDMs, with a special focus on 3HDMs. The reason being that FCNCs are easily forbidden within these setups, safeguarding the model against dangerous contributions to well-measured processes, while keeping the proliferation of free parameters of the Yukawa sector in check. On the other hand, the scalar sector still allows for a large number of parameters, possibly diluting the predictive power of the model, and making the exploration of its parametric space quite involved. Notwithstanding, the inherent arbitrariness can be reduced by taking into account a number of theoretical and experimental considerations, making the study of 3HDMs with Abelian flavour symmetry groups worthwhile. Given the simplicity of their implementation, and their closeness to well-established endeavours (such as the type-II 2HDM), it is the study of 3HDMs with Abelian groups acting as flavour symmetries which will lead our first steps into the flavour puzzle.

In this chapter, we will study various aspects of 3HDMs endowed with a flavour symmetry such that each scalar doublet couples to a different type of fermion, forbidding FCNCs at the tree-level (henceforth called 'democratic' 3HDM) [161–163]. We will start by presenting the model in the two most common realisations. In a tangential digression, we then review the custodial symmetry in the SM, and generalise this to the case of nHDMs. We present the results in a simple relation in terms of the physical masses and mixings of the scalar sector, rather than presenting basis-dependent relations between the quartic parameters of the scalar potential. For clarity and ease of comparison, we show the resulting relations between the quartic parameters for both democratic 3HDM implementations, for the custodial symmetry to hold. We will then analyse how, under certain assumptions, democratic 3HDMs can appear to mimic a damped type-II 2HDM, and see how the stringent constraints on the NP scale set by the experimental collaborations for the type-II 2HDM can be relaxed in this scenario. Finally, we leverage the fact that

experimental collaborations are not fully sensitive to the sign of the SM Higgs couplings to the down quarks and charged-leptons, to explore the possibility that these couplings could have the opposite sign of the SM prediction: the so-called wrong-sign limit. This chapter closely follows our works of refs. [164, 165]. It should be noted that the results related to experimental bounds which are presented here are now outdated. However, the main conclusions, in particular regarding the possibility of the democratic 3HDM to appear as a type-II 2HDM with softened bounds still holds, albeit possibly with a higher upper bound. Furthermore, we omit here the results gathered in ref. [164] regarding the direct searches for new scalars. That is not to understate the importance of taking these searches into account, especially since the  $\tau\tau$  channel can place very stringent bounds on the allowed pseudoscalar masses (see refs. [164, 166]). Nevertheless, these numerical studies do not destroy the concept behind Section 2.2, but rather complement it with further experimental constraints. As such, since the concept of relaxing experimental bounds while mimicking the type-II 2HDM Yukawa structure is less affected by experimental updates, we choose to present it as a proof-of-concept, and leave out the direct searches, as these are more impacted by the changes in experimental data as well as possible new signals [164, 166].

The democratic 3HDMs are defined through their Yukawa couplings, in which the RH up- and downtype quarks, as well as the charged-leptons each couple to a respective Higgs doublet. The Yukawa Lagrangian then takes the following form:

$$\mathcal{L}_Y = -Y_d \overline{Q}_L \phi_2 n_R - Y_u \overline{Q}_L \widetilde{\phi}_3 p_R - Y_\ell \overline{L}_L \phi_1 \ell_R, \qquad (2.1)$$

where  $Y_{d.u.\ell}$  are the Yukawa couplings in the down-quark, up-quark, and charged-lepton sectors. The up-type, down-type, and charged-lepton right-handed fields are denoted as  $p_R$ ,  $n_R$ , and  $\ell_R$ , respectively, whereas the left-handed  $SU(2)_L$  doublets for the quarks and leptons are  $Q_L = (p_L, n_L)^T$  and  $L_L = (\nu_L, e_L)^T$ . Finally,  $\widetilde{\phi}_3 = i\tau_2\phi_3^*$  is the  $SU(2)_L$  doublet responsible for the up-quark masses. There are two common ways to arrive at the above Lagrangian. The first is to impose a  $Z_3$  symmetry as follows [67] (with  $\omega = e^{2\pi i/3}$ )

$$\phi_1 \to \omega \, \phi_1 \,, \qquad \phi_2 \to \omega^2 \phi_2 \,, \qquad \ell_R \to \omega^2 \ell_R \,, \qquad n_R \to \omega \, n_R \,.$$
 (2.2)

The second possibility relies on a  $Z_2 \times Z_2'$  symmetry under which the fields transform as [162]

$$Z_2: \qquad \phi_1 \to -\phi_1 \,, \quad \ell_R \to -\ell_R$$
 (2.3a)

$$Z_2': \qquad \phi_2 \to -\phi_2 \,, \quad n_R \to -n_R \,.$$
 (2.3b)

Both in Eqs. (2.2) and (2.3), only the nontrivial transformations are explicitly displayed.

The inclusion of additional scalars in the theory has an impact on some observables which can be rather constraining. In particular, the effect of nonstandard scalars in the electroweak precision observables (specifically the  $\rho$  parameter) can lead to stringent constraints on the scalar sector. One easy way to circumvent this problem is to impose a custodial symmetry to minimize their impact. For this reason, we dedicate the next section to this topic.

# 2.1 Custodial Symmetry

To highlight the importance of the custodial limit, we recall that in the SM, the custodial symmetry (CS) ensures  $\rho = 1$  at the tree-level. The custodial symmetry is only an approximate symmetry of the SM since it is broken by the  $U(1)_Y$  gauge coupling, as well as the Yukawa couplings [167]. Because of this, at the loop level, the  $\rho$ -parameter deviates slightly from unity and the deviation is quite accurately predicted by the SM. As it happens, the experimental measurement is compatible with this SM prediction, leaving very little room for new physics (NP) to give an extra contribution. Such NP contributions are sometimes conveniently expressed in terms of the T-parameter, which has the following experimental limit [21]

$$T = 0.03 \pm 0.12$$
.

One noteworthy aspect is that the SM scalar sector respects CS perfectly. However, this is no longer guaranteed once the scalar sector is extended. Therefore, it is expected that the additional scalars will give rise to extra contributions to the T-parameter. The limit on the T-parameter will place constraints on the NP contributions, sometimes requiring a fine-tuned scalar spectrum to keep the value under control. Thus, models with n Higgs-doublets (nHDMs), although respecting  $\rho=1$  at the tree-level, can potentially drive the T-parameter away from the experimental bounds, if the scalar masses are arbitrarily chosen [168–171]. The study of custodial symmetry in the context of nHDMs has been performed earlier [172–176], but in this chapter we follow ref. [177]. This alternative approach enables us to intuitively identify the different custodial multiplets and at the end, the conditions for CS in nHDMs are concisely expressed in a single equation, in terms of the physical masses and mixings of the scalar sector.

The CS is an accidental global SU(2) symmetry (hereafter denoted as  $SU(2)_C$ ) which prevails even after the spontaneous breaking of the electroweak symmetry in the SM. Here, we follow the formulation of CS as in ref. [177], and confine ourselves to the  $SU(2)_L$  part of the electroweak gauge symmetry, that is, we work in the limit where the  $U(1)_Y$  gauge coupling goes to zero (g'=0). In this section, we will build our intuition first, by considering the simple example of the SM scalar sector. Then, we will extend our formalism to the case of a general nHDM and obtain conditions such that the scalar sector obeys the CS.

#### 2.1.1 SM Recap

In the SM, there is a single complex scalar doublet,  $\phi$ , which drives the EWSB. The scalar Lagragian of the SM is given by

$$\mathcal{L}_{\text{scalar}} = (D^{\mu}\phi)^{\dagger} (D_{\mu}\phi) - V(\phi), \qquad (2.4)$$

where  $V(\phi)$  is the scalar potential. In the limit g'=0, the gauge-covariant derivative for  $\phi$  is given by

$$D_{\mu}\phi = \left(\partial_{\mu} + ig\frac{\tau_a}{2}W_{\mu}^a\right)\phi, \tag{2.5}$$

where g is the  $SU(2)_L$  gauge coupling,  $W^a_\mu$  are the  $SU(2)_L$  gauge bosons, and  $\tau_a$  are the Pauli matrices. After the EWSB, the scalar doublet  $\phi$  can be explicitly expressed in terms of the component fields, as follows

$$\phi = \frac{1}{\sqrt{2}} \begin{pmatrix} \sqrt{2} \,\omega^+ \\ v + h + i\zeta \end{pmatrix} \,, \tag{2.6}$$

where v is the vev. Subsequently, the scalar kinetic terms can be conveniently decomposed as [177]

$$\mathcal{L}_{\text{kin}} = (D^{\mu}\phi)^{\dagger}(D_{\mu}\phi) = \mathcal{L}_{\text{mass}} + \mathcal{L}_{\text{quad}} + \mathcal{L}_{\text{mixed}} + \mathcal{L}_{\text{deriv}} + \mathcal{L}_{\text{cubic}} + \mathcal{L}_{\text{quartic}}. \tag{2.7}$$

Collectively denoting the gauge bosons as  $G^{a,b,...}_{\mu}$  and the component scalar fields as  $s_{i,j,...}$ , the meaning of the individual terms introduced in the above equation are given below

 $\mathscr{L}_{\mathrm{mass}}$ : these are the mass terms for the gauge bosons of the form  $v^2 G_{\mu}^{a\dagger} G^{a\mu}$ ,

 $\mathscr{L}_{\text{quad}}$ : these are the kinetic terms of the component scalar fields,  $(\partial^{\mu} s_i)^{\dagger} (\partial_{\mu} s_i)$ ,

 $\mathscr{L}_{\text{mixed}}$ : terms of the form  $(\partial^{\mu} s_i)^{\dagger} (ivG_{\mu}) + \text{h.c.}$ ,

 $\mathcal{L}_{\text{deriv}}$ : terms of the form  $(\partial^{\mu} s_i)^{\dagger} (iG_{\mu} s_j) + \text{h.c.}$ ,

 $\mathcal{L}_{\text{cubic}}$ : terms of the form  $(G^{a,\mu}s_i)^{\dagger}(vG_{\mu}^b) + \text{h.c.}$ ,

 $\mathscr{L}_{\text{quartic}}$ : terms of the form  $(G^{a,\mu}s_i)^{\dagger}(G_u^bs_j)$ .

To identify the custodial multiplets, we begin with  $\mathcal{L}_{\text{mass}}$  which, in the SM (with g'=0), is given by

$$\mathcal{L}_{\text{mass}} = \frac{g^2 v^2}{8} \left( W^{\mu +} W_{\mu}^- + W^{\mu -} W_{\mu}^+ + W^{3\mu} W_{\mu}^3 \right). \tag{2.8}$$

where

$$W_{\mu}^{\pm} = \frac{W_{\mu}^{1} \mp iW_{\mu}^{2}}{\sqrt{2}}.$$
 (2.9)

We can see from the above equation that the  $SU(2)_L$  gauge bosons have the same mass. This motivates us to identify a custodial multiplet of the gauge bosons as<sup>1</sup>

$$\mathbf{W} = \begin{pmatrix} -W^+ \\ W_3 \\ W^- \end{pmatrix} . \tag{2.10}$$

Note that the Lorentz indices have been suppressed here for simplicity as it has no bearing on the  $SU(2)_C$  transformations. In terms of the  $SU(2)_C$  triplet of Eq. (2.10),  $\mathcal{L}_{\text{mass}}$  can be rewritten as

$$\mathcal{L}_{\text{mass}} = \frac{g^2 v^2}{8} \left( \mathbf{W} \cdot \mathbf{W} \right), \tag{2.11}$$

<sup>&</sup>lt;sup>1</sup>the minus sign in the first entry of **W** comes from the details of SU(2) group theory, which are explained in Appendix A.1.

which is manifestly invariant under  $SU(2)_C$ . To identify the  $SU(2)_C$  multiplets of the scalar fields, let us turn our attention to  $\mathcal{L}_{\text{cubic}}$  and  $\mathcal{L}_{\text{mixed}}$ . First, in terms of the triplet  $\mathbf{W}$ ,  $\mathcal{L}_{\text{cubic}}$  can be expressed as

$$\mathcal{L}_{\text{cubic}} = \frac{g^2 v}{4} h\left(\mathbf{W} \cdot \mathbf{W}\right). \tag{2.12}$$

Thus,  $\mathscr{L}_{\text{cubic}}$  will also be  $SU(2)_C$  invariant if we identify the physical scalar, h, as a singlet of  $SU(2)_C$ . Next, we look into  $\mathscr{L}_{\text{mixed}}$ , which is given by

$$\mathcal{L}_{\text{mixed}} = \frac{gv}{2} \left[ i \left( \partial^{\mu} w^{-} \right) W_{\mu}^{+} - i \left( \partial^{\mu} w^{+} \right) W_{\mu}^{-} - \left( \partial^{\mu} \zeta \right) W_{\mu}^{3} \right]. \tag{2.13}$$

Given the identification of **W** in Eq. (2.10), the above equation encourages us to define an  $SU(2)_C$  triplet of scalar fields as follows:

$$\mathbf{T} = \begin{pmatrix} i\omega^+ \\ -\zeta \\ i\omega^- \end{pmatrix} . \tag{2.14}$$

In terms of W and T, Eq. (2.13) can be written as

$$\mathcal{L}_{\text{mixed}} = \frac{gv}{2} (\mathbf{W} \cdot \partial \mathbf{T}), \qquad (2.15)$$

which explicitly demonstrates the  $SU(2)_C$  invariance of  $\mathcal{L}_{mixed}$ . The other terms,  $\mathcal{L}_{quad}$ ,  $\mathcal{L}_{deriv}$ , and  $\mathcal{L}_{quartic}$ , when expressed in terms of  $\mathbf{W}$  and  $\mathbf{T}$ , can also be shown to be invariant under  $SU(2)_C$ . All these terms will be considered in detail in the next subsection, when we consider the nHDM generalisation of the above prescription.

Now, let us take a look at the  $SU(2)_C$  invariance of the scalar potential, which is given by

$$V(\phi) = \mu^2 \left(\phi^{\dagger} \phi\right) + \lambda \left(\phi^{\dagger} \phi\right)^2. \tag{2.16}$$

After the EWSB,  $\phi^{\dagger}\phi$  can be expressed as

$$\phi^{\dagger}\phi = \frac{1}{2}(\mathbf{T} \cdot \mathbf{T}) + \frac{v^2}{2} + \frac{h^2}{2} + vh.$$
 (2.17)

We can see that, our previous multiplet identifications of  $\mathbf{T}$  and h are compatible with the  $SU(2)_C$  invariance of the scalar potential. In other words, no additional conditions need to be imposed on the SM scalar potential to make it  $SU(2)_C$  invariant. It should be noted that, the  $SU(2)_C$  invariance of the scalar potential mandates that the scalars which are in the same  $SU(2)_C$  multiplet should have the same mass. This condition is trivially satisfied here in the SM as all the components of  $\mathbf{T}$  are Goldstone bosons with zero mass. This will no longer be true in nHDMs, where we will need to impose additional restrictions on the parameters of the scalar potential to ensure custodial invariance.

#### 2.1.2 Generalisation to nHDMs

We will now look at the scalar kinetic Lagrangian for a model with n complex scalar doublets  $\phi_k$  (k = 1, ..., n) and identify the different  $SU(2)_C$  multiplets. Thus we begin with

$$\mathscr{L}_{kin} = \sum_{k=1}^{n} (D^{\mu} \phi_k)^{\dagger} (D_{\mu} \phi_k), \qquad (2.18)$$

where, under the assumption of g' = 0, the gauge covariant derivative of  $\phi_k$  is given by

$$D_{\mu}\phi_{k} = \left(\partial_{\mu} + ig\frac{\tau_{a}}{2}W_{\mu}^{a}\right)\phi_{k}. \tag{2.19}$$

After the EWSB, the k-th scalar doublet is decomposed as

$$\phi_k = \frac{1}{\sqrt{2}} \begin{pmatrix} \sqrt{2}w_k^+ \\ v_k + h_k + iz_k \end{pmatrix} , \qquad (2.20)$$

where  $v_k$  is the vev of  $\phi_k$ , assumed to be real. Borrowing the terminology introduced in Eq. (2.7), we still have

$$\mathcal{L}_{\text{mass}} = \frac{g^2 v^2}{8} \left( \mathbf{W} \cdot \mathbf{W} \right), \tag{2.21}$$

where  $v = \sqrt{v_1^2 + v_2^2 + ... + v_n^2}$  is the total electroweak vev, and we have used Eq. (2.10) for the definition of **W**. This implies that  $\mathcal{L}_{\text{mass}}$  will still respect  $SU(2)_C$  once we identify the custodial triplet of the gauge bosons, as in the case of the SM. Similarly, for  $\mathcal{L}_{\text{cubic}}$  we have

$$\mathcal{L}_{\text{cubic}} = \frac{g^2}{4} \left( \mathbf{W} \cdot \mathbf{W} \right) \sum_{k=1}^{n} v_k h_k.$$
 (2.22)

Evidently,  $\mathcal{L}_{\text{cubic}}$  will also be custodially invariant if we identify  $h_k$  (k = 1, ..., n) as singlets of  $SU(2)_C$ . Next, we turn our attention to  $\mathcal{L}_{\text{mixed}}$ , which has the following form

$$\mathcal{L}_{\text{mixed}} = \frac{g}{2} \sum_{k=1}^{n} v_k \left[ i(\partial^{\mu} w_k^{-}) W_{\mu}^{+} - i(\partial^{\mu} w_k^{+}) W_{\mu}^{-} - (\partial^{\mu} z_k) W_{\mu}^{3} \right]. \tag{2.23}$$

Taking inspiration from Eq. (2.13), we now proceed to define a set of  $SU(2)_C$  triplets involving the scalar component fields as

$$\mathbf{T}_{k} \equiv \begin{pmatrix} iw_{k}^{+} \\ -z_{k} \\ iw_{k}^{-} \end{pmatrix}, \quad k = 1, ..., n.$$

$$(2.24)$$

<sup>&</sup>lt;sup>2</sup>The fact that the EWSB does not break CS implies  $h_k$  need to be singlets, otherwise the vev would necessarily break  $SU(2)_C$ . This is also implied by  $\mathcal{L}_{\text{mixed}}$ , and the remaining terms of  $\mathcal{L}_{\text{kin}}$ .

Following this identification, we can express  $\mathcal{L}_{\text{mixed}}$  as the sum of  $SU(2)_C$  invariants, given by

$$\mathcal{L}_{\text{mixed}} = \frac{g}{2} \sum_{k=1}^{n} v_k \left( \mathbf{W} \cdot \partial \mathbf{T}_k \right). \tag{2.25}$$

For the sake of completeness, we also express  $\mathcal{L}_{\text{quad}}$ ,  $\mathcal{L}_{\text{quartic}}$ , and  $\mathcal{L}_{\text{deriv}}$ , in terms of  $\mathbf{W}$ ,  $\mathbf{T}_k$ , and  $h_k$ , as follows

$$\mathcal{L}_{\text{quad}} = \frac{1}{2} \sum_{k=1}^{n} \left[ (\partial \mathbf{T}_k \cdot \partial \mathbf{T}_k) + (\partial^{\mu} h_k)(\partial_{\mu} h_k) \right], \qquad (2.26a)$$

$$\mathcal{L}_{\text{quartic}} = \frac{g^2}{8} (\mathbf{W} \cdot \mathbf{W}) \sum_{k=1}^{n} (\mathbf{T}_k \cdot \mathbf{T}_k + h_k^2), \qquad (2.26b)$$

$$\mathcal{L}_{\text{deriv}} = \frac{g}{2} \sum_{k=1}^{n} \left\{ h_k(\mathbf{W} \cdot \partial \mathbf{T}_k) + \partial h_k(\mathbf{T}_k \cdot \mathbf{W}) + (\mathbf{T}_k \times \partial \mathbf{T}_k) \cdot \mathbf{W} \right\}, \qquad (2.26c)$$

where  $(\mathbf{r}_1 \times \mathbf{r}_2) \cdot \mathbf{r}_3$  is the singlet combination of the SU(2) product of three triplets,  $\mathbf{r}_{1,2,3}$ , for which the explicit expression is given in Appendix A.1.

Thus, we can see that all the terms in the scalar kinetic Lagrangian are custodially invariant. However, the triplets  $\mathbf{T}_k$  are not expressed in terms of physical fields. Rotation of these fields from the Lagrangian basis to the physical basis will give rise to the Goldstone bosons, the physical charged-scalars, and pseudoscalars.<sup>3</sup> We would like to transfer the  $SU(2)_C$  invariance into the physical basis as well. For this, we need to rotate each triplet as a whole object, that is,

$$\mathbf{P}_{j} = \sum_{k=1}^{n} \mathcal{O}_{jk} \mathbf{T}_{k} \qquad j = 1, 2, \dots n,$$

$$(2.27)$$

where  $\mathbf{P}_{j}$  denotes the j-th triplet of  $SU(2)_{C}$  in the physical basis, and  $\mathcal{O}_{jk}$  are the elements of an orthogonal matrix. Note that, each triplet  $\mathbf{T}_{k}$ , contained a pseudoscalar field and a pair of charged fields. Consequently, Eq. (2.27) implies that the charged and pseudoscalar mass matrices should be rotated into the physical basis by means of the same rotation matrix, in order to preserve the  $SU(2)_{C}$  invariance of  $\mathcal{L}_{kin}$  in the physical basis as well. Now, for a charged-scalar and a pseudoscalar in the physical basis to be placed in the same triplet  $\mathbf{P}_{j}$ , they should have a common mass so that the mass terms for the members of  $\mathbf{P}_{j}$  can be concisely expressed in an  $SU(2)_{C}$  invariant form as  $M_{j}^{2}(\mathbf{P}_{j} \cdot \mathbf{P}_{j})$ . Thus, we can conclude that, in the physical basis, the diagonal mass matrices in the charged and pseudoscalar sectors must be equal. Also, from Eq. (2.27), we should recall that the rotations that bring the mass matrices of the charged and pseudoscalar sectors to their respective diagonal forms should also be the same. Putting this together, we can conclude that the mass matrix of the charged and pseudoscalar sectors should be equal in the Lagrangian basis as well, that is

$$M_C^2 = M_P^2$$
. (2.28)

 $<sup>^3</sup>$ Following Ref. [173], it is reasonable to have such a classification of the scalar spectrum because CP conservation follows for nHDMs with custodial symmetry.

Since the information about the scalar masses and the mixings comes from the scalar potential, the parameters of the scalar potential should adjust themselves so that Eq. (2.28) is satisfied for arbitrary values of the vevs. The arbitrariness of the vevs is important because the validity of the custodial symmetry should not depend on the exact values of the vevs, just as in the case of the SM.

#### 2.1.3 Validation of the Custodial Limit by Explicit Calculation

In  $SU(2)_C$  invariant models, we expect that no additional contribution to the T-parameter comes from the scalar sector. It would be rather reassuring to explicitly verify that this is indeed the case for nHDMs in the limit of Eq. (2.28). For this purpose, we use the one-loop formula for the NP contribution to the T-parameter for nHDMs given in refs. [170, 171]:

$$\alpha T = \frac{g^2}{64\pi^2 M_W^2} \left\{ \sum_{a=2}^n \sum_{b=2}^{2n} \left| \left( U^{\dagger} V \right)_{ab} \right|^2 F\left( m_a^2, \mu_b^2 \right) - \sum_{b=2}^{2n-1} \sum_{b'=b+1}^{2n} \left| \left( V^{\dagger} V \right)_{bb'} \right|^2 F\left( \mu_b^2, \mu_{b'}^2 \right) \right. \\ \left. + 3 \sum_{b=2}^n \left| \left( V^{\dagger} V \right)_{1b} \right|^2 \left[ F\left( M_Z^2, \mu_b^2 \right) - F\left( M_W^2, \mu_b^2 \right) \right] \right\}, \tag{2.29}$$

where

$$F(x,y) \equiv \begin{cases} \frac{x+y}{2} - \frac{xy}{x-y} \ln \frac{x}{y}, & x \neq y \\ 0, & x = y \end{cases},$$
 (2.30)

and  $\alpha$  is the fine-structure constant. The masses of the charged-scalars are denoted by  $m_a$ , and  $\mu_a$  are the masses of the physical neutral scalars, defined in such a way that  $a \leq n$  refers to the pseudoscalars, and a > n are the CP-even fields. Lastly,  $U^{\dagger}$  and  $V^{\dagger}$  are  $n \times n$  and  $2n \times n$  matrices that rotate the charged and neutral components  $(w_k^{\pm} \text{ and } \varphi_k^0 \equiv h_k + iz_k)$  into the physical basis  $(S^{\pm} \text{ and } S^0)$ , respectively, in such a way that the Goldstone bosons are located in the first row,

$$w_k^{\pm} = \sum_{a=1}^n U_{ka} S_a^{\pm}, \qquad \varphi_k^0 = \sum_{b=1}^{2n} V_{kb} S_b^0.$$
 (2.31)

We give the explicit structure of  $S^{\pm}$  and  $S^{0}$  as follows

$$S^{\pm} = \left(\omega^{\pm}, H_1^{\pm}, \dots, H_{n-1}^{\pm}\right)^T, \qquad S^0 = \left(\zeta, A_1, \dots, A_{n-1}, h, H_1, \dots, H_{n-1}\right)^T, \tag{2.32}$$

where  $\omega^{\pm}$  and  $\zeta$  are the charged and neutral unphysical Goldstone bosons, respectively,  $H_k^{\pm}$  is the k-th charged-scalar, and  $A_k$  the k-th pseudoscalar. For the CP-even scalars, h is the lightest scalar usually identified as the SM-like Higgs, and  $H_k$  denotes the k-th physical CP-even scalar. Following the definition of Eq. (2.27), and comparing with Eq. (2.31), we can relate the U and V matrices with the scalar rotation matrices as follows

$$U = \mathcal{O}_C^T, \quad V = \begin{pmatrix} i\mathcal{O}_P^T & \mathcal{O}_S^T \end{pmatrix}, \tag{2.33}$$

where the subscripts C, P, S refer to the charged, pseudoscalar, and scalar sectors respectively. The relevant combinations can be expressed as

$$U^{\dagger}V = \begin{pmatrix} i \mathcal{O}_C \mathcal{O}_P^T & \mathcal{O}_C \mathcal{O}_S^T \end{pmatrix}, \qquad V^{\dagger}V = \begin{pmatrix} \mathbb{1}_{n \times n} & -i \mathcal{O}_P \mathcal{O}_S^T \\ i \mathcal{O}_S \mathcal{O}_P^T & \mathbb{1}_{n \times n} \end{pmatrix}. \tag{2.34}$$

We must note that the last term of Eq. (2.29) vanishes in the limit  $g' \to 0$ , that is,  $M_Z = M_W$ . Therefore, we will focus on the first two terms in Eq. (2.29), and convince ourselves that they also vanish in the custodial limit of Eq. (2.28). Taking advantage of Eq. (2.34), we can rewrite the first two terms of Eq. (2.29) as

$$\alpha T = \frac{g^2}{64\pi^2 M_W^2} \left\{ \sum_{a=2}^n \sum_{b=2}^n \left| \left( i\mathcal{O}_C \mathcal{O}_P^T \right)_{ab} \right|^2 F\left( m_a^2, \mu_b^2 \right) + \sum_{a=2}^n \sum_{b=1}^n \left| \left( \mathcal{O}_C \mathcal{O}_S^T \right)_{ab} \right|^2 F\left( m_a^2, \mu_{n+b}^2 \right) - \sum_{a=2}^n \sum_{b=1}^n \left| \left( -i\mathcal{O}_P \mathcal{O}_S^T \right)_{ab} \right|^2 F\left( \mu_a^2, \mu_{n+b}^2 \right) \right\}.$$
(2.35)

In the custodial limit, we must have  $M_P^2 = M_C^2$ , and thus  $\mathcal{O}_P = \mathcal{O}_C$ , as well as  $m_a^2 = \mu_a^2$  (with a < n). In this way, the second and third terms of Eq. (2.35) cancel out, and  $\mathcal{O}_C \mathcal{O}_P^T = \mathcal{O}_P \mathcal{O}_P^T = \mathbb{1}_{n \times n}$  leads to a zero contribution from the first term, because of Eq. (2.30). We can also see in ref. [178] that, for the case of 2HDMs, the result also holds up to two-loops.

#### 2.1.4 Examples of the Custodial Limit: the 2HDM and Democratic 3HDMs

Having arrived at the condition for the custodial limit of nHDMs to hold, we devote this small section to apply it to the well-known case of 2HDMs to find the usual relation between the quartic parameters commonly found in the literature. Afterwards, we will perform the same computations for the case of our interest in this chapter, which are the two implementations of the democratic 3HDMs.

First, we explicitly demonstrate how Eq. (2.28) manifests itself for the simple case of a 2HDM scalar potential. Consider the 2HDM scalar potential with a softly-broken  $Z_2$  symmetry ( $\phi_1 \to \phi_1, \phi_2 \to -\phi_2$ ), which is commonly used in NFC models [47]:

$$V(\phi_{1}, \phi_{2}) = m_{11}^{2} \phi_{1}^{\dagger} \phi_{1} + m_{22}^{2} \phi_{2}^{\dagger} \phi_{2} - m_{12}^{2} (\phi_{1}^{\dagger} \phi_{2} + \phi_{2}^{\dagger} \phi_{1}) + \frac{\lambda_{1}}{2} (\phi_{1}^{\dagger} \phi_{1})^{2} + \frac{\lambda_{2}}{2} (\phi_{2}^{\dagger} \phi_{2})^{2} + \lambda_{3} (\phi_{1}^{\dagger} \phi_{1}) (\phi_{2}^{\dagger} \phi_{2}) + \lambda_{4} (\phi_{1}^{\dagger} \phi_{2}) (\phi_{2}^{\dagger} \phi_{1}) + \frac{\lambda_{5}}{2} \left\{ (\phi_{1}^{\dagger} \phi_{2})^{2} + (\phi_{2}^{\dagger} \phi_{1})^{2} \right\}.$$
 (2.36)

The charged and pseudoscalar mass matrices which transpire from the above scalar potential are given by

$$M_C^2 = \begin{pmatrix} \frac{m_{12}^2 v_2}{v_1} - \frac{1}{2}\lambda_4 v_2^2 - \frac{1}{2}\lambda_5 v_2^2 & -m_{12}^2 + \frac{1}{2}\lambda_4 v_1 v_2 + \frac{1}{2}\lambda_5 v_1 v_2 \\ -m_{12}^2 + \frac{1}{2}\lambda_4 v_1 v_2 + \frac{1}{2}\lambda_5 v_1 v_2 & \frac{m_{12}^2 v_1}{v_2} - \frac{1}{2}\lambda_4 v_1^2 - \frac{1}{2}\lambda_5 v_1^2 \end{pmatrix},$$
(2.37a)

$$M_P^2 = \begin{pmatrix} \frac{m_{12}^2 v_2}{v_1} - \lambda_5 v_2^2 & -m_{12}^2 + \lambda_5 v_1 v_2 \\ -m_{12}^2 + \lambda_5 v_1 v_2 & \frac{m_{12}^2 v_1}{v_2} - \lambda_5 v_1^2 \end{pmatrix}.$$
 (2.37b)

Thus, imposition of Eq. (2.28) for arbitrary values of the vevs will lead to the following relation

$$\lambda_4 = \lambda_5 \,, \tag{2.38}$$

which agrees with earlier results [168, 169, 176]. In passing, we wish to point out that even if we consider the general (CP-conserving) 2HDM potential [47]

$$V(\phi_{1},\phi_{2}) = m_{11}^{2}\phi_{1}^{\dagger}\phi_{1} + m_{22}^{2}\phi_{2}^{\dagger}\phi_{2} - (m_{12}^{2}\phi_{1}^{\dagger}\phi_{2} + \text{h.c.}) + \frac{\lambda_{1}}{2}(\phi_{1}^{\dagger}\phi_{1})^{2} + \frac{\lambda_{2}}{2}(\phi_{2}^{\dagger}\phi_{2})^{2} + \lambda_{3}(\phi_{1}^{\dagger}\phi_{1})(\phi_{2}^{\dagger}\phi_{2}) + \lambda_{4}(\phi_{1}^{\dagger}\phi_{2})(\phi_{2}^{\dagger}\phi_{1}) + \left\{ \frac{\lambda_{5}}{2}(\phi_{1}^{\dagger}\phi_{2})^{2} + \lambda_{6}(\phi_{1}^{\dagger}\phi_{1})(\phi_{1}^{\dagger}\phi_{2}) + \lambda_{7}(\phi_{2}^{\dagger}\phi_{2})(\phi_{1}^{\dagger}\phi_{2}) + \text{h.c.} \right\}, \quad (2.39)$$

the condition for custodial invariance is still given by Eq. (2.38). The reason for this will be discussed in more detail in Appendix A.2.

Second, to arrive at similar conditions for the democratic 3HDMs, we write down the explicit forms of the scalar potential which follow from the symmetry of Eqs. (2.2) and (2.3). After the computation of the structure of the charged and pseudoscalar mass matrices, impose Eq. (2.28) to extract the implications in terms of the parameters of the scalar potential.

The scalar potential for the  $Z_3$ -symmetric case given by Eq. (2.2) will be given by [179]

$$V_{Z_{3}} = m_{11}^{2}\phi_{1}^{\dagger}\phi_{1} + m_{22}^{2}\phi_{2}^{\dagger}\phi_{2} + m_{33}^{2}\phi_{3}^{\dagger}\phi_{3} - m_{12}^{2}(\phi_{1}^{\dagger}\phi_{2} + \phi_{2}^{\dagger}\phi_{1}) - m_{13}^{2}(\phi_{1}^{\dagger}\phi_{3} + \phi_{3}^{\dagger}\phi_{1}) - m_{23}^{2}(\phi_{2}^{\dagger}\phi_{3} + \phi_{3}^{\dagger}\phi_{2})$$

$$+\lambda_{1}(\phi_{1}^{\dagger}\phi_{1})^{2} + \lambda_{2}(\phi_{2}^{\dagger}\phi_{2})^{2} + \lambda_{3}(\phi_{3}^{\dagger}\phi_{3})^{2} + \lambda_{4}(\phi_{1}^{\dagger}\phi_{1})(\phi_{2}^{\dagger}\phi_{2}) + \lambda_{5}(\phi_{1}^{\dagger}\phi_{1})(\phi_{3}^{\dagger}\phi_{3}) + \lambda_{6}(\phi_{2}^{\dagger}\phi_{2})(\phi_{3}^{\dagger}\phi_{3})$$

$$+\lambda_{7}(\phi_{1}^{\dagger}\phi_{2})(\phi_{2}^{\dagger}\phi_{1}) + \lambda_{8}(\phi_{1}^{\dagger}\phi_{3})(\phi_{3}^{\dagger}\phi_{1}) + \lambda_{9}(\phi_{2}^{\dagger}\phi_{3})(\phi_{3}^{\dagger}\phi_{2}) + \lambda_{10}\left\{(\phi_{1}^{\dagger}\phi_{2})(\phi_{1}^{\dagger}\phi_{3}) + (\phi_{2}^{\dagger}\phi_{1})(\phi_{3}^{\dagger}\phi_{1})\right\}$$

$$+\lambda_{11}\left\{(\phi_{2}^{\dagger}\phi_{1})(\phi_{2}^{\dagger}\phi_{3}) + (\phi_{1}^{\dagger}\phi_{2})(\phi_{3}^{\dagger}\phi_{2})\right\} + \lambda_{12}\left\{(\phi_{3}^{\dagger}\phi_{1})(\phi_{3}^{\dagger}\phi_{2}) + (\phi_{1}^{\dagger}\phi_{3})(\phi_{2}^{\dagger}\phi_{3})\right\},$$

$$(2.40)$$

where soft-breaking terms have also been allowed. The explicit expressions for the elements of the  $3 \times 3$ symmetric mass matrix in the charged-scalar sector are given below<sup>4</sup>

$$(M_C^2)_{11} = \frac{m_{12}^2 v_2}{v_1} + \frac{m_{13}^2 v_3}{v_1} - \lambda_{10} v_2 v_3 - \frac{\lambda_{11} v_2^2 v_3}{2v_1} - \frac{\lambda_{12} v_2 v_3^2}{2v_1} - \frac{\lambda_7 v_2^2}{2} - \frac{\lambda_8 v_3^2}{2}, \qquad (2.41a)$$

$$(M_C^2)_{22} = \frac{m_{12}^2 v_1}{v_2} + \frac{m_{23}^2 v_3}{v_2} - \frac{\lambda_{10} v_1^2 v_3}{2v_2} - \lambda_{11} v_1 v_3 - \frac{\lambda_{12} v_1 v_3^2}{2v_2} - \frac{\lambda_7 v_1^2}{2} - \frac{\lambda_9 v_3^2}{2}, \qquad (2.41b)$$

$$(M_C^2)_{33} = \frac{m_{13}^2 v_1}{v_3} + \frac{m_{23}^2 v_2}{v_3} - \frac{\lambda_{10} v_1^2 v_2}{2v_3} - \frac{\lambda_{11} v_1 v_2^2}{2v_3} - \lambda_{12} v_1 v_2 - \frac{\lambda_8 v_1^2}{2} - \frac{\lambda_9 v_2^2}{2}, \qquad (2.41c)$$

$$(M_C^2)_{33} = \frac{m_{13}^2 v_1}{v_3} + \frac{m_{23}^2 v_2}{v_3} - \frac{\lambda_{10} v_1^2 v_2}{2v_3} - \frac{\lambda_{11} v_1 v_2^2}{2v_3} - \lambda_{12} v_1 v_2 - \frac{\lambda_8 v_1^2}{2} - \frac{\lambda_9 v_2^2}{2}, \qquad (2.41c)$$

$$(M_C^2)_{12} = (M_C^2)_{21} = -m_{12}^2 + \frac{1}{2}\lambda_{10}v_1v_3 + \frac{1}{2}\lambda_{11}v_2v_3 + \frac{1}{2}\lambda_7v_1v_2, \qquad (2.41d)$$

$$(M_C^2)_{13} = (M_C^2)_{31} = -m_{13}^2 + \frac{1}{2}\lambda_{10}v_1v_2 + \frac{1}{2}\lambda_{12}v_2v_3 + \frac{1}{2}\lambda_8v_1v_3, \qquad (2.41e)$$

$$(M_C^2)_{23} = (M_C^2)_{32} = -m_{23}^2 + \frac{1}{2}\lambda_{11}v_1v_2 + \frac{1}{2}\lambda_{12}v_1v_3 + \frac{1}{2}\lambda_9v_2v_3.$$
 (2.41f)

Similarly, for the pseudoscalar mass matrix we have

$$(M_P^2)_{11} = \frac{m_{12}^2 v_2}{v_1} + \frac{m_{13}^2 v_3}{v_1} - 2\lambda_{10} v_2 v_3 - \frac{\lambda_{11} v_2^2 v_3}{2v_1} - \frac{\lambda_{12} v_2 v_3^2}{2v_1}, \qquad (2.42a)$$

 $<sup>^4</sup>$ We have used the minimization conditions to trade  $m_{11}^2,\,m_{22}^2,\,$  and  $m_{33}^2$  in favor of the vevs.

$$(M_P^2)_{22} = \frac{m_{12}^2 v_1}{v_2} + \frac{m_{23}^2 v_3}{v_2} - \frac{\lambda_{10} v_1^2 v_3}{2v_2} - 2\lambda_{11} v_1 v_3 - \frac{\lambda_{12} v_1 v_3^2}{2v_2}, \qquad (2.42b)$$

$$(M_P^2)_{33} = \frac{m_{13}^2 v_1}{v_3} + \frac{m_{23}^2 v_2}{v_3} - \frac{\lambda_{10} v_1^2 v_2}{2v_3} - \frac{\lambda_{11} v_1 v_2^2}{2v_3} - 2\lambda_{12} v_1 v_2, \qquad (2.42c)$$

$$(M_P^2)_{12} = (M_P^2)_{21} = -m_{12}^2 + \lambda_{10}v_1v_3 + \lambda_{11}v_2v_3 - \frac{\lambda_{12}v_3^2}{2},$$
 (2.42d)

$$(M_P^2)_{13} = (M_P^2)_{31} = -m_{13}^2 + \lambda_{10}v_1v_2 + \lambda_{12}v_2v_3 - \frac{\lambda_{11}v_2^2}{2},$$
 (2.42e)

$$(M_P^2)_{23} = (M_P^2)_{32} = -m_{23}^2 + \lambda_{11}v_1v_2 + \lambda_{12}v_1v_3 - \frac{\lambda_{10}v_1^2}{2}.$$
 (2.42f)

For Eq. (2.28) to hold for any arbitrary values of the vevs, we should have

$$\lambda_7 = \lambda_8 = \lambda_9 = \lambda_{10} = \lambda_{11} = \lambda_{12} = 0, \qquad (2.43)$$

which should be read as the conditions for custodial invariance in a  $\mathbb{Z}_3$ -symmetric 3HDM potential.

Focusing now on the  $Z_2 \times Z_2$ -symmetric scalar potential of Eq. (2.3), the scalar potential takes the form [180]

$$V_{Z_{2}\times Z_{2}} = m_{11}^{2}\phi_{1}^{\dagger}\phi_{1} + m_{22}^{2}\phi_{2}^{\dagger}\phi_{2} + m_{33}^{2}\phi_{3}^{\dagger}\phi_{3}$$

$$-m_{12}^{2}(\phi_{1}^{\dagger}\phi_{2} + \phi_{2}^{\dagger}\phi_{1}) - m_{13}^{2}(\phi_{1}^{\dagger}\phi_{3} + \phi_{3}^{\dagger}\phi_{1}) - m_{23}^{2}(\phi_{2}^{\dagger}\phi_{3} + \phi_{3}^{\dagger}\phi_{2})$$

$$+\lambda_{1}(\phi_{1}^{\dagger}\phi_{1})^{2} + \lambda_{2}(\phi_{2}^{\dagger}\phi_{2})^{2} + \lambda_{3}(\phi_{3}^{\dagger}\phi_{3})^{2} + \lambda_{4}(\phi_{1}^{\dagger}\phi_{1})(\phi_{2}^{\dagger}\phi_{2}) + \lambda_{5}(\phi_{1}^{\dagger}\phi_{1})(\phi_{3}^{\dagger}\phi_{3})$$

$$+\lambda_{6}(\phi_{2}^{\dagger}\phi_{2})(\phi_{3}^{\dagger}\phi_{3}) + \lambda_{7}(\phi_{1}^{\dagger}\phi_{2})(\phi_{2}^{\dagger}\phi_{1}) + \lambda_{8}(\phi_{1}^{\dagger}\phi_{3})(\phi_{3}^{\dagger}\phi_{1}) + \lambda_{9}(\phi_{2}^{\dagger}\phi_{3})(\phi_{3}^{\dagger}\phi_{2})$$

$$+\lambda_{10}\left\{(\phi_{1}^{\dagger}\phi_{2})^{2} + (\phi_{2}^{\dagger}\phi_{1})^{2}\right\} + \lambda_{11}\left\{(\phi_{1}^{\dagger}\phi_{3})^{2} + (\phi_{3}^{\dagger}\phi_{1})^{2}\right\} + \lambda_{12}\left\{(\phi_{2}^{\dagger}\phi_{3})^{2} + (\phi_{3}^{\dagger}\phi_{2})^{2}\right\}, (2.44)$$

where, again, we have allowed terms that softly-break the symmetry. The elements of the charged-scalar mass matrix are given below:

$$(M_C^2)_{11} = \frac{m_{12}^2 v_2}{v_1} + \frac{m_{13}^2 v_3}{v_1} - \lambda_{10} v_2^2 - \frac{\lambda_7 v_2^2}{2} - \lambda_{11} v_3^2 - \frac{\lambda_8 v_3^2}{2}, \qquad (2.45a)$$

$$(M_C^2)_{22} = \frac{m_{12}^2 v_1}{v_2} + \frac{m_{23}^2 v_3}{v_2} - \lambda_{10} v_1^2 - \frac{\lambda_7 v_1^2}{2} - \lambda_{12} v_3^2 - \frac{\lambda_9 v_3^2}{2}, \qquad (2.45b)$$

$$(M_C^2)_{33} = \frac{m_{13}^2 v_1}{v_3} + \frac{m_{23}^2 v_2}{v_3} - \lambda_{11} v_1^2 - \frac{\lambda_8 v_1^2}{2} - \lambda_{12} v_2^2 - \frac{\lambda_9 v_2^2}{2}, \qquad (2.45c)$$

$$(M_C^2)_{12} = (M_C^2)_{21} = -m_{12}^2 + \lambda_{10}v_1v_2 + \frac{1}{2}\lambda_7v_1v_2,$$
 (2.45d)

$$(M_C^2)_{13} = (M_C^2)_{31} = -m_{13}^2 + \lambda_{11}v_1v_3 + \frac{1}{2}\lambda_8v_1v_3,$$
 (2.45e)

$$(M_C^2)_{23} = (M_C^2)_{32} = -m_{23}^2 + \lambda_{12}v_2v_3 + \frac{1}{2}\lambda_9v_2v_3.$$
 (2.45f)

For the case of the pseudoscalar mass matrix elements, we find

$$(M_P^2)_{11} = \frac{m_{12}^2 v_2}{v_1} + \frac{m_{13}^2 v_3}{v_1} - 2\lambda_{10}v_2^2 - 2\lambda_{11}v_3^2, \qquad (2.46a)$$

$$(M_P^2)_{22} = \frac{m_{12}^2 v_1}{v_2} + \frac{m_{23}^3 v_3}{v_2} - 2\lambda_{10}v_1^2 - 2\lambda_{12}v_3^2, \qquad (2.46b)$$

$$(M_P^2)_{33} = \frac{m_{13}^2 v_1}{v_3} + \frac{m_{23}^2 v_2}{v_3} - 2\lambda_{11}v_1^2 - 2\lambda_{12}v_2^2, \qquad (2.46c)$$

$$(M_P^2)_{12} = (M_P^2)_{21} = -m_{12}^2 + 2\lambda_{10}v_1v_2,$$
 (2.46d)

$$(M_P^2)_{13} = (M_P^2)_{31} = -m_{13}^2 + 2\lambda_{11}v_1v_3,$$
 (2.46e)

$$(M_P^2)_{23} = (M_P^2)_{32} = -m_{23}^2 + 2\lambda_{12}v_2v_3.$$
 (2.46f)

Following the reasoning presented for the  $Z_3$  case, the conditions for custodial invariance can be found using Eq. (2.28), which read

$$\lambda_7 = 2\lambda_{10}, \ \lambda_8 = 2\lambda_{11}, \ \lambda_9 = 2\lambda_{12}.$$
 (2.47)

# 2.2 Prospects for Light Charged-Scalars in Democratic 3HDMs

Now that we have seen the conditions to impose the custodial limit on democratic 3HDMs, and can be safeguarded against the nonstandard contributions to the T-parameter, we turn our analysis to the model's phenomenology. The additional (pseudo) scalar and charged-Higgs bosons can give rise to interesting signatures at the LHC as well as at various flavor physics experiments. Consistency with the strong constraints from the LHC and flavor observables often pushes the charged-Higgs boson mass in 2HDM towards the heavier end of the spectrum. It has been observed that a combination of flavor physics measurements can exclude charged-Higgs masses below  $\mathcal{O}(600~{\rm GeV})$  in 2HDM of Type-II [181],<sup>5</sup> where up and down-type quarks obtain their masses from two different Higgs doublets. This bound on the charged-scalar masses can be somewhat relaxed in Type-I 2HDM where a single Higgs doublet is responsible for generating masses of the up and down type quarks [184]. This is because in Type-I 2HDM all the fermionic couplings of the charged-scalar are proportional to  $\cot \beta$ , with  $\tan \beta$  being the ratio of the two vevs, as conventionally defined in 2HDMs. Therefore, the constraints on the nonstandard scalars can be easily evaded by choosing  $\tan \beta \gg 1$ . In this section, we aim to investigate the possibility of allowing lighter nonstandard scalars without compromising the essential feature of Type-II 2HDM *i.e.* two different doublets give masses to up- and down-type quarks.

To this end, we focus on the case unique to models with more than two Higgs doublets: democratic 3HDMs. As in the 2HDM case, it is possible to achieve an alignment limit corresponding to a physical scalar resembling the properties of 125 GeV SM-like Higgs boson [67, 185]. In contrast to 2HDM, the scalar spectrum is much broader here, leading to significant modifications in the flavour-changing neutral and charged current processes when compared to 2HDM. Here, we explore the phenomenological aspects of the alignment limit in democratic 3HDMs with an emphasis on the effects of flavour physics constraints on its parameter space, and show that these are notably relaxed compared to those in the Type-II 2HDM. Such a relaxation of constraints transpires from the presence of an additional suppression in the couplings of the charged-Higgs bosons in the model compared to Type-II 2HDM.

<sup>&</sup>lt;sup>5</sup>This bound has now increased to  $\sim \mathcal{O}(800)$  GeV [182], although lower values may still be viable [183].

#### 2.2.1 Scalar Sector

After the EWSB, the scalar doublets can be decomposed in terms of the component fields as in Eq. (2.20), where  $v_k$  denotes the vev of the field  $\phi_k$  ( $\langle \phi_k \rangle = v_k/\sqrt{2}$ ). For notational convenience, the vevs are expressed as

$$v_1 = v \cos \beta_1 \cos \beta_2 , \quad v_2 = v \sin \beta_1 \cos \beta_2 , \quad v_3 = v \sin \beta_2 ,$$
 (2.48)

where  $v = \sqrt{v_1^2 + v_2^2 + v_3^2}$  is the usual EW vev. The inclusion of three scalar doublets will give rise to four charged-scalar particles,  $H_{1,2}^{\pm}$ , three CP-even neutral ones  $h, H_{1,2}$ , as well as two CP-odd neutral particles  $A_{1,2}$ , where the remaining fields are the usual Goldstone bosons  $w^{\pm}, \zeta$ . These physical particles can be obtained by rotating the fields onto the mass basis. For the charged and pseudoscalar sectors, we can obtain the physical scalars by performing the following  $3 \times 3$  rotations,

$$\begin{pmatrix} w^{\pm} \\ H_1^{\pm} \\ H_2^{\pm} \end{pmatrix} = \mathcal{O}_{\gamma_2} \mathcal{O}_{\beta} \begin{pmatrix} w_1^{\pm} \\ w_2^{\pm} \\ w_3^{\pm} \end{pmatrix}, \qquad \begin{pmatrix} \zeta \\ A_1 \\ A_2 \end{pmatrix} = \mathcal{O}_{\gamma_1} \mathcal{O}_{\beta} \begin{pmatrix} z_1 \\ z_2 \\ z_3 \end{pmatrix}, \qquad (2.49)$$

where, the rotation matrices are defined as

$$\mathcal{O}_{\gamma_1} = \begin{pmatrix} 1 & 0 & 0 \\ 0 & \cos \gamma_1 & -\sin \gamma_1 \\ 0 & \sin \gamma_1 & \cos \gamma_1 \end{pmatrix}, \quad \mathcal{O}_{\gamma_2} = \begin{pmatrix} 1 & 0 & 0 \\ 0 & \cos \gamma_2 & -\sin \gamma_2 \\ 0 & \sin \gamma_2 & \cos \gamma_2 \end{pmatrix}, \tag{2.50}$$

and

$$\mathcal{O}_{\beta} = \begin{pmatrix} \cos \beta_2 \cos \beta_1 & \cos \beta_2 \sin \beta_1 & \sin \beta_2 \\ -\sin \beta_1 & \cos \beta_1 & 0 \\ -\cos \beta_1 \sin \beta_2 & -\sin \beta_1 \sin \beta_2 & \cos \beta_2 \end{pmatrix}. \tag{2.51}$$

For the CP-even sector, we can obtain the physical mass basis through

$$\begin{pmatrix} h \\ H_1 \\ H_2 \end{pmatrix} = \mathcal{O}_{\alpha} \begin{pmatrix} h_1 \\ h_2 \\ h_3 \end{pmatrix} \tag{2.52}$$

where

$$\mathcal{O}_{\alpha} = \mathcal{R}_3 \cdot \mathcal{R}_2 \cdot \mathcal{R}_1 \,, \tag{2.53a}$$

with

$$\mathcal{R}_{1} = \begin{pmatrix}
\cos \alpha_{1} & \sin \alpha_{1} & 0 \\
-\sin \alpha_{1} & \cos \alpha_{1} & 0 \\
0 & 0 & 1
\end{pmatrix}, \quad \mathcal{R}_{2} = \begin{pmatrix}
\cos \alpha_{2} & 0 & \sin \alpha_{2} \\
0 & 1 & 0 \\
-\sin \alpha_{2} & 0 & \cos \alpha_{2}
\end{pmatrix}, \quad \mathcal{R}_{3} = \begin{pmatrix}
1 & 0 & 0 \\
0 & \cos \alpha_{3} & \sin \alpha_{3} \\
0 & -\sin \alpha_{3} & \cos \alpha_{3}
\end{pmatrix}.$$
(2.53b)

Given the simplification of the scalar sector we will employ, we merely used this section to introduce notation, and do not dwell on the specific details of the scalar potential. A more detailed analysis of the scalar sector, including the expressions for the scalar potential parameters in terms of the physical parameters can be found in ref. [164].

The existence of nonstandard neutral CP-even scalars in nHDMs leads, in general, to a deviation of the couplings of the physical scalar h from the respective SM predictions. However, the data obtained from the LHC runs shows a good agreement of the experimental data to the SM prediction for the Higgs signal strengths [186, 187]. This motivates us to work in the alignment limit which is a set of conditions such that the lightest CP-even scalar mimics the SM-Higgs in its tree-level couplings, automatically respecting the agreement between the experimental data and the corresponding SM predictions for the Higgs signal strengths. For our democratic 3HDMs, the conditions for alignment are given by [67]

$$\alpha_1 = \beta_1, \qquad \alpha_2 = \beta_2. \tag{2.54}$$

As more data accumulate in the future runs of the High-Luminosity LHC (HL-LHC), the possibility of deviating from the alignment limit will become increasingly constrained, if no BSM signals are detected.

## 2.2.2 Quark Yukawa Sector

The quark Yukawa Lagrangian of the democratic 3HDMs can be written as

$$\mathcal{L} = -Y_d \overline{Q}_L \phi_2 n_R - Y_u \overline{Q}_L \widetilde{\phi}_3 p_R + \text{h.c.}, \qquad (2.55)$$

following Eq. (2.1). After EWSB, the mass matrices of the down and up-type quarks are given by

$$M_d = Y_d \frac{v_2}{\sqrt{2}} \; ; \quad M_u = Y_u \frac{v_3}{\sqrt{2}} \; .$$
 (2.56)

As usual, we can redefine the quark fields to rotate into the mass basis through

$$d_L = U_d n_L, \quad d_R = V_d n_R, \quad u_L = U_u p_L, \quad u_R = V_u p_R,$$
 (2.57)

which, in turn, will diagonalize the mass matrices through the bi-unitary transformation

$$D_d = U_d^{\dagger} M_d V_d = \text{diag}(m_d, m_s, m_b),$$
 (2.58a)

$$D_u = U_u^{\dagger} M_u V_u = \text{diag}(m_u, m_c, m_t). \tag{2.58b}$$

Similar to the SM, the CKM matrix is defined as  $V = U_u^{\dagger} U_d$ . As intended, our model does not have any FCNC at the tree-level, and the Higgs signal strengths will also be compatible with the corresponding SM expectations in the alignment limit. However, the presence of charged-scalars brings forth new channels for loop contributions to several flavour observables such as neutral meson oscillations and  $b \to s\gamma$ . In fact, these processes are quite restricted from experiments, and thus are usually used to place lower bounds on the nonstandard scalar masses, as their contributions must be kept in check. Thus, it becomes important to study the charged-scalar couplings to the fermions, as these will govern the vertices responsible for these processes at the one-loop level.

Given its importance, we focus on the original quark Yukawa Lagrangian containing the charged-Higgs couplings,

$$\mathcal{L}_{c}^{Q} = -Y_{d} \,\overline{p}_{L} \, n_{R} \, w_{2}^{+} + Y_{u}^{\dagger} \,\overline{p}_{R} \, n_{L} \, w_{3}^{+} + \text{h.c.}$$

$$= \frac{\sqrt{2}}{v} \overline{u} \left[ -\frac{1}{s_{\beta_{1}} c_{\beta_{2}}} w_{2}^{+} (V \, D_{d}) P_{R} + \frac{1}{s_{\beta_{2}}} w_{3}^{+} (D_{u} \, V) P_{L} \right] d + \text{h.c.},$$
(2.59a)

 $= \frac{\sqrt{2} \overline{u}}{v} \left[ -\frac{1}{s_{\beta_1} c_{\beta_2}} w_2^+(V D_d) P_R + \frac{1}{s_{\beta_2}} w_3^+(D_u V) P_L \right] d + \text{h.c.}, \qquad (2.59b)$ ep, we have rotated into the quark mass basis. Our goal is to arrive at couplings

where, in the last step, we have rotated into the quark mass basis. Our goal is to arrive at couplings among the physical fields, and so we further rewrite the Lagrangian in the scalar mass basis. Using  $X = \mathcal{O}_{\beta}^T \mathcal{O}_{\gamma_2}^T$ , Eq. (2.59b) becomes

$$\mathcal{L}_{c}^{Q} = \frac{\sqrt{2}}{v} H_{1}^{+} \overline{u} \left[ \frac{X_{32}}{s_{\beta_{2}}} (D_{u} V) P_{L} - \frac{X_{22}}{s_{\beta_{1}} c_{\beta_{2}}} (V D_{d}) P_{R} \right] d 
+ \frac{\sqrt{2}}{v} H_{2}^{+} \overline{u} \left[ \frac{X_{33}}{s_{\beta_{2}}} (D_{u} V) P_{L} - \frac{X_{23}}{s_{\beta_{1}} c_{\beta_{2}}} (V D_{d}) P_{R} \right] d + \text{h.c.},$$
(2.60)

which describes the vertices between the physical charged-scalars to the physical quarks. The same process can be repeated to obtain the leptonic couplings:

$$\mathcal{L}_{c}^{\ell} = -\frac{\sqrt{2}}{v} H_{1}^{+} \, \overline{\nu} \frac{X_{12}}{c_{\beta_{1}} c_{\beta_{2}}} D_{\ell} \, P_{R} \, \ell - \frac{\sqrt{2}}{v} H_{2}^{+} \, \overline{\nu} \frac{X_{13}}{c_{\beta_{1}} c_{\beta_{2}}} D_{\ell} \, P_{R} \, \ell + \text{h.c.} \,, \tag{2.61}$$

where,  $\ell \equiv (e, \mu, \tau)^T$ ,  $\nu \equiv (\nu_e, \nu_\mu, \nu_\tau)^T$  and  $D_\ell = \text{diag}(m_e, m_\mu, m_\tau)$ . In the following, we will focus mostly on the consequences of quark flavour observables. Hence, to better grasp the model's implications, it is helpful to substitute the  $X_{ij}$  elements explicitly following Eqs. (2.50) and (2.51), recasting the charged-Higgs couplings to quarks as

$$\mathcal{L}_{H_{1}^{\pm}}^{Q} = -\frac{\sqrt{2}}{v} H_{1}^{+} \overline{u} \left[ \cot \beta_{2} \sin \gamma_{2} (D_{u} V) P_{L} + \tan \beta_{2} \left( \frac{\cot \beta_{1} \cos \gamma_{2}}{\sin \beta_{2}} + \sin \gamma_{2} \right) (V D_{d}) P_{R} \right] d + \text{h.c.}, (2.62a)$$

$$\mathcal{L}_{H_{2}^{\pm}}^{Q} = -\frac{\sqrt{2}}{v} H_{2}^{+} \overline{u} \left[ \cot \beta_{2} \cos \gamma_{2} (D_{u} V) P_{L} - \tan \beta_{2} \left( \frac{\cot \beta_{1} \sin \gamma_{2}}{\sin \beta_{2}} - \cos \gamma_{2} \right) (V D_{d}) P_{R} \right] d + \text{h.c.}, (2.62b)$$

One noteworthy observation is the similarity between the democratic 3HDMs and the type-II 2HDM. In fact, both are NFC models, where the difference lies in the fact that, in the democratic 3HDMs, the lepton Yukawa couplings have a dedicated doublet, whereas in the type-II 2HDM the leptons share the doublet responsible for the down type quark masses. The resemblance can be made more explicit by noting that due to the charge assignments of the scalar doublets,  $\phi_1$  is responsible for the lepton masses,

which are generally much lower than the quark masses. Combining this with the relation between each individual vev and the EWSB seen in Eq. (2.48), it seems reasonable to assume  $v_1 \ll v_2, v_3$ , which is achieved by taking large values of  $\tan \beta_1$ , while still remaining in a perturbative regime for the  $\tau$ -Yukawa coupling. In this regime, where  $\cot \beta_1 \ll 1$ , the  $\cot \beta_1$  dependency of the charged-Higgs couplings of Eqs. (2.62a) and (2.62b) can be neglected, and the couplings become similar to those of the type-II 2HDM, relaxed by either  $\cos \gamma_2$  or  $\sin \gamma_2$ , which are always less than one. Indeed, by comparing with the corresponding couplings in the type-II 2HDM [47],

$$\mathcal{L}_{H^{\pm}}^{\text{2HDM-II}} = \frac{\sqrt{2}H^{+}}{v} \left[\cot\beta \,\overline{u}_{R} \left(D_{u} V\right) d_{L} + \tan\beta \,\overline{u}_{L} \left(V D_{d}\right) d_{R}\right] + \text{h.c.},$$
(2.63)

we can identify  $\tan \beta$  of 2HDM-II with  $\tan \beta_2$  of democratic 3HDMs, since both control the ratio  $v_u/v_d$ , where  $v_{u(d)}$  are the vevs of the scalars that couple to the up (down) quarks, respectively. If we further consider a scenario where either  $H_1^{\pm}$  or  $H_2^{\pm}$  is relatively heavy ( $\gtrsim 5$  TeV), while keeping the other relatively light ( $\lesssim 1$  TeV), then the heavy particle decouples and its contribution will be negligible, and our effective theory becomes similar to a type-II 2HDM scenario. The striking difference is that while one of the scalars is decoupled, the effective theory still retains some consequences of the full theory. In order to exemplify, we consider a scenario where  $H_2^{\pm}$  is decoupled and  $\tan \beta_1 \gg 1$ . In this case the  $H_1^{\pm}$  couplings of Eq. (2.62a) can be approximated as:

$$\mathcal{L}_{H_{1}^{\pm}}^{3\text{HDM}} \approx -\sin\gamma_{2} \cdot \frac{\sqrt{2}H_{1}^{+}}{v} \left[\cot\beta_{2}\,\overline{u}_{R}\left(D_{u}\,V\right)d_{L} + \tan\beta_{2}\,\overline{u}_{L}\left(V\,D_{d}\right)d_{R}\right] + \text{h.c.}$$

$$(2.64)$$

Comparing with Eq. (2.63), we notice the remarkable similarity with the type-II 2HDM except for the fact that the couplings are reduced in strength by a factor of  $\sin \gamma_2$ . This will play an important role in diluting the constraints from flavour data compared to those in the type-II 2HDM, which we will discuss next.

# 2.2.3 Constraints from Flavour Data

Since compliance with flavour data is continuously pushing the lower bound on the mass of the charged-Higgs of the type-II 2HDM upwards, the relaxation due to  $\gamma_2$  in this effective 2HDM can easily justify lower masses for new charged-particles, while still remaining within the experimental limits for the NP contributions to the flavour processes.

In order to make the discussion concrete, we analyze the resulting bounds coming from flavour data. We restrict ourselves to the analysis of the NP contributions to the radiative decay  $b \to s\gamma$ , as well as the bounds coming from the B meson oscillations,  $\Delta M_{B_{s,d}}$ .<sup>6</sup> We make use of the flavourKit [188] functionalities within SPheno [189, 190], compiled by SARAH [191], explicitly retaining contributions up to one-loop only. In order to gain some qualitative insights into the processes and phenomenologies at hand, we refer the reader to Appendix A.3, where we provide analytic expressions for the relevant processes. It is, however, easy to note that in models with no tree-level FCNCs, the only one-loop NP

<sup>&</sup>lt;sup>6</sup>The constraints from  $\Delta M_K$  are much weaker.

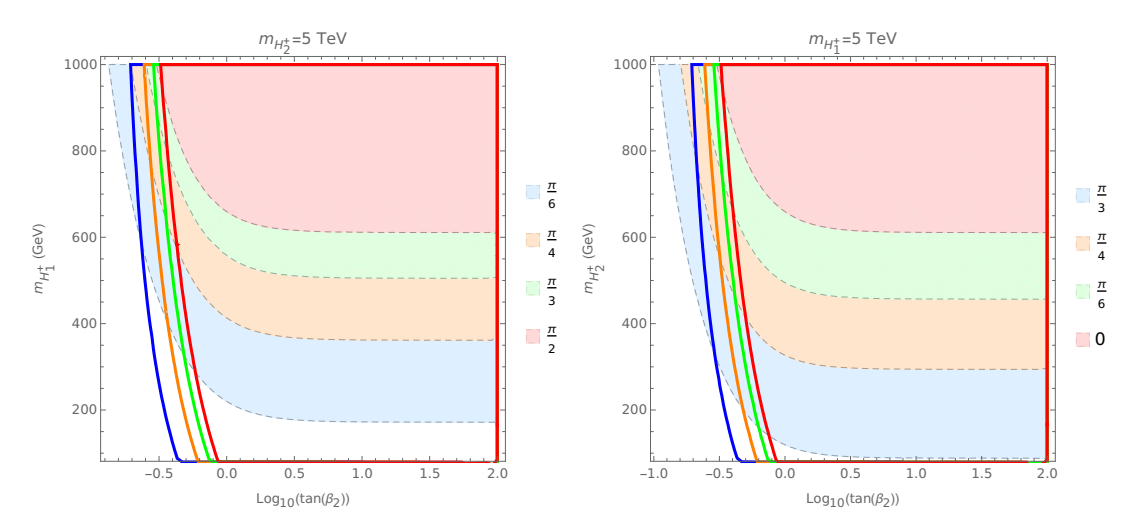


Figure 2.1: The experimentally allowed regions for the  $b\to s\gamma$  branching ratio (colored regions), as well as the boundaries placed by the neutral meson oscillations  $\Delta M_{B_s}$  and  $\Delta M_{B_d}$ , shown by the solid lines. The allowed region for the meson oscillations lies within the boundaries. The color labels denote the value of  $\gamma_2$  used in the analysis. The results are shown in the  $\tan\beta_2$  vs the lighter charged-Higgs mass plane. Left:  $m_{H_2^+}=5$  TeV,  $\tan\beta_1=10,\ \gamma_2=\{\pi/6,\pi/4,\pi/3,\pi/2\}$ . The 2HDM-II limiting case is  $\gamma_2=\pi/2$ . Right:  $m_{H_1^+}=5$  TeV,  $\tan\beta_1=10,\ \gamma_2=\{\pi/3,\pi/4,\pi/6,0\}$ . The 2HDM-II limiting case is  $\gamma_2=0$ . Notice the different arrangement of  $\gamma_2$  values due to the difference between the trigonometric functions of Eqs. (2.62a) and (2.62b).

contributions to both  $b \to s\gamma$  as well as  $\Delta M_{B_{s,d}}$  will come from the charged-Higgs couplings. Therefore, these observables will be governed by a set of five parameters, namely,  $(\tan \beta_1, \tan \beta_2, \gamma_2, m_{H_1^+}, m_{H_2^+})$ .

As we mentioned earlier, democratic 3HDMs where one charged-Higgs is decoupled from EW scale dynamics may become a relaxed type-II 2HDM effective scenario. Namely, a remnant of the full theory survives as a damping of the usual type-II 2HDM charged-scalar couplings, which will in turn result in a relaxation of the bounds which are found for the type-II 2HDM. As such, we initially focus on this case where one of the charged-scalars is decoupled, featuring the relaxation of the bounds.

Our point is clearly exemplified in Fig. 2.1 where we note that the type-II 2HDM bounds coincide with the more restrictive case of these models' limit ( $\gamma_2 = \pi/2$  for the bounds on  $H_1^{\pm}$ , and  $\gamma_2 = 0$  for  $H_2^{\pm}$ ). As we can see, for our benchmark of  $\tan \beta_1 = 10$ , the constraints on the charged-scalar masses are, at worst, comparable to the corresponding bounds in type-II 2HDM for appropriate values of  $\gamma_2$ . But the important point is that by changing the values of  $\gamma_2$ , the bounds can be considerably diluted. Even while keeping away from the extremal cases, the bounds can be easily relaxed by a factor of 2, by taking  $\gamma_2 = \pi/4$ , as clearly seen in the plots. From Fig. 2.1 we also note that there is an asymmetry in the bounds on  $H_1^{\pm}$  and  $H_2^{\pm}$  when we are away from the type-II 2HDM limit. This feature can be attributed to the  $\tan \beta_1$  dependency of the charged-Higgs couplings. Moreover, considering the particular nature of the  $\tan \beta_2$  dependence of both the  $b \to s \gamma$  and  $\Delta M_{B_{s,d}}$  bounds, we see that for a intermediate range  $2 \lesssim \tan \beta_2 \lesssim 30$ , the bounds on the charged-Higgs masses are practically independent of  $\tan \beta_2$ . Thus, by choosing  $\tan \beta_2$  in this range, we can lift the assumption of a decoupled charged-Higgs, and instead analyze the interplay between both contributions to the flavour data, placing the bounds on the  $m_{H_1^+}$ - $m_{H_2^+}$  plane. The results can be seen in Fig. 2.2, where we show the region compatible with the  $b \to s \gamma$  constraints, on the charged-Higgs mass plane, while taking  $\tan \beta_2 = 2$  as a benchmark. We have

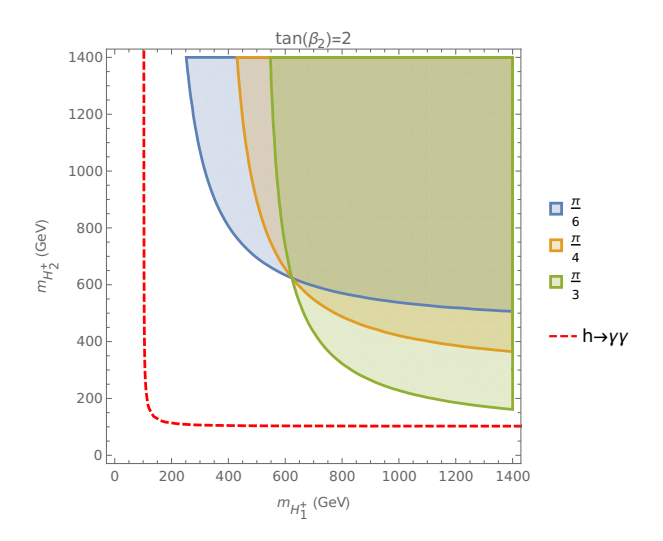


Figure 2.2: The experimentally allowed regions at 95% C.L. from the  $b \to s \gamma$  branching ratio (colored regions), where the region of interest is already in agreement with  $\Delta M_{B_s}$  and  $\Delta M_{B_d}$ . The color labels denote the values of  $\gamma_2$  used in the analysis. The results are shown in the  $m_{H_1}^+$ - $m_{H_2}^+$  plane, and  $\tan \beta_1 = 10$ ,  $\tan \beta_2 = 2$ ,  $\gamma_2 = \{\pi/6, \pi/4, \pi/3\}$ . In dashed line we display the  $h \to \gamma \gamma$  bounds studied below where we set  $m_{H_i}^+ = m_{H_i} = m_{A_i}$ , i = 1, 2. The allowed region at 95% C.L. from the  $h \to \gamma \gamma$  constraint lies above the dashed line.

checked explicitly that the  $\Delta M_{B_{s,d}}$  constraints are also satisfied on the region of interest of Fig. 2.2, *i.e.*, they do not impose additional restrictions in the  $m_{H_1^+}$ - $m_{H_2^+}$  plane. The intersection point between all the different values of  $\gamma_2$  coincides with the type-II 2HDM bound on its charged-Higgs mass. Evidently, considerably light charged-scalars with masses as low as  $\mathcal{O}$  (200 GeV), can be allowed from flavour data by taking the other charged-scalar to be heavier, while still keeping away from extreme values of  $\gamma_2$ .

Now that we have established that relatively light charged-scalars can successfully pass through the stringent constraints imposed by the flavour data, it will be interesting if we can say something about the masses of the neutral nonstandard scalars in relation to those of the charged-scalars. This is where the constraints from the electroweak  $\rho$ -parameter become useful. Following the earlier discussion on the custodial symmetry, the neutral scalars are expected to have masses such that the impact of NP on the  $\rho$ -parameter is minimized. This can be easily achieved in the democratic 3HDMs by making use of Eq. (2.28), or through the explicit results on the quartic couplings given in Section 2.1.4. In this way, we can be sure that the  $\rho$ -parameter measurements will not pose a problem for the scalar spectrum. Nonetheless, our present goal is not to fully explore the available parametric space, but rather to showcase that a lighter scalar spectrum can be accommodated. As such, we take an simplistic approach and further take the nonstandard CP-even neutral scalars to be tier-wise degenerate with the charged and CP-odd neutral scalars:  $m_{H_1^+} \approx m_{H_1} \approx m_{A_1} = M_1$  (say) and  $m_{H_2^+} \approx m_{H_2} \approx m_{A_2} = M_2$  (say). Under this assumption, the scalar spectrum conveniently breaks down into two degenerate tiers of nonstandard masses. This spectrum of masses and mixings can be easily achieved with a simplified scalar potential of the following form, which has an enhanced symmetry in its quartic part [176]:

$$V = m_{11}^{2}(\phi_{1}^{\dagger}\phi_{1}) + m_{22}^{2}(\phi_{2}^{\dagger}\phi_{2}) + m_{33}^{2}(\phi_{3}^{\dagger}\phi_{3}) - \left(m_{12}^{2}(\phi_{1}^{\dagger}\phi_{2}) + m_{23}^{2}(\phi_{2}^{\dagger}\phi_{3}) + m_{13}^{2}(\phi_{1}^{\dagger}\phi_{3}) + \text{h.c.}\right) + \lambda(\phi_{1}^{\dagger}\phi_{1} + \phi_{2}^{\dagger}\phi_{2} + \phi_{3}^{\dagger}\phi_{3})^{2}.$$

$$(2.65)$$

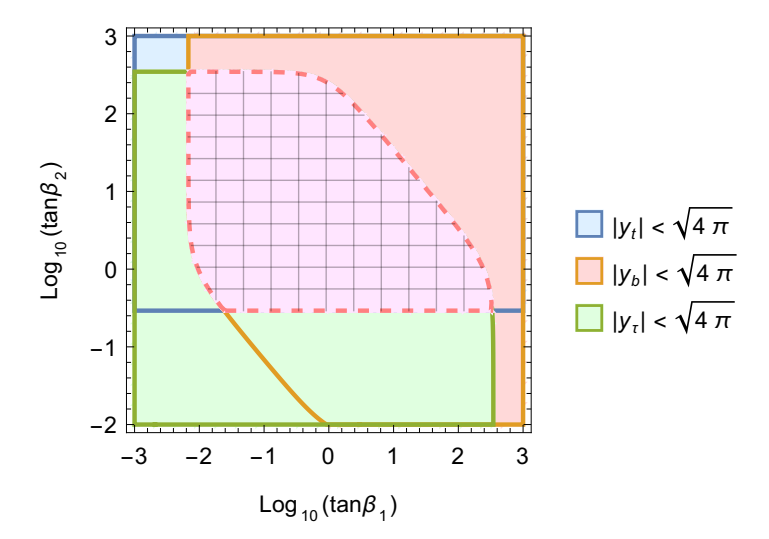


Figure 2.3: The allowed regions from the perturbativity conditions of the Yukawa couplings. The individual color labels denote the regions allowed from the top, bottom and  $\tau$  Yukawa couplings and the hatched region represents the combined perturbative regime.

In the above potential there are seven parameters which can be traded in favor of the seven physical parameters,  $(v, \beta_1, \beta_2, m_h, M_1, M_2, \alpha)$ . At this point, it is worthwhile to remark that the potential of Eq. (2.65) contains only one quartic parameter,<sup>7</sup>  $\lambda$ , and thus we can easily see that it is manifestly compatible with the unitarity and vacuum stability constraints.<sup>8</sup>

Next, we extract the top, bottom, and  $\tau$  Yukawa couplings as

$$y_t = \frac{\sqrt{2} m_t}{v \sin \beta_2}, \quad y_b = \frac{\sqrt{2} m_b}{v \sin \beta_1 \cos \beta_2}, \quad y_\tau = \frac{\sqrt{2} m_\tau}{v \cos \beta_1 \cos \beta_2},$$
 (2.66)

which follow from our convention that  $\phi_3$ ,  $\phi_2$ , and  $\phi_1$  couple to up-type quarks, down-type quarks, and charged-leptons respectively. For the perturbativity of Yukawa couplings, we should have  $|y_t|, |y_b|, |y_\tau| < \sqrt{4\pi}$ . The resulting constraint from perturbativity has been displayed in Fig. 2.3. Throughout this chapter, we use values of  $\tan \beta_{1,2}$  which are consistent with this perturbative region.

At this point one might naturally wonder whether such light charged-scalars would leave observable imprints in loop induced Higgs decays such as  $h \to \gamma \gamma$ . After the 13 TeV run of the LHC, updated constraints on the Higgs to diphoton signal strength has been reported by both the ATLAS [192] and CMS [193] collaborations at 139 fb<sup>-1</sup> luminosity. It is thus important that we check whether such light charged-scalars can negotiate the bound arising from the measurement of the Higgs to diphoton signal strength. To do that, we need to calculate the  $hH_i^+H_i^-$  couplings which, for the potential of Eq. (2.65) are given below:

$$g_{hH_{i}^{+}H_{i}^{-}} = -\frac{m_{h}^{2}}{v}, \quad (i = 1, 2). \tag{2.67}$$

<sup>&</sup>lt;sup>7</sup>This potential should be taken as a simplification for the underlying analysis. Indeed, the scalar potential should be invariant under some subgroup of SU(3), and thus have at least two different quartic couplings. Nonetheless, we take this limit as a proof-of-concept, and argue that there should be a parametric region (even if only neighbouring) which does not alter significantly the results.

<sup>&</sup>lt;sup>8</sup>For more general analysis of unitarity and boundedness from below conditions for this model, please see Ref. [166].

Using this, we can easily write down the expression for the diphoton signal strength as follows:

$$\mu_{\gamma\gamma} = \frac{|F_W(\tau_W) + \frac{4}{3}F_t(\tau_t) + \sum_{i=1}^2 \kappa_i F_{i+}(\tau_{i+})|^2}{|F_W(\tau_W) + \frac{4}{3}F_t(\tau_t)|^2},$$
(2.68)

where,  $\kappa_i = -m_h^2/2m_{H_i^+}^2$ ,  $\tau_x = (2m_x/m_h)^2$ ,  $\left(x = W, t, H_i^+\right)$  and the loop functions are given by [194],

$$F_W(x) = 2 + 3x + 3x(2 - x)f(x), (2.69a)$$

$$F_t(x) = -2x [1 + (1-x)f(x)],$$
 (2.69b)

$$F_{i+}(x) = -x [1 - xf(x)].$$
 (2.69c)

with,  $f(x) = \left[\sin^{-1}\left(\sqrt{1/x}\right)\right]^2$  for x>1. It is interesting to note that in the limiting potential of Eq. (2.65), the charged-Higgs couplings to the SM-like Higgs in Eq. (2.67) are completely independent of any mixing angles and fixed to a constant value. Therefore, the charged-Higgs contribution to the loop-induced Higgs to diphoton channel will always be suppressed by the charged-Higgs masses when the charged-Higgses are much larger than the SM-like Higgs. We display our results in Fig. 2.2 in the  $(m_{H_1^+}-m_{H_2^+})$  mass plane, where we see that the current Higgs data mainly discards the parameter space where both or any one of the charged-Higgs masses are below  $\mathcal{O}$  (200 GeV). In Fig. 2.2, the region below the red dashed line is excluded by the current data at 95% C.L [192].

# 2.3 Wrong Sign Yukawa

Scalar extensions of the SM also face severe constraints from the measurements of the Higgs signal strengths [195]. For nHDMs, these constraints can be greatly alleviated by staying in the proximity of the alignment limit, where the lightest CP-even scalar has the same couplings as the SM Higgs boson at the tree-level. However, an intriguing possibility may arise if we keep in mind that the current Higgs data is not very sensitive to the sign of the down quark and charged-lepton Yukawa couplings. Here, we are after a relatively less-explored possibility where the sign of the down-type Yukawa couplings is opposite to what is predicted by the SM. Such an exotic possibility can be accommodated in a 2HDM framework with, for example, a type-II Yukawa structure and is quite well studied in the literature [196–199]. In this section, we want to point out that democratic 3HDMs can also accommodate this possibility, with much more freedom, due to the increased number of parameters.

To establish the  $\kappa$  notation, we define the Higgs coupling modifiers as follows [73, 74]

$$\kappa_X = \frac{g_{hXX}}{g_{hXX}^{SM}} \,, \tag{2.70}$$

where the field h, in the context of nHDMs, denotes the lightest CP-even scalar, and 'X' can represent either the massive vector bosons or fermions.

To illustrate the details of the wrong-sign limit, we briefly revisit the example of a type-II 2HDM where the coupling modifiers have the expression given in Table 2.1.<sup>9</sup> These coupling modifiers can be

 $<sup>^9\</sup>mathrm{We}$  note here that for the 2HDM case we are using the standard convention for  $\alpha$ , such that the alignment limit is

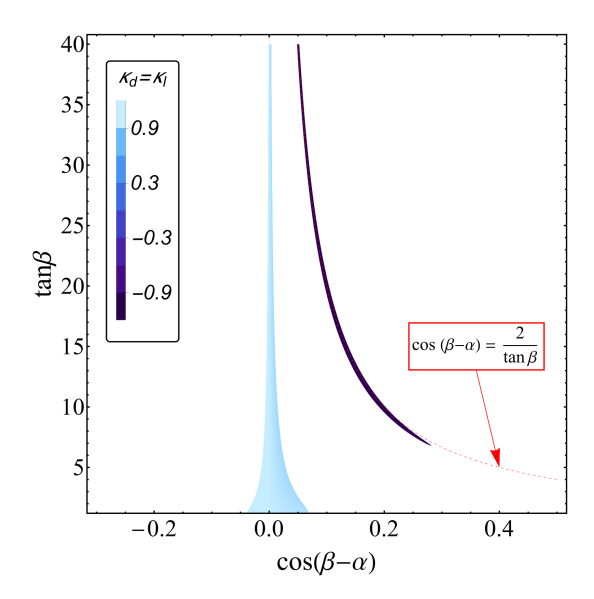


Figure 2.4: The allowed region at 95% CL from the current data on Higgs signal strengths in the type-II 2HDM. It should be noted that when considering the  $h \to \gamma \gamma$  decay, the charged-Higgs contribution has been neglected with the understanding that it can be safely decoupled in the presence of the soft-breaking parameter in the scalar potential [200–202]. For illustration, the line corresponding to  $\cos(\beta - \alpha) = 2/\tan\beta$  has also been plotted in the same graph, which reinforces our intuitions from Eq. (2.72).

conveniently rewritten as follows

$$\kappa_V^{\rm II} = \sin\left(\beta - \alpha\right),\tag{2.71a}$$

$$\kappa_u^{\text{II}} = \sin(\beta - \alpha) + \cot\beta\cos(\beta - \alpha),$$
(2.71b)

$$\kappa_d^{\text{II}} = \kappa_\ell^{\text{II}} = \sin(\beta - \alpha) - \tan\beta\cos(\beta - \alpha).$$
(2.71c)

Model	$\kappa_V$	$\kappa_u$	$\kappa_d$	$\kappa_\ell$
type-II 2HDM	$\sin{(\alpha - \beta)}$	$\frac{\cos\alpha}{\sin\beta}$	$-\frac{\sin\alpha}{\cos\beta}$	$-\frac{\sin\alpha}{\cos\beta}$
democratic 3HDMs	$\cos \alpha_2 \cos \beta_2 \cos (\alpha_1 - \beta_1) + \sin \alpha_2 \sin \beta_2$	$\frac{\sin \alpha_2}{\sin \beta_2}$	$\frac{\sin \alpha_1}{\sin \beta_1} \frac{\cos \alpha_2}{\cos \beta_2}$	$\frac{\cos \alpha_1}{\cos \beta_1} \frac{\cos \alpha_2}{\cos \beta_2}$

**Table 2.1:** The coupling modifiers for the type-II 2HDM and democratic 3HDMs. In the 2HDM case,  $\tan \beta = v_2/v_1$  and  $\alpha$  is a suitably defined rotation angle in the CP-even scalar sector [47]. Similarly, in the case of 3HDMs,  $\alpha_1$  and  $\alpha_2$  are two suitably defined rotation angles in the CP-even scalar sector [67].

Now let us consider the limit

$$\cos\left(\beta - \alpha\right) = \frac{r}{\tan\beta},\tag{2.72}$$

where r is a real number and  $\tan \beta \gg |r|$ . In such a scenario, Eq. (2.71) can be approximated as

$$\kappa_V^{\rm II} \approx 1, \qquad \kappa_u^{\rm II} \approx 1, \qquad \kappa_{d,\ell}^{\rm II} \approx 1 - r.$$
(2.73)

given by  $\cos(\beta - \alpha) = 0$ . However, for the case of democratic 3HDMs, the angles  $\alpha_{1,2}$  are defined in a way such that the alignment conditions read  $\sin(\alpha_i - \beta_i) = 0$ , with i = 1, 2 [67].

The wrong-sign limit, in particular, arises for r = 2, in which case Eq. (2.73) takes the form

$$\kappa_V^{\text{II}} \approx 1, \qquad \kappa_u^{\text{II}} \approx 1, \qquad \kappa_{d,\ell}^{\text{II}} \approx -1.$$
(2.74)

Such a possibility is allowed because the current LHC Higgs data is not sensitive enough to probe the sign of the bottom-quark Yukawa coupling in the loop-induced vertices such as hgg and  $h\gamma\gamma$ . To demonstrate this explicitly, we use the current Higgs data [195], and display the  $2\sigma$ -allowed region in the  $\cos(\beta - \alpha)$  vs  $\tan \beta$  plane in Fig. 2.4. The dark-blue region corresponds to the wrong-sign limit in the type-II 2HDM.<sup>10</sup>

Now, we will demonstrate that such wrong-sign scenarios are also entertained in democratic 3HDMs with much greater flexibility in terms of the number of free parameters. To illustrate this, we again purposefully rewrite the Higgs coupling modifiers in Table 2.1 for democratic 3HDMs as follows

$$\kappa_{V} = \frac{\cos(\alpha_{1} - \beta_{1})}{1 + \tan^{2}\beta_{2}} \left(\cos(\alpha_{2} - \beta_{2}) - \sin(\alpha_{2} - \beta_{2}) \tan\beta_{2}\right) 
+ \frac{\tan^{2}\beta_{2}}{1 + \tan^{2}\beta_{2}} \left(\cos(\alpha_{2} - \beta_{2}) + \sin(\alpha_{2} - \beta_{2}) \cot\beta_{2}\right),$$

$$\kappa_{u} = \cos(\alpha_{2} - \beta_{2}) + \sin(\alpha_{2} - \beta_{2}) \cot\beta_{2},$$
(2.75a)

$$\kappa_d = \left(\cos\left(\alpha_2 - \beta_2\right) + \sin\left(\alpha_2 - \beta_2\right)\cot\beta_2, \qquad (2.75c)$$

$$\kappa_d = \left(\cos\left(\alpha_1 - \beta_1\right) + \sin\left(\alpha_1 - \beta_1\right)\cot\beta_1\right) \left(\cos\left(\alpha_2 - \beta_2\right) - \tan\beta_2\sin\left(\alpha_2 - \beta_2\right)\right), \quad (2.75c)$$

$$\kappa_{\ell} = \left(\cos\left(\alpha_{1} - \beta_{1}\right) - \sin\left(\alpha_{1} - \beta_{1}\right) \tan\beta_{1}\right) \left(\cos\left(\alpha_{2} - \beta_{2}\right) - \tan\beta_{2}\sin\left(\alpha_{2} - \beta_{2}\right)\right). (2.75d)$$

In a similar way to the 2HDM scenario, we focus our attention to the limit

$$\sin\left(\alpha_2 - \beta_2\right) = \frac{r_2}{\tan\beta_2},\tag{2.76}$$

where  $r_2$  is a real number, and  $\tan \beta_2 \gg |r_2|$ . In this limit,  $\kappa_V \approx \kappa_u \approx 1$ , but  $\kappa_d$  and  $\kappa_\ell$  take the following form

$$\kappa_d = (1 - r_2) \left( \cos(\alpha_1 - \beta_1) + \sin(\alpha_1 - \beta_1) \cot \beta_1 \right) = (1 - r_2) \frac{\sin \alpha_1}{\sin \beta_1},$$
(2.77a)

$$\kappa_{\ell} = (1 - r_2) \left( \cos \left( \alpha_1 - \beta_1 \right) - \sin \left( \alpha_1 - \beta_1 \right) \tan \beta_1 \right) = (1 - r_2) \frac{\cos \alpha_1}{\cos \beta_1}. \tag{2.77b}$$

If we further consider the limit

$$\sin\left(\alpha_1 - \beta_1\right) = \frac{r_1}{\tan\beta_1},\tag{2.78}$$

where, again,  $r_1$  is a real number, and  $\tan \beta_1 \gg |r_1|$ , then Eq. (2.77) can be further simplified to

$$\kappa_d = (1 - r_2), \tag{2.79a}$$

$$\kappa_{\ell} = (1 - r_2)(1 - r_1). \tag{2.79b}$$

The limits that can be obtained for different values of  $r_1$  and  $r_2$  have been listed in Table 2.2, where we can

 $<sup>^{10}</sup>$ In a recent 2HDM fit [203], it was claimed that the wrong-sign limit is disfavoured by the current Higgs data at  $2\sigma$ , and only allowed within  $3\sigma$ . However, we have used a more updated dataset and our result for 2HDM agrees with the most updated fit from ATLAS [195] (in Fig. 20b, we can see the wrong-sign limit is still allowed).

see that all the wrong-sign possibilities that can be obtained from 2HDMs with NFC are encompassed by a democratic 3HDM. All these features have been clearly depicted in Figs. 2.5 and 2.6, where the darker shade corresponds to the wrong-sign limit. Thus, we can see that the democratic 3HDM gives more leeway for the wrong-sign limit, when compared to the 2HDM.

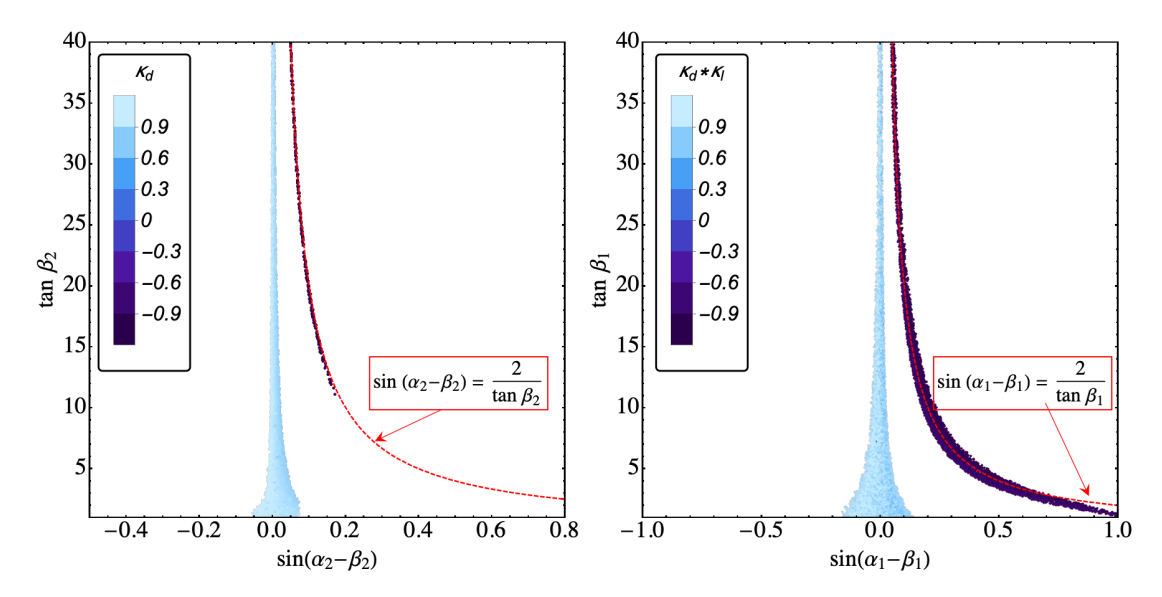


Figure 2.5: The allowed region at 95% CL from the current data on Higgs signal strengths in democratic 3HDM. As before, the charged-Higgs contribution to  $h \to \gamma \gamma$  decay is neglected with the understanding that it can be safely decoupled in the presence of the soft-breaking parameter in the scalar potential [200–202]. The contours corresponding to Eqs. (2.76) and (2.78) for  $r_1 = r_2 = 2$  are also displayed for ease of comparison.

	$r_1 = 0$	$r_1 = 2$
$r_2 = 0$	$ \kappa_d = 1  \kappa_\ell = 1 $	$\kappa_d \approx 1  \kappa_\ell \approx -1$
	(alignment limit)	(wrong-sign limit in the type-X 2HDM)
$r_2 = 2$	$\kappa_d \approx -1  \kappa_\ell \approx -1$	$\kappa_d \approx -1  \kappa_\ell \approx 1$
	(wrong-sign limit in the type-II 2HDM)	(wrong-sign limit in the type-Y 2HDM)

**Table 2.2:** Wrong-sign possibilities in democratic 3HDMs. It should be noted that  $\kappa_u \approx \kappa_V \approx 1$  in all the cases.

So far, we have obtained the wrong-sign limit in the democratic 3HDM following the 2HDM prescription. However, a democratic Yukawa structure can entertain more exotic possibilities. As usual, we start by investigating how to impose  $\kappa_u \approx 1$ . One possibility is to set  $\tan \beta_2 \gg 1$  together with  $\cos (\alpha_2 - \beta_2) \approx 1$ , as was done in Eq. (2.76), leading to Eq. (2.77). Now, instead of going to the limit of Eq. (2.78), one can choose

$$\sin(\alpha_1 - \beta_1) \approx \pm 1$$
,  $\tan \beta_1 \approx 1$ . (2.80)

In this way, using  $\cos(\alpha_1 - \beta_1) \approx 0$ , we get

$$\kappa_V \approx \kappa_u \approx 1,$$
(2.81a)

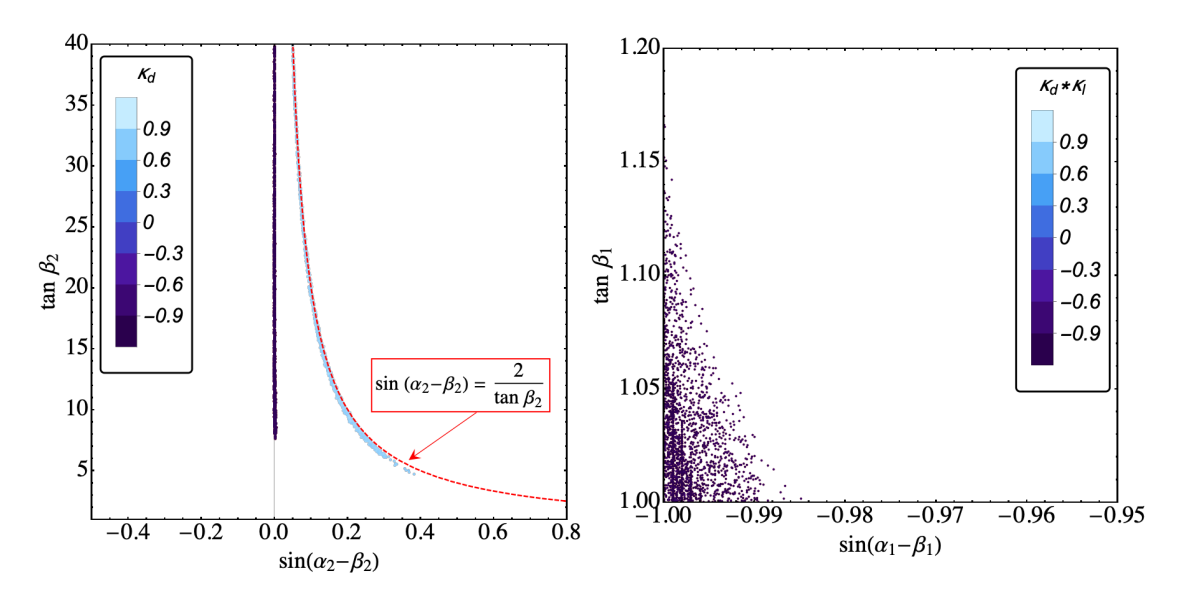


Figure 2.6: The allowed region at 95% CL from the current data on Higgs signal strengths for  $\sin(\alpha_1 - \beta_1) \approx -1$  is displayed separately in this plot. All the points shown in the left panel in the  $\sin(\alpha_2 - \beta_2)$  vs.  $\tan \beta_2$  plane are sampled from the  $\sin(\alpha_1 - \beta_1) \approx -1$  region as displayed in the right panel. The contour corresponding to Eq. (2.76) for  $r_2 = 2$  is displayed for easy comparison.

$$\kappa_d \approx -\kappa_\ell \approx \pm (1 - r_2),$$
(2.81b)

where, as before,  $r_2 \approx 0$  and  $r_2 \approx 2$  can give us two different possibilities. As such, we see that it is possible to achieve a wrong-sign limit in the democratic 3HDMs without the requirement of large  $\tan \beta_1$ . If we follow the usual path to the wrong-sign limit, we see that  $\sin (\alpha_1 - \beta_1) \approx 1$  is allowed in Fig. 2.5. The possibility with  $\sin (\alpha_1 - \beta_1) \approx -1$  is separately showcased in Fig. 2.6 for better visibility.

At this point it will be quite natural to wonder how such wrong-sign possibilities can be probed in experiments. An obvious way to sense the wrong-sign limit will be to measure the Higgs signal strengths that involve hgg and  $h\gamma\gamma$  effective vertices with increasing precision to the extent that the interference terms from the lighter fermions in the loop start to become relevant. Alternatively, the decay  $h \to \Upsilon\gamma$  was suggested as a probe for the sign of  $\kappa_b$  [204, 205]. Similarly,  $h \to \tau^+\tau^-\gamma$  [206] may serve as a probe for the sign of  $\kappa_\tau$ . Additionally, if we know the UV complete model responsible for the wrong-sign Yukawas, then we can perform a targeted search for the nonstandard particles. For instance, in this case the wrong-sign limit is arising within an nHDM framework. Thus, one can look for nonstandard scalars whose phenomenologies in the wrong-sign limit will be presumably different from the corresponding alignment limit counterparts [207].

But the crucial point is, even if we stay agnostic about the origin of the wrong-sign Yukawas, we should still remember that any departure from the SM couplings will introduce an energy scale beyond which unitarity will be violated [208]. Therefore, the wrong-sign limits as described in, e.g., Eq. (2.74) will inevitably call for NP below the unitarity violation scale. For the arrangement of couplings appearing in Eq. (2.74), the earliest onset of unitarity violation will occur in the  $b\bar{b} \to W_L W_L$  scattering and the

maximum energy cut-off before which the NP must intervene, will be given by [72]

$$E_{\text{max}} = \frac{2\sqrt{2}\pi}{G_F m_b} \approx 180 \text{ TeV}. \tag{2.82}$$

# 2.4 Discussion

We dedicated this chapter to the study of different aspects of democratic 3HDMs. Namely, we focused on the impact of custodial symmetry, as well as the Yukawa sector, whether in the alignment limit, or in wrong-sign limits. As such, our goal is to provide the ingredients for constructing democratic 3HDMs which are safeguarded against the T-parameter constraints, while showcasing the interesting Yukawa structures allowed by the Higgs and flavour data. The custodial limit serves as a systematic guideline for alleviating the stringent constraints arising from the electroweak T-parameter. We have followed an alternative approach to find the general condition for the custodial symmetry to be prevalent in the scalar sector of an nHDM. We used these results to extract the model specific conditions for democratic 3HDMs which usually comes in two different avatars – one with a  $Z_3$  symmetry and the other with a  $Z_2 \times Z_2'$  symmetry.

We then analyse a 3HDM where we assume some flavour symmetry is employed to ensure a democratic Yukawa structure, requiring each type of SM fermion to be coupled to a particular Higgs doublet, thus eliminating FCNCs at tree level. We do not dedicate time to separate the different possible avatars of democratic 3HDMs, since we employ a simplification on the scalar potential which renders all possible incarnations of the model indistinguishable. Hence, our study of the flavour constraints, under this simplification, apply to all democratic 3HDMs (if all soft-breaking terms are allowed). We have discussed the characteristics of the Yukawa sector, focusing on the alignment limit, where the lightest CP-even Higgs boson of the model possesses SM-like tree-level couplings and hence can serve as a candidate for the 125 GeV scalar observed at the LHC. The alignment limit is also phenomenologically well-motivated in view of the increasingly precise measurements of the signal strengths of the 125 GeV SM-like Higgs boson at the LHC.

The presence of additional Higgs bosons in the model gives rise to distinctive signatures in various experiments looking for direct or indirect signals of BSM physics. From the phenomenological point of view, we have put an emphasis on analysing the effect of the flavour physics constraints on the parameter space of democratic 3HDMs. The leading BSM contribution to flavour observables like  $\mathrm{BR}(b \to s \gamma)$  and  $\Delta M_{B_{s,d}}$  comes from the loops containing the charged-Higgs bosons. The Yukawa coupling structure of the charged-scalars bears a close resemblance to those of the Type-II 2HDM. However, the key difference from Type-II 2HDM is that the fermionic couplings of the charged-scalars feature an additional suppression effect. Thus, even in the limit of an effective Type-II 2HDM, with one of the charged-Higgs taken to be decoupled from the spectrum, the couplings of the other charged-Higgs retains the suppression factor. This produces a significant relaxation of the bounds coming from flavour observables in this model compared to Type-II 2HDM. It is observed that, in these models, charged-Higgs masses as low as 200 GeV are allowed by the flavour data, whereas in the case of Type-II 2HDM the lower bound

on charged-Higgs mass from the same flavour physics constraints stands at  $\mathcal{O}$  (600 GeV). We show that there is a limiting case where we can take the nonstandard scalars to be tier-wise degenerate, and the couplings of the charged-Higgs bosons to the 125 GeV SM-like Higgs assumes a constant value. Therefore, the contribution to  $h \to \gamma \gamma$  decay from charged-Higgs loop, being suppressed by a factor of  $m_h^2/m_{H^\pm}^2$ , i=1,2, does not produce any additional constraint on the relevant parameter space.

Finally, we turn our attention to the possibility of democratic 3HDMs to accommodate the wrong-sign limit, where the signs of the down-type Yukawa couplings are opposite to the corresponding SM predictions. We find that a democratic 3HDM covers all the wrong-sign scenarios that can possibly arise from a 2HDM framework with NFC. In the recent fits of the Higgs couplings [195, 209, 210] in the kappa formalism [73, 74], the results are often reported with an implicit assumption about the signs of the kappas. Our discussion on the wrong-sign limit highlights the importance of presenting the fit results without any inherent assumptions about the signs of the coupling modifiers because, otherwise we can miss potentially interesting and unconventional limits brought in by many different BSM scenarios. To emphasize the last point, we have also argued how the wrong-sign limit inevitably leads to an upper limit on the energy scale for the onset of NP.

On a cautionary note, we emphasize that these analyses are relevant to highlight certain aspects of BSM models, but can be supplemented by a more complete phenomenological study. In particular, the flavour constraints analysis takes a simplified approach to the scalar potential, to maintain a good handle on how to interpret the resulting parametric constraints. Nonetheless, a dedicated study of the different implementations of democratic 3HDMs can also lead to interesting distinguishing characteristics [211]. Furthermore, while light charged-scalars can successfully circumvent the flavour constraints from  $\Delta M$  and  $b \to s\gamma$ , under our simplistic scalar potential (also in the custodial limit), this will mandate the pseudoscalars to be light, which might impose additional constraints from direct searchers [164, 166].

# Softly-Broken nHDMs with Large Discrete Symmetry Groups

Abelian groups can effectively constraint the Yukawa interactions of the model, but fall short in the scalar sector, allowing for a lot of arbitrariness. One way to counter this deficiency is to investigate more restrictive symmetries, which include irreps with larger dimensions (*i.e.*, doublets, triplets, and so forth). We will generically call these large groups. These symmetries are able to introduce a lot of structure into the models, effectively reducing the amount of freedom by large amounts, eventually to the point of fixing the possible directions of minima and leading to relations between the scalar spectrum. A straightforward downfall of such rigid predictions is running in conflict with experiment, without the means to avoid it. One remedy is the inclusion of soft-breaking terms in the theory. These allow for a window to elude the unacceptable phenomenological consequences of large groups, while still retaining some of their rigidity. As such, our next steps focus on the study of large groups in the context of nHDMs.

Numerous pieces of evidence suggest that the SM cannot be the ultimate theoretical construction of the microscopic world. In the absence of direct compelling hints of how NP beyond the SM should look like, theorists explore different avenues. A very active direction of research is the study of non-minimal scalar sectors (for a selection of topics see the recent reviews [47, 51, 212, 213]). The simple idea that Higgs doublets can come in generations, just like fermions, alleviates some of the problems of the SM and also leads to a surprisingly rich list of phenomena. After a decades-long study of 2HDMs [47], the community is exploring other scalar sectors, such as 3HDMs.

First proposed by S. Weinberg in 1976 [214], the 3HDMs equipped with various global symmetries, exact or softly-broken, were studied in hundreds of papers, see a brief historical overview in [51]. However, a systematic study of all the opportunities offered by the 3HDMs is still lacking. One obvious reason for that is the very large number of free parameters. The most general renormalizable scalar potential of the N-Higgs-doublet model can be written, at the tree level, as

$$V = \mu_{ij}(\phi_i^{\dagger}\phi_j) + \lambda_{ij,kl}(\phi_i^{\dagger}\phi_j)(\phi_k^{\dagger}\phi_l), \quad i, j, k, l = 1, \dots, N,$$
(3.1)

with 54 free parameters for N=3. If one includes the quark Yukawa sector, the total number of free parameters exceeds one hundred. Certainly, it is possible, for any particular point in the entire parameter space, to numerically minimize the potential, compute all scalar masses and couplings, track down the fermion sector and its interaction with new scalars. But the real challenge is to make sense of these case-by-case calculations and to identify all the essentially distinct phenomenological situations which may be hiding in various parts of the very-large-dimensional parameter space. The richness of the 3HDM is just too vast to grasp and visualize with a straightforward (numerical) approach.

One popular way to tame the proliferation of free parameters is to assume that the multi-Higgs model is equipped with an additional global symmetry group. In early 1980's, this approach seemed promising because one hoped to link the mixing angles of the Cabibbo-Kobayashi-Maskawa matrix with quark mass ratios [51]. Later it turned out that this direct approach exploiting the exact symmetry groups could not lead to a viable quark sector [110, 215], but softly-broken symmetries seemed to offer sufficient flexibility and interesting predictions. In the case of the 3HDM scalar sector, several continuous and discrete symmetry groups have been implemented, starting from Weinberg's model, which has the symmetry group  $\mathbb{Z}_2 \times \mathbb{Z}_2$ . The full classification of discrete symmetry groups usable in the scalar sector of the 3HDM was established in [216]. If one focuses on the Higgs potential alone, one can observe accidental symmetries which go beyond Higgs family transformations. They were classified in [176] and a deeper analysis of the so-called maximally symmetric 3HDM was presented in [71]. The CP properties of the 3HDM scalar sector were also explored by using basis-independent methods [53, 217–220].

The investigation of the 3HDMs with softly-broken global symmetry group G depends on the group itself. Let us focus on the attractive case of large discrete groups G, with Higgs doublets transforming as an irreducible triplet representation. Four such cases are known<sup>1</sup> [216]:  $G = A_4$ ,  $S_4$ ,  $\Delta(54)$ , and  $\Sigma(36)$ -symmetric 3HDMs. In any of these four cases, the Higgs potential invariant under G has the following form:

$$V_0 = -m^2 (\phi_1^{\dagger} \phi_1 + \phi_2^{\dagger} \phi_2 + \phi_3^{\dagger} \phi_3) + V_4, \qquad (3.2)$$

while the G-symmetric quartic potential  $V_4$  contains several terms. All possible minima of this potential for the symmetry groups  $A_4$ ,  $S_4$ ,  $\Delta(54)$ , and  $\Sigma(36)$  are known and were put together in [221] (see also [222]).

If one wants to explore a 3HDM with a softly-broken group G, one needs to introduce all possible quadratic terms:

$$V_{\text{soft}} = m_{11}^2 \phi_1^{\dagger} \phi_1 + m_{22}^2 \phi_2^{\dagger} \phi_2 + m_{33}^2 \phi_3^{\dagger} \phi_3 + \left( m_{12}^2 \phi_1^{\dagger} \phi_2 + m_{23}^2 \phi_2^{\dagger} \phi_3 + m_{31}^2 \phi_3^{\dagger} \phi_1 + h.c. \right)$$
(3.3)

with complex  $m_{ij}^2$  for  $i \neq j$ . In total, there are nine free parameters here. Exploring in detail the emerging phenomenology in all corners of this 9-dimensional soft-breaking parameter space and visualizing the results would be very challenging. However these free parameters do not play equal roles. Some parameters may trigger structural changes, while others will only shift the numerical values of the observables.

<sup>&</sup>lt;sup>1</sup>The 3HDM with a  $\Delta(27)$  triplet leads to the same potential as the potential for a  $\Delta(54)$  group, so it is implicitly included in the  $\Delta(54)$  case.

Some phenomena may happen along generic directions in this soft-breaking parameter space, while other effects may take place only along some very particular directions. One could even think of plotting a phase diagram of the phenomenology of the resulting 3HDM with softly-broken G, but describing it in its full dimensionality seems very hard.

In short, one needs a guiding principle and a set of efficient methods to make sense of multi-Higgs models with softly-broken large discrete symmetry groups.

This is the main goal of this chapter. We will show that the nine soft-breaking free parameters can be split into two families: five parameters which preserve the vev alignment of the exactly symmetric parent model, and the four parameters which drive this alignment away in orthogonal directions. Focusing on the vev-preserving parameters, we will show which structural features of the fully symmetric model stay unchanged and which get modified, and how to track the effect of each of these parameters. In particular, we will find that, although the models with vev-preserving soft-breaking terms do not possess any exact symmetry, their scalar sector phenomenology "inherits" some of the features from the parent G-symmetric model. These results help develop qualitative and quantitative intuition when building multi-Higgs models with softly-broken large discrete symmetry groups.

These phenomena will be illustrated, following ref. [223], with the example of the largest discrete symmetry group possible in the 3HDM scalar sector, the group  $\Sigma(36)$ , which is not as well known as the  $A_4$ ,  $S_4$ , or  $\Delta(54)$ -symmetric 3HDMs. After presenting the  $\Sigma(36)$ -symmetric 3HDM (together with the analysis of its minima and scalar spectrum), we go through the method to include soft-breaking terms which preserve the vacuum alignment. This includes the general formalism, and its application to a particular example, as well as the study of the modified scalar spectrum. Finally, we study the conditions for the preserved minimum to remain global, and the implications of breaking the symmetry (softly) on the decoupling limits, and the decays of nonstandard scalars.

# 3.1 $\Sigma(36)$ -Symmetric 3HDM

#### 3.1.1 The Scalar Potential and its Minima

 $\Sigma(36)$  is the largest discrete symmetry group which can be imposed on the scalar sector of the 3HDM without leading to accidental continuous symmetries [216]. Group-theoretically, it is defined as a  $\mathbb{Z}_4$  permutation acting on generators of the abelian group  $\mathbb{Z}_3 \times \mathbb{Z}_3$ :

$$\Sigma(36) \simeq (\mathbb{Z}_3 \times \mathbb{Z}_3) \rtimes \mathbb{Z}_4. \tag{3.4}$$

The generators of the  $\mathbb{Z}_3 \times \mathbb{Z}_3$  "core" and the generator of  $\mathbb{Z}_4$  are

$$a = \begin{pmatrix} 1 & 0 & 0 \\ 0 & \omega & 0 \\ 0 & 0 & \omega^2 \end{pmatrix}, \quad b = \begin{pmatrix} 0 & 1 & 0 \\ 0 & 0 & 1 \\ 1 & 0 & 0 \end{pmatrix}, \quad d = \frac{i}{\sqrt{3}} \begin{pmatrix} 1 & 1 & 1 \\ 1 & \omega^2 & \omega \\ 1 & \omega & \omega^2 \end{pmatrix}, \tag{3.5}$$

where  $\omega = \exp(2\pi i/3)$ . The orders of these generators are:

$$a^3 = 1$$
,  $b^3 = 1$ ,  $d^4 = 1$ .

Notice that  $d^2$  is a transformation which transposes two doublets; thus,  $\Sigma(36)$  contains all permutations of the three doublets. Had we imposed symmetry under  $d^2$  but not d, we would end up with the more familiar symmetry group  $\Delta(54)$ , first used within the 3HDMs back in late 1970's [224] and explored later in [225–228]. For more details on the relation between  $\Delta(54)$  and  $\Sigma(36)$  and the subtleties of their definitions, see Appendix B.1.

The scalar potential of 3HDM invariant under  $\Sigma(36)$  has the following form:

$$V_{0} = -m^{2} \left[ \phi_{1}^{\dagger} \phi_{1} + \phi_{2}^{\dagger} \phi_{2} + \phi_{3}^{\dagger} \phi_{3} \right] + \lambda_{1} \left[ \phi_{1}^{\dagger} \phi_{1} + \phi_{2}^{\dagger} \phi_{2} + \phi_{3}^{\dagger} \phi_{3} \right]^{2}$$

$$-\lambda_{2} \left[ |\phi_{1}^{\dagger} \phi_{2}|^{2} + |\phi_{2}^{\dagger} \phi_{3}|^{2} + |\phi_{3}^{\dagger} \phi_{1}|^{2} - (\phi_{1}^{\dagger} \phi_{1})(\phi_{2}^{\dagger} \phi_{2}) - (\phi_{2}^{\dagger} \phi_{2})(\phi_{3}^{\dagger} \phi_{3}) - (\phi_{3}^{\dagger} \phi_{3})(\phi_{1}^{\dagger} \phi_{1}) \right]$$

$$+\lambda_{3} \left( |\phi_{1}^{\dagger} \phi_{2} - \phi_{2}^{\dagger} \phi_{3}|^{2} + |\phi_{2}^{\dagger} \phi_{3} - \phi_{3}^{\dagger} \phi_{1}|^{2} + |\phi_{3}^{\dagger} \phi_{1} - \phi_{1}^{\dagger} \phi_{2}|^{2} \right). \tag{3.6}$$

It has four real free parameters. The first two lines of Eq. (3.6) are invariant under the entire SU(3) transformation group of the three Higgs doublets. The positive sign of  $\lambda_2$  guarantees that the minimum corresponds to a neutral vacuum, but the minimization of these two lines alone would lead to several neutral Nambu-Goldstone bosons. The last term with the coefficient  $\lambda_3$  selects the discrete  $\Sigma(36)$  group out of it and renders those Higgs bosons massive.

The potential of Eq. (3.6) is also CP invariant. Apart from the standard CP symmetry  $\phi_i \to \phi_i^*$ , it is also invariant under many other CP transformations of the form of the standard CP combined with any of the symmetries from  $\Sigma(36)$ . Unlike the  $\Delta(54)$  3HDM, the absence of CP violation in  $\Sigma(36)$  3HDM is not an assumption but is a consequence of the  $\mathbb{Z}_4$  subgroup which forbids any form of CP violation in 3HDM, explicit or spontaneous [221, 229].

An important feature of the entire  $\Delta(54)$  family of 3HDM models, including  $\Sigma(36)$  3HDM, is the rigid structure of its minima. Depending on the values of the parameters, the global minimum of the potential can only correspond to the following vev alignments [221]:

alignment A: 
$$A_1 = (\omega, 1, 1), A_2 = (1, \omega, 1), A_3 = (1, 1, \omega)$$
 (3.7a)

alignment 
$$A'$$
:  $A'_1 = (\omega^2, 1, 1), \quad A'_2 = (1, \omega^2, 1), \quad A'_3 = (1, 1, \omega^2)$  (3.7b)

alignment B: 
$$B_1 = (1, 0, 0), B_2 = (0, 1, 0), B_3 = (0, 0, 1)$$
 (3.7c)

alignment C: 
$$C_1 = (1, 1, 1), \quad C_2 = (1, \omega, \omega^2), \quad C_3 = (1, \omega^2, \omega)$$
 (3.7d)

Notice that, due to the global symmetry of the 3HDM potential under simultaneous phase rotation of the three doublets, other possible configurations can be reduced to these ones; for example,  $(\omega, \omega^2, 1) = \omega(1, \omega, \omega^2)$  also corresponds to the alignment  $C_2$ . The phase rigidity is reflected in the fact that the relative phases between vevs are calculable and are not sensitive to the exact numerical values of the coefficients. This rigidity was behind the "geometric CP-violation" proposal back in 1984 [230] which was

revisited in more detail in [231–233], and also shown to be compatible with viable Yukawa sectors [234–236].

None of the minima of the  $\Sigma(36)$ -symmetric 3HDM breaks the symmetry group completely [221]. There are six family symmetries and six CP-type symmetries which are preserved at each vev alignment. Other, spontaneously broken, symmetries link different vacua, which, despite looking differently, represent the same physics. For  $\lambda_3 < 0$ , the global minima are at the six points A and A', which are related by the broken symmetries from  $\Sigma(36)$ . For  $\lambda_3 > 0$ , the degenerate global minima are at points B or C. Thus, we have two essentially distinct phenomenological situations in the  $\Sigma(36)$ -symmetric 3HDM.<sup>2</sup>

Further insights into the structural properties of the model, including the vev alignments, symmetry and CP properties, can be gained if one pays attention not only to the transformations from the symmetry group G but also to the transformations from SU(3) which leave G invariant, or "symmetries of symmetries" in the language of [237]. The potential remains form-invariant under such transformations, only up to reparametrization of coefficients, which may provide additional links between different regimes of the same model.

#### 3.1.2 The Physical Higgs Bosons

Three Higgs doublets contain 12 real fields. When expanding the potential around a neutral vacuum, one absorbs, as usual, three of them in the longitudinal components of the  $W^{\pm}$  and Z-bosons. What remains is two pairs of charged Higgses and five neutral Higgs bosons. At points B or C, the Higgs boson masses are

$$\begin{split} m_{h_{SM}}^2 &= 2\lambda_1 v^2 = 2m^2 \,, \\ m_{H^\pm}^2 &= \frac{1}{2}\lambda_2 v^2 \quad \text{(double degenerate)} \,, \\ m_h^2 &= \frac{1}{2}\lambda_3 v^2 \quad \text{(double degenerate)} \,, \\ m_H^2 &= 3m_h^2 = \frac{3}{2}\lambda_3 v^2 \quad \text{(double degenerate)} \,. \end{split} \tag{3.9}$$

At points A and A', which are the minima for  $\lambda_3 < 0$ , the Higgs masses are

$$\begin{split} m_{h_{SM}}^2 &= 2(\lambda_1 + \lambda_3)v^2 = 2m^2 \,, \\ m_{H^\pm}^2 &= \frac{1}{2}(\lambda_2 - 3\lambda_3)v^2 \quad \text{(double degenerate)} \,, \\ m_h^2 &= -\frac{1}{2}\lambda_3v^2 \quad \text{(double degenerate)} \,, \\ m_H^2 &= 3m_h^2 = -\frac{3}{2}\lambda_3v^2 \quad \text{(double degenerate)} \,. \end{split} \tag{3.10}$$

$$b.A_1 = A_3, \quad b^2.A_1 = A_2 \quad a.b.d.A_1 = A_1',$$
 (3.8)

and the same is true for the alignments of types B and C. On the other hand, there are no group elements which are able to take a point from B to A or A', making these two distinct.

<sup>&</sup>lt;sup>2</sup>The alignments  $A_i$  and  $A'_i$  are connected through symmetry actions:

Identification of the SM-like Higgs boson is unambiguous. It is a straightforward exercise to show that, if the quadratic potential of an nHDM has the form  $m^2 \sum_i \phi_i^{\dagger} \phi_i$ , then whatever the quartic potential is, the model automatically incorporates the exact scalar alignment [238]. This means that the direction along the vev alignment is a mass eigenstate which, therefore, couples to the WW and ZZ pairs just as in the SM. The other neutral Higgs bosons do not couple to gauge-boson pairs.

The fact that the symmetry group  $\Sigma(36)$  is not broken completely by the vacuum configuration means that one can classify the physical Higgs bosons according to their conserved charges. For example, the vev alignment (1,0,0) corresponding to point B preserves the symmetry group  $S_3$  generated by a and  $d^2$ . Thus, within each subspace of physical scalar fields (the charged, the light neutral, and the heavy neutral Higgses) we can construct states which are eigenstates of parity under  $d^2$  or which have definite  $Z_3$ -charges under a. Either of these numbers is conserved. Thus, the lightest pair of states from the second and third doublet is stable against decay to the SM fields (provided they do not couple to fermions).

# 3.1.3 The Scalar Sector of $\Sigma(36)$ 3HDM: a Summary

To summarize the above observations, we list here the structural features of the  $\Sigma(36)$ -symmetric 3HDM scalar sector.

- The vev alignment at the global minimum can only be of types (3.7).
- Spontaneous CP violation is impossible.
- The model contains automatic scalar alignment, with the SM-like Higgs  $h_{SM}$ .
- All charged Higgses are degenerate, and the four non-SM-like neutral Higgs bosons are pair-wise degenerate.
- The masses of the two pairs of the neutral Higgses are related as  $m_H^2 = 3m_h^2$ .
- Since the full symmetry group  $\Sigma(36)$  is broken only partially at any of the vev alignments, the lightest non-SM-like Higgs bosons are stable against decay to the SM fields.

# 3.2 Alignment Preserving Soft-Breaking

The exact discrete symmetry group  $\Sigma(36)$  leads to very rigid predictions which could easily run in conflict with experiment. It is customary to introduce some flexibility to a model via soft-breaking terms, which in the case of 3HDM involve up to 9 new free parameters, see Eq. (3.3). The main challenge then is to understand how these soft-breaking terms change the structural properties of the  $\Sigma(36)$  scalar sector outlined in the previous section.

Of course, for any specific set of  $m_{ij}^2$ , one could numerically compute the vevs and the properties of the physical scalar bosons. But, as we already mentioned, the large number of free parameters makes it difficult and impractical to blindly track down, via a numerical scan, the modifications of the observables in the entire space of soft-breaking parameters. It is even not clear how these numerical results should be

presented. Thus, the real challenge is to comprehend all these dependences, to construct a clear vision of which parameters govern numerical deviations and which drive structural changes.

In this section, we take the first step towards this vision. We identify the soft-breaking terms which preserve the vev alignments and then study the effects of such terms. An important consequence is that the automatic scalar alignment with the SM-like Higgs is preserved. The analytical derivations are corroborated by numerical computation and accompanied with a qualitative discussion.

## 3.2.1 How to Preserve the vev Alignment

Suppose we pick up one of the vev alignments listed in Eq. (3.7). Which terms in  $V_{\text{soft}}$  can we introduce to keep the alignment intact?

A straightforward way to answer this question for all alignments, one by one, is to write down the extremum conditions, solve them and deduce the relations among the parameters  $m_{ij}^2$  which protect the chosen vev alignment. This method is not very enlightening. First, it requires direct computations of derivatives for each individual case. Second, when it leads to certain constraints on the soft-breaking parameters  $m_{ij}^2$ , it may remain obscure within what range one is allowed to vary them. Finally, there may arise particular points which may require special treatment.

Instead, we propose here a simple method which leads to a clear picture for any vev alignment. Furthermore, it can be applied not only to the  $\Sigma(36)$  3HDM, but to any multi-Higgs potential with the trivial quadratic part, which includes  $A_4$ ,  $S_4$  and  $\Delta(54)$  3HDMs.

First, we remind the reader that, when we have a function which depends on the complex variable z and its conjugate  $z^*$ , we can differentiate it with respect to z and  $z^*$  independently. Writing z = x + iy, we define the antiholomorphic derivative operator as

$$\frac{\partial}{\partial z^*} = \frac{1}{2} \left( \frac{\partial}{\partial x} + i \frac{\partial}{\partial y} \right), \quad \frac{\partial z}{\partial z^*} = 0, \quad \frac{\partial z^*}{\partial z^*} = 1.$$
 (3.11)

The  $\Sigma(36)$ -invariant potential  $V_0 = -m^2 \phi_i^{\dagger} \phi_i + V_4$  depends on the complex variables  $\phi_i$  and  $\phi_i^{\dagger}$ . Here, the index i can run over six entries: three upper and three lower components of the doublets. However, since the minimum is neutral, one can suppress the upper components and assume that  $\phi_i = \phi_i^0$ , i = 1, 2, 3.

The extremization condition for the  $\Sigma(36)$ -symmetric potential is:

$$\frac{\partial V_0}{\partial \phi_i^*} = -m^2 \phi_i + \frac{\partial V_4}{\partial \phi_i^*} = 0. \tag{3.12}$$

Therefore, at the extremum point, we have

$$\frac{\partial V_4}{\partial \phi_i^*} \bigg|_{V_0 \text{ extremum}} = m^2 \phi_i \bigg|_{V_0 \text{ extremum}}.$$
(3.13)

Now, we add the soft-breaking terms of Eq. (3.3), which we write compactly as

$$V_{\text{soft}} = \phi_i^{\dagger} M_{ij} \phi_j , \quad M_{ij} = \begin{pmatrix} m_{11}^2 & m_{12}^2 & (m_{31}^2)^* \\ (m_{12}^2)^* & m_{22}^2 & m_{23}^2 \\ m_{31}^2 & (m_{23}^2)^* & m_{33}^2 \end{pmatrix} , \tag{3.14}$$

with hermitean matrix M. Extremization condition for the full potential  $V = V_0 + V_{\text{soft}}$  is

$$\frac{\partial V}{\partial \phi_i^*} = M_{ij}\phi_j - m^2\phi_i + \frac{\partial V_4}{\partial \phi_i^*} = 0.$$
(3.15)

In general, the extremum point may have shifted with respect to the symmetric case, so we cannot use the relation of Eq. (3.13). But we now require that the soft-breaking terms preserve the vev alignment up to rescaling:  $v|_{V \text{ extremum}} = \zeta \cdot v|_{V_0 \text{ extremum}}$ . Because of this feature and because the quadratic and quartic terms are homogeneous functions with degrees 2 and 4, respectively, we can now state that

$$\frac{\partial V_4}{\partial \phi_i^*} \bigg|_{V \text{ extremum}} = \zeta^2 \cdot m^2 \phi_i \bigg|_{V \text{ extremum}}. \tag{3.16}$$

Therefore, at the point of the extremum of V we can simplify Eq. (3.15) as

$$M_{ij}\phi_i = (1 - \zeta^2)m^2\phi_i. {3.17}$$

We conclude that the soft-breaking terms preserve a vev alignment of the original symmetric model if and only if this vev alignment is an eigenvector of the corresponding matrix M. This offers us a method of writing down the most general soft-breaking terms which preserve any given vev alignment of the symmetric model.

# 3.2.2 An Example

Let us illustrate this method with point  $C_1$  whose vev alignment is (1, 1, 1). We want to establish the form of M which would preserve this alignment. Suppose  $\mu_1$ ,  $\mu_2$ ,  $\mu_3$  are the eigenvalues of M, and the complex vectors  $\vec{n}_1$ ,  $\vec{n}_2$ ,  $\vec{n}_3$  are the corresponding orthonormal eigenvectors. Then M can be written as

$$M_{ij} = \mu_1 \, n_{1i} n_{1j}^* + \mu_2 \, n_{2i} n_{2j}^* + \mu_3 \, n_{3i} n_{3j}^* \,. \tag{3.18}$$

Given one eigenvector, which is already known,

$$n_1 = \frac{1}{\sqrt{3}} \begin{pmatrix} 1\\1\\1 \end{pmatrix}, \tag{3.19}$$

we can select two other eigenvectors in the subspace orthogonal to  $\vec{n}_1$ . Let us define two orthonormal vectors in this subspace, for example,

$$e_2 = \frac{1}{\sqrt{2}} \begin{pmatrix} 0\\1\\-1 \end{pmatrix}$$
 and  $e_3 = \frac{1}{\sqrt{6}} \begin{pmatrix} -2\\1\\1 \end{pmatrix}$ . (3.20)

Both  $\{\vec{n}_2, \vec{n}_3\}$  and  $\{\vec{e}_2, \vec{e}_3\}$  form a basis. Therefore, the two eigenvectors  $\vec{n}_2$  and  $\vec{n}_3$  can be obtained from  $\vec{e}_2$  and  $\vec{e}_3$  with an appropriate unitary transformation within this space:

$$\vec{n}_i = \mathcal{U}_{ij}\vec{e}_j$$
,  $i, j = 2, 3$ , where  $\mathcal{U} = \begin{pmatrix} \cos\theta & e^{i\xi}\sin\theta \\ -e^{-i\xi}\sin\theta & \cos\theta \end{pmatrix}$ . (3.21)

Notice that multiplying  $\vec{n}_2$  and  $\vec{n}_3$  with additional phase factors does not affect M. Thus, the most general soft-breaking terms preserving the vev alignment of point A are described with the matrix M in Eq. (3.18) with the following free parameters:

$$\mu_1 = m^2 (1 - \zeta^2), \quad \mu_2, \quad \mu_3, \quad \theta, \quad \xi.$$
 (3.22)

If we insist not only on keeping the vev alignment, but also want to preserve the value of v, we set  $\mu_1 = 0$  and are left with 4 parameters, which we recast in the following more convenient form:

$$\Sigma = \mu_2 + \mu_3, \quad \delta = \mu_2 - \mu_3, \quad \theta, \quad \xi.$$
 (3.23)

All these parameters can vary in their full domains of definitions.

The explicit expressions for the matrix M and individual  $m_{ij}^2$  soft-breaking parameters which preserve the vev alignment  $C_1$  and the value of v are

$$M_{11} = m_{11}^2 = \frac{1}{3} \left( \Sigma - \delta \cos 2\theta \right)$$

$$M_{22} = m_{22}^2 = \frac{1}{3} \left[ \Sigma + \delta \left( \frac{\sqrt{3}}{2} \sin 2\theta \cos \xi + \frac{1}{2} \cos 2\theta \right) \right]$$

$$M_{33} = m_{22}^2 = \frac{1}{3} \left[ \Sigma + \delta \left( -\frac{\sqrt{3}}{2} \sin 2\theta \cos \xi + \frac{1}{2} \cos 2\theta \right) \right]$$

$$M_{12} = m_{12}^2 = \frac{1}{6} \left[ -\Sigma + \delta \left( -\sqrt{3} \sin 2\theta e^{i\xi} + \cos 2\theta \right) \right]$$

$$M_{31} = m_{31}^2 = \frac{1}{6} \left[ -\Sigma + \delta \left( \sqrt{3} \sin 2\theta e^{-i\xi} + \cos 2\theta \right) \right]$$

$$M_{23} = m_{23}^2 = \frac{1}{6} \left[ -\Sigma - \delta \left( i\sqrt{3} \sin 2\theta \sin \xi + 2 \cos 2\theta \right) \right]. \tag{3.24}$$

In a similar fashion, we parametrize the soft-breaking terms which preserve all other vev alignments of the  $\Sigma(36)$  3HDM, see Appendix B.2 for the full list. Here we only remark that, in each case, there exists ambiguity in choosing the basis vectors  $\vec{e}_2$  and  $\vec{e}_3$  with respect to which we parametrize the matrix  $M_{ij}$  via angles  $\theta$  and  $\xi$ . We resolve this ambiguity by choosing such vectors that the neutral physical

Higgs boson masses to be given below take exactly the same form at all minima.

# 3.2.3 Physical Scalars in the Softly-Broken $\Sigma(36)$ 3HDM

Parametrizing the vev-preserving soft-breaking terms as outlined above, we computed in each case the mass matrices of the physical Higgs bosons. A remarkable observation is that for all vev alignments and with the above choices of the parametrization procedure, we could obtain *universal* formulas for masses of the physical Higgs bosons, valid for all the vev alignments of the parent  $\Sigma(36)$ -symmetric model.

- The scalar alignment feature is preserved. Indeed, since the vev alignment was the eigenvector of the parent model at its minimum and since it is an eigenvector of the matrix of the soft-breaking terms, it will remain an eigenvector of the Hessian matrix of the softly-broken case.
- Since we select  $\mu_1 = 0$  to preserve not only the alignment but also the value of v, the mass of the SM-like Higgs boson is unchanged:  $m_{h_{SM}}^2 = 2(\lambda_1 + \lambda_3)v^2$  for cases A and A' and  $m_{h_{SM}}^2 = 2\lambda_1v^2$  for cases B and C, just as in Eqs. (3.10) and (3.9).
- The non-standard Higgs bosons cease to be mass degenerate. For the charged Higgs bosons, we write  $m_{H_i^{\pm}}^2 = m_{H_i^{\pm}}^2 \big|_{\Sigma(36)} + \Delta m_{H_i^{\pm}}^2$ , where  $m_{H_i^{\pm}}^2 \big|_{\Sigma(36)}$  are their masses in the parent  $\Sigma(36)$ -symmetric model given by Eqs. (3.10) and (3.9), and observe the following universal corrections:

$$\Delta m_{H_1^{\pm}}^2 = \mu_2 = \frac{\Sigma + \delta}{2}, \quad \Delta m_{H_2^{\pm}}^2 = \mu_3 = \frac{\Sigma - \delta}{2}.$$
 (3.25)

The four non-SM-like neutral Higgs bosons have the following masses:

$$m_{h_1}^2 = \frac{1}{2} \left( 2|\lambda_3|v^2 + \Sigma - \sqrt{(\lambda_3 v^2)^2 + \delta^2 + 2x|\lambda_3||\delta|v^2} \right), \tag{3.26}$$

$$m_{h_2}^2 = \frac{1}{2} \left( 2|\lambda_3|v^2 + \Sigma - \sqrt{(\lambda_3 v^2)^2 + \delta^2 - 2x|\lambda_3||\delta|v^2} \right), \tag{3.27}$$

$$m_{H_1}^2 = \frac{1}{2} \left( 2|\lambda_3|v^2 + \Sigma + \sqrt{(\lambda_3 v^2)^2 + \delta^2 - 2x|\lambda_3||\delta|v^2} \right), \tag{3.28}$$

$$m_{H_2}^2 = \frac{1}{2} \left( 2|\lambda_3|v^2 + \Sigma + \sqrt{(\lambda_3 v^2)^2 + \delta^2 + 2x|\lambda_3||\delta|v^2} \right), \tag{3.29}$$

where the quantity  $x \in [0, 1]$  is

$$x = \sqrt{1 - (\sin 2\theta \sin \xi)^2}. \tag{3.30}$$

Here, we write  $|\lambda_3|$  to cover both cases A and A'  $(\lambda_3 < 0)$  and cases B and C  $(\lambda_3 > 0)$ .

Apart from splitting, the mass patterns demonstrate two remarkable features. The first is the unexpected similarity between the cases A + A' and B + C. Indeed, cases A and A' are linked by a symmetry of the parent model, and therefore, one expects that the appropriately parametrized soft-terms would lead to the same results for points A and A'. In a similar way, symmetries link cases B and C. However, there is no symmetry of the model which links the vev alignments from points A or A' to points B or C. Indeed, we see that the expressions for the SM-like and charged Higgs masses are not identical. Whether this intriguing feature can be explained from the "symmetries of symmetries" perspective of [237] is an open

question which deserves a closer look.<sup>3</sup>

The second feature is that the masses depend not on four, but on three independent soft-breaking parameters:  $\Sigma$ ,  $\delta$ , and the combination  $\sin 2\theta \sin \xi$ . In the example of point C, this combination quantifies the imaginary part of  $m_{ij}^2$  in Eq. (3.24). This means that, in the 4D space of vev-preserving soft-breaking parameters, there exist lines of identical Higgs spectra. Moving along these lines, one can adjust additional features of the model, keeping the masses fixed.

It is interesting to observe that, at  $\sin 2\theta \sin \xi = 1$  leading to x = 0, the four neutral Higgses again combine into two mass-degenerate pairs. The origin of this degeneracy is the special form of the softbreaking terms which satisfy  $\sin 2\theta \sin \xi = 1$ . Such soft-breaking terms, in fact, respect several of the symmetries of the vacuum. Within the same example  $C_1$ , the soft-breaking matrix takes the form

$$M = \frac{\Sigma}{6} \begin{pmatrix} 2 & -1 & -1 \\ -1 & 2 & -1 \\ -1 & -1 & 2 \end{pmatrix} + \frac{\delta\sqrt{3}}{6} \begin{pmatrix} 0 & -i & i \\ i & 0 & -i \\ -i & i & 0 \end{pmatrix}, \tag{3.31}$$

which is invariant under cyclic permutations as well as an exchange of any two doublets followed by a CP transformation. These residual symmetries form the group  $S_3$  and force the neutral scalars to be pairwise degenerate.

The third observation is the remarkable form of neutral mass splittings:

$$m_{h_2}^2 - m_{h_1}^2 = m_{H_2}^2 - m_{H_1}^2. (3.32)$$

It can be viewed as yet another structural feature inherited from the parent symmetric model.

#### 3.2.4 Global vs. Local Minimum

The potential of the parent  $\Sigma(36)$ -invariant 3HDM contains six distinct minima which are linked by the broken symmetry generators and are degenerate. When we introduce soft-breaking terms, we destroy the symmetry, and the six minima are not equivalent anymore. Therefore, one can wonder if the minimum which one selects to construct the vev-preserving soft-breaking terms represents the global or a local minimum. The answer turns out surprisingly simple: the chosen minimum remains the global one if  $\mu_2 > 0$  and  $\mu_3 > 0$ . Additionally, we verified numerically and found that for negative, but small values of either  $\mu_2$  or  $\mu_3$ , the minimum can remain global. The smallness can be quantified relative to the coefficient of the SU(3)-invariant quadratic term,  $m^2$ .

This feature has a simple explanation. Suppose we select one particular minimum out of the six degenerate minima and add generic soft-breaking terms which preserve this minimum. The depth of the potential at this particular minimum does not change because  $\langle \phi_i^{\dagger} \rangle M_{ij} \langle \phi_j \rangle = 0$  (we used here  $\mu_1 = 0$ ). At all other points, be they extrema or not, the soft-breaking terms add  $\langle \phi_i^{\dagger} \rangle M_{ij} \langle \phi_j \rangle$  to the potential. If  $\mu_2 > 0$  and  $\mu_3 > 0$ , this extra contribution is strictly positive everywhere away from the chosen minimum

<sup>&</sup>lt;sup>3</sup> Following the idea of [237], there may be outer automorphisms which relate different parametric regions, while describing the same system until a physical identification of the fields. This could be in the origin of the similarity between the two disconnected cases of A + A' and B + C.

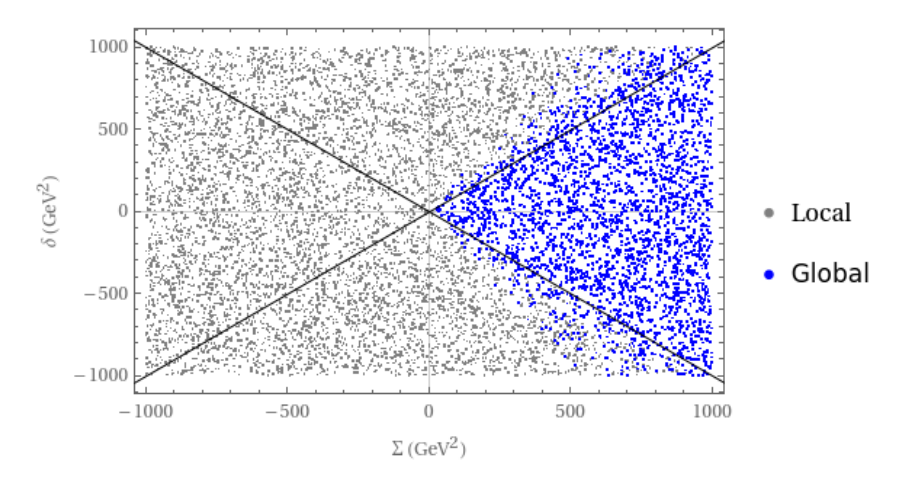


Figure 3.1: The effect of the vev-preserving alignment parameters of Eq. (3.23) on the depth of the chosen minimum. The entire four-parameter scan is projected onto the  $(\Sigma, \delta)$  plane within the range  $-10^3 \text{ GeV}^2 \leq \Sigma, \delta \leq 10^3 \text{ GeV}^2$ . Blue (gray) dots correspond to soft-breaking parameter sets leading to the global (local) minimum. The black lines are the borders where  $\mu_2$  or  $\mu_3$  changes sign.

direction. Therefore, the chosen minimum is automatically the global one.

It is possible to construct examples in which the global minimum is not unique. For example, one can set  $\mu_2 = 0$  and construct such M that the corresponding eigenvector coincides with another minimum of the  $\Sigma(36)$  symmetric model. In this case, the soft-breaking terms will keep unchanged at least two of the previously degenerate minima.

By the same logic, one can also select a small  $\mu_2 < 0$  (keeping  $\mu_3 > 0$ ) and select the eigenvector not to pass through any other minima. Then, it is possible to find the values of angles  $\theta$ ,  $\xi$  which will result in a second minimum at the same depth as the selected one. By continuity arguments, we see that the selected minimum can remain the global one even if  $\mu_2 < 0$ .

This analysis is corroborated by a numerical scan over the vev-preserving soft-breaking parameter space, which proceeds as follows. We take a reference  $\Sigma(36)$ -symmetric parent model by selecting parameters  $\lambda_2 > 0$  (required for the minimum to be neutral) and  $\lambda_3$  and then expressing  $m^2$  and  $\lambda_1$  via known v and the SM-like Higgs mass  $m_h$ . Once the reference model is fixed, we select a vev alignment and add soft-breaking terms  $V_{\text{soft}}$  which preserve the vev alignment selected as well as its magnitude (that is, we set  $\mu_1 = 0$ ). We then scan over the soft-breaking parameters  $\mu_2$ ,  $\mu_3$  in the range from  $-10^6 \text{ GeV}^2$  to  $10^6 \text{ GeV}^2$  and over  $\theta, \xi$  in their entire domains. At each point, we numerically search for the global minimum and, with this information, we can determine whether the selected vev alignment stays the global minimum or becomes a local minimum with a given choice of soft-breaking terms. Also, at each vev alignment, we numerically compute the masses of the physical scalars; for the minimum we have selected, these masses are found to agree with Eqs. (3.25)–(3.29).

We found that for all points with  $\mu_2, \mu_3 > 0$ , the chosen minimum remains the global one upon the addition of soft-breaking terms. We also verify that it is the only global minimum of the resulting potential, not a degenerate global minimum. If  $\mu_2$  or  $\mu_3$  is significantly negative, the selected minimum unavoidably becomes local. However we also found many points where one of the two parameters,  $\mu_2$  or  $\mu_3$ , is slightly negative, but the minimum remains global. Thus, requiring  $\mu_2, \mu_3 > 0$  is a sufficient but not necessary assumption for staying in the global minimum. We illustrate this observation with the scatter plot in Fig. 3.1, where we start with the symmetric model with  $\lambda_2 = 0.6$ ,  $\lambda_3 = -0.7$ , select a minimum of type A, perform a four-parameter scan over soft-breaking parameters, and project the results onto the  $(\Sigma, \delta)$  plane. We focus here on relatively small values of these two parameters. At the black lines,  $\mu_2$  or  $\mu_3$  changes sign. However the boundary between "always local" and "always global" parameter space regions does not coincide with the black lines and is in fact blurred. A very similar picture is observed for other parameters of the symmetric model.

What we gain from this exercise is the following insight: if one wants to build a softly-broken  $\Sigma(36)$  3HDM with a vacuum at the brink of absolute tree-level stability, one should explore the parameter space regions along these lines.

#### 3.2.5 Decoupling Limits

Decoupling limit in multi-Higgs models refers to the regime in which additional, non-SM scalars are very heavy, so that we are left at the electroweak scale with the single Higgs particle whose tree-level properties approach the properties if the SM Higgs [63]. Decoupling limit is a weaker statement than the exact decoupling theorem, which requires all the effects induced by heavy non-standard particles to asymptotically disappear in the large mass limit. It is well known that, in the 2HDM and 3HDM, certain decays of the SM-like Higgs boson receive finite corrections from the charged Higgs boson loops even if their masses are very large [200, 239]. Thus, it is worth scrutinizing the properties of the SM-like Higgs boson in the decoupling limit.

In the 3HDM, we can also define in a similar manner the 2HDM-like limit, when two neutral and a pair of charged Higgses are heavy and decouple from the remaining relatively light 2HDM-like sector. Similarly to the distinction between the decoupling theorem and decoupling limit, decays of the scalars in this 2HDM-like sector may show deviations with respect to the 2HDM which would mimic the mass spectrum of the 3HDM with one generation of very heavy Higgses. This comparison would require a dedicated work.

Whether a multi-Higgs model can exhibit the SM decoupling limit depends on its symmetry content. The recent studies [201, 202, 240] proved that a symmetry-constrained multi-Higgs-doublet model allows for the decoupling limit only when the vev alignment preserves the symmetry group. In the 3HDMs with Higgs doublets in the 3D irreducible representation of the global symmetry group G, including the case of  $\Sigma(36)$ , the vev alignment unavoidably breaks the symmetry group, which makes the decoupling limit unattainable. This is also clearly seen by the single quadratic parameter  $m^2$  in the  $\Sigma(36)$ -invariant 3HDM.

The presence of soft-breaking terms lead to models without any exact symmetry and, therefore, can display the decoupling regime. If both  $\mu_2, \mu_3 \gg |\lambda_3| v^2$ , one can expand the neutral Higgs masses Eqs. (3.25)–(3.29) as

$$m_{h_1,h_2}^2 \approx \mu_2 + |\lambda_3| v^2 \mp \frac{x}{2} |\lambda_3| v^2, \quad m_{H_1,H_2}^2 \approx \mu_3 + |\lambda_3| v^2 \mp \frac{x}{2} |\lambda_3| v^2.$$
 (3.33)

One observes the natural scale separation for the two heavy "multiplets": the squared-masses of  $H_1^{\pm}$ ,

 $h_1$  and  $h_2$  stay at the scale  $\mu_2$ , while  $H_2^{\pm}$ ,  $H_1$  and  $H_2$  reside at the scale  $\mu_3$ . Within each multiplet, one observes the same mass splitting pattern:

$$m_{H_1^{\pm}}^2 - m_{h_1}^2 = \frac{1}{2}v^2 \left[\lambda_2 + \lambda_3 f(x)\right], \quad m_{h_2}^2 - m_{h_1}^2 = x|\lambda_3|v^2,$$
 (3.34)

with f(x) = x + 1 for  $\lambda_3 > 0$  (points B and C) and f(x) = 2 - x for  $\lambda_3 < 0$  (points A and A'), and exactly the same splitting for  $H_2^{\pm}$ ,  $H_1$ ,  $H_2$ . Notice that since  $0 \le x \le 1$ , the function f(x) lies between 1 and 2 for any choice of the minimum.

Thus, we observe another structural feature of the softly-broken model driven by the large symmetry of the parent model: in the SM-like decoupling limit, the decoupled sector has a rigid structure of its mass spectrum.

For the 2HDM-like decoupling limit, we assume that  $\mu_3$  is large, while  $\mu_2$  is of the same order of magnitude as  $\lambda_3 v^2$ . The approximate results of Eq. (3.33) driven by large  $|\delta|$  remain valid, but the mass scales of  $h_i$  and  $H_i$  are now different. The heavy scalars may be dynamically decoupled from the lighter degrees of freedom, but this does not mean their spectrum can be arbitrary. In fact, the heavy scalars display the same pattern of mass splitting shown in Eq. (3.34) as the lighter Higgses. Put simply, decoupling does not imply structural independence of the two sectors.

We also stress that the 2HDM-like model emerging after decoupling of the heavier scalars is not the general 2HDM but a rather constrained version of it. It closely resembles the 2HDM equipped with an approximate  $\mathbb{Z}_2$  symmetry and further constrained by additional relations among parameters. Investigation of the phenomenological features of the resulting 2HDM-like model deserves a dedicated study.

#### 3.2.6 Decays of Non-Standard Higgses

In the parent  $\Sigma(36)$  3HDM, each of the possible minima is still invariant under a subgroup of  $\Sigma(36)$ . As a result, the scalar spectrum contains states stabilized against decay by these residual symmetries. In particular, tree-level trilinear couplings of such states to  $h_{SM}$  pairs are all vanishing. However, the vev alignment preserving soft-breaking terms, in general, remove all the symmetries from the model. As a result, the Higgses which were previously stabilized by residual symmetries are not protected anymore and can decay to the SM-like Higgses and further to the SM fields.

To understand how these decays proceed, suppose that  $h_1$  is the lightest non-SM-like scalar. In the parent symmetric model, we had very few trilinear couplings involving  $h_1$ . With the soft-breaking terms, one adds a few more terms, but the interaction vertices  $h_1h_{SM}h_{SM}$  and  $h_1h_{SM}h_{SM}h_{SM}$  which could generate tree-level decays of  $h_1$  are still absent. Thus, there is no tree-level path to the decay of  $h_1$ .

Next, we checked scalar combinations which could lead to one-loop decays through the diagrams shown in Fig. 3.2. We found that there exist matching trilinear and quartic couplings ( $h_1XY$  and  $XYh_{SM}h_{SM}$  for topology 1,  $h_1h_{SM}XY$  and  $XYh_{SM}$  for topology 2) which share the same pairs of scalars XY. These matching pairs appear only with soft-breaking terms; they were absent in the symmetric model.

These diagrams induce decay of  $h_1$ , which may be suppressed due to a number of reasons (loop factors,

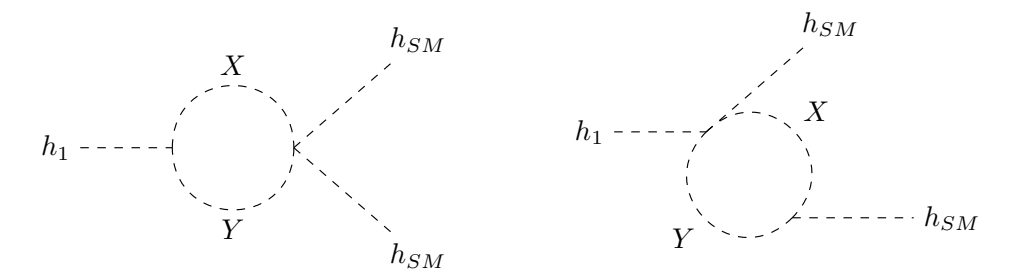


Figure 3.2: Scalar loop diagrams inducing  $h_1 \to h_{SM} h_{SM}$  decays in the softly-broken  $\Sigma(36)$  3HDM, where X, Y denote any scalar field.

small couplings, subthreshold effects for  $m_{h_1} < 2m_{h_{SM}}$ ). If this suppression is significant, it may lead to displaced vertex signals which could be seen at colliders. Calculation of these decays should be an important part of a detailed phenomenological study of the softly-broken  $\Sigma(36)$  3HDM.

#### 3.3 Discussion

Historically, multi-Higgs-doublet models with large symmetry groups triggered interest thanks to the opportunities they offered to link hierarchical quark masses and mixing patterns as well as the amount of CP violation with symmetry group properties. It turned out, however, that large exact discrete symmetry groups are too restrictive and run into conflict with quark properties [110, 215]. This obstacle can be avoided if the large symmetry group is softly-broken by quadratic terms in the potential. However, the large number of new free parameters associated with the general soft-breaking terms come makes a straightforward analysis of their consequences — and even the presentations of the results — rather cumbersome. One needs additional methods capable of indicating which directions in the soft-breaking parameter space are linked to which kind of phenomenological signals.

We dedicated this chapter to such methods. Relying on the fact that multi-Higgs models with large discrete symmetry groups lead to very specific vev alignments, we asked which soft-breaking terms could preserve a chosen alignment and found a general constructive answer through an eigenvector-based procedure.

We illustrated this procedure with the 3HDM example based on the softly-broken symmetry group  $\Sigma(36)$ . Out of the nine soft-breaking parameters, we identified five which preserve the vev alignment and four which break it. Focusing on the vev-alignment preserving terms, we investigated scalar alignment, physical Higgs masses and their relations, the global vs. local minimum distinction, stable vs. unstable scalars, existence of the SM-like and 2HDM-like decoupling limits. Remarkably, although the softly-broken model does not possess any exact symmetry, we found that is still possesses several structural properties inherited from the parent  $\Sigma(36)$ -symmetric 3HDM. They included scalar alignment, certain relations among Higgs masses, and peculiar form of decoupling to a 2HDM-like model (that is, decoupling does not imply complete independence).

The vision which emerges from this study will guide further detailed phenomenological studies of softly-broken symmetry models. If one asks for specific signatures from softly-broken symmetries, this procedure will indicate which parameters must be taken into account and which are inessential.

# Diluting Quark Hierarchies with $D_4$

Non-Abelian symmetries can severely reduce the freedom of the scalar sector of the theory, such that the inclusion of soft-breaking terms may become necessary to comply with experimental data. However, these theories can still end up being restrictive to the point of introducing interesting correlations, even in the softly-broken regime. Besides the study of the scalar potential, it is also necessary to investigate if the Yukawa sector can be correctly accommodated. Interestingly, it is possible to connect the emerging correlations between different sectors of the theory, fruit of the restrictive nature of the symmetries. Thus, we now turn to the Yukawa sector of a model endowed with a non-Abelian symmetry.

The SM successfully explains the mechanism responsible for the fermion masses but does not justify them. The arbitrariness of the Yukawa couplings makes the SM adaptable to any spectrum of fermion masses and mixings brought in by the experimental measurements. As it happens, the observed quark masses span five orders of magnitudes, with the third generation of quarks being much heavier than the first two. Furthermore, the quark mixings obey the following hierarchical pattern [108]:

$$V \approx \begin{pmatrix} 1 - \lambda^2/2 & -\lambda & \mathcal{O}(\lambda^3) \\ \lambda & 1 - \lambda^2/2 & \mathcal{O}(\lambda^2) \\ \mathcal{O}(\lambda^3) & \mathcal{O}(\lambda^2) & 1 \end{pmatrix}, \tag{4.1}$$

where  $\lambda \approx 0.22$  is the Cabibbo mixing parameter and the matrix, V, is known as the CKM matrix [19, 20, 83]. Within the ambit of SM, such hierarchies can only originate from some conspiracies within the Yukawa couplings themselves [241] and indeed the hierarchical structure of the masses and mixing are completely disconnected. This aspect of the SM has, for decades, fueled speculations that there might exist a deeper theoretical framework which can offer a more natural insight into the flavour structure. This chapter, which follows ref. [242], presents an extension of the SM with a  $D_4$  symmetry, which can make the quark flavour structure appear more instinctive (for other works on flavour models using  $D_4$  symmetry, see [? ? ? ? ? ? ? ? ? ? ? ? ? ]). An essential ingredient of our model is that the primary sources of masses for the third generation of quarks have been disentangled from those for the first two generations of quarks. The hierarchies in the quark masses and mixings are then chiefly attributed to

the hierarchies in the vacuum expectation values of the different scalar fields. This allows us to relax the Yukawa hierarchies in the quark sector considerably along with some new and interesting implications for the CKM matrix.

We start by laying out some of the basics of  $D_4$  symmetry [88]. The discrete group  $D_4$  has five irreducible representations which we label as  $\mathbf{1}_{++}$ ,  $\mathbf{1}_{--}$ ,  $\mathbf{1}_{-+}$ ,  $\mathbf{1}_{+-}$ , and  $\mathbf{2}$ . For the two-dimensional representation of  $D_4$ , we opt to work in a basis in which the generators of  $D_4$  are given by

$$a = \begin{bmatrix} 0 & -1 \\ 1 & 0 \end{bmatrix}, \qquad b = \begin{bmatrix} 1 & 0 \\ 0 & -1 \end{bmatrix}, \tag{4.2}$$

where a is of order 4 and b is of order 2. In this basis, the relevant tensor products in the explicit component form are given by [243]

$$\begin{bmatrix} x_1 \\ x_2 \end{bmatrix}_{\mathbf{2}} \otimes \begin{bmatrix} y_1 \\ y_2 \end{bmatrix}_{\mathbf{2}} = \begin{bmatrix} x_1 y_1 + x_2 y_2 \end{bmatrix}_{\mathbf{1}_{++}} \oplus \begin{bmatrix} x_1 y_2 - x_2 y_1 \end{bmatrix}_{\mathbf{1}_{+-}} \\
\oplus \begin{bmatrix} x_1 y_2 + x_2 y_1 \end{bmatrix}_{\mathbf{1}_{--}} \oplus \begin{bmatrix} x_1 y_1 - x_2 y_2 \end{bmatrix}_{\mathbf{1}_{-+}}, \qquad (4.3a)$$

$$\mathbf{1}_{\mathbf{7},\mathbf{8}} \otimes \mathbf{1}_{\mathbf{7}',\mathbf{8}'} = \mathbf{1}_{\mathbf{7}',\mathbf{8}',\mathbf{8}'}. \qquad (4.3b)$$

Now we will specify the  $D_4$  transformations of the different fields in our model. The *i*-th generation of left-handed quark doublet is denoted by  $Q_{iL} \equiv (p_{iL}, n_{iL})^T$ . The right-handed charged quark singlets are denoted by  $p_{iR}$  and  $n_{iR}$  in the up and down sectors, respectively. We have four scalar doublets in our model, which we symbolize as  $\phi_1$ ,  $\phi_2$ ,  $\phi_u$  and  $\phi_d$ . These fields are assumed to transform under the  $D_4$  symmetry as follows:

$$\mathbf{2}: \begin{bmatrix} Q_{1L} \\ Q_{2L} \end{bmatrix}, \begin{bmatrix} \phi_1 \\ \phi_2 \end{bmatrix}, \quad \mathbf{1}_{++}: n_{1R}, \quad \mathbf{1}_{+-}: n_{2R}, n_{3R}, \phi_u, \\ \mathbf{1}_{-+}: Q_{3L}, p_{1R}, \quad \mathbf{1}_{--}: p_{2R}, p_{3R}, \phi_d.$$
 (4.4)

As we will see shortly, because of the above transformations,  $\phi_u$  and  $\phi_d$  will couple exclusively to the up and down type quarks respectively, justifying their labelling. The Yukawa Lagrangian in the up and down quark sectors are then given by

$$\begin{split} -\mathcal{L}_{u} &= A_{u}(\overline{Q}_{1L}\widetilde{\phi}_{1} - \overline{Q}_{2L}\widetilde{\phi}_{2})p_{1R} + B_{u}(\overline{Q}_{1L}\widetilde{\phi}_{2} + \overline{Q}_{2L}\widetilde{\phi}_{1})p_{2R} + C_{u}(\overline{Q}_{1L}\widetilde{\phi}_{2} + \overline{Q}_{2L}\widetilde{\phi}_{1})p_{3R} \\ &+ X_{u}\overline{Q}_{3L}\phi_{u}p_{2R} + Y_{u}\overline{Q}_{3L}\phi_{u}p_{3R} \,, \\ -\mathcal{L}_{d} &= A_{d}(\overline{Q}_{1L}\phi_{1} + \overline{Q}_{2L}\phi_{2})n_{1R} + B_{d}(\overline{Q}_{1L}\phi_{2} - \overline{Q}_{2L}\phi_{1})n_{2R} + C_{d}(\overline{Q}_{1L}\phi_{2} - \overline{Q}_{2L}\phi_{1})n_{3R} \\ &+ X_{d}\overline{Q}_{3L}\phi_{d}n_{2R} + Y_{d}\overline{Q}_{3L}\phi_{d}n_{3R} \,, \end{split} \tag{4.5b}$$

where  $\widetilde{\phi}_k = i\sigma_2 \phi_k^*$  with  $\sigma_2$  being the second Pauli matrix. For an intuitive understanding of the upcoming results, we will assume the Yukawa parameters to be real. As such, we will not deliberate so much on the complex phase of the CKM matrix. We will treat the phase as an independent parameter which, as we have checked, can be easily accommodated by allowing the Yukawa couplings to be complex. The mass

matrices in the up and down sector that transpire from Eq. (4.5) are

$$M_{u} = \begin{pmatrix} A_{u}v_{1} & B_{u}v_{2} & C_{u}v_{2} \\ -A_{u}v_{2} & B_{u}v_{1} & C_{u}v_{1} \\ 0 & X_{u}v_{u} & Y_{u}v_{u} \end{pmatrix}, \quad M_{d} = \begin{pmatrix} A_{d}v_{1} & B_{d}v_{2} & C_{d}v_{2} \\ A_{d}v_{2} & -B_{d}v_{1} & -C_{d}v_{1} \\ 0 & X_{d}v_{d} & Y_{d}v_{d} \end{pmatrix}, \tag{4.6}$$

where  $v_1, v_2, v_u$  and  $v_d$  represents the vevs of  $\phi_1, \phi_2, \phi_u$  and  $\phi_d$  respectively with the total electroweak vev, v, being defined through the relation

$$v^2 = v_1^2 + v_2^2 + v_2^2 + v_d^2 \approx (174 \text{ GeV})^2$$
. (4.7)

The diagonal mass matrices can then be obtained via the following biunitary transformations:

$$D_u = U_u^{\dagger} M_u V_u = \operatorname{diag}(m_u, \ m_c, \ m_t), \qquad (4.8a)$$

$$D_d = U_d^{\dagger} M_d V_d = \text{diag}(m_d, m_s, m_b).$$
 (4.8b)

Following this convention for the biunitary transformations, the CKM matrix will be given by

$$V_{\rm CKM} = U_u^{\dagger} U_d \,. \tag{4.9}$$

The matrices  $U_u$  and  $U_d$  are obtained by diagonalizing  $M_u M_u^{\dagger}$  and  $M_d M_d^{\dagger}$  respectively, and, as a matter of fact, both  $M_u M_u^{\dagger}$  and  $M_d M_d^{\dagger}$  can be fully diagonalized analytically with

$$O_{\beta} = \begin{pmatrix} \cos \beta & -\sin \beta & 0 \\ \sin \beta & \cos \beta & 0 \\ 0 & 0 & 1 \end{pmatrix}, \quad O_{\theta}^{u,d} = \begin{pmatrix} 1 & 0 & 0 \\ 0 & \cos \theta_{u,d} & -\sin \theta_{u,d} \\ 0 & \sin \theta_{u,d} & \cos \theta_{u,d} \end{pmatrix}, \tag{4.10}$$

where  $\tan \beta = v_2/v_1$  and  $\theta_{u,d}$  will be defined shortly. As a first step, we notice that  $M_u M_u^{\dagger}$  and  $M_d M_d^{\dagger}$ can be block-diagonalized using  $O_{\beta}$  as

$$O_{\beta}M_{u}M_{u}^{\dagger}O_{\beta}^{\dagger} = \begin{pmatrix} A_{u}^{2}v_{12}^{2} & 0 & 0\\ 0 & (B_{u}^{2} + C_{u}^{2})v_{12}^{2} & (C_{u}Y_{u} + B_{u}X_{u})v_{12}v_{u}\\ 0 & (C_{u}Y_{u} + B_{u}X_{u})v_{12}v_{u} & (Y_{u}^{2} + X_{u}^{2})v_{u}^{2} \end{pmatrix}, \qquad (4.11a)$$

$$O_{\beta}^{\dagger}M_{d}M_{d}^{\dagger}O_{\beta} = \begin{pmatrix} A_{d}^{2}v_{12}^{2} & 0 & 0\\ 0 & (B_{d}^{2} + C_{d}^{2})v_{12}^{2} & -(C_{d}Y_{d} + B_{d}X_{d})v_{12}v_{d}\\ 0 & -(C_{d}Y_{d} + B_{d}X_{d})v_{12}v_{d} & (Y_{d}^{2} + X_{d}^{2})v_{d}^{2} \end{pmatrix}, \qquad (4.11b)$$

$$O_{\beta}^{\dagger} M_d M_d^{\dagger} O_{\beta} = \begin{pmatrix} A_d^2 v_{12}^2 & 0 & 0 \\ 0 & (B_d^2 + C_d^2) v_{12}^2 & -(C_d Y_d + B_d X_d) v_{12} v_d \\ 0 & -(C_d Y_d + B_d X_d) v_{12} v_d & (Y_d^2 + X_d^2) v_d^2 \end{pmatrix},$$
(4.11b)

where  $v_{12}^2 = v_1^2 + v_2^2$  is the total vev that is primarily responsible for the light quark masses. Quite clearly, the remaining  $2 \times 2$  block in the up and down sectors can be diagonalized using  $O_{\theta}^{u}$  and  $O_{\theta}^{d}$ , respectively, given:

$$\tan 2\theta_u = \frac{2(C_u Y_u + B_u X_u) v_{12} v_u}{(Y_u^2 + X_u^2) v_u^2 - (B_u^2 + C_u^2) v_{12}^2},$$
(4.12a)

$$\tan 2\theta_u = \frac{2(C_u Y_u + B_u X_u) v_{12} v_u}{(Y_u^2 + X_u^2) v_u^2 - (B_u^2 + C_u^2) v_{12}^2},$$

$$\tan 2\theta_d = -\frac{2(C_d Y_d + B_d X_d) v_{12} v_d}{(Y_d^2 + X_d^2) v_d^2 - (B_d^2 + C_d^2) v_{12}^2}.$$
(4.12a)

Thus, the full diagonalization in the up and down sectors can be expressed as

$$D_u^2 = O_\theta^u O_\beta(M_u M_u^\dagger) O_\beta^\dagger O_\theta^{u\dagger} \equiv \operatorname{diag}(m_u^2, m_c^2, m_t^2), \qquad (4.13a)$$

$$D_d^2 = O_\theta^d O_\beta^\dagger (M_d M_d^\dagger) O_\beta O_\theta^{d\dagger} \equiv \operatorname{diag}(m_d^2, m_s^2, m_b^2). \tag{4.13b}$$

Following our convention in Eq. (4.8),

$$U_u^{\dagger} = O_{\theta}^u O_{\beta}, \qquad U_d^{\dagger} = O_{\theta}^d O_{\beta}^{\dagger}.$$
 (4.14)

and, from Eq. (4.9), the CKM matrix is

$$V_{\text{CKM}} = \begin{pmatrix} \cos 2\beta & -\cos \theta_d \sin 2\beta & -\sin 2\beta \sin \theta_d \\ \cos \theta_u \sin 2\beta & \cos 2\beta \cos \theta_d \cos \theta_u + \sin \theta_d \sin \theta_u & \cos 2\beta \cos \theta_u \sin \theta_d - \cos \theta_d \sin \theta_u \\ \sin 2\beta \sin \theta_u & -\cos \theta_u \sin \theta_d + \cos 2\beta \cos \theta_d \sin \theta_u & \cos \theta_d \cos \theta_u + \cos 2\beta \sin \theta_d \sin \theta_u \end{pmatrix}. \tag{4.15}$$

To make the connection between Eqs. (4.15) and (4.1) apparent, we assume that  $v_{12}$  is responsible for the masses of the first two generations of quarks whereas  $v_u$  and  $v_d$  primarily contribute to the third generation masses in the up and down sector, respectively. Therefore, it is quite natural to expect  $v_{12} \ll v_{u,d}$ . From Eq. (4.11) we identify the first generation quark masses as

$$m_u^2 = A_u^2 v_{12}^2, \qquad m_d^2 = A_d^2 v_{12}^2.$$
 (4.16)

Furthermore, using the vev hierarchy  $v_{u,d} \gg v_{12}$  we can approximate Eq. (4.12) as

$$\theta_u \approx \frac{\left(C_u Y_u + B_u X_u\right)}{\left(Y_u^2 + X_u^2\right)} \frac{v_{12}}{v_u} \approx \mathcal{O}\left(\frac{v_{12}}{v_u}\right),$$
(4.17a)

$$\theta_d \approx -\frac{(C_d Y_d + B_d X_d)}{(Y_d^2 + {X_d}^2)} \frac{v_{12}}{v_d} \approx \mathcal{O}\left(\frac{v_{12}}{v_d}\right),$$
(4.17b)

where we are implicitly assuming that the involved Yukawa couplings have similar orders of magnitude. It is also quite reasonable to take  $v_{12} \sim \mathcal{O}(1 \text{ GeV})$  and  $v_{u,d} \sim \mathcal{O}(100 \text{ GeV})$  so that the ratio  $v_{12}/v_{u,d}$ comes out to be  $\mathcal{O}(\lambda^2)$ . Therefore, from Eq. (4.17) we conclude

$$\sin \theta_{u,d} \approx \mathcal{O}\left(\lambda^2\right), \qquad \cos \theta_{u,d} \approx \mathcal{O}\left(1\right).$$
 (4.18)

Moreover, if we identify  $\sin 2\beta$  as the Cabibbo mixing, namely,

$$\sin 2\beta = \lambda \,, \tag{4.19}$$

then Eq. (4.15) resembles Eq. (4.1). All these intuitive results will be validated later by providing explicit numerical benchmarks.

Given the structure of the CKM matrix predicted by the model as a function of  $\beta$  and  $\theta_{u,d}$ , shown in Eq. (4.15), it is possible to extract the quark mixing angles by comparing the CKM matrix with the standard parametrization [244]. This, in turn, allows us to find the following best-fit values of  $\beta$  and  $\theta_{u,d}$  such that the quark mixing angles are compatible with the observed values [245]:

$$\sin 2\beta \approx 0.2265$$
,  $\theta_u \approx \pm 0.025$ ,  $\theta_d \approx \mp 0.016$ . (4.20)

As expected, the above values for  $\sin 2\beta$  and  $\theta_{u,d}$  conform well to our intuitive expectations of Eqs. (4.18) and (4.19). Fixing  $\sin 2\beta$  at its best-fit value, in Fig. 4.1 we display one region in  $\sin \theta_u$ -  $\sin \theta_d$  plane allowed by the experimental uncertainties.

For the sake of completeness, we also calculate the mass eigenvalues for the second and third generation of quarks by diagonalizing the  $2 \times 2$  submatrices in Eq. (4.11). In the up quark sector, we can compare the traces to write

$$m_c^2 + m_t^2 = (B_u^2 + C_u^2)v_{12}^2 + (Y_u^2 + X_u^2)v_u^2. (4.21)$$

Keeping in mind the hierarchies,  $v_u \gg v_{12}$  and  $m_t \gg m_c$ , the above relation can be approximated to express the top quark mass as

$$m_t^2 \approx (Y_u^2 + X_u^2)v_u^2$$
. (4.22)

Again, from the determinant of the  $2 \times 2$  block in Eq. (4.11a), we may write

$$m_c^2 m_t^2 = (B_u Y_u - C_u X_u)^2 v_{12}^2 v_u^2$$
. (4.23)

Using the expression for  $m_t$  from Eq. (4.22), we can extract the charm quark mass as

$$m_c^2 \approx \frac{(B_u Y_u - C_u X_u)^2}{(Y_u^2 + X_u^2)} v_{12}^2$$
. (4.24)

Following the same steps in the down sector, we can obtain

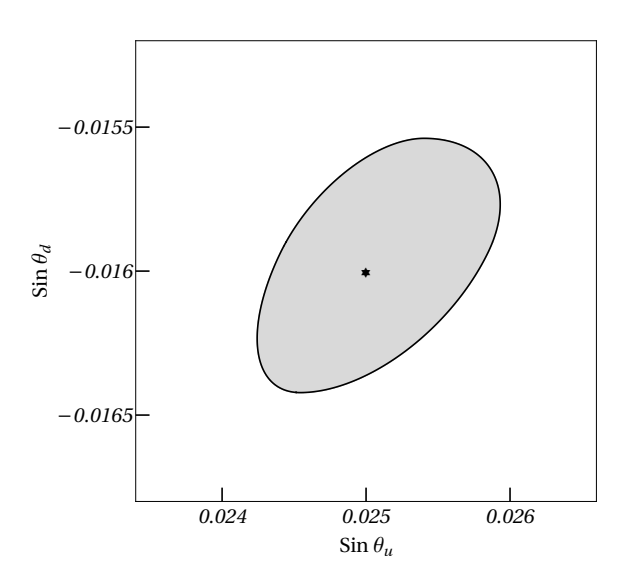
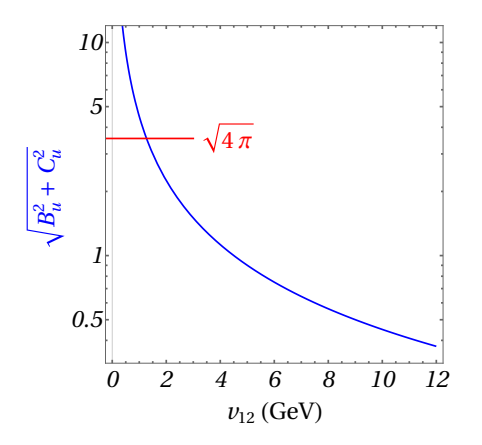


**Figure 4.1:** A representative allowed region in the  $\sin \theta_u$ -  $\sin \theta_d$  plane from the mixing angle uncertainties, with  $\sin 2\beta \approx 0.2265$ . The best-fit point in the  $\sin \theta_u$ -  $\sin \theta_d$  plane is marked with a star  $(\star)$ .

$$m_s^2 \approx \frac{(B_d Y_d - C_d X_d)^2}{(Y_d^2 + X_d^2)} v_{12}^2,$$
 (4.25)

$$m_b^2 \approx (Y_d^2 + X_d^2)v_d^2$$
. (4.26)

At this point, we wish to emphasize that, assuming the Yukawas couplings to be similar for a particular



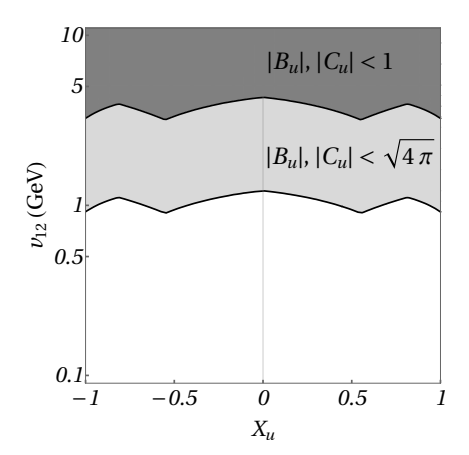


Figure 4.2: Left: Value of  $\sqrt{B_u^2 + C_u^2}$  compatible with the experimental values for the quark masses and mixing angles, for a benchmark point of  $X_u = 0.9$ , as a function of  $v_{12}$ . In red, an approximate perturbativity bound is shown. Right:  $|B_u|$  and  $|C_u|$  are perturbative in the light-grey shaded region in the  $X_u$ -  $v_{12}$  plane. In a darker shade, we show the region where  $B_u, C_u \leq 1$ , to showcase the behaviour with  $v_{12}$  more explicitly. We have assumed  $v_u = 150$  GeV and  $\sin \theta_u = 0.025$  for both cases.

sector, an obvious outcome of our model is

$$\frac{m_c}{m_t} \approx \frac{v_{12}}{v_u} \sim \mathcal{O}\left(\lambda^2\right) \,, \qquad \frac{m_s}{m_b} \approx \frac{v_{12}}{v_d} \sim \mathcal{O}\left(\lambda^2\right) \,, \tag{4.27}$$

which agrees with the observations.

From Eqs. (4.22) and (4.24), we see that the third and second generation masses are controlled by  $v_u$  and  $v_{12}$ , respectively. We can wonder how perturbativity may affect the model at hand, since  $m_t \approx \mathcal{O}(v_u)$  and  $m_c \approx \mathcal{O}(v_{12})$  already [246]. Fig. 4.2 illustrates how arbitrarily low values of  $v_{12}$  may jeopardize the perturbativity of the theory. Given Eqs. (4.21) and (4.22), the value of  $\sqrt{B_u^2 + C_u^2}$  is approximately independent of  $Y_u$  and  $X_u$ . So, by choosing a benchmark example of  $v_u = 150$  GeV and  $X_u = 0.9$ , we can see from Fig. 4.2 that to have  $B_u$  and  $C_u$  in the perturbative regime, we should have  $v_{12} \gtrsim \mathcal{O}(1 \text{ GeV})$ .

Finally, to provide explicit justification to these intuitive expectations, we consider the following benchmark

$$\begin{split} v_{12} &= 2 \text{ GeV}, & v_u &= 150 \text{ GeV}, & v_d \approx 88 \text{ GeV}, \\ A_u &\approx 1.08 \times 10^{-3}, & B_u \approx 1.69, & C_u \approx 1.50, & X_u \approx 1.04, & Y_u \approx 0.49, \\ A_d &\approx 2.34 \times 10^{-3}, & B_d \approx 3.65 \times 10^{-2}, & C_d \approx 4.41 \times 10^{-2}, & X_d \approx 4.73 \times 10^{-2}, & Y_d \approx -3.20 \times 10^{-3}, \end{split} \tag{4.28}$$

which results in the following values of the quark masses and mixing angles

$$m_u = 2.2 \text{ MeV}, \qquad m_c = 1.27 \text{ GeV}, \qquad m_t = 173 \text{ GeV},$$
 (4.29a)

$$m_d = 4.7 \text{ MeV}, \qquad m_s = 0.093 \text{ GeV}, \qquad m_b = 4.18 \text{ GeV}$$
 (4.29b)

$$\sin \theta_{12} = 0.2265$$
,  $\sin \theta_{13} = 0.0036$ ,  $\sin \theta_{23} = 0.041$ , (4.29c)

which are in agreement with the corresponding observations [245].

In passing, let us highlight the most notable outcomes of our construction:

- The hierarchy of the Yukawa couplings is diluted by two orders of magnitude, at least. Recall that, in the SM,  $m_t = 174$  GeV and  $m_{u,d} \sim \mathcal{O}\left(10^{-3} \text{ GeV}\right)$  imply that the quark Yukawa couplings span five orders of magnitudes. We dampen this problem by assuming that the first two generations of quarks receive their masses from  $v_{12}$  which is of  $\mathcal{O}(1 \text{ GeV})$ . This means, the first generation Yukawas are, at worst, of  $\mathcal{O}\left(10^{-3}\right)$  whereas the second generation Yukawas can be of  $\mathcal{O}(1)$ . This feature is quite evident from the benchmark values given in Eq. (4.28).
- We have introduced  $\phi_{u,d}$  dedicated for masses of the third generation of quarks. Quite naturally, we expect,  $v_{u,d} \sim \mathcal{O}$  (100 GeV) so that the top-Yukawa is of  $\mathcal{O}$  (1). Thus, we should have the ratio  $v_{12}/v_{u,d} \sim \mathcal{O}(\lambda^2)$ . It is very interesting to note that, this automatically conforms to  $m_2/m_3 \approx v_{12}/v_{u,d} \sim \mathcal{O}(\lambda^2)$  where  $m_k$  is the mass for the k-th generation of quark.
- The quark mixing becomes connected with the dynamics of the scalar sector. Indeed, the Cabibbo part of the quark-mixing stems purely from the ratio  $v_2/v_1$  (see Eq. (4.19)). The smallness of the off-Cabibbo elements of the CKM matrix is further connected to the vev hierarchy  $v_{12} \ll v_{u,d}$ . Thus, contrary to the SM, the fact that the third generation of quarks are much heavier than the first two generations, is intimately connected to the smallness of the off-Cabibbo elements.

Finally, apart from the connection between quark mixing and the scalar dynamics, this construction will have other observable consequences too. The design of the model comes at the cost of making the scalar potential substantially more involved, containing four scalar doublets. This means that the Higgs boson observed at the LHC is not the only fundamental scalar in nature, it is just the first one in series of many others to follow. The physical Higgs bosons will emerge from mixings among the four scalar doublets. Expanding the scalar doublets as

$$\phi_k = \begin{pmatrix} \varphi_k^+ \\ v_k + (h_k + iz_k)/\sqrt{2} \end{pmatrix}, \qquad k = 1, 2, u, d,$$
 (4.30)

after the spontaneous symmetry breaking, the SM-like Higgs boson, h, can be extracted as [56–58, 67] (recall the discussion in Section 1.2.1):

$$h = \frac{1}{v}(v_1h_1 + v_2h_2 + v_uh_u + v_dh_d). \tag{4.31}$$

In the alignment limit, this particular linear combination of the component fields will mimic the SM Higgs in its tree-level couplings and will not induce FCNCs at the tree-level. However, the other physical neutral scalars, in general, will possess tree-level FCNCs which means they have to be quite heavy to evade the experimental constraints.

To have some intuitions on the FCNC couplings, we analyze the matrices,  $N_d^{1,2,d}$ , which control them in the down sector [59]:

$$\mathcal{L}_{ddh_i} \supset h_i \left( \overline{d_L} N_d^i d_R + \text{h.c.} \right), \quad \text{where} \quad N_d^i = \frac{1}{\sqrt{2}} U_d \Gamma_i V_d^{\dagger}.$$
 (4.32)

The off-diagonal entries of  $N_d^i$  are responsible for the flavour-changing couplings with the flavour-basis scalars,  $\phi_i$ . A further rotation to the scalar physical basis is required to compute the actual FCNC couplings with the massive scalars, and will come with a suppression stemming from the fact that  $\phi_d$  $(\phi_u)$  does not couple to the up-type (down-type) quarks.

We can approximate  $V_d$  from  $M^{\dagger}M$ :

$$M^{\dagger}M = \begin{pmatrix} A_d^2 v_{12}^2 & 0 & 0 \\ 0 & B_d^2 v_{12}^2 + X_d^2 v_d^2 & B_d C_d v_{12}^2 + X_d Y_d v_d^2 \\ 0 & B_d C_d v_{12}^2 + X_d Y_d v_d^2 & C_d^2 v_{12}^2 + Y_d^2 v_d^2 \end{pmatrix} \approx \begin{pmatrix} A_d^2 v_{12}^2 & 0 & 0 \\ 0 & X_d^2 v_d^2 & X_d Y_d v_d^2 \\ 0 & X_d Y_d v_d^2 & Y_d^2 v_d^2 \end{pmatrix}, (4.33)$$

given that  $v_d \gg v_{12}$ . The diagonalisation relies on a single angle,  $\alpha_d$ ,

$$V_d = \begin{pmatrix} 1 & 0 & 0 \\ 0 & \cos \alpha_d & -\sin \alpha_d \\ 0 & \sin \alpha_d & \cos \alpha_d \end{pmatrix}, \quad \text{with} \quad \tan \alpha_d \approx \frac{X_d}{Y_d},$$
 (4.34)

which allows us to write

$$N_d^1 \approx \frac{1}{\sqrt{2}v_{12}} \begin{pmatrix} m_d \cos \beta & -m_s \sin \beta & m_b \theta_d \sin \beta \\ -m_d \sin \beta & -m_s \cos \beta & m_b \theta_d \cos \beta \\ -m_d \theta_d \sin \beta & -m_s \theta_d \cos \beta & m_b \theta_d^2 \cos \beta \end{pmatrix}, \tag{4.35a}$$

$$N_d^2 \approx \frac{1}{\sqrt{2}v_{12}} \begin{pmatrix} m_d \sin \beta & m_s \cos \beta & -m_b \theta_d \cos \beta \\ m_d \cos \beta & -m_s \sin \beta & m_b \theta_d \sin \beta \\ m_b \theta_d \cos \beta & -m_s \theta_d \sin \beta & m_b \theta_d^2 \sin \beta \end{pmatrix}, \tag{4.35b}$$

$$N_d^2 \approx \frac{1}{\sqrt{2}v_{12}} \begin{pmatrix} m_d \sin \beta & m_s \cos \beta & -m_b \theta_d \cos \beta \\ m_d \cos \beta & -m_s \sin \beta & m_b \theta_d \sin \beta \\ m_b \theta_d \cos \beta & -m_s \theta_d \sin \beta & m_b \theta_d^2 \sin \beta \end{pmatrix}, \tag{4.35b}$$

$$N_d^d \approx \frac{1}{\sqrt{2}v_d} \begin{pmatrix} 0 & 0 & 0 \\ 0 & 0 & -m_b \theta_d \\ 0 & 0 & m_b \end{pmatrix}. \tag{4.35c}$$

From the above expressions, we note that the magnitude of the largest off-diagonal element, for our chosen benchmarks of Eqs. (4.20) and (4.28), is 0.033. On top of this, the flavour constraints may be further relaxed if we remember the following points:

- The actual FCNC matrices that control the couplings of the physical neutral scalars are orthogonal linear combinations (dictated by the scalar potential) of  $N_d^1$ ,  $N_d^2$ ,  $N_d^d$  and  $N_d^u$  where  $N_d^u=0$  simply because  $h_u$  does not couple to the down-type quarks.
- A cancellation may be arranged between the scalar and pseudoscalar diagrams appearing in the FCNC process [247].

Furthermore, it should also be noted that low values of the vevs, especially  $v_{12} \sim \mathcal{O}(1 \text{ GeV})$ , will not necessarily imply the existence of light nonstandard scalars if we include terms that softly break the  $D_4$ symmetry in the scalar potential [200–202]. The complete analysis of the scalar potential would be quite complex, although with possibly interesting phenomenology. However, we note that the  $D_4$  group is a subgroup of larger groups, such that there is, in principle, a parametric region (if we include soft-breaking terms) which complies with theoretical constraints and allows for the decoupling limit. Nevertheless, this design can be considered as a proof-of-concept for the idea that it might be possible to ascribe the quark flavour hierarchies primarily to the hierarchies in the vevs all of which add together to constitute the total electroweak vev.<sup>1</sup>

 $<sup>^{1}</sup>$ This is in stark contrast with the Froggatt-Nielsen mechanism [107], where flavon vevs are usually much higher than the electroweak scale.

## Crossed 2HDMs

Interestingly, flavour symmetries are not the only way to introduce flavour relations in a theory. Flavour symmetries rely on enlarging the gauge group with global symmetries, such that the model becomes a subset of the parametric space of the initial theory (through symmetry arguments, which also protect the ensuing relations from higher-order perturbations). This serves the purpose of reducing the free parameters of the theory, and can lead to testable correlations between observables. On the other hand, since these symmetries are global, the successes of the gauge principle is emulated, but not fully mimicked. The requirement that theories must be locally-invariant under some (continuous) symmetry forcibly leads to the existence of gauge bosons, and a plethora of phenomena whose low-energy consequences may be hard to mitigate. As such, enlarging the SM's gauge group can lead to interesting predictions for NP processes. That is to be expected, but it is not the only consequence. Inspecting the idea behind gauge extensions, it becomes obvious that the matter content of the theory must now be embedded onto a larger framework, to accommodate the new symmetries. Depending on the framework itself, this can easily lead to sources of flavour which stem not from an ad hoc horizontal symmetry, but rather from the embedding of the SM onto the gauge extension. As an example, SU(5) extensions require the SM (RH) down-type quarks and (LH) charged-leptons to be on the same SU(5) multiplet. If one takes the minimal scalar content, this forcibly leads to relations between their Yukawa interactions at the UV scale:  $Y_{\ell} = Y_d^T$ . In this way, we see that gauge extensions are able to introduce relations in the flavour sector of the SM, in a way that no flavour symmetry could, since they cannot connect particles with different quantum numbers. One more straightforward example is the case of the MSSM, whose holomorphicity requirement leads to a type-II 2HDM Yukawa structure. Now that we have seen that SM extensions can lead to similar successes of introducing flavour symmetries, we devote this chapter to the study of a class of 2HDMs whose Yukawa structure is constrained by symmetries which cannot, at the low-energy, be taken as flavour symmetries, but whose origin could, in principle, come from UV completions.

The SM features a minimal scalar content, and thus the quark mass matrices become proportional to the corresponding Yukawa matrices. Hence, diagonalizing the quark mass matrices will automatically

ensure the simultaneous diagonalization of the Yukawa matrices, and the SM Higgs boson has only diagonal couplings, proportional to the quark masses.

This straightforward picture may get perturbed even in the minimal BSM theories, such as the 2HDM, where the diagonalization of the fermion mass matrices will no longer guarantee the diagonalization of the Yukawa matrices. In other words, a 2HDM, in general, will contain FCNCs mediated by neutral scalars at the tree-level. Given that the FCNC couplings are, a priori, unknown, the analysis of the physical implications of a general 2HDM contains a lot of inherent arbitrariness.

As a simple way out, one tries to avoid the tree-level FCNCs altogether by appropriate adjustments in the Yukawa sector, as in NFC models, for example. An interesting alternative to completely eliminating the tree-level FCNCs is to accommodate them in a controlled manner. This was achieved by Branco, Grimus and Lavoura (BGL) [101], where the scalar FCNC couplings were related to the rows or columns of the CKM matrix [47, 248, 249]. In these BGL models, flavour symmetries were introduced to appropriately texturize the Yukawa matrices. In this chapter, we make an effort similar to BGL models, but with the additional assumption that the RH quark mixing is physical. In this way, we aim to connect, through (approximate) flavour-universal symmetries, the scalar FCNC couplings to the quark mixing parameters, thereby reducing the arbitrariness in the Yukawa sector to a considerable degree.

This chapter also addresses the philosophical relevance of 2HDMs in the present era. A major part of the popularity of 2HDMs may be attributed to minimal supersymmetry relying on a 2HDM scalar structure. However, current trends in the LHC Higgs data point towards a not so bright future for minimal supersymmetry. In such a case, one may question the aesthetic appeal of 2HDM, if it lacks the possibility to be embedded in a larger theory. However, the minimal left-right symmetric model (LRSM) also results in a 2HDM Yukawa structure at the electroweak scale [250], which will be very different from its canonical counterparts and can have quite distinct implications.

We will closely follow ref. [251], and present a brief overview of the general 2HDM Yukawa sector in Section 5.1, including, for convenience, an alternative notation. This is the usual notation of the LRSM, which helps the connection between 2HDM and LRSM become clear. This notation is particularly helpful in uncovering new models, which is done in Section 5.2. Some specificities of these models are shown in Section 5.3, and we include a small phenomenological analysis in Section 5.4. Lastly, we summarise our findings in Section 5.5.

#### 5.1 Yukawa Sector of 2HDMs:

## Some Generalities and Reducible Yukawa Couplings

In an effort to make each chapter self-contained, we go through some generalities of the Yukawa sector of 2HDMs, and establish the notation for the chapter. This should help make our goal clear, as well as introduce the bidoublet notation which will be helpful in our efforts.

#### 5.1.1 Quark Masses, Mixings and Couplings

We denote the quark fields in the original Lagrangian with primes:

$$Q'_{L} = \begin{pmatrix} u'_{L} \\ d'_{L} \end{pmatrix}, \qquad u'_{R}, \qquad d'_{R}, \tag{5.1}$$

where the generation index is suppressed. The Higgs boson multiplets  $\phi_1$  and  $\phi_2$  have a hypercharge assignment that yields the following general Yukawa couplings:

$$-\mathcal{L}_Y = \sum_{a=1}^2 \left[ \overline{Q}'_L \Gamma_a \phi_a d'_R + \overline{Q}'_L \Delta_a \widetilde{\phi}_a u'_R \right] + \text{h.c.}, \tag{5.2}$$

where  $\Gamma_a$  and  $\Delta_a$  denote matrices in the generation space, and

$$\widetilde{\phi}_a = i\sigma_2 \phi_a^* \,. \tag{5.3}$$

After SSB, we decompose the two  $SU(2)_L$  scalar doublets in their component form as follows:

$$\phi_a = \frac{1}{\sqrt{2}} \begin{pmatrix} \sqrt{2}w_a^+ \\ v_a + h_a + iz_a \end{pmatrix}, \qquad (a = 1, 2).$$
 (5.4)

We will assume that the vevs are real, and use the usual notations

$$\tan \beta = v_2/v_1$$
, and  $v = \sqrt{v_1^2 + v_2^2}$ . (5.5)

The quark mass matrices are given by

$$M_d = \frac{1}{\sqrt{2}} (\Gamma_1 v_1 + \Gamma_2 v_2) ,$$
 (5.6a)

$$M_u = \frac{1}{\sqrt{2}} (\Delta_1 v_1 + \Delta_2 v_2) .$$
 (5.6b)

These can be diagonalized through bi-unitary transformations:

$$U_u^{\dagger} M_u V_u = D_u = \operatorname{diag}(m_u, m_c, m_t). \tag{5.7a}$$

$$U_d^{\dagger} M_d V_d = D_d = \operatorname{diag}(m_d, m_s, m_b), \qquad (5.7b)$$

The usual CKM matrix is given by

$$V_L \equiv V_{CKM}^L = U_u^{\dagger} U_d \,, \tag{5.8}$$

and controls the couplings of the quarks with the SM charged-currents. Similarly, we can define a mixing matrix for the right-handed quarks:

$$V_R \equiv V_{CKM}^R = V_u^{\dagger} V_d \,. \tag{5.9}$$

Our aim is to search for models in which the Higgs couplings to quarks are entirely determined by  $V_L$  and  $V_R$ . Although  $V_R$  is unphysical in the SM, in models which feature RH charged-currents, this mixing becomes physical and measurable.

In order to discuss the Yukawa couplings, we first summarize the spectrum of the scalar bosons. The charged  $(\omega^{\pm})$  and the neutral  $(\zeta)$  Goldstone bosons can be extracted using the following rotations

$$\begin{pmatrix} \omega^{\pm} \\ H^{\pm} \end{pmatrix} = \begin{pmatrix} \cos \beta & \sin \beta \\ -\sin \beta & \cos \beta \end{pmatrix} \begin{pmatrix} w_1^{\pm} \\ w_2^{\pm} \end{pmatrix}, \qquad \begin{pmatrix} \zeta \\ A \end{pmatrix} = \begin{pmatrix} \cos \beta & \sin \beta \\ -\sin \beta & \cos \beta \end{pmatrix} \begin{pmatrix} z_1 \\ z_2 \end{pmatrix}, \tag{5.10}$$

where,  $H^{\pm}$  and A stand for the physical charged scalar and pseudoscalar respectively. In the CP even sector, we apply the same rotation to obtain

$$\begin{pmatrix} H_0 \\ S \end{pmatrix} = \begin{pmatrix} \cos \beta & \sin \beta \\ -\sin \beta & \cos \beta \end{pmatrix} \begin{pmatrix} h_1 \\ h_2 \end{pmatrix}. \tag{5.11}$$

The states  $H_0$  and S are not mass eigenstates in general. However, in the alignment limit [67? -69], they become physical scalars and  $H_0$  can be readily identified with Higgs scalar observed at the LHC because it possesses SM-like couplings at the tree-level. Thus the quark couplings of  $H_0$  are entirely flavour diagonal. Without the assumption of the alignment limit, the mass eigenstates would be superpositions of  $H_0$  and S, controlled by the parameters of the scalar potential. Hence, the quark couplings of the lightest scalar field would not be flavour diagonal due to the  $H_0$ -S mixture. Nonetheless, assuming the alignment limit holds, only the other neutral scalars, S and A, can have flavour-changing couplings to quarks, which will be an important theme in the subsequent discussion.

Defining  $N_d$  and  $N_u$  as [59]

$$N_d = \frac{1}{\sqrt{2}} U_d^{\dagger} \left( \sin \beta \, \Gamma_1 - \cos \beta \, \Gamma_2 \right) V_d \,, \tag{5.12a}$$

$$N_u = \frac{1}{\sqrt{2}} U_u^{\dagger} \Big( \sin \beta \, \Delta_1 - \cos \beta \, \Delta_2 \Big) V_u \,, \tag{5.12b}$$

the quark couplings with the different scalars can be written in the form

$$-\mathcal{L}_{Y} = \sqrt{2} \left[ \overline{u} \left( N_{u}^{\dagger} V_{L} P_{L} - V_{L} N_{d} P_{R} \right) d H^{+} + \text{h.c.} \right] + \frac{H_{0}}{v} \left( \overline{u} D_{u} u + \overline{d} D_{d} d \right)$$

$$- S \left\{ \overline{d} \left( N_{d} P_{R} + N_{d}^{\dagger} P_{L} \right) d + \overline{u} \left( N_{u} P_{R} + N_{u}^{\dagger} P_{L} \right) u \right\}$$

$$- i A \left\{ \overline{d} \left( N_{d} P_{R} - N_{d}^{\dagger} P_{L} \right) d - \overline{u} \left( N_{u} P_{R} - N_{u}^{\dagger} P_{L} \right) u \right\},$$

$$(5.12c)$$

where  $P_L$  and  $P_R$  are the chirality projection operators.

#### 5.1.2 Reducible Yukawa Couplings

From Eq. (5.12), we see that the couplings of the Higgs bosons depend on the four diagonalizing matrices  $U_u$ ,  $U_d$ ,  $V_u$  and  $V_d$ , as well as the matrices that appear in the Yukawa couplings. We now show that there is a class of models in which the Yukawa couplings are reducible, by which we mean that the

couplings are completely specified by the quark masses, and the left and right CKM matrices,  $V_L$  and  $V_R$ . The only dependence to the parameters of the Higgs potential is through the implicit dependence on the angle  $\beta$ . Clearly, this requires  $N_d$  and  $N_u$  to be able to be written in terms of  $V_L$  and  $V_R$ , apart from possible numerical factors.

The key to this reduction lies in the following observation. Suppose, in a given model, it is possible to write

$$\sin \beta \, \Gamma_1 - \cos \beta \, \Gamma_2 = \frac{\sqrt{2}}{v} (A_d M_d + B_d M_u), \qquad (5.13a)$$

$$\sin \beta \,\Delta_1 - \cos \beta \,\Delta_2 = \frac{\sqrt{2}}{v} (A_u M_u + B_u M_d), \qquad (5.13b)$$

with the numerical factors  $A_d$ ,  $B_d$ ,  $A_u$ ,  $B_u$ . Then Eq. (5.12) can be rewritten as

$$N_d = \frac{1}{v} U_d^{\dagger} \left( A_d M_d + B_d M_u \right) V_d$$
  
= 
$$\frac{1}{v} \left( A_d D_d + B_d V_L^{\dagger} D_u V_R \right), \qquad (5.14a)$$

$$N_u = \frac{1}{v} \left( A_u D_u + B_u V_L D_d V_R^{\dagger} \right). \tag{5.14b}$$

Therefore, if Eq. (5.13) holds, the Yukawa couplings will be completely determined by the quark masses and LH and RH mixing matrices.

However, it should be clear that it is not possible to write relations of the form of Eq. (5.13) in the most general case. Four general matrices,  $\Gamma_{1,2}$  and  $\Delta_{1,2}$ , cannot be written in terms of two matrices,  $M_d$  and  $M_u$ . Therefore, it is necessary to have only two independent Yukawa matrices. In order to achieve this, it is necessary to introduce some condition to restrict the Yukawa matrices.

We noticed in Eq. (5.12c) that the couplings of the neutral Higgs bosons, S and A, to the up-type and down-type quarks are governed by the matrices  $N_u$  and  $N_d$  respectively. From Eq. (5.14), we see that the parts governed by  $A_u$  and  $A_d$  are proportional to the diagonal mass matrices in the respective sector, and are therefore flavour diagonal. Thus, FCNC occurs only through the parts  $B_u$  and  $B_d$ , and are absent in a model where these parts vanish. In such models, the Higgs couplings are even independent of the quark mixing matrices. The conventional type-I and type-II 2HDMs constitute examples of this category, which will be discussed in Section 5.2.1. But the aim of this chapter is to uncover other interesting models where Eq. (5.13) holds, and  $B_u$  and  $B_d$  do not vanish.

#### 5.1.3 Notational Digression

In order to find nontrivial examples of 2HDMs where Eq. (5.13) holds we find it convenient to write the two doublets together, into what we will abusively call a bidoublet:

$$\Phi = \begin{pmatrix} \widetilde{\phi}_1 & \phi_2 \end{pmatrix} . \tag{5.15}$$

The transformation properties of the Higgs-doublets under the SM gauge symmetry can be expressed in a concise manner using the bidoublet:

$$\Phi \xrightarrow{SU(2)_L \times \mathrm{U}(1)_Y} \Sigma_L \Phi e^{-\frac{i}{2}\sigma_3\theta(x)}, \qquad (5.16)$$

where  $\Sigma_L$  denotes an element of  $SU(2)_L$  and the appearance of  $\sigma_3$  on the right takes care of the fact that the hypercharges of  $\phi_k$  and  $\widetilde{\phi}_k$  are opposite. It should now be noted that one can construct additional bidoublets as well, all of which have the same transformation properties under  $SU(2)_L \times U(1)_Y$  as  $\Phi$ :

$$\widetilde{\Phi} = \sigma_2 \Phi^* \sigma_2 \equiv \begin{pmatrix} \widetilde{\phi}_2 & \phi_1 \end{pmatrix}, \tag{5.17a}$$

$$\Psi = \Phi \sigma_3 \equiv \begin{pmatrix} \widetilde{\phi}_1 & -\phi_2 \end{pmatrix}, \qquad (5.17b)$$

$$\widetilde{\Psi} = \sigma_2 \Psi^* \sigma_2 \equiv \left( -\widetilde{\phi}_2 \quad \phi_1 \right).$$
 (5.17c)

In keeping with the bidoublet notation for the Higgs multiplets, the right-handed quark fields can be written in a column with two components. Note that the gauge transformation on this column can also be written in a succinct form:

$$\begin{pmatrix} u_R' \\ d_R' \end{pmatrix} \xrightarrow{SU(2)_L \times U(1)_Y} e^{+\frac{i}{6}\theta(x)} e^{+\frac{i}{2}\sigma_3\theta(x)} \begin{pmatrix} u_R' \\ d_R' \end{pmatrix} , \qquad (5.18)$$

whereas the transformation of the left-handed quark doublets are given by

$$Q_L' \xrightarrow{SU(2)_L \times U(1)_Y} \Sigma_L e^{+\frac{i}{6}\theta(x)} Q_L'. \tag{5.19}$$

The four different Yukawa coupling matrices that appeared in Eq. (5.2) are now encrypted in the couplings of the quarks with these four different bidoublets given in Eqs. (5.15) and (5.17):

$$-\mathcal{L}_{Y} = \left[ Y_{\Phi} \overline{Q}_{L} \Phi \begin{pmatrix} u_{R}' \\ d_{R}' \end{pmatrix} + \widetilde{Y}_{\Phi} \overline{Q}_{L} \widetilde{\Phi} \begin{pmatrix} u_{R}' \\ d_{R}' \end{pmatrix} + Y_{\Psi} \overline{Q}_{L} \Psi \begin{pmatrix} u_{R}' \\ d_{R}' \end{pmatrix} + \widetilde{Y}_{\Psi} \overline{Q}_{L} \widetilde{\Psi} \begin{pmatrix} u_{R}' \\ d_{R}' \end{pmatrix} \right] + \text{h.c.}.$$
 (5.20)

Comparing Eqs. (5.2) and (5.20), it is easy to see the relations between the two different sets of notations:

$$\Gamma_1 = \widetilde{Y}_{\Phi} + \widetilde{Y}_{\Psi}, \qquad \qquad \Gamma_2 = Y_{\Phi} - Y_{\Psi}, \qquad (5.21a)$$

$$\Delta_1 = Y_{\Phi} + Y_{\Psi}, \qquad \Delta_2 = \widetilde{Y}_{\Phi} - \widetilde{Y}_{\Psi}. \qquad (5.21b)$$

#### 5.2 Crossed 2HDMs

We will now proceed to construct nontrivial examples of 2HDMs where Eq. (5.13) holds. But first, let us recover the conventional 2HDMs which prevent any FCNC at the tree level. We note that by restricting ourselves to the quark sector, all four NFC 2HDMs are encompassed by the Type-I and Type-II.

#### 5.2.1 Retrieving Type-I and Type-II 2HDMs

In type-I 2HDM, only  $\phi_1$  is odd under a  $Z_2$  symmetry while all other fields are even. Consequently, only  $\phi_2$  couples to all the fermions. In the bidoublet notation, we can write this  $Z_2$  symmetry as

$$\Phi \to -\Phi \sigma_3 = -\Psi. \tag{5.22}$$

The above transformation will affect the remaining bidoublet structures as

$$\Psi \to -\Psi \sigma_3 = -\Phi, \qquad \widetilde{\Phi} \to \widetilde{\Phi} \sigma_3 = -\widetilde{\Psi}, \qquad \widetilde{\Psi} \to \widetilde{\Psi} \sigma_3 = -\widetilde{\Phi}.$$
 (5.23)

The Yukawa Lagrangian of Eq. (5.20) will remain unaffected by the above transformation if

$$Y_{\Phi} = -Y_{\Psi} \quad \text{and} \quad \widetilde{Y}_{\Phi} = -\widetilde{Y}_{\Psi} \,, \tag{5.24}$$

which, in view of Eq. (5.21), implies

$$\Gamma_1 = \Delta_1 = 0. \tag{5.25}$$

It is easy to see that in this model,  $A_u = A_d = -\cot \beta$ ,  $B_u = B_d = 0$ . Since the  $B_{u,d}$  coefficients are zero, there is no FCNC in this model.

In type-II 2HDM,  $\phi_1 \to -\phi_1$  and  $d'_R \to -d'_R$  under the  $Z_2$  symmetry. Thus,  $\phi_1$  will couple only to the down-type quarks whereas  $\phi_2$  will couple to the up-type quarks. This can be ensured via the following transformations in the bidoublet notation:

$$\Phi \to -\Phi \sigma_3$$
 and  $\begin{pmatrix} u_R' \\ d_R' \end{pmatrix} \to \sigma_3 \begin{pmatrix} u_R' \\ d_R' \end{pmatrix}$ . (5.26)

It is then easily seen that to keep the Yukawa Lagrangian of Eq. (5.20) invariant under the above transformations, we must require

$$Y_{\Phi} = Y_{\Psi} = 0,$$
 (5.27)

since

$$Y_{X}\overline{Q}'_{L}X\begin{pmatrix} u'_{R} \\ d'_{R} \end{pmatrix} \rightarrow -Y_{X}\overline{Q}'_{L}X\sigma_{3}^{2}\begin{pmatrix} u'_{R} \\ d'_{R} \end{pmatrix},$$

$$\widetilde{Y}_{X}\overline{Q}'_{L}\widetilde{X}\begin{pmatrix} u'_{R} \\ d'_{R} \end{pmatrix} \rightarrow \widetilde{Y}_{X}\overline{Q}'_{L}\widetilde{X}\sigma_{3}^{2}\begin{pmatrix} u'_{R} \\ d'_{R} \end{pmatrix},$$

$$(5.28)$$

with  $X = \Phi, \Psi$ . This, in view of Eq. (5.21), translates into

$$\Delta_1 = \Gamma_2 = 0, \tag{5.29}$$

and we find  $A_d = \tan \beta$ ,  $A_u = -\cot \beta$ ,  $B_u = B_d = 0$  in this model.

Note that we could have defined the  $Z_2$  symmetry differently, by omitting the minus sign in the transformation law of right-handed quarks from Eq. (5.26). That would not have given us a new model: it would have just interchanged the roles of  $\phi_1$  and  $\phi_2$ .

These examples have no tree-level FCNCs, as anticipated. Next, we will go through examples which we dub as "crossed 2HDMs" (or "x2HDMs"), since they feature a connection between the  $\Gamma$  and  $\Delta$  matrices (equivalently, since they connect quarks across hypercharges).

#### 5.2.2 First Example of Crossed 2HDM:

#### Connection with Left-Right Symmetry

Consider a symmetry under which the nontrivial transformations are

$$\Phi \to \Phi \Sigma_R^{\dagger}, \qquad \begin{pmatrix} u_R' \\ d_R' \end{pmatrix} \to \Sigma_R \begin{pmatrix} u_R' \\ d_R' \end{pmatrix} , \qquad (5.30)$$

where  $\Sigma_R$  is any SU(2) matrix. Since  $2 \times 2$  unitary matrices have the property

$$\Sigma_R^* = \sigma_2 \, \Sigma_R \, \sigma_2 \,, \tag{5.31}$$

we can find the implied transformations of the remaining bidoublets. It is easily seen that  $\Psi$  (and  $\widetilde{\Psi}$ ) do not transform similarly to  $\Phi$ , because of the presence of  $\sigma_3$ , which won't commute with a general SU(2) element,  $\Sigma_R^{\dagger}$ :

$$\Psi = \Phi \sigma_3 \to \Phi \Sigma_R^{\dagger} \sigma_3 \neq \Phi \sigma_3 \Sigma_R^{\dagger} \,. \tag{5.32}$$

On the other hand, for  $\widetilde{\Phi}$ , we can use

$$\Phi \to \Phi \Sigma_R^{\dagger} \Rightarrow \Phi^* \to \Phi^* \Sigma_R^T, \tag{5.33}$$

together with

$$\Sigma_R^* = \sigma_2 \Sigma_R \sigma_2 \Rightarrow \Sigma_R^{\dagger} = \sigma_2 \Sigma_R^T \sigma_2 \,, \tag{5.34}$$

to find

$$\widetilde{\Phi} = \sigma_2 \Phi^* \sigma_2 \to \sigma_2 \Phi^* \Sigma_R^T \sigma_2 = (\sigma_2 \Phi^* \sigma_2) \left( \sigma_2 \Sigma_R^T \sigma_2 \right) = \widetilde{\Phi} \Sigma_R^{\dagger}, \tag{5.35}$$

such that it is clear that, under the transformation of Eq. (5.30),  $\widetilde{\Phi}$  transforms the same way as  $\Phi$ , but  $\Psi$  and  $\widetilde{\Psi}$  do not. Thus, the Yukawa couplings associated with  $\Psi$  and  $\widetilde{\Psi}$  are not invariant under this symmetry. It should be noted that this symmetry should be considered as an approximate symmetry, since it does not commute with the hypercharge symmetry (the  $\Sigma_R$  element will mix up- and down-type

quarks, such that the transformation property of Eq. (5.18) is no longer verified, and similarly for  $\widetilde{\phi}_i$  and  $\phi_i$ ). Imposing the symmetry of Eq. (5.30) on the Yukawa Lagrangian of Eq. (5.20), we will obtain the following restrictions on the Yukawa matrices:

$$Y_{\Psi} = \widetilde{Y}_{\Psi} = 0, \tag{5.36}$$

leading to

$$\Gamma_1 = \Delta_2 \equiv \Gamma \text{ (say)}, \qquad \Gamma_2 = \Delta_1 \equiv \Delta \text{ (say)}.$$
 (5.37)

In this case, we will have the following mass matrices

$$M_d = \frac{v}{\sqrt{2}} (\cos \beta \Gamma + \sin \beta \Delta) , \qquad M_u = \frac{v}{\sqrt{2}} (\cos \beta \Delta + \sin \beta \Gamma) .$$
 (5.38)

Inverting these equations and comparing with Eq. (5.13), one obtains

$$A_d = A_u = \tan 2\beta$$
,  $B_d = B_u = -\sec 2\beta$ . (5.39)

Plugging this into the definitions Eq. (5.14), we find

$$N_d = \frac{1}{v} \left( \tan 2\beta \ D_d - \sec 2\beta \ V_L^{\dagger} D_u V_R \right) , \qquad (5.40a)$$

$$N_u = \frac{1}{v} \left( \tan 2\beta \ D_u - \sec 2\beta \ V_L D_d V_R^{\dagger} \right) . \tag{5.40b}$$

As such, the FCNC couplings of the neutral Higgs bosons are fully controlled by the quark mixing parameters and  $\tan \beta$ . This is a crossed 2HDM, which we will call x2HDM-1 in subsequent discussion.

The symmetry of Eq. (5.30), which was used to arrive at this model, is qualitatively different from those introduced in Sec. 5.2.1. The point is that the transformations produce linear superpositions of the SM doublets  $\tilde{\phi}_1$  and  $\phi_2$ . Since these two objects have opposite hypercharges, such mixing is not allowed by gauge symmetry. So, a symmetry of this sort can be imposed on the Yukawa sector only, although it will be violated by the gauge interactions, and therefore can only be an approximate symmetry of the full Lagrangian. We call these *crossed* symmetries because it connects across different hypercharges.

However, the particular transformations of Eq. (5.30) can easily be promoted to be a symmetry of the full Lagrangian. These transformations are easily seen as the transformations of the relevant fields under an  $SU(2)_R$  symmetry. Thus, in effect, the imposition of the symmetry of Eq. (5.30) implies that the Yukawa couplings have a symmetry  $SU(2)_L \times SU(2)_R \times U(1)$ , which is the gauge symmetry of the LRSMs [? ? ?]. We can therefore extend the symmetry to the entire Lagrangian and build a LRSM. In fact, our Yukawa couplings are no different than the usual ones encountered in the LRSMs that involve a bidoublet Higgs multiplet  $\Phi$  transforming as the (2,2,0) representation of the gauge group. In the context of LRSMs, it was noted [252] that the fermion couplings with Higgs bosons depend only on  $V_L$  and  $V_R$ .

#### 5.2.3 One Other Example of a Crossed 2HDM

So far, our approach may appear as a convoluted exercise to connect the LRSM with 2HDM. However, the notations that we adopted here can be used to uncover new types of 2HDMs which were previously unknown.

As an example, we introduce a  $Z_2$  symmetry in the following form:<sup>1</sup>

$$\Phi \to \Phi \, \sigma_1 \,, \qquad \begin{pmatrix} u_R' \\ d_R' \end{pmatrix} \to \sigma_1 \begin{pmatrix} u_R' \\ d_R' \end{pmatrix} \,.$$
 (5.41)

Note that, this also does not commute with the hypercharge symmetry, and therefore should be considered as an approximate symmetry. This symmetry, when imposed on the Yukawa Lagrangian of Eq. (5.20), implies the following<sup>2</sup>

$$\widetilde{Y}_{\Phi} = Y_{\Psi} = 0, \tag{5.42}$$

which means

$$\Gamma_1 = -\Delta_2 \equiv \Gamma \quad (\text{say}), \qquad \Gamma_2 = \Delta_1 \equiv \Delta \quad (\text{say}).$$
 (5.43)

This model will be called x2HDM-2. As a consequence of Eq. (5.43), the quark mass matrices will now become,

$$M_d = (\cos \beta \Gamma + \sin \beta \Delta)v/\sqrt{2}, \qquad M_u = (\cos \beta \Delta - \sin \beta \Gamma)v/\sqrt{2}.$$
 (5.44)

Inverting these equations and comparing with Eq. (5.13), one obtains

$$A_d = A_u = 0$$
,  $B_u = -B_d = 1$ . (5.45)

As a result, the matrices  $N_u$  and  $N_d$  are given by

$$N_d = -\frac{1}{v} V_L^{\dagger} D_u V_R , \qquad (5.46a)$$

$$N_u = \frac{1}{v} V_L D_d V_R^{\dagger}. \tag{5.46b}$$

This is an intriguing case where the Yukawa couplings with physical Higgs bosons are independent of  $\tan \beta$ , the ratio of the two vevs.

One may consider other relations among the Yukawa matrices  $Y_{\Phi}$ ,  $\widetilde{Y}_{\Phi}$ ,  $Y_{\Psi}$  and  $\widetilde{Y}_{\Psi}$ , which can potentially give rise to different structures of  $N_u$  and  $N_d$ . Not all relations will produce new models. For

<sup>&</sup>lt;sup>1</sup>Note that  $\sigma_1$  is not an element of SU(2), since det  $\sigma_1 = -1$ , and thus this case does not fall into the umbrella of the previous example.

<sup>&</sup>lt;sup>2</sup>In  $\widetilde{\Phi}$  and  $\Psi$ , the  $\sigma_1$  needs to anti-commute with a single  $\sigma_{i\neq 1}$  until it reaches the one from the RH quarks transformation, leading to a minus sign. For the case of  $\widetilde{\Psi}$ , it anti-commutes twice, and the minus sign is no longer present. Thus, under this symmetry,  $\widetilde{\Phi} \to -\widetilde{\Phi}\sigma_1$ ,  $\Psi \to -\Psi\sigma_1$  and  $\widetilde{\Psi} \to \widetilde{\Psi}\sigma_1$ .

example, changing  $\sigma_1$  to  $\sigma_2$  (and indeed to any linear combination of  $\sigma_1$  and  $\sigma_2$ ) in Eq. (5.41) produces the same restrictions on Yukawa couplings as those shown in Eq. (5.43). Some other conditions might result in equations which imply only an interchange of the names  $\phi_1$  and  $\phi_2$ , and therefore a redefinition of  $\beta$ . But there is no reason why more models cannot be produced which have different physical implications. However, it is not always straightforward to motivate arbitrary relations between the Yukawa matrices from symmetries.

#### 5.3 Some Specificities on the x2HDMs

It has been pointed out that, unlike the symmetries in Eqs. (5.22) and (5.26), the ones shown in Eqs. (5.30) and (5.41) mix fields with different hypercharges. Therefore, these symmetries do not commute with the  $U(1)_Y$  part of the SM gauge symmetry. Thus, as previously stated, it should be considered as an approximate symmetry, imposed only on the Yukawa sector, and can prevail in the Lagrangian only in the limit when the  $U(1)_Y$  gauge coupling (g') vanishes. This approximate character or, in other words, the interference with the SM hypercharge gauge group can be explicitly seen through the computation of the renormalization group equations of the Yukawa couplings. If the relations of Eq. (5.37) or Eq. (5.43) are imposed at a certain scale, then they will evolve with the change of scale according to the formulas [47]

$$16\pi^{2} \frac{d}{d \ln \mu} (\Delta_{1} - \Gamma_{2}) = -g^{2} \Delta, \qquad 16\pi^{2} \frac{d}{d \ln \mu} (\Gamma_{1} \mp \Delta_{2}) = g^{2} \Gamma, \qquad (5.47)$$

where we assume the presence of right-handed neutrinos with appropriate Yukawa interactions involving the doublet Higgs bosons, and extend the symmetry to the leptonic sector.

By taking a closer look at the relations of both x2HDMs, it is possible to extract one characteristic which is general to all x2HDMs. Suppose the inversion of Eq. (5.6) yields the solutions

$$\Gamma = p_1 M_u + p_2 M_d$$
,  $\Delta = q_1 M_u + q_2 M_d$ , (5.48)

for some assignment of  $\Gamma$  and  $\Delta$  from among the four Yukawa matrices. We can now form the traces of the hermitian matrices  $\Gamma^{\dagger}\Gamma$  and  $\Delta^{\dagger}\Delta$ , each of which will contain four terms. Since  $\text{Tr}(M_u^{\dagger}M_u) \approx m_t^2$ , we expect this term to dominate. If it indeed does, then

$$\frac{\text{Tr}(\Gamma^{\dagger}\Gamma)}{\text{Tr}(\Delta^{\dagger}\Delta)} = \frac{p_1^2}{q_1^2} + \text{(small terms)}.$$
 (5.49)

This means that there should a strong correlation between the square root of the left side of this equation and  $|p_1/q_1|$ . For all x2HDMs presented here,  $|p_1/q_1| = |\tan \beta|$ . The correlation is shown in Fig. 5.1, for the parametric region compatible with the experimental data for quark masses and mixings, and where we apply a perturbative bound such that  $|\Gamma_{ab}|$ ,  $|\Delta_{ab}| \leq 1$ .

We notice from Fig. 5.1 the weakening of the correlation as we move away from  $\tan \beta = 1$ . This can be understood as a direct consequence of the strong hierarchy between the up and down-quark masses.

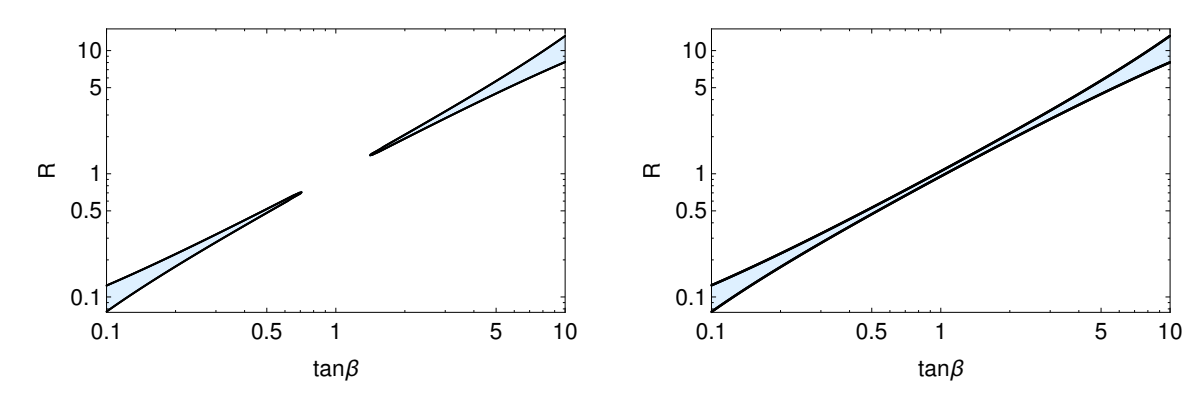


Figure 5.1: Plot of tan  $\beta$  vs  $R = \sqrt{\text{Tr}(\Gamma^{\dagger}\Gamma)/\text{Tr}(\Delta^{\dagger}\Delta)}$  for randomly generated Γ and Δ. The shaded region is consistent with the observed quark masses and mixings, in the x2HDM-1 (left) and x2HDM-2 (right). We impose a perturbativity limit of  $|\Gamma_{ab}|, |\Delta_{ab}| \leq 1$ .

For  $\tan \beta \approx 1$ , we need to arrange a cancellation in the expression for  $M_d$  to reproduce such a strong hierarchy. This will approximately fix  $\tan \beta$ . However, for  $\tan \beta$  far away from unity (*i.e.*, for either  $\sin \beta$  or  $\cos \beta$  close to zero), the matrices  $\Gamma$  and  $\Delta$  in Eqs. (5.38) and (5.44) effectively serve as independent sources of masses for the up and down-type quarks.

One particular aspect of the x2HDM-1 can easily be seen by looking at Eq. (5.38). Namely, for  $\tan \beta = 1$  we will have  $M_u = M_d$  leading to unacceptable phenomenological results. Therefore we must be away from  $\tan \beta = 1$  to reproduce realistic values for the physical quark masses and mixings. Additionally, problems in the region surrounding  $\tan \beta = 1$  can be understood by inverting Eq. (5.38) to obtain  $\Gamma$  and  $\Delta$  in terms of  $M_u$  and  $M_d$ . These expression will have terms proportional to  $\sec 2\beta$ , which is large near the  $\tan \beta = 1$  region, leading to non-perturbative Yukawa couplings. One may then naturally wonder how close can  $\tan \beta$  be to unity so that the observed values of the quark masses and mixings are recovered while, at the same time, the elements of Yukawa matrices in Eq. (5.37) are kept under the perturbative limit,  $|\Gamma_{ab}|, |\Delta_{ab}| \leq 1$ . From Fig. 5.1 (left), we can read the forbidden region in  $\tan \beta$  as follows:

$$0.75 \lesssim \tan \beta \lesssim 1.33. \tag{5.50}$$

We argued earlier that the x2HDM-1 is the low-energy limit of the left-right symmetric model. In this connection, it should be pointed out that our results on  $\tan \beta$  are equally applicable in the case of LRSM where  $\tan \beta$  will obviously be redefined as the ratio of the two vevs of the bidoublet.

### 5.4 Phenomenology of x2HDMs

Our goal was to relate the FCNC parameters to the LH and RH quark mixing parameters. Having achieved that goal, we now briefly turn our attention to the consequences of experimental constraints on the models. More specifically, by relating  $N_d$  with  $V_R$ , we greatly reduce the free parameters of the model, yet these FCNC contributions are still present at the tree-level. As such, as our first objective, we set out to neutralize these contributions to minimize the impact they have on neutral meson mixing.

We expect this to lead to a very constrained  $V_R$ , due to the high experimental precision of  $\Delta M_P$ , where  $P=K,B_s,B_d$ . Interestingly, the coupling structure of the x2HDMs is such that these are the same couplings that drive the fermionic decays of the nonstandard scalars of the model. Thus, by finding one  $V_R$  compatible with  $\Delta F=2$  flavour observables, the models will have a distinct prediction for the ratio of fermionic non-SM scalar decays: Br  $(S,A\to \overline{f}f)$ /Br  $(S,A\to \overline{b}b)$ . As mentioned earlier, we work under the assumption of the alignment limit, where  $H_0$  is a SM-like Higgs particle with flavour-diagonal couplings. Thus, all NP FCNC come exclusively from S and A.

To tame the tree-level effects of the nonstandard scalars in  $\Delta M_P$ , we first write the relevant expression for the NP contribution to the meson mass difference ( $\Delta M_P^{\rm NP}$ ) as [247, 253]

$$2M_{P}\Delta M_{P}^{\text{NP}} = \left| \left( \frac{1}{M_{A}^{2}} - \frac{1}{M_{S}^{2}} \right) \left[ \left( (N_{d}^{*})_{ji} \right)^{2} + \left( (N_{d})_{ij} \right)^{2} \right] \frac{5}{3} M_{P}^{0,F} - \left( \frac{1}{M_{A}^{2}} + \frac{1}{M_{S}^{2}} \right) 2(N_{d})_{ij} (N_{d}^{*})_{ji} \left( \frac{M_{A}^{0,F}}{3} - 2M_{P}^{0,F} \right) \right|,$$
 (5.51)

where  $P = \overline{q}_i q_j$  , and

$$M_P^{0,F} = -f_P^2 \frac{M_P^4}{\left(m_{q_i} + m_{q_i}\right)^2}, \qquad M_A^{0,F} = f_P^2 M_P^2.$$
 (5.52)

In the above,  $m_{q_i}$  is the mass of the quark  $q_i$ , whereas  $f_P$  and  $M_P$  are the decay constant and the mass of the meson P, respectively.

Clearly, in the limit  $M_S = M_A$ , there is a cancellation in the first term of Eq. (5.51). In order to sufficiently dilute the contribution of the second term of Eq. (5.51), we must require  $(N_d)_{ij}(N_d^*)_{ji} \sim 0$ , which leads to  $\Delta M_P^{\rm NP} \sim 0$ . Ignoring the possible phases of  $V_R$ , we can constrain the three Euler angles through the three conditions above. This should fix  $V_R$  to a precise degree, depending on the different solutions one can find for the constraints. One specific example which effectively has a negligible NP contribution to  $\Delta M_{K,B_d,B_s}$  is:

$$V_R \approx \begin{pmatrix} 1. & 3.92461 \times 10^{-4} & 2.30929 \times 10^{-8} \\ -3.92461 \times 10^{-4} & 1. & 3.07822 \times 10^{-4} \\ 9.77154 \times 10^{-8} & -3.07822 \times 10^{-4} & 1. \end{pmatrix} . \tag{5.53}$$

Using this  $V_R$ , we have explicitly checked that the  $\Delta F = 2$  contributions to K,  $B_s$ , and  $B_d$  oscillations are under control for  $M_S = M_A \sim \mathcal{O}(\text{TeV})$ , even for regions near  $\tan \beta \sim 1$ . It is interesting to note that, in other examples, some of the off-diagonal terms can be  $\mathcal{O}(1)$ , such as the case

$$V_R \approx \begin{pmatrix} 7.35844 \times 10^{-3} & 0.999973 & 1.01105 \times 10^{-8} \\ -0.999973 & 7.35844 \times 10^{-3} & 3.07814 \times 10^{-4} \\ 3.07806 \times 10^{-4} & -2.27514 \times 10^{-6} & 1. \end{pmatrix} . \tag{5.54}$$

Now that we have established that TeV-scale nonstandard scalars can successfully negotiate the stringent  $\Delta F = 2$  flavour constraints, it is interesting to find distinctive features of these scalars. To this end, we notice that the decays  $S, A \to \overline{q}_i q_j$  will be governed by the elements of  $N_u$  and  $N_d$  which are now

almost fixed because  $V_R$  is approximately defined in Eq. (5.53). Of course,  $V_R$  can take other forms, as was seen in Eq. (5.54), which will affect the decays of the scalars. Nonetheless, the RH mixing will be restricted to a few different shapes, in turn restricting the branching ratios themselves.<sup>3</sup> In the following, we focus on the case of Eq. (5.53). This is a consequence of the reducible Yukawa parameters structure of the x2HDMs, leaving all flavour couplings to be governed by  $V_L$  and  $V_R$ . Thus, we can wonder what are the effects of flavour data in the nonstandard scalar branching ratios. By taking, as an example, Eq. (5.53), we are fully equipped to compute the relevant two-body scalar decays into a quark anti-quark pair. For benchmark values of  $M_S = M_A = 1.5$  TeV, the results are shown in Table 5.1 for x2HDM-2, where the FCNCs are independent of  $\tan \beta$ , leading to fixed values of the branching ratios for any particular  $V_R$ . The results for x2HDM-1 are shown in Fig. 5.2, due to the explicit dependence on tan  $\beta$ . In the case of x2HDM-2, the nonstandard scalars will preferably decay into down-type quarks, because the couplings are proportional to the up-type masses, whereas the up-type decays are proportional to the down-type masses, as seen in Eq. (5.46). For the x2HDM-1, the same does not necessarily hold, as there are two contributions for flavour-diagonal decays, as shown in Eq. (5.40). The different dependence on  $\tan \beta$  of both contributions will make the  $S \to \bar{t}t$  or  $S \to \bar{b}b$  predominance be determined by  $V_R$  as well as  $\tan \beta$ . In fact, for  $V_R$  given in Eq. (5.53), we find  $S \to \bar{t}t$  starts competing with  $S \to \bar{b}b$  for a region of  $\tan \beta$ . Nonetheless, the behaviour of  $S \to \overline{q}_i q_j$  will be precisely defined by the classes of  $V_R$  allowed by  $\Delta M_P$ .

x2HDM-2	$\frac{H \to ss}{H \to bb}$	$\frac{H \to \mathrm{bs}}{H \to \mathrm{bb}}$	$\frac{H \to cc}{H \to bb}$	$\frac{H \to \mathrm{tc}}{H \to \mathrm{bb}}$	$\frac{H \to \mathrm{tt}}{H \to \mathrm{bb}}$
$H \equiv S$	$5 \times 10^{-5}$	$8 \times 10^{-4}$	$3\times10^{-7}$	$5 \times 10^{-7}$	$5 \times 10^{-4}$
$H \equiv A$					$6 \times 10^{-4}$

**Table 5.1:** Relative branching ratios for the two body fermionic decays of S and A for the x2HDM-2, normalized by the branching ratio of the decay into a  $\bar{b}b$  pair, for  $M_S = M_A = 1.5$  TeV. One of the quarks in each process is to be taken to be an antiquark. We have not marked which one, because the result is independent of this choice.

#### 5.5 Discussion

In this chapter, we studied some properties of a minimal extension of the SM, the 2HDM, and, in particular, focused on the study of the FCNCs of the model. We studied different variants of the 2HDM, resulting from the imposition of different symmetries on the Yukawa interactions of the model. Since these symmetries do not commute with the full gauge group of the SM Lagrangian (in practice, they are broken by the hypercharge), they are effectively approximate symmetries of the theory. Taking advantage that the renormalization group equations of the 2HDM are well-known, assuming the symmetry to be a true symmetry of the Lagrangian at an energy scale  $\mu$ , it is possible to compute the evolution of the deviation from the symmetric situation with respect to the energy scale.

<sup>&</sup>lt;sup>3</sup>This holds while neglecting the possible phases of  $V_R$ . A full analysis would require knowledge of the covering theories, as new processes could help constraint the RH mixing.

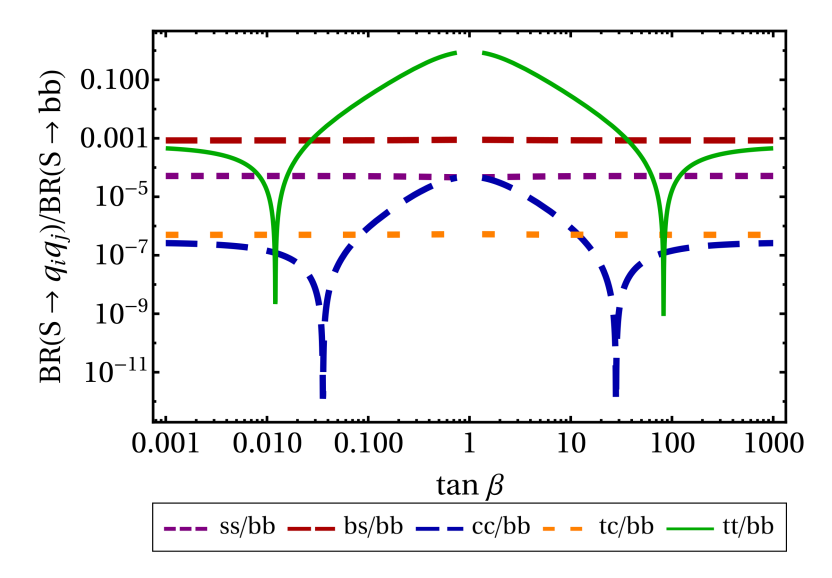


Figure 5.2: Log-log plot of relative branching ratios for the S decay into quark-antiquark pairs, normalized by its branching ratio into a  $\bar{b}b$  quark pair, as a function of  $\tan \beta$ , for the x2HDM-1, with  $M_S = M_A = 1.5$  TeV. The region for  $\tan \beta$  which was excluded in Fig. 5.1 is intentionally kept out in these plots. The relative branching ratios for A are very similar.

We advocate the bidoublet notation, widely popular in the context of left-right symmetric theories, applied to the context of the 2HDM. While it may seem a convoluted exercise which increases the problem's complexity, we argue for its benefits. Namely, imposing simple symmetries on the bidoublet, we are able to recover the paradigmatic type-I and type-II 2HDM models, as well as formulate two new 2HDM variants, which until now remained unstudied.

Throughout this chapter, our main goal was to search for models where the general arbitrariness of the FCNC couplings was reduced, following the motivation of BGL models, by relating these couplings with the quark mixing matrices. We find a class of new models, where the FCNCs are controlled by the left- and right-handed quark mixings. Due to the particular relations between the Yukawa matrices of the model, we name this new class of models the crossed 2HDM (x2HDM). In one of these such models, the x2HDM-1, we show that it is possible to impose a symmetry on the Yukawa sector such that the FCNCs are fully controlled by the left- and right-handed CKMs, as well as the ratio between the scalar doublets vevs. We also point out that, while this symmetry is approximate in the 2HDM context, it is automatically imposed when dealing with the LRSM. As such, this model can be taken as the electroweak scale incarnation of the LRSM, given that the LRSM relies on a 2HDM structure. Following up on this intimate connection between the x2HDM-1 and the LRSM, a comprehensive flavour analysis, when paired up with the RGE study, may lead to valuable insight on the validity of some LRSMs. Furthermore, it is important to note that some of the conclusions obtained for the x2HDM-1 are equally valid or extendable to the LRSM, such as the excluded region for the Higgs-doublets' (the bidoublet's in the LRSM context) vevs. We also present a second model, dubbed x2HDM-2, where the FCNC structure is further simplified, being entirely controlled by the left- and right-handed CKMs, independent of the vev ratio. While we do not present a UV-completion for this model, we consider this model as a valuable argument for the benefits of a change of outlook (in this case, notations), to uncover new interesting possibilities.

We have also performed a phenomenological analysis of the x2HDMs, to showcase their predictive

power. In the paradigm of the alignment limit, as well as assuming  $M_S = M_A$ , the tree-level contributions to the  $\Delta F = 2$  processes are simplified, but still remain. As such, the restrictive flavour data on  $\Delta M_K$ ,  $\Delta M_{B_s}$ , and  $\Delta M_{B_d}$ , constrain the model. However, the same couplings are responsible not only for the neutral meson oscillations, but also for other flavour processes such as the two-body fermionic decays of the nonstandard scalars of the theory. As such, a specific example for  $V_R$  is shown, which was obtained by requiring the compatibility of the models with  $\Delta F = 2$  data. It leads to specific values for the branching ratios of both S and A for the x2HDM-2, and a distinctive pattern of these quantities as a function of tan  $\beta$  for the x2HDM of type 1.

As a final note, hopefully, the explicit relation between the x2HDM-1 and the LRSM, together with the economical structure of the FCNCs of both x2HDMs, as well as the benefits of a change in notation for uncovering models, will lead to a renewed aesthetic motivation for the study of 2HDMs, apart from the supersymmetric embedding.

## Modular Symmetries and Stabilisers

Non-Abelian discrete symmetries were introduced to understand the theoretical origin of large lepton mixing angles observed in neutrino oscillation experiments. A popular approach is that the lepton flavour mixing is realised by the SSB of discrete flavour symmetries [254, 255]. This approach requires the introduction of new scalars called flavons. They get vacuum expectation values, leading to SSB of the symmetry, and Yukawa couplings appear as the effective consequence of the vevs of flavons (see, e.g., [94, 95, 256] for some recent reviews).

However, as alluded to previously, other paths can be taken. The idea of modular invariance [129, 130] has been suggested as a key ingredient in solutions to the flavour problem [131]. In these promising scenarios, a modular symmetry associated with transformations of a modulus field can lead to very predictive models of flavour. In order to apply the methodology of residual flavour symmetries, it is relevant to consider all their fixed points or stabilizers [257, 258]: special values for the modulus field where part of the modular transformations are preserved. Furthermore, if multiple residual symmetries are desired, multiple modular symmetries, each with its respective modulus, can be employed - as proposed in [137] and expanded upon in [259–261]. Given the importance of modular invariance for model-building, we dedicate the following three chapters to this topic.

Although it is still not clear how the modulus gains a vev in flavour models, some particularly interesting values of  $\tau$ , which are invariant under specific modular transformations, have taken some relevance in the literature. These are called fixed points of the relevant modular transformation, and may play important role in modular symmetry breaking and lead to special mixing patterns. In ref. [137], it has been explicitly proven that modular forms at a stabiliser preserve a residual subgroup of the finite modular symmetry and are eigenvectors of representation matrices of the relevant elements in the subgroup.

The use of fixed points in the full domain of the finite modular symmetry becomes relevant when flavons come into play. Indeed, the use of  $\tau$  outside of the fundamental domain may be recast as a point inside the fundamental domain, with an appropriate change of basis [141]. This is no longer permitted if we include flavons since, after the SSB, the basis is fixed by the particular choice of flavon vev. In this way, in the presence of flavons (which is needed for most models which make use of multiple modular

symmetries), the full set of fixed points becomes relevant for model building based on residual symmetries.

In this chapter, we introduce an algorithm to find stabilisers and then perform a systematic scan to find stabilisers for each element of finite modular groups for N=2 to 5, i.e.  $\Gamma_{2,3,4,5}$ . A recent work [262] has similarly studied the fixed points for  $\Gamma_{3,4}$  ( $A_4, S_4$ ), and showcases their usefulness for model building. Our results extend the list by adding the stabilizers for  $\Gamma_{2,5}$ .

As it was already presented in the introduction, we will not go through the basics of modular symmetries here, but will give some relevance to the domains and their fixed points in Section 6.1. Section 6.2 starts with an explanation of the algorithm, followed by its systematic application for  $\Gamma_N$  with  $N \leq 5$ . We present the results in figures showing the stabilisers in the domains of the respective modular symmetries and we list them in tables displaying each group element and respective stabilisers.

#### 6.1 Domain, Fixed Points, and Residual Symmetries

Given its relevance for our present objective, we now discuss the target space of the modular symmetry, and some definitions and properties of the fixed points.

We label the fundamental domain of  $\Gamma$  and  $\Gamma(N)$  as  $\mathcal{D}$  and  $\mathcal{D}(N)$ , respectively. The fundamental domain  $\mathcal{D}$  is defined as follows. Given a point  $\tau$  in the upper complex plane, acting all modular transformations of  $\Gamma$  on  $\tau$  forms an orbit of the point  $\tau$ . The fundamental domain  $\mathcal{D}$  of  $\Gamma$  represents a minimal (and connected) region of  $\tau$ , where every orbit intersects  $\mathcal{D}$  in no more than one point. Similarly, one defines the fundamental domain  $\mathcal{D}(N)$  of  $\Gamma(N)$ .

Acting  $\Gamma$  on  $\mathcal{D}$  generates  $\mathcal{C} \equiv \mathbb{C}_+ \cup \{\text{cusps}\}$ , namely, the upper complex plane  $(\text{Im}(\tau) > 0)$  with cusps on the real axis. On the other hand, acting  $\Gamma(N)$  on  $\mathcal{D}(N)$  generates the same space. Therefore, we have

$$C = \Gamma D = \Gamma(N)D(N). \tag{6.1}$$

Since  $\Gamma_N$  represents the quotient group  $\Gamma/\Gamma(N)$ , we further have  $\Gamma \mathcal{D} = \Gamma(N)\Gamma_N \mathcal{D}$ . Comparing with the former equation, we obtain

$$\mathcal{D}(N) = \Gamma_N \mathcal{D} \,. \tag{6.2}$$

In other words, the fundamental domain of  $\Gamma(N)$ ,  $\mathcal{D}(N)$ , forms the full target space of  $\Gamma_N$ . Any transformation  $\gamma \in \Gamma_N$  acting on  $\mathcal{D}(N)$  leaves  $\mathcal{D}(N)$  invariant,  $\gamma \mathcal{D}(N) = \mathcal{D}(N)$ . On the other hand, acting each element  $\gamma$  of  $\Gamma_N$  on the fundamental domain of  $\Gamma$  generates another fundamental domain of  $\Gamma$ , i.e.,  $\gamma \mathcal{D} \neq \mathcal{D}$ . In other words, acting with  $\Gamma_N$  on  $\mathcal{D}$  generates the target space of  $\Gamma_N$ : a (finite) collection of fundamental domains of  $\Gamma$ , which make up the fundamental domain of  $\Gamma(N)$ . The full upper complex plane (plus cusps),  $\mathcal{C}$ , can be then generated by acting  $\Gamma(N)$  on  $\mathcal{D}(N)$ .

Given an element  $\gamma$  in the modular group  $\Gamma_N$ , a stabiliser of  $\gamma$  (which may not be unique) corresponds to a fixed point  $\tau_{\gamma}$  either in the interior or in the boundary of the fundamental domain  $\mathcal{D}(N)$ , which satisfies  $\gamma \tau_{\gamma} = \tau_{\gamma}$ . Some of the properties satisfied by stabilisers are discussed below.

• Since each orbit of  $\Gamma$  intersects the interior of  $\mathcal{D}$  in no more than one point, a stabiliser of  $\gamma \in \Gamma_N$ 

should be located only on either an edge or cusp of one fundamental domain of  $\Gamma$ .

- A stabiliser of  $\gamma$  is also a stabiliser of  $\gamma^2, \gamma^3, \dots$ , since  $\gamma^2 \tau_{\gamma} = \gamma \tau_{\gamma} = \tau_{\gamma}$ . Therefore, once the modular field  $\tau$  gains a vev at such a stabiliser,  $\langle \tau \rangle = \tau_{\gamma}$ , an Abelian residual modular symmetry  $Z_{\gamma} = \{1, \gamma, \gamma^2, \dots\}$  is preserved.
- Given a stabiliser  $\tau_{\gamma}$  of  $\gamma$ ,  $\gamma_{1}\tau_{\gamma}$  is a stabiliser of the conjugate  $\gamma_{1}\gamma\gamma_{1}^{-1}$ . This is simply proven as  $\gamma_{1}\gamma\gamma_{1}^{-1}\gamma_{1}\tau_{\gamma} = \gamma_{1}\gamma\tau_{\gamma} = \gamma_{1}\tau_{\gamma}$ . A specific consequence is that if there is an element  $\gamma_{1}$  which is not equal to  $\gamma$  but permutes with  $\gamma$ ,  $\gamma = \gamma_{1}\gamma\gamma_{1}^{-1}$ , and then both  $\tau_{\gamma}$  and  $\gamma_{1}\tau_{\gamma}$  are stabilisers of  $\gamma$ . Therefore, one modular transformation of  $\Gamma_{N}$  may have several different stabilisers in  $\mathcal{D}(N)$ .

Given a, b, c and d for any element  $\gamma \in \Gamma_N$  with a, b, c and d being integers and ad - bc = 1, the most general  $2 \times 2$  matrix of  $\gamma$  should be written as

$$\gamma = \eta \begin{pmatrix} Nn_a + a & Nn_b + b \\ Nn_c + c & Nn_d + d \end{pmatrix}, \tag{6.3}$$

where  $n_a$ ,  $n_b$ ,  $n_c$  and  $n_d$  are any integers and satisfy  $Nn_an_d + an_d + dn_a = Nn_bn_c + bn_c + cn_b$  and  $\eta = \pm 1$ . Stabilisers of  $\gamma$  can be obtained by solving the following equations

$$\frac{(Nn_a+a)\tau + Nn_b + b}{(Nn_c+c)\tau + Nn_d + d} = \tau.$$

$$(6.4)$$

Solutions of  $\tau$  must be located in  $\mathcal{D}(N)$ , which is always achieved by selecting a typical set of integers  $n_a$ ,  $n_b$ ,  $n_c$  and  $n_d$ . Using these conditions, we are, in principle, able to obtain full lists of stabilisers for all modular transformations of  $\Gamma_N$ .

Here, we show stabilisers for the generator S of  $\Gamma_2$ , where  $S^2 = e$ . The element S can be represented as

$$S = \begin{pmatrix} 0 & 1 \\ -1 & 0 \end{pmatrix} = \begin{pmatrix} 0 & 1 \\ -1 & 2 \end{pmatrix} = \begin{pmatrix} 0 & 1 \\ -1 & -2 \end{pmatrix}, \tag{6.5}$$

where we have taken  $n_a = n_b = n_c = 0$ , and  $n_d = 0, 1, -1$ , from left to right. For these possibilities, we solve  $S\tau = \tau$  and obtain

$$\tau_{S,1} = i, \quad \tau_{S,2} = 1, \quad \tau_{S,3} = -1,$$
(6.6)

where  $\tau_{S,1}$ ,  $\tau_{S,2}$  are different stabilisers of S in  $\mathcal{D}(2)$ . Given the relation  $\tau = \tau + N$ , we find that  $\tau_{S,2} = \tau_{S,3}$ . It should be obvious that some choices of  $n_a, n_b, n_c, n_d$  lead to stabilisers outside  $\mathcal{D}(N)$ , making it such that not all sets of integers are fruitful, and making this list finite.

Modular forms of a given weight k and for a given level N are simply holomorphic functions (of  $\tau$ ) which transform in a specific way under  $\Gamma_N$ :

$$Y_I(\gamma \tau) = (c\tau + d)^k \rho(\gamma) Y_I(\tau). \tag{6.7}$$

Modular forms are particularly important, as they are the building blocks of models based on invariance under a modular symmetry, similar to irreducible representations.

It is obvious that acting  $\gamma$  on a modular form at its stabiliser leaves the modular form invariant, i.e.,

$$\gamma: Y_I(\tau_\gamma) \to Y_I(\gamma \tau_\gamma) = Y_I(\tau_\gamma). \tag{6.8}$$

Following the standard transformation property Eq. (6.7),  $Y_I(\gamma \tau_{\gamma}) = (c\tau_{\gamma} + d)^k \rho_I(\gamma) Y_I(\tau_{\gamma})$ , we obtain

$$\rho_I(\gamma)Y_I(\tau_\gamma) = (c\tau_\gamma + d)^{-k}Y_I(\tau_\gamma), \qquad (6.9)$$

where  $\rho_I(\gamma)$  is the representation matrix of  $\gamma$ . This equation lead us to the following important properties for the stabiliser and the modular form [137]:

- A modular form multiplet at a stabiliser, that is  $Y_I(\tau_{\gamma})$ , is an eigenvector of the representation matrix  $\rho_I(\gamma)$  with corresponding eigenvalue  $(c\tau_{\gamma}+d)^{-k}$ .
- The stabiliser  $\tau_{\gamma}$  satisfies  $|c\tau_{\gamma}+d|=1$  since  $(c\tau_{\gamma}+d)^{-k}$  is an eigenvalue of a unitary matrix.

A special case is that when  $(c\tau_{\gamma} + d)^{-k} = 1$  is satisfied,  $\rho(\gamma)Y(\tau_{\gamma}) = Y(\tau_{\gamma})$ , and we recover the residual flavour symmetry generated by  $\gamma$ . In general, the eigenvalue does not need to be fixed at 1 in the framework of modular symmetry.

### 6.2 Fixed Points of Finite Modular Groups

A straightforward way to understand how to find an extensive list of stabilisers, is to make use of disjoint sections of the domain of  $\Gamma_N$ . In the following, we take  $\mathcal{D}$  to be the domain defined as  $\{\tau \in \mathbb{C} : |\tau| > 1, |\text{Re}(\tau)| < 1/2\}$ , combined with a suitable choice of boundaries. These disjoint (barring boundaries) regions are obtained by acting all elements of  $\Gamma_N$  on  $\mathcal{D}$ , and span the fundamental domain of the congruence group (cf. Eq. (6.2)). As such, all points in  $\gamma \mathcal{D}$  for  $\gamma \in \Gamma_N$  are bijectively related to points in  $\mathcal{D}$ , in a one-to-one mapping. This is the property we exploit to find an extensive list of all stabilisers in  $\Gamma_N$ .

Since, with suitable boundaries, acting any element  $\gamma$  on  $\tau$  will transform it from  $\mathcal{D}_{\tau}$  to  $\gamma \mathcal{D}_{\tau}$ , then for any non-boundary point to be a stabiliser ( $\gamma \tau = \tau$ ), it would require  $\gamma \mathcal{D}_{\tau} = \mathcal{D}_{\tau}$ , and thus  $\gamma = e$  (recall that the definition of  $\mathcal{D}$  requires any orbit of  $\tau$  to intersect  $\mathcal{D}$  only once). On the other hand, for a point  $\tau$  on the boundary of  $\mathcal{D}$ , it is possible to act  $\gamma$  such that the point remains on  $\mathcal{D}$ , if  $\mathcal{D}$  and  $\gamma \mathcal{D}$  share a border. This is succintly put in the first properties satisfied by stabilisers, shown in Section 6.1. Hence, if it is possible to find  $\gamma_1 \tau = \gamma_2 \tau$ , with  $\gamma_1 \neq \gamma_2$ , for any boundary point, then  $\gamma_1 \gamma_2^{-1} \tau = \tau$ .

Exploring the boundaries<sup>1</sup> of  $\mathcal{D}$ , there are four well-known stabilisers [141] (where they appear with different notation):

• 
$$\tau_1 = i, \, \gamma_1 = S, \, \gamma_2 = e$$
,

<sup>&</sup>lt;sup>1</sup>In what follows, since we are no longer interest in the definition of a fundamental domain, we drop the requirement of appropriate boundaries for  $\mathcal{D}$ , such that  $\pm 1/2 + i\sqrt{3}/2$  are both in  $\mathcal{D}$ .

• 
$$\tau_2 = \frac{1}{2} + \frac{i\sqrt{3}}{2}$$
,  $\gamma_1 = T$ ,  $\gamma_2 = S$ ,

• 
$$\tau_3 = -\frac{1}{2} + \frac{i\sqrt{3}}{2}, \ \gamma_1 = T^{N-1}, \ \gamma_2 = S,$$

• 
$$\tau_4 = i\infty$$
,  $\gamma_1 = T$ ,  $\gamma_2 = e$ .

Given the stabilisers in  $\mathcal{D}$ , it is possible to propagate these onto the remaining sections, by acting all elements of  $\Gamma_N$  on the stabilisers. Since these will span the entire (fundamental) domain of  $\Gamma_N$ , a list of stabilisers arises, containing all non-equivalent possibilities. It is noteworthy to say that, while the specific methodology holds for any choice of domain, the upper complex plane has a many-to-one mapping to the domain of  $\Gamma_N$ . Namely, due to the relation  $T^N = e$ , we have

$$\tau = \frac{\tau}{1 + n_1 N \tau} + n_2 N, \qquad n_1, n_2 \in \mathbb{Z}. \tag{6.10}$$

Thus, there is an infinite number of points in the upper complex plane which are equivalent to each other, for  $\Gamma_N$ . As such, the lists obtained show the stabilisers  $\tau$ , where  $\tau$  belongs to our chosen domain. That is not to say that there are no other points in  $\mathcal{C}$  which stabilise a certain element of  $\Gamma_N$ , but rather that those elements are equivalent to one of the stabilisers given here. One may also naively think that a certain point is not stabilised by its corresponding element. Again, this is due to the redundancy of points in  $\mathcal{C}$ , shown in Eq. (6.10).

Lastly, after finding the full list of stabilisers, one needs to find the element  $\gamma$  for which  $\gamma \tau = \tau$ . The methodology for the whole process is a straightforward 3-step computation:

- 1. Take  $\tau = \tau_i$ , where  $\tau_i = \gamma_i \tau_i$ , i = 1, ..., 4 is a stabiliser of  $\mathcal{D}$ ;
- 2. Act  $\gamma$  on  $\tau$ :  $\tau' = \gamma \tau$ . Compute  $\gamma^{-1}$ ;
- 3. The element that stabilises  $\tau'$  is given by  $\gamma^{-1}\gamma_i \gamma$ .

The idea behind this simple process is exemplified in Fig. 6.1. By comparing with the methodology exposed above, we see that we act  $\gamma$  on  $\tau = i$ , to find  $\tau'$ . Then, the element that stabilises  $\tau'$  is  $\gamma^{-1}\gamma_i\gamma$ , where each action is represented by an arrow. Namely,  $\gamma^{-1}$ ,  $\gamma_i$ , and  $\gamma$  are shown by arrows 1, 2, and 3, respectively.<sup>2</sup>

In the following subsections, we show the fundamental domain<sup>3</sup>  $\mathcal{D}(N)$  of  $\Gamma(N)$  for N=2,3,4,5. The complete lists of stabilisers for all elements of  $\Gamma_N$  are found both in the domain, and separately in a table with its corresponding stabilising element. A given element can be stabilised by more than one stabiliser, and further, a stabiliser for a specific element necessarily also stabilises powers of that element and therefore preserves the associated cyclic subgroup. The elements are listed according to their conjugacy classes. In general, stabilisers are located at special points in the complex plane, namely in intersections or midway points in the domains of each group. Given that there are redundancies in

<sup>&</sup>lt;sup>2</sup>This procedure is also presented in [262]. Here, we complement their results by applying the methodology for additional groups, and present the results in terms of the final element of  $\Gamma_N$  which stabilises  $\tau$ , such that there is an unequivocal identification of the elements which stabilise each point.

<sup>&</sup>lt;sup>3</sup>Domains at the top (e.g.  $\mathcal{D}$ ) continue to complex  $+\infty$ , whereas domains represented at the edges overlap and points should not be double counted. For simplicity, we represent both boundaries in the figures.

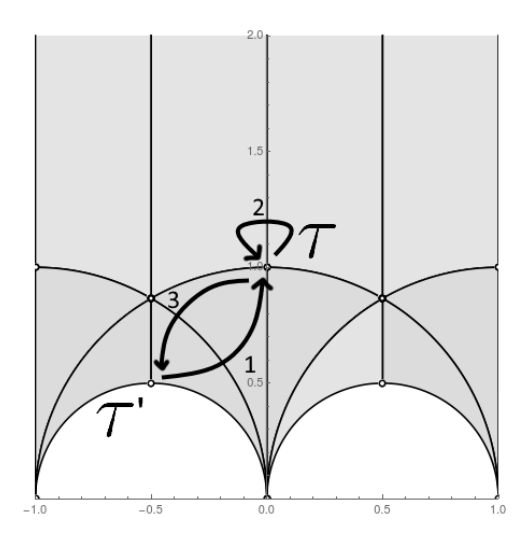


Figure 6.1: An example of the applied methodology to find the stabilisers of  $\Gamma_N$ . The example shown is for  $\Gamma_2$ , where the arrows denote the actions of different elements,  $\gamma^{-1}$ ,  $\gamma_i$ ,  $\gamma$ , for 1,2,3 respectively, following the convention of the text.

the boundaries of  $\mathcal{D}(N)$ , we choose to keep only one choice for the stabiliser in the table (we opt for the right-most  $\tau$ , i.e. the one with largest real part), and also show a list of equivalences between relevant boundary points for  $\Gamma_N$ .

Even though these finite modular groups can be generated by a minimal set of 2 elements S and T, it was convenient for us to identify each group element through 3 (related) generators S, T and C = ST (note that while the order of T is N, for  $\Gamma_N$ , the order of S is 2 and the order of C is 3, regardless). For a given irreducible representation (the doublet of  $\Gamma_2$  and triplets of the remaining groups) we present in a specific basis the elements S and T in the respective subsection, as well as an example of what is the modular form for that representation at a given stabiliser.

#### **6.2.1** $\Gamma_2$

In the framework of modular symmetry,  $\Gamma_2$  is obtained by fixing N=2, such that we have  $S^2=(ST)^3=T^2=e$ .  $\Gamma_2$  is isomorphic to  $S_3$ , the group of permutations of 3 objects and the symmetry of the equilateral triangle. We relate the generators S and T to a conventional set of generators in cycle notation, e.g. S=(12) and T=(31), where the equalities between generators of the modular group and of the cycle notation generators of  $S_3$  (or the symmetries of the triangle) are taken in the sense of the isomorphism relating them. The 6 elements are then  $\{e, S, T, ST, TS, TST\}$  with STS=TST=(23). The conjugacy classes are the  $\{e\}$ , the 3-cycles (3-fold rotations of the triangle)  $\{ST, TS\} = \{(123), (321)\}$  and the 2-cycles (reflections of the triangle)  $\{S, T, TST\} = \{(12), (31), (23)\}$ . We recall also our definition of  $C \equiv ST$ .

We depict the fundamental domain of  $\Gamma(2)$  and the location of the stabilisers in the complex plane in Fig. 6.2. Table 6.1 has a complete list of stabilisers. For  $S_3$ , the relevant redundancies are:

$$\frac{1}{2} + \frac{i}{2} = -\frac{1}{2} + \frac{i}{2}, \qquad 1 = -1. \tag{6.11}$$

For the sake of clarity, we show here a proof of the first redundancy shown, since it also helps understand why  $\tau = \frac{1}{2} + \frac{i}{2}$  is a stabiliser of T. Although we are adressing this issue specifically for  $\Gamma_2$ , the reasoning holds for the remaining modular symmetries here shown. Let us start with the element  $\gamma = STSTS$ . It is easily seen that  $\gamma$  stabilises  $\tau = \frac{1}{2} + \frac{i}{2}$ :

$$\frac{1}{2} + \frac{i}{2} \xrightarrow{S} -1 + i \xrightarrow{T} i \xrightarrow{S} i \xrightarrow{T} 1 + i \xrightarrow{\tau = \tau + N} -1 + i \xrightarrow{S} \frac{1}{2} + \frac{i}{2}. \tag{6.12}$$

Additionally, it can be shown that  $\gamma = T$ , for the case of  $\Gamma_2$ :

$$\gamma = (STSTS)(TT^{-1}) = (STSTST)T = T, \tag{6.13}$$

where we used  $T^{-1}=T$ , and  $(ST)^3=e$ . Hence, we see that, for  $\Gamma_2$ ,  $\gamma\tau_{\gamma}=-\frac{1}{2}+\frac{i}{2}=\frac{1}{2}+\frac{i}{2}$ , and  $T\tau_{\gamma}=\tau_{\gamma}$ , for  $\tau_{\gamma}=\frac{1}{2}+\frac{i}{2}$ .

This could also be shown using Eq. (6.10), by taking  $n_1 = -1$ ,  $n_2 = 0$ , and obviously N = 2. Although this may not always be possible by a single application of Eq. (6.10), multiple consecutive applications of this relation would link any two redundant points.

In this way, the table shows  $\tau = (1+i)/2$  (with larger real part than  $\tau = (-1+i)/2$ ), and this list of equivalences complements the table, by stating these points are identical in  $\Gamma_2$ , and thus any of the two are effectively stabilisers of the corresponding element. As stated above, this game could be endlessly played, since there is an infinite number of redundancies in  $\mathcal{C}$ . However, here, we restrict ourselves to the redundancies belonging to the fundamental domains of our choice (up to the redundancies of the boundaries and cusps, since we relaxed the condition of appropriate choice of boundaries) of the respective groups, shown in Figs. 6.2 to 6.5.

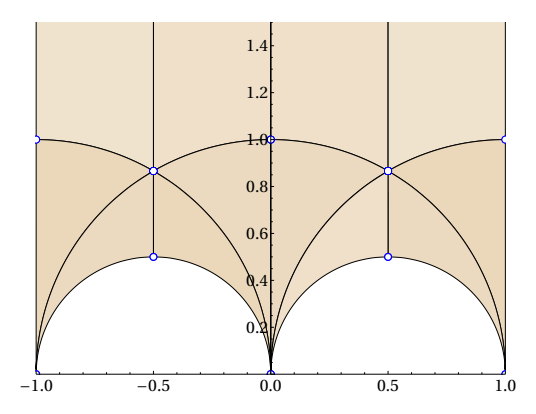


Figure 6.2: The fundamental domain  $\mathcal{D}(2)$  of  $\Gamma(2)$  (i.e., the full target space of  $\Gamma_2 \simeq S_3$ ) with the stabilisers of modular transformations of  $\Gamma_2$  denoted as dots.

For the doublet irreducible representation in a T-diagonal basis, the S and T generators take the form

$$\rho_{\mathbf{2}}(S) = \frac{1}{2} \begin{bmatrix} -1 & \sqrt{3} \\ \sqrt{3} & 1 \end{bmatrix}, \quad \rho_{\mathbf{2}}(T) = \begin{bmatrix} 1 & 0 \\ 0 & -1 \end{bmatrix}, \tag{6.14}$$

where here and in following subsection we use square brackets for representation matrices to distinguish

	$\gamma$	$ au_{\gamma}$		$\gamma$	$ au_{\gamma}$
$\mathcal{C}_2$	TC T S	$ \begin{vmatrix} 0 & 1+i \\ i\infty & \frac{1}{2} + \frac{i}{2} \\ i & 1 \end{vmatrix} $	$\mathcal{C}_3$	TS	$ \begin{array}{c ccccccccccccccccccccccccccccccccccc$

Table 6.1: The non-identity elements of  $\Gamma_2$  and respective stabilisers.

from the  $2 \times 2$  operators acting in the upper complex plane such as (6.5). For the doublet of  $\Gamma_2$  (S<sub>3</sub>), modular forms at stabilisers for S and T take the form:

$$Y_{\mathbf{2}}(\tau_S) \propto \frac{1}{2} \begin{bmatrix} -\sqrt{3} \\ 1 \end{bmatrix}, \ \frac{1}{2} \begin{bmatrix} 1 \\ \sqrt{3} \end{bmatrix}, \quad Y_{\mathbf{2}}(\tau_T) \propto \begin{bmatrix} 1 \\ 0 \end{bmatrix}, \begin{bmatrix} 0 \\ 1 \end{bmatrix}.$$
 (6.15)

These forms are directly determined following the discussion after Eq. (6.9). Only the overall factor cannot be determined.

### **6.2.2** $\Gamma_3$

 $\Gamma_3$  has the presentation  $S^2 = (ST)^3 = T^3 = e$ . It is isomorphic to  $A_4$ , the group of even permutations of four objects and the symmetry group of the tetrahedron. For  $\Gamma_3$ , S can be interpreted geometrically as a reflection and T as a 3-fold rotation. We consider 3 generators S, T and C = ST as described before. The list of equivalences between the relevant boundary points of the domain shown in Fig. 6.3 is:

$$\frac{3}{2} + \frac{i}{2\sqrt{3}} = \frac{1}{2} + \frac{i}{2\sqrt{3}} = -\frac{1}{2} + \frac{i}{2\sqrt{3}} = -\frac{3}{2} + \frac{i}{2\sqrt{3}}, 
\frac{3}{2} + \frac{i}{2} = -\frac{3}{2} + \frac{i}{2}, \qquad \frac{3}{2} + \frac{i\sqrt{3}}{2} = -\frac{3}{2} + \frac{i\sqrt{3}}{2}.$$
(6.16)

These relations complement Table 6.2.

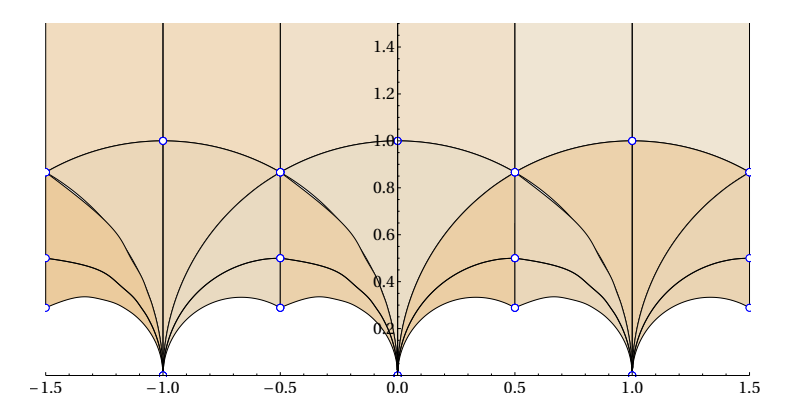


Figure 6.3: The fundamental domain  $\mathcal{D}(3)$  of  $\Gamma(3)$  with the stabilisers of modular transformations of  $\Gamma_3$  denoted as dots.

	$\gamma$	$ au_{\gamma}$	(		$\gamma$	$ au_{\gamma}$	Y		$\gamma$	$ au_{\gamma}$	,
$\mathcal{C}_2$	$C^2$ $T^2$ $TC$ $CT$	$-\frac{1}{2} + \frac{i\sqrt{3}}{2}$ $i\infty$ $0$ $-1$	$1$ $\frac{3}{2} + \frac{i}{2\sqrt{3}}$ $\frac{3}{2} + \frac{i\sqrt{3}}{2}$ $\frac{1}{2} + \frac{i\sqrt{3}}{2}$	$\mathcal{C}_3$	$egin{array}{c} C & & & & & \\ T & & & & & \\ CS & & & & \\ TS & & & & \end{array}$	$ \begin{array}{c} -\frac{1}{2} + \frac{i\sqrt{3}}{2} \\ i\infty \\ 0 \\ -1 \end{array} $	$1$ $\frac{3}{2} + \frac{i}{2\sqrt{3}}$ $\frac{3}{2} + \frac{i\sqrt{3}}{2}$ $\frac{1}{2} + \frac{i\sqrt{3}}{2}$	$\mathcal{C}_4$	$T^2C$ $S$ $TCT$	$-1+i$ $i$ $-\frac{1}{2}+\frac{i}{2}$	$\frac{\frac{1}{2} + \frac{i}{2}}{\frac{3}{2} + \frac{i}{2}}$ $1 + i$

**Table 6.2:** The non-identity elements of  $\Gamma_3$  and respective stabilisers.

The generators S and T for the triplet of  $A_4$  in a T-diagonal basis have the representation matrices:

$$\rho_{\mathbf{3}}(S) = \frac{1}{3} \begin{bmatrix} -1 & 2 & 2\\ 2 & -1 & 2\\ 2 & 2 & -1 \end{bmatrix}, \quad \rho_{\mathbf{3}}(T) = \begin{bmatrix} 1 & 0 & 0\\ 0 & \omega^2 & 0\\ 0 & 0 & \omega \end{bmatrix}.$$
 (6.17)

Note that this particular choice for the generators has been taken in the literature (see e.g. [263]). Following the discussion after Eq. (6.9), we obtain modular forms at stabilisers for S and T as

$$Y_{\mathbf{3}}(\tau_S) \propto \begin{bmatrix} 1\\1\\1 \end{bmatrix}, x \begin{bmatrix} 2\\-1\\-1 \end{bmatrix} + y \begin{bmatrix} 0\\1\\-1 \end{bmatrix}, Y_{\mathbf{3}}(\tau_T) \propto \begin{bmatrix} 1\\0\\0 \end{bmatrix}, \begin{bmatrix} 0\\1\\0 \end{bmatrix}, \begin{bmatrix} 0\\0\\1 \end{bmatrix}.$$
 (6.18)

Here, since  $\rho_{\mathbf{3}}(S)$  has degenerate eigenvalues,  $[2, -1, -1]^T$  and  $[0, 1, -1]^T$  and any of their linear combinations are eigenvectors of  $\rho_{\mathbf{3}}(S)$ . To further determine the coefficients x and y, we have to consider either correlations of modular forms (e.g.,  $Y_2^2 + 2Y_1Y_3 = 0$  for weight k = 2 [131]) or explicit expressions of modular forms.

#### **6.2.3** $\Gamma_4$

 $\Gamma_4$  is isomorphic to  $S_4$ , which is the group of all permutations of four objects, and the symmetry group of the cube and of the octahedron. Here, S can be interpreted geometrically as a reflection whereas T can be interpreted as a 4-fold rotation. In the framework of modular symmetry, the  $\Gamma_4$  modular group is obtained in the series of  $\Gamma_N$  by fixing N=4. In other words, its generators satisfy  $S^2=(ST)^3=T^4=e$ . In former works, it is common to use three generators S', T' and U' (we will use the primes to distinguish between these and the  $SL(2,\mathbb{Z})$  matrices), which satisfy  $S'^2=T'^3=U'^2=(S'T')^3=(S'U')^2=(T'U')^2=e$ , to generate  $S_4$ . These generators can be represented by S and T as

$$S' = T^2, \ T' = ST, \ U' = TST^2S.$$
 (6.19)

In the upper complex plane with the requirement  $\tau = \tau + 4$ , S', T' and U' can be represented by two by two matrices such as

$$S' = \begin{pmatrix} 1 & 2 \\ 0 & 1 \end{pmatrix}, \ T' = \begin{pmatrix} 0 & 1 \\ -1 & -1 \end{pmatrix}, \ U' = \begin{pmatrix} 1 & -1 \\ 2 & -1 \end{pmatrix}. \tag{6.20}$$

Due to the identification in Eq. (6.3), these representation matrices are not unique. It is convenient to write out other three elements of  $S_4$ ,  $T'S' = ST^{-1}$ ,  $S'T' = TST^{-1}S$  and  $S'T'S' = T^{-1}STS$ . They are order-three elements of  $S_4$  and will be used for our later discussion. The two by two representation matrices for them are given by

$$T'S' = \begin{pmatrix} 0 & 1 \\ -1 & 1 \end{pmatrix}, \ S'T' = \begin{pmatrix} 2 & -1 \\ 3 & -1 \end{pmatrix}, \ S'T'S' = \begin{pmatrix} -2 & -1 \\ 3 & 1 \end{pmatrix}. \tag{6.21}$$

We list the target space of  $\Gamma_4$ , namely, the fundamental domain  $\mathcal{D}(4)$ , in Fig. 6.4. The list of stabilisers is shown in Table 6.3, and the redundancies of the domain shown in Fig. 6.4 are

$$2 = -2, 2 + i = -2 + i, \frac{2}{5} + \frac{i}{5} = -\frac{2}{5} + \frac{i}{5},$$
  

$$\pm \frac{7}{5} + \frac{i}{5} = \pm \frac{3}{5} + \frac{i}{5}, \frac{8}{5} + \frac{i}{5} = -\frac{8}{5} + \frac{i}{5}, \frac{3}{2} = \frac{1}{2} = -\frac{1}{2} = -\frac{3}{2}. (6.22)$$

We note that the  $\pm$  in the equation above mean only that the two stabilisers with positive real part are equivalent, and that the two stabilisers with negative real part are equivalent, without further equivalences.

It may be instructive to show an example of how the redundancies appear, and why certain elements are stabilised by transformations which seemingly do not leave  $\tau$  invariant. We take, as an example, the point  $\tau = 3/2$ , which is stabilised by T and its powers. The reasoning is as follows:

- $\gamma(i\infty) = 3/2$  with  $\gamma = T^2ST^2S$ .
- The inverse relation must also hold:  $\gamma^{-1} = ST^2ST^2$ , such that  $\gamma^{-1}(3/2) = i\infty$ .
- Hence, since  $T(i\infty) = i\infty$ , we have that  $\gamma T \gamma^{-1}(3/2) = (3/2)$ .
- Using  $T^4 = S^2 = (ST)^3 = e$ , we can show  $\gamma T \gamma^{-1} = T^3$ , such that  $T^3(3/2) = (3/2)$ .
- If  $T^3(3/2) = (3/2)$ , then  $T^6$  and  $T^9$  must also stabilise  $\tau = 3/2$ . But, due to  $T^4 = e$ , we have  $T^6 = T^2$  and  $T^9 = T$ . As such, any power of T stabilises  $\tau = 3/2$ , which leads to  $3/2 = 3/2 + 1 = 3/2 + 2 = 3/2 + 3 \Leftrightarrow 3/2 = 1/2 = -1/2 = -3/2$ .

The remaining redundancies are obtained in similar ways.

By inverting the relations of Eq. (6.19), it is possible to find S and T as a function of S', T', and U':

$$S = S'T'S'U', T = S'T'S'U'T'.$$
(6.23)

For completeness, we show here for the triplet irreducible representations, in a T'-diagonal basis, the representations matrices for both choices of generators:

$$\rho_{\mathbf{3}^{(\prime)}}(S') = \frac{1}{3} \begin{bmatrix} -1 & 2 & 2 \\ 2 & -1 & 2 \\ 2 & 2 & -1 \end{bmatrix}, \quad \rho_{\mathbf{3}^{(\prime)}}(T') = \begin{bmatrix} 1 & 0 & 0 \\ 0 & \omega^2 & 0 \\ 0 & 0 & \omega \end{bmatrix}, \quad \rho_{\mathbf{3}^{(\prime)}}(U') = (-) \begin{bmatrix} 1 & 0 & 0 \\ 0 & 0 & 1 \\ 0 & 1 & 0 \end{bmatrix}, \quad (6.24)$$

and

$$\rho_{\mathbf{3}^{(\prime)}}(S) = (-)\frac{1}{3} \begin{bmatrix} -1 & 2\omega^2 & 2\omega \\ 2\omega & 2 & -\omega^2 \\ 2\omega^2 & -\omega & 2 \end{bmatrix}, \quad \rho_{\mathbf{3}^{(\prime)}}(T) = (-)\frac{1}{3} \begin{bmatrix} -1 & 2\omega & 2\omega^2 \\ 2\omega & 2\omega^2 & -1 \\ 2\omega^2 & -1 & 2\omega \end{bmatrix}, \tag{6.25}$$

where  $\omega = e^{2i\pi/3}$ .

For the triplet 3 of  $\Gamma_4$  ( $S_4$ ), modular forms at stabilisers for S and T take the form:

$$Y_{\mathbf{3}}(\tau_S) \propto \begin{bmatrix} 2 \\ -\omega \\ -\omega^2 \end{bmatrix}, x \begin{bmatrix} -\omega \\ 2 \\ 0 \end{bmatrix} + y \begin{bmatrix} \omega \\ 0 \\ 2 \end{bmatrix}, Y_{\mathbf{3}}(\tau_T) \propto \begin{bmatrix} 1 \\ 1 \\ 1 \end{bmatrix}, \begin{bmatrix} 1 - \sqrt{3} \\ \sqrt{3} - 2 \\ 1 \end{bmatrix}, \begin{bmatrix} 1 + \sqrt{3} \\ -\sqrt{3} - 2 \\ 1 \end{bmatrix}, (6.26)$$

where, as in  $\Gamma_3$ , we use x, y as placeholder normalization factors that can be found (for a specified weight). We note that  $Y_3(\tau_{S'})$  and  $Y_3(\tau_{T'})$  are the same as  $Y_3(\tau_S)$  and  $Y_3(\tau_T)$ , respectively, in Eq. (6.18). In turn,  $Y_3(\tau_{U'})$  is given by (using x, y factors):

$$Y_{\mathbf{3}}(\tau_{U'}) \propto \begin{bmatrix} 0\\1\\-1 \end{bmatrix}, x \begin{bmatrix} 1\\0\\0 \end{bmatrix} + y \begin{bmatrix} 0\\1\\1 \end{bmatrix}.$$
 (6.27)

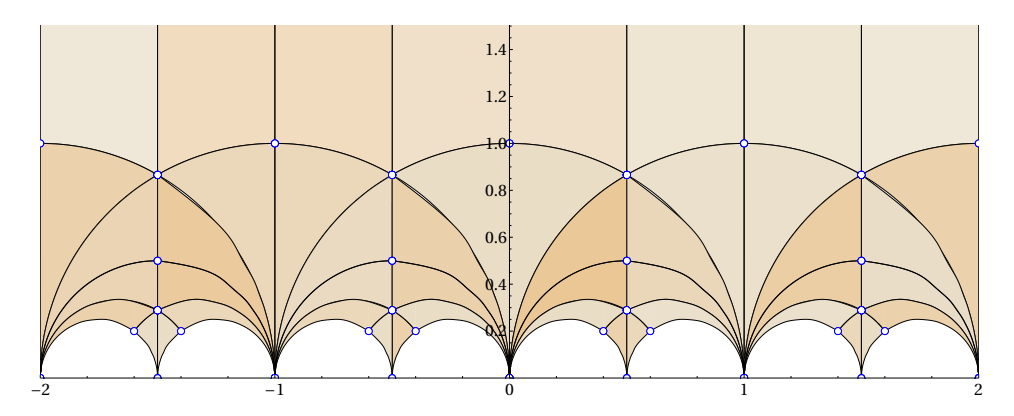


Figure 6.4: The fundamental domain  $\mathcal{D}(4)$  of  $\Gamma(4)$  with the stabilisers of modular transformations of  $\Gamma_4$  denoted as dots.

	$\gamma$	$ au_{\gamma}$		$\gamma$	$ au_{\gamma}$
$\mathcal{C}_2$	$T^{2}CT$ $T^{2}CS$ $TCTS$ $S$ $CTC$ $C^{2}T$	$ \frac{2}{5} + \frac{i}{5} \qquad 2 + i  1 + i \qquad -\frac{3}{5} + \frac{i}{5}  -\frac{3}{2} + \frac{i}{2} \qquad \frac{1}{2} + \frac{i}{2}  i \qquad \frac{8}{5} + \frac{i}{5}  -\frac{1}{2} + \frac{i}{2} \qquad \frac{3}{2} + \frac{i}{2}  -1 + i \qquad \frac{7}{5} + \frac{i}{5} $	$\mathcal{C}_3$	$C^2$ $C$ $T^2C$ $CTCS$ $TCT$ $C^2TS$ $TCS$ $TCS$	$-\frac{1}{2} + \frac{i\sqrt{3}}{2}  \frac{3}{2} + \frac{i}{2\sqrt{3}}$ $-\frac{1}{2} + \frac{i\sqrt{3}}{2}  \frac{3}{2} + \frac{i}{2\sqrt{3}}$ $-\frac{3}{2} + \frac{i\sqrt{3}}{2}  \frac{1}{2} + \frac{i}{2\sqrt{3}}$ $-\frac{3}{2} + \frac{i\sqrt{3}}{2}  \frac{1}{2} + \frac{i}{2\sqrt{3}}$ $-\frac{1}{2} + \frac{i}{2\sqrt{3}}  \frac{3}{2} + \frac{i\sqrt{3}}{2}$ $-\frac{1}{2} + \frac{i}{2\sqrt{3}}  \frac{3}{2} + \frac{i\sqrt{3}}{2}$ $-\frac{1}{2} + \frac{i}{2\sqrt{3}}  \frac{3}{2} + \frac{i\sqrt{3}}{2}$ $-\frac{3}{2} + \frac{i}{2\sqrt{3}}  \frac{1}{2} + \frac{i\sqrt{3}}{2}$ $-\frac{3}{2} + \frac{i}{2\sqrt{3}}  \frac{1}{2} + \frac{i\sqrt{3}}{2}$
$\mathcal{C}_4$	$T^2$ $CTS$ $CTCT$	$i\infty  \frac{3}{2}$ $0  2$ $-1  1$	$\mathcal{C}_5$	$T$ $T^3$ $CS$ $TC$ $T^2S$ $CT$	$i\infty  \frac{3}{2}$ $i\infty  \frac{3}{2}$ $i\infty  \frac{3}{2}$ $0  2$ $0  2$ $-1  1$ $-1  1$

**Table 6.3:** The non-identity elements of  $\Gamma_4$  and respective stabilisers.

#### **6.2.4** $\Gamma_5$

 $\Gamma_5$  is isomorphic to  $A_5$ , which is the group of even permutations of five objects and the symmetry group of the dodecahedron and of the icosahedron. The generators satisfy  $S^2 = (ST)^3 = T^5 = e$ . S can be interpreted geometrically as a reflection, with T interpreted as a 5-fold rotation. With 60 elements, we can generate the group with a minimal generating set of two elements but it is more helpful to also consider three as we have done previously, with C = ST. We note that the domain shown in Fig. 6.5 appears to be missing some sections (it is no longer symmetric around the cusps). This is due to the equivalence of some points of the complex plane (brought on by  $T^N = e$ ). The stabilisers are compiled in Table 6.4, where the stabilisers have equivalent values within the boundary of the domain shown in Fig. 6.5, given by:<sup>4</sup>

$$\begin{split} \frac{5}{2} &= -\frac{5}{2}, \qquad -\frac{12}{5} = -\frac{7}{5} = -\frac{2}{5} = \frac{3}{5} = \frac{8}{5}, \\ \frac{5}{2} + \frac{i}{2} &= -\frac{5}{2} + \frac{i}{2}, \qquad \frac{5}{2} + i\frac{\sqrt{3}}{2} = -\frac{5}{2} + i\frac{\sqrt{3}}{2}, \qquad \frac{5}{2} + \frac{i}{2\sqrt{3}} = -\frac{5}{2} + \frac{i}{2\sqrt{3}}, \\ \pm \frac{33}{14} + i\frac{\sqrt{3}}{14} &= \pm \frac{23}{14} + i\frac{\sqrt{3}}{14}, \qquad \pm \frac{19}{14} + i\frac{\sqrt{3}}{14} = \pm \frac{9}{14} + i\frac{\sqrt{3}}{14}, \qquad \frac{5}{14} + i\frac{\sqrt{3}}{14} = -\frac{5}{14} + i\frac{\sqrt{3}}{14}, \\ \frac{5}{13} + \frac{i}{13} &= -\frac{5}{13} + \frac{i}{13}, \qquad \pm \frac{18}{13} + \frac{i}{13} = \pm \frac{8}{13} + \frac{i}{13}, \qquad \pm \frac{31}{13} + \frac{i}{13} = \pm \frac{21}{13} + \frac{i}{13}, \end{split}$$

In Eq.(6.28), most of the equivalences are due to the redundancy between the outer-most boundaries (that is,  $\text{Re}(\tau) = \pm 5/2$ ). The only exception is -0.4 = 0.6 (the remaining follow trivially), which can be shown to be equivalent by making use of  $\gamma_1 = \begin{pmatrix} -2 & -1 \\ 5 & 2 \end{pmatrix}$ , and  $\gamma_2 = \begin{pmatrix} 3 & 1 \\ 5 & 2 \end{pmatrix}$ . It can be seen that  $\gamma_2^2 = e$ , and  $\gamma_2 \cdot \gamma_1 = T^4$ , where  $\gamma_1$ ,  $\gamma_2 \in \Gamma_5$ . Choosing  $\tau = i\infty$ , we have that  $\gamma_1 i\infty = -2/5$ , and  $\gamma_2 i\infty = 3/5$ . In this way,  $-2/5 = \gamma_1 i\infty = \gamma_2 \cdot \gamma_2 \cdot \gamma_1 i\infty = \gamma_2 T^4 i\infty = \gamma_2 i\infty = 3/5$ . Hence, -2/5 = 3/5, and the remaining follow by acting T on this equivalence.

$$\frac{15}{26} + \frac{i}{26\sqrt{3}} = \frac{15}{38} + i\frac{\sqrt{3}}{38} = -\frac{15}{38} + i\frac{\sqrt{3}}{38} = -\frac{15}{26} + \frac{i}{26\sqrt{3}},$$

$$\pm \frac{41}{26} + \frac{i}{26\sqrt{3}} = \pm \frac{53}{38} + i\frac{\sqrt{3}}{38} = \pm \frac{23}{38} + i\frac{\sqrt{3}}{38} = \pm \frac{11}{26} + \frac{i}{26\sqrt{3}},$$

$$\pm \frac{91}{38} + i\frac{\sqrt{3}}{38} = \mp \frac{63}{26} + \frac{i}{26\sqrt{3}} = \pm \frac{61}{38} + i\frac{\sqrt{3}}{38} = \pm \frac{37}{26} + \frac{i}{26\sqrt{3}}.$$
(6.28)

In these equivalences, we stress the  $\pm$  and the  $\mp$  are not interchangeable. Each equivalence featuring these symbols is a compact form encoding only two (not four) separate equivalences.

In terms of the generators S and T, in a T-diagonal basis, for the triplet irreducible representations of  $A_5$ , we have the following representation matrices:

$$\rho_{\mathbf{3}}(S) = \frac{1}{\sqrt{5}} \begin{bmatrix} 1 & -\sqrt{2} & -\sqrt{2} \\ -\sqrt{2} & -\phi_g & \phi_g - 1 \\ -\sqrt{2} & \phi_g - 1 & -\phi_g \end{bmatrix}, \quad \rho_{\mathbf{3}}(T) = \begin{bmatrix} 1 & 0 & 0 \\ 0 & \omega_5 & 0 \\ 0 & 0 & \omega_5^4 \end{bmatrix}, \\
\rho_{\mathbf{3}'}(S) = \frac{1}{\sqrt{5}} \begin{bmatrix} -1 & \sqrt{2} & \sqrt{2} \\ \sqrt{2} & 1 - \phi_g & \phi_g \\ \sqrt{2} & \phi_g & 1 - \phi_g \end{bmatrix}, \quad \rho_{\mathbf{3}'}(T) = \begin{bmatrix} 1 & 0 & 0 \\ 0 & \omega_5^2 & 0 \\ 0 & 0 & \omega_5^3 \end{bmatrix}, \quad (6.29)$$

where 
$$\phi_g = \frac{(1+\sqrt{5})}{2}$$
.

For the triplets of  $\Gamma_5$  ( $A_5$ ), the modular forms at stabilisers of the generators are:

$$Y_{\mathbf{3}}(\tau_{S}) \propto \begin{bmatrix} -2\phi_{g} \\ \sqrt{2} \\ \sqrt{2} \end{bmatrix}, \quad x \begin{bmatrix} \phi_{g} - 1 \\ \sqrt{2} \\ 0 \end{bmatrix} + y \begin{bmatrix} \phi_{g} - 1 \\ 0 \\ \sqrt{2} \end{bmatrix}, \quad Y_{\mathbf{3}}(\tau_{T}) \propto \begin{bmatrix} 1 \\ 0 \\ 0 \end{bmatrix}, \quad \begin{bmatrix} 0 \\ 1 \\ 0 \end{bmatrix}, \quad \begin{bmatrix} 0 \\ 0 \\ 1 \end{bmatrix},$$

$$Y_{\mathbf{3}'}(\tau_{S}) \propto \begin{bmatrix} 2\phi_{g} - 2 \\ \sqrt{2} \\ \sqrt{2} \end{bmatrix}, \quad x \begin{bmatrix} -\phi_{g} \\ \sqrt{2} \\ 0 \end{bmatrix} + y \begin{bmatrix} -\phi_{g} \\ 0 \\ \sqrt{2} \end{bmatrix}, \quad Y_{\mathbf{3}'}(\tau_{T}) \propto \begin{bmatrix} 1 \\ 0 \\ 0 \end{bmatrix}, \quad \begin{bmatrix} 0 \\ 1 \\ 0 \end{bmatrix}, \quad \begin{bmatrix} 0 \\ 0 \\ 1 \end{bmatrix}, \quad (6.30)$$

where (again) x, y are placeholder normalization factors that can be found (for a specified weight).

### 6.3 Discussion

In this chapter, we have described and employed an algorithm for identifying stabilisers  $\tau_{\gamma}$  for finite modular groups. We used the algorithm to find all inequivalent stabilisers for each group element  $\gamma \in \Gamma_{2,3,4,5}$ , *i.e.*, for finite modular groups with N up to 5. We have shown the stabilisers in the domains of the respective modular symmetries, in the upper complex plane, and the Tables 6.1-6.4 list our findings. The stabilisers listed are complete in the sense that we present all inequivalent stabilisers. Nevertheless, we note that these have infinite multiplicities in the upper complex plane, but we show the explicit multiplicities in the domains shown within the figures. Given that each group element by itself generates a specific cyclic subgroup of the finite modular symmetry, our work provides stabilisers for each of these

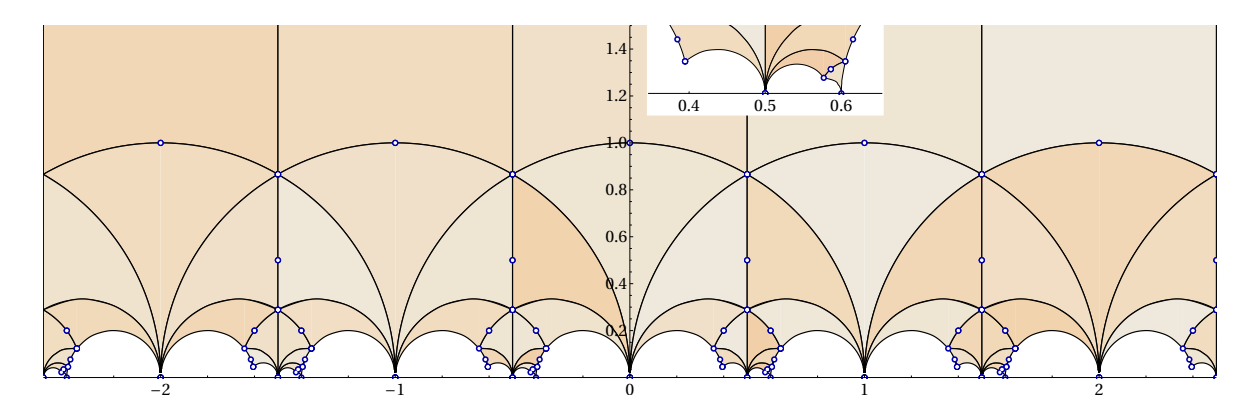


Figure 6.5: The fundamental domain  $\mathcal{D}(5)$  of  $\Gamma(5)$  with the stabilisers of modular transformations of  $\Gamma_5$  denoted as dots. In the box on top, we show a zoomed section of the domain around the cusp  $\tau = 1/2$ , where there are many small-sized intricacies. We show only one zoomed section as the remaining areas surrounding the half-integer cusps are identical.

cyclic subgroups, and is therefore useful to applications of finite modular symmetries that are broken to residual subgroups. In particular, this work is intended to assist model-building efforts when finite modular symmetries are used as flavour symmetries, to account for fermion masses and mixing.

6.3 Discussion 137

	$\gamma$	$ au_{\gamma}$	,		γ	$ au_{\gamma}$	
$\mathcal{C}_2$	$\begin{array}{c c} \gamma \\ \hline T^3CTC \\ CTCT^2 \\ CTCTC \\ CT^2C \\ \hline T^3CT^2 \\ T^2CT \\ TS \\ TCS \\ CT^2CS \\ T^2CTC \\ C^2T^2 \\ T^3C \\ CT^2CT \\ T^3CTS \\ T^3CTS \\ T^3CS \\ TCT^2 \\ C \\ \end{array}$	$-\frac{3}{2} + \frac{i}{2\sqrt{3}} - \frac{3}{2} + \frac{i}{2\sqrt{3}} - \frac{1}{2} + \frac{i}{2\sqrt{3}} - \frac{1}{2} + \frac{i}{2\sqrt{3}}$	$\frac{\frac{19}{14} + \frac{i\sqrt{3}}{14}}{\frac{19}{14} + \frac{i\sqrt{3}}{14}}$ $\frac{33}{14} + \frac{i\sqrt{3}}{14}$	$\mathcal{C}_3$	$\begin{array}{c} C^2T \\ T^2CT^2CS \\ CT^2CTS \\ T^2CT^2 \\ S \\ CT^2CTC \\ CTCT^2C \\ T^2CT^2CT \\ C^2T^2CT \\ TCTS \\ CTCT^2CT \\ TCTS \\ CTCT^2CT \\ CTC \\ T^3CT \\ T^2CS \\ TCT^2CTS \end{array}$	$-1+i$ $-\frac{8}{13}+\frac{i}{13}$ $-\frac{12}{5}+\frac{i}{5}$ $-\frac{12}{29}+\frac{i}{29}$ $-\frac{70}{29}+\frac{i}{29}$ $-\frac{2}{5}+\frac{i}{5}$ $-\frac{3}{5}+\frac{i}{5}$ $\frac{5}{13}+\frac{i}{13}$ $-\frac{3}{2}+\frac{i}{2}$ $-\frac{21}{13}+\frac{i}{13}$ $-\frac{7}{5}+\frac{i}{5}$ $-\frac{1}{2}+\frac{i}{2}$ $-2+i$ $-\frac{41}{29}+\frac{i}{29}$	$\frac{46}{29} + \frac{i}{29}$ $\frac{3}{2} + \frac{i}{2}$ $\frac{2}{5} + \frac{i}{5}$ $2 + i$ $i$ $\frac{12}{5} + \frac{i}{5}$ $\frac{8}{5} + \frac{i}{5}$ $\frac{5}{2} + \frac{i}{2}$ $\frac{18}{13} + \frac{i}{13}$ $\frac{1}{2} + \frac{i}{2}$ $\frac{31}{13} + \frac{i}{13}$ $\frac{17}{29} + \frac{i}{29}$ $1 + i$
	$C^2$ $TCT^2C$ $CTCTS$	$-\frac{1}{2} + \frac{i\sqrt{3}}{2}$ $\frac{5}{14} + \frac{i\sqrt{3}}{14}$ $\frac{5}{14} + \frac{i\sqrt{3}}{14}$	$\frac{91}{38} + \frac{i\sqrt{3}}{38}$ $\frac{5}{2} + \frac{i}{2\sqrt{3}}$ $\frac{5}{2} + \frac{i}{2\sqrt{3}}$		TCT <sup>2</sup> CTS	$-\frac{8}{5} + \frac{i}{5}$	<del>5</del> + <del>5</del>
	T	$i\infty$	8 5		$T^2$	$i\infty$	<u>8</u> 5
	$T^4$	$i\infty$	8 5		$T^3$	$i\infty$	8 5
	TC	0	$\frac{5}{2}$		CTS	0	$\frac{5}{2}$
	CS	0	$\frac{5}{2}$		TCTC	0	$\frac{5}{2}$
	$C^2TS$	$-\frac{1}{2}$	2		$C^2T^2CTS$	$-\frac{1}{2}$	2
$\mathcal{C}_4$	TCT	$-\frac{1}{2}$	2	$\mathcal{C}_5$	$TCT^2CT$	$-\frac{1}{2}$	2
	$T^3S$	-1	$\frac{3}{2}$	C5	$C^2T^2C$	-1	$\frac{3}{2}$
	CT	-1	$\frac{3}{2}$		CTCT	-1	$\frac{3}{2}$
	$T^2S$	$-\frac{3}{2}$	1		$T^2CTS$	$-\frac{3}{2}$	1
	$CT^2$	$-\frac{3}{2}$	1		$TCT^2CS$	$-\frac{3}{2}$	1
	CTCS	-2	$\frac{1}{2}$		$T^2CT^2C$	-2	$\frac{1}{2}$
	$T^2C$	-2	$\frac{1}{2}$		$CTCT^2CS$	-2	$\frac{1}{2}$

Table 6.4: The non-identity elements of  $\Gamma_5$  and respective stabilisers.

# 7

## Littlest Modular Seesaw and its SU(5) Extension

One piece of the flavour puzzle that has received a lot of attention is the lightness of neutrino masses. Although the type I seesaw mechanism can qualitatively explain the smallness of neutrino masses through heavy right-handed neutrinos (RHNs), if one doesn't make other assumptions, it contains too many parameters to make any particular predictions for neutrino mass and mixing. The sequential dominance (SD) [264, 265] of right-handed neutrinos proposes that the mass spectrum of heavy Majorana neutrinos is strongly hierarchical, i.e.  $M_{\rm atm} \ll M_{\rm sol} \ll M_{\rm dec}$ , where the lightest RHN with mass  $M_{\rm atm}$  is responsible for the atmospheric neutrino mass, that with mass  $M_{\rm sol}$  gives the solar neutrino mass, and a third largely decoupled RHN gives a suppressed lightest neutrino mass. It leads to an effective two right-handed neutrino (2RHN) model [266, 267] with a natural explanation for the physical neutrino mass hierarchy, with normal ordering and the lightest neutrino being approximately massless,  $m_1 = 0$ .

A very predictive minimal seesaw model with two right-handed neutrinos and one texture zero is the so-called constrained sequential dominance (CSD) model [268–277]. The CSD(n) scheme assumes that the two columns of the Dirac neutrino mass matrix are proportional to (0,1,-1) and (1,n,2-n) respectively, in the RHN diagonal basis, where the parameter n was initially assumed to be a positive integer, but in general may be a real number. For example, the CSD(3) (also called Littlest Seesaw model) [270–274], or CSD(4) models [275, 276] and CSD(-1/2) [278] can give rise to phenomenologically viable predictions for lepton mixing parameters and the two neutrino mass squared differences  $\Delta m_{21}^2$  and  $\Delta m_{31}^2$ , corresponding to special constrained cases of TM<sub>1</sub> lepton mixing. Remarkably, modular symmetry suggests CSD(1 +  $\sqrt{6} \approx 3.45$ ) [257, 279], where the three required moduli have been incorporated into complete models of leptons at the field theory level [280], or in 10-dimensional orbifolds [281]. However, leveraging the modular construction to accommodate the quark sector in a non-trivial manner proves more complicated. The origin of all quark and lepton masses and mixing may be addressed by combining Grand Unified Theories (GUTs) with modular symmetry groups, for example SU(5) GUT models at

level 2 [282, 283], level 3 [284–286] and level 4 [279, 287, 288]. To this end, an SU(5) extension of the Littlest Modular Seesaw was proposed in [290].

This chapter follows refs. [280, 290], where Section 7.1 is devoted to the Littlest Modular Seesaw construction of ref. [280], with Section 7.1.1 presenting the fields and their respective assignments under the modular symmetries. The ensuing charged-lepton and neutrino sectors are the focus of Section 7.1.2 and Section 7.1.3, respectively. Analytical results for the leptonic mixing angles and the neutrino masses are given in Section 7.1.4 and a numerical analysis is done in Section 7.1.5. We also show alternative constructions, which employ weightons to provide an explanation for the hierarchy of the charged-lepton masses in Section 7.1.6. Section 7.2 is dedicated to the SU(5) extension proposed in ref. [290]. A brief introduction of the SU(5) embedding of the model, shown in Section 7.2.1. Following, we present the model in Section 7.2.2, including the numerical results. Finally, we conclude in Section 7.3.

### 7.1 The Littlest Modular Seesaw

In this section, we go through the first complete model of the Littlest Modular Seesaw (LMS), based on  $CSD(1-\sqrt{6}) \approx CSD(-1.45)$ , within a consistent framework based on multiple modular symmetries. We also study related possibility based on  $CSD(1+\sqrt{6}) \approx CSD(3.45)$ , intermediate between CSD(3) and CSD(4). In each case, three  $S_4$  modular symmetries are introduced, each with their respective modulus field at a distinct stabilizer, leading to three separate residual subgroups. The result, in the symmetry basis, is a diagonal charged-lepton mass matrix and a LMS scenario of a particular kind. In order to account for the hierarchy of the charged-lepton masses, we subsequently introduce a weighton field, where this model is implemented by upgrading the modular symmetries to the respective double covers,  $S'_4$ . Using a semi-analytical approach, we perform a  $\chi^2$  analysis of each case and show that good agreement with neutrino oscillation data is obtained, for both possible octants of atmospheric angle, including predictive relations between the leptonic mixing angles and the ratio of light neutrino masses, which non-trivially agree with the experimental values. It is noteworthy that in this very predictive setup, all the models fit the experimental data remarkably well, depending on the choice of stabilizers and data set, in one case to within approximately  $1\sigma$ .

The Littlest Modular Seesaw relies on multiple modular symmetries to impose the CSD(n) structure, with bi-triplet flavons which acquire vacuum expectation values in such a way that the three  $S_4$  modular symmetries are broken down to a diagonal  $S_4$  subgroup which effectively mimics a single modular symmetry, with different moduli, depending on the invariant considered [137]. The inclusion of flavons (with non-zero vevs) will spontaneously break the modular symmetry, and thus it is no longer always possible to perform a modular group action  $\gamma$  such that only the fundamental domain may be considered [141]. In the low-energy theory, the whole domain is relevant, and we can make use of all of the different fixed points [257, 258]. This is also possible to understand in the context of multiple modular symmetries, by recalling that the bi-triplets break the multiple modular symmetries into a diagonal subgroup. As such,

<sup>&</sup>lt;sup>1</sup>Also flipped  $SU(5) \times A_4$  [286] and  $SO(10) \times A_4$  [289] modular models have been considered.

<sup>&</sup>lt;sup>2</sup>Here, we do not dwell on the choice of normalisations for the modular forms [291]. We assume the canonical renormalisation effect due to the (minimal) Kähler potential (see also [156]) to be absorbed into the modular form normalisation. The relevance of this for the concept of *naturalness* requires a dedicated study [158, 292].

the group action will transform all moduli simultaneously, and consequently it is no longer possible to send all moduli to the fundamental domain in general.

#### 7.1.1Symmetries and Stabilisers

The model features three commuting  $S_4$  modular symmetries, which we label as  $S_4^A$ ,  $S_4^B$ ,  $S_4^C$ . At low energies, due to the vevs of fields  $\Phi_{AC}$  and  $\Phi_{BC}$ , they are broken down to the diagonal subgroup, as described in [137]. Table 7.1 contains the transformation properties (representations and modular weights) under the modular symmetries of the fields and of the relevant modular forms, where we also take usual SU(2) doublets  $H_{u,d}$  to transform trivially under all flavour symmetries, and so we omit them from Table 7.1. These assignments are very similar to those used in [137].<sup>3</sup>

Field	$S_4^A$	$S_4^B$	$S_4^C$	$k_A$	$k_B$	$k_C$				~			
_							Yuk/Mass	$S_4^A$	$S_4^B$	$S_4^C$	$2k_A$	$2k_B$	$2k_C$
L	1	1	3	0	0	0	$Y_e(\tau_C)$	1	1	3′	0	0	6
$e^c$	1	1	<b>1</b> '	0	0	6		_			-	-	
$\mu^c$	1	1	<b>1</b> '	0	0	4	$Y_{\mu}(\tau_C)$	1	1	<b>3</b> '	0	0	4
$\tau^c$	1	1	1′	0	0	2	$Y_{\tau}(\tau_C)$	1	1	<b>3</b> '	0	0	2
	_		1	_	_	_	$Y_A( au_A)$	3′	1	1	4	0	0
$N_A^c$	1′	1	1	4	0	0	$Y_B(\tau_B)$	1	<b>3</b> '	1	0	2	0
$N_B^c$	1	<b>1</b> '	1	0	2	0	, ,						
$\Phi_{AC}$	3	1	3	0	0	0	$M_A( au_A)$	1	1	1	8	0	0
				_			$M_B(\tau_B)$	1	1	1	0	4	0
$\Phi_{BC}$	1	3	3	0	0	0							

Table 7.1: Transformation properties of fields and modular forms (Yuk/Mass) under the modular symmetries.

Our goal is to achieve a CSD(3.45) [257] structure from the multiple modular symmetries. To that end, the desired directions of the modular forms are obtained for these representations and weights at specific stabilizers [137, 257, 258]. Namely, following the basis of [137], we compute the modular forms:<sup>4</sup>

$$\tau_A = \frac{1}{2} + \frac{i}{2} : Y_{\mathbf{3}'}^{(4)}(\tau_A) = (0, -1, 1),$$
(7.1)

for one of the Dirac mass matrix columns, and

$$\tau_B = \frac{3}{2} + \frac{i}{2}: Y_{\mathbf{3}'}^{(2)}(\tau_B) = (1, 1 - \sqrt{6}, 1 + \sqrt{6}), (7.2)$$

or

$$\tau_B = -\frac{1}{2} + \frac{i}{2}: Y_{3'}^{(2)}(\tau_B) = (1, 1 + \sqrt{6}, 1 - \sqrt{6}), (7.3)$$

for the other. These specific modular forms lead to the desired CSD structure. In the same basis, we want to enforce a diagonal structure for the charged-lepton Yukawa coupling matrices. This can be easily achieved through the weights 2, 4, and 6 modular forms transforming as 3', for  $\tau_C = \omega \equiv e^{2\pi i/3}$ :

$$Y_{\mathbf{3'}}^{(2)}(\tau_C) = (0, 1, 0) \tag{7.4a}$$

<sup>&</sup>lt;sup>3</sup>We note there is a typo in [137] where RH leptons and the respective modular forms should have primes, as the modular form  $Y_{\tau}(\tau_C)$  (weight 2) only exists as a 3'.

<sup>4</sup>This choice is not unique, and  $\tau_A' = (-3+i)/2$  also gives the same modular form.

$$\tau_C = \omega : Y_{3'}^{(4)}(\tau_C) = (0, 0, 1) (7.4b)$$

$$Y_{\mathbf{3'}}^{(6)}(\tau_C) = (1, 0, 0) \tag{7.4c}$$

A subtlety should be noted here. Indeed, for weight 6, there are two independent 3' modular forms, which could spoil the diagonal arrangement of the charged-leptons. Nevertheless, for  $\tau = \omega$ , one of them vanishes, introducing no further parameters.

In Appendix C.2 it is shown that  $\tau_A$  and  $\tau'_A$  are stabilisers of U, and that  $\tau_B$  (either version) is a stabiliser of SU in our chosen basis. It is also shown that the respective modular forms we are using are eigenvectors of the 3' representation matrices.

For clarity, we note that the basis in which the modular forms are computed in the present work follows reference [137], which is different from [257]. To be precise, although the  $S_4$  basis used here and [137] is the same as that in [257], the basis of modular generators is different, and hence the modular forms differ also. However the physics should be and is basis independent, and indeed the Yukawa alignments shown above can be achieved for different values of the modulus field in the two different bases. It is useful to present the different stabilisers for both the cases which lead to the desired modular forms, which are shown in Table 7.2.<sup>5</sup> To explicitly show that these two cases are nothing more than a basis transformation, we note that we can find a single modular action, which takes the form

$$\gamma = \begin{pmatrix} 1 & 0 \\ 1 & 1 \end{pmatrix}, \tag{7.5}$$

which leads to

$$\gamma \circ \frac{-1+i}{2} = i, \quad \gamma \circ \frac{3+i}{2} = \frac{-8+i}{13}, \quad \gamma \circ \frac{1+i}{2} = \frac{-2+i}{5}, \quad \gamma \circ \frac{-3+i}{2} = 2+i, \tag{7.6}$$

where we have used that  $(-2+i)/5 \equiv (2+i)/5$  and  $(-8+i)/13 \equiv (8+i)/13$ , both of which can be understood by the application of  $ST^2S$  on  $\pm 2+i$ , given  $T^4=e$ . In this way, the full domain is relevant, since we can no longer perform individual modular actions on each modular symmetry. However, it is still possible to perform a modular transformation on the diagonal subgroup, which acts on all the individual modular symmetries simultaneously. The choice of  $\gamma$  in Eq. (7.5) will also transform the charged-lepton stabiliser from the left to the right cusp ( $\omega$  to  $-\omega^2$ ), which leads to the same modular forms. As such, both cases will feature the same mass matrices, as expected.

 $<sup>^5</sup>$ Note that with multiple moduli, transforming under a diagonal  $S_4$  subgroup, it is meaningful to have fixed points outside the fundamental domain. This can be understood for a case with two moduli, one inside and one outside the fundamental domain, the relative difference in residual subgroups is relevant - the transformation of the diagonal  $S_4$  subgroup that brings one inside takes the other one outside.

**Table 7.2:** Relevant stabilisers to obtain the desired modular forms to achieve either a CSD(3.45) or a CSD(-1.45) model, both for basis 1 (used throughout this chapter), and basis 2 used in [257]. Note that the convention of **3** and **3**' is exchanged.

#### 7.1.2 Charged-Leptons

With the fields and assignments of the previous subsection, we write the respective lepton sector superpotential as

$$w_{\ell} = \frac{1}{\Lambda} \left[ L\Phi_{AC}Y_{A}(\tau_{A})N_{A}^{c} + L\Phi_{BC}Y_{B}(\tau_{B})N_{B}^{c} \right] H_{u}$$

$$+ \left[ LY_{e}(\tau_{C})e^{c} + LY_{\mu}(\tau_{C})\mu^{c} + LY_{\tau}(\tau_{C})\tau^{c} \right] H_{d}$$

$$+ \frac{1}{2}M_{A}(\tau_{A})N_{A}^{c}N_{A}^{c} + \frac{1}{2}M_{B}(\tau_{B})N_{B}^{c}N_{B}^{c} + M_{AB}(\tau_{A}, \tau_{B})N_{A}^{c}N_{B}^{c} .$$

$$(7.7)$$

Expanding the superpotential of Eq. (7.7), we can find the mass matrices for the fields after the electroweak symmetry breaking, where we are assuming the minimal form of the Kähler potential.<sup>6</sup> Due to the nature of the  $S_4$  tensor products in our chosen basis, and the particular structure chosen for the bi-triplets vevs, the  $\mathbf{3} \otimes \mathbf{3}$  tensor products are non-diagonal:

$$(\mathbf{a} \otimes \mathbf{b})_1 = a_1 b_1 + a_2 b_3 + a_3 b_2,$$
 (7.8)

$$(\mathbf{a} \otimes \langle \Phi \rangle \otimes \mathbf{b})_1 \propto a_1 b_1 + a_2 b_3 + a_3 b_2.$$
 (7.9)

Hence, the charged-lepton mass matrix is simply given by

$$M_{l} = v_{d} \begin{pmatrix} (Y_{e})_{1} & (Y_{\mu})_{1} & (Y_{\tau})_{1} \\ (Y_{e})_{3} & (Y_{\mu})_{3} & (Y_{\tau})_{3} \\ (Y_{e})_{2} & (Y_{\mu})_{2} & (Y_{\tau})_{2} \end{pmatrix},$$

$$(7.10)$$

where we omit the  $\tau_c$  dependency for clarity, and  $v_d$  stands for  $\langle H_d \rangle$ . Plugging in the specific shapes of the modular forms given in Eqs. (7.4a)-(7.4c) we arrive at a diagonal charged-lepton mass matrix when  $\tau_C = \omega$ :

$$M_l = v_d \begin{pmatrix} y_e & 0 & 0 \\ 0 & y_\mu & 0 \\ 0 & 0 & y_\tau \end{pmatrix}, \tag{7.11}$$

<sup>&</sup>lt;sup>6</sup>The choice of the minimal Kähler potential is common in modular flavour constructions, as a generic Kähler potential compatible with modular invariance would reduce the predictive power of the model [156]. However, in principle it should be possible to modify the model, for example by replacing the modular group associated with the lepton doublets by a traditional flavour symmetry, in order to incorporate the Quasi-Eclectic mechanism in which such corrections are controlled [293].

where  $v_d$   $y_{e,\mu,\tau}$  are the electron, muon, and tau masses respectively. For now, the hierarchical masses of the charged-leptons are not addressed. In order to naturally deal with this issue, we present two modifications of this model in Section 7.1.6, where a weighton is responsible for the hierarchy of the masses, without affecting the remaining predictions of the model. Other mechanisms to address the hierarchies rely on small displacements from the fixed points [158, 292, 294–297]. However, our set-up relies on residual symmetries that are preserved in the fixed point to make the model predictive.

#### 7.1.3 Neutrinos

We now turn to the Majorana mass terms for the neutrinos,  $N_A^c$  and  $N_B^c$ . From Table 7.1, we see that  $N_A^c N_A^c$  as well as  $N_B^c N_B^c$  are  $S_4^A \times S_4^B \times S_4^C$  singlets. As such, we just need to cancel out the weight with a singlet Yukawa modular form. From [141, 142] we see that the Yukawa modular forms of weight 4 do have a singlet representation, needed for the  $M_A(\tau_A)$  term.<sup>7</sup> Due to the properties of the modular terms, this implies that there is also a singlet modular form of weight 8, required for  $M_B(\tau_B)$ . Conversely, as  $N_A^c N_B^c$  transforms non-trivially under both  $S_4^A$  and under  $S_4^B$ , there are no one-dimensional modular forms of weight 2 and the respective term is forbidden by the symmetries, and the RH neutrino mass matrix is diagonal:

$$M_R = \begin{pmatrix} M_A(\tau_A) & 0\\ 0 & M_B(\tau_B) \end{pmatrix}. \tag{7.12}$$

Finally, we need to check the shape of the Dirac mass matrices. Given the vevs for the bi-triplets  $\Phi_{AC}$ ,  $\Phi_{BC}$ , the tensor products after SSB will mimic those of the usual  $S_4$  (the diagonal  $S_4$  preserved by the bi-triplets symmetry breaking), as explained in [137, 259–261]. This feature is preserved also in the weighton versions of the model, that are using  $S'_4$ . The Dirac mass matrix is then given by:

$$M_D = v_u \begin{pmatrix} (Y_A)_1 & (Y_B)_1 \\ (Y_A)_3 & (Y_B)_3 \\ (Y_A)_2 & (Y_B)_2 \end{pmatrix}, \tag{7.13}$$

where, as usual,  $v_u$  denotes the  $H_u$  vev, and the  $3 \times 2$  structure comes from the CSD with just two RH neutrinos. Choosing specific stabilisers for the two remaining moduli fields, we can achieve a new CSD(3.45) structure with  $n = 1 + \sqrt{6}$ :

$$M_D = v_u \begin{pmatrix} 0 & b \\ a & b \left( 1 + \sqrt{6} \right) \\ -a & b \left( 1 - \sqrt{6} \right) \end{pmatrix}, \qquad \tau_A = -\frac{3}{2} + \frac{i}{2}, \quad \tau_B = \frac{3}{2} + \frac{i}{2}.$$
 (7.14)

<sup>&</sup>lt;sup>7</sup>Although we use a different basis, the assignments of the representations are identical, as can be seen by the weight 2 modular forms. Furthermore, we have explicitly checked that the tensor product of  $\left(Y_{3'}^{(2)} \otimes Y_{3'}^{(2)}\right)_1$  does not vanish for the relevant  $\tau_A$  nor any of  $\tau_B$ . This ensures a non-zero  $M_A$  and  $M_B$ .

We can similarly achieve the case CSD(-1.45) with  $n = 1 - \sqrt{6}$  already discussed in [257]:

$$M_D = v_u \begin{pmatrix} 0 & b \\ a & b \left( 1 - \sqrt{6} \right) \\ -a & b \left( 1 + \sqrt{6} \right) \end{pmatrix}, \qquad \tau_A = -\frac{3}{2} + \frac{i}{2}, \quad \tau_B = -\frac{1}{2} + \frac{i}{2}. \tag{7.15}$$

The type-I seesaw mechanism will lead to an effective mass matrix for the light neutrinos:

$$m_{\nu} = M_{D} \cdot M_{R}^{-1} \cdot M_{D}^{T} = v_{u}^{2} \begin{pmatrix} \frac{b^{2}}{M_{B}} & \frac{b^{2}n}{M_{B}} & \frac{b^{2}(2-n)}{M_{B}} \\ . & \frac{a^{2}}{M_{A}} + \frac{b^{2}n^{2}}{M_{B}} & -\frac{a^{2}}{M_{A}} + \frac{b^{2}n(2-n)}{M_{B}} \\ . & . & \frac{a^{2}}{M_{A}} + \frac{b^{2}(2-n)^{2}}{M_{B}} \end{pmatrix},$$
(7.16)

where  $n = 1 + \sqrt{6} \approx 3.45$  or  $n = 1 - \sqrt{6} \approx -1.45$ .

#### 7.1.4 Analytical Results

The effective mass matrix for the light neutrinos can be split into two contributions,

$$m_{\nu} = \frac{v_{u}^{2}}{M_{A}}|a|^{2} \begin{pmatrix} 0 & 0 & 0\\ 0 & 1 & -1\\ 0 & -1 & 1 \end{pmatrix} + \frac{v_{u}^{2}}{M_{B}}|b|^{2}e^{i\beta} \begin{pmatrix} 1 & n & 2-n\\ n & n^{2} & n(2-n)\\ 2-n & n(2-n) & (2-n)^{2} \end{pmatrix}.$$
(7.17)

It is worth noting that the above neutrino mass matrix in the diagonal charged-lepton mass basis is determined effectively by two real parameters,  $m_a = v_u^2 \frac{|a|^2}{M_A}$ ,  $m_b = v_u^2 \frac{|b|^2}{M_B}$ , one phase  $\beta$  and a discrete choice of  $n = 1 \pm \sqrt{6}$ . For a given choice of n, the remaining three real parameters determine all the parameters in the neutrino sector, namely all the neutrino masses and the entire PMNS matrix.

These two terms above can be simultaneously block-diagonalized by the following Tri-bimaximal mixing matrix,

$$\mathcal{U}_{\text{TBM}} = \begin{pmatrix} -\sqrt{\frac{2}{3}} & \sqrt{\frac{1}{3}} & 0\\ \sqrt{\frac{1}{6}} & \sqrt{\frac{1}{3}} & \sqrt{\frac{1}{2}}\\ \sqrt{\frac{1}{6}} & \sqrt{\frac{1}{3}} & -\sqrt{\frac{1}{2}} \end{pmatrix}, \tag{7.18}$$

leading to

$$m_{\nu}' = \mathcal{U}_{\text{TBM}}^T \cdot m_{\nu} \cdot \mathcal{U}_{\text{TBM}} = \frac{v_u^2}{M_A} |a|^2 \begin{pmatrix} 0 & 0 & 0 \\ 0 & 0 & 0 \\ 0 & 0 & 2 \end{pmatrix} + \frac{v_u^2}{M_B} |b|^2 e^{i\beta} \begin{pmatrix} 0 & 0 & 0 \\ 0 & 3 & \sqrt{6}(n-1) \\ 0 & \sqrt{6}(n-1) & 2(n-1)^2 \end{pmatrix}.$$
(7.19)

We diagonalize the remaining (2,2) block through the matrix

$$\mathcal{U}_{\alpha} = \begin{pmatrix} 1 & 0 & 0 \\ 0 & c_{\alpha} & e^{i\gamma}s_{\alpha} \\ 0 & -e^{-i\gamma}s_{\alpha} & c_{\alpha} \end{pmatrix}, \tag{7.20}$$

such that

$$\mathcal{U}_{\alpha}^{T} \cdot m_{\nu}' \cdot \mathcal{U}_{\alpha} = \operatorname{diag}(0, m_{1}, m_{2}). \tag{7.21}$$

To ensure that  $m_1, m_2$  are real and positive, we use the phase matrix,  $P_{\nu}$ , such that:

$$\mathcal{U}_{\nu}^{T} \cdot m_{\nu} \cdot \mathcal{U}_{\nu} = \operatorname{diag}(0, |m_{1}|, |m_{2}|), \tag{7.22}$$

where

$$\mathcal{U}_{\nu} \equiv (\mathcal{U}_{\text{TBM}} \mathcal{U}_{\alpha} P_{\nu}) = \begin{pmatrix}
-\sqrt{\frac{2}{3}} & \frac{c_{\alpha}}{\sqrt{3}} & e^{i\gamma} \frac{s_{\alpha}}{\sqrt{3}} \\
\sqrt{\frac{1}{6}} & \frac{c_{\alpha}}{\sqrt{3}} - e^{-i\gamma} \frac{s_{\alpha}}{\sqrt{2}} & \frac{c_{\alpha}}{\sqrt{2}} + e^{i\gamma} \frac{s_{\alpha}}{\sqrt{3}} \\
\sqrt{\frac{1}{6}} & \frac{c_{\alpha}}{\sqrt{3}} + e^{-i\gamma} \frac{s_{\alpha}}{\sqrt{2}} & -\frac{c_{\alpha}}{\sqrt{2}} + e^{i\gamma} \frac{s_{\alpha}}{\sqrt{3}}
\end{pmatrix} \cdot \begin{pmatrix}
1 & 0 & 0 \\
0 & e^{i\phi_{2}} & 0 \\
0 & 0 & e^{i\phi_{3}}
\end{pmatrix}.$$
(7.23)

As this is effectively a  $2 \times 2$  diagonalization, it is possible to find analytical relations for  $\alpha$ . Namely, by requiring a vanishing  $(\mathcal{U}_{\alpha}^T m_{\nu}' \mathcal{U}_{\alpha})_{23}$  element we find [271]:

$$t \equiv \tan 2\alpha = \frac{2y}{z\cos(\varphi - \gamma) - x\cos\gamma},$$

$$\tan \gamma = \frac{z\sin\varphi}{x + z\cos\varphi}, \quad \text{with} \quad \varphi = \phi_z - \beta,$$

$$(7.24)$$

$$\tan \gamma = \frac{z \sin \varphi}{x + z \cos \varphi}, \quad \text{with } \varphi = \phi_z - \beta,$$
 (7.25)

where we defined

$$m'_{\nu} = \begin{pmatrix} 0 & 0 & 0 \\ 0 & xe^{i\beta} & ye^{i\beta} \\ 0 & ye^{i\beta} & ze^{i\phi_z} \end{pmatrix}, \tag{7.26}$$

with

$$x = 3m_b$$
,  $y = \sqrt{6}(n-1)m_b$ ,  $z = |2(m_a + e^{i\beta}(n-1)^2 m_b)|$ ,  $m_a = v_u^2 \frac{|a|^2}{M_A}$ ,  $m_b = v_u^2 \frac{|b|^2}{M_B}$ . (7.27)

To relate this to the PMNS matrix in its standard parametrization, we must also take into account the charged-lepton rotation. In our specific realisation, the modular representations of the charged-leptons were chosen in such a way that its mass matrix is already diagonal. As such, the LH rotation is, in general, a diagonal phase matrix

$$\mathcal{U}_{\ell} = \begin{pmatrix} e^{i\delta_{e}} & 0 & 0\\ 0 & e^{i\delta_{\mu}} & 0\\ 0 & 0 & e^{i\delta_{\tau}} \end{pmatrix},$$
(7.28)

which can be used to match the standard parametrization [21]:<sup>8</sup>

$$\mathcal{U}_{\text{PMNS}} = \begin{pmatrix} c_{12}c_{13} & s_{12}c_{13} & s_{13}e^{-i\delta} \\ -s_{12}c_{23} - c_{12}s_{13}s_{23}e^{i\delta} & c_{12}c_{23} - s_{12}s_{13}s_{23}e^{i\delta} & c_{13}s_{23} \\ s_{12}s_{23} - c_{12}s_{13}c_{23}e^{i\delta} & -c_{12}s_{23} - s_{12}s_{13}c_{23}e^{i\delta} & c_{13}c_{23} \end{pmatrix} \cdot \begin{pmatrix} e^{i\eta_{1}} & 0 & 0 \\ 0 & e^{i\eta_{2}} & 0 \\ 0 & 0 & 1 \end{pmatrix}, \quad (7.29)$$

which has the measured mixing angles and CP-violating phase, and  $s_{ij}$  ( $c_{ij}$ ) denotes  $\sin \theta_{ij}$  ( $\cos \theta_{ij}$ ).

Now, we can relate our Unitary matrix  $\mathcal{U}_{\nu}$  to  $\mathcal{U}_{PMNS}$  and find out the relations between the measured neutrino data, and our model's parameters. The resulting relations are

$$\sin \theta_{13} = \frac{\sin \alpha}{\sqrt{3}} = \frac{1}{\sqrt{6}} \sqrt{1 - \sqrt{\frac{1}{1 + t^2}}},\tag{7.30}$$

$$\tan \theta_{12} = \frac{\cos \alpha}{\sqrt{2}} = \frac{1}{\sqrt{2}} \sqrt{1 - 3\sin^2 \theta_{13}},$$
(7.31)

$$\tan \theta_{23} = \frac{|1 + \epsilon_{\alpha}|}{|1 - \epsilon_{\alpha}|},\tag{7.32}$$

where

$$\epsilon_{\alpha} = \sqrt{\frac{2}{3}} e^{i\gamma} \tan \alpha = \sqrt{\frac{2}{3}} e^{i\gamma} \frac{\sqrt{1+t^2}-1}{t}.$$
 (7.33)

Note that the mixing angles depend only on two parameters, with  $\theta_{13}$  and  $\theta_{12}$  depending only on t. Since the mixing is unaffected by an overall factor, we can factorise  $m_b$  in Eq. (7.26), leading to

$$m'_{\nu} = m_b \begin{pmatrix} 0 & 0 & 0 \\ 0 & x'e^{i\beta} & y'e^{i\beta} \\ 0 & y'e^{i\beta} & z'e^{i\phi_z} \end{pmatrix}, \tag{7.34}$$

where

$$x' = 3,$$
  $y' = \sqrt{6(n-1)},$   $z' = \left| 2\left(\frac{1}{r} + e^{i\beta}(n-1)^2\right) \right|,$  (7.35)

$$\phi_z = \arg\left(\frac{1}{r} + e^{i\beta}(n-1)^2\right), \qquad r = \frac{m_b}{m_a}, \tag{7.36}$$

where we note how  $\phi_z$  and z' depend on r and  $\beta$ . For fixed n, the mixing angles themselves will depend solely on r and  $\beta$ .

To obtain the neutrinos masses, we proceed as in [271] by taking the trace and determinant of the hermitian combination  $H'_{\nu} = {m'_{\nu}}^{\dagger} m'_{\nu}$ , and equating it to the sum and product of the squared masses, respectively. Given that the littlest seesaw paradigm leads to Normal Ordering, the obtained masses can be readily equated to the  $\Delta m^2_{21}$  and  $\Delta m^2_{31}$  observables. Defining the combinations of parameters, that depend on those of Eqs. (7.25) and (7.35)-(7.36),

$$\Sigma \equiv \frac{m_b^2}{2} \left( x'^2 + 2y'^2 + z'^2 \right), \tag{7.37}$$

<sup>&</sup>lt;sup>8</sup>Indeed, the RH fields rotate away the possible phases of  $M_l$  and, as such, when we write down  $m_{\nu}$  we are already in a basis where  $M_l$  is diagonal and positive. The LH rotation was used to enforce the reality of a. In general, this won't be the basis where the light neutrino masses are real.  $\mathcal{U}_l$  is then required to rotate into the standard parametrization basis.

$$\delta M \equiv \frac{m_b^2}{2} \sqrt{x'^2 (4y'^2 - 2z'^2) + x'^4 + 8x'y'^2 z' \cos \varphi + 4y'^2 z'^2 + z'^4}, \tag{7.38}$$

then

$$\Delta m_{21}^2 = m_2^2 = \Sigma - \delta M, (7.39)$$

$$\Delta m_{31}^2 = m_3^2 = \Sigma + \delta M,$$
 (7.40)

which are functions of r and  $\beta$ , and with the overall factor given by  $m_b$ , which cancels out in the ratio. As such,  $\Delta m_{21}^2/\Delta m_{31}^2$ , the 3 mixing angles, and the CP-phase are all functions of just two effective parameters.

The CP-phase of the PMNS matrix, as well as the physical Majorana phase (since there is one massless neutrino, only  $\eta_2$  of Eq. (7.29) is physical<sup>9</sup>) can be extracted through careful combinations of the elements [244], and lead to

$$\delta = -\arg\left(\operatorname{sign}(t)e^{i\beta}\left(4\left(\sqrt{t^2+1}-1\right)+\left(-2+3e^{2i\gamma}\right)t^2\right)\right),\tag{7.41}$$

$$\eta_2 = (-\gamma - \delta - (\phi_3 - \phi_2)).$$
(7.42)

#### 7.1.5 Numerical Results

Using the analytical expressions, we plot the allowed experimental ranges for the lepton mixing parameters in the  $(r, \beta)$  plane. We present both the case where  $\tau_B = (3+i)/2$  and  $\tau_B = (-1+i)/2$ , corresponding to the modular forms of Eqs (7.2) and (7.3). The results shown correspond to the Nu-Fit 5.1 values [30, 298] without SK atmospheric data in Fig. 7.1 and with SK atmospheric data in Fig. 7.2. In both Figures, the top (bottom) row displays the  $3\sigma$  ( $1\sigma$ ) ranges of Table 7.3, with the left and right columns showing the  $n = 1 + \sqrt{6}$  and  $n = 1 - \sqrt{6}$  cases, respectively.<sup>10</sup>

We note the significant differences between the two possibilities:  $n = 1 + \sqrt{6}$  and  $n = 1 - \sqrt{6}$ . This corresponds to a change of sign in the effective parameter t, which does not affect the predictions for r,  $\theta_{13}$ ,  $\theta_{12}$ , but does affect the prediction for  $\theta_{23}$  and  $\delta$ . This can be understood by noting that the change of sign corresponds to changing from the tangent to a cotangent in the  $\theta_{23}$  expression (7.32), and for  $\delta$  (7.41) to adding  $\pi$ .

While qualitatively both possibilities are similarly successful in reproducing the experimental data at  $3\sigma$ , it is visible from the plots how the  $1\sigma$  range clearly favours different cases. It is worth emphasising how  $n=1+\sqrt{6}$  case is able to fit all observables at  $1\sigma$ , with the exception of  $\theta_{12}$ , for which the  $1\sigma$  contour is just slightly above the intersection of all other observables, which include the very narrow contours from  $\theta_{13}$  and from the mass ratio. To better quantify this, we define

$$\chi^2 = \sum_i \left( \frac{x_i^{\text{pred}} - x_i^{\text{exp}}}{\sigma_i} \right)^2 \tag{7.43}$$

<sup>&</sup>lt;sup>9</sup>This is made clear when computing  $m_{ee}$ . Alternatively, we can always rotate  $\nu_1$  to absorb  $\eta_1$ , but this will not influence the second and third columns

<sup>&</sup>lt;sup>10</sup>The results for  $n=1-\sqrt{6}$  match the results of [257], as expected.

		without SK a	tmospheric data	with SK atı	mospheric data
		bfp $\pm 1\sigma$	$3\sigma$ range	bfp $\pm 1\sigma$	$3\sigma$ range
	$\sin^2 \theta_{12}$	$0.304^{+0.013}_{-0.012}$	$0.269 \rightarrow 0.343$	$0.304^{+0.012}_{-0.012}$	$0.269 \rightarrow 0.343$
	$\theta_{12}/^{\circ}$	$33.44^{+0.77}_{-0.74}$	$31.27 \rightarrow 35.86$	$33.45^{+0.77}_{-0.75}$	$31.27 \rightarrow 35.87$
ng	$\sin^2 \theta_{23}$	$0.573^{+0.018}_{-0.023}$	$0.405 \rightarrow 0.620$	$0.450^{+0.019}_{-0.016}$	$0.408 \rightarrow 0.603$
Normal Ordering	$\theta_{23}/^{\circ}$	$49.2^{+1.0}_{-1.3}$	$39.5 \rightarrow 52.0$	$42.1_{-0.9}^{+1.1}$	$39.7 \rightarrow 50.9$
mal (	$\sin^2 \theta_{13}$	$0.02220^{+0.00068}_{-0.00062}$	$0.02034 \to 0.02430$	$0.02240^{+0.00062}_{-0.00062}$	$0.02060 \to 0.02435$
Nor	$\theta_{13}/^{\circ}$	$8.57^{+0.13}_{-0.12}$	$8.20 \rightarrow 8.97$	$8.62^{+0.12}_{-0.12}$	$8.25 \rightarrow 8.98$
	$\delta/^{\circ}$	$194^{+52}_{-25}$	$105 \rightarrow 405$	$230^{+36}_{-25}$	$144 \rightarrow 350$
	$\frac{\Delta m_{21}^2}{10^{-5} \text{ eV}^2}$	$7.42_{-0.20}^{+0.21}$	$6.82 \rightarrow 8.04$	$7.42_{-0.20}^{+0.21}$	$6.82 \rightarrow 8.04$
	$\frac{\Delta m_{3\ell}^2}{10^{-3} \text{ eV}^2}$	$+2.515^{+0.028}_{-0.028}$	$+2.431 \rightarrow +2.599$	$+2.510^{+0.027}_{-0.027}$	$+2.430 \to +2.593$

Table 7.3: Normal Ordering NuFit 5.1 values [30, 298] for the neutrino observables.

and list the respective  $\chi^2$  values in Table 7.4. For the  $n=1+\sqrt{6}$  case,  $\chi^2=1.87$  can be obtained. Table 7.4 also gives the predictions for  $m_{ee}$  for the best-fit point in each case, where [21]:

$$m_{ee} = \left| \sum_{i} \mathcal{U}_{ei}^{2} m_{i} \right|, \tag{7.44}$$

which, in our case (since we are working in a basis where the charged-leptons are already diagonal, positive, and ordered) can be extracted simply from

$$m_{ee} = \left| (m_{\nu})_{1,1} \right|.$$
 (7.45)

From Eq. (7.16), we can see that this is identically  $m_b$ .

	Go	odness o	of fit ag	ainst NuFit	5.1 values wi	thout SK at	mospheri	ic data		
n	$\chi^2$	r	$\beta/\pi$	$m_b/10^{-3}$	$m_2^2/10^{-5}$	$m_3^2/10^{-3}$	$\theta_{12}$	$\theta_{23}$	$\theta_{13}$	δ
$1+\sqrt{6}$	29.47	0.076	1.26	2.33	7.19	2.53	34.29	43.06	8.78	262
$1-\sqrt{6}$	4.96	0.073	0.76	2.23	7.45	2.51	34.34	48.26	8.55	284
	C	Goodness	of fit a	gainst NuFit	5.1 results	with SK atm	ospheric	data		
n	$\chi^2$	r	$\beta/\pi$	$m_b/10^{-3}$	$m_2^2/10^{-5}$	$m_3^2/10^{-3}$	$\theta_{12}$	$\theta_{23}$	$\theta_{13}$	δ
$1+\sqrt{6}$	1.87	0.074	1.24	2.30	7.42	2.51	34.33	42.03	8.62	257
$1-\sqrt{6}$	25.79	0.077	0.74	2.33	7.15	2.52	34.28	46.76	8.82	277

**Table 7.4:** Our  $\chi^2$  values for the different cases  $n=1+\sqrt{6}$  and  $n=1-\sqrt{6}$ . Note that from Eq. (7.16) and the definition Eq. (7.27), the output parameter  $m_{ee}$  is directly equal to the input parameter  $m_b$ . The neutrino squared-masses  $m_2^2$  and  $m_3^2$  are given in eV<sup>2</sup>.

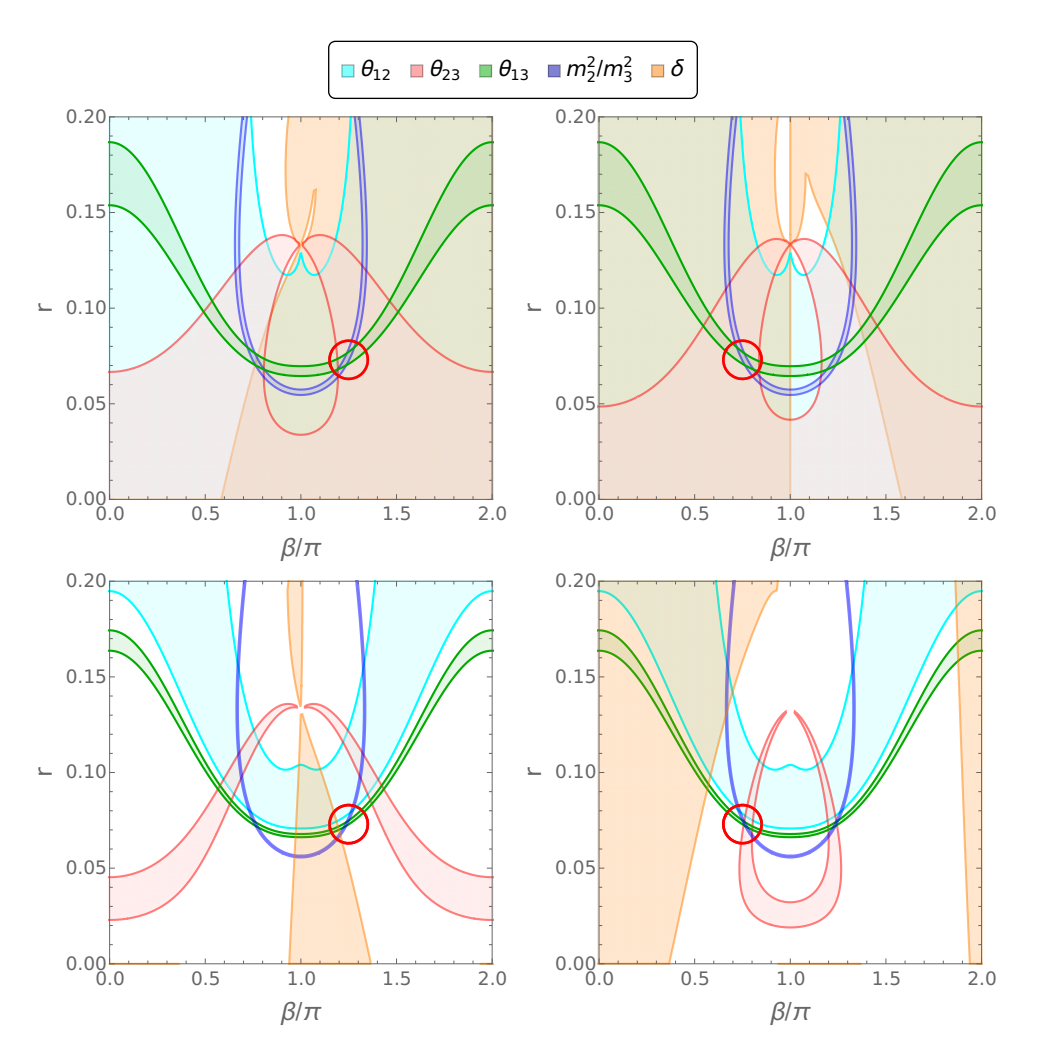


**Figure 7.1:** Allowed  $3\sigma$  (top) and  $1\sigma$  (bottom) experimental ranges in the  $(r, \beta)$  plane using NuFit 5.1 values without SK atmospheric data for the  $n = 1 + \sqrt{6}$  case (left) and for the  $n = 1 - \sqrt{6}$  case (right). The red circle indicates the best fit region.

#### 7.1.6 Weighton Models

We now modify the model presented to include a weighton field  $\phi$ . In order to preserve the features of the previous model (particularly the diagonal charged-lepton mass matrix) we employ  $S'_4$  modular symmetries [142] instead of  $S_4$ .

#### Weighton Model 1

The assignments of the fields under the symmetries are listed in Table 7.5. Notice that this implementation of the weighton is distinguished from the standard one as the weighton is assigned to non-trivial representations of  $S'_4^A$ ,  $S'_4^B$ , and  $S'_4^C$ . Due to this and the representations of the charged-leptons, the invariant terms have the desired modular forms  $Y_\tau$ ,  $Y_\mu$  and  $Y_e$  respectively for the field combinations  $L\tau^c$ ,  $L\mu^c\phi$  and  $Le^c\phi^3$ . This is shown (in green) in Table 7.6, where other possibilities are not invariant.

Since there are no charged-leptons with weights under  $S'_4^{A,B}$ , the charged-leptons Yukawa modular forms must be singlets under  $S'_4^{A,B}$  with weight 0 under these symmetries.

By having chosen the weighton to have a negative weight under  $S_4^{\prime C}$ , there are no additional con-

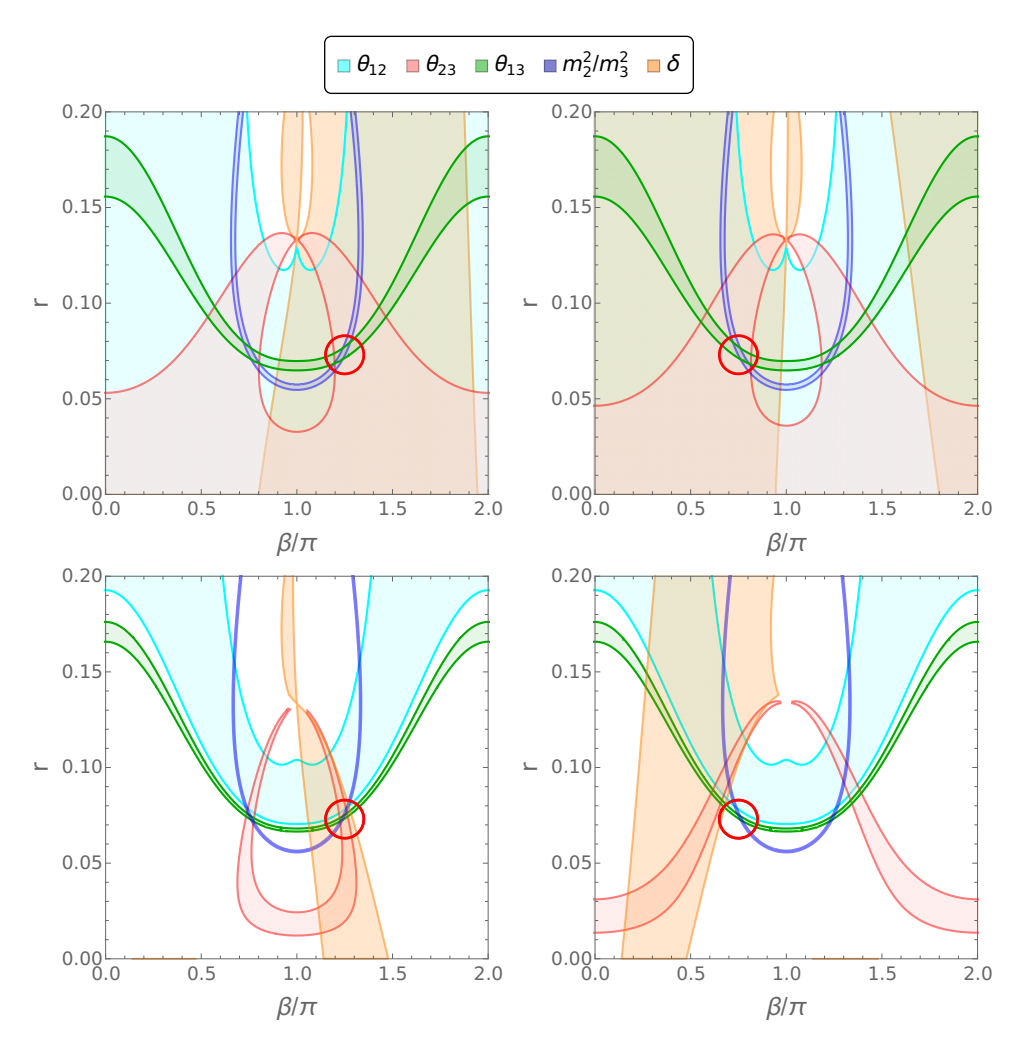


**Figure 7.2:** As in Fig. 7.1 but using the NuFit 5.1 values with SK atmospheric data. **Left:**  $n = 1 + \sqrt{6}$ , **right:**  $n = 1 - \sqrt{6}$ , **top:**  $3\sigma$ , **bottom:**  $1\sigma$ .

tributions beyond the leading order ones, as the Yukawa modular forms also have positive weight. An alternative solution, where the weighton has a positive weight under  $S_4^{\prime C}$ , is presented below.

#### Weighton Model 2

In this subsection we provide an alternative weighton model, that does not require assigning large modular weights to the charged-lepton fields.

This allows fields (in particular charged-lepton fields) to be assigned as distinct non-trivial singlets of the underlying modular symmetries, as shown in Table 7.7.

Table 7.8 shows the assignments of the different field combinations and clarifies how the non-trivial singlet choices of the charged-leptons allow only one coupling at leading order of powers of  $\phi$ , with the next leading order term appearing only with the insertion of additional  $\phi^4$ .<sup>11</sup> We estimate this suppression factor should to be around  $10^{-5}$  by assuming  $\mathcal{O}(1)$  couplings for the charged-leptons.<sup>12</sup>

<sup>&</sup>lt;sup>11</sup>Since the weighton is charged under  $S_4^{\prime C}$ , and the 1D irreps have at most  $\mathbf{r}^4 = \mathbf{1}$ , there will always be corrections to the leading terms with 4 more weighton insertions.

<sup>&</sup>lt;sup>12</sup>Namely, we take  $\langle \phi \rangle/M = \epsilon = 6.5 \times 10^{-2}$ , to have  $m_{\mu} \sim 0.92 \, \epsilon \, m_{\tau}$  and  $m_e \sim 1.08 \, \epsilon^3 \, m_{\tau}$ .

Field	$S'_4^A$	$S'_4^B$	$S'_4^C$	$k_A$	$k_B$	$k_C$							
L	1	1	3	0	0	0	Yuk/Mass	$S'_4^A$	$S'_4^B$	$S'_4^C$	$k_A$	$k_B$	$k_C$
$e^c$	î	$\hat{1}$	<b>1</b> '	0	0	12	$Y_e( au_C)$	1	1	3′	0	0	6
$\mu^c$	$\widehat{1}'$	$\widehat{1}'$	<b>1</b> '	0	0	6	$Y_{\mu}(\tau_C)$	1	1	<b>3</b> '	0	0	4
$\tau^c$	1	1	<b>1</b> '	0	0	2	$Y_{ au}( au_C)$	1	1	<b>3</b> '	0	0	2
$N_A^c$	1′	1	1	4	0	0	$Y_A( au_A)$	3′	1	1	4	0	0
$N_B^c$	1	<b>1</b> '	1	0	2	0	$Y_B( au_B)$	1	<b>3</b> '	1	0	2	0
$\Phi_{AC}$	3	1	3	0	0	0	$M_A( au_A)$	1	1	1	8	0	0
$\Phi_{BC}$	1	3	3	0	0	0	$M_B( au_B)$	1	1	1	0	4	0
$\phi$	î	$\widehat{1}$	$\hat{1}$	0	0	-2							

Table 7.5: Assignments of fields for the weighton version of the model.

	$\phi^0$	$\phi^1$	$\phi^2$	$\phi^3$	$\phi^4$
$Le^c$	$\left(\widehat{1}_{0},\widehat{1}_{0},\widehat{3}_{12}^{\prime} ight)$	$(\mathbf{1'}_0,\mathbf{1'}_0,3_{10})$	$\left(\widehat{1}_{0}^{\prime},\widehat{1}_{0}^{\prime},\widehat{3}_{8}\right)$	$({f 1}_0,{f 1}_0,{f 3'}_6)$	$\left(\widehat{1}_{0},\widehat{1}_{0},\widehat{3}_{4}^{\prime}\right)$
	$(\widehat{1}_0', \widehat{1}_0', \widehat{3}_6)$	$\left(1_{0},1_{0},3_{4}^{\prime}\right)$	$(\widehat{1}_0,\widehat{1}_0,\widehat{3}_2')$	$({\bf 1'}_0,{\bf 1'}_0,{\bf 3}_0)$	$\left(\widehat{\widehat{1}}_{0}^{\prime},\widehat{1}_{0}^{\prime},\widehat{3}_{-2}^{\prime} ight)$
$L\tau^c$	$({f 1}_0,{f 1}_0,{f 3'}_2)$	$\left(\widehat{1}_{0},\widehat{1}_{0},\widehat{3}_{0}'\right)$	$({f 1'}_0,{f 1'}_0,{f 3}_{-2})$	$\left(\widehat{1}_0',\widehat{1}_0',\widehat{3}_{-4}\right)$	$({f 1}_0,{f 1}_0,{f 3'}_{-6})$

**Table 7.6:** Irreps of the leptonic tensor products with different powers of the weighton. The invariant combinations are highlighted in green.

Field	$S'_4^A$	$S'_4^B$	$S'_4^C$	$k_A$	$k_B$	$k_C$							
L	1	1	3	0	0	0	Yuk/Mass	$S'_4^A$	$S'_4^B$	$S'_4^C$	$k_A$	$k_B$	$k_C$
$e^c$	î	$\widehat{1}$	<b>1</b> '	0	0	0	$Y_e( au_C)$	1	1	3′	0	0	6
$\mu^c$	$\widehat{1}'$	$\widehat{1}'$	<b>1</b> '	0	0	2	$Y_{\mu}(\tau_C)$	1	1	<b>3</b> '	0	0	4
$ au^c$	1	1	<b>1</b> '	0	0	2	$Y_{\tau}(\tau_C)$	1	1	<b>3</b> '	0	0	2
$N_A^c$	1′	1	1	4	0	0	$Y_A( au_A)$	3′	1	1	4	0	0
$N_B^c$	1	<b>1</b> '	1	0	2	0	$Y_B( au_B)$	1	<b>3</b> '	1	0	2	0
$\Phi_{AC}$	3	1	3	0	0	0	$M_A( au_A)$	1	1	1	8	0	0
$\Phi_{BC}$	1	3	3	0	0	0	$M_B( au_B)$	1	1	1	0	4	0
φ	î	î	$\hat{1}$	0	0	2							

Table 7.7: Assignments of fields for the alternative weighton version of the model.

## 7.2 SU(5) Extension

In this section, we consider an SU(5) GUT model with three modular  $S_4$  symmetries, which can lead to a predictive Littlest Modular Seesaw model of leptons [280], while at the same time accommodating the quark masses and CKM mixing parameters. In order to provide a natural explanation of mass and mixing hierarchies, we employ two weighton fields [143, 144], resulting in a triangular form of hierarchical downtype and quark and charged-lepton Yukawa matrices as in [288]. The resulting hierarchical triangular forms preserve the successes of the Littlest Seesaw model while allowing down-type contributions to the CKM angles, with the weightons providing the hierarchical suppressions in all charged-fermion sectors, including the up-type quark Yukawa matrix. We present benchmark points which demonstrate the viability of the approach, and show how higher order operators may be controlled by judicious use of the modular weights across all three  $S_4$  sectors.

	$\phi^0$	$\phi^1$	$\phi^2$	$\phi^3$	$\phi^4$
$Le^c$	$\left(\widehat{1}_{0},\widehat{1}_{0},\widehat{3}_{0}^{\prime}\right)$	$({\bf 1'}_0,{\bf 1'}_0,{\bf 3}_2)$	$\left(\widehat{1}_{0}^{\prime},\widehat{1}_{0}^{\prime},\widehat{3}_{4}\right)$	$({f 1}_0,{f 1}_0,{f 3'}_6)$	$\left(\widehat{1}_{0},\widehat{1}_{0},\widehat{3}_{8}^{\prime} ight)$
$L\mu^c$	$\left(\widehat{1}_0',\widehat{1}_0',\widehat{3}_2 ight)$	$\left(1_{0},1_{0},3_{4}^{\prime}\right)$	$\left(\widehat{1}_{0},\widehat{1}_{0},,\widehat{3}_{6}^{\prime} ight)$	$({\bf 1'}_0,{\bf 1'}_0,{\bf 3}_8)$	$\left(\widehat{1}_{0}^{\prime},\widehat{1}_{0}^{\prime},\widehat{3}_{10}\right)$
$L\tau^c$	$(1_0,1_0,\mathbf{3'}_2)$	$\left(\widehat{1}_{0},\widehat{1}_{0},\widehat{3}_{4}^{\prime} ight)$	$(\mathbf{1'}_0,\mathbf{1'}_0,3_6)$	$\left(\widehat{1}_{0}^{\prime},\widehat{1}_{0}^{\prime},\widehat{3}_{8}\right)$	$(1_0,1_0,\mathbf{3'}_{10})$
$L\Phi_{AC}N_A^c$	$(\mathbf{3'}_4,1_0,1_0)$	$\left(\widehat{3}_{4}^{\prime},\widehat{1}_{0},\widehat{1}_{2} ight)$	$({\bf 3}_4,{\bf 1'}_0,{\bf 1'}_4)$	$\left(\widehat{3}_{4},\widehat{1}_{0}^{\prime},\widehat{1}_{6}^{\prime} ight)$	$({f 3'}_4,{f 1}_0,{f 1}_8)$
$L\Phi_{BC}N_B^c$	$(1_0, \mathbf{3'}_2, 1_0)$	$\left(\widehat{1}_{0},\widehat{3}_{2}^{\prime},\widehat{1}_{2} ight)$	$({\bf 1'}_0,{\bf 3}_2,{\bf 1'}_4)$	$\left(\widehat{1}_{0}^{\prime},\widehat{3}_{2},\widehat{1}_{6}^{\prime}\right)$	$({f 1}_0,{f 3'}_2,{f 1}_8)$
$N_A^c N_A^c$	$(1_8,1_0,1_0)$	$\left(\widehat{1}_{8},\widehat{1}_{0},\widehat{1}_{2} ight)$	$({\bf 1'}_8,{\bf 1'}_0,{\bf 1'}_4)$	$\left(\widehat{1}_{8}^{\prime},\widehat{1}_{0}^{\prime},\widehat{1}_{6}^{\prime}\right)$	$({f 1}_8,{f 1}_0,{f 1}_8)$
$N_B^c N_B^c$	$({f 1}_0,{f 1}_4,{f 1}_0)$	$\left(\widehat{1}_{0},\widehat{1}_{4},\widehat{1}_{2} ight)$	$({\bf 1'}_0,{\bf 1'}_4,{\bf 1'}_4)$	$\left(\widehat{1}_{0}^{\prime},\widehat{1}_{4}^{\prime},\widehat{1}_{6}^{\prime}\right)$	$(1_0,1_4,1_8)$
$N_A^c N_B^c$	$({\bf 1'}_4,{\bf 1'}_2,{\bf 1}_0)$	$\left(\widehat{1}_{4}^{\prime},\widehat{1}^{\prime}{}_{2},\widehat{1}_{2} ight)$	$({\bf 1}_4,{\bf 1}_2,{\bf 1'}_4)$	$\left(\widehat{1}_{4},\widehat{1}_{2},\widehat{1}_{6}^{\prime}\right)$	$({f 1'}_4,{f 1'}_2,{f 1}_8)$
$N_A^c \Phi_{AC} N_A^c$	$(3_8,1_0,3_0)$	$\left(\widehat{3}_{8},\widehat{1}_{0},\widehat{3}_{2} ight)$	$({\bf 3'}_8,{\bf 1'}_0,{\bf 3'}_4)$	$\left(\widehat{3}_{8}^{\prime},\widehat{1}_{0}^{\prime},\widehat{3}_{6}^{\prime}\right)$	$(3_8,1_0,3_8)$
$N_B^c \Phi_{AC} N_B^c$	$(3_0,1_4,3_0)$	$\left(\widehat{3}_{0},\widehat{1}_{4},\widehat{3}_{2} ight)$	$({\bf 3'}_0,{\bf 1'}_4,{\bf 3'}_4)$	$\left(\widehat{3}_{0}^{\prime},\widehat{1}_{4}^{\prime},\widehat{3}_{6}^{\prime}\right)$	$({f 3}_0,{f 1}_4,{f 3}_8)$
$N_A^c \Phi_{AC} N_B^c$	$(\mathbf{3'}_4,\mathbf{1'}_2,3_0)$	$\left(\widehat{3}_{4}^{\prime},\widehat{1}_{2}^{\prime},\widehat{3}_{2} ight)$	$({f 3}_4,{f 1}_2,{f 3'}_4)$	$\left(\widehat{3}_{4},\widehat{1}_{2},\widehat{3}_{6}^{\prime}\right)$	$(\mathbf{3'}_4,\mathbf{1'}_2,3_8)$
$N_A^c \Phi_{BC} N_A^c$	$(1_8, 3_0, 3_0)$	$\left(\widehat{f 1}_{8},\widehat{f 3}_{0},\widehat{f 3}_{2} ight)$	$({\bf 1'}_8,{\bf 3'}_0,{\bf 3'}_4)$	$\left(\widehat{1}_{8}^{\prime},\widehat{3}_{0}^{\prime},\widehat{3}_{6}^{\prime}\right)$	$({f 1}_8,{f 3}_0,{f 3}_8)$
$N_B^c \Phi_{BC} N_B^c$	$(1_0, 3_4, 3_0)$	$\left(\widehat{f 1}_0,\widehat{f 3}_4,\widehat{f 3}_2 ight)$	$({\bf 1'}_0,{\bf 3'}_4,{\bf 3'}_4)$	$\left(\widehat{1}_{0}^{\prime},\widehat{3}_{4}^{\prime},\widehat{3}_{6}^{\prime}\right)$	$({f 1}_0,{f 3}_4,{f 3}_8)$
$N_A^c \Phi_{BC} N_B^c$	$(\mathbf{1'}_4,\mathbf{3'}_2,3_0)$	$\left(\widehat{1}_{4}^{\prime},\widehat{3}_{2}^{\prime},\widehat{3}_{2} ight)$	$({f 1}_4,{f 3}_2,{f 3'}_4)$	$\left(\widehat{1}_{4},\widehat{3}_{2},\widehat{3}_{6}^{\prime}\right)$	$({f 1'}_4,{f 3'}_2,{f 3}_8)$

**Table 7.8:** Irreps of the leptonic tensor products with different powers of the weighton following the new assignments. The invariant combinations are highlighted in green.

## 7.2.1 SU(5) Details

We are extending the Littlest Modular Seesaw to a grand unified setting, and a straightforward possibility is to extend the gauge symmetry to an SU(5) framework. We briefly review some SU(5) details and set our conventions. Further details about Grand Unified Theories can be found in [5, 299]. We furnish a  $\bf{10}$  and a  $\bf{\overline{5}}$  SU(5) representations with the usual SM fields (including singlet heavy neutrinos) as follows:

$$T = \begin{pmatrix} 0 & u_{G}^{c} & -u_{B}^{c} & u_{R} & d_{R} \\ 0 & u_{G}^{c} & u_{B} & d_{B} \\ 0 & u_{G} & d_{G} \\ 0 & 0 & e^{c} \\ 0 & 0 \end{pmatrix} \sim \mathbf{10}, \qquad F = \begin{pmatrix} d_{R}^{c} \\ d_{B}^{c} \\ d_{G}^{c} \\ e^{-} \\ -\nu \end{pmatrix} \sim \overline{\mathbf{5}}, \quad N^{c} \sim \mathbf{1}, \tag{7.46}$$

where the 10 is an anti-symmetric representation of SU(5), and so we omit the lower entries.

The relevant tensor products for the Yukawa terms are

$$Y_{\ell}, Y_d: F \otimes T = \overline{\mathbf{5}} \otimes \mathbf{10} = \mathbf{5} \oplus \mathbf{45},$$
 (7.47a)

$$Y_u: T \otimes T = \mathbf{10} \otimes \mathbf{10} = \overline{\mathbf{5}} \oplus \overline{\mathbf{45}} \oplus \overline{\mathbf{50}},$$
 (7.47b)

$$Y_D: F \otimes N = \overline{\mathbf{5}} \otimes \mathbf{1} = \mathbf{5},$$
 (7.47c)

where  $Y_{u,d}$  are the quark Yukawa matrices, and  $Y_{\ell}$  and  $Y_{D}$  are the charged-lepton and Dirac neutrino mass matrices, respectively. We see that we must include scalars in a  $\overline{\bf 5}$  representation to have a non-zero  $Y_{D}$ , which automatically also leads to a non-zero  $Y_{\ell}$  and  $Y_{d}$ . A minimal choice which provides a non-zero  $Y_{u}$  is to include a scalar in a  $\bf 5$  representation. As we can see, these gauge assignments (required for the low-energy theory to be SM-like), relate the charged-leptons and down quarks, placing them in a single

SU(5) multiplet. More specifically, if we include only a  $\overline{\bf 5}$  scalar field, responsible for the Yukawas for the (low-energy) charged-leptons and down quarks, we unavoidably find (at the UV scale)

$$Y_d = Y_\ell^T \,. \tag{7.48}$$

This simple relation is not viable, and can be relaxed by the inclusion of a second scalar multiplet. Introducing a  $\overline{\bf 45}$ , provides a splitting between  $Y_{\ell}$  and  $Y_{d}$  [300]. With the inclusion of these two multiplets, the mass matrices are given by:

$$Y_{\ell} = (Y_{\overline{5}} - 3Y_{\overline{45}}) , \qquad Y_{d} = (Y_{\overline{5}} + Y_{\overline{45}})^{T} ,$$
 (7.49)

relations which can be inverted to yield

$$Y_{\overline{5}} = \frac{1}{4} (Y_{\ell} + 3Y_d^T) , \qquad Y_{\overline{45}} = \frac{1}{4} (Y_d^T - Y_{\ell}) .$$
 (7.50)

As a consequence, we see that the Yukawa matrices for the down quarks and charged-leptons become general. Nonetheless, we also see that texture zeroes (by which we mean vanishing entries in both  $Y_{\overline{5}}$  and  $Y_{\overline{45}}$  due to symmetry purposes and not fortuitous cancellations) are shared by both matrices, up to transposition. Thus, even though we include a second scalar multiplet to avoid the stringent relation  $Y_d = Y_\ell^T$ , the connection between charged-leptons and down quarks lingers on (a situation we will denote as  $Y_\ell \sim Y_d^T$  during the rest of the chapter). A second consequence of the choice of SU(5) as a gauge symmetry comes from the terms responsible for the up quarks Yukawa matrix. Since T contains both the LH and RH quarks, the Yukawa terms are given by  $T_iH_5T_j$ , and are thus necessarily symmetric.

In summary, for our purposes here, in order to convert the Littlest Modular Seesaw into SU(5) grand unification, we need to consider non-trivial constraints on the Yukawa couplings. As had already been mentioned above, we will have symmetrical up quark Yukawa couplings and introduce additional scalars to make the Yukawa couplings of the charged-lepton and down quarks viable. However, the modular symmetries will lead to texture zeroes in the charged-lepton mass matrices, which are preserved up to transposition, retaining consequences of the SU(5) unification. Naturally, as a SUSY GUT, a complete formulation of our model should have anomaly cancellation, and therefore the  $\overline{\bf 45}$  should be accompanied by a  $\bf 45$ . Also, in terms of SU(5) GUT related predictions, we expect that proton decay will be relevant. Although such considerations are beyond the scope of the present work, they can be suppressed analogously to non-modular flavoured SU(5) GUTs e.g. [301, 302]. The reason is that the mechanisms used do not employ non-trivial representations of the flavour symmetry, and therefore can be applied in the presence of modular flavour symmetries.

#### 7.2.2 The Model

The littlest modular seesaw model is a simple implementation of multiple modular symmetries that economically explains the leptonic sector flavour observables. The inclusion of an symmetry based explanation for the quark observables is a desirable next step. One interesting possibility is to take advantage

of the SU(5) link between charged-leptons and down quarks. The inclusion of a  $\overline{\bf 45}$  decouples this connection, except that it retains the symmetry protected zeroes in the mass matrices. We leverage this fact to design a model in which the symmetries still safeguard the littlest modular seesaw against large contributions from the leptonic sector, while enhancing the contribution of the down sector to the quark mixing. To retain the successes of the  $CSD(1\pm\sqrt{6})$  lepton mixing predictions, the structure for  $Y_\ell$  cannot have large deviations from the diagonal shape. On the other hand, given the connection between the lepton and down-quark sectors  $(Y_d \sim Y_\ell^T)$ , we need to be careful not to suppress the  $Y_d$  contribution to the quark mixing. To this end, our goal is to employ lower and upper triangular Yukawa matrices for the charged-lepton and down-quark sectors, respectively. The point of the triangular shape for  $Y_\ell$  is to suppress the corrections to the lepton mixing (compared to the diagonal structure in the unspoiled CSD(n) framework). This suppression can be understood through a simplistic illustration of the  $2 \times 2$  case: taking the matrix

$$Y = \begin{pmatrix} m_{11} & x \\ 0 & m_{22} \end{pmatrix} , (7.51)$$

we compute the Hermitian matrices (assuming real Yukawas, for simplicity)  $H_{\ell} = YY^T$  and  $H_d = Y^TY^{13}$ . The ensuing rotation angles are, assuming  $m_{22}^2 \gg m_{11}^2$ :

$$\tan(2\theta_{\ell}) \approx \frac{2x}{m_{22}} \frac{m_{11}}{m_{22}}, \qquad \tan(2\theta_{d}) \approx \frac{2x}{m_{22}}.$$
 (7.52)

Clearly, we see that in the lower triangular case, the mixing will be suppressed due to hierarchical nature of the fermion masses, whereas the mixing in the upper triangular case can be  $\mathcal{O}(1)$ .<sup>14</sup>

The UV nature of the model requires the running of the measured masses to some high scale. Here, we make use of the values shown in [303], obtained from [302, 304], for  $\tan \beta = 5$  and a GUT scale at  $2 \times 10^{16}$  GeV:<sup>15</sup>

$$y_{e} = (1.97 \pm 0.024) \times 10^{-6} , \quad y_{\mu} = (4.16 \pm 0.050) \times 10^{-4} , \quad y_{\tau} = (7.07 \pm 0.073) \times 10^{-3} ,$$

$$y_{u} = (2.92 \pm 1.81) \times 10^{-6} , \quad y_{c} = (1.43 \pm 0.100) \times 10^{-3} , \quad y_{t} = (0.534 \pm 0.0341) \times 10^{0} ,$$

$$y_{d} = (4.81 \pm 1.06) \times 10^{-6} , \quad y_{s} = (9.52 \pm 1.03) \times 10^{-5} , \quad y_{b} = (6.95 \pm 0.175) \times 10^{-3} ,$$

$$\theta_{12} = (13.027 \pm 0.0814)^{\circ} , \qquad \theta_{23} = (2.054 \pm 0.384)^{\circ} , \qquad \theta_{13} = (0.1802 \pm 0.0281)^{\circ} ,$$

$$(7.54a)$$

together with

$$\delta = (69.21 \pm 6.19)^{\circ}. \tag{7.54b}$$

For the neutrino observables, we use the NuFit 5.2 infrared values [30, 298]. 16

$$H_{\text{lower}} = \begin{pmatrix} |m_{11}|^2 & m_{11} x^* \\ m_{11}^* x & |m_{22}|^2 + |x|^2 \end{pmatrix}, \qquad H_{\text{upper}} = \begin{pmatrix} |m_{11}|^2 + |x|^2 & m_{22} x^* \\ m_{22}^* x & |m_{22}|^2 \end{pmatrix}, \tag{7.53}$$

together with  $m_{22} \gg m_{11}$ , rather than their unphysical Yukawa shapes. Regardless, we feel no confusion will arise throughout the chapter.

 $<sup>^{13}</sup>$ In this work, we follow the left-right convention for the Yukawa matrices.

 $<sup>^{14}</sup>$ Due to the RH rotation freedom in the SM, we can more accurately describe the lower and upper triangular forms through their hermitian combinations

<sup>&</sup>lt;sup>15</sup>We consider for simplicity that SU(5) is broken at  $2 \times 10^{16}$  GeV, and use the SM field content for calculating the running.

 $<sup>^{16}</sup>$ We assume the neutrino observables have negligible running, as done in [302]. See [305] for a comprehensive analysis.

Taking the Cabibbo angle as a measure,  $\lambda \sim 0.227$ , the experimental values are approximately

$$y_e \sim \lambda^{8.9}$$
,  $y_\mu \sim \lambda^{5.3}$ ,  $y_\tau \sim \lambda^{3.3}$ ,  
 $y_u \sim \lambda^{8.6}$ ,  $y_c \sim \lambda^{4.4}$ ,  $y_t \sim \lambda^{0.4}$ ,  
 $y_d \sim \lambda^{8.2}$ ,  $y_s \sim \lambda^{6.2}$ ,  $y_b \sim \lambda^{3.4}$ ,  
 $\theta_{12} \sim \lambda^1$ ,  $\theta_{23} \sim \lambda^{2.3}$ ,  $\theta_{13} \sim \lambda^{3.9}$ . (7.55)

We wish to have  $\mathcal{O}(1)$  coefficients controlling the fermionic masses and mixings. Consequently, we can exploit the smallness of the quark mixing angles and naively use Eq. (7.52) to populate the entries of the Yukawa matrices, such that these are, by design, suppressed in such a way that both the quark mass hierarchy and the CKM matrix come out naturally:

$$Y_{u} \sim \begin{pmatrix} \lambda^{8} & \lambda^{5} & \lambda^{4} \\ \lambda^{5} & \lambda^{4} & \lambda^{2} \\ \lambda^{4} & \lambda^{2} & \lambda^{0} \end{pmatrix}, \qquad Y_{d}^{T} \sim \begin{pmatrix} \lambda^{8} & 0 & 0 \\ \lambda^{7} & \lambda^{6} & 0 \\ \lambda^{7} & \lambda^{5} & \lambda^{3} \end{pmatrix}, \qquad Y_{\ell} \sim \begin{pmatrix} \lambda^{9} & 0 & 0 \\ - & \lambda^{5} & 0 \\ - & - & \lambda^{3} \end{pmatrix}, \tag{7.56}$$

where the off-diagonal non-zero entries of  $Y_{\ell}$  are undetermined and denoted as "-", since the lower triangular shape suppresses the contributions to the leptonic mixing, and the main driver behind the PMNS mixing matrix comes from the Dirac neutrino structure, in the modular CSD( $1 \pm \sqrt{6}$ ) set-up. As for the neutrino sector, due to the built-in suppression mechanism in the form of the Type-I seesaw, we do not require any specific suppressions. We stress that the matrices shown in Eq. (7.56) are derived merely from the experimental values, and are not necessarily attainable in a specific set-up. Indeed, the SU(5) gauge symmetry, assuming the same order of magnitude for all Yukawas, will forbid different suppressions in  $Y_{\ell}$  and  $Y_{d}^{T}$ , as we will see later.

Our model relies on an SU(5) gauge symmetry, supplemented by 3 distinct  $S_4$  modular symmetries. The assignments of the fields are given in Table 7.9, both for the gauge and modular symmetries. We note that although we use non-integer weights for the fields, only even-weighted Yukawa modular forms are considered, consistent with the requirement of invariance under the  $S_4$  modular group. Indeed, rational modular weights for the fields are also obtained from top-down constructions in [145, 306, 307]. As such, the present framework continues to be that of modular invariance, and not that of metaplectic models [138, 308], since we do not consider half-integer modular forms.

Motivated by the modular CSD( $1 \pm \sqrt{6}$ ) structure, we do not take the values for the moduli as free parameters, and set them to the relevant stabilisers [257, 258]. As such, we take (using  $\omega \equiv e^{2\pi i/3}$ )

$$\tau_A = \frac{1}{2} + \frac{i}{2}, \qquad \tau_B = \frac{3}{2} + \frac{i}{2}, \qquad \tau_C = \omega, 
\tau_A = \frac{1}{2} + \frac{i}{2}, \qquad \tau_B' = -\frac{1}{2} + \frac{i}{2}, \qquad \tau_C = \omega,$$
(7.57a)

$$\tau_A = \frac{1}{2} + \frac{i}{2}, \qquad \tau_B' = -\frac{1}{2} + \frac{i}{2}, \qquad \tau_C = \omega,$$
(7.57b)

where the choice of Eq. (7.57a) corresponds to the  $CSD(1+\sqrt{6})$  case, whereas Eq. (7.57b) gives rise to  $CSD(1-\sqrt{6})$ . In the basis of [257, 279], these correspond to more familiar fixed points:

$$\tau_A = 2 + i, \qquad \tau_B = i, \qquad \qquad \tau_C = -\omega^2, \qquad (7.57c)$$

Field	SU(5)	$S_4^A$	$k_A$	$S_4^B$	$k_B$	$S_4^C$	$k_C$
F	$\overline{5}$	1	$+\frac{1}{2}$	1	$+\frac{1}{2}$	3	-3
$T_1$	10	1	+1	1	+1	1′	+3
$T_2$	10	1	$+\frac{1}{2}$	1	$+\frac{1}{2}$	1′	+3
$T_3$	10	1	0	1	0	1′	+3
$N_A^c$	1	1′	$+\frac{9}{2}$	1	$+\frac{1}{2}$	1	-1
$N_B^c$	1	1	$+\frac{1}{2}$	1′	$+\frac{5}{2}$	1	-1
$\Phi_{AC}$	1	3	0	1	0	3	0
$\Phi_{BC}$	1	1	0	3	0	3	0
$\phi_T$	1	1	$-\frac{1}{2}$	1	$-\frac{1}{2}$	1	0
$\phi_F$	1	1	$-\frac{1}{2}$	1	$-\frac{1}{2}$	1	+2
$H_5$	5	1	0	1	0	1	0
$H_{\overline{5}}$	$\overline{5}$	1	0	1	0	1	0
$H_{\overline{45}}$	$\overline{45}$	1	0	1	0	1	0

**Table 7.9:** Assignments of the fields under the SU(5) gauge symmetry and the representations and weights under the 3 modular symmetries  $(S_4^A, S_4^B, S_4^C)$  considered. We omit fields that are necessary for a consistent UV completion, such as messenger fields to complete the non-renormalizable terms, as well as the driving fields responsible for the bi-triplet and weighton vevs.

$$\tau_A = 2 + i, \qquad \tau_B' = -\frac{8}{13} + \frac{i}{13}, \qquad \tau_C = -\omega^2.$$
(7.57d)

We emphasise that the fixed points in Eq. (7.57c) arise from the well known single modulus fixed points  $\tau = i$  and  $\tau = -\omega^2$ . With three moduli, the two fixed points i and i+2 are simply related but inequivalent.

The superpotential responsible for the up-quark mass matrix comes from  $T_iH_5T_i$  couplings:

$$w_{u} = H_{5} \left\{ T_{1} \left[ y_{uu} Y_{1}^{(6)} \left( \tau_{C} \right) \left( \frac{\phi_{T}^{4}}{\Lambda^{4}} \right) + y_{uu}' Y_{1}^{(12)} \left( \tau_{C} \right) \left( \frac{\phi_{F}^{3} \phi_{T}}{\Lambda^{4}} \right) \right] T_{1} + T_{2} \left[ y_{cc} Y_{1}^{(6)} \left( \tau_{C} \right) \left( \frac{\phi_{T}^{2}}{\Lambda^{2}} \right) \right] T_{2} \right.$$

$$\left. + y_{tt} Y_{1}^{(6)} \left( \tau_{C} \right) \left[ T_{3} T_{3} \right] + T_{1} \left[ y_{uc} Y_{1}^{(6)} \left( \tau_{C} \right) \left( \frac{\phi_{T}^{3}}{\Lambda^{3}} \right) + y_{uc}' Y_{1}^{(12)} \left( \tau_{C} \right) \left( \frac{\phi_{F}^{3}}{\Lambda^{3}} \right) \right] T_{2} \right.$$

$$\left. + T_{1} \left[ y_{ut} Y_{1}^{(6)} \left( \tau_{C} \right) \left( \frac{\phi_{T}^{2}}{\Lambda^{2}} \right) \right] T_{3} + T_{2} \left[ y_{ct} Y_{1}^{(6)} \left( \tau_{C} \right) \left( \frac{\phi_{T}}{\Lambda} \right) \right] T_{3} \right\},$$

$$(7.58)$$

where we suppress  $Y_1^{(0)}(\tau_{A,B})$  from the notation, and  $\Lambda$  stands for the relevant UV scale for a particular non-renormalizable operator, which we take to be universal for notational convenience. The contributions to  $Y_d$  (and similarly for  $Y_\ell$ ) come from the couplings to both  $H_{\overline{5}}$  and  $H_{\overline{45}}$ . The superpotential will read the same for both scalars, with  $H_{\overline{5}}$  and  $H_{\overline{45}}$  exchanged, and different Yukawa couplings:

$$w_{\ell,d} = H_{\overline{5}} \left\{ F \left[ y_{11}^{\overline{5}} Y_{\mathbf{3}'}^{(6)} \left( \tau_C \right) \left( \frac{\phi_F^3}{\Lambda^3} \right) + y_{12}^{\overline{5}} Y_{\mathbf{3}}^{(4)} \left( \tau_C \right) \left( \frac{\phi_F^2 \phi_T}{\Lambda^3} \right) + y_{13}^{\overline{5}} Y_{\mathbf{3}'}^{(2)} \left( \tau_C \right) \left( \frac{\phi_F \phi_T^2}{\Lambda^2} \right) \right] T_1 \right\}$$

$$+F\left[y_{22}^{\overline{5}}Y_{3}^{(4)}(\tau_{C})\left(\frac{\phi_{F}^{2}}{\Lambda^{2}}\right)+y_{23}^{\overline{5}}Y_{3'}^{(2)}(\tau_{C})\left(\frac{\phi_{F}\phi_{T}}{\Lambda^{2}}\right)\right]T_{2}+F\left[y_{33}^{\overline{5}}Y_{3'}^{(2)}(\tau_{C})\left(\frac{\phi_{F}}{\Lambda}\right)\right]T_{3}\right\} (7.59)$$

$$+\left(\overline{5}\to\overline{45}\right).$$

The relevant modular forms (for  $\tau_C = \omega$ ) are given by

$$Y_{\mathbf{3'}}^{(2)}(\tau_C) = \begin{pmatrix} 0 \\ 1 \\ 0 \end{pmatrix}, \quad Y_{\mathbf{3,3'}}^{(4)}(\tau_C) = \begin{pmatrix} 0 \\ 0 \\ 1 \end{pmatrix}, \quad Y_{\mathbf{3,3'}}^{(6)}(\tau_C) = \begin{pmatrix} 1 \\ 0 \\ 0 \end{pmatrix}, \quad Y_{\mathbf{1}}^{(6)}(\tau_C) = Y_{\mathbf{1}}^{(12)}(\tau_C) = 1, \quad (7.60)$$

and thus, the resulting Yukawa matrices are

$$Y_{u} = \begin{pmatrix} y_{uu}\epsilon_{T}^{4} + y'_{uu}\epsilon_{F}^{3}\epsilon_{T} & y_{uc}\epsilon_{T}^{3} + y'_{uc}\epsilon_{F}^{3} & y_{ut}\epsilon_{T}^{2} \\ \vdots & y_{cc}\epsilon_{T}^{2} & y_{ct}\epsilon_{T} \\ \vdots & \vdots & y_{tt} \end{pmatrix},$$
(7.61a)

$$Y_{u} = \begin{pmatrix} y_{uu}\epsilon_{T}^{4} + y'_{uu}\epsilon_{F}^{3}\epsilon_{T} & y_{uc}\epsilon_{T}^{3} + y'_{uc}\epsilon_{F}^{3} & y_{ut}\epsilon_{T}^{2} \\ . & y_{cc}\epsilon_{T}^{2} & y_{ct}\epsilon_{T} \end{pmatrix},$$

$$Y_{d} = \begin{pmatrix} y_{dd}\epsilon_{F}^{3} & y_{ds}\epsilon_{F}^{2}\epsilon_{T} & y_{db}\epsilon_{F}\epsilon_{T}^{2} \\ 0 & y_{ss}\epsilon_{F}^{2} & y_{sb}\epsilon_{F}\epsilon_{T} \\ 0 & 0 & y_{bb}\epsilon_{F} \end{pmatrix},$$

$$Y_{\ell} = \begin{pmatrix} y_{ee}\epsilon_{F}^{3} & 0 & 0 \\ y_{\mu e}\epsilon_{F}^{2}\epsilon_{T} & y_{\mu\mu}\epsilon_{F}^{2} & 0 \\ y_{\tau e}\epsilon_{F}\epsilon_{T}^{2} & y_{\tau\mu}\epsilon_{F}\epsilon_{T} & y_{\tau\tau}\epsilon_{F} \end{pmatrix}.$$

$$(7.61b)$$

The superpotentials of Eqs. (7.58) and (7.59) responsible for the quark and charged-lepton masses rely on non-renormalizable operators, through multiple weighton insertions. After the weighton fields acquire a non-zero vev,  $\epsilon_{F,T} = \langle \phi_{F,T} \rangle / \Lambda$ , the quarks and charged-leptons get contributions to their masses a la Froggatt-Nielsen, as per the weighton mechanism. If we assume  $\mathcal{O}(1)$  coefficients, together with  $\epsilon_F \sim \lambda^3$ , and  $\epsilon_T \sim \lambda^2$ , we see that the mass matrices are close to those of Eq. (7.56):

$$Y_{u} \sim \begin{pmatrix} \epsilon_{T}^{4} + \epsilon_{F}^{3} \epsilon_{T} & \epsilon_{T}^{3} + \epsilon_{F}^{3} & \epsilon_{T}^{2} \\ . & \epsilon_{T}^{2} & \epsilon_{T} \\ . & . & 1 \end{pmatrix}, \quad Y_{d} \sim \begin{pmatrix} \epsilon_{F}^{3} & \epsilon_{F}^{2} \epsilon_{T} & \epsilon_{F} \epsilon_{T}^{2} \\ 0 & \epsilon_{F}^{2} & \epsilon_{F} \epsilon_{T} \\ 0 & 0 & \epsilon_{F} \end{pmatrix}, \quad Y_{\ell} \sim \begin{pmatrix} \epsilon_{F}^{3} & 0 & 0 \\ \epsilon_{F}^{2} \epsilon_{T} & \epsilon_{F}^{2} & 0 \\ \epsilon_{F} \epsilon_{T}^{2} & \epsilon_{F} \epsilon_{T} & \epsilon_{F} \end{pmatrix}, \quad (7.62)$$

where the up quark Yukawa matrix is symmetric. We see that we are unable to get different suppressions for  $Y_{\ell}$  and  $Y_d$ , due to the SU(5) nature of the model. Nonetheless, if we identify  $\epsilon_T \sim \lambda^2$  and  $\epsilon_F \sim \lambda^3$ , all the entries would have the desired suppressions, except for the (1,2) entries of both  $Y_u$  and  $Y_d$  which carry an extra suppression of  $\lambda$ , and so does the (1,1) entry of  $Y_d$  (yielding, however, the correct suppression for  $Y_{\ell}$ ). As such, we expect from the start that the model is able to fit the quark masses and mixings, as well as the charged-lepton masses, with  $\mathcal{O}(1)$  coefficients, as the model is designed such that the weighton insertions could be responsible for most of the observed hierarchies.

We turn now to the neutrino sector. The neutrino Dirac Yukawa matrix comes from  $FH_5N^c$  couplings. Due to the requirement of invariance under the modular symmetries, we see that  $Y_D$  can only be non-zero via couplings to the bi-triplets  $\Phi_{AC}$  and  $\Phi_{BC}$ . The allowed superpotential for the neutrino Dirac Yukawa

matrix reads

$$w_D = H_5 \left\{ a Y_{\mathbf{3'}}^{(4)} \left( \tau_A \right) F \left( \frac{\phi_F^2}{\Lambda^2} \frac{\langle \Phi_{AC} \rangle}{\Lambda} \right) N_A^c + b Y_{\mathbf{3'}}^{(2)} \left( \tau_B \right) F \left( \frac{\phi_F^2}{\Lambda^2} \frac{\langle \Phi_{BC} \rangle}{\Lambda} \right) N_B^c \right\}.$$
 (7.63)

Given the moduli of Eq. (7.57), the relevant Yukawa modular forms are

$$Y_{\mathbf{3'}}^{(4)}(\tau_A) = \begin{pmatrix} 0 \\ -1 \\ 1 \end{pmatrix}, \qquad Y_{\mathbf{3'}}^{(2)}(\tau_B) = \begin{pmatrix} 1 \\ 1 - \sqrt{6} \\ 1 + \sqrt{6} \end{pmatrix}, \qquad Y_{\mathbf{3'}}^{(2)}(\tau_B') = \begin{pmatrix} 1 \\ 1 + \sqrt{6} \\ 1 - \sqrt{6} \end{pmatrix}. \tag{7.64}$$

After both the bi-triplets and the weighton acquire a non-zero vev, the terms of Eq. (7.63) populate the neutrino Dirac Yukawa matrix as

$$Y_D \propto \epsilon_F^2 \begin{pmatrix} 0 & b \\ a & b \left( 1 \pm \sqrt{6} \right) \\ -a & b \left( 1 \mp \sqrt{6} \right) \end{pmatrix}. \tag{7.65}$$

Lastly, we analyse the relevant terms for the RH neutrino mass matrix. The modular assignments of Table 7.9 do not allow for the presence of bare mass terms, otherwise allowed by gauge invariance. However, similarly for the remaining fermions, we can build non-renormalizable terms which will generate mass terms for the heavy neutrinos below an appropriately large scale. The relevant Yukawa modular forms here will transform as  $\mathbf{1}^{(\prime)}$  and, as it happened for  $\tau = \omega$ , there are vanishing modular forms at  $\tau_A$  and  $\tau_B$ . We find that, up to weight 10, the relevant non-zero modular forms are

$$Y_{\mathbf{1}}^{(4)}, \quad Y_{\mathbf{1}'}^{(6)}, \quad Y_{\mathbf{1}}^{(8)}, \quad Y_{\mathbf{1}'}^{(10)}.$$
 (7.66)

The Majorana superpotential is given by

$$w_{M} = \frac{1}{2} M_{A} Y_{\mathbf{1}}^{(8)} (\tau_{A}) \left( \frac{\phi_{F} \phi_{T}}{\Lambda^{2}} \right) N_{A}^{c} N_{A}^{c} + \frac{1}{2} M_{B} Y_{\mathbf{1}}^{(4)} (\tau_{B}) \left( \frac{\phi_{F} \phi_{T}}{\Lambda^{2}} \right) N_{B}^{c} N_{B}^{c},$$
 (7.67)

where, as usual, we omit any modular form of weight 0. Any mixed term is forbidden by the modular symmetries. The ensuing Majorana mass matrix is then given by

$$M_M = \epsilon_F \epsilon_T \begin{pmatrix} M_A & 0 \\ 0 & M_B \end{pmatrix} . \tag{7.68}$$

Through the type-I seesaw mechanism, we arrive at a situation similar to that of Section 7.1.3, and the

effective mass matrix for the light neutrinos becomes

$$m_{\nu} = M_{D} \cdot M_{R}^{-1} \cdot M_{D}^{T} = \frac{v_{u}^{2} \epsilon_{F}^{3}}{\epsilon_{T}} \begin{pmatrix} \frac{b^{2}}{M_{B}} & \frac{b^{2}n}{M_{B}} & \frac{b^{2}(2-n)}{M_{B}} \\ . & \frac{a^{2}}{M_{A}} + \frac{b^{2}n^{2}}{M_{B}} & -\frac{a^{2}}{M_{A}} + \frac{b^{2}n(2-n)}{M_{B}} \\ . & . & \frac{a^{2}}{M_{A}} + \frac{b^{2}(2-n)^{2}}{M_{B}} \end{pmatrix},$$
(7.69)

with  $n=1\pm\sqrt{6}$ , as desired for the CSD(1  $\pm\sqrt{6}$ ) predictions. This can be written in more compact notation as

$$m_{\nu} = m_a \begin{pmatrix} 0 & 0 & 0 \\ 0 & 1 & -1 \\ 0 & -1 & 1 \end{pmatrix} + m_b e^{i\beta} \begin{pmatrix} 1 & n & 2-n \\ n & n^2 & n(2-n) \\ 2-n & n(2-n) & (2-n)^2 \end{pmatrix}.$$
 (7.70)

where  $m_a = \left\| \frac{v_u^2 \epsilon_F^3}{\epsilon_T} \frac{a^2}{M_A} \right\|$  and  $m_b = \left\| \frac{v_u^2 \epsilon_F^3}{\epsilon_T} \right\|$  are real parameters and  $\beta$  is an undetermined phase. This shows that the neutrino mass matrix is completely determined by three real parameters  $m_a$ ,  $m_b$  and  $\beta$ , where  $n = 1 \pm \sqrt{6}$ , making it a highly predictive scheme, which successfully describes the current data as recently discussed [309].

We note as a final remark that, due to the choice of assignments of Table 7.9, the superpotentials of Eqs. (7.58), (7.59), (7.63), and (7.67) do not have higher order corrections stemming for further insertions of weightons. A more technical note is shown in Appendix C.4, where we highlight the importance of having only one way to generate the couplings of Eq (7.63).

We expect the model to be compatible with experiment, due to its design. For completeness, we show here one point to showcase that indeed we can get the UV values for the quark masses and mixings with  $\mathcal{O}(1)$  coefficients, and negligible  $\chi^2$ :

$$y_{uu} = 1.1533 e^{-0.524i}, \quad y'_{uu} = 1.0001 e^{-2.24i}, \quad y_{uc} = 0.97294 e^{-2.59i},$$

$$y'_{uc} = 0.93204 e^{0.0393i}, \quad y_{ut} = 0.97272 e^{1.20i}, \quad y_{cc} = 1.0264 e^{1.53i},$$

$$y_{ct} = 0.92436 e^{-0.461i}, \quad y_{tt} = 0.53034 e^{-2.34i},$$

$$y_{dd} = 2.6549 e^{1.10i}, \quad y_{ds} = 2.1282 e^{0.555i}, \quad y_{db} = 1.0022 e^{-1.07i},$$

$$y_{ss} = 0.62888 e^{-2.97i}, \quad y_{sb} = 0.93386 e^{2.76i}, \quad y_{bb} = 0.56589 e^{1.10i},$$

$$\epsilon_T = 4.877 \times 10^{-2} \approx 0.946 \lambda^2, \quad \epsilon_F = 1.224 \times 10^{-2} \approx 1.046 \lambda^3.$$

As expected, we see that  $\epsilon_F \sim \lambda^3$ , and  $\epsilon_T \sim \lambda^2$ . Moreover, we see that we can easily fit the quark masses and mixings with  $\mathcal{O}(1)$  Yukawas, due to having the correct suppressions on the Yukawa matrices. As mentioned earlier, the (1,1) and (1,2) entries of  $Y_d$  have an extra  $\lambda$  suppression comparing to our naïve guess. In that sense, the associated couplings  $(y_{dd} \text{ and } y_{ds})$  need to be larger to compensate. That

is clearly seen in the numerical result of Eq. (7.71), in the relative hierarchy between  $y_{dd,ds}$  and the remaining Yukawas.

Turning now to the neutrino and charged-leptons, we provide a leptonic benchmark, assuming the same values for the weighton suppressions as obtained in the quark sector, namely, taking  $\epsilon_T$  and  $\epsilon_F$  from Eq. (7.71), and imposing  $y_{ij} \leq 3$ . We then find, for the  $n = 1 + \sqrt{6}$  case, and taking into account the SK-atmospheric data:

$$y_{ee} = 1.0756e^{0.00i}, \quad y_{\mu e} = 3.0000e^{0.14i}, \quad y_{\tau e} = 3.0000e^{2.06i},$$

$$y_{\mu \mu} = 2.8652e^{-0.83i}, \quad y_{\tau \mu} = 2.9998e^{-0.06i}, \quad y_{\tau \tau} = 0.5586e^{-0.96i},$$

$$r = 7.317 \times 10^{-2}, \qquad \beta = 1.2378$$

$$(7.72)$$

which yields predictions for the neutrino masses and lepton mixing parameters (which are very close to the LMS best-fit point) with  $\chi^2 \sim 1.9$ . In other words the extra off-diagonal charged-lepton Yukawa couplings are practically irrelevant since they have negligible effect on the lepton mixing angles. This is of course expected since the off-diagonal entries in the charged-lepton Yukawa matrix are confined to the lower triangular entries as shown in Eq. (7.61b). Since these lower off-diagonal entries are all suppressed relative to the diagonal element in the same row, one may diagonalise the Yukawa matrix using a perturbative approximation in which the right-handed mixing angles may be estimated as the ratio of the off-diagonal elements to the diagonal elements. Moreover, in this approximation, the left-handed charged-lepton mixing angles which are relevant ones for physical lepton mixing, are zero, since the upper triangular off-diagonal elements are just zero. Going beyond the perturbative approximation, there will be contributions to the physical lepton mixing angles from these non-zero off-diagonal entries in the lower triangular positions but they are highly suppressed. This is explicitly shown in Table 7.10, where we show the comparison between the point using the full  $Y_\ell$  of Eq. (7.72), and a point assuming a diagonal  $Y_\ell$ , which leads to the same structure of [280]. As we can see, the difference between the results is negligible, and the neutrino predictions analysis performed in [280] holds.

Goodness of fit against NuFit 5.2 results with SK atmospheric data											
$Y_{\ell}$	n	$\chi^2$	r	$\beta/\pi$	$m_b/10^{-3}$	$m_2^2/10^{-5}$	$m_3^2/10^{-3}$	$\theta_{12}$	$\theta_{23}$	$\theta_{13}$	δ
diagonal	$1 + \sqrt{6}$	2.08	0.0734	1.239	2.297	7.41	2.51	34.33	41.95	8.59	256
full	$1+\sqrt{6}$	1.87	0.0732	1.238	2.292	7.41	2.51	34.33	42.19	8.58	254

**Table 7.10:** Neutrino observables and input parameters for the case where the off-diagonal contributions are absent (top) and allowed (bottom). The neutrino squared-masses  $m_2^2$  and  $m_3^2$  are given in eV<sup>2</sup>.

This good fit to the flavour observables in an SU(5) unified model is obtained through a combination of Georgi-Jarlskog factors, the upper / lower diagonal form for the matrices of the down quarks and charged-leptons respectively, and the weighton mechanism, and demonstrate clearly some of the advantages of employing (multiple) modular symmetries in theories of flavour.

### 7.3 Discussion

This chapter was dedicated to the first complete model of the littlest modular seesaw, based on  $CSD(1-\sqrt{6}) \approx CSD(-1.45)$ , within a consistent framework based on multiple modular symmetries, as well as a related possibility based on  $CSD(1+\sqrt{6}) \approx CSD(3.45)$ . In each case, three  $S_4$  modular symmetries are introduced, each with their respective modulus field at a distinct stabilizer, leading to three separate residual subgroups. Of the three moduli, two are responsible implementing the viable Littlest Seesaw leading to Trimaximal 1 mixing, which correlates non-trivially with the observed ratio of neutrino masses. The remaining modulus guarantees the charged-lepton mass matrix is diagonal in the same basis, preserving the predictive power of the model. The result, in the symmetry basis, is a diagonal charged-lepton mass matrix and a LMS scenario of a particular kind.

Using a semi-analytical approach, we performed a  $\chi^2$  analysis of each case case and showed that good agreement with neutrino oscillation data is obtained, for both possible octants of atmospheric angle, including predictive relations between the leptonic mixing angles and the ratio of light neutrino masses, which non-trivially agree with the experimental values. It is noteworthy that in this very predictive setup, all the models fit the experimental data very well, depending on the choice of stabilizers and data set, in one case to within approximately  $1\sigma$ . This is a remarkable achievement, given that the neutrino mass matrix in the diagonal charged-lepton mass basis is determined effectively by two real parameters,  $m_a$ ,  $m_b$  and one phase  $\beta$  together with a discrete choice of  $n = 1 \pm \sqrt{6}$ . For a given choice of n, the remaining three real parameters determine all the parameters in the neutrino sector, namely all the neutrino masses and the entire PMNS matrix.

By extending the model to include a weighton and swapping the  $\Gamma_4$  with its double cover group  $\Gamma'_4 \simeq S'_4$ , we are able to also account for the hierarchy of the charged-leptons using modular symmetries, without altering the neutrino predictions.

On the other hand, the LMS only aims to provide a solution to a part of the flavour puzzle, as it does not take the quarks into account. Indeed, a grand unified theory of flavour is a desirable goal, but not easy to achieve. The connections between families imposed by unification restrict the solutions to the flavour problem. Given the predictive success of the LMS, we tackled the challenge by embedding the littlest modular seesaw model into an SU(5) unification framework. We surmounted the typical difficulty arising from the relation between charged-leptons and down quarks by employing Georgi-Jarlskog factors arising from appropriate SU(5) multiplets, and, from the modular flavour symmetry, constructing an upper-diagonal matrix in the flavour symmetry basis for the down quarks. Due to this, the contributions to quark mixing are sizeable at the same time that the transposed charged-lepton matrix is lower-diagonal, such that its off-diagonal entry contributions to the leptonic mixing are suppressed by the hierarchical charged-lepton mass ratios. We employ also two weightons, which enable us to justify the hierarchical entries in the mass matrices through the use of the modular weights, a mechanism which is reminiscent of typical Froggatt-Nielsen, but without requiring the introduction of an extra symmetry. The use of weightons was an optional feature without the SU(5) embedding, but is central in our GUT construction.

# Quarks at the $S_4$ Modular Cusp

One unique characteristic of the modular framework is the fact that fermion mass hierarchies may follow from the properties of the modular forms, without fine-tuning [158]. This mechanism was recently employed in Refs. [296, 297, 310–314] and will also be explored in the present work. It relies on the vev of the modulus taking a value close to one of the symmetric points. Indeed, fermion mass matrices are strongly constrained at or in the vicinity of the points of residual symmetry (see also [141, 263, 294, 295, 315–319]). As an example, for the viable fine-tuning-free model presented in Ref. [158],  $\tau$  is driven by lepton data to the vicinity of the cusp  $\omega$ . The numerical fit region corresponds to a ring around the latter, with a small radius  $|u| \simeq 0.007$ , where  $u \equiv (\tau - \omega)/(\tau - \omega^2)$ . While the best-fit point  $\tau \simeq -0.496 + 0.877i$  follows from a fit of low-energy lepton data, such peculiar values of  $\tau$  may instead be selected, in a top-down approach, by a dynamical principle [320, 321].

At present, a vast number of modular flavour models can be found in the literature, including:

- models of flavour based on the groups  $\Gamma_2 \simeq S_3$  [323–326],  $\Gamma_3 \simeq A_4$  [257, 263, 327–367],  $\Gamma_4 \simeq S_4$  [141, 143, 257, 368–375],  $\Gamma_5 \simeq A_5$  [143, 315, 374, 376], and  $\Gamma_7 \simeq PSL(2, \mathbb{Z}_7)$  [377],
- models of flavour based on the "double cover" groups  $\Gamma_3' \simeq T'$  [157, 378–381],  $\Gamma_4' \simeq S_4'$  [142, 382, 383] and  $\Gamma_5' \simeq A_5'$  [308, 384–386] and on  $\Gamma_6' \simeq S_3 \times T'$  [314, 387] (see also [388], considering a generalisation to other finite modular groups),
- models exploring the interplay of modular and gCP symmetries [389–394],
- models of quark-lepton unification [279, 282, 283, 285, 287–289, 303, 308, 313, 314, 364, 382, 391, 394–403],
- models with multiple moduli, first considered phenomenologically in [141, 263] and further developed in [137, 258–261, 280, 281, 362, 404, 405], and
- models relating modular flavour symmetries and inflation [406, 407].

<sup>&</sup>lt;sup>1</sup>For explanations of the fermion mass hierarchies relying on extra (weighted) scalars, with modular weights playing the role of Froggatt-Nielsen charges [107], see instead [143, 144, 322].

The outcomes of this (mostly) bottom-up strategy should eventually be linked with the top-down results of UV-complete theories [140, 145–149, 151–153, 284, 306, 307, 320, 321, 408–431], building towards a more predictive setup (see also [156, 293]).

Many of the models built so far have focused on the lepton sector, while fitting the quark sector — either independently of leptons or in an unified manner — has proven to be a challenge (see, e.g., [297]). If no explanation for hierarchical parameters is sought, modular models have been found to fit the 10 quark sector parameters (6 masses, 3 angles, 1 CPV phase) using a minimum of 9 real parameters. This has been achieved, using fine-tuned parameters, for the modular groups  $S'_4$  [382],  $A_4$  [391] (with a marginal fit), and  $S_4$  [394]. Instead, as mentioned above, there is a recent effort to additionally derive the quark mass hierarchies from the closeness of  $\tau$  to a symmetric point, via the mechanism of Ref. [158]. In this context, in which fine-tuning can be avoided, the community has so far considered:

- the modular group  $A_4$ , with  $\tau \simeq \omega$  [296] or  $\tau \simeq i\infty$  [297],
- the modular group  $S_4'$ , with  $\tau \simeq i\infty$  [311, 313],
- the modular group  $\Gamma_6 \simeq S_3 \times A_4$ , with  $\tau \simeq i \infty$  [310],
- the modular group  $\Gamma_6' \simeq S_3 \times A_4'$ , with  $\tau \simeq i \infty$  [314], and
- the multiple modular group  $A_4 \times A_4 \times A_4$ , assuming a common vev  $\tau$  for the three moduli, with either  $\tau \simeq \omega$  or  $\tau \simeq i\infty$  [312].<sup>2</sup>

With the exception of Ref. [310], which relies on discrete choices for the parameters, these models can fit the quark data with a minimum of 11 real parameters (case p=1 in Ref. [311]), in a phenomenological approach. Here and in what follows, "phenomenological" refers to the fact that some parameters are chosen to be real, despite the fact that they are complex in general — their reality is not guaranteed by e.g. a consistent combination of modular and gCP symmetries. Therefore, taking into account the ignored (but allowed) phases, the number of real parameters rises to a minimum of 13 in these models. It is hoped that a modular model can be built with a number of parameters coming close to the previously-found minimum of 9, while explaining the quark mass hierarchies.

In this work, we look into the restrictions on viable and minimal  $S_4^{(\prime)}$  modular flavour models of the quark sector where the proximity of the modulus to the point of residual  $\mathbb{Z}_3^{ST}$  symmetry (the cusp) plays a fundamental role in determining quark mass hierarchies. Although we focus on the quark case, all analytical results are also applicable to other fermions, e.g. the charged leptons. In Section 8.1 we expose our rationale, identifying the mass matrices which i) are minimal in terms of parameters, and ii) are hierarchical in a way which may be attributed to the properties of modular multiplets in the vicinity of the cusp. These matrices are expanded and explored analytically in Section 8.2. Our numerical results, showing which models can be fitted to data, are collected in Section 8.3, while some illustrative benchmarks are discussed in Section 8.4. We summarise and conclude in Section 8.5.

<sup>&</sup>lt;sup>2</sup>Refs. [313] and [314] also explore quark-lepton unification, from a bottom-up and grand unified theory perspective, respectively.

## 8.1 Framework

The framework of modular-invariant theories has already been presented in the introduction. Nonetheless, we feel its repetition here adds to the readability of this chapter, as it helps set up notation for the following analysis, as well as recall some properties of modular invariance which will be explored here. The familiar reader may feel free to skip to Section 8.1.1.

For a given element  $\gamma$  of the modular group  $\Gamma$ , with generators

$$S = \begin{pmatrix} 0 & 1 \\ -1 & 0 \end{pmatrix}, \quad T = \begin{pmatrix} 1 & 1 \\ 0 & 1 \end{pmatrix}, \quad R = \begin{pmatrix} -1 & 0 \\ 0 & -1 \end{pmatrix}, \tag{8.1}$$

obeying  $S^2 = R$ ,  $(ST)^3 = R^2 = 1$ , and RT = TR, the modulus  $\tau$  transforms via fractional linear transformations, as

$$\gamma = \begin{pmatrix} a & b \\ c & d \end{pmatrix} \in \Gamma : \quad \tau \to \gamma \tau = \frac{a\tau + b}{c\tau + d},$$
(8.2)

while matter superfields  $\psi_i$  transform as weighted multiplets [129–131],

$$\psi_i \to (c\tau + d)^{-k} \rho_{ij}(\gamma) \psi_j$$
, (8.3)

where  $\rho$  is a representation of  $\Gamma$  and k is the modular weight of  $\psi$ . To employ the modular symmetry as a flavour symmetry, we start by fixing an integer level N > 1 and assuming that  $\rho(\gamma) = \mathbb{1}$  for elements of the principal congruence subgroup  $\Gamma(N)$ . Hence,  $\rho$  is an "almost trivial" representation of the full modular group and a unitary representation of the finite quotient  $\Gamma'_N \equiv \Gamma / \Gamma(N) \simeq SL(2, \mathbb{Z}_N)$ . Moreover, if matter fields transform trivially under R, it is effectively a representation of the smaller group  $\Gamma_N \equiv \Gamma / \langle \Gamma(N) \cup \mathbb{Z}_2^R \rangle$ .

By requiring the invariance of the superpotential under modular transformations, one finds that couplings  $Y_{I_1...I_n}(\tau)$  appearing in terms of the type  $\psi_{I_1}...\psi_{I_n}$  must be special holomorphic functions of  $\tau$  — modular forms of level N — obeying

$$Y_{I_1...I_n}(\tau) \xrightarrow{\gamma} Y_{I_1...I_n}(\gamma \tau) = (c\tau + d)^{k_Y} \rho_Y(\gamma) Y_{I_1...I_n}(\tau).$$
 (8.4)

Modular forms carry weights  $k_Y = k_{I_1} + \ldots + k_{I_n}$  and furnish unitary representations  $\rho_Y$  of the finite modular group such that  $\rho_Y \otimes \rho_{I_1} \otimes \ldots \otimes \rho_{I_n} \supset \mathbf{1}$ . Modular symmetry may thus constrain the Yukawa structures of a model in a predictive way, since the modular forms span finite-dimensional linear spaces of relatively low dimensionalities, for small values of k and N. We will focus on the case N=4 and  $\Gamma_4' \simeq S_4'$ , although our reasoning can be straightforwardly extended to the other finite modular groups. The group theory and modular forms for  $S_4'$  are summarised in Appendix D. Crucially, these forms can

be written in terms of only two functions,  $\theta$  and  $\varepsilon$  [142], defined by

$$\theta(\tau) \equiv 1 + 2\sum_{k=1}^{\infty} q^{(2k)^2} = 1 + 2q^4 + 2q^{16} + \dots,$$

$$\varepsilon(\tau) \equiv 2\sum_{k=1}^{\infty} q^{(2k-1)^2} = 2q + 2q^9 + 2q^{25} + \dots,$$
(8.5)

with  $q \equiv \exp(\pi i \tau/2)$ , and satisfying  $\varepsilon(\omega)/\theta(\omega) = (1-i)/(1+\sqrt{3})$ .

The vev of  $\tau$  is restricted to the upper half-plane and plays the role of a spurion, parameterising all modular symmetry breaking in the absence of flavons. In such a case, the value of  $\tau$  can always be restricted to the fundamental domain  $\mathcal{D}$  of the modular group  $\Gamma$  [141]. In a CP-invariant modular theory, an additional  $\mathbb{Z}_2^{\text{CP}}$  symmetry is preserved for  $\text{Re }\tau=0$  or for  $\tau$  on the border of  $\mathcal{D}$ , while is broken at generic values of  $\tau$  [139, 142]. All three symmetric points  $\tau_{\text{sym}}=i,\,\omega,\,i\infty$  preserve the CP symmetry. Finally, a  $\mathbb{Z}_2^R$  symmetry is always preserved, as the R generator is unbroken for any value of  $\tau$ .

At each of the symmetric points  $\tau_{\rm sym} = i$ ,  $\omega$ ,  $i\infty$ , flavour textures can be further constrained by the residual symmetry group, which may enforce the presence of multiple zero entries in the mass matrices. As  $\tau$  moves away from the symmetric value, these entries will generically become non-zero. The magnitudes of such (residual-)symmetry-breaking entries are controlled by the size of the departure  $\epsilon$  of  $\tau$  from  $\tau_{\rm sym}$  and by the field transformation properties under the residual symmetry group, which may depend on modular weights [158]. Indeed, the zero entries of fermion mass matrices are expected to become  $\mathcal{O}(|\epsilon|^l)$ . The exponents l are extracted from products of factors which correspond to representations of the residual symmetry group and thus are not additional independent parameters (see Ref. [158] for further details).

For the left cusp and N=4, one may choose the small-magnitude parameter  $\epsilon$  as

$$\epsilon(\tau) \equiv 1 - \frac{1 + \sqrt{3}}{1 - i} \frac{\varepsilon(\tau)}{\theta(\tau)}, \text{ such that } \epsilon(\omega) = 0.$$
(8.6)

This parameter can be related to the previously-defined  $u = (\tau - \omega)/(\tau - \omega^2)$ , via a u-expansion [320], resulting in  $\epsilon \simeq 2.82 \, u$  — an approximation valid in the vicinity of the left cusp. Both  $|\epsilon|$  and |u| thus quantify the deviation of  $\tau$  from the point of residual  $\mathbb{Z}_3^{ST}$  symmetry. Note that the right cusp,  $\omega + 1 = \exp(\pi i/3)$ , is equivalent to the left cusp since they are related by the modular T transformation. Additionally, the vicinity of the right cusp can be mapped to the vicinity of the left cusp  $\omega$ , by the inverse of the T transformation, without affecting observables. While the resulting points may lie outside of the fundamental domain  $\mathcal{D}$ , the corresponding |u| will be small and the results of Ref. [158] apply. Finally, note that if a fit of masses and mixing is possible in the vicinity of the right cusp within  $\mathcal{D}$ , then such a fit is also possible in the vicinity of the left cusp within  $\mathcal{D}$ , with  $\tau \to -\tau^*$ , using the conjugated values of the superpotential constants, leading only to a sign flip of CPV phases [141].

#### 8.1.1 Quark Mass Matrices

We are interested in finding quark mass matrices M whose singular values — the quark masses — are hierarchical as a consequence of the proximity of  $\tau$  to the cusp  $\omega$ , i.e. due to the smallness of  $\epsilon$  (the

absolute value is implied, unless stated otherwise). As shown in Ref. [158], for  $\tau \simeq \omega$  the only possible hierarchical massive spectra are of the type 1 :  $\epsilon$  :  $\epsilon^2$ , since no higher powers of  $\epsilon$  are attainable. The irrep pairs leading to such spectra have been identified therein for the case of a common weight across generations of a given isospin multiplet. Here, we lift this requirement and allow for different weights across generations.

Quark masses enter the superpotential W via a modular-invariant bilinear,

$$W \supset Q_i M(\tau)_{ij} q_i^c, \tag{8.7}$$

where i, j = 1, 2, 3 and we adopt a left-right convention. The quark superfield doublets  $Q \sim \bigoplus_{\alpha} (\mathbf{r}_{\alpha}, k_{\alpha})$  and quark superfield singlets  $q^c \sim \bigoplus_{\beta} (\mathbf{r}_{\beta}^c, k_{\beta}^c)$  of a given sector (up or down) transform according to

$$Q_{\alpha} \xrightarrow{\gamma} (c\tau + d)^{-k_{\alpha}} \rho_{\mathbf{r}_{\alpha}}(\gamma) Q_{\alpha},$$

$$q_{\beta}^{c} \xrightarrow{\gamma} (c\tau + d)^{-k_{\beta}^{c}} \rho_{\mathbf{r}_{\beta}^{c}}(\gamma) q_{\beta}^{c},$$

$$(8.8)$$

under a modular transformation  $\gamma \in \Gamma$ , with  $\alpha$  and  $\beta$  labelling different irreps and weights. To each pair  $(\alpha, \beta)$  corresponds a sub-block of the matrix M. A finite number of modular forms of weight  $k_{\alpha} + k_{\beta}^{c}$  may contribute to it.

#### The Issue of Normalisations

Let us comment on the relative size of modular forms contributing to M. Taking an agnostic point of view, we do not attribute physical significance to the absolute normalisation of modular form multiplets in the vicinity of the cusp. Indeed, note that modular forms always appear together with superpotential constants that can absorb their normalisation. Therefore, one can only meaningfully discuss the magnitude of these constants after some normalisation has been fixed for the modular forms. In practice, in this work we will choose to normalise modular multiplets at the fit value of  $\tau$  using the Euclidean norm. From the bottom-up perspective, constrained by group theory alone, this is a valid (albeit arbitrary) choice of normalisation.

To guarantee that fermion mass textures and hierarchies in our setup originate from the properties of modular forms, they should then originate from the relations between the entries of a modular form multiplet — the direction of the "vector" — and not from the relative norms of independent modular forms — the (arbitrary) sizes of the "vectors". So, a priori, different sub-blocks of M may contribute on the same footing to the mass matrix, and should not be  $\epsilon$ -suppressed among themselves.<sup>3</sup>

To illustrate this last point, consider as an example  $Q \sim (\mathbf{2},0) \oplus (\mathbf{1},2)$  and  $q^c \sim (\mathbf{2},4) \oplus (\mathbf{1},2)$ . Employing the results of Ref. [158] summarised in Table 8.1, one finds the decompositions  $Q \rightsquigarrow \mathbf{1}_1 \oplus \mathbf{1}_2 \oplus \mathbf{1}_2$  and  $q^c \rightsquigarrow \mathbf{1}_2 \oplus \mathbf{1}_0 \oplus \mathbf{1}_2$  under the residual  $\mathbb{Z}_3$  symmetry group at the cusp. In an appropriate basis, if one considers that sub-blocks of M are on the same footing, the mass matrix will schematically have the

<sup>&</sup>lt;sup>3</sup>This philosophy differs from what is considered in Refs. [310–312].

$S_4'$ irrep <b>r</b>	$1,1',\widehat{1},\widehat{1}'$	$2,\widehat{2}$	$3,3',\widehat{3},\widehat{3}'$
$\mathbb{Z}_3$ decomposition	$1_k$	$1_{k+1}\oplus1_{k+2}$	$1_k \oplus 1_{k+1} \oplus 1_{k+2}$

**Table 8.1:** Decompositions of  $\Gamma'_4 \simeq S'_4$  weighted multiplets  $(\mathbf{r}, k)$  under the residual symmetry group  $\mathbb{Z}_3^{ST}$  at the cusp [158]. Subscripts are understood modulo 3.

structure

$$M \sim \begin{pmatrix} 1 & \epsilon & 1 \\ \epsilon & \epsilon^2 & \epsilon \\ \hline 1 & \epsilon & 1 \end{pmatrix}, \text{ instead of } \begin{pmatrix} 1 & \epsilon & 1 \\ \epsilon & \epsilon^2 & \epsilon \\ \hline \epsilon & \epsilon^2 & \epsilon \end{pmatrix}$$
 (8.9)

as one may expect from the residual decomposition analysis.<sup>4</sup> In particular,  $M_{33}$  is populated by a modular singlet  $Y_1^{(4)}$ , whose norm, we argue, should not play a role in producing fermion mass hierarchies in a bottom-up approach. In other words, even though  $Y_1^{(4)}$  vanishes at the cusp, one is free to normalise it as  $Y_1^{(4)} = 1$  elsewhere. Similarly, the doublet  $Y_2^{(6)}$  which, following the definition given in Appendix D.2, reads  $Y_2^{(6)} \sim (\epsilon^2, \epsilon)$  in an appropriate basis, may be normalised to read  $Y_2^{(6)} \sim (\epsilon, 1)$  in the vicinity of the cusp. Nevertheless, we stress that the arbitrariness in these normalisations cannot change the ratios or relative suppressions between entries of modular multiplets. These are what one can reliably use to justify mass hierarchies.

#### Minimal Quark Mass Matrices

It should be clear that, once the above viewpoint is adopted, a fully hierarchical M cannot contain four or more sub-blocks. It follows that either Q or  $q^c$  (or both) must furnish some triplet representation(s)  $\mathbf{3}^*$  of the finite modular group  $S_4'$ . From the outset, it is not immediately important which of the two must be a triplet, since the spectrum is insensitive to transposition, i.e. to the exchange of irrep and weight assignments of Q and  $q^c$ . Under the residual  $\mathbb{Z}_3^{ST}$  group at the cusp, one has  $(\mathbf{3}^*, k) \rightsquigarrow \mathbf{1}_k \oplus \mathbf{1}_{k+1} \oplus \mathbf{1}_{k+2}$  [158], as shown in Table 8.1. For any weight, this decomposition spans all three  $\mathbb{Z}_3$  irreps. To avoid more than one large mass in the vicinity of the symmetric point, the partners of  $\mathbf{3}^*$  need to decompose into a direct sum of three copies of the same  $\mathbb{Z}_3$  irrep. This automatically precludes using doublet or triplet irreps for these fields, cf. Table 8.1. Therefore, if (say)  $Q \sim (\mathbf{3}^*, k)$ , then  $q^c \sim \bigoplus_{\beta} (\mathbf{1}_{\beta}, k_{\beta})$  with all  $k_{\beta}$  equal modulo 3. As such, the desired mass matrix can only originate from modular form triplets of weight  $k_Y + 3n$ , with  $n \in \mathbb{Z}$ .

We proceed in a systematic way and restrict our attention to mass matrices that i) do not lead to massless quarks, by imposing det  $M \neq 0$ , and that ii) involve at most 4 parameters in the corresponding sector (excluding  $\tau$ ). Note that in the presence of a gCP symmetry, this maximum number of real parameters (4 in each sector and 2 from  $\tau$ ) already matches the number of quark observables (6 masses, 3 angles, and 1 CPV phase). To list all viable matrices, one starts by counting the number of linearly independent  $S'_4$  triplet modular forms available at each weight. This counting is given in Table 8.2, with each sub-table corresponding to a different weight modulo 3.

<sup>&</sup>lt;sup>4</sup>Working out this particular example, one additionally finds that  $M_{12} = M_{21} = 0$  even though these entries can be as large as  $\mathcal{O}(\epsilon)$ .

	<b>3</b> (3')	$3'$ $(\widehat{3})$		<b>3</b> (3')	$3'$ $(\widehat{3})$		<b>3</b> (3')	<b>3</b> ′ (3)
k = 1	0	1	k=2	0	1	k = 3	1	1
k = 4	1	1	k = 5	1	2	k = 6	1	2
k = 7	2	2	k = 8	2	2	k = 9	2	3
k = 10	2	3	k = 11	3	3	k = 12	3	3

**Table 8.2:** Counting of linearly independent  $S'_4$  modular forms for a given weight k and triplet representation. For even (odd) weights, the counting refers to the triplet representation shown outside (within) the parentheses.

	$M_1$	$M_2$	$M_3$	$M_4$	$M_5$	$M_6$
$(\mathbf{r}_1, k_1)$	$(\widehat{3},1)$	(3, 4)	(3', 2)	(3', 2)	$(\widehat{3}',3)$	$(\widehat{3}',3)$
$(\mathbf{r}_2, k_2)$	(3',4)	$({\bf 3}',4)$	$(\widehat{3}', 5)$	$(\widehat{3}', 5)$	$(\widehat{3},3)$	<b>(3</b> , 6)
$(\mathbf{r}_3, k_3)$	$(\widehat{3}',7)$	$(\widehat{3}',7)$	$(\widehat{3}, 5)$	<b>(3</b> , 8)	(3', 6)	(3', 6)

**Table 8.3:** Modular weights and representations for the minimal  $S'_4$  quark mass matrices viable in the vicinity of the cusp.

Viable minimal matrices involve at most 4 independent triplet modular forms, for 3 different  $(\mathbf{r}, k)$  pairs chosen from the same sub-table. Therefore, any  $(\mathbf{r}, k)$  pair for which there are "3" or more independent forms is excluded. The only possibilities correspond to either selecting three "1" entries (2 possible three-parameter matrices), or two "1" entries together with a single "2" entry (18 four-parameter matrices). However, not all of these 20 matrices are viable, since some of the modular forms turn out to be proportional to each other across weights, leading to a massless quark. Indeed, the fact that  $Y_3^{(1)} \propto Y_3^{(4)}$  and  $Y_3^{(3)} \propto Y_3^{(6)}$  means that all three-parameter matrices have zero determinant. We are left with only 6 viable four-parameter matrices  $M_i$  ( $i = 1, \ldots, 6$ ), defined in Table 8.3 via the weights and irreps of the forms entering them.

Being more explicit, note that e.g. a variant of the matrix  $M_1$  with  $(\mathbf{r}_2,k_2)=(\mathbf{3},4)$  or a variant of  $M_6$  with  $(\mathbf{r}_1,k_1)=(\widehat{\mathbf{3}},3)$  are excluded since  $Y_{\mathbf{3}}^{(4)}\propto Y_{\widehat{\mathbf{3}}}^{(1)}$  and  $Y_{\mathbf{3}}^{(6)}\propto Y_{\widehat{\mathbf{3}}}^{(3)}$ , as previously indicated, leading to a zero eigenvalue. Furthermore, one can exclude the variant of  $M_1$  with  $(\mathbf{r}_3,k_3)=(\widehat{\mathbf{3}},7)$ , since it turns out that  $Y_{\widehat{\mathbf{3}},1}^{(7)}\propto Y_{\mathbf{3}'}^{(4)}-3\frac{Y_{\mathbf{1}}^{(6)}}{Y_{\widehat{\mathbf{1}}'}^{(3)}}Y_{\widehat{\mathbf{3}}}^{(1)}$ , while  $Y_{\widehat{\mathbf{3}},2}^{(7)}\propto Y_{\mathbf{3}'}^{(4)}$ . A similar situation happens for, e.g., the variant of  $M_4$  with  $(\mathbf{r}_3,k_3)=(\mathbf{3}',8)$ , where  $Y_{\mathbf{3}',1}^{(8)}\propto Y_{\widehat{\mathbf{3}}'}^{(5)}+\frac{24}{17}\frac{Y_{\mathbf{1}}^{(6)}}{Y_{\widehat{\mathbf{1}}'}^{(3)}}Y_{\mathbf{3}'}^{(2)}$  and  $Y_{\mathbf{3}',2}^{(8)}\propto Y_{\widehat{\mathbf{3}}'}^{(5)}$ .

The matrices  $M_i$   $(i=1,\ldots,6)$ , that we consider in what follows, are the minimal mass matrices, involving at most four superpotential parameters and no massless fermions, where the quark mass hierarchies may stem from the proximity of  $\tau$  to the cusp, assuming our choice of modular form normalisation. In the limit where  $\tau$  is brought to the symmetric point  $(\epsilon \to 0)$ , all of them lead to a single massive quark. Furthermore, since  $Y_3^{(1)} \propto Y_3^{(4)}$  and  $Y_3^{(3)} \propto Y_3^{(6)}$ ,  $M_1$  and  $M_2$  as well as  $M_5$  and  $M_6$  are effectively the same matrices and need not be considered separately. In Section 8.2, we derive approximate analytical expressions for fermion mass ratios for each of the  $M_i$ .

#### 8.1.2 Assignments, Transposition, and gCP

Before proceeding, note that the up and down sectors are connected by the quark doublets Q. Therefore, it is not obvious whether one may choose independently  $M_u$  and  $M_d$  from the above list of 6 matrices, i.e. whether one may find modular  $S'_4$  assignments for Q,  $u^c$  and  $d^c$  leading to every possible matrix pair.

Let us consider separately the cases  $Q \sim 3^*$  and  $q^c \sim 3^*$  ( $q^c = u^c, d^c$ ). If one takes  $Q \sim 3^*$ , there is still freedom to adjust the singlets  $u^c_{\beta}$  and  $d^c_{\beta}$  independently so that each product  $Q u^c_{\beta}$  and  $Q d^c_{\beta}$  carries the desired weight and furnishes the desired triplet representation.<sup>5</sup> As such, any choice  $(M_u, M_d) = (M_i, M_j)$  with  $i, j = 1, \ldots, 6$  is possible in principle — their compatibility with quark mixing will be discussed in Section 8.3. The same is not true for the case where  $u^c$  and  $d^c$  are triplets, as shown below.

In the case where  $q^c$  are triplets, one has  $Q \sim \bigoplus_{\alpha} (\mathbf{1}_{\alpha}, k_{\alpha})$  with all  $k_{\alpha}$  equal modulo 3.<sup>6</sup> These 1-dimensional irreps are shared by  $M_u$  and  $M_d$ . It follows that the modular forms that feature in  $M_u$  and  $M_d$  must differ by a common weight,  $k_u^c - k_d^c$ , and by a single 1-dimensional irrep factor. In other words, if  $M_u$  is built from modular forms furnishing the representations  $(\mathbf{r}_1, \mathbf{r}_2, \mathbf{r}_3)$ , those entering  $M_d$  must correspond to  $(\mathbf{r}_1, \mathbf{r}_2, \mathbf{r}_3) \otimes \mathbf{1}^*$ , where  $\mathbf{1}^*$  is some 1-dimensional irrep. This reduces the possible pairs  $(M_u, M_d)$  in the  $q^c \sim \mathbf{3}^*$  case to

$$(M_1^T, M_4^T), \quad (M_2^T, M_5^T), \quad (M_3^T, M_6^T),$$

$$(M_4^T, M_1^T), \quad (M_5^T, M_2^T), \quad (M_6^T, M_3^T), \quad \text{and} \quad (M_i^T, M_i^T) \text{ with } i = 1, \dots, 6.$$

$$(8.10)$$

Note that the relevant mass matrices must be transposed with respect to the previous case of  $Q \sim 3^*$ .

Finally let us comment on the number of real parameters brought about by these models in the presence or absence of a gCP symmetry. Each mass matrix will be a function of four superpotential parameters  $\alpha_i$  (i = 1, ..., 4) which can be complex, in general. Schematically (q = u, d),

$$M_q \sim \begin{pmatrix} | & | & | \\ \alpha_1 Y_1 & \alpha_2 Y_2 & \alpha_3 Y_3 + \alpha_4 Y_4 \\ | & | & | \end{pmatrix}$$
 or its transpose, (8.11)

where the  $Y_i$  denote the triplet modular forms after a Clebsch-Gordan rearrangement. Further details are given in the next section, see Eq. (8.13). Imposing gCP, all  $\alpha_i$  are made real<sup>7</sup> and the number of real parameter matches the number of observables, as previously commented:  $(4 \times 2) + 2 = 10$ , independently of whether Q or  $q^c$  is a triplet. Lifting the requirement of gCP in the case  $Q \sim 3^*$  generically leads to one extra physical phase in each matrix, since the  $u^c_\beta$  and  $d^c_\beta$  can be rephased independently to absorb all  $\arg(\alpha_{1,2,3})$ . Therefore, in each sector we are left with  $\alpha_4$  as the only complex parameter, for a total of  $(5 \times 2) + 2 = 12$  degrees of freedom in the quark model. Instead, the absence of gCP in the  $q^c \sim 3^*$ 

<sup>5</sup>Indeed, this is an underconstrained problem, as there are classes of assignments that lead to the same quark mass matrix. For example, the choices  $Q \sim (\mathbf{3}, k), \ q^c \sim (\widehat{\mathbf{1}}', -k+1) \oplus (\mathbf{1}', -k+4) \oplus (\widehat{\mathbf{1}}, -k+7)$  and  $Q \sim (\mathbf{3}', k), \ q^c \sim (\widehat{\mathbf{1}}, -k+1) \oplus (\mathbf{1}, -k+4) \oplus (\widehat{\mathbf{1}}', -k+7)$  both generate  $M_1$ .

<sup>&</sup>lt;sup>6</sup>The ordering of singlets is unphysical: any permutation corresponds to a weak basis choice affecting both sectors simultaneously and thus cannot impact quark mixing.

<sup>&</sup>lt;sup>7</sup>In our case, CP invariance implies the reality of superpotential parameters, as we are considering a symmetric basis for the generators of  $S'_4$  as well as real Clebsch-Gordan coefficients [139, 142].

(transpose) case allows, in general, for (5+7)+2=14 real degrees of freedom, since one may only absorb the phases  $\arg(\alpha_{1,2,3})$  in one of the sectors, via the rephasing of the  $Q_{\alpha}$ , and a global phase in the other sector, via  $q^c$  rephasing. In light of this proliferation of free real parameters, we will not consider the latter class of models — transpose case without gCP — in what follows.

## 8.2 Analytical Results for the Mass Matrices

In this section, we derive approximate analytical expressions for the fermion mass ratios for each of the minimal  $S'_4$  quark matrices identified in the previous section. The superpotential of interest reads (q = u, d):

$$W_{q} = \alpha_{1} \left( Y_{\mathbf{r}_{1}}^{(k_{1})} Q q_{1}^{c} \right)_{\mathbf{1}} H_{q} + \alpha_{2} \left( Y_{\mathbf{r}_{2}}^{(k_{2})} Q q_{2}^{c} \right)_{\mathbf{1}} H_{q}$$

$$+ \alpha_{3} \left( Y_{\mathbf{r}_{3},1}^{(k_{3})} Q q_{3}^{c} \right)_{\mathbf{1}} H_{q} + \alpha_{4} \left( Y_{\mathbf{r}_{3},2}^{(k_{3})} Q q_{3}^{c} \right)_{\mathbf{1}} H_{q} ,$$

$$(8.12)$$

where we set  $\alpha_{1,2,3}$  real and non-negative without loss of generality (since only  $|\alpha_{1,2,3}|^2$  will enter in the expressions for  $M_q M_q^{\dagger}$  whose eigenvalues are the corresponding quark masses squared and whose diagonalising unitary matrix enters the expression for the CKM quark mixing matrix), while  $\alpha_4 \in \mathbb{C}$  in general, covering the no-gCP case. The weights and representations of the modular forms entering  $W_q$  have been summarised in Table 8.3 for each of the six quark mass matrices  $M_i$  (i = 1, ..., 6) under consideration. Before taking into account the canonical normalisation of the fields (see also Section 8.3), these matrices take the form

$$M_{i} = v_{q} \begin{bmatrix} \alpha_{1} \\ \sqrt{3} \\ y_{3} & 0 & 0 \\ y_{2} & 0 & 0 \end{bmatrix}_{Y_{\mathbf{r}_{1}^{(k_{1})}}} + \frac{\alpha_{2}}{\sqrt{3}} \begin{pmatrix} 0 & y_{1} & 0 \\ 0 & y_{3} & 0 \\ 0 & y_{2} & 0 \end{pmatrix}_{Y_{\mathbf{r}_{2}^{(k_{2})}}} + \frac{\alpha_{3}}{\sqrt{3}} \begin{pmatrix} 0 & 0 & y_{1} \\ 0 & 0 & y_{3} \\ 0 & 0 & y_{2} \end{pmatrix}_{Y_{\mathbf{r}_{3},1}^{(k_{3})}} + \frac{\alpha_{4}}{\sqrt{3}} \begin{pmatrix} 0 & 0 & y_{1} \\ 0 & 0 & y_{3} \\ 0 & 0 & y_{2} \end{pmatrix}_{Y_{\mathbf{r}_{3},2}^{(k_{3})}} \end{bmatrix},$$

$$(8.13)$$

in the left-right convention. In what follows, we expand each of these matrices in leading order in  $|\epsilon|$  and obtain approximate expressions for q-quark masses and quark mass ratios. Masses are defined by the ordering  $m_1 \ll m_2 \ll m_3$ , which may require appropriate permutations in the diagonalisation of the Hermitian products  $M_q M_q^{\dagger}$ .

Note that these results apply not just within the quark sector but to any fermionic sector of the theory where hierarchical structures may be required (e.g. the charged-lepton sector). We further assume an appropriate rotation of left-handed fields and the rephasing of right-handed fields, in order to move to a common "ST-diagonal" weak basis where the power structure in  $|\epsilon|$  is apparent, see also Appendix D.2. Here, we consider  $\epsilon \in \mathbb{C}$  as defined in Eq. (8.6) (the absolute value is no longer implied).

## Mass Matrix $M_1$

Keeping only the leading term in  $|\epsilon|$  element-wise, this matrix is given by the product

$$M_{1} \simeq v_{q} \, \widetilde{\alpha}_{1} \begin{pmatrix} \frac{\epsilon}{\sqrt{3}} & -\sqrt{3} \, \epsilon & -\frac{\epsilon}{\sqrt{3}} \left( 7 - \frac{\widetilde{\alpha}_{4}}{\widetilde{\alpha}_{3}} \right) \\ -\frac{\epsilon^{2}}{6} & \frac{7\epsilon^{2}}{6} & -\frac{\epsilon^{2}}{6} \left( 49 + \frac{\widetilde{\alpha}_{4}}{\widetilde{\alpha}_{3}} \right) \\ 1 & 1 & 1 + \frac{\widetilde{\alpha}_{4}}{\widetilde{\alpha}_{3}} \end{pmatrix} \cdot \begin{pmatrix} 1 & 0 & 0 \\ 0 & \widetilde{\alpha}_{2} & 0 \\ 0 & 0 & \widetilde{\alpha}_{3} \end{pmatrix},$$
(8.14)

after accounting for the canonical normalisation of the fields, with

$$\frac{\widetilde{\alpha}_{1}}{\sqrt{2 \operatorname{Im} \tau}} = \left(\sqrt{3} - 1\right) |\theta|^{2} \alpha_{1} \simeq 0.73 |\theta|^{2} \alpha_{1},$$

$$\frac{\widetilde{\alpha}_{2}}{(2 \operatorname{Im} \tau)^{3/2}} = \left(9 - 5\sqrt{3}\right) |\theta|^{6} \frac{\alpha_{2}}{\alpha_{1}} \simeq 0.34 |\theta|^{6} \frac{\alpha_{2}}{\alpha_{1}},$$

$$\frac{\widetilde{\alpha}_{3}}{(2 \operatorname{Im} \tau)^{3}} = 18\sqrt{\frac{2}{37}} \left(26 - 15\sqrt{3}\right) |\theta|^{12} \frac{\alpha_{3}}{\alpha_{1}} \simeq 0.08 |\theta|^{12} \frac{\alpha_{3}}{\alpha_{1}},$$

$$\frac{\widetilde{\alpha}_{4}}{(2 \operatorname{Im} \tau)^{3}} = 18\sqrt{2} \left(26 - 15\sqrt{3}\right) |\theta|^{12} \frac{\alpha_{4}}{\alpha_{1}} \simeq 0.49 |\theta|^{12} \frac{\alpha_{4}}{\alpha_{1}}.$$
(8.15)

The ensuing masses and mass ratios are given by

$$m_3 \simeq v_q \,\widetilde{\alpha}_1 \, \sqrt{1 + \widetilde{\alpha}_2^2 + |\widetilde{\alpha}_3 + \widetilde{\alpha}_4|^2} \,,$$
 (8.16)

$$\frac{m_2}{m_3} \simeq \frac{4}{\sqrt{3}} \frac{\sqrt{(1+|\widetilde{\alpha}_3 - \widetilde{\alpha}_4|^2)} \,\widetilde{\alpha}_2^2 + 4\widetilde{\alpha}_3^2}{1+\widetilde{\alpha}_2^2 + |\widetilde{\alpha}_3 + \widetilde{\alpha}_4|^2} |\epsilon|, \qquad (8.17)$$

$$\frac{m_1}{m_3} \simeq \frac{32}{3} \frac{\widetilde{\alpha}_2 \widetilde{\alpha}_3}{\sqrt{1 + \widetilde{\alpha}_2^2 + |\widetilde{\alpha}_3 + \widetilde{\alpha}_4|^2} \sqrt{(1 + |\widetilde{\alpha}_3 - \widetilde{\alpha}_4|^2) \, \widetilde{\alpha}_2^2 + 4\widetilde{\alpha}_3^2}} |\epsilon|^2, \tag{8.18}$$

while for the determinant one obtains

$$|\det M_1| \simeq \frac{128}{3\sqrt{3}} v_q^3 \widetilde{\alpha}_1^3 \widetilde{\alpha}_2 \widetilde{\alpha}_3 |\epsilon|^3.$$
 (8.19)

In modular models with a single modulus, the small value of  $|\epsilon|$  is shared by both the up and down sectors. It is challenging to fit both up- and down-quark mass hierarchies using the same power structure,  $1: |\epsilon|: |\epsilon|^2$ , in  $M_u$  and  $M_d$ . An additional suppression of quark mass ratios in one of the sectors may be arranged if, e.g., one of the superpotential constants is sufficiently larger than the others. Namely, the useful limit corresponds to taking the constant which is absent from the determinant to be large. Accordingly, in the limit  $|\tilde{\alpha}_4| \gg \tilde{\alpha}_2, \tilde{\alpha}_3$  one finds

$$m_3 \simeq v_q \widetilde{\alpha}_1 |\widetilde{\alpha}_4|, \qquad \frac{m_2}{m_3} \simeq \frac{4}{\sqrt{3}} \widetilde{\alpha}_2 \left| \frac{\epsilon}{\widetilde{\alpha}_4} \right|, \qquad \frac{m_1}{m_3} \simeq \frac{32}{3} \widetilde{\alpha}_3 \left| \frac{\epsilon}{\widetilde{\alpha}_4} \right|^2,$$
 (8.20)

illustrating how a different hierarchy may arise in both sectors (see also [296]).

## Mass Matrix $M_2$

The results for  $M_2$  coincide with those for  $M_1$ , provided one redefines the  $\widetilde{\alpha}_{1,\dots,4}$  as

$$\frac{\widetilde{\alpha}_{1}}{(2 \operatorname{Im} \tau)^{2}} = 6 \left(7 - 4\sqrt{3}\right) |\theta|^{8} \alpha_{1} \simeq 0.43 |\theta|^{8} \alpha_{1},$$

$$\widetilde{\alpha}_{2} = \frac{1}{\sqrt{3}} \frac{\alpha_{2}}{\alpha_{1}} \simeq 0.58 \frac{\alpha_{2}}{\alpha_{1}},$$

$$\frac{\widetilde{\alpha}_{3}}{(2 \operatorname{Im} \tau)^{3/2}} = 3\sqrt{\frac{2}{37}} \left(3\sqrt{3} - 5\right) |\theta|^{6} \frac{\alpha_{3}}{\alpha_{1}} \simeq 0.14 |\theta|^{6} \frac{\alpha_{3}}{\alpha_{1}},$$

$$\frac{\widetilde{\alpha}_{4}}{(2 \operatorname{Im} \tau)^{3/2}} = 3\sqrt{2} \left(3\sqrt{3} - 5\right) |\theta|^{6} \frac{\alpha_{4}}{\alpha_{1}} \simeq 0.83 |\theta|^{6} \frac{\alpha_{4}}{\alpha_{1}}.$$
(8.21)

This can be traced to the fact that the modular forms entering the second columns of  $M_1$  and  $M_2$  are proportional to each other,  $Y_3^{(4)} \propto Y_{\widehat{3}}^{(1)}$ , as previously indicated.

## Mass Matrix $M_3$

This mass matrix has the approximate form

$$M_{3} \simeq v_{q} \, \widetilde{\alpha}_{1} \begin{pmatrix} -\frac{\epsilon^{2}}{2} & \frac{3 \, \epsilon^{2}}{2} & -\frac{\epsilon^{2}}{2} \left( 5 - \frac{\widetilde{\alpha}_{4}}{\widetilde{\alpha}_{3}} \right) \\ 1 & 1 & 1 - \frac{\widetilde{\alpha}_{4}}{\widetilde{\alpha}_{3}} \\ \frac{\epsilon}{\sqrt{3}} & -\frac{\epsilon}{\sqrt{3}} & -\frac{\epsilon}{\sqrt{3}} \left( 5 + \frac{\widetilde{\alpha}_{4}}{\widetilde{\alpha}_{3}} \right) \end{pmatrix} \cdot \begin{pmatrix} 1 & 0 & 0 \\ 0 & \widetilde{\alpha}_{2} & 0 \\ 0 & 0 & \widetilde{\alpha}_{3} \end{pmatrix}, \tag{8.22}$$

with

$$\frac{\tilde{\alpha}_{1}}{2 \operatorname{Im} \tau} = 2\sqrt{14 - 8\sqrt{3}} |\theta|^{4} \alpha_{1} \simeq 0.76 |\theta|^{4} \alpha_{1},$$

$$\frac{\tilde{\alpha}_{2}}{(2 \operatorname{Im} \tau)^{3/2}} = \left(9 - 5\sqrt{3}\right) |\theta|^{6} \frac{\alpha_{2}}{\alpha_{1}} \simeq 0.34 |\theta|^{6} \frac{\alpha_{2}}{\alpha_{1}},$$

$$\frac{\tilde{\alpha}_{3}}{(2 \operatorname{Im} \tau)^{3/2}} = \frac{3}{\sqrt{10}} \left(3\sqrt{3} - 5\right) |\theta|^{6} \frac{\alpha_{3}}{\alpha_{1}} \simeq 0.19 |\theta|^{6} \frac{\alpha_{3}}{\alpha_{1}},$$

$$\frac{\tilde{\alpha}_{4}}{(2 \operatorname{Im} \tau)^{3/2}} = 3 \left(3\sqrt{3} - 5\right) |\theta|^{6} \frac{\alpha_{4}}{\alpha_{1}} \simeq 0.59 |\theta|^{6} \frac{\alpha_{4}}{\alpha_{1}}.$$
(8.23)

For the quark masses and mass ratios, one finds (after applying the 2-3 permutation matrix on the diagonal matrix with the singular values of  $M_3$ )

$$m_3 \simeq v_q \,\widetilde{\alpha}_1 \, \sqrt{1 + \widetilde{\alpha}_2^2 + |\widetilde{\alpha}_3 - \widetilde{\alpha}_4|^2} \,,$$
 (8.24)

$$\frac{m_2}{m_3} \simeq \frac{2}{\sqrt{3}} \frac{\sqrt{(1+|2\widetilde{\alpha}_3+\widetilde{\alpha}_4|^2)} \, \widetilde{\alpha}_2^2 + 9\widetilde{\alpha}_3^2}{1+\widetilde{\alpha}_2^2+|\widetilde{\alpha}_3-\widetilde{\alpha}_4|^2} |\epsilon|, \qquad (8.25)$$

$$\frac{m_1}{m_3} \simeq \frac{8 \,\widetilde{\alpha}_2 \widetilde{\alpha}_3}{\sqrt{1 + \widetilde{\alpha}_2^2 + |\widetilde{\alpha}_3 - \widetilde{\alpha}_4|^2} \sqrt{(1 + |2\widetilde{\alpha}_3 + \widetilde{\alpha}_4|^2)} \,\widetilde{\alpha}_2^2 + 9\widetilde{\alpha}_3^2} |\epsilon|^2, \tag{8.26}$$

whereas for the determinant,

$$|\det M_3| \simeq \frac{16}{\sqrt{3}} v_q^3 \widetilde{\alpha}_1^3 \widetilde{\alpha}_2 \widetilde{\alpha}_3 |\epsilon|^3,$$
 (8.27)

which is independent of  $\widetilde{\alpha}_4$ . Accordingly, taking the limit  $|\widetilde{\alpha}_4| \gg \widetilde{\alpha}_2, \widetilde{\alpha}_3$  one finds

$$m_3 \simeq v_q \widetilde{\alpha}_1 |\widetilde{\alpha}_4|, \qquad \frac{m_2}{m_3} \simeq \frac{2}{\sqrt{3}} \widetilde{\alpha}_2 \left| \frac{\epsilon}{\widetilde{\alpha}_4} \right|, \qquad \frac{m_1}{m_3} \simeq 8 \widetilde{\alpha}_3 \left| \frac{\epsilon}{\widetilde{\alpha}_4} \right|^2.$$
 (8.28)

#### Mass Matrix $M_4$

This mass matrix has the approximate form

$$M_{4} \simeq v_{q} \, \widetilde{\alpha}_{1} \begin{pmatrix} -\frac{\epsilon^{2}}{2} & \frac{3 \, \epsilon^{2}}{2} & -\frac{\epsilon^{2}}{2} \left( 5 + \frac{\widetilde{\alpha}_{4}}{\widetilde{\alpha}_{3}} \right) \\ 1 & 1 & 1 + \frac{\widetilde{\alpha}_{4}}{\widetilde{\alpha}_{3}} \\ \frac{\epsilon}{\sqrt{3}} & -\frac{\epsilon}{\sqrt{3}} & -\frac{\epsilon}{\sqrt{3}} \left( 5 - \frac{\widetilde{\alpha}_{4}}{\widetilde{\alpha}_{3}} \right) \end{pmatrix} \cdot \begin{pmatrix} 1 & 0 & 0 \\ 0 & \widetilde{\alpha}_{2} & 0 \\ 0 & 0 & \widetilde{\alpha}_{3} \end{pmatrix}, \tag{8.29}$$

with

$$\frac{\widetilde{\alpha}_{1}}{2 \operatorname{Im} \tau} = 2\sqrt{14 - 8\sqrt{3}} |\theta|^{4} \alpha_{1} \simeq 0.76 |\theta|^{4} \alpha_{1},$$

$$\frac{\widetilde{\alpha}_{2}}{(2 \operatorname{Im} \tau)^{3/2}} = \left(9 - 5\sqrt{3}\right) |\theta|^{6} \frac{\alpha_{2}}{\alpha_{1}} \simeq 0.34 |\theta|^{6} \frac{\alpha_{2}}{\alpha_{1}},$$

$$\frac{\widetilde{\alpha}_{3}}{(2 \operatorname{Im} \tau)^{3}} = \frac{18}{\sqrt{5}} \left(26 - 15\sqrt{3}\right) |\theta|^{12} \frac{\alpha_{3}}{\alpha_{1}} \simeq 0.15 |\theta|^{12} \frac{\alpha_{3}}{\alpha_{1}},$$

$$\frac{\widetilde{\alpha}_{4}}{(2 \operatorname{Im} \tau)^{3}} = 18\sqrt{2} \left(26 - 15\sqrt{3}\right) |\theta|^{12} \frac{\alpha_{4}}{\alpha_{1}} \simeq 0.49 |\theta|^{12} \frac{\alpha_{4}}{\alpha_{1}}.$$
(8.30)

The quark masses and ratios follow:

$$m_3 \simeq v_q \,\widetilde{\alpha}_1 \, \sqrt{1 + \widetilde{\alpha}_2^2 + |\widetilde{\alpha}_3 + \widetilde{\alpha}_4|^2} \,,$$
 (8.31)

$$\frac{m_2}{m_3} \simeq \frac{2}{\sqrt{3}} \frac{\sqrt{(1+|2\widetilde{\alpha}_3 - \widetilde{\alpha}_4|^2)} \, \widetilde{\alpha}_2^2 + 9\widetilde{\alpha}_3^2}{1+\widetilde{\alpha}_2^2 + |\widetilde{\alpha}_3 + \widetilde{\alpha}_4|^2} |\epsilon|, \qquad (8.32)$$

$$\frac{m_1}{m_3} \simeq \frac{8 \,\widetilde{\alpha}_2 \widetilde{\alpha}_3}{\sqrt{1 + \widetilde{\alpha}_2^2 + |\widetilde{\alpha}_3 + \widetilde{\alpha}_4|^2} \sqrt{(1 + |2\widetilde{\alpha}_3 - \widetilde{\alpha}_4|^2)} \,\widetilde{\alpha}_2^2 + 9\widetilde{\alpha}_3^2} |\epsilon|^2, \tag{8.33}$$

and the determinant reads

$$|\det M_4| \simeq \frac{16}{\sqrt{3}} v_q^3 \widetilde{\alpha}_1^3 \widetilde{\alpha}_2 \widetilde{\alpha}_3 |\epsilon|^3.$$
 (8.34)

In the limit  $|\widetilde{\alpha}_4| \gg \widetilde{\alpha}_2, \widetilde{\alpha}_3$ , one finds

$$m_3 \simeq v_q \widetilde{\alpha}_1 |\widetilde{\alpha}_4|, \qquad \frac{m_2}{m_3} \simeq \frac{2}{\sqrt{3}} \widetilde{\alpha}_2 \left| \frac{\epsilon}{\widetilde{\alpha}_4} \right|, \qquad \frac{m_1}{m_3} \simeq 8\widetilde{\alpha}_3 \left| \frac{\epsilon}{\widetilde{\alpha}_4} \right|^2.$$
 (8.35)

## Mass Matrix $M_5$

This mass matrix has the approximate form

$$M_{5} \simeq v_{q} \, \widetilde{\alpha}_{1} \begin{pmatrix} 1 & 1 & 1 + \frac{\widetilde{\alpha}_{4}}{\widetilde{\alpha}_{3}} \\ \sqrt{3} \, \epsilon & -\frac{\epsilon}{\sqrt{3}} & -\sqrt{3} \, \epsilon \left(1 - \frac{\widetilde{\alpha}_{4}}{\widetilde{\alpha}_{3}}\right) \\ -\frac{\epsilon^{2}}{2} & \frac{5 \, \epsilon^{2}}{6} & -\frac{\epsilon^{2}}{2} \left(5 + \frac{\widetilde{\alpha}_{4}}{\widetilde{\alpha}_{3}}\right) \end{pmatrix} \cdot \begin{pmatrix} 1 & 0 & 0 \\ 0 & \widetilde{\alpha}_{2} & 0 \\ 0 & 0 & \widetilde{\alpha}_{3} \end{pmatrix},$$
(8.36)

with

$$\frac{\widetilde{\alpha}_{1}}{(2 \operatorname{Im} \tau)^{3/2}} = 2 \left( 3\sqrt{3} - 5 \right) |\theta|^{6} \alpha_{1} \simeq 0.39 |\theta|^{6} \alpha_{1},$$

$$\widetilde{\alpha}_{2} = \sqrt{\frac{3}{2}} \frac{\alpha_{2}}{\alpha_{1}} \simeq 1.23 \frac{\alpha_{2}}{\alpha_{1}},$$

$$\frac{\widetilde{\alpha}_{3}}{(2 \operatorname{Im} \tau)^{3/2}} = \frac{6}{\sqrt{13}} \left( 3\sqrt{3} - 5 \right) |\theta|^{6} \frac{\alpha_{3}}{\alpha_{1}} \simeq 0.33 |\theta|^{6} \frac{\alpha_{3}}{\alpha_{1}},$$

$$\frac{\widetilde{\alpha}_{4}}{(2 \operatorname{Im} \tau)^{3/2}} = 3 \left( 3\sqrt{3} - 5 \right) |\theta|^{6} \frac{\alpha_{4}}{\alpha_{1}} \simeq 0.59 |\theta|^{6} \frac{\alpha_{4}}{\alpha_{1}}.$$
(8.37)

For quark masses and mass ratios, one finds

$$m_3 \simeq v_q \,\widetilde{\alpha}_1 \, \sqrt{1 + \widetilde{\alpha}_2^2 + |\widetilde{\alpha}_3 + \widetilde{\alpha}_4|^2} \,,$$
 (8.38)

$$\frac{m_2}{m_3} \simeq \frac{2}{\sqrt{3}} \frac{\sqrt{(4+|\widetilde{\alpha}_3 - 2\widetilde{\alpha}_4|^2)} \, \widetilde{\alpha}_2^2 + 9\widetilde{\alpha}_3^2}{1+\widetilde{\alpha}_2^2 + |\widetilde{\alpha}_3 + \widetilde{\alpha}_4|^2} |\epsilon|, \qquad (8.39)$$

$$\frac{m_1}{m_3} \simeq \frac{8\widetilde{\alpha}_2\widetilde{\alpha}_3}{\sqrt{1+\widetilde{\alpha}_2^2+|\widetilde{\alpha}_3+\widetilde{\alpha}_4|^2}\sqrt{(4+|\widetilde{\alpha}_3-2\widetilde{\alpha}_4|^2)\widetilde{\alpha}_2^2+9\widetilde{\alpha}_3^2}} |\epsilon|^2, \tag{8.40}$$

while for the determinant one obtains

$$|\det M_5| \simeq \frac{16}{\sqrt{3}} v_q^3 \widetilde{\alpha}_1^3 \widetilde{\alpha}_2 \widetilde{\alpha}_3 |\epsilon|^3.$$
 (8.41)

In the limit  $|\widetilde{\alpha}_4| \gg \widetilde{\alpha}_2, \widetilde{\alpha}_3$ , one finds

$$m_3 \simeq v_q \widetilde{\alpha}_1 |\widetilde{\alpha}_4|, \qquad \frac{m_2}{m_3} \simeq \frac{4}{\sqrt{3}} \widetilde{\alpha}_2 \left| \frac{\epsilon}{\widetilde{\alpha}_4} \right|, \qquad \frac{m_1}{m_3} \simeq 4 \widetilde{\alpha}_3 \left| \frac{\epsilon}{\widetilde{\alpha}_4} \right|^2.$$
 (8.42)

#### Mass Matrix $M_6$

The results for  $M_6$  coincide with those for  $M_5$ , provided one redefines the  $\widetilde{\alpha}_{1,\dots,4}$  as

$$\frac{\widetilde{\alpha}_{1}}{(2 \operatorname{Im} \tau)^{3/2}} = 2 \left( 3\sqrt{3} - 5 \right) |\theta|^{6} \alpha_{1} \simeq 0.39 |\theta|^{6} \alpha_{1},$$

$$\frac{\widetilde{\alpha}_{2}}{(2 \operatorname{Im} \tau)^{3/2}} = 3 \left( 9 - 5\sqrt{3} \right) |\theta|^{6} \frac{\alpha_{2}}{\alpha_{1}} \simeq 1.02 |\theta|^{6} \frac{\alpha_{2}}{\alpha_{1}},$$

$$\frac{\widetilde{\alpha}_{3}}{(2 \operatorname{Im} \tau)^{3/2}} = \frac{6}{\sqrt{13}} \left( 3\sqrt{3} - 5 \right) |\theta|^{6} \frac{\alpha_{3}}{\alpha_{1}} \simeq 0.33 |\theta|^{6} \frac{\alpha_{3}}{\alpha_{1}},$$

$$\frac{\widetilde{\alpha}_{4}}{(2 \operatorname{Im} \tau)^{3/2}} = 3 \left( 3\sqrt{3} - 5 \right) |\theta|^{6} \frac{\alpha_{4}}{\alpha_{1}} \simeq 0.59 |\theta|^{6} \frac{\alpha_{4}}{\alpha_{1}}.$$
(8.43)

		Observable	Best-fit $\pm 1\sigma$ range
Observable	Best-fit $\pm 1\sigma$ range	$(m_u/m_c)/10^{-3}$	$2.04 \pm 1.27$
$y_u / 10^{-6}$	$2.92 \pm 1.81$	$\left(m_c/m_t\right)/10^{-3}$	$2.68 \pm 0.25$
$y_c / 10^{-3}$	$1.43 \pm 0.100$	$\left(m_d/m_s\right)/10^{-2}$	$5.05 \pm 1.24$
$y_t$	$0.534 \pm 0.0341$	$(m_s/m_b)/10^{-2}$	$1.37 \pm 0.15$
$y_d / 10^{-6}$	$4.81 \pm 1.06$	θ <sub>12</sub> (°)	$13.027 \pm 0.0814$
$y_s / 10^{-5}$	$9.52 \pm 1.03$	$\theta_{23}\left(^{\circ}\right)$	$2.054 \pm 0.384$
$y_b / 10^{-3}$	$6.95\pm0.175$	$\theta_{13}\left(^{\circ}\right)$	$0.1802 \pm 0.0281$
		$\delta_{ ext{CP}}\left( angle ight)$	$69.21 \pm 6.19$

**Table 8.4:** Best-fit values and  $1\sigma$  ranges for the quark Yukawa couplings (left), quark mass ratios, mixing angles and CPV phase (right) at the high-energy scale of  $2 \times 10^{16}$  GeV for  $\tan \beta = 5$ . The values and uncertainties of Yukawa couplings, mixing angles and the CPV phase are reproduced from [303] and obtained from Refs. [302, 304].

This can be traced to the fact that the modular forms entering the second columns of  $M_5$  and  $M_6$  are proportional to each other,  $Y_3^{(6)} \propto Y_{\widehat{\mathbf{3}}}^{(3)}$ , as previously indicated.

In the following section, we confront the above flavour textures with quark data. We analyse some benchmarks in more detail in Section 8.4.

## 8.3 Numerical Results for the Mass Matrices

In the preceding sections, we have identified the minimal structures that can be assigned to  $M_u$  and  $M_d$ , each depending on 4 independent parameters. The resulting  $S_4'$  quark modular models may lead to hierarchical masses near the cusp and do not present more free parameters than observables when gCP is imposed. The next step is to verify numerically if any of these models can actually achieve a good fit of quark data, summarised in Table 8.4. To quantify the goodness of fit, we consider the sum of one-dimensional  $\chi^2$  functions in a Gaussian approximation,

$$\chi^{2}(\vec{p}) = \sum_{j=1}^{8} \left( \frac{\Theta_{j}(\vec{p}) - \Theta_{j}^{\text{b.f.}}}{\sigma_{j}} \right)^{2}, \qquad (8.44)$$

which we seek to minimise, and define  $N\sigma \equiv \sqrt{\chi^2}$ . Here,  $\Theta_j$  correspond to the values of the 8 observables in the right-hand side of Table 8.4, as predicted by the model under consideration, for a given set of parameters  $\vec{p}$ , while  $\Theta_j^{\text{b.f.}}$  denotes their high-energy best-fit values and  $\sigma_j$  are the corresponding  $1\sigma$  uncertainties. Note that if a model successfully reproduces dimensionless observables, the mass scales in each sector can be easily recovered by a common rescaling of the corresponding superpotential parameters.

For the  $\chi^2$  minimisation procedure,  $\tau$  is scanned within the fundamental domain  $\mathcal{D}$  and kept close to

the cusps, in the regions

$$|\text{Re}\,\tau| > \frac{1}{2} - 0.025\,,\qquad \text{Im}\,\tau < \sqrt{1 - (\text{Re}\,\tau)^2} + 0.05\,,$$
 (8.45)

in agreement with our goal.<sup>8</sup> For the left cusp, the region includes values of  $|\epsilon|$  as large as 0.1. A priori, no constraints are imposed on the ranges of superpotential parameters, i.e. they can be arbitrarily large or small. Hence, in this first step, we are not concerned with the particular normalisation of modular forms, which can be absorbed in the superpotential parameters. Additionally, these parameters can absorb the effects of canonically normalising the fields, due to the assumed minimal-form Kähler potential,

$$K(\tau, \overline{\tau}; \psi, \overline{\psi}) \supset -\Lambda_K^2 \log(2 \operatorname{Im} \tau) + \sum_{\psi \in \{Q_\alpha, u_\beta^c, d_{\beta'}^c\}} \frac{|\psi|^2}{(2 \operatorname{Im} \tau)^{k_\psi}},$$
(8.46)

with  $\Lambda_K$  having mass dimension one. Namely, fields are scaled as  $\psi \to \sqrt{(2 \operatorname{Im} \tau)^{k_{\psi}}} \psi$  to yield canonical kinetic terms. Mass matrices will be affected accordingly, with each contribution being scaled by a factor  $\sqrt{(2 \operatorname{Im} \tau)^{k_Y}}$ . Note that this factor depends only on the weight  $k_Y$  of the corresponding modular form and has been taken into account in the dictionary between the  $\alpha_i$  and  $\widetilde{\alpha}_i$  (i = 1, ..., 4) of Section 8.1.1. The impact of modular form and canonical field normalisations on fine-tuning will be discussed in Section 8.4.1.

In what follows, we present our numerical results, starting with the cases where gCP is imposed and  $\delta_{\text{CP}}$  is either absent from (Section 8.3.1) or present in (Section 8.3.2) the fit. Lifting gCP allows for 11-parameter phenomenological fits (Section 8.3.3) or 12-parameter gCP-consistent fits (Section 8.3.4). Finally, we consider fits with an additional modulus and gCP (Section 8.3.5). In the summary tables, 9+ indicates a value of  $\sqrt{\chi^2} > 9$ , while 5+ refers to values in the range  $5 < \sqrt{\chi^2} < 9$ . For fits with a minimum below  $5\sigma$ , the value of  $\sqrt{\chi^2}$  is given explicitly. As will be shown already in Section 8.3.2, a fit of the 10 quark observables is not possible within the 10-parameter models. Moreover, even in the presence of additional parameters, fitting the quark data in the vicinity of the cusps is not guaranteed.

#### 8.3.1 Fits without $\delta_{CP}$ in the Presence of gCP

We start by considering the minimal cases resulting from the imposition of a gCP symmetry, such that the complexity of the mass matrices may only originate from non-CP conserving values of the modulus, via the modular forms. It may be challenging to obtain sizeable CP violation in the vicinity of the cusps if  $\tau$  is the only source of CP violation (see also [296]). Therefore, we first exclude the CPV phase from the list of fit observables, checking if the models can reproduce the quark masses and mixing angles. As a result, fits near the left and right cusps are equivalent (see also the comment in Section 8.1).

Our results are summarised in Tables 8.5a and 8.5b for the cases where the left- or right-handed quarks are  $S_4'$  triplets, respectively. A value of  $N\sigma = \sqrt{\chi^2} = 0.0$  indicates that one can reproduce the central values for all the observables under consideration. As discussed in Sections 8.1.1 and 8.2, the matrices  $M_1$  and  $M_2$  are equivalent up to a redefinition of superpotential parameters. Hence, these cases

<sup>&</sup>lt;sup>8</sup>A model not fitting the quark data in these regions may yet be viable for other values of  $\tau \in \mathcal{D}$ .

$M_u$	$M_{1,2}$	$M_3$	$M_4$	$M_{5,6}$	$M_u$ $M_d$	$M_{1,2}^T$	$M_3^T$	$M_4^T$	$M_{5,6}^T$
$M_{1,2}$	0.0 9+	9+	9+	9+	$M_{1,2}^T$				
$M_3$	9+	0.0	0.0	9+		_			
	9+				$M_4^T$	0.0	_	1.0	_
$M_{5,6}$	9+	9+	9+	0.0	$M_{5,6}^T$	0.0	1.5	_	1.4
(8	a) Models	s with (	$Q \sim 3^*$		(1	<b>b)</b> Model	s with q	$q^c \sim oldsymbol{3}^*$	

**Table 8.5:** Values of  $\sqrt{\chi^2}$  for quark fits of 10-parameter (gCP) models, without  $\delta_{\text{CP}}$ , depending on which fields are taken as triplets of  $S_4'$ . Note that some pairs  $(M_u, M_d) = (M_i^T, M_j^T)$  are not allowed, as discussed in Section 8.1.2.

are grouped in the tables. The same goes for  $M_5$  and  $M_6$ . Recall that in the context of  $q^c \sim 3^*$  models only some combinations  $(M_i^T, M_j^T)$  are meaningful, cf. Section 8.1.2.

It is interesting to note that, among these 10-parameter models, some can easily fit quark masses and mixing while others cannot fit them at all (at  $9\sigma$  or worse). This can be understood by verifying that, for those cases, the CKM matrix approaches a non-viable form in the limit of vanishing  $|\epsilon|$ . In other words, the diagonalisation of the mass matrices requires permutations which do not cancel in the product defining the CKM matrix. This is not so for  $q^c \sim 3^*$  models, since the transpositions lead to democratic-like  $M_q M_q^{\dagger}$  matrices for both sectors, in the same limit.

Finally, we have verified that the CPV character of  $\tau$  is not relevant for the goodness of fit in these scenarios. Namely, we have checked that fits of masses and mixing are still possible, with the same  $\chi^2$  values, for CP-conserving values of  $\tau$ , i.e. imposing either Re  $\tau = \pm 1/2$  or  $|\tau|^2 = 1$  for the same value of  $|\epsilon|$  (but possibly different values of the other parameters).

## 8.3.2 Fits with $\delta_{CP}$ in the Presence of gCP

We now include the CPV phase in the list of fit observables. To be more precise, and in the context of this section alone, we consider  $J_{\text{CP}} = (2.31 \pm 0.57) \times 10^{-5}$ , with  $J_{\text{CP}} \equiv c_{12}c_{13}^2c_{23}s_{12}s_{13}s_{23}\sin\delta_{\text{CP}}$  ( $c_{ij} = \cos\theta_{ij}$ ,  $s_{ij} = \sin\theta_{ij}$ ), in the search for models with sufficient CP violation, since  $\delta_{\text{CP}}$  itself may not be a good indicator of the latter when mixing angles driven to very small values. By including a CPV observable in the fit, differences may arise depending on which cusp the modulus approaches. We thus analyse both cusps separately.

Our results are summarised in Tables 8.6a and 8.6b for the cases where the left- or right-handed quarks are  $S'_4$  triplets, respectively. As one may expect, results are globally worse in the presence of an extra constraint. Moreover, these results suggest that the proximity to an enhanced symmetry point (either  $\omega$  or  $\omega + 1$ ) places too big a strain on the models for them to be able to comply with all quark data below the  $4\sigma$  level. By comparing Tables 8.5 and 8.6, one sees that this failure is driven by the CPV observable.

$M_u$	$M_{1,2}$	$M_3$	$M_4$	$M_{5,6}$	$M_u$	$M_{1,2}^T$	$M_3^T$	$M_4^T$	$M_{5,6}^T$
$M_{1,2}$	4.1 9+	9+	9+	9+	$M_{1,2}^{T} \ M_{3}^{T} \ M_{4}^{T} \ M_{5,6}^{T}$	4.0	_	4.3	4.3
$M_3$	9+	4.1	4.1	9+	$M_3^T$	_	4.2	_	4.1
	9+				$M_4^T$	4.0	_	4.2	_
$M_{5,6}$	9+	9+	9+	4.1	$M_{5,6}^T$	4.0	4.3	_	4.3
(8	a) Models	s with (	$Q \sim 3^*$			b) Model			

**Table 8.6:** Values of  $\sqrt{\chi^2}$  for quark fits of 10-parameter (gCP) models, including  $\delta_{\text{CP}}$ , depending on which fields are taken as triplets of  $S_4'$ . All entries apply to both cusps.

To illustrate the strain placed on the models by the addition of the CPV observable to the fit, consider Fig. 8.1, where a no- $\delta_{\rm CP}$  fit point for the  $M_{u,d} \sim M_1$  model (black dot) is shown in the  $\tau$  plane. One may quantify the magnitude of CP violation through the value of  $J_{\rm CP}$  in this plane, by varying the value of  $\tau$  for this point while keeping the other parameters fixed. Note that this variation is done for illustrative purposes only, as it spoils the values of observables. One concludes that reaching the correct magnitude for  $J_{\rm CP}$  (green band) calls for relatively large values of  $|\epsilon|$ , i.e. seems incompatible with the required closeness to the cusp.

#### 8.3.3 Fits with 11 Parameters

So far, we have seen that the models of interest cannot comply with all quark data in the presence of a gCP symmetry. Lifting the assumption of gCP leads to new sources of complexity in the mass matrices, which may result in phenomenologically acceptable models. As discussed at the end of Section 8.1.2, these models in general will be described by 2 additional physical phases in the  $Q \sim 3^*$  case, namely the phases of the  $\alpha_4$  in the up and down sectors. We focus exclusively on this case in what follows, since the  $q^c \sim 3^*$  scenario brings about too many additional parameters (4 new phases).

We start by following a phenomenological approach, allowing only one of the  $\alpha_4$  parameters to be complex, in turn, for a total of 11 parameters. Our results are summarised in Table 8.7. They are, in practice, independent of the cusp (left vs. right) and of which sector (up vs. down) contains the phenomenological phase. By lifting gCP in this explicit way — such that  $\tau$  is not the only source of CP violation — models can be found which fit all the quark data. Nonetheless, note that the presence of more degrees of freedom than observables is not a sufficient condition for the model to be viable in the vicinity of the cusps (cf. also the discussion in Section 8.3.1).

#### 8.3.4 12-Parameter Fits without gCP

Consistently allowing both  $\alpha_4$  to be complex results in a total of 12 parameters but leads to no apparent qualitative improvement with respect to the phenomenological case. In particular, the results

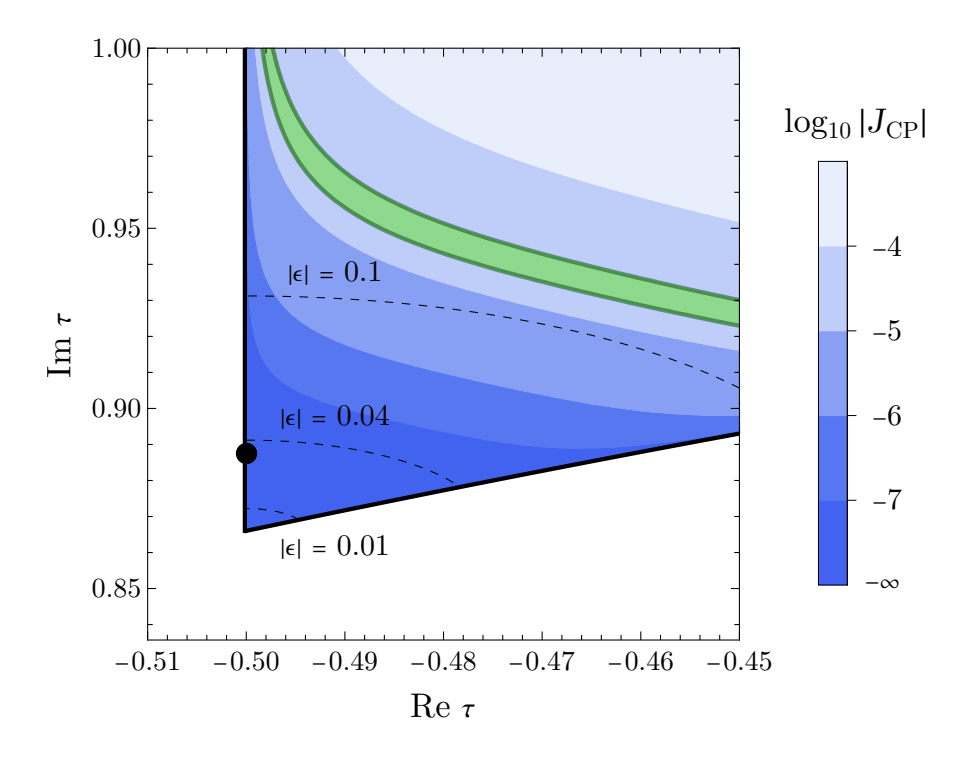


Figure 8.1: Magnitude of CP violation for different values of the modulus  $\tau$  in the vicinity of the left cusp and for a fixed set of superpotential parameters. The model considered corresponds to  $M_{u,d} \sim M_1$  and can fit quark masses and mixing angles — but not  $\delta_{\rm CP}$  — at the value of  $\tau$  marked by the black dot. The green band represents the  $1\sigma$ -allowed range for the  $J_{\rm CP}$  invariant.

as shown in Table 8.7 apply also to this general case.

It may be possible to reduce the number of degrees of freedom if, for instance, the value of the modulus is selected by a dynamical principle in a top-down approach. In Ref. [320], simple modular-invariant supergravity-motivated potentials were considered and global CP-breaking minima were found in the vicinities of the cusps. The selected values of  $\tau$  follow a series,

$$\tau \simeq \mp 0.484 + 0.884 i, \ \mp 0.492 + 0.875 i, \ \mp 0.495 + 0.872 i, \dots,$$
corresponding to  $|\epsilon(\tau)| \simeq 0.04, \ 0.02, \ 0.01, \dots,$ 

$$(8.47)$$

which approaches the cusps. The goodness of fit is in general expected to decrease. We find that for the first of the values in Eq. (8.47), the viable fits remain acceptable, while this ceases to be the case as one gets closer to the cusps. The corresponding results of these top-down inspired 10-parameter models are summarised in Tables 8.8a and 8.8b.

## 8.3.5 Fits with Two Moduli in the Presence of gCP

Finally, we consider a phenomenologically-motivated analysis where we allow for two distinct moduli to co-exist,  $\tau_u$  coupling to up-type quarks and  $\tau_d$  coupling to down-type quarks. Such a situation may arise, for instance, in the context of symplectic modular invariance, see [393]. Since now we have an extra complex parameter, gCP is imposed to keep the total number of parameters as small as possible: 12 for the minimal quark mass matrices identified. The presence of an extra modulus allows for an independent

$M_u$ $M_d$	$M_{1,2}$	$M_3$	$M_4$	$M_{5,6}$
$M_{1,2}$	0.0	9+	9+	9+
$M_3$	9+	0.0	0.0	9+
$M_4$	9+	0.0	0.0	9+
$M_{5,6}$	9+	9+	9+	0.0

**Table 8.7:** Values of  $\sqrt{\chi^2}$  for quark fits of 11-parameter (phenomenological) and 12-parameter (consistent) models with  $Q \sim \mathbf{3}^*$ . These results apply to both cusps and are independent of which sector holds the new phase.

$M_u$	$M_{1,2}$	$M_3$	$M_4$	$M_{5,6}$	$M_u$	$M_{1,2}$	$M_3$	$M_4$	$M_{5,6}$
$M_{1,2}$	0.1	9+	9+	9+	$M_{1,2}$ $M_3$	5+	9+	9+	9+
$M_3$	9+	2.1	2.1	9+	$M_3$	9+	5+	5+	9+
$M_4$	9+	2.1	2.1	9+	$M_4$	9+	5+	5+	9+
$M_{5,6}$	9+	9+	9+	2.1	$M_{5,6}$	9+	9+	9+	5+
(8	$\mathbf{a)} \ \tau = \mp 0$	0.484 +	0.884 i		(t	$\tau = \mp 0$	0.492 +	0.875 i	

**Table 8.8:** Values of  $\sqrt{\chi^2}$  for quark fits of models in the absence of gCP, with  $Q \sim 3^*$  and fixing  $\tau$  to top-down selected values (10 free parameters). These results apply independently of the cusp considered.

source of CP violation in this scenario. Moreover, assuming that both moduli are near a cusp allows to decouple the explanation of quark mass hierarchies in the up and down sectors, which are now each controlled by their own small parameter,  $|\epsilon_u|$  and  $|\epsilon_d|$ , respectively.<sup>9</sup>

Our results are summarised in Tables 8.9a and 8.9b. It is interesting to note that some of the models can fit all the quark data at less than  $3\sigma$ , including the CPV phase  $\delta_{\rm CP}$ , with the moduli being the only source of CP violation (all other parameters are real). Results vary depending on which cusps (left vs. right)  $\tau_u$  and  $\tau_d$  approach. There are four options for each of the considered cases ( $Q \sim 3^*$  vs.  $q^c \sim 3^*$ ). Overall, one notices that fits are typically better whenever both moduli are in the vicinity of the same cusp.

## 8.4 A Closer Look at Natural Hierarchies

In the previous section we checked whether the proposed quark models could fit the known quark data for values of  $\tau$  close to the cusps. Even if a good fit is possible, it may be that the proximity of  $\tau$  to

<sup>&</sup>lt;sup>9</sup>Indeed, it is difficult to fit both quark sectors with a structure of the type  $1 : |\epsilon| : |\epsilon|^2$ ,  $\mathcal{O}(1)$  coefficients, and a common value of  $|\epsilon|$ .

$M_u$ $M_d$	$M_{1,2}$	$M_3$	$M_4$	$M_{5,6}$
$M_{1,2}$	0.0	9+	9+	9+
$M_3$	9+	0.0	0.0	9+
$M_4$	9+	0.0	0.0	9+
$M_{5,6}$	9+	9+	9+	0.0

(a) Models with  $Q \sim \mathbf{3}^*$ 

$M_u$ $M_d$	$M_{1,2}^T$	$M_3^T$	$M_4^T$	$M^T_{5,6}$
$M_{1,2}^T$	[0.0, 0.4]	_	[0.0, 2.8]	[0.0, 0.7]
$M_3^T$	_	$[0.0, 3.4]^*$	_	$[1.1, 3.4]^*$
$M_4^T$	$[1.3, 4.5]^{***}$	_	[0.1, 3.0]	_
$M_{5,6}^T$	[0.0, 1.4]	$[0.0, 3.4]^*$	_	$[0.0, 3.3]^{**}$
$> 3\sigma$ onl	y if: *cusps differ	$^{**}(\tau_u,\tau_d)\simeq 0$	$(\omega+1,\omega),$ *** $(\tau$	$(\tau_u, \tau_d) \simeq (\omega, \omega).$

(b) Models with  $q^c \sim 3^*$ 

**Table 8.9:** Values and ranges of  $\sqrt{\chi^2}$  for quark fits of 2-moduli 12-parameter (gCP) models, depending on which fields are taken as triplets of  $S_4'$ . In Table 8.9a, fits below  $9\sigma$  are only possible for both moduli near the same cusp. In Table 8.9b, entries show the minimum and maximum fit  $\sqrt{\chi^2}$  across the 4 different possibilities  $(\tau_u, \tau_d) \simeq (\omega, \omega)$ ,  $(\omega, \omega+1)$ ,  $(\omega+1, \omega)$ ,  $(\omega+1, \omega+1)$ .

a point of residual symmetry is not the main driver behind quark mass hierarchies, since superpotential parameters were not constrained.

In what follows, we analyse a particular model in more detail, looking into potential sources of finetuning, namely i) hierarchies between superpotential parameters, which depend heavily on normalisation choices, and ii) cancellations between superpotential parameters. The latter can be analysed e.g. via a Barbieri-Giudice (BG) measure of fine-tuning [432] (discussed below in Eq. (8.49)). We perform this analysis for the model with both  $M_u$  and  $M_d$  taking the form  $M_1$ , in the vicinity of the left cusp  $\omega$ . In what follows, we still denote the superpotential constants as  $\alpha_i$  in the up sector, while for the down sector we use the notation  $\beta_i$  instead. Our results are summarised in Table 8.10.

We consider benchmarks for the following five cases:

- gCP (masses): gCP is imposed, but only mass ratios are considered in the fit,
- gCP (all): gCP is imposed (all observables are considered in the fit),
- pheno phase: a phenomenological phase is added to the up-quark sector,
- no gCP: a fit of the model in the absence of gCP (two new phases), and
- two moduli: a fit of the model with gCP imposed, in the presence of an extra modulus  $(\tau_{u,d} = \tau_{1,2})$ .

As anticipated from the previous discussion, in the presence of gCP and with a single modulus, one is able to fit quark mass ratios but not all quark data satisfactorily. In particular, the observed strength of CP violation cannot be accommodated. This can be remedied by introducing a single (phenomenological) phase, e.g., for  $\alpha_4$  in the up sector, as shown in the third data column of Table 8.10. It follows that a fit is also possible in the absence of gCP, with independent phases for  $\alpha_4$  and  $\beta_4$ , in the up and down sectors respectively (see the fourth data column). Finally, in the presence of gCP, a fit of all quark data — including CP violation — is possible with two moduli, one for each sector (recall the results of Section 8.3.5).

## 8.4.1 Hierarchical Parameters

If the proximity to the cusp, i.e. the smallness of  $|\epsilon|$ , is to explain quark mass hierarchies, one expects superpotential parameters to be of the same order, within each sector. However, as discussed in Section 8.1.1, these parameters may absorb the different choices of modular form normalisations. Therefore, we report the (ratios between) products of superpotential parameters by the Euclidean norm of the corresponding modular form,  $\alpha_i ||Y_i||$ . These products are what (partly) determines the magnitude of the columns of mass matrices. Requiring superpotential parameters to be of the same order then means that the aforementioned ratios should be  $\mathcal{O}(1)$ . If one chooses to normalise the forms using the Euclidean norm at the fit value of the modulus (moduli), then all  $||Y_i|| = 1$  in Table 8.10.

The magnitude of the columns of mass matrices is also affected by the canonical normalisation of fields. As mentioned in Section 8.3, bringing the kinetic terms to a canonical form results in a rescaling

of each contribution to the mass matrix by a factor of  $\sqrt{(2 \text{Im } \tau)^{k_{Y_i}}}$ . Recall that the reported  $\alpha_i$  and  $\beta_i$  are defined via Eq. (8.13), prior to taking into account this effect. These additional factors are tied to the specificities of the model and may play a role in naturally enhancing or suppressing mass hierarchies.

As noted in the previous sections, it is quite restrictive to use a single modulus and, correspondingly, a single value of  $|\epsilon|$ , common to both quark sectors. Some extra hierarchy in the parameters may be necessary to accommodate all mass ratios, as evidenced by the "gCP (masses)" benchmark (first data column of Table 8.10). Here, one can check that  $\tilde{\alpha}_4 \gg \tilde{\alpha}_2, \tilde{\alpha}_3$ , resulting in an extra suppression of mass ratios in the up sector, now controlled by powers of  $|\epsilon/\tilde{\alpha}_4|$ , as anticipated in Section 8.1.1. By adding mixing and CPV constraints to the fit, the limit of interest becomes less transparent, as one may be driven to regions of parameter space with small  $\tilde{\alpha}_2$  ("gCP (masses)" benchmark, second column) or small  $\tilde{\alpha}_1$  ("pheno phase" and "no gCP" benchmarks, third and fourth columns).

#### 8.4.2 The Role of $|\epsilon|$ and Possible Cancellations

The above single-modulus benchmarks feature values of  $|\epsilon| \sim 0.03 - 0.05$ , whereas for the two-moduli case one can fit the data with  $|\epsilon_1| \sim 0.01$  and  $\epsilon_2 \sim 0.03$ . A simple way to inspect how hierarchies are controlled by the appropriate powers of  $|\epsilon|$  is to look into the ratios

$$(m_c/m_t)/|\epsilon|, \quad (m_u/m_t)/|\epsilon|^2, \quad (m_s/m_b)/|\epsilon|, \quad (m_d/m_b)/|\epsilon|^2,$$
 (8.48)

which we report in Table 8.10 for each benchmark. These ratios are non-linear functions of the parameters, encoding also the effects of canonical field normalisation, cf. Eqs. (8.16) to (8.18). One expects these ratios to be  $\mathcal{O}(1)$  if the proximity to the cusp is to single-handedly explain the quark hierarchies. The fact that these values are relatively small in the up sector for the single-modulus benchmarks shows that either hierarchies or cancellations of superpotential constants, together with the effect of canonical field rescalings, play an important role in driving the up-quark mass hierarchies. An exception is the two-moduli case, where the values of these ratios can be milder, thanks to the freedom in varying separately  $\tau_u$  and  $\tau_d$ .

One way to gauge how reliant a model is on parameter-driven cancellations is to compute the BG measure of fine-tuning [432], which allows one to identify regions of parameter space where small changes lead to large deviations in model predictions. We employ the definition

$$\max BG \frac{m_i}{m_j} \equiv \max_{\substack{p = \alpha, \beta \\ k = 2, 3, 4}} \left| \frac{\partial \ln m_i / m_j}{\partial \ln p_k / p_1} \right|, \tag{8.49}$$

singling out the largest effect on mass ratios across superpotential parameters. Note that this measure is not suitable for angular variables. BG values are reported in Table 8.10 for the benchmarks above. Overall, one finds acceptable values with the exception perhaps of the two-moduli benchmark, featuring an apparently tuned ratio  $m_c/m_t$ . We have checked that this effect is driven by quark mixing and CP

<sup>&</sup>lt;sup>10</sup>In the two-moduli case, we take these factors to be  $\sqrt{(2 \operatorname{Im} \tau_1)^{k_{Y_i}}(2 \operatorname{Im} \tau_2)^{k_{Y_i}}}$ , inspired by the diagonal ( $\tau_3 = 0$ ) scenario in [393]. Note that, in the absence of a complete model, this is a purely heuristic choice.

violation, to the extent that a fit of quark mass ratios alone is possible in this scenario, for similar values of  $|\epsilon_u|$  and  $|\epsilon_d|$ , with all BG  $\sim 1$ , with  $\mathcal{O}(0.1-1)$  ratios of  $\alpha_i ||Y_i||$ , and with the quantities in Eq. (8.48) within the interval [0.2, 0.7].

## 8.5 Discussion

Obtaining an economical and fine-tuning-free description of the quark sector — *i.e.* of quark mass hierarchies, mixing and CP violation — within the modular flavour approach still remains a serious challenge. In this chapter, we have spelled out the challenges for building viable and minimal  $S'_4$  modular-invariant quark models where the proximity to the point of residual  $\mathbb{Z}_3^{ST}$  symmetry plays a role in determining mass hierarchies, via powers of a small parameter  $|\epsilon|$  [158].

We argue that, in a bottom-up approach, the absolute normalisations of the modular forms are arbitrary and should not determine hierarchies.<sup>11</sup> These can instead follow from the relative magnitudes of modular multiplet components. We thus identify four minimal mass matrix patterns,  $M_{1,2}$ ,  $M_3$ ,  $M_4$  and  $M_{5,6}$ , where the quark mass hierarchies may stem from the proximity of  $\tau$  to the cusp (the smallness of  $|\epsilon|$ ). These involve at most four superpotential parameters and do not lead to massless fermions. Approximate analytical expressions have been derived for the quark masses and mass ratios, for each of these structures. These results are directly applicable to other fermions, e.g. the charged lepton sector.

Two main hurdles to overcome in this class of models are i) the different hierarchies observed in the up and down sectors, which call for different values of  $|\epsilon|$ , and ii) the suppression of CP violation whenever  $\tau$  is the only source of CP symmetry breaking, already alluded to in Ref. [296]. The former indicates that, to explain quark mass ratios in the single-modulus case, one may need to tolerate some hierarchy among superpotential couplings. As for the latter, we find that the observed strength of quark CP violation cannot be adequately fitted in the minimal 10-parameter scenarios, featuring a gCP symmetry. Instead, we are able to fit quark data with 11 parameters in a phenomenological approach, by explicitly adding a complex phase in one of the sectors. The consistent lifting of the gCP symmetry leads to models with 12 parameters — one less than previous constructions in the literature — which can also fit quark data. Note that having as many parameters as observables does not automatically guarantee a viable fit (see e.g. Table 8.8b). Curiously, a 12-parameter fit including the correct amount of CP violation can be achieved near the cusp and in the presence of gCP, provided different moduli are responsible for each of the quark sectors.

In summary, these results illustrate how the demand for explanatory power and for the absence of different kinds of tuning may restrict models of flavour based on modular invariance. It is hoped that these requirements select only a few viable models that provide a clear understanding of the puzzling flavour structures of fundamental fermions.

<sup>&</sup>lt;sup>11</sup>See ref. [291] for a recent discussion on the subject.

	gCP (masses)	gCP (all)	pheno phase	no gCP	two moduli
$\operatorname{Re}  au_1$	-0.4772	-0.4823	-0.4992	-0.4978	-0.4969
$\operatorname{Im} \tau_1$	0.8861	0.8784	0.8852	0.8850	0.8692
$\operatorname{Re}  au_2$	_	_	_	-	-0.4939
$\operatorname{Im}\tau_2$	_	_	_	_	0.8856
$ \epsilon_1 $	0.0486	0.0348	0.0306	0.0306	0.0072
$ \epsilon_2 $	-	-	-	-	0.0328
$\frac{\alpha_2 \ Y_{\mathbf{3'}}^{(4)}\ }{\alpha_1 \ Y_{\widehat{3}_{(7)}}^{(1)}\ }$	2.725	0.009	70.93	35.79	0.329
$\frac{\alpha_3 \ Y_{3',1}^{(i)}\ }{\alpha_1 \ Y_{\widehat{3}}^{(1)}\ }$	2.128	2.975	214.0	54.52	4.341
$\frac{\alpha_4 \ Y_{3',2}^{(7)}\ }{\alpha_1 \ Y_{3'}^{(1)}\ }$	41.86	3.979	$211.0e^{0.890i}$	$141.5  e^{-0.356  i}$	2.555
$\frac{\beta_2 \ Y_{3'}^{(4)}\ }{\beta_1 \ Y_{\widehat{3}}^{(1)}\ }$	3.001	5.700	7.689	5.360	2.806
$\frac{\beta_3 \ Y_{3',1}^{(7)}\ }{\beta_1 \ Y_{\widehat{3}}^{(1)}\ }$	6.261	0.729	2.261	1.098	0.578
$\frac{\beta_4 \ Y_{3',2}^{(7)}\ }{\beta_1 \ Y_{\widehat{3}}^{(1)}\ }$	1.174	1.433	1.043	$1.337  e^{0.676  i}$	0.258
$(m_u/m_c)/10^{-3}$	2.042	1.897	2.040	2.042	2.041
$(m_c/m_t) / 10^{-3}$	2.678	1.824	2.678	2.678	2.678
$(m_d/m_s)/10^{-2}$	5.053	5.059	5.053	5.053	5.052
$(m_s/m_b) / 10^{-2}$	1.370	1.390	1.370	1.370	1.370
$ heta_{12}\left( ^{\circ} ight)$	15.42	13.05	13.03	13.03	13.03
$ heta_{23}\left( ^{\circ} ight)$	10.00	$4.08 \times 10^{-5}$	2.055	2.054	2.054
$ heta_{13}\left( ^{\circ} ight)$	1.226	0.208	0.180	0.180	0.180
$\delta_{\mathrm{CP}}\left(^{\circ} ight)$	0.0026	69.24	69.21	69.21	69.21
$J_{\rm CP} / 10^{-5}$	0.0042	$5.33 \times 10^{-5}$	2.314	2.313	2.313
$\left(m_c/m_t\right)/\left \epsilon\right $	0.055	0.052	0.088	0.088	0.371
$(m_u/m_t) /  \epsilon ^2$	0.002	0.003	0.006	0.006	0.105
$\left(m_s/m_b\right)/\left \epsilon\right $	0.282	0.400	0.448	0.448	0.418
$\left(m_d/m_b\right)/\left \epsilon\right ^2$	0.293	0.582	0.739	0.739	0.643
$\max BG m_c/m_t$	0.998	1.144	0.988	1.022	4.084
$\max  \mathrm{BG}   m_u/m_t$	2.004	1.000	0.972	1.862	2.173
$\max  \mathrm{BG}   m_s/m_b$	0.841	1.229	1.089	0.759	1.167
$\max\mathrm{BG}\ m_d/m_b$	1.018	2.096	1.098	0.959	1.211
$N\sigma$ (masses)	0.0	3.4	0.0	0.0	0.0
$N\sigma$ (angles)	51.8	5.5	0.0	0.0	0.0
$N\sigma~(\delta_{ m CP})$	11.2	0.0	0.0	0.0	0.0
$N\sigma$ (total)	52.9	6.4	0.0	0.0	0.0

**Table 8.10:** Fit benchmarks (see text) for the model with both  $M_{u,d} \sim M_1$ . Here,  $\tau_1 = \tau$  and  $\epsilon_1 = \tau$ , while  $\tau_{1,2} = \tau_{u,d}$  and  $\epsilon_{1,2} = \epsilon_{u,d}$  in the two-moduli case. All moduli are in the vicinity of the left cusp.

## Conclusions

Seemingly mocking the words of Isidor Isaac Rabi - "Who ordered that?", the puzzle of flavour remains an open question of particle physics, without an ultimate solution in sight. A principle akin to the gauge principle, where the origin of flavour could be traced to properties of a symmetry, would be a godsend. For decades now, a lot of work has been dedicated in attempts to see if and how such a principle could comply with Nature.

In this thesis, we have tackled different proposals for solutions to the flavour puzzle. While we did not exhaust all different avenues which have been proposed in the literature over the past decades, we hope these studies have contributed to the common effort in unravelling the underlying nature of flavour. The main conclusions can be summarised as follows.

#### Democratic 3HDMs

We dedicated Chapter 2 to the study of democratic 3HDMs. After decades of increasingly more extensive studies of the 2HDMs, recent years have seen the community turn their attention to 3HDMs. Democratic 3HDMs arise as an interesting class of 3HDMs, since they comprise the only flavour-universal NFC nHDMs which require at least 3 Higgs doublets, and thus cannot be accommodated in a 2HDM. In this sense, they provide the perfect test grounds to see how the phenomenology of increasingly more complex models can differ from the well-known results of the 2HDMs. To this end, we explored various aspects of democratic 3HDMs. First, we note that the custodial symmetry in the scalar potential is an automatic feature of the SM, but which does not need to be respected in nHDMs. On the other hand, experimental measurements hint that this symmetry is (mostly) respected by Nature, making it desirable for BSM models to respect it, lest they run into conflict with experiment. Hence, we study the implementation of custodial symmetry in nHDMs, in such a way that we can provide a simple, easily implementable, and, most importantly, basis-independent condition for custodial symmetry to hold  $M_C^2 = M_P^2$ .

Armed with this knowledge, we set out to see how the additional degrees of freedom of the 3HDM can help alleviate some of the bounds that flavour observables place on 2HDMs. We explore the similarity between a parametric region of democratic 3HDMs, and the well-known type-II 2HDM, to the sense that, in this region, the democratic 3HDM can be seen as a damped type-II 2HDM. This dampening of the interaction strengths allows for a lowering of the stringent bounds that charged-scalars face in the type-II 2HDM, especially in the case of a partial decoupling of one of the nonstandard set of scalars of the 3HDM. Interestingly, this regime of partial decoupling is not essential to evade the experimental bounds on neutral meson oscillations and of  $b \to s\gamma$ , and we find that it is also possible for both nonstandard charged-scalars to be relatively light.

Lastly, we investigate extremal violations of the alignment limit, where instead of requiring the SM-like Higgs couplings to fermions to be exactly (or close to) the SM-values, we exploit the fact that experiments are mildly insensitive to the sign of these couplings, and require some to have an opposite sign. Also here, the democratic 3HDMs are interesting in the fact that all different possibilities for wrong-sign limits in the different types of NFC 2HDMs can be accommodated in different parametric regions of democratic 3HDMs. It is interesting to note that, unlike the cases of 2HDMs, it is possible to find wrong-sign limits in democratic 3HDMs which do not require large discrepancies between (all) the different vevs.

#### Discrete Symmetries and their Soft-Breaking

The study of non-Abelian groups as flavour symmetries is enticing. Not only does the observed pattern of neutrino oscillations hints at a non-Abelian structure, but the added structure that these groups introduce in the theory is highly restrictive, allowing for the possibility of very predictive models. Unfortunately, these constraints lead to phenomenological implications which can, more often than not, run into conflict with experiment. Introducing an explicit breaking of the underlying symmetry would defeat the original purpose of introducing the flavour symmetry itself, albeit could help evade the problematic phenomenological implications of the symmetry. An interesting middle ground is the introduction of soft-breaking terms in the theory. Even while keeping agnostic of their origin, these terms do not respect the symmetry (they are not invariant under the group transformation), but are not able to generate couplings of lower mass dimension which were forbidden by the symmetry (akin to the introduction of SSB). In this way, it is possible to alleviate the restrictions on the scalar spectrum or the vev alignment, while keeping the quartic terms (for example) symmetry protected. On the other hand, if we include all possible soft-breaking terms, we reintroduce many parameters back into the theory, which we were actively trying to avoid by including non-Abelian symmetries. As such, a study to show how the different directions in the soft-breaking space are linked with different phenomenological implications is missing.

We dedicate Chapter 3 to a first step in classifying the different directions in which the introduction of soft-breaking parameters impacts the scalar sector of the theory. Hopefully, in time, this study can be expanded, such that a guiding principle to the inclusion of soft-breaking terms fully arises. It is interesting to note that, for a  $\Sigma(36)$ -symmetric 3HDM, which generally has 9 soft-breaking parameters, 5 of these preserve the vacuum alignment. Remarkably, by studying this subset of parameters, we found that the softly-broken model, despite not exhibiting any exact symmetry, inherits structural properties from the parent model.

While non-Abelian symmetries were mostly motivated by the neutrino mixing pattern, this does not

entail that they are completely without purpose for the quark sector. In Chapter 4, we present a model which makes use of  $D_4$  to relegate almost entirely the quark mixing pattern to scalar dynamics, instead of relying on the freedom of the Yukawa sector to do such. In this way, the CKM and the scalar sector are intrinsically linked, and the experimental knowledge of the quark mixing pattern could, in principle, constraint the scalar dynamics. Indeed, contrary to the SM where the hierarchies of the quark masses and those of the quark mixing are completely disentangled, here they are linked, and caused by large hierarchies between the vevs of different scalars. This feature is similar to what is usually found in Froggatt-Nielsen constructions. However, unlike those models, in this model all of the scalar vevs lie at the EW scale.

#### Other Sources of Flavour

Most of the studies on the flavour puzzle have focused on the case where the flavour symmetry commutes with the gauge symmetry. However, it is quite interesting to note that the gauge structure itself can be a source of relations between the Yukawa coefficients of different sectors (or even between generations). These constructions have received considerably less attention by part of the community. In Chapter 5, we take the example of a 2HDM, and employ flavour symmetries which do not commute with the gauge structure (namely, they're broken by the hypercharge) to arrive at two different 2HDMs which, by virtue of the flavour symmetries connecting fields across hypercharges, we dub crossed-2HDMs (x2HDMs). The most interesting aspect of these models is that they are extensions of BGL-type constructions, where the FCNCs are fully controlled by the LH and RH quark mixing matrices (whereas in BGL constructions, only the LH mixing is physical). By virtue of this, compliance with flavour data can lead to precise expectations for the decays of the nonstandard scalars. Ultimately, it would be desirable to discover the covering theories of these models, such that these relations would be entirely imposed by the gauge structure of the model. The x2HDM of the first type has a well-known covering theory, which is the LRSM. In this way, it is a low-energy avatar of the LRSM, and the phenomenological studies can be complemented by new processes due to the extended gauge structure, to further constraint the parametric space, and make the estimations for the nonstandard decays more precise. On the other hand, the covering theory which leads to the x2HDM of the second type still remains elusive. Interestingly, the FCNCs in this model are independent of the ratio of the vevs, leading to a more restrictive scenario, and thus this model could be more easily falsified in case new decay channels were discovered.

#### Modular Symmetries

A new avenue to tackle the flavour puzzle has emerged recently - modular symmetries. Being a recent proposal, the field is still in its infancy, but the advances are quite fast-paced. We focus on two classes of models which employ modular symmetries. First, we investigate the idea of having multiple modular symmetries which are broken, via the SSB of flavons, to a diagonal modular group. The advantage of this type of construction is that the full domain of the modular symmetry (the quotient group  $\Gamma_N$ ) becomes relevant. In turn, this allows us to make use of the full list of residual symmetries to arrive at the desired mixing patterns. Given the relevance of the residual symmetries for these models, we dedicate Chapter 6

to present a methodology to find a full list of stabilisers for a given  $\Gamma_N$ , and show the ensuing list of these points for these symmetries, with  $N \leq 5$ .

Afterwards, we leverage these fixed points to construct a modular version of the Littlest seesaw, which makes use of a constrained sequential dominance framework to arrive at a highly predictive scenario for the neutrino sector. This is the focus of Chapter 7. We complement this construction by presenting additional constructions, which not only feature the CSD( $1 \pm \sqrt{6}$ ) framework for neutrinos (made possible with modular symmetries), but which also leverage the weights of modular invariant theories to provide a FN-type construction to explain the charged-lepton hierarchies, without the need of explicitly including the  $U(1)_{\rm FN}$  symmetry - the weighton mechanism. We then extend the construction to include quarks. Aiming to connect the quark and leptonic sectors, we extend the gauge structure to an SU(5) GUT, such that the texture zeroes are shared between the charged-lepton and down-quark sectors, up to transposition. Interestingly, we can exploit this connection to minimize the impact the off-diagonal terms have on the neutrino mixing (effectively preserving the findings of the previous model), while still providing sizeable contributions to the quark mixing, by having these matrices to be lower and upper triangular, respectively. The SU(5) extension presented includes the weighton mechanism from the start, further providing a connection between the mass and mixing hierarchies of the quarks, as well as an explanation for the hierarchies of the charged-lepton masses.

Finally, we explore another possibility for a natural explanation of the quark hierarchies. Making use of a single modular symmetry, only the fundamental domain is relevant, and, as a consequence, only three fixed points exist. An enticing proposal is that the hierarchies of the fermions can be related to a proximity to these fixed points, where the deviation of the modulus from these points effectively acts as a spurion. Depending on the fixed points (more accurately, on the preserved subgroup of each stabiliser), the fermionic masses have well-defined behaviours, such that the hierarchical nature of the masses appears as powers of the spurion. Although promising models for leptons exist, the application of this idea to quarks still remains elusive. We dedicated Chapter 8 to an comprehensive study of all possible predictive models which may lead to natural quark hierarchical masses, in  $\Gamma'_4$  models near  $\tau = \omega$ .

The flavour puzzle stands out as a tantalizing taunt, simultaneously mocking our best efforts to make sense of it, all the while alluring us with promising solutions. This work represents, at most, a small droplet in the quest to understand if there is any symmetry principle for the flavour puzzle. In the end, only time and a communal effort will tell if such a principle exists, or if this is all the ramblings of many a madman.



# Democratic 3HDMs: Custodial Symmetry and Flavour Observables

## A.1 Brief Note on SU(2) Triplets

A real SU(2) triplet in the Cartesian basis is expressed as follows:

$$\mathbf{A}_{\mathrm{Car}} = \begin{pmatrix} A_1 \\ A_2 \\ A_3 \end{pmatrix} \tag{A.1}$$

The generators of SU(2) in this basis are given by

$$T_{1} = \begin{pmatrix} 0 & 0 & 0 \\ 0 & 0 & -i \\ 0 & i & 0 \end{pmatrix}, \quad T_{2} = \begin{pmatrix} 0 & 0 & i \\ 0 & 0 & 0 \\ -i & 0 & 0 \end{pmatrix}, \quad T_{3} = \begin{pmatrix} 0 & -i & 0 \\ i & 0 & 0 \\ 0 & 0 & 0 \end{pmatrix}. \tag{A.2}$$

which make the transformation real. Now we want to migrate to a basis where  $T_3$  is diagonal. We will call this the spherical basis and the SU(2) triplet in this basis will be denoted by  $\mathbf{A}_{\mathrm{Sph}}$ . We note that the unitary matrix

$$\mathcal{U} = \frac{1}{\sqrt{2}} \begin{pmatrix} -1 & i & 0\\ 0 & 0 & \sqrt{2}\\ 1 & i & 0 \end{pmatrix}, \tag{A.3}$$

diagonalizes  $T_3$  as follows

$$\mathcal{U} \cdot T_3 \cdot \mathcal{U}^{\dagger} = \begin{pmatrix} 1 & 0 & 0 \\ 0 & 0 & 0 \\ 0 & 0 & -1 \end{pmatrix} = T_3'. \tag{A.4}$$

This implies that  $\mathbf{A}_{\mathrm{Sph}}$  will be related to  $\mathbf{A}_{\mathrm{Car}}$  via the following relation

$$\mathbf{A}_{Sph} = \mathcal{U}\mathbf{A}_{Car} = \begin{pmatrix} \frac{1}{\sqrt{2}}(-A_1 + iA_2) \\ A_3 \\ \frac{1}{\sqrt{2}}(A_1 + iA_2) \end{pmatrix}. \tag{A.5}$$

where we have used Eq. (A.1). Now let us define

$$A_{\pm} = \frac{1}{\sqrt{2}} (A_1 \mp iA_2), \tag{A.6}$$

where  $A_{+}$  and  $A_{-}$  are implicitly understood to be the complex conjugates of each other. In terms of these we can write the SU(2) triplet in the spherical basis as

$$A_{\rm Sph} = \begin{pmatrix} -A_+ \\ A_3 \\ A_- \end{pmatrix}. \tag{A.7}$$

Thus, the SU(2) invariant combination of two triplets, in these two bases, will be given by

$$\mathbf{A} \cdot \mathbf{B} = A_1 B_1 + A_2 B_2 + A_3 B_3 = A_+ B_- + A_- B_+ + A_3 B_3. \tag{A.8}$$

In a similar manner, the SU(2) invariant combination of three triplets is expressed as

$$(\mathbf{A} \times \mathbf{B}) \cdot \mathbf{C} = (A_2 B_3 - B_2 A_3) C_1 + (A_3 B_1 - B_3 A_1) C_2 + (A_1 B_2 - B_1 A_2) C_3$$
$$= i [A_3 (B_- C_+ - C_- B_+) + B_3 (C_- A_+ - A_- C_+) + C_3 (A_- B_+ - B_- A_+)] . \quad (A.9)$$

## A.2 Custodially Invariant Scalar Potential

In this Appendix, we try to enumerate the terms in the scalar potential of a CS-invariant nHDM. Since we have doublets only, the renormalizable scalar potential can contain only quadratic and quartic terms.

In n doublets, there are 4n real fields. After the symmetry breaking, there will be n triplets of the CS, including one that contains the unphysical Goldstone modes. In addition, there will be n CS singlets, composed by the tree real parts of the neutral components of  $\phi_k$ . It is then easy to see that

$$\phi_k^{\dagger} \phi_k = \frac{1}{2} \mathbf{T}_k \cdot \mathbf{T}_k + \text{CS singlets},$$
 (A.10a)

$$\phi_j^{\dagger} \phi_k + \phi_k^{\dagger} \phi_j = \mathbf{T}_j \cdot \mathbf{T}_k + \text{CS singlets},$$
 (A.10b)

with  $j \neq k$ . These are the quadratic forms which are CS invariant [168, 172, 174]. The total number of terms of the first kind is n, and of the second kind is  $\frac{1}{2}n(n-1)$ , making a total of  $\frac{1}{2}n(n+1)$ , which is also exactly the number of different quadratic terms of the form  $\mathbf{T}_j \cdot \mathbf{T}_k$  that we can get, with unrestricted j and k. In fact, if we insist on only real parameters in the scalar potential, there is no additional restriction arising from the CS: the terms shown in Eq. (A.10) are the only ones that are Hermitian and gauge invariant.

A large subset of the quartic CS invariants can be constructed as combinations of the quadratics. We can enumerate these kinds of terms as follows:

$$(\phi_i^{\dagger}\phi_i)^2$$
 : :  $n \text{ terms},$  (A.11a)

$$(\phi_i^{\dagger}\phi_i)(\phi_i^{\dagger}\phi_j)$$
 :  $(i \neq j)$ :  $N \text{ terms},$  (A.11b)

$$(\phi_i^{\dagger}\phi_i)^2 \qquad : : \qquad n \text{ terms}, \tag{A.11a}$$
 
$$(\phi_i^{\dagger}\phi_i)(\phi_j^{\dagger}\phi_j) \qquad : (i \neq j) : \qquad N \text{ terms}, \tag{A.11b}$$
 
$$(\phi_i^{\dagger}\phi_j + \phi_j^{\dagger}\phi_i)^2 \qquad : (i \neq j) : \qquad N \text{ terms}, \tag{A.11c}$$

$$(\phi_i^{\dagger}\phi_j + \phi_j^{\dagger}\phi_i)(\phi_k^{\dagger}\phi_l + \phi_l^{\dagger}\phi_k) : (\{i.j\} \neq \{k,l\}) : \frac{1}{2}N(N-1) \text{ terms}, \tag{A.11d}$$

$$(\phi_i^{\dagger}\phi_i)(\phi_k^{\dagger}\phi_l + \phi_l^{\dagger}\phi_k)$$
 :  $(k \neq l)$ :  $nN$  terms, (A.11e)

where,  $N=\frac{1}{2}n(n-1)$ . The total number of such terms is  $\frac{1}{8}n(n+1)(n^2+n+2)$ . The number of such terms arising from pairs of dot product type combinations of n triplets of CS comes out to be exactly the same. For nHDMs with  $n \geq 4$ , as discussed in Ref. [173], it is possible to obtain a new gauge invariant quantity that is truly independent of the combinations listed in Eq. (A.11) and corresponding to it we have the following CS invariant:

$$\operatorname{Im}(\phi_{i}^{\dagger}\phi_{j})\operatorname{Im}(\phi_{k}^{\dagger}\phi_{l}) + \operatorname{Im}(\phi_{i}^{\dagger}\phi_{l})\operatorname{Im}(\phi_{j}^{\dagger}\phi_{k}) + \operatorname{Im}(\phi_{i}^{\dagger}\phi_{k})\operatorname{Im}(\phi_{l}^{\dagger}\phi_{j})$$

$$= -\frac{1}{4}\left[ (\mathbf{T}_{i} \times \mathbf{T}_{j}) \cdot \mathbf{T}_{k}h_{l} - (\mathbf{T}_{j} \times \mathbf{T}_{k}) \cdot \mathbf{T}_{l}h_{i} + (\mathbf{T}_{k} \times \mathbf{T}_{l}) \cdot \mathbf{T}_{i}h_{j} - (\mathbf{T}_{l} \times \mathbf{T}_{i}) \cdot \mathbf{T}_{j}h_{k} \right] \quad (A.12)$$

with  $i \neq j \neq k \neq l$ . However, the term in Eq. (A.12) does not contribute to the mass matrices and therefore complies with Eq. (2.28). It should be noted that in the most general gauge invariant potential, many more quartic terms are possible. Thus, the quartic coefficients,  $\lambda_i$ , need to be correlated in such a way so that the terms in the quartic part of the scalar potential can be expressed in terms of the  $SU(2)_C$ invariant quantities listed in Eqs. (A.11) and (A.12).

#### **A.3** Flavour Observables in Democratic 3HDMs

#### A.3.1 Computing $b \to s\gamma$

The nonstandard contributions to the one-loop  $b \to s\gamma$  amplitude in democratic 3HDMs are shown in Fig. A.1. Since the one-loop contributions come from the charged scalar only, the NP amplitudes will depend only on the parameters  $\tan \beta_1$ ,  $\tan \beta_2$ ,  $m_{H_1^+}$ ,  $m_{H_2^+}$  and  $\gamma_2$ . To find the amplitudes, we simply extend the analysis of a NFC 2HDM [433, 434] for a scenario with two different  $H^+$ . Following Ref. [435],

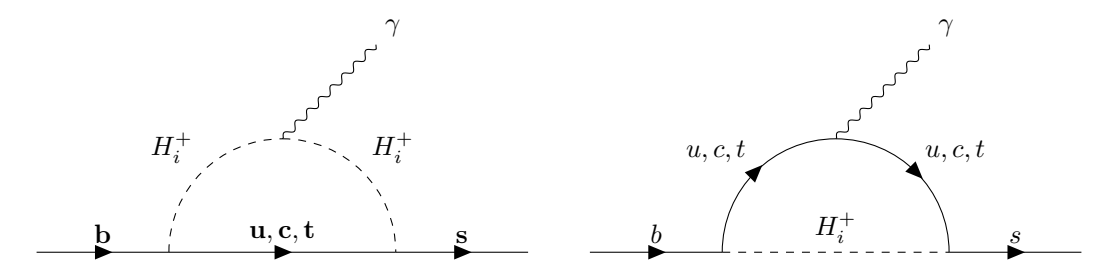


Figure A.1: NP contributions to  $b \to s\gamma$  in democratic 3HDMs.  $H_i^{\pm}$  stands for both charged scalars

the branching ratio for  $b \to s \gamma$  is controlled by the  $C_{7L}^{\rm eff}$  and  $C_{7R}^{\rm eff}$  Wilson coefficients:

$$\frac{\mathrm{BR}\left(b \to s\gamma\right)}{\mathrm{BR}\left(b \to ce\overline{\nu}\right)} = \frac{6\alpha}{\pi B} \left| \frac{V_{ts}^* V_{tb}}{V_{cb}} \right|^2 \left[ \left| C_{7L}^{\mathrm{eff}} \right|^2 + \left| C_{7R}^{\mathrm{eff}} \right|^2 \right],\tag{A.13}$$

where the normalization by BR  $(b \to ce\overline{\nu})$  helps canceling some of the hadronic uncertainties. The effective Wilson coefficients read

$$C_{7L}^{\text{eff}} = \eta^{16/23} C_{7L} + \frac{8}{3} \left( \eta^{14/23} - \eta^{16/23} \right) C_{8L} + \sum_{i=1}^{8} h_i \eta^{a_i}, \qquad (A.14a)$$

$$C_{7R}^{\text{eff}} = \eta^{16/23} C_{7R} + \frac{8}{3} \left( \eta^{14/23} - \eta^{16/23} \right) C_{8R},$$
 (A.14b)

where, as in the usual analysis of 2HDMs [435], the leading log QCD corrections in the SM are described by

$$a_{i} = \begin{pmatrix} \frac{14}{23}, & \frac{16}{23}, & \frac{6}{23}, & -\frac{2}{23}, & 0.4086, & -0.4230, & -0.8994, & 0.1456 \end{pmatrix},$$

$$h_{i} = \begin{pmatrix} \frac{626126}{272277}, & -\frac{56281}{51730}, & -\frac{3}{7}, & -\frac{1}{14}, & -0.6494, & -0.0380, & -0.0186, & -0.0057 \end{pmatrix},$$
(A.14d)

$$h_i = \left(\frac{626126}{272277}, -\frac{56281}{51730}, -\frac{3}{7}, -\frac{1}{14}, -0.6494, -0.0380, -0.0186, -0.0057\right), (A.14d)$$

and  $\eta = \alpha_s(M_Z)/\alpha_s(\mu)$ , where  $\mu$  is the QCD renormalization scale,  $\mu \approx 221$  MeV. Taking into account the absence of tree-level FCNCs, the coefficients in Eqs. (A.14a) and (A.14b) can be recast as

$$C_{7L} = A_{\gamma}^{\text{SM}} + A_{\gamma L}^{+}, \qquad C_{7R} = \frac{m_s}{m_h} A_{\gamma}^{\text{SM}} + A_{\gamma R}^{+},$$
 (A.15a)

$$C_{8L} = A_g^{\text{SM}} + A_{gL}^+, \qquad C_{8R} = \frac{m_s}{m_b} A_g^{\text{SM}} + A_{gR}^+,$$
 (A.15b)

where the  $A^+$  terms correspond to our NP (charged-Higgs) contributions. These contributions can be further broken down into

$$A_{\gamma L,R}^{+} = \frac{1}{V_{ts}^{*} V_{tb}} \sum_{q=u,c,t} V_{qs}^{*} V_{qb} \left[ C_{1L,R}(y_q) + \frac{2}{3} C_{2L,R}(y_q) \right], \tag{A.16a}$$

$$A_{gL,R}^{+} = \frac{1}{V_{ts}^{*} V_{tb}} \sum_{q=u,c,t} V_{qs}^{*} V_{qb} C_{2L,R}(y_q), \tag{A.16b}$$

with  $y_q = m_q^2/M_{H^+}^2$  and

$$C_{1L,R}(y_q) = \frac{y_q}{4} \left( \left[ \overline{\mathcal{F}}_2(y_q) - \overline{\mathcal{F}}_1(y_q) \right] \left( \frac{m_{s,b}^2}{m_q^2} Y^2 + X^2 \right) + 2XY \left[ \overline{\mathcal{F}}_1(y_q) - \overline{\mathcal{F}}_0(y_q) \right] \right), \text{ (A.17a)}$$

$$C_{2L,R}(y_q) = \frac{y_q}{4} \left( \left[ \mathcal{F}_2(y_q) - \mathcal{F}_1(y_q) \right] \left( \frac{m_{s,b}^2}{m_q^2} Y^2 + X^2 \right) - 2XY \mathcal{F}_1(y_q) \right), \tag{A.17b}$$

in which X and Y are the charged-Higgs coupling to left- and right-handed quarks, respectively, and the loop functions are given by

$$\mathcal{F}_k(t) = \int_0^1 dx \frac{(1-x)^k}{x + (1-x)t} = \frac{1}{(k+1)t} {}_{2}F_1\left(1, 1; k+2; \frac{t-1}{t}\right), \tag{A.18a}$$

$$\overline{\mathcal{F}}_k(t) = \int_0^1 dx \frac{x^k}{x + (1 - x)t} = \frac{1}{(k+1)t} \, _2F_1\left(1, \ k+1; k+2; \frac{t-1}{t}\right),\tag{A.18b}$$

where  ${}_{p}F_{q}\left(a,\ b;c;d\right)$  is the Hypergeometric Function. Finally, the SM amplitude is given by (keeping only the top contribution)

$$A_{\gamma}^{\text{SM}} = \left[ \frac{(2-3x_t)}{2} \overline{\mathcal{F}}_1(x_t) + \frac{(2+x_t)}{2} \overline{\mathcal{F}}_2(x_t) + x_t \overline{\mathcal{F}}_0(x_t) + \frac{4}{3} \mathcal{F}_0(x_t) - \frac{(6-x_t)}{3} \mathcal{F}_1(x_t) + \frac{(2+x_t)}{3} \mathcal{F}_2(x_t) \right] - \frac{23}{36}, \tag{A.19a}$$

$$A_g^{\text{SM}} = \left[ 2\mathcal{F}_0(x_t) - \frac{(6-x_t)}{2}\mathcal{F}_1(x_t) + \frac{(2+x_t)}{2}\mathcal{F}_2(x_t) \right] - \frac{1}{3}, \tag{A.19b}$$

where  $x_t = m_t^2/M_W^2$ . So far, we have presented the analysis of the  $b \to s\gamma$  processes in a 2HDM where FCNCs are absent. To extend these results to our model, we redefine Eqs. (A.16) and (A.17) to account for both charged-Higgs contributions:

$$A_{\gamma L,R}^{+} = \frac{1}{V_{ts}^{*} V_{tb}} \sum_{q=u,c,t} V_{qs}^{*} V_{qb} \sum_{i=1,2} \left[ C_{1L,R}^{i}(y_{q}^{i}) + \frac{2}{3} C_{2L,R}^{i}(y_{q}^{i}) \right], \tag{A.20a}$$

$$A_{gL,R}^{+} = \frac{1}{V_{ts}^{*}V_{tb}} \sum_{q=u,c,t} V_{qs}^{*}V_{qb} \sum_{i=1,2} C_{2L,R}^{i}(y_{q}^{i}), \tag{A.20b}$$

where now  $y_q^i = m_q^2/M_{H_i^+}^2$ , and

$$C_{1L,R}^{i}(y_q) = \frac{y_q}{4} \left( \left[ \overline{\mathcal{F}_2}(y_q) - \overline{\mathcal{F}_1}(y_q) \right] \left( \frac{m_{s,b}^2}{m_q^2} Y_i^2 + X_i^2 \right) + 2X_i Y_i \left[ \overline{\mathcal{F}_1}(y_q) - \overline{\mathcal{F}_0}(y_q) \right] \right), \quad (A.21a)$$

$$C_{2L,R}^{i}(y_q) = \frac{y_q}{4} \left( \left[ \mathcal{F}_2(y_q) - \mathcal{F}_1(y_q) \right] \left( \frac{m_{s,b}^2}{m_q^2} Y_i^2 + X_i^2 \right) - 2X_i Y_i \mathcal{F}_1(y_q) \right), \tag{A.21b}$$

where we can see the  $X_i$  and  $Y_i$  couplings now carry an index, denoting the  $H_1^+$  and  $H_2^+$  chiral ( $P_L$  and  $P_R$ ) couplings to quarks. In the present model, these couplings can be extracted from Eqs. (2.62a) and (2.62b):

$$X_1 = -\cot \beta_2 \sin \gamma_2,\tag{A.22a}$$

$$Y_1 = -\tan \beta_2 \left( \frac{\cot \beta_1 \cos \gamma_2}{\sin \beta_2} + \sin \gamma_2 \right), \tag{A.22b}$$

$$X_2 = \cot \beta_2 \cos \gamma_2, \tag{A.22c}$$

$$X_2 = \cot \beta_2 \cos \gamma_2,$$

$$Y_2 = -\tan \beta_2 \left( \frac{\cot \beta_1 \sin \gamma_2}{\sin \beta_2} - \cos \gamma_2 \right).$$
(A.22d)

We now have all the relevant information needed to compute the  $b \to s\gamma$  branching ratio in our model. As advertised, the only dependencies on the BSM degrees of freedom is through  $\tan \beta_1$ ,  $\tan \beta_2$ ,  $\gamma_2$ , which control the couplings, the charged-Higgs masses,  $m_{H_1^+}$  and  $m_{H_2^+}$ , which will affect the loop functions. Finally, the SM prediction for the  $b \to s\gamma$  branching ratio can be found in ref. [436], and the experimental values in [96].

#### Neutral Meson Mixing: $\Delta M_{Ba}$ A.3.2

A very restrictive aspect of BSM models comes from neutral meson oscillations. These processes, for models without tree-level FCNCs, are forbidden at tree-level, but may have sizable one-loop contributions. The left panel in Fig. A.2 represents the SM contribution for such processes, whereas the other two diagrams represent the additional contributions in democratic 3HDMs. To obtain some qualitative

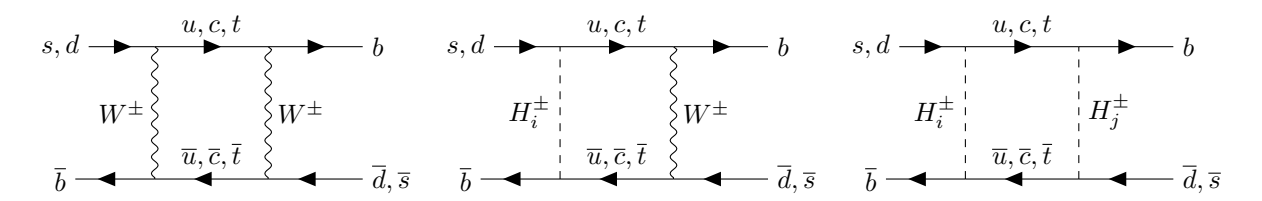


Figure A.2: Contributions to  $\Delta M_{B_q}$  in democratic 3HDMs.  $H_i^{\pm}$  stands for both charged scalars (i=1,2). The first box diagram corresponds to the SM amplitude. The diagrams with interchanged internal lines are not shown explicitly.

intuitions we write the effective  $\Delta F = 2$  Lagrangian as:

$$\mathcal{L}_{\text{eff}}^{\Delta F=2} = \frac{G_F^2 M_W^2}{16\pi^2} \sum_{\substack{a,b=u,c,t\\i,j=H_1^{\pm},H_2^{\pm}}} \lambda_a \lambda_b \ \omega_a \omega_b \left( \frac{S(y_a,y_b)}{4} + X_{ia} X_{ib} \left[ I_1(y_a,y_b,y_i) + X_{ja} X_{jb} I_2(y_a,y_b,y_i,y_j) \right] \right) O_F.$$
(A.23)

The SM contribution is encoded in  $S(y_a, y_b)$ , normalized by a factor of 4 to account for the summation on the charged Higgs. The  $I_1(y_a, y_b, y_i)$  contributions are due to the mixed  $W^{\pm} - H_i^{\pm}$  boxes, and  $I_2(y_a, y_b, y_i, y_j)$  are the  $H_i^{\pm} - H_j^{\pm}$  boxes in Fig. A.2. The above expression is valid in the zero external momenta approximation, where the down-type quark masses are taken to be zero. We use  $X_{ia}$  to denote the coupling between the charged-Higgs  $H_i^\pm$  and the up-quark a, which, as seen in Eq. (A.22a), are flavour universal, i.e.,  $X_{1a} = X_1 = -\cot \beta_2 \sin \gamma_2$  and  $X_{2a} = X_2 = \cot \beta_2 \cos \gamma_2$  for  $H_1^{\pm}$  and  $H_2^{\pm}$ , respectively. The quantities  $y_a$  and  $y_i$  stand for the ratios  $m_a^2/M_W^2$  and  $m_{H_i^+}^2/M_W^2$  respectively. The specificities of the neutral meson under consideration are contained in the CKM elements  $\lambda_a$ , and the dimension-6 operators  $O_F$ . For a generic meson  $P = (\overline{q_1}, q_2)$ , these are defined as

$$\lambda_a = (V_{a \, q_2}^* V_{a \, q_1}), \qquad O_F = (\overline{q}_1 \gamma^{\mu} P_L q_2)^2.$$
 (A.24)

Finally, the loop functions are given by

$$f(x) = \frac{(x^2 - 8x + 4) \ln x + 3(x - 1)}{(x - 1)^2}, \qquad S(y_a, y_b) = \frac{f(y_a, y_b)}{y_a - y_b},$$

$$g(x, y, z) = \frac{x(x - 4) \ln x}{(x - 1)(x - y)(x - z)}, \qquad h(x, y, w, z) = \frac{x^2 \ln x}{(x - y)(x - w)(x - z)},$$
(A.25a)

$$g(x,y,z) = \frac{x(x-4)\ln x}{(x-1)(x-y)(x-z)}, \qquad h(x,y,w,z) = \frac{x^2\ln x}{(x-y)(x-w)(x-z)}, \tag{A.25b}$$

$$I_1(y_a, y_b, y_i) = g(y_a, y_b, y_i) + g(y_b, y_i, y_a) + g(y_i, y_a, y_b),$$
(A.25c)

$$I_2(y_a, y_b, y_i, y_j) = h(y_a, y_b, y_i, y_j) + h(y_b, y_a, y_i, y_j) + h(y_i, y_a, y_b, y_j) + h(y_j, y_a, y_b, y_i).$$
(A.25d)

The limiting cases where, for instance, the same Higgs runs in the  $I_2$  box diagram should be carefully dealt with, as the loop functions are only apparently divergent for  $x_i = x_j$ , but indeed have a well-defined limit.

Finally, we can obtain  $\Delta M_P$  from the effective Lagrangian,

$$\Delta M_P = 2|M_{12}^P|, \qquad M_{12}^P = -\frac{1}{2M_P} \langle P^0 | \mathcal{L}_{\text{eff}}^{\Delta F=2} | \overline{P}^0 \rangle, \tag{A.26a}$$

$$\langle P^0 | O_F^P | \overline{P}^0 \rangle = \frac{2}{3} f_P^2 M_P^2 B_P, \tag{A.26b}$$

where  $M_P$  is the meson mass,  $f_P$  its decay constant, and  $B_P$  is its bag parameter. The 2HDM limit (with no tree-level FCNCs) of Eq. (A.23) can be easily extracted, taking some care on the symmetry factors. As in the  $b \to s\gamma$  computations, it would be possible to parametrize these results to match numerical results with higher-order corrections. The experimental values which will determine the experimentally allowed region are taken from [96], whereas the relevant hadronic parameters can be found in [437].

# B

# $\Sigma(36)$ and Alignment Preserving Soft-Breaking Terms

### **B.1** $\Sigma(36)$ vs. $\Delta(54)$ 3HDM

To avoid confusion, let us clarify the definition of the group  $\Sigma(36)$ . If one understands the generators a, b, and d given in Eq. (3.5) as transformations, from SU(3), then the group generated by them is

$$\Sigma(36\varphi) \simeq \Delta(27) \rtimes \mathbb{Z}_4$$
, (B.1)

which has order  $|\Sigma(36\varphi)| = 108$ . However, SU(3) contains its center, the group  $\mathbb{Z}_3$  generated by  $\omega(1,1,1)$ , which belongs to the global group hypercharge transformation group. Factoring SU(3) by its center brings us to  $PSU(3) \simeq SU(3)/\mathbb{Z}_3$ . The group  $\Sigma(36) \simeq \Sigma(36\varphi)/\mathbb{Z}_3$  of order 36 is understood as the subgroup of PSU(3).

When defining a group in PSU(3), one can still write a generator g as a unitary  $3 \times 3$  matrix, which is understood as a representative point of the entire coset  $g \cdot \mathbb{Z}_3$ . Thus, one can still use the generators a, b, and d as in Eq. (3.5), provided one considers their relations up to any possible transformation from the center. It is in this sense that we say that the generators a and b commute: their commutator  $aba^{-1}b^{-1}$  produces an element from the center of SU(3), which becomes an identity element of PSU(3). For more discussion of these subtle distinctions, see [216, 229].

We remark that the traditional notation of symmetry groups in the scalar sector of 3HDM inadvertently confuses the two spaces. That is, when one defines the  $A_4$  3HDM, the group  $A_4$  is understood as a subgroup of PSU(3) (the center of  $A_4$  is trivial), while when one speaks of  $\Delta(27)$  3HDM, one uses  $\Delta(27)$  which is a subgroup of SU(3) (the groups  $\Sigma(36\varphi)$ ,  $\Delta(54)$ , and  $\Delta(27)$  are related, and have the same center).

The symmetry group  $\Sigma(36)$  is twice larger than the more familiar group  $\Delta(54)$  (which is, in fact, just  $(\mathbb{Z}_3 \times \mathbb{Z}_3) \rtimes \mathbb{Z}_2$  inside PSU(3)). One would obtain the  $\Delta(54)$ -symmetric 3HDM, if one required invariance

under the generator  $d^2$ , not d itself.  $\Delta(54)$  allows for additional terms in the potential which are absent in Eq. (3.6).

In the CP-violating version of  $\Delta(54)$  3HDM, the three points A would not be linked with A' by a symmetry transformation. The same would apply to the points B and C. Thus, in CP-violating  $\Delta(54)$  3HDM, depending on the values of the parameters, the minimum could be at A, A', B, or C. For the CP-conserving  $\Delta(54)$ , points A and A' become related by a (generalized) CP symmetry transformation, so the minimum can be either at points A + A' or B or C. With the enhanced family symmetry  $\Sigma(36)$  points B and C become equivalent, too.

# B.2 Alignment Preserving Soft-Breaking Terms for all the Minima

For completeness, we list here the explicit expressions for eigenvectors and the parametrization of the soft-breaking terms  $M_{ij}$  for all the minima of the  $\Sigma(36)$  symmetric model.

We begin the case considered in the main text and then use it to build all other cases of type C, A and A':

• For point  $C_1$  with the alignment (1,1,1) we use

$$n_1 = \frac{1}{\sqrt{3}} \begin{pmatrix} 1\\1\\1 \end{pmatrix}, \quad e_2 = \frac{1}{\sqrt{2}} \begin{pmatrix} 0\\1\\-1 \end{pmatrix}, \quad e_3 = \frac{1}{\sqrt{6}} \begin{pmatrix} -2\\1\\1 \end{pmatrix},$$
 (B.2)

and construct the vectors  $\vec{n}_2$ ,  $\vec{n}_3$  using the matrix in Eq. (3.21). The hermitean matrix  $M_{ij}$  has the following elements:

$$M_{11} = m_{11}^2 = \frac{1}{3} \left( \Sigma - \delta \cos 2\theta \right)$$

$$M_{22} = m_{22}^2 = \frac{1}{3} \left[ \Sigma + \delta \left( \frac{\sqrt{3}}{2} \sin 2\theta \cos \xi + \frac{1}{2} \cos 2\theta \right) \right]$$

$$M_{33} = m_{22}^2 = \frac{1}{3} \left[ \Sigma + \delta \left( -\frac{\sqrt{3}}{2} \sin 2\theta \cos \xi + \frac{1}{2} \cos 2\theta \right) \right]$$

$$M_{12} = m_{12}^2 = \frac{1}{6} \left[ -\Sigma + \delta \left( -\sqrt{3} \sin 2\theta e^{i\xi} + \cos 2\theta \right) \right]$$

$$M_{31} = m_{31}^2 = \frac{1}{6} \left[ -\Sigma + \delta \left( \sqrt{3} \sin 2\theta e^{-i\xi} + \cos 2\theta \right) \right]$$

$$M_{23} = m_{23}^2 = \frac{1}{6} \left[ -\Sigma - \delta \left( i\sqrt{3} \sin 2\theta \sin \xi + 2 \cos 2\theta \right) \right].$$
(B.3)

• For point  $C_2$  with the alignment  $(1, \omega, \omega^2)$  we use:

$$n_1 = \frac{1}{\sqrt{3}} \begin{pmatrix} 1 \\ \omega \\ \omega^2 \end{pmatrix}, \quad e_2 = \frac{1}{\sqrt{2}} \begin{pmatrix} 0 \\ \omega \\ -\omega^2 \end{pmatrix}. \quad e_3 = \frac{1}{\sqrt{6}} \begin{pmatrix} -2 \\ \omega \\ \omega^2 \end{pmatrix}. \tag{B.4}$$

The hermitean matrix  $M_{ij}$  can now be easily expressed as

$$M_{ij}\Big|_{C_2} = \begin{pmatrix} \dots & \omega^2 \dots & \omega \dots \\ \omega \dots & \dots & \omega^2 \dots \\ \omega^2 \dots & \omega \dots & \dots \end{pmatrix},$$
(B.5)

where dots indicate the corresponding element of the matrix  $M_{ij}$  at point  $C_1$  given in Eq. (B.3).

• For point  $C_3$  with the alignment  $(1, \omega^2, \omega)$  we use:

$$n_1 = \frac{1}{\sqrt{3}} \begin{pmatrix} 1 \\ \omega^2 \\ \omega \end{pmatrix}, \quad e_2 = \frac{1}{\sqrt{2}} \begin{pmatrix} 0 \\ \omega^2 \\ -\omega \end{pmatrix}. \quad e_3 = \frac{1}{\sqrt{6}} \begin{pmatrix} -2 \\ \omega^2 \\ \omega \end{pmatrix}. \tag{B.6}$$

The elements of the hermitean matrix  $M_{ij}$  are now

$$M_{ij}\Big|_{C_3} = \begin{pmatrix} \dots & \omega \dots & \omega^2 \dots \\ \omega^2 \dots & \dots & \omega \dots \\ \omega \dots & \omega^2 \dots & \dots \end{pmatrix},$$
(B.7)

• For point  $A_1$  with the alignment  $(\omega, 1, 1)$  we use:

$$n_1 = \frac{1}{\sqrt{3}} \begin{pmatrix} \omega \\ 1 \\ 1 \end{pmatrix}, \quad e_2 = \frac{1}{\sqrt{2}} \begin{pmatrix} 0 \\ 1 \\ -1 \end{pmatrix}. \quad e_3 = \frac{1}{\sqrt{6}} \begin{pmatrix} -2\omega \\ 1 \\ 1 \end{pmatrix}.$$
 (B.8)

The hermitean matrix  $M_{ij}$  is now

$$M_{ij}\Big|_{A_1} = \begin{pmatrix} \dots & \omega \dots & \omega \dots \\ \omega^2 \dots & \dots & \dots \\ \omega^2 \dots & \dots & \dots \end{pmatrix}, \tag{B.9}$$

• For point  $A_2$  with the alignment  $(1, \omega, 1)$  we use:

$$n_1 = \frac{1}{\sqrt{3}} \begin{pmatrix} 1 \\ \omega \\ 1 \end{pmatrix}, \quad e_2 = \frac{1}{\sqrt{2}} \begin{pmatrix} 0 \\ \omega \\ -1 \end{pmatrix}. \quad e_3 = \frac{1}{\sqrt{6}} \begin{pmatrix} -2 \\ \omega \\ 1 \end{pmatrix}. \tag{B.10}$$

The hermitean matrix  $M_{ij}$  is now

$$M_{ij}\Big|_{A_2} = \begin{pmatrix} \dots & \omega^2 \dots & \dots \\ \omega \dots & \omega \dots & \omega \dots \\ \dots & \omega^2 \dots & \dots \end{pmatrix}, \tag{B.11}$$

• For point  $A_3$  with the alignment  $(1,1,\omega)$  we use:

$$n_1 = \frac{1}{\sqrt{3}} \begin{pmatrix} 1\\1\\\omega \end{pmatrix}, \quad e_2 = \frac{1}{\sqrt{2}} \begin{pmatrix} 0\\1\\-\omega \end{pmatrix}. \quad e_3 = \frac{1}{\sqrt{6}} \begin{pmatrix} -2\\1\\\omega \end{pmatrix}. \tag{B.12}$$

The hermitean matrix  $M_{ij}$  is now

$$M_{ij}\Big|_{A_3} = \begin{pmatrix} \dots & \dots & \omega^2 \dots \\ \dots & \dots & \omega^2 \dots \\ \omega \dots & \omega \dots & \dots \end{pmatrix}, \tag{B.13}$$

• For points  $A'_1$ ,  $A'_2$ ,  $A'_3$ , we obtain the relevant expressions by performing complex conjugation (not hermitean conjugation!) of the corresponding expressions for points  $A_1$ ,  $A_2$ ,  $A_3$ .

Finally, for points of type B we use a slightly different choice of basis eigenvectors.

• For point  $B_1$  with alignment (1,0,0) we use

$$n_1 = \begin{pmatrix} 1 \\ 0 \\ 0 \end{pmatrix}, \quad e_2 = \frac{1}{\sqrt{2}} \begin{pmatrix} 0 \\ 1 \\ i \end{pmatrix}, \quad e_3 = \frac{1}{\sqrt{2}} \begin{pmatrix} 0 \\ i \\ 1 \end{pmatrix}.$$
 (B.14)

The resulting matrix  $M_{ij}$  has the following elements:

$$M_{11} = M_{12} = M_{13} = 0$$

$$M_{22} = \frac{1}{2} (\Sigma - \delta \sin 2\theta \sin \xi)$$

$$M_{33} = \frac{1}{2} (\Sigma + \delta \sin 2\theta \sin \xi)$$

$$M_{23} = \frac{1}{2} \delta (\sin 2\theta \cos \xi - i \cos 2\theta) .$$
(B.15)

The motivation for the choice (B.12) is the following. In all previous cases, by setting  $\sin 2\theta \sin \xi = 1$ , we obtain soft-breaking terms which respect several symmetries of the vacuum which, in turn, leads to pairwise mass degenerate neutral scalars, see the discussion around Eq. (3.31). We want to achieve the same feature for points B. This can be done if M is diagonal (the preserved symmetries being the generator a in Eq. (3.5) and the ordinary CP). The choice of Eq. (B.14) is exactly the one which produces diagonal M for  $\sin 2\theta \sin \xi = 1$ .

• For point  $B_2$  with alignment (0,1,0) we use

$$n_1 = \begin{pmatrix} 0 \\ 1 \\ 0 \end{pmatrix}, \quad e_2 = \frac{1}{\sqrt{2}} \begin{pmatrix} i \\ 0 \\ 1 \end{pmatrix}, \quad e_3 = \frac{1}{\sqrt{2}} \begin{pmatrix} 1 \\ 0 \\ i \end{pmatrix}.$$
 (B.16)

The resulting matrix  $M_{ij}$  has the following elements:

$$M_{21} = M_{22} = M_{23} = 0$$

$$M_{33} = \frac{1}{2} (\Sigma - \delta \sin 2\theta \sin \xi)$$

$$M_{11} = \frac{1}{2} (\Sigma + \delta \sin 2\theta \sin \xi)$$

$$M_{31} = \frac{1}{2} \delta (\sin 2\theta \cos \xi - i \cos 2\theta) .$$
(B.17)

• For point  $B_3$  with alignment (0,0,1) we use

$$n_1 = \begin{pmatrix} 0 \\ 0 \\ 1 \end{pmatrix}, \quad e_2 = \frac{1}{\sqrt{2}} \begin{pmatrix} 1 \\ i \\ 0 \end{pmatrix}, \quad e_3 = \frac{1}{\sqrt{2}} \begin{pmatrix} i \\ 1 \\ 0 \end{pmatrix}.$$
 (B.18)

The resulting matrix  $M_{ij}$  has the following elements:

$$M_{31} = M_{32} = M_{33} = 0$$

$$M_{11} = \frac{1}{2} (\Sigma - \delta \sin 2\theta \sin \xi)$$

$$M_{22} = \frac{1}{2} (\Sigma + \delta \sin 2\theta \sin \xi)$$

$$M_{12} = \frac{1}{2} \delta (\sin 2\theta \cos \xi - i \cos 2\theta) .$$
(B.19)



# $S_4$ Group Theory and the Littlest Modular Seesaw

## C.1 Group Theory of $S_4$

In this appendix we summarize some relevant group theoretical details of  $S_4$  (see [137] and references therein). The products of irreps follow:

$$1' \otimes 1' = 1, \ 1' \otimes 2 = 2, \ 1' \otimes 3 = 3', \ 1' \otimes 3' = 3,$$
$$2 \otimes 2 = 1 \oplus 1' \oplus 2, \ 2 \otimes 3 = 2 \otimes 3' = 3 \oplus 3',$$
$$3 \otimes 3 = 3' \otimes 3' = 1 \oplus 2 \oplus 3 \oplus 3', \ 3 \otimes 3' = 1' \oplus 2 \oplus 3 \oplus 3'. \tag{C.1}$$

In the basis we are using, the representation matrices for T, S and U are shown in Table C.1.

	$\rho(T)$	$\rho(S)$	$\rho(U)$
1	1	1	1
1′	1	1	-1
2	$\left[\begin{array}{cc} \left(\begin{array}{cc} \omega & 0 \\ 0 & \omega^2 \end{array}\right)\right]$	$\left(\begin{array}{cc} 1 & 0 \\ 0 & 1 \end{array}\right)$	$\begin{pmatrix} 0 & 1 \\ 1 & 0 \end{pmatrix}$
3	$\left[\begin{array}{cccc} 1 & 0 & 0 \\ 0 & \omega^2 & 0 \\ 0 & 0 & \omega \end{array}\right]$	$ \frac{1}{3} \begin{pmatrix} -1 & 2 & 2 \\ 2 & -1 & 2 \\ 2 & 2 & -1 \end{pmatrix} $	$\left(\begin{array}{ccc} 1 & 0 & 0 \\ 0 & 0 & 1 \\ 0 & 1 & 0 \end{array}\right)$
3′	$ \left(\begin{array}{ccc} 1 & 0 & 0 \\ 0 & \omega^2 & 0 \\ 0 & 0 & \omega \end{array}\right) $	$ \begin{array}{c cccc} \frac{1}{3} & -1 & 2 & 2 \\ 2 & -1 & 2 \\ 2 & 2 & -1 \end{array} $	$-\left(\begin{array}{ccc} 1 & 0 & 0 \\ 0 & 0 & 1 \\ 0 & 1 & 0 \end{array}\right)$

**Table C.1:** In the basis used, the representation matrices for T, S and U, with  $\omega = e^{2\pi i/3}$ .

In this basis, the product of 3 dimensional irreps a and b:

$$(ab)_{\mathbf{1}_{i}} = a_{1}b_{1} + a_{2}b_{3} + a_{3}b_{2},$$

$$(ab)_{\mathbf{2}} = (a_{2}b_{2} + a_{1}b_{3} + a_{3}b_{1}, \ a_{3}b_{3} + a_{1}b_{2} + a_{2}b_{1})^{T},$$

$$(ab)_{\mathbf{3}_{i}} = (2a_{1}b_{1} - a_{2}b_{3} - a_{3}b_{2}, 2a_{3}b_{3} - a_{1}b_{2} - a_{2}b_{1}, 2a_{2}b_{2} - a_{3}b_{1} - a_{1}b_{3})^{T},$$

$$(ab)_{\mathbf{3}_{i}} = (a_{2}b_{3} - a_{3}b_{2}, a_{1}b_{2} - a_{2}b_{1}, a_{3}b_{1} - a_{1}b_{3})^{T},$$

$$(C.2)$$

for

$$\mathbf{1_i} = \mathbf{1}, \ \mathbf{3_i} = \mathbf{3}, \ \mathbf{3_j} = \mathbf{3}' \ \text{for} \ a \sim b \sim \mathbf{3}, \ \mathbf{3}',$$

$$\mathbf{1_i} = \mathbf{1}', \ \mathbf{3_i} = \mathbf{3}', \ \mathbf{3_j} = \mathbf{3} \ \text{for} \ a \sim \mathbf{3}, \ b \sim \mathbf{3}'.$$
(C.3)

The expressions for the product of 2 dimensional irreps  $a = (a_1, a_2)^T$  and  $b = (b_1, b_2)^T$  are:

$$(ab)_{\mathbf{1}} = a_1b_2 + a_2b_1, \quad (ab)_{\mathbf{1}'} = a_1b_2 - a_2b_1, \quad (ab)_{\mathbf{2}} = (a_2b_2, a_1b_1)^T.$$
 (C.4)

### C.2 Stabilizers and Residual Symmetry

In the basis we work in, we can make the following mapping of modular generators [137]:

$$S = T_{\tau}^2, \qquad T = S_{\tau} T_{\tau}, \qquad U = T_{\tau} S_{\tau} T_{\tau}^2 S_{\tau}, \tag{C.5}$$

where  $S_{\tau}$  and  $T_{\tau}$  are the usual modular generators of the full modular group  $\Gamma$ :

$$S_{\tau} = \begin{pmatrix} 0 & 1 \\ -1 & 0 \end{pmatrix}, \qquad T_{\tau} = \begin{pmatrix} 1 & 1 \\ 0 & 1 \end{pmatrix} \tag{C.6}$$

which act on the modulus field as

$$\gamma \tau = \frac{a\tau + b}{c\tau + d}, \qquad \gamma = \begin{pmatrix} a & b \\ c & d \end{pmatrix}.$$
(C.7)

With the requirement that  $\tau = \tau + 4$ , which must hold true for  $\Gamma_4$ , we can compute the corresponding  $\gamma$  for U and SU [137]:

$$\gamma(U) = \begin{pmatrix} 1 & -1 \\ 2 & -1 \end{pmatrix}, \qquad \gamma(SU) = \begin{pmatrix} 5 & -3 \\ 2 & -1 \end{pmatrix}. \tag{C.8}$$

Now, due to  $T_{\tau}^4 = 1$ , the choice of  $\gamma(g)$  is not unique. Indeed, any element of  $S_4$ ,  $\gamma(g)$ :

$$\gamma(g) = \begin{pmatrix} a & b \\ c & d \end{pmatrix}, \quad ad - bc = 1, \quad a, b, c, d \in \mathbb{Z}, \tag{C.9}$$

is equivalent to

$$\gamma'(g) = (\pm 1) \begin{pmatrix} 4k_a + a & 4k_b + b \\ 4k_c + c & 4k_d + d \end{pmatrix}, \qquad 4k_a k_d + ak_d + dk_a = 4k_b k_c bk_c + ck_d, \quad k_x \in \mathbb{Z}$$
 (C.10)

where the constraint comes from requiring that  $\gamma'(g)$  also satisfies ad - bc = 1.

By choosing the following sets of integers, we arrive at equivalent representations of the  $\gamma(U)$  and  $\gamma(SU)$  matrices:

$$\gamma_1(U) = \begin{pmatrix} 1 & -1 \\ 2 & -1 \end{pmatrix} \equiv \gamma(U),$$
(C.11)

$$\gamma_2(U) = \begin{pmatrix} -3 & -5 \\ 2 & 3 \end{pmatrix}, \quad k_a = -1 \quad k_b = -1 \quad k_c = 0 \quad k_d = 1,$$
(C.12)

$$\gamma_1(SU) = \begin{pmatrix} -1 & -1 \\ 2 & 1 \end{pmatrix}, \quad k_a = -1 \quad k_b = 1 \quad k_c = -1 \quad k_d = 0,$$
(C.13)

$$\gamma_2(SU) = \begin{pmatrix} -3 & 5 \\ -2 & 3 \end{pmatrix}, \quad k_a = -2 \quad k_b = 2 \quad k_c = -1 \quad k_d = 1.$$
(C.14)

Using these matrices, it is straightforward to show that

$$\gamma_1(U)\tau_A = \tau_A, \quad \tau_A = \frac{1+i}{2} \tag{C.15}$$

$$\gamma_2(U)\tau_A' = \tau_A', \quad \tau_A' = \frac{-3+i}{2}$$
(C.16)

$$\gamma_1(SU)\tau_B = \tau_B, \quad \tau_B = \frac{-1+i}{2} \tag{C.17}$$

$$\gamma_2(SU)\tau_B = \tau_B, \quad \tau_B = \frac{3+i}{2}. \tag{C.18}$$

In other words,  $\tau_A$  and  $\tau'_A$  are stabilisers of the modular generator U, and that  $\tau_B$  (either version) is a stabiliser of the modular generator SU in our chosen basis.

To further corroborate that the stabilisers are leaving an unbroken subgroup, we can check that the respective modular forms are eigenvectors of the appropriate representation matrices. From Appendix C.1, we have

$$\rho_{\mathbf{3'}}(S) = \frac{1}{3} \begin{pmatrix} -1 & 2 & 2 \\ 2 & -1 & 2 \\ 2 & 2 & -1 \end{pmatrix}, \quad \rho_{\mathbf{3'}}(U) = -\begin{pmatrix} 1 & 0 & 0 \\ 0 & 0 & 1 \\ 0 & 1 & 0 \end{pmatrix}, \quad \rho_{\mathbf{3'}}(SU) = \frac{1}{3} \begin{pmatrix} 1 & -2 & -2 \\ -2 & -2 & 1 \\ -2 & 1 & -2 \end{pmatrix}, \quad (C.19)$$

from which is straightforward to arrive at

$$\rho_{\mathbf{3}'}(U) \cdot \begin{pmatrix} 0 \\ -1 \\ 1 \end{pmatrix} = (+1) \begin{pmatrix} 0 \\ -1 \\ 1 \end{pmatrix}, \qquad \rho_{\mathbf{3}'}(SU) \cdot \begin{pmatrix} 1 \\ 1 \pm \sqrt{6} \\ 1 \mp \sqrt{6} \end{pmatrix} = (-1) \begin{pmatrix} 1 \\ 1 \pm \sqrt{6} \\ 1 \mp \sqrt{6} \end{pmatrix}, \tag{C.20}$$

agreeing with the expected results. We note that both modular forms  $\begin{pmatrix} 1 & 1 \pm \sqrt{6} & 1 \mp \sqrt{6} \end{pmatrix}$  have an eigenvalue -1, which is a consequence of [137]

$$(c\tau + d)^{-2k} = (2\tau_{SU} + 1)^{-2k} = (-1)^k, \tag{C.21}$$

where k = 1 for  $Y_{3'}^{(2)}$ . As such, we preserve a residual flavour symmetry U by the modular form of  $\tau_A$  (eigenvalue +1), whereas the modular forms of  $\tau_B$  (eigenvalue -1) do not preserve the residual flavour symmetry SU, but do preserve the corresponding residual modular symmetry, taking into account the automorphy factor.

### C.3 $S_4$ : Another Basis and Modular Forms at $\tau = \omega$

The generators of  $S_4$  obey

$$S^2 = (ST)^3 = T^4 = 1. (C.22)$$

We follow the  $S_4$  basis of [141], where the representation matrices are

1 : 
$$\rho(S) = 1$$
,  $\rho(T) = 1$ , (C.23a)

$$\mathbf{1}' : \rho(S) = -1, \quad \rho(T) = -1,$$
 (C.23b)

$$\mathbf{2} \quad : \quad \rho(S) = \begin{pmatrix} 0 & \omega \\ \omega^2 & 0 \end{pmatrix}, \quad \rho(T) = \begin{pmatrix} 0 & 1 \\ 1 & 0 \end{pmatrix}, \tag{C.23c}$$

$$\mathbf{3} : \rho(S) = \frac{1}{3} \begin{pmatrix} -1 & 2\omega^2 & 2\omega \\ 2\omega & 2 & -\omega^2 \\ 2\omega^2 & -\omega & 2 \end{pmatrix}, \quad \rho(T) = \frac{1}{3} \begin{pmatrix} -1 & 2\omega & 2\omega^2 \\ 2\omega & 2\omega^2 & -1 \\ 2\omega^2 & -1 & 2\omega \end{pmatrix}, \quad (C.23d)$$

$$\mathbf{3'} : \rho(S) = -\frac{1}{3} \begin{pmatrix} -1 & 2\omega^2 & 2\omega \\ 2\omega & 2 & -\omega^2 \\ 2\omega^2 & -\omega & 2 \end{pmatrix}, \quad \rho(T) = -\frac{1}{3} \begin{pmatrix} -1 & 2\omega & 2\omega^2 \\ 2\omega & 2\omega^2 & -1 \\ 2\omega^2 & -1 & 2\omega \end{pmatrix}. \quad (C.23e)$$

The tensor products are given by

$$1 \otimes \mathbf{r} = \mathbf{r}, \tag{C.24a}$$

$$\mathbf{1}' \otimes \mathbf{1}' = \mathbf{1}, \tag{C.24b}$$

$$\mathbf{1}' \otimes \mathbf{2} = \mathbf{2}, \tag{C.24c}$$

$$\mathbf{1}' \otimes \mathbf{3} = \mathbf{3}', \tag{C.24d}$$

$$\mathbf{1}' \otimes \mathbf{3}' = \mathbf{3}, \tag{C.24e}$$

$$\mathbf{2} \otimes \mathbf{2} = \mathbf{1} \oplus \mathbf{1}' \oplus \mathbf{2}, \tag{C.24f}$$

$$\mathbf{2} \otimes \mathbf{3} = \mathbf{3} \oplus \mathbf{3}', \tag{C.24g}$$

$$\mathbf{2} \otimes \mathbf{3}' = \mathbf{3} \oplus \mathbf{3}', \tag{C.24h}$$

$$\mathbf{3} \otimes \mathbf{3} = \mathbf{1} \oplus \mathbf{2} \oplus \mathbf{3} \oplus \mathbf{3}', \tag{C.24i}$$

$$\mathbf{3} \otimes \mathbf{3'} = \mathbf{1'} \oplus \mathbf{2} \oplus \mathbf{3} \oplus \mathbf{3'}, \tag{C.24j}$$

where we only show the relevant Clebsch-Gordan coefficients for our model, and the remaining can be found in [141]:

$$(\mathbf{3} \otimes \mathbf{3})_{\mathbf{1}} = \alpha_1 \beta_1 + \alpha_2 \beta_3 + \alpha_3 \beta_2. \tag{C.25}$$

Using this basis, the relevant fixed points for our model are

$$\tau_{C} = \omega, Y_{\mathbf{3},\mathbf{3'}}^{(k)}(\tau_{C}) = \begin{pmatrix} \delta_{0}^{\text{mod}(k,6)} \\ \delta_{2}^{\text{mod}(k,6)} \\ \delta_{4}^{\text{mod}(k,6)} \end{pmatrix}, (C.26a)$$

$$\tau_{A} = \frac{1}{2} + \frac{i}{2}, Y_{\mathbf{3'}}^{(4)}(\tau_{A}) = \begin{pmatrix} 0 \\ -1 \\ 1 \end{pmatrix}, (C.26b)$$

$$\tau_A = \frac{1}{2} + \frac{i}{2}, \qquad Y_{3'}^{(4)}(\tau_A) = \begin{pmatrix} 0\\ -1\\ 1 \end{pmatrix},$$
(C.26b)

$$\tau_B = \frac{3}{2} + \frac{i}{2}, \qquad Y_{\mathbf{3'}}^{(2)}(\tau_B) = \begin{pmatrix} 1\\ 1 - \sqrt{6}\\ 1 + \sqrt{6} \end{pmatrix},$$
(C.26c)

$$\tau_B' = -\frac{1}{2} + \frac{i}{2}, \qquad Y_{\mathbf{3'}}^{(2)}(\tau_B') = \begin{pmatrix} 1\\ 1 + \sqrt{6}\\ 1 - \sqrt{6} \end{pmatrix}.$$
 (C.26d)

As for the modular forms we have, at the lowest weight in  $S_4$ ,

$$Y_{\mathbf{2}}^{(2)}(\tau_C) = \begin{pmatrix} 0 \\ 1 \end{pmatrix}, \qquad Y_{\mathbf{3}}^{(2)}(\tau_C) = \begin{pmatrix} 0 \\ 1 \\ 0 \end{pmatrix}.$$
 (C.27)

Higher weight modular forms are obtained through the tensor products of lower-weight modular forms:

$$Y^{(k)} = Y^{(k-2)} \otimes Y^{(2)} = \bigotimes^{k/2} Y^{(2)}, \qquad (C.28)$$

which can be easily computed for at  $\tau = \omega$ , and we see that, up to weight 12:

$$k = 2$$
 :  $Y_{\mathbf{2}}^{(2)}(\tau_C) = \begin{pmatrix} 0 \\ 1 \end{pmatrix}$  ,  $Y_{\mathbf{3}}^{(2)}(\tau_C) = \begin{pmatrix} 0 \\ 1 \\ 0 \end{pmatrix}$  , (C.29a)

$$k = 4$$
 :  $Y_{\mathbf{2}}^{(4)}(\tau_C) = \begin{pmatrix} 1\\0 \end{pmatrix}$  ,  $Y_{\mathbf{3}}^{(4)}(\tau_C) = \begin{pmatrix} 0\\0\\1 \end{pmatrix}$  , (C.29b)

$$k = 6$$
 :  $Y_{\mathbf{1}}^{(6)}(\tau_C) = (1)$  ,  $Y_{\mathbf{1}'}^{(6)}(\tau_C) = (1)$  ,  $Y_{\mathbf{3}}^{(2)}(\tau_C) = \begin{pmatrix} 1\\0\\0 \end{pmatrix}$  , (C.29c)

$$k = 8$$
 :  $Y_{\mathbf{2}}^{(8)}(\tau_C) = \begin{pmatrix} 0 \\ 1 \end{pmatrix}$  ,  $Y_{\mathbf{3}}^{(8)}(\tau_C) = \begin{pmatrix} 0 \\ 1 \\ 0 \end{pmatrix}$  , (C.29d)

$$k = 10$$
 :  $Y_{\mathbf{2}}^{(10)}(\tau_C) = \begin{pmatrix} 1\\0 \end{pmatrix}$  ,  $Y_{\mathbf{3}}^{(10)}(\tau_C) = \begin{pmatrix} 0\\0\\1 \end{pmatrix}$  , (C.29e)

$$k = 12$$
 :  $Y_{\mathbf{1}}^{(12)}(\tau_C) = (1)$  ,  $Y_{\mathbf{1}'}^{(12)}(\tau_C) = (1)$  ,  $Y_{\mathbf{3}}^{(2)}(\tau_C) = \begin{pmatrix} 1\\0\\0 \end{pmatrix}$  , (C.29f)

where we only show the non-vanishing modular forms. It is clear that the pattern repeats, such that the non-vanishing modular forms at k=2,4,6 and k=8,10,12 are identical, respectively. Additionally, given Eq. (C.28), and that the modular forms of weight 6 and 12 are identical, then there is no difference in computing  $Y^{(2)} \otimes Y^{(6)}$  and  $Y^{(2)} \otimes Y^{(12)}$ . Thus, at  $\tau = \omega$ , it becomes obvious that the modular forms are given by:

$$Y_{\mathbf{1}}^{(k)}(\tau_C) = \left(\delta_0^{\text{mod}(k,6)}\right), \qquad Y_{\mathbf{1}'}^{(k)}(\tau_C) = \left(\delta_0^{\text{mod}(k,6)}\right),$$
 (C.30a)

$$Y_{\mathbf{2}}^{(k)}(\tau_C) = \begin{pmatrix} \delta_4^{\text{mod}(k,6)} \\ \delta_2^{\text{mod}(k,6)} \end{pmatrix}, \qquad Y_{\mathbf{3},\mathbf{3}'}^{(k)}(\tau_C) = \begin{pmatrix} \delta_0^{\text{mod}(k,6)} \\ \delta_2^{\text{mod}(k,6)} \\ \delta_4^{\text{mod}(k,6)} \end{pmatrix}, \tag{C.30b}$$

assuming they exist in at a certain modular weight. This is useful for model building at fixed points, since it allows us to easily identify the shape of the modular forms of higher weights, without the need for actual computation.

# C.4 Possible Corrections to the CSD(n) Structure

At first glance, the assignments of the model shown in the main text appear more convoluted than necessary. Indeed, it is possible to find a seemingly simpler model, which includes all the terms and invariants we find in the main text. However, it is important to check if there are (non-negligible) corrections to any of the structures found for the relevant Yukawa matrices. In this Appendix, we show a simple example of this. Table C.2 shows one possible set of assignments for the fields that also lead to

the structures found in the main text for  $Y_u$  and  $Y_d$ . Namely, we find

$$Y_{u} = \begin{pmatrix} y_{uu}\epsilon_{T}^{4} + y'_{uu}\epsilon_{F}^{3}\epsilon_{T} & y_{uc}\epsilon_{T}^{3} + y'_{uc}\epsilon_{F}^{3} & y_{ut}\epsilon_{T}^{2} \\ . & y_{cc}\epsilon_{T}^{2} & y_{ct}\epsilon_{T} \\ . & . & y_{tt} \end{pmatrix},$$
(C.31a)

$$Y_{u} = \begin{pmatrix} y_{uu}\epsilon_{T}^{4} + y'_{uu}\epsilon_{F}^{3}\epsilon_{T} & y_{uc}\epsilon_{T}^{3} + y'_{uc}\epsilon_{F}^{3} & y_{ut}\epsilon_{T}^{2} \\ & . & y_{cc}\epsilon_{T}^{2} & y_{ct}\epsilon_{T} \\ & . & . & y_{tt} \end{pmatrix},$$

$$Y_{d} = \begin{pmatrix} y_{dd}\epsilon_{F}^{3} & y_{ds}\epsilon_{F}^{2}\epsilon_{T} & y_{db}\epsilon_{F}\epsilon_{T}^{2} \\ 0 & y_{ss}\epsilon_{F}^{2} & y_{sb}\epsilon_{F}\epsilon_{T} \\ 0 & 0 & y_{bb}\epsilon_{F} \end{pmatrix} \qquad Y_{\ell} = \begin{pmatrix} y_{ee}\epsilon_{F}^{3} & 0 & 0 \\ y_{\mu e}\epsilon_{F}^{2}\epsilon_{T} & y_{\mu\mu}\epsilon_{F}^{2} & 0 \\ y_{\tau e}\epsilon_{F}\epsilon_{T}^{2} & y_{\tau\mu}\epsilon_{F}\epsilon_{T} & y_{\tau\tau}\epsilon_{F} \end{pmatrix} .$$
(C.31a)

as we do with the model in the main text. Moreover, the charges of the weightons  $(\phi_F, \phi_T)$  under  $S_4^A$ will forbid higher-order corrections to these matrices.

Field	SU(5)	$S_4^A$	$k_A$	$S_4^B$	$k_B$	$S_4^C$	$k_C$
F	5	1	$+\frac{1}{2}$	1	0	3	0
$T_1$	10	1	+1	1	0	1′	0
$T_2$	10	1	$+\frac{1}{2}$	1	0	1′	0
$T_3$	10	1	0	1	0	1′	0
$N_A^c$	1	1	4	1	0	1	0
$N_B^c$	1	1	0	1	+2	1	0
$\Phi_{AC}$	1	3	0	1	0	3	0
$\Phi_{BC}$	1	1	0	3	0	3	0
$\phi_T$	1	1	$-\frac{1}{2}$	1	0	1	0
$\phi_F$	1	1	$-\frac{1}{2}$	1	0	1	+2
$H_5$	5	1	0	1	0	1	0
$H_{\overline{5}}$	$\overline{5}$	1	0	1	0	1	0
$H_{\overline{45}}$	$\overline{45}$	1	0	1	0	1	0

Table C.2: A seemingly simpler assignment under the three modular symmetries, but which lead to non-negligible contributions which spoil the CSD(n) structure. As in the main text, we do not show the messenger fields nor any necessary driving fields.

As we can see from the weight assignments for the RH neutrinos, here the SU(5) singlets will have bare mass terms, at the renormalizable level, contrary to what we see in Eq. (7.67). Mixed terms are still forbidden by the absence of the  $Y_1^{(2)}$  modular form, needed to make a  $N_A^c N_B^c$  term invariant.

The last ingredient needed is to reproduce the Dirac mass matrix compatible with the CSD(n) structure. There, we find that the invariants

$$w_D \supset H_5 \left\{ a Y_{3'}^{(4)}(\tau_A) F\left(\frac{\phi_T}{\Lambda} \frac{\langle \Phi_{AC} \rangle}{\Lambda}\right) N_A^c + b Y_{3'}^{(2)}(\tau_B) F\left(\frac{\phi_T}{\Lambda} \frac{\langle \Phi_{BC} \rangle}{\Lambda}\right) N_B^c \right\}$$
 (C.32)

are present, as required, similarly to Eq. (7.63). On the other hand, we can now make another set of invariants, by replacing  $\phi_T$  with  $\phi_F$ . If we follow the same tensor product contractions as the terms in  $w_D$ , these would be forbidden by the absence of the  $Y_1^{(2)}$  modular form. However, we can contract the term as (we show the example for  $FN_A^c$ )

$$\left(\left(\left(Y_{\mathbf{3'}}^{(2)}(\tau_C)\otimes(F\phi_F)\right)_{\mathbf{3}}\otimes\langle\Phi_{AC}\rangle\otimes Y_{\mathbf{3}}^{(4)}(\tau_A)\right)_{\mathbf{1'}}\otimes(N_A^c)_{\mathbf{1'}}\right)_{\mathbf{1}},\tag{C.33}$$

which spoil the  $Y_D$  structure. At first glance, we could argue that we could choose the model's messengers such that the terms in Eq. (C.32) are present, but those of Eq. (C.33) are absent. However, we checked that, for the simplest choice of messengers, both terms are necessarily present. This is shown in the diagrams of Fig. C.1, where we can clearly see that the same set of messengers lead to the existence of both terms. The assignments of the model presented in the main text are mostly motivated to eliminate

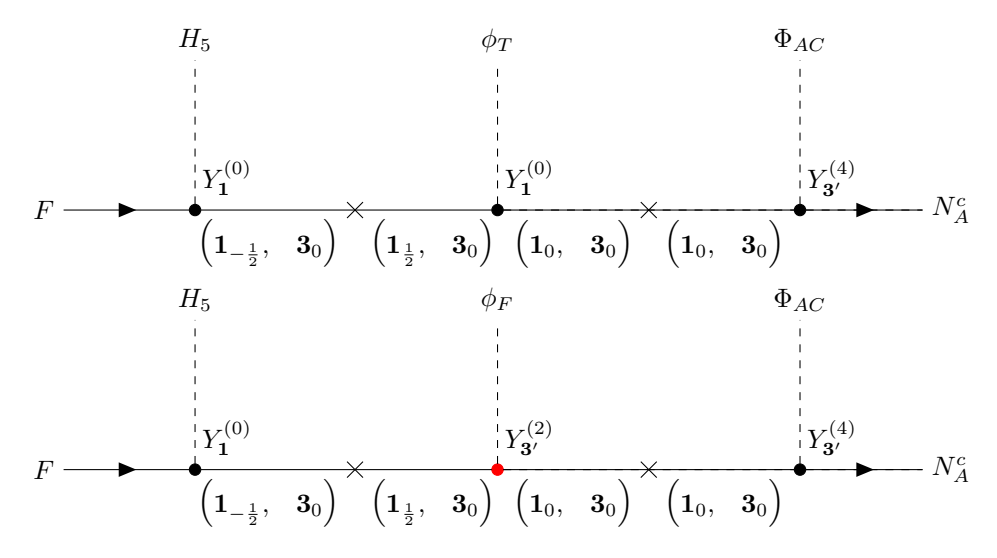


Figure C.1: The diagrams leading to the desired (top) and undesired (bottom) terms for  $w_D$ . The modular forms refer to  $S_4^A$ , as the remaining are trivial. The messengers are fermionic SU(5) singlets, represented by the  $S_4^A$  and  $S_4^C$  representations and weights, and assumed to transform trivially under  $S_4^B$ .

these terms, and keep an unspoiled  $Y_D$ , such that the corrections to the  $\mathrm{CSD}(n)$  structure arise solely from the non-diagonal  $Y_\ell$ , in a suppressed manner.

## C.5 Driving Superpotential for the Weighton Fields

Our goal in this appendix is to show that it is possible to arrange a scalar potential for the weighton fields such that they can function as the FN suppression. We follow ref. [144] and arrange a superpotential to drive the weighton fields. Given the choice of weights, we can take the driving field  $\chi$  to transform as  $\chi \sim (\mathbf{1}_4, \mathbf{1}_4, \mathbf{1}_0)$  under  $S_4^{A,B,C}$  respectively. Making use of the bi-triplets, we can write

$$W_{\text{driving}} = \chi \left[ -Y_{\mathbf{1}}^{(4)}(\tau_A)Y_{\mathbf{1}}^{(4)}(\tau_B)Y_{\mathbf{1}}^{(0)}(\tau_C)M^2 + Y_{\mathbf{3'}}^{(2)}(\tau_A) \left\langle \Phi_{AC} \right\rangle \left\langle \Phi_{BC} \right\rangle^T Y_{\mathbf{3'}}^{(2)}(\tau_B) \quad \frac{\phi_T^4}{M_{fl}^2} + \left( Y_{\mathbf{3'}}^{(2)}(\tau_A) \left\langle \Phi_{AC} \right\rangle Y_{\mathbf{3'}}^{(2)}(\tau_C) \right) \left( Y_{\mathbf{3'}}^{(2)}(\tau_B) \left\langle \Phi_{BC} \right\rangle Y_{\mathbf{3'}}^{(2)}(\tau_C) \right) \quad \frac{\phi_T^2 \phi_F^2}{M_{fl}^2}$$

$$+ \left( Y_{\mathbf{3'}}^{(2)}(\tau_A) \langle \Phi_{AC} \rangle Y_{\mathbf{3'}}^{(4)}(\tau_C) \right) \left( Y_{\mathbf{3'}}^{(2)}(\tau_B) \langle \Phi_{BC} \rangle Y_{\mathbf{3'}}^{(4)}(\tau_C) \right) \quad \frac{\phi_F^4}{M_{fl}^2} \quad \left[ (C.34) \right]$$

where  $M^2$  is a dimensionful scale, and  $M_{fl}$  is the scale suppression due to the non-renormalizable nature of the dimension 5 operators. Since these terms are each governed by an arbitrary coefficient, the choice of  $\langle \phi_F \rangle \sim \lambda^3$  and  $\langle \phi_T \rangle \sim \lambda^2$  can originate from suitable choices of the superpotential constants.



# Modular $S'_4$ and Hierarchies at the Cusp

### D.1 Group Theory

The homogeneous finite modular group  $S_4' \equiv SL(2, \mathbb{Z}_4)$ , with group ID [48, 30] in the computer algebra system GAP [438, 439], is a group of 48 elements defined by the three generators S, T and R satisfying:

$$S^2 = R$$
,  $T^4 = (ST)^3 = R^2 = 1$ ,  $TR = RT$ . (D.1)

It admits 10 irreducible representations, denoted by

$$1, \hat{1}, 1', \hat{1}', 2, \hat{2}, 3, \hat{3}, 3', \hat{3}',$$
 (D.2)

where irreps without a hat have a direct correspondence with  $S_4$  irreps. The working basis for the representation matrices of the group generators coincides with the one used in Ref. [142], where also Clebsch-Gordan coefficients can be found. The chosen basis is symmetric and thus convenient for the study of modular symmetry extended by a gCP symmetry [139, 142].

#### D.2 Modular Forms

Modular multiplets for the homogeneous finite modular group  $S_4'$  can be written in terms of the two functions  $\theta(\tau)$  and  $\varepsilon(\tau)$  defined in Eq. (8.5), and can be found in section 3 and appendix D of Ref. [142], for weights up to k=10. We make use of the modular multiplets  $Y_{\mathbf{r}}^{(k)}(\tau)$  given therein, which we reproduce here for convenience, up to weight k=8. Note that the dimensionality of the linear spaces of  $S_4'$  modular forms of weight k is given by 2k+1, in agreement with these results.

Of particular relevance to our study is an ST-diagonal basis, where the power structure in  $\epsilon \sim \tau - \omega$  becomes apparent. Such a basis can be defined by  $\rho_{2^*}(ST) = \operatorname{diag}(\omega, \omega^2)$  and  $\rho_{3^*}(ST) = \operatorname{diag}(1, \omega, \omega^2)$  for all doublets  $2^*$  and triplets  $3^*$  of  $S_4'$ . For modular forms in these representations, the relative suppressions of modular multiplet elements are physically significant, as argued in Section 8.1.1. Therefore, we additionally present the profile of modular doublets and triplets in the ST-diagonal basis, in the vicinity of the cusp  $\omega$ , ignoring multiplet normalisation, i.e. the  $\mathcal{O}(\epsilon^0)$  term is scaled to 1, and keeping only the leading term in each entry. This approximate proportionality is denoted by the symbol " $\chi$ ". Some modular forms vanish at  $\tau = \omega$ , e.g.  $Y_2^{(6)}$  for which the overall factor of  $\epsilon$  is shown explicitly.

Note finally that whenever there is more than one multiplet for the same weight k and irrep  $\mathbf{r}$ , one is also free to choose the basis of the corresponding subspace — in a bottom-up approach there is no known rule to select which are the "correct" linear combinations of the multiplets one should consider. Moreover, one of these combinations may vanish at a certain  $\tau$  (e.g. the cusp). While the triplets of interest, as defined in [142], do not vanish at  $\tau = \omega$ , one may find a linear combination of these forms (with the same k and  $\mathbf{r}$ ) that does. In this specific basis, normalising the  $\epsilon$ -suppressed form may then suggest a different  $\epsilon$  power structure for the triplet. Such a basis choice may be a source of fine-tuning, and we do not consider it further in this work.

#### Weight 1

$$Y_{\widehat{\mathbf{3}}}^{(1)}(\tau) = \begin{pmatrix} \sqrt{2} \,\varepsilon\,\theta \\ \varepsilon^2 \\ -\theta^2 \end{pmatrix} \xrightarrow[ST\text{-diag.}]{} \begin{pmatrix} \frac{1}{\sqrt{3}} \,\epsilon \\ 1 \\ -\frac{1}{6} \,\epsilon^2 \end{pmatrix}.$$

#### Weight 2

$$Y_{\mathbf{2}}^{(2)}(\tau) = \begin{pmatrix} \frac{1}{\sqrt{2}} \left(\theta^4 + \varepsilon^4\right) \\ -\sqrt{6} \, \varepsilon^2 \, \theta^2 \end{pmatrix} \xrightarrow{\text{ST-diag.}} \begin{pmatrix} -\frac{2}{\sqrt{3}} \, \epsilon \\ 1 \end{pmatrix},$$

$$Y_{\mathbf{3'}}^{(2)}(\tau) = \begin{pmatrix} \frac{1}{\sqrt{2}} \left(\theta^4 - \varepsilon^4\right) \\ -2 \, \varepsilon \, \theta^3 \\ -2 \, \varepsilon^3 \, \theta \end{pmatrix} \xrightarrow{\text{ST-diag.}} \begin{pmatrix} -\frac{1}{2} \, \epsilon^2 \\ \frac{1}{\sqrt{3}} \, \epsilon \\ 1 \end{pmatrix}.$$

$$Y_{\widehat{\mathbf{1}}'}^{(3)}(\tau) = \sqrt{3} \left( \varepsilon \, \theta^5 - \varepsilon^5 \, \theta \right) \,,$$

$$Y_{\widehat{\mathbf{3}}}^{(3)}(\tau) = \begin{pmatrix} \varepsilon^5 \, \theta + \varepsilon \, \theta^5 \\ \frac{1}{2\sqrt{2}} \left( 5 \, \varepsilon^2 \, \theta^4 - \varepsilon^6 \right) \\ \frac{1}{2\sqrt{2}} \left( \theta^6 - 5 \, \varepsilon^4 \, \theta^2 \right) \end{pmatrix} \xrightarrow{\underbrace{\otimes}} \begin{pmatrix} 1 \\ \frac{5}{6} \, \epsilon^2 \\ -\frac{1}{\sqrt{3}} \, \epsilon \end{pmatrix},$$

$$Y_{\widehat{\mathbf{3}}'}^{(3)}(\tau) = \frac{1}{2} \begin{pmatrix} -4\sqrt{2} \, \varepsilon^3 \, \theta^3 \\ \theta^6 + 3 \, \varepsilon^4 \, \theta^2 \\ \frac{3}{2} \, \varepsilon^2 \, \theta^4 - \varepsilon^6 \end{pmatrix} \xrightarrow{\underbrace{\otimes}} \begin{pmatrix} 1 \\ -\frac{1}{2} \, \epsilon^2 \\ \sqrt{3} \, \epsilon \end{pmatrix}.$$

#### Weight 4

$$\begin{split} Y_{\mathbf{1}}^{(4)}(\tau) &= \frac{1}{2\sqrt{3}} \left(\theta^8 + 14\,\varepsilon^4\,\theta^4 + \varepsilon^8\right) \;, \\ Y_{\mathbf{2}}^{(4)}(\tau) &= \begin{pmatrix} \frac{1}{4} \left(\theta^8 - 10\,\varepsilon^4\,\theta^4 + \varepsilon^8\right) \\ \sqrt{3} \left(\varepsilon^2\,\theta^6 + \varepsilon^6\,\theta^2\right) \end{pmatrix} \xrightarrow{ST\text{-diag.}} \begin{pmatrix} 1 \\ -\frac{4}{3}\,\epsilon^2 \end{pmatrix} \;, \\ Y_{\mathbf{3}}^{(4)}(\tau) &= \frac{3}{2\sqrt{2}} \begin{pmatrix} \sqrt{2} \left(\varepsilon^2\,\theta^6 - \varepsilon^6\,\theta^2\right) \\ \varepsilon^3\,\theta^5 - \varepsilon^7\,\theta \\ -\varepsilon\,\theta^7 + \varepsilon^5\,\theta^3 \end{pmatrix} \xrightarrow{ST\text{-diag.}} \begin{pmatrix} \frac{1}{\sqrt{3}}\,\epsilon \\ 1 \\ -\frac{1}{6}\,\epsilon^2 \end{pmatrix} \;, \\ Y_{\mathbf{3'}}^{(4)}(\tau) &= \begin{pmatrix} \frac{1}{4} \left(\theta^8 - \varepsilon^8\right) \\ \frac{1}{2\sqrt{2}} \left(\varepsilon\,\theta^7 + 7\,\varepsilon^5\,\theta^3\right) \\ \frac{1}{2\sqrt{2}} \left(7\,\varepsilon^3\,\theta^5 + \varepsilon^7\,\theta\right) \end{pmatrix} \xrightarrow{ST\text{-diag.}} \begin{pmatrix} -\sqrt{3}\,\epsilon \\ 1 \\ \frac{7}{6}\,\epsilon^2 \end{pmatrix} \;. \end{split}$$

$$\begin{split} Y_{\widehat{\mathbf{2}}}^{(5)}(\tau) &= \begin{pmatrix} \frac{3}{2} \left( \varepsilon^3 \, \theta^7 - \varepsilon^7 \, \theta^3 \right) \\ \frac{\sqrt{3}}{4} \left( \varepsilon \, \theta^9 - \varepsilon^9 \, \theta \right) \end{pmatrix} \xrightarrow{\sum} \begin{pmatrix} \frac{2}{\sqrt{3}} \, \epsilon \\ 1 \end{pmatrix} \,, \\ Y_{\widehat{\mathbf{3}},1}^{(5)}(\tau) &= \begin{pmatrix} \frac{6\sqrt{2}}{\sqrt{5}} \, \varepsilon^5 \, \theta^5 \\ \frac{3}{8\sqrt{5}} \left( 5 \, \varepsilon^2 \, \theta^8 + 10 \, \varepsilon^6 \, \theta^4 + \varepsilon^{10} \right) \\ -\frac{3}{8\sqrt{5}} \left( \theta^{10} + 10 \, \varepsilon^4 \, \theta^6 + 5 \, \varepsilon^8 \, \theta^2 \right) \end{pmatrix} \xrightarrow{\sum} \begin{pmatrix} -\frac{5}{2} \, \epsilon^2 \\ -\frac{5}{\sqrt{3}} \, \epsilon \\ 1 \end{pmatrix} \,, \\ Y_{\widehat{\mathbf{3}},2}^{(5)}(\tau) &= \begin{pmatrix} \frac{3}{4} \left( \varepsilon \, \theta^9 - 2 \, \varepsilon^5 \, \theta^5 + \varepsilon^9 \, \theta \right) \\ \frac{3}{\sqrt{2}} \left( -\varepsilon^2 \, \theta^8 + \varepsilon^6 \, \theta^4 \right) \\ \frac{3}{\sqrt{2}} \left( -\varepsilon^4 \, \theta^6 + \varepsilon^8 \, \theta^2 \right) \end{pmatrix} \xrightarrow{\sum} \begin{pmatrix} -\frac{1}{2} \, \epsilon^2 \\ \frac{1}{\sqrt{3}} \, \epsilon \\ 1 \end{pmatrix} \,, \end{split}$$

$$Y_{\widehat{\mathbf{3}}'}^{(5)}(\tau) = \begin{pmatrix} 2\left(\varepsilon^3\,\theta^7 + \varepsilon^7\,\theta^3\right) \\ \frac{1}{4\sqrt{2}}\left(\theta^{10} - 14\,\varepsilon^4\,\theta^6 - 3\,\varepsilon^8\,\theta^2\right) \\ \frac{1}{4\sqrt{2}}\left(3\,\varepsilon^2\,\theta^8 + 14\,\varepsilon^6\,\theta^4 - \varepsilon^{10}\right) \end{pmatrix} \xrightarrow{\bigotimes} \begin{cases} \frac{3}{2}\,\epsilon^2 \\ -\frac{1}{\sqrt{3}}\,\epsilon \\ 1 \end{cases}.$$

#### Weight 6

$$\begin{split} Y_{\mathbf{1}}^{(6)}(\tau) &= \frac{1}{4\sqrt{6}} \left(\theta^{12} - 33\,\varepsilon^{4}\,\theta^{8} - 33\,\varepsilon^{8}\,\theta^{4} + \varepsilon^{12}\right)\,, \\ Y_{\mathbf{1}'}^{(6)}(\tau) &= \frac{3}{2}\sqrt{\frac{3}{2}} \left(\varepsilon^{2}\,\theta^{10} - 2\,\varepsilon^{6}\,\theta^{6} + \varepsilon^{10}\,\theta^{2}\right)\,, \\ Y_{\mathbf{2}}^{(6)}(\tau) &= \begin{pmatrix} \frac{1}{8} \left(\theta^{12} + 15\,\varepsilon^{4}\,\theta^{8} + 15\,\varepsilon^{8}\,\theta^{4} + \varepsilon^{12}\right) \\ -\frac{\sqrt{3}}{4} \left(\varepsilon^{2}\,\theta^{10} + 14\,\varepsilon^{6}\,\theta^{6} + \varepsilon^{10}\,\theta^{2}\right) \end{pmatrix} \xrightarrow{\sum_{ST\text{-diag.}}} \epsilon \begin{pmatrix} -\frac{2}{\sqrt{3}}\,\epsilon \\ 1 \end{pmatrix}\,, \\ Y_{\mathbf{3}}^{(6)}(\tau) &= \begin{pmatrix} \frac{3}{2} \left(\varepsilon^{2}\,\theta^{10} - \varepsilon^{10}\,\theta^{2}\right) \\ \frac{3}{4\sqrt{2}} \left(5\,\varepsilon^{3}\,\theta^{9} - 6\,\varepsilon^{7}\,\theta^{5} + \varepsilon^{11}\,\theta\right) \\ \frac{3}{4\sqrt{2}} \left(\varepsilon\,\theta^{11} - 6\,\varepsilon^{5}\,\theta^{7} + 5\,\varepsilon^{9}\,\theta^{3}\right) \end{pmatrix} \xrightarrow{\sum_{ST\text{-diag.}}} \begin{pmatrix} 1 \\ \frac{5}{6}\,\epsilon^{2} \\ -\frac{1}{\sqrt{3}}\,\epsilon \end{pmatrix}\,, \\ Y_{\mathbf{3}',1}^{(6)}(\tau) &= \begin{pmatrix} -\frac{3}{8\sqrt{13}} \left(\theta^{12} - 3\,\varepsilon^{4}\,\theta^{8} + 3\,\varepsilon^{8}\,\theta^{4} - \varepsilon^{12}\right) \\ \frac{3\sqrt{2}}{\sqrt{13}} \left(3\,\varepsilon^{5}\,\theta^{7} + \varepsilon^{9}\,\theta^{3}\right) \\ \frac{3\sqrt{2}}{\sqrt{13}} \left(\varepsilon^{3}\,\theta^{9} + 3\,\varepsilon^{7}\,\theta^{5}\right) \end{pmatrix} \xrightarrow{\sum_{ST\text{-diag.}}} \begin{pmatrix} 1 \\ -\frac{5}{2}\,\epsilon^{2} \\ -\sqrt{3}\,\epsilon \end{pmatrix}\,, \\ Y_{\mathbf{3}',2}^{(6)}(\tau) &= \begin{pmatrix} 3 \left(\varepsilon^{4}\,\theta^{8} - \varepsilon^{8}\,\theta^{4}\right) \\ -\frac{3}{4\sqrt{2}} \left(\varepsilon\,\theta^{11} + 2\,\varepsilon^{5}\,\theta^{7} - 3\,\varepsilon^{9}\,\theta^{3}\right) \\ \frac{3}{4\sqrt{2}} \left(3\,\varepsilon^{3}\,\theta^{9} - 2\,\varepsilon^{7}\,\theta^{5} - \varepsilon^{11}\,\theta\right) \end{pmatrix} \xrightarrow{\sum_{ST\text{-diag.}}} \begin{pmatrix} 1 \\ -\frac{1}{2}\,\epsilon^{2} \\ \sqrt{3}\,\epsilon \end{pmatrix}\,. \end{split}$$

$$\begin{split} Y_{\widehat{\mathbf{1}}'}^{(7)}(\tau) &= \frac{1}{4} \sqrt{\frac{3}{2}} \left( -\varepsilon^{13} \, \theta - 13 \, \varepsilon^9 \, \theta^5 + 13 \, \varepsilon^5 \, \theta^9 + \varepsilon \, \theta^{13} \right) \,, \\ Y_{\widehat{\mathbf{2}}}^{(7)}(\tau) &= \begin{pmatrix} \frac{3}{2} \left( \varepsilon^3 \, \theta^{11} - \varepsilon^{11} \, \theta^3 \right) \\ -\frac{\sqrt{3}}{8} \left( \varepsilon \, \theta^{13} - 11 \, \varepsilon^5 \, \theta^9 + 11 \, \varepsilon^9 \, \theta^5 - \varepsilon^{13} \, \theta \right) \end{pmatrix} \xrightarrow{ST\text{-diag.}} \begin{pmatrix} 1 \\ \frac{4}{3} \, \epsilon^2 \end{pmatrix} \,, \\ Y_{\widehat{\mathbf{3}},1}^{(7)}(\tau) &= \begin{pmatrix} \frac{12}{\sqrt{13}} \left( \varepsilon^5 \, \theta^9 + \varepsilon^9 \, \theta^5 \right) \\ \frac{3}{8\sqrt{26}} \left( \varepsilon^2 \, \theta^{12} + 45 \, \varepsilon^6 \, \theta^8 + 19 \, \varepsilon^{10} \, \theta^4 - \varepsilon^{14} \right) \\ \frac{3}{8\sqrt{26}} \left( \theta^{14} - 19 \, \varepsilon^4 \, \theta^{10} - 45 \, \varepsilon^8 \, \theta^6 - \varepsilon^{12} \, \theta^2 \right) \end{pmatrix} \xrightarrow{ST\text{-diag.}} \begin{pmatrix} \sqrt{3} \, \epsilon \\ 1 \\ -\frac{5}{6} \, \epsilon^2 \end{pmatrix} \,, \end{split}$$

$$Y_{\widehat{\mathbf{3}},2}^{(7)}(\tau) = \begin{pmatrix} \frac{3}{8} \left( \varepsilon \, \theta^{13} - \varepsilon^{5} \, \theta^{9} - \varepsilon^{9} \, \theta^{5} + \varepsilon^{13} \, \theta \right) \\ \frac{3}{4\sqrt{2}} \left( \varepsilon^{2} \, \theta^{12} + 6 \, \varepsilon^{6} \, \theta^{8} - 7 \, \varepsilon^{10} \, \theta^{4} \right) \\ \frac{3}{4\sqrt{2}} \left( 7 \, \varepsilon^{4} \, \theta^{10} - 6 \, \varepsilon^{8} \, \theta^{6} - \varepsilon^{12} \, \theta^{2} \right) \end{pmatrix} \xrightarrow{\bigotimes} \begin{cases} -\sqrt{3} \, \epsilon \\ 1 \\ \frac{7}{6} \, \epsilon^{2} \end{cases}, \\ Y_{\widehat{\mathbf{3}}',1}^{(7)}(\tau) = \begin{pmatrix} \frac{3}{4\sqrt{37}} \left( 7 \, \varepsilon^{3} \, \theta^{11} + 50 \, \varepsilon^{7} \, \theta^{7} + 7 \, \varepsilon^{11} \, \theta^{3} \right) \\ -\frac{3}{4\sqrt{74}} \left( \theta^{14} + 14 \, \varepsilon^{4} \, \theta^{10} + 49 \, \varepsilon^{8} \, \theta^{6} \right) \\ \frac{3}{4\sqrt{74}} \left( 49 \, \varepsilon^{6} \, \theta^{8} + 14 \, \varepsilon^{10} \, \theta^{4} + \varepsilon^{14} \right) \end{pmatrix} \xrightarrow{\bigotimes} \begin{cases} -\sqrt{3} \, \epsilon \\ 1 \\ -\frac{49}{6} \, \epsilon^{2} \end{cases}, \\ Y_{\widehat{\mathbf{3}}',2}^{(7)}(\tau) = \begin{pmatrix} \frac{9}{4} \left( \varepsilon^{3} \, \theta^{11} - 2 \, \varepsilon^{7} \, \theta^{7} + \varepsilon^{11} \, \theta^{3} \right) \\ \frac{9}{4\sqrt{2}} \left( \varepsilon^{4} \, \theta^{10} - 2 \, \varepsilon^{8} \, \theta^{6} + \varepsilon^{12} \, \theta^{2} \right) \\ -\frac{9}{4\sqrt{2}} \left( \varepsilon^{2} \, \theta^{12} - 2 \, \varepsilon^{6} \, \theta^{8} + \varepsilon^{10} \, \theta^{4} \right) \end{pmatrix} \xrightarrow{\bigotimes} \begin{cases} \frac{1}{\sqrt{3}} \, \epsilon \\ 1 \\ -\frac{1}{6} \, \epsilon^{2} \end{cases}. \end{cases}$$

$$\begin{split} Y_{\mathbf{1}}^{(8)}(\tau) &= \frac{1}{8\sqrt{6}} \left( \theta^{16} + 28\,\varepsilon^4\,\theta^{12} + 198\,\varepsilon^8\,\theta^8 + 28\,\varepsilon^{12}\,\theta^4 + \varepsilon^{16} \right) \,, \\ Y_{\mathbf{2},1}^{(8)}(\tau) &= \begin{pmatrix} \frac{9}{16\sqrt{82}} \left( \theta^{16} - 130\,\varepsilon^8\,\theta^8 + \varepsilon^{16} \right) \\ \frac{3}{8}\sqrt{\frac{3}{82}} \left( 5\,\varepsilon^2\,\theta^{14} + 91\,\varepsilon^6\,\theta^{10} + 91\,\varepsilon^{10}\,\theta^6 + 5\,\varepsilon^{14}\,\theta^2 \right) \end{pmatrix} \xrightarrow{ST\text{-diag.}} \begin{pmatrix} -\frac{34}{\sqrt{3}}\,\epsilon \\ 1 \end{pmatrix} \,, \\ Y_{\mathbf{2},2}^{(8)}(\tau) &= \begin{pmatrix} \frac{9}{4} \left( \varepsilon^4\,\theta^{12} - 2\,\varepsilon^8\,\theta^8 + \varepsilon^{12}\,\theta^4 \right) \\ \frac{3\sqrt{3}}{8} \left( \varepsilon^2\,\theta^{14} - \varepsilon^6\,\theta^{10} - \varepsilon^{10}\,\theta^6 + \varepsilon^{14}\,\theta^2 \right) \end{pmatrix} \xrightarrow{ST\text{-diag.}} \begin{pmatrix} \frac{2}{\sqrt{3}}\,\epsilon \\ 1 \end{pmatrix} \,, \\ Y_{\mathbf{3},1}^{(8)}(\tau) &= \begin{pmatrix} 9\,\sqrt{\frac{2}{5}} \left( \varepsilon^6\,\theta^{10} - \varepsilon^{10}\,\theta^6 + \varepsilon^{14}\,\theta^2 \right) \end{pmatrix} \xrightarrow{ST\text{-diag.}} \begin{pmatrix} -\frac{5}{2}\,\epsilon^2 \\ 1 \end{pmatrix} \,, \\ Y_{\mathbf{3},1}^{(8)}(\tau) &= \begin{pmatrix} 9\,\sqrt{\frac{2}{5}} \left( \varepsilon^6\,\theta^{10} - \varepsilon^{10}\,\theta^6 \right) \\ \frac{9}{16\sqrt{5}} \left( 5\,\varepsilon^3\,\theta^{13} + 5\,\varepsilon^7\,\theta^9 - 9\,\varepsilon^{11}\,\theta^5 - \varepsilon^{15}\,\theta \right) \\ -\frac{9}{16\sqrt{5}} \left( \varepsilon\,\theta^{15} + 9\,\varepsilon^5\,\theta^{11} - 5\,\varepsilon^9\,\theta^7 - 5\,\varepsilon^{13}\,\theta^3 \right) \end{pmatrix} \xrightarrow{ST\text{-diag.}} \begin{pmatrix} -\frac{5}{2}\,\epsilon^2 \\ -\frac{5}{\sqrt{3}}\,\epsilon \\ 1 \end{pmatrix} \,, \\ Y_{\mathbf{3},2}^{(8)}(\tau) &= \begin{pmatrix} -\frac{9}{8} \left( \varepsilon^2\,\theta^{14} - 3\,\varepsilon^6\,\theta^{10} + 3\,\varepsilon^{10}\,\theta^6 - \varepsilon^{14}\,\theta^2 \right) \\ \frac{9}{2\sqrt{2}} \left( \varepsilon^3\,\theta^{13} - 2\,\varepsilon^7\,\theta^9 + \varepsilon^{11}\,\theta^5 \right) \\ \frac{9}{2\sqrt{2}} \left( \varepsilon^5\,\theta^{11} - 2\,\varepsilon^9\,\theta^7 + \varepsilon^{13}\,\theta^3 \right) \end{pmatrix} \xrightarrow{ST\text{-diag.}} \begin{pmatrix} -\frac{1}{2}\,\epsilon^2 \\ \frac{1}{\sqrt{3}}\,\epsilon \\ 1 \end{pmatrix} \,, \\ Y_{\mathbf{3},1}^{(8)}(\tau) &= \begin{pmatrix} \frac{3}{200\sqrt{2}} \left( \varepsilon\,\theta^{15} + 273\,\varepsilon^5\,\theta^{11} + 715\,\varepsilon^9\,\theta^7 + 35\,\varepsilon^{13}\,\theta^3 \right) \\ \frac{3}{200\sqrt{2}} \left( 35\,\varepsilon^3\,\theta^{13} + 715\,\varepsilon^7\,\theta^9 + 273\,\varepsilon^{11}\,\theta^5 + \varepsilon^{15}\,\theta \right) \end{pmatrix} \xrightarrow{ST\text{-diag.}} \begin{pmatrix} \frac{1}{7\sqrt{3}}\,\epsilon \\ \frac{41}{7\sqrt{3}}\,\epsilon \\ 1 \end{pmatrix} \,, \\ Y_{\mathbf{3},2}^{(8)}(\tau) &= \begin{pmatrix} 3 \left( \varepsilon^4\,\theta^{12} - \varepsilon^{12}\,\theta^4 \right) \\ \frac{3}{8\sqrt{2}} \left( \varepsilon\,\theta^{15} - 15\,\varepsilon^5\,\theta^{11} + 11\,\varepsilon^9\,\theta^7 + 3\,\varepsilon^{13}\,\theta^3 \right) \\ \frac{3}{8\sqrt{2}} \left( 3\,\varepsilon^3\,\theta^{13} + 11\,\varepsilon^7\,\theta^9 - 15\,\varepsilon^{11}\,\theta^5 + \varepsilon^{15}\,\theta \right) \end{pmatrix} \xrightarrow{ST\text{-diag.}} \begin{pmatrix} \frac{1}{2}\,\varepsilon^2 \\ -\frac{1}{\sqrt{3}}\,\epsilon \\ 1 \end{pmatrix} \,. \end{split}$$

# **Bibliography**

- [1] S. L. Glashow, Partial Symmetries of Weak Interactions, Nucl. Phys. 22 (1961) 579–588.
- [2] S. Weinberg, A Model of Leptons, Phys. Rev. Lett. 19 (1967) 1264–1266.
- [3] A. Salam, Weak and Electromagnetic Interactions, Conf. Proc. C 680519 (1968) 367–377.
- [4] C.-N. Yang and R. L. Mills, Conservation of Isotopic Spin and Isotopic Gauge Invariance, Phys. Rev. 96 (1954) 191–195.
- [5] R. Slansky, Group Theory for Unified Model Building, Phys. Rept. 79 (1981) 1–128.
- [6] R. J. Crewther, P. Di Vecchia, G. Veneziano, and E. Witten, Chiral Estimate of the Electric Dipole Moment of the Neutron in Quantum Chromodynamics, Phys. Lett. B 88 (1979) 123.
  [Erratum: Phys.Lett.B 91, 487 (1980)].
- [7] M. Pospelov and A. Ritz, Theta vacua, QCD sum rules, and the neutron electric dipole moment, Nucl. Phys. B 573 (2000) 177–200, [hep-ph/9908508].
- [8] χQCD Collaboration, J. Liang, A. Alexandru, T. Draper, K.-F. Liu, B. Wang, G. Wang, and Y.-B. Yang, Nucleon electric dipole moment from the θ term with lattice chiral fermions, Phys. Rev. D 108 (2023), no. 9 094512, [arXiv:2301.04331].
- [9] G. 't Hooft and M. J. G. Veltman, Regularization and Renormalization of Gauge Fields, Nucl. Phys. B 44 (1972) 189–213.
- [10] P. W. Higgs, Broken Symmetries and the Masses of Gauge Bosons, Phys. Rev. Lett. 13 (1964) 508–509.
- [11] P. W. Higgs, Broken symmetries, massless particles and gauge fields, Phys. Lett. 12 (1964) 132–133.
- [12] F. Englert and R. Brout, Broken Symmetry and the Mass of Gauge Vector Mesons, Phys. Rev. Lett. 13 (1964) 321–323.
- [13] T. W. B. Kibble, Symmetry breaking in nonAbelian gauge theories, Phys. Rev. 155 (1967) 1554–1561.
- [14] G. S. Guralnik, C. R. Hagen, and T. W. B. Kibble, Global Conservation Laws and Massless Particles, Phys. Rev. Lett. 13 (1964) 585–587.

- [15] S. Weinberg, Physical Processes in a Convergent Theory of the Weak and Electromagnetic Interactions, Phys. Rev. Lett. 27 (1971) 1688–1691.
- [16] S. Weinberg, General Theory of Broken Local Symmetries, Phys. Rev. D 7 (1973) 1068–1082.
- [17] P. Ramond, Journeys beyond the standard model, vol. 101. 1999.
- [18] S. Weinberg, The quantum theory of fields. Vol. 2: Modern applications. Cambridge University Press, 8, 2013.
- [19] N. Cabibbo, Unitary Symmetry and Leptonic Decays, Phys. Rev. Lett. 10 (1963) 531–533.
- [20] M. Kobayashi and T. Maskawa, CP Violation in the Renormalizable Theory of Weak Interaction, Prog. Theor. Phys. 49 (1973) 652–657.
- [21] Particle Data Group Collaboration, R. L. Workman et al., Review of Particle Physics, PTEP 2022 (2022) 083C01.
- [22] B. Pontecorvo, Neutrino Experiments and the Problem of Conservation of Leptonic Charge, Zh. Eksp. Teor. Fiz. 53 (1967) 1717–1725.
- [23] V. N. Gribov and B. Pontecorvo, Neutrino astronomy and lepton charge, Phys. Lett. B 28 (1969) 493.
- [24] L. Wolfenstein, Neutrino Oscillations in Matter, Phys. Rev. D 17 (1978) 2369–2374.
- [25] S. P. Mikheyev and A. Y. Smirnov, Resonance Amplification of Oscillations in Matter and Spectroscopy of Solar Neutrinos, Sov. J. Nucl. Phys. 42 (1985) 913–917.
- [26] Z. Maki, M. Nakagawa, and S. Sakata, Remarks on the unified model of elementary particles, Prog. Theor. Phys. 28 (1962) 870–880.
- [27] G. 't Hooft, Symmetry Breaking Through Bell-Jackiw Anomalies, Phys. Rev. Lett. 37 (1976) 8–11.
- [28] E. Majorana, Teoria simmetrica dell'elettrone e del positrone, Nuovo Cim. 14 (1937) 171–184.
- [29] P. F. de Salas, D. V. Forero, S. Gariazzo, P. Martínez-Miravé, O. Mena, C. A. Ternes, M. Tórtola, and J. W. F. Valle, 2020 global reassessment of the neutrino oscillation picture, JHEP 02 (2021) 071, [arXiv:2006.11237].
- [30] I. Esteban, M. C. Gonzalez-Garcia, M. Maltoni, T. Schwetz, and A. Zhou, The fate of hints: updated global analysis of three-flavor neutrino oscillations, JHEP 09 (2020) 178, [arXiv:2007.14792].
- [31] F. Capozzi, E. Di Valentino, E. Lisi, A. Marrone, A. Melchiorri, and A. Palazzo, *Unfinished fabric of the three neutrino paradigm*, *Phys. Rev. D* **104** (2021), no. 8 083031, [arXiv:2107.00532].
- [32] S. M. Bilenky, J. Hosek, and S. T. Petcov, On Oscillations of Neutrinos with Dirac and Majorana Masses, Phys. Lett. B 94 (1980) 495–498.

- [33] P. Langacker, S. T. Petcov, G. Steigman, and S. Toshev, Implications of the Mikheev-Smirnov-Wolfenstein (MSW) Mechanism of Amplification of Neutrino Oscillations in Matter, Nucl. Phys. B 282 (1987) 589–609.
- [34] J. Schechter and J. W. F. Valle, Neutrinoless Double beta Decay in SU(2) x U(1) Theories, Phys. Rev. D 25 (1982) 2951.
- [35] G. 't Hooft and M. J. G. Veltman, One loop divergencies in the theory of gravitation, Ann. Inst. H. Poincare A Phys. Theor. 20 (1974) 69–94.
- [36] J. D. Simon, The Faintest Dwarf Galaxies, Ann. Rev. Astron. Astrophys. 57 (2019), no. 1 375–415, [arXiv:1901.05465].
- [37] P. Salucci, The distribution of dark matter in galaxies, Astron. Astrophys. Rev. 27 (2019), no. 1 2, [arXiv:1811.08843].
- [38] S. W. Allen, A. E. Evrard, and A. B. Mantz, Cosmological Parameters from Observations of Galaxy Clusters, Ann. Rev. Astron. Astrophys. 49 (2011) 409-470, [arXiv:1103.4829].
- [39] N. A. Bahcall, R. Cen, R. Dave, J. P. Ostriker, and Q. Yu, The Mass-to-light function: Antibias and omega(m), Astrophys. J. 541 (2000) 1, [astro-ph/0002310].
- [40] Planck Collaboration, N. Aghanim et al., Planck 2018 results. VIII. Gravitational lensing, Astron. Astrophys. 641 (2020) A8, [arXiv:1807.06210].
- [41] A. A. Starobinsky, A New Type of Isotropic Cosmological Models Without Singularity, Phys. Lett. B 91 (1980) 99–102.
- [42] A. H. Guth, The Inflationary Universe: A Possible Solution to the Horizon and Flatness Problems, Phys. Rev. D 23 (1981) 347–356.
- [43] R. D. Peccei and H. R. Quinn, CP Conservation in the Presence of Instantons, Phys. Rev. Lett. 38 (1977) 1440–1443.
- [44] S. Weinberg, A New Light Boson?, Phys. Rev. Lett. 40 (1978) 223–226.
- [45] F. Wilczek, Problem of Strong P and T Invariance in the Presence of Instantons, Phys. Rev. Lett. 40 (1978) 279–282.
- [46] P. Langacker, Grand Unified Theories and Proton Decay, Phys. Rept. 72 (1981) 185.
- [47] G. C. Branco, P. M. Ferreira, L. Lavoura, M. N. Rebelo, M. Sher, and J. P. Silva, *Theory and phenomenology of two-Higgs-doublet models*, *Phys. Rept.* **516** (2012) 1–102, [arXiv:1106.0034].
- [48] C.-W. Chiang and K. Yagyu, Models with higher weak-isospin Higgs multiplets, Phys. Lett. B 786 (2018) 268–271, [arXiv:1808.10152].
- [49] T. D. Lee, A Theory of Spontaneous T Violation, Phys. Rev. D 8 (1973) 1226–1239.

- [50] F. J. Botella and J. P. Silva, Jarlskog like invariants for theories with scalars and fermions, Phys. Rev. D 51 (1995) 3870–3875, [hep-ph/9411288].
- [51] I. P. Ivanov, Building and testing models with extended Higgs sectors, Prog. Part. Nucl. Phys. 95 (2017) 160-208, [arXiv:1702.03776].
- [52] A. Barroso, P. M. Ferreira, and R. Santos, Charge and CP symmetry breaking in two Higgs doublet models, Phys. Lett. B 632 (2006) 684-687, [hep-ph/0507224].
- [53] C. C. Nishi, CP violation conditions in N-Higgs-doublet potentials, Phys. Rev. D 74 (2006) 036003, [hep-ph/0605153]. [Erratum: Phys.Rev.D 76, 119901 (2007)].
- [54] B. W. Lee, C. Quigg, and H. B. Thacker, The Strength of Weak Interactions at Very High-Energies and the Higgs Boson Mass, Phys. Rev. Lett. 38 (1977) 883–885.
- [55] B. W. Lee, C. Quigg, and H. B. Thacker, Weak Interactions at Very High-Energies: The Role of the Higgs Boson Mass, Phys. Rev. D 16 (1977) 1519.
- [56] H. Georgi and D. V. Nanopoulos, Suppression of Flavor Changing Effects From Neutral Spinless Meson Exchange in Gauge Theories, Phys. Lett. B 82 (1979) 95–96.
- [57] L. Lavoura and J. P. Silva, Fundamental CP violating quantities in a SU(2) x U(1) model with many Higgs doublets, Phys. Rev. D 50 (1994) 4619–4624, [hep-ph/9404276].
- [58] S. Davidson and H. E. Haber, Basis-independent methods for the two-Higgs-doublet model, Phys. Rev. D 72 (2005) 035004, [hep-ph/0504050]. [Erratum: Phys.Rev.D 72, 099902 (2005)].
- [59] F. J. Botella, G. C. Branco, and M. N. Rebelo, Minimal Flavour Violation and Multi-Higgs Models, Phys. Lett. B 687 (2010) 194–200, [arXiv:0911.1753].
- [60] H. E. Haber and Y. Nir, Multiscalar Models With a High-energy Scale, Nucl. Phys. B 335 (1990) 363–394.
- [61] H. E. Haber, Nonminimal Higgs sectors: The Decoupling limit and its phenomenological implications, in Joint U.S.-Polish Workshop on Physics from Planck Scale to Electro-Weak Scale (SUSY 94), 12, 1994. hep-ph/9501320.
- [62] I. F. Ginzburg, M. Krawczyk, and P. Osland, Resolving SM like scenarios via Higgs boson production at a photon collider. 1. 2HDM versus SM, hep-ph/0101208.
- [63] J. F. Gunion and H. E. Haber, The CP conserving two Higgs doublet model: The Approach to the decoupling limit, Phys. Rev. D 67 (2003) 075019, [hep-ph/0207010].
- [64] M. Carena, I. Low, N. R. Shah, and C. E. M. Wagner, Impersonating the Standard Model Higgs Boson: Alignment without Decoupling, JHEP 04 (2014) 015, [arXiv:1310.2248].
- [65] M. Carena, H. E. Haber, I. Low, N. R. Shah, and C. E. M. Wagner, Complementarity between Nonstandard Higgs Boson Searches and Precision Higgs Boson Measurements in the MSSM, Phys. Rev. D 91 (2015), no. 3 035003, [arXiv:1410.4969].

- [66] P. S. Bhupal Dev and A. Pilaftsis, Maximally Symmetric Two Higgs Doublet Model with Natural Standard Model Alignment, JHEP 12 (2014) 024, [arXiv:1408.3405]. [Erratum: JHEP 11, 147 (2015)].
- [67] D. Das and I. Saha, Alignment limit in three Higgs-doublet models, Phys. Rev. D 100 (2019), no. 3 035021, [arXiv:1904.03970].
- [68] D. Das and I. Saha, Search for a stable alignment limit in two-Higgs-doublet models, Phys. Rev. D 91 (2015), no. 9 095024, [arXiv:1503.02135].
- [69] G. Bhattacharyya, D. Das, P. B. Pal, and M. N. Rebelo, Scalar sector properties of two-Higgs-doublet models with a global U(1) symmetry, JHEP 10 (2013) 081, [arXiv:1308.4297].
- [70] A. Pilaftsis, Symmetries for standard model alignment in multi-Higgs doublet models, Phys. Rev. D 93 (2016), no. 7 075012, [arXiv:1602.02017].
- [71] N. Darvishi, M. R. Masouminia, and A. Pilaftsis, Maximally symmetric three-Higgs-doublet model, Phys. Rev. D 104 (2021), no. 11 115017, [arXiv:2106.03159].
- [72] G. Bhattacharyya, D. Das, and P. B. Pal, Modified Higgs couplings and unitarity violation, Phys. Rev. D 87 (2013) 011702, [arXiv:1212.4651].
- [73] LHC Higgs Cross Section Working Group Collaboration, A. David, A. Denner, M. Duehrssen, M. Grazzini, C. Grojean, G. Passarino, M. Schumacher, M. Spira, G. Weiglein, and M. Zanetti, LHC HXSWG interim recommendations to explore the coupling structure of a Higgs-like particle, arXiv:1209.0040.
- [74] LHC Higgs Cross Section Working Group Collaboration, J. R. Andersen et al., Handbook of LHC Higgs Cross Sections: 3. Higgs Properties, arXiv:1307.1347.
- [75] A. Milagre and L. Lavoura, Unitarity constraints on large multiplets of arbitrary gauge groups, Nucl. Phys. B 1004 (2024) 116542, [arXiv:2403.12914].
- [76] A. Zee, Quantum Field Theory in a Nutshell: Second Edition. Princeton University Press, 2, 2010.
- [77] W. Grimus and L. Lavoura, The Seesaw mechanism at arbitrary order: Disentangling the small scale from the large scale, JHEP 11 (2000) 042, [hep-ph/0008179].
- [78] P. Minkowski,  $\mu \to e \gamma$  at a Rate of One Out of  $10^9$  Muon Decays?, Phys. Lett. B **67** (1977) 421-428.
- [79] M. Gell-Mann, P. Ramond, and R. Slansky, Complex Spinors and Unified Theories, Conf. Proc. C 790927 (1979) 315–321, [arXiv:1306.4669].
- [80] T. Yanagida, Horizontal gauge symmetry and masses of neutrinos, Conf. Proc. C 7902131 (1979) 95–99.

- [81] R. N. Mohapatra and G. Senjanovic, Neutrino Mass and Spontaneous Parity Nonconservation, Phys. Rev. Lett. 44 (1980) 912.
- [82] J. Schechter and J. W. F. Valle, Neutrino Masses in SU(2) x U(1) Theories, Phys. Rev. D 22 (1980) 2227.
- [83] S. L. Glashow, J. Iliopoulos, and L. Maiani, Weak Interactions with Lepton-Hadron Symmetry, Phys. Rev. D 2 (1970) 1285–1292.
- [84] Gargamelle Neutrino Collaboration, F. J. Hasert et al., Observation of Neutrino Like Interactions Without Muon Or Electron in the Gargamelle Neutrino Experiment, Phys. Lett. B 46 (1973) 138–140.
- [85] A. D. Sakharov, Violation of CP Invariance, C asymmetry, and baryon asymmetry of the universe, Pisma Zh. Eksp. Teor. Fiz. 5 (1967) 32–35.
- [86] M. B. Gavela, P. Hernandez, J. Orloff, and O. Pene, Standard model CP violation and baryon asymmetry, Mod. Phys. Lett. A 9 (1994) 795–810, [hep-ph/9312215].
- [87] Z.-z. Xing, Quark Mass Hierarchy and Flavor Mixing Puzzles, Int. J. Mod. Phys. A 29 (2014) 1430067, [arXiv:1411.2713].
- [88] H. Ishimori, T. Kobayashi, H. Ohki, Y. Shimizu, H. Okada, and M. Tanimoto, Non-Abelian Discrete Symmetries in Particle Physics, Prog. Theor. Phys. Suppl. 183 (2010) 1–163, [arXiv:1003.3552].
- [89] G. Altarelli and F. Feruglio, Discrete Flavor Symmetries and Models of Neutrino Mixing, Rev. Mod. Phys. 82 (2010) 2701–2729, [arXiv:1002.0211].
- [90] S. F. King, A. Merle, S. Morisi, Y. Shimizu, and M. Tanimoto, Neutrino Mass and Mixing: from Theory to Experiment, New J. Phys. 16 (2014) 045018, [arXiv:1402.4271].
- [91] M. Tanimoto, Neutrinos and flavor symmetries, AIP Conf. Proc. 1666 (2015), no. 1 120002.
- [92] S. T. Petcov, Discrete Flavour Symmetries, Neutrino Mixing and Leptonic CP Violation, Eur. Phys. J. C 78 (2018), no. 9 709, [arXiv:1711.10806].
- [93] F. Feruglio and A. Romanino, Lepton flavor symmetries, Rev. Mod. Phys. 93 (2021), no. 1 015007, [arXiv:1912.06028].
- [94] S. F. King, Unified Models of Neutrinos, Flavour and CP Violation, Prog. Part. Nucl. Phys. 94 (2017) 217–256, [arXiv:1701.04413].
- [95] Z.-z. Xing, Flavor structures of charged fermions and massive neutrinos, Phys. Rept. **854** (2020) 1–147, [arXiv:1909.09610].
- [96] Particle Data Group Collaboration, P. A. Zyla et al., Review of Particle Physics, PTEP 2020 (2020), no. 8 083C01.

- [97] S. L. Glashow and S. Weinberg, Natural Conservation Laws for Neutral Currents, Phys. Rev. D 15 (1977) 1958.
- [98] E. A. Paschos, Diagonal Neutral Currents, Phys. Rev. D 15 (1977) 1966.
- [99] T. P. Cheng and M. Sher, Mass Matrix Ansatz and Flavor Nonconservation in Models with Multiple Higgs Doublets, Phys. Rev. D 35 (1987) 3484.
- [100] H. Fritzsch, Calculating the Cabibbo Angle, Phys. Lett. B 70 (1977) 436–440.
- [101] G. C. Branco, W. Grimus, and L. Lavoura, Relating the scalar flavor changing neutral couplings to the CKM matrix, Phys. Lett. B 380 (1996) 119–126, [hep-ph/9601383].
- [102] A. J. Buras, P. Gambino, M. Gorbahn, S. Jager, and L. Silvestrini, Universal unitarity triangle and physics beyond the standard model, Phys. Lett. B 500 (2001) 161–167, [hep-ph/0007085].
- [103] G. D'Ambrosio, G. F. Giudice, G. Isidori, and A. Strumia, *Minimal flavor violation: An Effective field theory approach*, *Nucl. Phys. B* **645** (2002) 155–187, [hep-ph/0207036].
- [104] T. Abe, R. Sato, and K. Yagyu, Muon specific two-Higgs-doublet model, JHEP 07 (2017) 012, [arXiv:1705.01469].
- [105] I. P. Ivanov and C. C. Nishi, Abelian symmetries of the N-Higgs-doublet model with Yukawa interactions, JHEP 11 (2013) 069, [arXiv:1309.3682].
- [106] B. L. Gonçalves, M. Knauss, and M. Sher, Lepton flavor specific extended Higgs model, Phys. Rev. D 107 (2023), no. 9 095001, [arXiv:2301.08641].
- [107] C. D. Froggatt and H. B. Nielsen, Hierarchy of Quark Masses, Cabibbo Angles and CP Violation, Nucl. Phys. B 147 (1979) 277–298.
- [108] L. Wolfenstein, Parametrization of the Kobayashi-Maskawa Matrix, Phys. Rev. Lett. 51 (1983) 1945.
- [109] S. Dimopoulos, Natural Generation of Fermion Masses, Phys. Lett. B 129 (1983) 417–428.
- [110] M. Leurer, Y. Nir, and N. Seiberg, Mass matrix models, Nucl. Phys. B 398 (1993) 319–342, [hep-ph/9212278].
- [111] L. E. Ibanez and G. G. Ross, Fermion masses and mixing angles from gauge symmetries, Phys. Lett. B 332 (1994) 100–110, [hep-ph/9403338].
- [112] P. Binetruy and P. Ramond, Yukawa textures and anomalies, Phys. Lett. B 350 (1995) 49–57, [hep-ph/9412385].
- [113] E. Dudas, S. Pokorski, and C. A. Savoy, Yukawa matrices from a spontaneously broken Abelian symmetry, Phys. Lett. B 356 (1995) 45–55, [hep-ph/9504292].

- [114] K. S. Babu and T. Enkhbat, Fermion mass hierarchy and electric dipole moments, Nucl. Phys. B 708 (2005) 511–531, [hep-ph/0406003].
- [115] Z.-z. Xing, Flavor structures of charged fermions and massive neutrinos, Phys. Rept. 854 (2020) 1–147, [arXiv:1909.09610].
- [116] K. S. Babu, TASI Lectures on Flavor Physics, in Theoretical Advanced Study Institute in Elementary Particle Physics: The Dawn of the LHC Era, pp. 49–123, 2010. arXiv:0910.2948.
- [117] K. S. Babu, S. M. Barr, and I. Gogoladze, Family Unification with SO(10), Phys. Lett. B 661 (2008) 124–128, [arXiv:0709.3491].
- [118] M. Fernández Navarro, S. F. King, and A. Vicente, *Tri-unification: a separate SU(5) for each fermion family*, *JHEP* **05** (2024) 130, [arXiv:2311.05683].
- [119] M. Reig, J. W. F. Valle, C. A. Vaquera-Araujo, and F. Wilczek, A Model of Comprehensive Unification, Phys. Lett. B 774 (2017) 667–670, [arXiv:1706.03116].
- [120] C. Hagedorn, Leptonic CP violation theory, J. Phys. Conf. Ser. 888 (2017), no. 1 012027.
- [121] S. F. King, Models of Neutrino Mass, Mixing and CP Violation, J. Phys. G 42 (2015) 123001, [arXiv:1510.02091].
- [122] R. N. Mohapatra and C. C. Nishi, S<sub>4</sub> Flavored CP Symmetry for Neutrinos, Phys. Rev. D 86 (2012) 073007, [arXiv:1208.2875].
- [123] T. Neder, Lepton Mixing Predictions from (Generalised) CP and Discrete Flavour Symmetry, J. Phys. Conf. Ser. 631 (2015), no. 1 012019, [arXiv:1503.09041].
- [124] S. F. King and C. Luhn, A New family symmetry for SO(10) GUTs, Nucl. Phys. B 820 (2009) 269-289, [arXiv:0905.1686].
- [125] C. S. Lam, Determining Horizontal Symmetry from Neutrino Mixing, Phys. Rev. Lett. 101 (2008) 121602, [arXiv:0804.2622].
- [126] I. Girardi, S. T. Petcov, A. J. Stuart, and A. V. Titov, Leptonic Dirac CP Violation Predictions from Residual Discrete Symmetries, Nucl. Phys. B 902 (2016) 1–57, [arXiv:1509.02502].
- [127] S. F. King and C. Luhn, Neutrino Mass and Mixing with Discrete Symmetry, Rept. Prog. Phys. 76 (2013) 056201, [arXiv:1301.1340].
- [128] F. Feruglio, Pieces of the Flavour Puzzle, Eur. Phys. J. C 75 (2015), no. 8 373, [arXiv:1503.04071].
- [129] S. Ferrara, D. Lust, A. D. Shapere, and S. Theisen, Modular Invariance in Supersymmetric Field Theories, Phys. Lett. B 225 (1989) 363.
- [130] S. Ferrara, . D. Lust, and S. Theisen, Target Space Modular Invariance and Low-Energy Couplings in Orbifold Compactifications, Phys. Lett. B 233 (1989) 147–152.

- [131] F. Feruglio, Are neutrino masses modular forms?, pp. 227-266. 2019. arXiv:1706.08749.
- [132] T. Kobayashi and M. Tanimoto, Modular flavor symmetric models, 7, 2023. arXiv:2307.03384.
- [133] F. Feruglio, A. Strumia, and A. Titov, Modular invariance and the QCD angle, JHEP 07 (2023) 027, [arXiv:2305.08908].
- [134] J. T. Penedo and S. T. Petcov, Finite modular symmetries and the strong CP problem, arXiv:2404.08032.
- [135] S. T. Petcov and M. Tanimoto, A<sub>4</sub> modular invariance and the strong CP problem, arXiv:2404.00858.
- [136] R. de Adelhart Toorop, F. Feruglio, and C. Hagedorn, Finite Modular Groups and Lepton Mixing, Nucl. Phys. B 858 (2012) 437–467, [arXiv:1112.1340].
- [137] I. de Medeiros Varzielas, S. F. King, and Y.-L. Zhou, Multiple modular symmetries as the origin of flavor, Phys. Rev. D 101 (2020), no. 5 055033, [arXiv:1906.02208].
- [138] X.-G. Liu, C.-Y. Yao, B.-Y. Qu, and G.-J. Ding, Half-integral weight modular forms and application to neutrino mass models, Phys. Rev. D 102 (2020), no. 11 115035, [arXiv:2007.13706].
- [139] P. P. Novichkov, J. T. Penedo, S. T. Petcov, and A. V. Titov, Generalised CP Symmetry in Modular-Invariant Models of Flavour, JHEP 07 (2019) 165, [arXiv:1905.11970].
- [140] A. Baur, H. P. Nilles, A. Trautner, and P. K. S. Vaudrevange, *Unification of Flavor, CP, and Modular Symmetries, Phys. Lett. B* **795** (2019) 7–14, [arXiv:1901.03251].
- [141] P. P. Novichkov, J. T. Penedo, S. T. Petcov, and A. V. Titov, Modular S<sub>4</sub> models of lepton masses and mixing, JHEP 04 (2019) 005, [arXiv:1811.04933].
- [142] P. P. Novichkov, J. T. Penedo, and S. T. Petcov, Double cover of modular S<sub>4</sub> for flavour model building, Nucl. Phys. B **963** (2021) 115301, [arXiv:2006.03058].
- [143] J. C. Criado, F. Feruglio, and S. J. D. King, Modular Invariant Models of Lepton Masses at Levels 4 and 5, JHEP 02 (2020) 001, [arXiv:1908.11867].
- [144] S. J. D. King and S. F. King, Fermion mass hierarchies from modular symmetry, JHEP 09 (2020) 043, [arXiv:2002.00969].
- [145] H. P. Nilles, S. Ramos-Sanchez, and P. K. S. Vaudrevange, Lessons from eclectic flavor symmetries, Nucl. Phys. B 957 (2020) 115098, [arXiv:2004.05200].
- [146] H. P. Nilles, S. Ramos-Sánchez, and P. K. S. Vaudrevange, Eclectic Flavor Groups, JHEP 02 (2020) 045, [arXiv:2001.01736].

- [147] H. P. Nilles, S. Ramos-Sánchez, and P. K. S. Vaudrevange, Eclectic flavor scheme from ten-dimensional string theory – I. Basic results, Phys. Lett. B 808 (2020) 135615, [arXiv:2006.03059].
- [148] A. Baur, M. Kade, H. P. Nilles, S. Ramos-Sanchez, and P. K. S. Vaudrevange, Completing the eclectic flavor scheme of the  $\mathbb{Z}_2$  orbifold, JHEP 06 (2021) 110, [arXiv:2104.03981].
- [149] H. Ohki, S. Uemura, and R. Watanabe, Modular flavor symmetry on a magnetized torus, Phys. Rev. D 102 (2020), no. 8 085008, [arXiv:2003.04174].
- [150] T. Kobayashi, S. Nagamoto, and S. Uemura, Modular symmetry in magnetized/intersecting D-brane models, PTEP 2017 (2017), no. 2 023B02, [arXiv:1608.06129].
- [151] T. Kobayashi, S. Nagamoto, S. Takada, S. Tamba, and T. H. Tatsuishi, Modular symmetry and non-Abelian discrete flavor symmetries in string compactification, Phys. Rev. D 97 (2018), no. 11 116002, [arXiv:1804.06644].
- [152] T. Kobayashi and S. Tamba, Modular forms of finite modular subgroups from magnetized D-brane models, Phys. Rev. D 99 (2019), no. 4 046001, [arXiv:1811.11384].
- [153] Y. Almumin, M.-C. Chen, V. Knapp-Pérez, S. Ramos-Sánchez, M. Ratz, and S. Shukla, Metaplectic Flavor Symmetries from Magnetized Tori, JHEP 05 (2021) 078, [arXiv:2102.11286].
- [154] M.-C. Chen, M. Fallbacher, M. Ratz, and C. Staudt, On predictions from spontaneously broken flavor symmetries, Phys. Lett. B 718 (2012) 516–521, [arXiv:1208.2947].
- [155] M.-C. Chen, M. Fallbacher, Y. Omura, M. Ratz, and C. Staudt, Predictivity of models with spontaneously broken non-Abelian discrete flavor symmetries, Nucl. Phys. B 873 (2013) 343–371, [arXiv:1302.5576].
- [156] M.-C. Chen, S. Ramos-Sánchez, and M. Ratz, A note on the predictions of models with modular flavor symmetries, Phys. Lett. B 801 (2020) 135153, [arXiv:1909.06910].
- [157] X.-G. Liu and G.-J. Ding, Neutrino Masses and Mixing from Double Covering of Finite Modular Groups, JHEP 08 (2019) 134, [arXiv:1907.01488].
- [158] P. P. Novichkov, J. T. Penedo, and S. T. Petcov, Fermion mass hierarchies, large lepton mixing and residual modular symmetries, JHEP 04 (2021) 206, [arXiv:2102.07488].
- [159] D. Marzocca and A. Romanino, Stable fermion mass matrices and the charged lepton contribution to neutrino mixing, JHEP 11 (2014) 159, [arXiv:1409.3760].
- [160] Y. Reyimuaji and A. Romanino, Can an unbroken flavour symmetry provide an approximate description of lepton masses and mixing?, JHEP 03 (2018) 067, [arXiv:1801.10530].
- [161] G. Cree and H. E. Logan, Yukawa alignment from natural flavor conservation, Phys. Rev. D 84 (2011) 055021, [arXiv:1106.4039].

- [162] A. G. Akeroyd, S. Moretti, K. Yagyu, and E. Yildirim, Light charged Higgs boson scenario in 3-Higgs doublet models, Int. J. Mod. Phys. A 32 (2017), no. 23n24 1750145, [arXiv:1605.05881].
- [163] H. E. Logan, S. Moretti, D. Rojas-Ciofalo, and M. Song, CP violation from charged Higgs bosons in the three Higgs doublet model, JHEP 07 (2021) 158, [arXiv:2012.08846].
- [164] M. Chakraborti, D. Das, M. Levy, S. Mukherjee, and I. Saha, Prospects for light charged scalars in a three-Higgs-doublet model with Z3 symmetry, Phys. Rev. D 104 (2021), no. 7 075033, [arXiv:2104.08146].
- [165] D. Das, M. Levy, P. B. Pal, A. M. Prasad, I. Saha, and A. Srivastava, Democratic three-Higgs-doublet models: The custodial limit and wrong-sign Yukawa coupling, Phys. Rev. D 107 (2023), no. 5 055035, [arXiv:2301.00231].
- [166] R. Boto, J. C. Romão, and J. a. P. Silva, Current bounds on the type-Z Z3 three-Higgs-doublet model, Phys. Rev. D 104 (2021), no. 9 095006, [arXiv:2106.11977].
- [167] S. Willenbrock, Symmetries of the standard model, in Theoretical Advanced Study Institute in Elementary Particle Physics: Physics in  $D \ge 4$ , pp. 3–38, 10, 2004. hep-ph/0410370.
- [168] A. Pomarol and R. Vega, Constraints on CP violation in the Higgs sector from the rho parameter, Nucl. Phys. B 413 (1994) 3–15, [hep-ph/9305272].
- [169] H. E. Haber and D. O'Neil, Basis-independent methods for the two-Higgs-doublet model III: The CP-conserving limit, custodial symmetry, and the oblique parameters S, T, U, Phys. Rev. D 83 (2011) 055017, [arXiv:1011.6188].
- [170] W. Grimus, L. Lavoura, O. M. Ogreid, and P. Osland, A Precision constraint on multi-Higgs-doublet models, J. Phys. G 35 (2008) 075001, [arXiv:0711.4022].
- [171] W. Grimus, L. Lavoura, O. M. Ogreid, and P. Osland, *The Oblique parameters in multi-Higgs-doublet models*, *Nucl. Phys. B* **801** (2008) 81–96, [arXiv:0802.4353].
- [172] K. Olaussen, P. Osland, and M. A. Solberg, Symmetry and Mass Degeneration in Multi-Higgs-Doublet Models, JHEP 07 (2011) 020, [arXiv:1007.1424].
- [173] C. C. Nishi, Custodial SO(4) symmetry and CP violation in N-Higgs-doublet potentials, Phys. Rev. D 83 (2011) 095005, [arXiv:1103.0252].
- [174] M. A. Solberg, Conditions for the custodial symmetry in multi-Higgs-doublet models, JHEP 05 (2018) 163, [arXiv:1801.00519].
- [175] B. Grzadkowski, M. Maniatis, and J. Wudka, The bilinear formalism and the custodial symmetry in the two-Higgs-doublet model, JHEP 11 (2011) 030, [arXiv:1011.5228].
- [176] N. Darvishi and A. Pilaftsis, Classifying Accidental Symmetries in Multi-Higgs Doublet Models, Phys. Rev. D 101 (2020), no. 9 095008, [arXiv:1912.00887].

- [177] A. Kundu, P. Mondal, and P. B. Pal, Custodial symmetry, the Georgi-Machacek model, and other scalar extensions, Phys. Rev. D 105 (2022), no. 11 115026, [arXiv:2111.14195].
- [178] S. Hessenberger and W. Hollik, Two-loop corrections to the ρ parameter in Two-Higgs-Doublet Models, Eur. Phys. J. C 77 (2017), no. 3 178, [arXiv:1607.04610].
- [179] M. P. Bento, H. E. Haber, J. C. Romão, and J. a. P. Silva, Multi-Higgs doublet models: physical parametrization, sum rules and unitarity bounds, JHEP 11 (2017) 095, [arXiv:1708.09408].
- [180] V. Keus, S. F. King, and S. Moretti, Three-Higgs-doublet models: symmetries, potentials and Higgs boson masses, JHEP 01 (2014) 052, [arXiv:1310.8253].
- [181] M. Misiak and M. Steinhauser, Weak radiative decays of the B meson and bounds on  $M_{H^{\pm}}$  in the Two-Higgs-Doublet Model, Eur. Phys. J. C 77 (2017), no. 3 201, [arXiv:1702.04571].
- [182] O. Atkinson, M. Black, C. Englert, A. Lenz, A. Rusov, and J. Wynne, *The flavourful present and future of 2HDMs at the collider energy frontier*, *JHEP* **11** (2022) 139, [arXiv:2202.08807].
- [183] A. de Giorgi, F. Koutroulis, L. Merlo, and S. Pokorski, Flavour and Higgs physics in Z2-symmetric 2HD models near the decoupling limit, Nucl. Phys. B 994 (2023) 116323, [arXiv:2304.10560].
- [184] A. Arbey, F. Mahmoudi, O. Stal, and T. Stefaniak, Status of the Charged Higgs Boson in Two Higgs Doublet Models, Eur. Phys. J. C 78 (2018), no. 3 182, [arXiv:1706.07414].
- [185] D. Das and U. K. Dey, Analysis of an extended scalar sector with  $S_3$  symmetry, Phys. Rev. D 89 (2014), no. 9 095025, [arXiv:1404.2491]. [Erratum: Phys.Rev.D 91, 039905 (2015)].
- [186] CMS Collaboration, A. M. Sirunyan et al., Combined measurements of Higgs boson couplings in proton-proton collisions at  $\sqrt{s} = 13$  TeV, Eur. Phys. J. C 79 (2019), no. 5 421, [arXiv:1809.10733].
- [187] **ATLAS** Collaboration, G. Aad et al., Combined measurements of Higgs boson production and decay using up to 80 fb<sup>-1</sup> of proton-proton collision data at  $\sqrt{s} = 13$  TeV collected with the ATLAS experiment, Phys. Rev. D **101** (2020), no. 1 012002, [arXiv:1909.02845].
- [188] W. Porod, F. Staub, and A. Vicente, A Flavor Kit for BSM models, Eur. Phys. J. C 74 (2014), no. 8 2992, [arXiv:1405.1434].
- [189] W. Porod, SPheno, a program for calculating supersymmetric spectra, SUSY particle decays and SUSY particle production at e+ e- colliders, Comput. Phys. Commun. 153 (2003) 275–315, [hep-ph/0301101].
- [190] W. Porod and F. Staub, SPheno 3.1: Extensions including flavour, CP-phases and models beyond the MSSM, Comput. Phys. Commun. 183 (2012) 2458–2469, [arXiv:1104.1573].
- [191] F. Staub, SARAH 4: A tool for (not only SUSY) model builders, Comput. Phys. Commun. 185 (2014) 1773-1790, [arXiv:1309.7223].

- [192] **ATLAS** Collaboration, Measurement of the properties of Higgs boson production at  $\sqrt{s}$ =13 TeV in the  $H \to \gamma \gamma$  channel using 139 fb<sup>-1</sup> of pp collision data with the ATLAS experiment, .
- [193] **CMS** Collaboration, Measurements of Higgs boson properties in the diphoton decay channel at  $\sqrt{s}$  = 13 TeV, .
- [194] J. F. Gunion, H. E. Haber, G. L. Kane, and S. Dawson, The Higgs Hunter's Guide, vol. 80. 2000.
- [195] **ATLAS** Collaboration, Combined measurements of Higgs boson production and decay using up to  $139 \text{ fb}^{-1}$  of proton-proton collision data at  $\sqrt{s} = 13 \text{ TeV}$  collected with the ATLAS experiment, .
- [196] D. Fontes, J. C. Romão, and J. a. P. Silva, A reappraisal of the wrong-sign  $hb\bar{b}$  coupling and the study of  $h \to Z\gamma$ , Phys. Rev. D **90** (2014), no. 1 015021, [arXiv:1406.6080].
- [197] A. Biswas and A. Lahiri, Alignment, reverse alignment, and wrong sign Yukawa couplings in two Higgs doublet models, Phys. Rev. D 93 (2016), no. 11 115017, [arXiv:1511.07159].
- [198] P. M. Ferreira, R. Guedes, M. O. P. Sampaio, and R. Santos, Wrong sign and symmetric limits and non-decoupling in 2HDMs, JHEP 12 (2014) 067, [arXiv:1409.6723].
- [199] P. M. Ferreira, R. Guedes, J. F. Gunion, H. E. Haber, M. O. P. Sampaio, and R. Santos, The Wrong Sign limit in the 2HDM, in 2nd Large Hadron Collider Physics Conference, 10, 2014. arXiv:1410.1926.
- [200] G. Bhattacharyya and D. Das, Nondecoupling of charged scalars in Higgs decay to two photons and symmetries of the scalar potential, Phys. Rev. D 91 (2015) 015005, [arXiv:1408.6133].
- [201] S. Carrolo, J. C. Romão, J. a. P. Silva, and F. Vazão, Symmetry and decoupling in multi-Higgs boson models, Phys. Rev. D 103 (2021), no. 7 075026, [arXiv:2102.11303].
- [202] F. Faro, J. C. Romao, and J. P. Silva, Nondecoupling in Multi-Higgs doublet models, Eur. Phys. J. C 80 (2020), no. 7 635, [arXiv:2002.10518].
- [203] O. Atkinson, M. Black, A. Lenz, A. Rusov, and J. Wynne, Cornering the Two Higgs Doublet Model Type II, JHEP 04 (2022) 172, [arXiv:2107.05650].
- [204] T. Modak, J. C. Romão, S. Sadhukhan, J. a. P. Silva, and R. Srivastava, Constraining wrong-sign hbb couplings with  $h \to \Upsilon \gamma$ , Phys. Rev. D **94** (2016), no. 7 075017, [arXiv:1607.07876].
- [205] A. Batra, S. Mandal, and R. Srivastava,  $h \to \Upsilon \gamma$  Decay: Smoking Gun Signature of Wrong-Sign  $hb\bar{b}$  Coupling, arXiv:2209.01200.
- [206] I. Galon, A. Rajaraman, and T. M. P. Tait,  $H \to \tau^+ \tau^- \gamma$  as a probe of the  $\tau$  magnetic dipole moment, JHEP 12 (2016) 111, [arXiv:1610.01601].
- [207] S. Kanemura, T. Mondal, and K. Yagyu, Exploring wrong sign scenarios in the Yukawa-Aligned 2HDM, JHEP 02 (2023) 237, [arXiv:2211.08803].

- [208] S. D. Joglekar, S matrix derivation of the Weinberg model, Annals Phys. 83 (1974) 427.
- [209] ATLAS Collaboration, G. Aad et al., Combined measurements of Higgs boson production and decay using up to 80 fb<sup>-1</sup> of proton-proton collision data at √s = 13 TeV collected with the ATLAS experiment, Phys. Rev. D 101 (2020), no. 1 012002, [arXiv:1909.02845].
- [210] **CMS** Collaboration, Measurement of Higgs boson decay to a pair of muons in proton-proton collisions at  $\sqrt{s} = 13 \text{ TeV}$ ,.
- [211] R. Boto, D. Das, L. Lourenco, J. C. Romao, and J. P. Silva, Fingerprinting the type-Z three-Higgs-doublet models, Phys. Rev. D 108 (2023), no. 1 015020, [arXiv:2304.13494].
- [212] S. Kanemura, K. Tsumura, K. Yagyu, and H. Yokoya, Fingerprinting nonminimal Higgs sectors, Phys. Rev. D 90 (2014) 075001, [arXiv:1406.3294].
- [213] G. Arcadi, A. Djouadi, and M. Raidal, Dark Matter through the Higgs portal, Phys. Rept. 842 (2020) 1–180, [arXiv:1903.03616].
- [214] S. Weinberg, Gauge Theory of CP Violation, Phys. Rev. Lett. 37 (1976) 657.
- [215] R. González Felipe, I. P. Ivanov, C. C. Nishi, H. Serôdio, and J. a. P. Silva, *Constraining multi-Higgs flavour models*, Eur. Phys. J. C 74 (2014), no. 7 2953, [arXiv:1401.5807].
- [216] I. P. Ivanov and E. Vdovin, Classification of finite reparametrization symmetry groups in the three-Higgs-doublet model, Eur. Phys. J. C 73 (2013), no. 2 2309, [arXiv:1210.6553].
- [217] I. de Medeiros Varzielas, S. F. King, C. Luhn, and T. Neder, Spontaneous CP violation in multi-Higgs potentials with triplets of  $\Delta(3n^2)$  and  $\Delta(6n^2)$ , JHEP 11 (2017) 136, [arXiv:1706.07606].
- [218] I. P. Ivanov, C. C. Nishi, J. a. P. Silva, and A. Trautner, *Basis-invariant conditions for CP symmetry of order four, Phys. Rev. D* **99** (2019), no. 1 015039, [arXiv:1810.13396].
- [219] I. P. Ivanov, C. C. Nishi, and A. Trautner, Beyond basis invariants, Eur. Phys. J. C 79 (2019), no. 4 315, [arXiv:1901.11472].
- [220] I. de Medeiros Varzielas and I. P. Ivanov, Recognizing symmetries in a 3HDM in a basis-independent way, Phys. Rev. D 100 (2019), no. 1 015008, [arXiv:1903.11110].
- [221] I. P. Ivanov and C. C. Nishi, Symmetry breaking patterns in 3HDM, JHEP 01 (2015) 021, [arXiv:1410.6139].
- [222] I. de Medeiros Varzielas, S. F. King, C. Luhn, and T. Neder, Minima of multi-Higgs potentials with triplets of  $\Delta(3n^2)$  and  $\Delta(6n^2)$ , Phys. Lett. B 775 (2017) 303–310, [arXiv:1704.06322].
- [223] I. de Medeiros Varzielas, I. P. Ivanov, and M. Levy, Exploring multi-Higgs models with softly broken large discrete symmetry groups, Eur. Phys. J. C 81 (2021), no. 10 918, [arXiv:2107.08227].

- [224] G. Segre and H. A. Weldon, Mass Hierarchies and a Formula for the Cabibbo Angle in  $SU(2)_L \times U(1)$ , Phys. Lett. B 83 (1979) 351–354.
- [225] W. Grimus and P. O. Ludl, Principal series of finite subgroups of SU(3), J. Phys. A 43 (2010) 445209, [arXiv:1006.0098].
- [226] A. Merle and R. Zwicky, Explicit and spontaneous breaking of SU(3) into its finite subgroups, JHEP 02 (2012) 128, [arXiv:1110.4891].
- [227] C. Hagedorn, A. Meroni, and L. Vitale, Mixing patterns from the groups  $\Sigma(n\phi)$ , J. Phys. A 47 (2014) 055201, [arXiv:1307.5308].
- [228] S.-j. Rong, Lepton mixing patterns from the group Σ(36×3) with a generalized CP transformation, Phys. Rev. D 95 (2017), no. 7 076014, [arXiv:1604.08482].
- [229] I. P. Ivanov, V. Keus, and E. Vdovin, Abelian symmetries in multi-Higgs-doublet models, J. Phys. A 45 (2012) 215201, [arXiv:1112.1660].
- [230] G. C. Branco, J. M. Gerard, and W. Grimus, GEOMETRICAL T VIOLATION, Phys. Lett. B 136 (1984) 383–386.
- [231] I. de Medeiros Varzielas and D. Emmanuel-Costa, Geometrical CP Violation, Phys. Rev. D 84 (2011) 117901, [arXiv:1106.5477].
- [232] I. de Medeiros Varzielas, D. Emmanuel-Costa, and P. Leser, Geometrical CP Violation from Non-Renormalisable Scalar Potentials, Phys. Lett. B 716 (2012) 193–196, [arXiv:1204.3633].
- [233] I. P. Ivanov and L. Lavoura, Geometrical CP violation in the N-Higgs-doublet model, Eur. Phys. J. C 73 (2013), no. 4 2416, [arXiv:1302.3656].
- [234] G. Bhattacharyya, I. de Medeiros Varzielas, and P. Leser, A common origin of fermion mixing and geometrical CP violation, and its test through Higgs physics at the LHC, Phys. Rev. Lett. 109 (2012) 241603, [arXiv:1210.0545].
- [235] I. de Medeiros Varzielas and D. Pidt, Towards realistic models of quark masses with geometrical CP violation, J. Phys. G 41 (2014) 025004, [arXiv:1307.0711].
- [236] I. de Medeiros Varzielas and D. Pidt, Geometrical CP violation with a complete fermion sector, JHEP 11 (2013) 206, [arXiv:1307.6545].
- [237] M. Fallbacher and A. Trautner, Symmetries of symmetries and geometrical CP violation, Nucl. Phys. B 894 (2015) 136–160, [arXiv:1502.01829].
- [238] P. M. Ferreira, I. P. Ivanov, E. Jiménez, R. Pasechnik, and H. Serôdio, *CP4 miracle: shaping Yukawa sector with CP symmetry of order four, JHEP* **01** (2018) 065, [arXiv:1711.02042].
- [239] A. Arhrib, M. Capdequi Peyranere, W. Hollik, and S. Penaranda, Higgs decays in the two Higgs doublet model: Large quantum effects in the decoupling regime, Phys. Lett. B 579 (2004) 361–370, [hep-ph/0307391].

- [240] M. Nebot, Bounded masses in two Higgs doublets models, spontaneous CP violation and Z<sub>2</sub> symmetry, Phys. Rev. D 102 (2020), no. 11 115002, [arXiv:1911.02266].
- [241] F. J. Botella, G. C. Branco, M. N. Rebelo, and J. I. Silva-Marcos, What if the masses of the first two quark families are not generated by the standard model Higgs boson?, Phys. Rev. D 94 (2016), no. 11 115031, [arXiv:1602.08011].
- [242] A. Srivastava, M. Levy, and D. Das, Diluting quark flavor hierarchies using dihedral symmetry, Eur. Phys. J. C 82 (2022), no. 3 205, [arXiv:2107.03756].
- [243] D. Das, Relating the Cabibbo angle to  $\tan \beta$  in a two Higgs-doublet model, Phys. Rev. D 100 (2019), no. 7 075004, [arXiv:1908.03961].
- [244] S. Antusch, J. Kersten, M. Lindner, and M. Ratz, Running neutrino masses, mixings and CP phases: Analytical results and phenomenological consequences, Nucl. Phys. B 674 (2003) 401–433, [hep-ph/0305273].
- [245] Particle Data Group Collaboration, P. A. Zyla et al., Review of Particle Physics, PTEP 2020 (2020), no. 8 083C01.
- [246] M. S. Chanowitz, M. A. Furman, and I. Hinchliffe, Weak Interactions of Ultraheavy Fermions. 2., Nucl. Phys. B 153 (1979) 402–430.
- [247] M. Nebot and J. a. P. Silva, Self-cancellation of a scalar in neutral meson mixing and implications for the LHC, Phys. Rev. D 92 (2015), no. 8 085010, [arXiv:1507.07941].
- [248] G. Bhattacharyya, D. Das, and A. Kundu, Feasibility of light scalars in a class of two-Higgs-doublet models and their decay signatures, Phys. Rev. D 89 (2014) 095029, [arXiv:1402.0364].
- [249] F. J. Botella, G. C. Branco, A. Carmona, M. Nebot, L. Pedro, and M. N. Rebelo, Physical Constraints on a Class of Two-Higgs Doublet Models with FCNC at tree level, JHEP 07 (2014) 078, [arXiv:1401.6147].
- [250] R. N. Mohapatra, G. Yan, and Y. Zhang, Ameliorating Higgs induced flavor constraints on TeV scale W<sub>R</sub>, Nucl. Phys. B 948 (2019) 114764, [arXiv:1902.08601].
- [251] G. C. Branco, D. Das, M. Levy, and P. B. Pal, Crossed two Higgs-doublet models: reduction of Yukawa parameters in the low-scale limit of left-right symmetry and other avatars, Phys. Rev. D 102 (2020), no. 3 035007, [arXiv:2004.11291].
- [252] N. G. Deshpande, J. F. Gunion, B. Kayser, and F. I. Olness, Left-right symmetric electroweak models with triplet Higgs, Phys. Rev. D 44 (1991) 837–858.
- [253] D. Atwood, L. Reina, and A. Soni, Phenomenology of two Higgs doublet models with flavor changing neutral currents, Phys. Rev. D 55 (1997) 3156–3176, [hep-ph/9609279].

- [254] G. Altarelli and F. Feruglio, Tri-bimaximal neutrino mixing from discrete symmetry in extra dimensions, Nucl. Phys. B 720 (2005) 64–88, [hep-ph/0504165].
- [255] G. Altarelli and F. Feruglio, Tri-bimaximal neutrino mixing, A(4) and the modular symmetry, Nucl. Phys. B 741 (2006) 215–235, [hep-ph/0512103].
- [256] F. Feruglio and A. Romanino, Lepton flavor symmetries, Rev. Mod. Phys. 93 (2021), no. 1 015007, [arXiv:1912.06028].
- [257] G.-J. Ding, S. F. King, X.-G. Liu, and J.-N. Lu, Modular S<sub>4</sub> and A<sub>4</sub> symmetries and their fixed points: new predictive examples of lepton mixing, JHEP 12 (2019) 030, [arXiv:1910.03460].
- [258] I. de Medeiros Varzielas, M. Levy, and Y.-L. Zhou, Symmetries and stabilisers in modular invariant flavour models, JHEP 11 (2020) 085, [arXiv:2008.05329].
- [259] S. F. King and Y.-L. Zhou, Trimaximal  $TM_1$  mixing with two modular  $S_4$  groups, Phys. Rev. D 101 (2020), no. 1 015001, [arXiv:1908.02770].
- [260] I. de Medeiros Varzielas and J. a. Lourenço, Two A4 modular symmetries for Tri-Maximal 2 mixing, Nucl. Phys. B 979 (2022) 115793, [arXiv:2107.04042].
- [261] I. de Medeiros Varzielas and J. a. Lourenço, Two A5 modular symmetries for Golden Ratio 2 mixing, Nucl. Phys. B 984 (2022) 115974, [arXiv:2206.14869].
- [262] G.-J. Ding, S. F. King, X.-G. Liu, and J.-N. Lu, Modular S<sub>4</sub> and A<sub>4</sub> symmetries and their fixed points: new predictive examples of lepton mixing, JHEP 12 (2019) 030, [arXiv:1910.03460].
- [263] P. P. Novichkov, S. T. Petcov, and M. Tanimoto, Trimaximal Neutrino Mixing from Modular A4 Invariance with Residual Symmetries, Phys. Lett. B 793 (2019) 247–258, [arXiv:1812.11289].
- [264] S. F. King, Atmospheric and solar neutrinos with a heavy singlet, Phys. Lett. B 439 (1998) 350–356, [hep-ph/9806440].
- [265] S. F. King, Atmospheric and solar neutrinos from single right-handed neutrino dominance and U(1) family symmetry, Nucl. Phys. B 562 (1999) 57–77, [hep-ph/9904210].
- [266] S. F. King, Large mixing angle MSW and atmospheric neutrinos from single right-handed neutrino dominance and U(1) family symmetry, Nucl. Phys. B 576 (2000) 85–105, [hep-ph/9912492].
- [267] P. H. Frampton, S. L. Glashow, and T. Yanagida, Cosmological sign of neutrino CP violation, Phys. Lett. B 548 (2002) 119–121, [hep-ph/0208157].
- [268] S. F. King, Predicting neutrino parameters from SO(3) family symmetry and quark-lepton unification, JHEP 08 (2005) 105, [hep-ph/0506297].
- [269] S. Antusch, S. F. King, C. Luhn, and M. Spinrath, Trimaximal mixing with predicted θ<sub>13</sub> from a new type of constrained sequential dominance, Nucl. Phys. B 856 (2012) 328–341, [arXiv:1108.4278].

- [270] S. F. King, Minimal predictive see-saw model with normal neutrino mass hierarchy, JHEP 07 (2013) 137, [arXiv:1304.6264].
- [271] S. F. King, Littlest Seesaw, JHEP 02 (2016) 085, [arXiv:1512.07531].
- [272] S. F. King and C. Luhn, Littlest Seesaw model from  $S_4 \times U(1)$ , JHEP **09** (2016) 023, [arXiv:1607.05276].
- [273] P. Ballett, S. F. King, S. Pascoli, N. W. Prouse, and T. Wang, Precision neutrino experiments vs the Littlest Seesaw, JHEP 03 (2017) 110, [arXiv:1612.01999].
- [274] S. F. King, S. Molina Sedgwick, and S. J. Rowley, Fitting high-energy Littlest Seesaw parameters using low-energy neutrino data and leptogenesis, JHEP 10 (2018) 184, [arXiv:1808.01005].
- [275] S. F. King, Minimal see-saw model predicting best fit lepton mixing angles, Phys. Lett. B 724 (2013) 92-98, [arXiv:1305.4846].
- [276] S. F. King, A model of quark and lepton mixing, JHEP 01 (2014) 119, [arXiv:1311.3295].
- [277] F. Björkeroth and S. F. King, Testing constrained sequential dominance models of neutrinos, J. Phys. G 42 (2015), no. 12 125002, [arXiv:1412.6996].
- [278] P.-T. Chen, G.-J. Ding, S. F. King, and C.-C. Li, A New Littlest Seesaw Model, J. Phys. G 47 (2020), no. 6 065001, [arXiv:1906.11414].
- [279] G.-J. Ding, S. F. King, and C.-Y. Yao, Modular  $S_4 \times SU(5)$  GUT, Phys. Rev. D **104** (2021), no. 5 055034, [arXiv:2103.16311].
- [280] I. de Medeiros Varzielas, S. F. King, and M. Levy, Littlest modular seesaw, JHEP 02 (2023) 143, [arXiv:2211.00654].
- [281] F. J. de Anda and S. F. King, Modular flavour symmetry and orbifolds, JHEP 06 (2023) 122, [arXiv:2304.05958].
- [282] T. Kobayashi, Y. Shimizu, K. Takagi, M. Tanimoto, and T. H. Tatsuishi, Modular S<sub>3</sub>-invariant flavor model in SU(5) grand unified theory, PTEP 2020 (2020), no. 5 053B05, [arXiv:1906.10341].
- [283] X. Du and F. Wang, SUSY breaking constraints on modular flavor S<sub>3</sub> invariant SU(5) GUT model, JHEP **02** (2021) 221, [arXiv:2012.01397].
- [284] F. J. de Anda, S. F. King, and E. Perdomo, SU(5) grand unified theory with  $A_4$  modular symmetry, Phys. Rev. D 101 (2020), no. 1 015028, [arXiv:1812.05620].
- [285] P. Chen, G.-J. Ding, and S. F. King, SU(5) GUTs with  $A_4$  modular symmetry, JHEP **04** (2021) 239, [arXiv:2101.12724].
- [286] G. Charalampous, S. F. King, G. K. Leontaris, and Y.-L. Zhou, Flipped SU(5) with modular A4 symmetry, Phys. Rev. D 104 (2021), no. 11 115015, [arXiv:2109.11379].

- [287] Y. Zhao and H.-H. Zhang, Adjoint SU(5) GUT model with modular S<sub>4</sub> symmetry, JHEP 03 (2021) 002, [arXiv:2101.02266].
- [288] S. F. King and Y.-L. Zhou, Twin modular  $S_4$  with SU(5) GUT, JHEP **04** (2021) 291, [arXiv:2103.02633].
- [289] G.-J. Ding, S. F. King, and J.-N. Lu, SO(10) models with  $A_4$  modular symmetry, JHEP 11 (2021) 007, [arXiv:2108.09655].
- [290] I. de Medeiros Varzielas, S. F. King, and M. Levy, A modular SU (5) littlest seesaw, JHEP 05 (2024) 203, [arXiv:2309.15901].
- [291] S. T. Petcov, On the normalisation of the modular forms in modular invariant theories of flavour, Phys. Lett. B 850 (2024) 138540, [arXiv:2311.04185].
- [292] I. de Medeiros Varzielas, M. Levy, J. T. Penedo, and S. T. Petcov, Quarks at the modular S<sub>4</sub> cusp, JHEP 09 (2023) 196, [arXiv:2307.14410].
- [293] M.-C. Chen, V. Knapp-Perez, M. Ramos-Hamud, S. Ramos-Sanchez, M. Ratz, and S. Shukla, Quasi-eclectic modular flavor symmetries, Phys. Lett. B 824 (2022) 136843, [arXiv:2108.02240].
- [294] H. Okada and M. Tanimoto, Modular invariant flavor model of A<sub>4</sub> and hierarchical structures at nearby fixed points, Phys. Rev. D 103 (2021), no. 1 015005, [arXiv:2009.14242].
- [295] F. Feruglio, V. Gherardi, A. Romanino, and A. Titov, Modular invariant dynamics and fermion mass hierarchies around  $\tau = i$ , JHEP 05 (2021) 242, [arXiv:2101.08718].
- [296] S. T. Petcov and M. Tanimoto,  $A_4$  modular flavour model of quark mass hierarchies close to the fixed point  $\tau = \omega$ , Eur. Phys. J. C 83 (2023), no. 7 579, [arXiv:2212.13336].
- [297] S. T. Petcov and M. Tanimoto,  $A_4$  modular flavour model of quark mass hierarchies close to the fixed point  $\tau = i\infty$ , JHEP **08** (2023) 086, [arXiv:2306.05730].
- [298] "NuFit webpage." http://www.nu-fit.org.
- [299] G. G. Ross, GRAND UNIFIED THEORIES. 1985.
- [300] H. Georgi and C. Jarlskog, A New Lepton Quark Mass Relation in a Unified Theory, Phys. Lett. B 86 (1979) 297–300.
- [301] S. Antusch, I. de Medeiros Varzielas, V. Maurer, C. Sluka, and M. Spinrath, Towards predictive flavour models in SUSY SU(5) GUTs with doublet-triplet splitting, JHEP 09 (2014) 141, [arXiv:1405.6962].
- [302] F. Björkeroth, F. J. de Anda, I. de Medeiros Varzielas, and S. F. King, Towards a complete  $A_4 \times SU(5)$  SUSY GUT, JHEP **06** (2015) 141, [arXiv:1503.03306].
- [303] H. Okada and M. Tanimoto, Quark and lepton flavors with common modulus τ in A4 modular symmetry, Phys. Dark Univ. 40 (2023) 101204, [arXiv:2005.00775].

- [304] S. Antusch and V. Maurer, Running quark and lepton parameters at various scales, JHEP 11 (2013) 115, [arXiv:1306.6879].
- [305] T. Geib and S. F. King, Comprehensive renormalization group analysis of the littlest seesaw model, Phys. Rev. D 97 (2018), no. 7 075010, [arXiv:1709.07425].
- [306] A. Baur, H. P. Nilles, S. Ramos-Sanchez, A. Trautner, and P. K. S. Vaudrevange, Top-down anatomy of flavor symmetry breakdown, Phys. Rev. D 105 (2022), no. 5 055018, [arXiv:2112.06940].
- [307] A. Baur, H. P. Nilles, S. Ramos-Sanchez, A. Trautner, and P. K. S. Vaudrevange, The first string-derived eclectic flavor model with realistic phenomenology, JHEP 09 (2022) 224, [arXiv:2207.10677].
- [308] C.-Y. Yao, X.-G. Liu, and G.-J. Ding, Fermion masses and mixing from the double cover and metaplectic cover of the A<sub>5</sub> modular group, Phys. Rev. D 103 (2021), no. 9 095013, [arXiv:2011.03501].
- [309] F. Costa and S. F. King, Neutrino Mixing Sum Rules and the Littlest Seesaw, Universe 9 (2023), no. 11 472, [arXiv:2307.13895].
- [310] S. Kikuchi, T. Kobayashi, K. Nasu, S. Takada, and H. Uchida, Quark hierarchical structures in modular symmetric flavor models at level 6, Phys. Rev. D 107 (2023), no. 5 055014, [arXiv:2301.03737].
- [311] Y. Abe, T. Higaki, J. Kawamura, and T. Kobayashi, Quark masses and CKM hierarchies from S'<sub>4</sub> modular flavor symmetry, Eur. Phys. J. C 83 (2023), no. 12 1140, [arXiv:2301.07439].
- [312] S. Kikuchi, T. Kobayashi, K. Nasu, S. Takada, and H. Uchida, Quark mass hierarchies and CP violation in A<sub>4</sub> × A<sub>4</sub> × A<sub>4</sub> modular symmetric flavor models, JHEP 07 (2023) 134, [arXiv:2302.03326].
- [313] Y. Abe, T. Higaki, J. Kawamura, and T. Kobayashi, Quark and lepton hierarchies from S4' modular flavor symmetry, Phys. Lett. B 842 (2023) 137977, [arXiv:2302.11183].
- [314] Y. Abe, T. Higaki, J. Kawamura, and T. Kobayashi, Fermion hierarchies in SU(5) grand unification from  $\Gamma'_6$  modular flavor symmetry, JHEP **08** (2023) 097, [arXiv:2307.01419].
- [315] P. P. Novichkov, J. T. Penedo, S. T. Petcov, and A. V. Titov, Modular A<sub>5</sub> symmetry for flavour model building, JHEP 04 (2019) 174, [arXiv:1812.02158].
- [316] S. Kikuchi, T. Kobayashi, M. Tanimoto, and H. Uchida, Texture zeros of quark mass matrices at fixed point τ = ω in modular flavor symmetry, Eur. Phys. J. C 83 (2023), no. 7 591, [arXiv:2207.04609].

- [317] K. Hoshiya, S. Kikuchi, T. Kobayashi, and H. Uchida, Quark and lepton flavor structure in magnetized orbifold models at residual modular symmetric points, Phys. Rev. D 106 (2022), no. 11 115003, [arXiv:2209.07249].
- [318] F. Feruglio, Universal Predictions of Modular Invariant Flavor Models near the Self-Dual Point, Phys. Rev. Lett. 130 (2023), no. 10 101801, [arXiv:2211.00659].
- [319] F. Feruglio, Fermion masses, critical behavior and universality, JHEP 03 (2023) 236, [arXiv:2302.11580].
- [320] P. P. Novichkov, J. T. Penedo, and S. T. Petcov, Modular flavour symmetries and modulus stabilisation, JHEP 03 (2022) 149, [arXiv:2201.02020].
- [321] V. Knapp-Perez, X.-G. Liu, H. P. Nilles, S. Ramos-Sanchez, and M. Ratz, Matter matters in moduli fixing and modular flavor symmetries, Phys. Lett. B 844 (2023) 138106, [arXiv:2304.14437].
- [322] H. Kuranaga, H. Ohki, and S. Uemura, Modular origin of mass hierarchy: Froggatt-Nielsen like mechanism, JHEP 07 (2021) 068, [arXiv:2105.06237].
- [323] T. Kobayashi, K. Tanaka, and T. H. Tatsuishi, Neutrino mixing from finite modular groups, Phys. Rev. D 98 (2018), no. 1 016004, [arXiv:1803.10391].
- [324] H. Okada and Y. Orikasa, Modular S<sub>3</sub> symmetric radiative seesaw model, Phys. Rev. D 100 (2019), no. 11 115037, [arXiv:1907.04716].
- [325] S. Mishra, Neutrino mixing and Leptogenesis with modular S<sub>3</sub> symmetry in the framework of type III seesaw, arXiv:2008.02095.
- [326] D. Meloni and M. Parriciatu, A simplest modular  $S_3$  model for leptons, JHEP **09** (2023) 043, [arXiv:2306.09028].
- [327] J. C. Criado and F. Feruglio, Modular Invariance Faces Precision Neutrino Data, SciPost Phys. 5 (2018), no. 5 042, [arXiv:1807.01125].
- [328] T. Kobayashi, N. Omoto, Y. Shimizu, K. Takagi, M. Tanimoto, and T. H. Tatsuishi, Modular A<sub>4</sub> invariance and neutrino mixing, JHEP 11 (2018) 196, [arXiv:1808.03012].
- [329] H. Okada and M. Tanimoto, CP violation of quarks in A<sub>4</sub> modular invariance, Phys. Lett. B 791 (2019) 54-61, [arXiv:1812.09677].
- [330] T. Nomura and H. Okada, A two loop induced neutrino mass model with modular A<sub>4</sub> symmetry, Nucl. Phys. B 966 (2021) 115372, [arXiv:1906.03927].
- [331] H. Okada and Y. Orikasa, A radiative seesaw model in modular A<sub>4</sub> symmetry, arXiv:1907.13520.
- [332] T. Nomura and H. Okada, A modular A<sub>4</sub> symmetric model of dark matter and neutrino, Phys. Lett. B 797 (2019) 134799, [arXiv:1904.03937].

- [333] G.-J. Ding, S. F. King, and X.-G. Liu, Modular A<sub>4</sub> symmetry models of neutrinos and charged leptons, JHEP 09 (2019) 074, [arXiv:1907.11714].
- [334] T. Kobayashi, T. Nomura, and T. Shimomura, Type II seesaw models with modular A<sub>4</sub> symmetry, Phys. Rev. D 102 (2020), no. 3 035019, [arXiv:1912.00637].
- [335] T. Nomura, H. Okada, and O. Popov, A modular A<sub>4</sub> symmetric scotogenic model, Phys. Lett. B 803 (2020) 135294, [arXiv:1908.07457].
- [336] T. Asaka, Y. Heo, T. H. Tatsuishi, and T. Yoshida, Modular A<sub>4</sub> invariance and leptogenesis, JHEP 01 (2020) 144, [arXiv:1909.06520].
- [337] D. Zhang, A modular A<sub>4</sub> symmetry realization of two-zero textures of the Majorana neutrino mass matrix, Nucl. Phys. B **952** (2020) 114935, [arXiv:1910.07869].
- [338] T. Nomura, H. Okada, and S. Patra, An inverse seesaw model with A<sub>4</sub> -modular symmetry, Nucl. Phys. B 967 (2021) 115395, [arXiv:1912.00379].
- [339] X. Wang, Lepton flavor mixing and CP violation in the minimal type-(I+II) seesaw model with a modular A<sub>4</sub> symmetry, Nucl. Phys. B **957** (2020) 115105, [arXiv:1912.13284].
- [340] P. T. P. Hutauruk, D. W. Kang, J. Kim, and H. Okada, Muon g-2, dark matter, and neutrino mass explanations in a modular A4 symmetry, Phys. Dark Univ. 44 (2024) 101440, [arXiv:2012.11156].
- [341] H. Okada and Y. Shoji, A radiative seesaw model with three Higgs doublets in modular A<sub>4</sub> symmetry, Nucl. Phys. B **961** (2020) 115216, [arXiv:2003.13219].
- [342] G.-J. Ding and F. Feruglio, Testing Moduli and Flavon Dynamics with Neutrino Oscillations, JHEP 06 (2020) 134, [arXiv:2003.13448].
- [343] M. K. Behera, S. Mishra, S. Singirala, and R. Mohanta, Implications of A4 modular symmetry on neutrino mass, mixing and leptogenesis with linear seesaw, Phys. Dark Univ. 36 (2022) 101027, [arXiv:2007.00545].
- [344] T. Nomura and H. Okada, Modular  $A_4$  symmetric inverse seesaw model with  $SU(2)_L$  multiplet fields, arXiv:2007.15459.
- [345] M. K. Behera, S. Singirala, S. Mishra, and R. Mohanta, A modular A 4 symmetric scotogenic model for neutrino mass and dark matter, J. Phys. G 49 (2022), no. 3 035002, [arXiv:2009.01806].
- [346] T. Asaka, Y. Heo, and T. Yoshida, Lepton flavor model with modular A<sub>4</sub> symmetry in large volume limit, Phys. Lett. B 811 (2020) 135956, [arXiv:2009.12120].
- [347] K. I. Nagao and H. Okada, Lepton sector in modular A4 and gauged U(1)R symmetry, Nucl. Phys. B 980 (2022) 115841, [arXiv:2010.03348].

- [348] M. Abbas, Modular A<sub>4</sub> Invariance Model for Lepton Masses and Mixing, Phys. Atom. Nucl. 83 (2020), no. 5 764–769.
- [349] M. Kashav and S. Verma, Broken scaling neutrino mass matrix and leptogenesis based on A<sub>4</sub> modular invariance, JHEP 09 (2021) 100, [arXiv:2103.07207].
- [350] H. Okada, Y. Shimizu, M. Tanimoto, and T. Yoshida, Modulus τ linking leptonic CP violation to baryon asymmetry in A<sub>4</sub> modular invariant flavor model, JHEP 07 (2021) 184, [arXiv:2105.14292].
- [351] M. Tanimoto and K. Yamamoto, Electron EDM arising from modulus τ in the supersymmetric modular invariant flavor models, JHEP 10 (2021) 183, [arXiv:2106.10919].
- [352] K. I. Nagao and H. Okada, Modular A4 symmetry and light dark matter with gauged U(1)B-L, Phys. Dark Univ. 36 (2022) 101039, [arXiv:2108.09984].
- [353] T. Kobayashi, H. Okada, and Y. Orikasa, Dark matter stability at fixed points in a modular A4 symmetry, Phys. Dark Univ. 37 (2022) 101080, [arXiv:2111.05674].
- [354] A. Dasgupta, T. Nomura, H. Okada, O. Popov, and M. Tanimoto, Dirac Radiative Neutrino Mass with Modular Symmetry and Leptogenesis, arXiv:2111.06898.
- [355] T. Nomura, H. Okada, and Y.-h. Qi, Zee model in a modular A<sub>4</sub> symmetry, arXiv:2111.10944.
- [356] T. Kobayashi, T. Shimomura, and M. Tanimoto, Soft supersymmetry breaking terms and lepton flavor violations in modular flavor models, Phys. Lett. B 819 (2021) 136452, [arXiv:2102.10425].
- [357] H. Okada and Y.-h. Qi, Zee-Babu model in modular A<sub>4</sub> symmetry, arXiv:2109.13779.
- [358] H. Otsuka and H. Okada, Radiative neutrino masses from modular A<sub>4</sub> symmetry and supersymmetry breaking, arXiv:2202.10089.
- [359] Y. H. Ahn, S. K. Kang, R. Ramos, and M. Tanimoto, Confronting the prediction of leptonic Dirac CP-violating phase with experiments, Phys. Rev. D 106 (2022), no. 9 095002, [arXiv:2205.02796].
- [360] T. Nomura and H. Okada, A radiative seesaw model in a supersymmetric modular A<sub>4</sub> group, arXiv: 2201.10244.
- [361] T. Kobayashi, H. Otsuka, M. Tanimoto, and K. Yamamoto, Lepton flavor violation, lepton  $(g 2)_{\mu,e}$  and electron EDM in the modular symmetry, JHEP **08** (2022) 013, [arXiv:2204.12325].
- [362] T. Kobayashi, H. Otsuka, M. Tanimoto, and K. Yamamoto, Modular symmetry in the SMEFT, Phys. Rev. D 105 (2022), no. 5 055022, [arXiv:2112.00493].
- [363] D. W. Kang, J. Kim, T. Nomura, and H. Okada, Natural mass hierarchy among three heavy Majorana neutrinos for resonant leptogenesis under modular A<sub>4</sub> symmetry, JHEP 07 (2022) 050, [arXiv:2205.08269].

- [364] T. Nomura, H. Okada, and Y. Shoji,  $SU(4)_C \times SU(2)_L \times U(1)_R$  models with modular  $A_4$  symmetry, arXiv:2206.04466.
- [365] J. Kim and H. Okada, Fermi-LAT GeV excess and muon g-2 in a modular  $A_4$  symmetry, arXiv:2302.09747.
- [366] M. R. Devi, Retrieving texture zeros in 3+1 active-sterile neutrino framework under the action of A<sub>4</sub> modular-invariants, arXiv:2303.04900.
- [367] P. Mishra, M. K. Behera, P. Panda, M. Ghosh, and R. Mohanta, Exploring models with modular symmetry in neutrino oscillation experiments, JHEP 09 (2023) 144, [arXiv:2305.08576].
- [368] J. T. Penedo and S. T. Petcov, Lepton Masses and Mixing from Modular S<sub>4</sub> Symmetry, Nucl. Phys. B 939 (2019) 292–307, [arXiv:1806.11040].
- [369] T. Kobayashi, Y. Shimizu, K. Takagi, M. Tanimoto, and T. H. Tatsuishi, New A<sub>4</sub> lepton flavor model from S<sub>4</sub> modular symmetry, JHEP 02 (2020) 097, [arXiv:1907.09141].
- [370] T. Kobayashi, Y. Shimizu, K. Takagi, M. Tanimoto, and T. H. Tatsuishi, A<sub>4</sub> lepton flavor model and modulus stabilization from S<sub>4</sub> modular symmetry, Phys. Rev. D 100 (2019), no. 11 115045, [arXiv:1909.05139]. [Erratum: Phys.Rev.D 101, 039904 (2020)].
- [371] H. Okada and Y. Orikasa, Neutrino mass model with a modular S<sub>4</sub> symmetry, arXiv:1908.08409.
- [372] X. Wang and S. Zhou, The minimal seesaw model with a modular S<sub>4</sub> symmetry, JHEP **05** (2020) 017, [arXiv:1910.09473].
- [373] X. Wang, Dirac neutrino mass models with a modular S<sub>4</sub> symmetry, Nucl. Phys. B **962** (2021) 115247, [arXiv:2007.05913].
- [374] J. Gehrlein and M. Spinrath, Leptonic Sum Rules from Flavour Models with Modular Symmetries, JHEP 03 (2021) 177, [arXiv:2012.04131].
- [375] T. Nomura and H. Okada, Linear seesaw model with a modular S<sub>4</sub> flavor symmetry \*, Chin. Phys. C 46 (2022), no. 5 053101, [arXiv:2109.04157].
- [376] G.-J. Ding, S. F. King, and X.-G. Liu, Neutrino mass and mixing with  $A_5$  modular symmetry, Phys. Rev. D 100 (2019), no. 11 115005, [arXiv:1903.12588].
- [377] G.-J. Ding, S. F. King, C.-C. Li, and Y.-L. Zhou, Modular Invariant Models of Leptons at Level 7, JHEP 08 (2020) 164, [arXiv:2004.12662].
- [378] H. Okada and Y. Orikasa, Lepton mass matrix from double covering of A 4 modular flavor symmetry\*, Chin. Phys. C 46 (2022), no. 12 123108, [arXiv:2206.12629].
- [379] G.-J. Ding, F. R. Joaquim, and J.-N. Lu, Texture-zero patterns of lepton mass matrices from modular symmetry, JHEP 03 (2023) 141, [arXiv:2211.08136].

- [380] P. Mishra, M. K. Behera, and R. Mohanta, Neutrino phenomenology, W-mass anomaly, and muon (g-2) in a minimal type-III seesaw model using a T' modular symmetry, Phys. Rev. D 107 (2023), no. 11 115004, [arXiv:2302.00494].
- [381] G.-J. Ding, S. F. King, C.-C. Li, X.-G. Liu, and J.-N. Lu, Neutrino mass and mixing models with eclectic flavor symmetry Δ(27) × T', JHEP 05 (2023) 144, [arXiv:2303.02071].
- [382] X.-G. Liu, C.-Y. Yao, and G.-J. Ding, Modular invariant quark and lepton models in double covering of S<sub>4</sub> modular group, Phys. Rev. D 103 (2021), no. 5 056013, [arXiv:2006.10722].
- [383] G.-J. Ding, X.-G. Liu, and C.-Y. Yao, A minimal modular invariant neutrino model, JHEP 01 (2023) 125, [arXiv:2211.04546].
- [384] X. Wang, B. Yu, and S. Zhou, Double covering of the modular A<sub>5</sub> group and lepton flavor mixing in the minimal seesaw model, Phys. Rev. D 103 (2021), no. 7 076005, [arXiv:2010.10159].
- [385] M. K. Behera and R. Mohanta, Inverse seesaw in  $A_5'$  modular symmetry, J. Phys. G 49 (2022), no. 4 045001, [arXiv:2108.01059].
- [386] M. K. Behera and R. Mohanta, Linear Seesaw in A5' Modular Symmetry With Leptogenesis, Front. in Phys. 10 (2022) 854595, [arXiv:2201.10429].
- [387] C.-C. Li, X.-G. Liu, and G.-J. Ding, Modular symmetry at level 6 and a new route towards finite modular groups, JHEP 10 (2021) 238, [arXiv:2108.02181].
- [388] X.-G. Liu and G.-J. Ding, Modular flavor symmetry and vector-valued modular forms, JHEP 03 (2022) 123, [arXiv:2112.14761].
- [389] T. Kobayashi, Y. Shimizu, K. Takagi, M. Tanimoto, T. H. Tatsuishi, and H. Uchida, CP violation in modular invariant flavor models, Phys. Rev. D 101 (2020), no. 5 055046, [arXiv:1910.11553].
- [390] H. Okada and M. Tanimoto, Spontaneous CP violation by modulus  $\tau$  in  $A_4$  model of lepton flavors, JHEP 03 (2021) 010, [arXiv:2012.01688].
- [391] C.-Y. Yao, J.-N. Lu, and G.-J. Ding, Modular Invariant A<sub>4</sub> Models for Quarks and Leptons with Generalized CP Symmetry, JHEP **05** (2021) 102, [arXiv:2012.13390].
- [392] X. Wang and S. Zhou, Explicit perturbations to the stabilizer  $\tau = i$  of modular  $A_5'$  symmetry and leptonic CP violation, JHEP 07 (2021) 093, [arXiv:2102.04358].
- [393] G.-J. Ding, F. Feruglio, and X.-G. Liu, *CP symmetry and symplectic modular invariance*, *SciPost Phys.* **10** (2021), no. 6 133, [arXiv:2102.06716].
- [394] B.-Y. Qu, X.-G. Liu, P.-T. Chen, and G.-J. Ding, Flavor mixing and CP violation from the interplay of an S4 modular group and a generalized CP symmetry, Phys. Rev. D 104 (2021), no. 7 076001, [arXiv:2106.11659].

- [395] T. Kobayashi, Y. Shimizu, K. Takagi, M. Tanimoto, T. H. Tatsuishi, and H. Uchida, Finite modular subgroups for fermion mass matrices and baryon/lepton number violation, Phys. Lett. B 794 (2019) 114–121, [arXiv:1812.11072].
- [396] H. Okada and M. Tanimoto, Towards unification of quark and lepton flavors in A<sub>4</sub> modular invariance, Eur. Phys. J. C 81 (2021), no. 1 52, [arXiv:1905.13421].
- [397] J.-N. Lu, X.-G. Liu, and G.-J. Ding, Modular symmetry origin of texture zeros and quark lepton unification, Phys. Rev. D 101 (2020), no. 11 115020, [arXiv:1912.07573].
- [398] M. Abbas, Fermion masses and mixing in modular A4 Symmetry, Phys. Rev. D 103 (2021), no. 5 056016, [arXiv:2002.01929].
- [399] T. Nomura, H. Okada, and Y. Orikasa, Quark and lepton flavor model with leptoquarks in a modular A<sub>4</sub> symmetry, Eur. Phys. J. C 81 (2021), no. 10 947, [arXiv:2106.12375].
- [400] G.-J. Ding, S. F. King, J.-N. Lu, and B.-Y. Qu, Leptogenesis in SO(10) models with A<sub>4</sub> modular symmetry, JHEP 10 (2022) 071, [arXiv:2206.14675].
- [401] X. K. Du and F. Wang, Flavor structures of quarks and leptons from flipped SU(5) GUT with A<sub>4</sub> modular flavor symmetry, JHEP 01 (2023) 036, [arXiv:2209.08796].
- [402] P. Beneš, H. Okada, and Y. Orikasa, Towards unification of lepton and quark mass matrices from double covering of modular A<sub>4</sub> flavor symmetry, arXiv:2212.07245.
- [403] T. Nomura and H. Okada, Quark and lepton model with flavor specific dark matter and muon g-2 in modular  $A_4$  and hidden U(1) symmetries, arXiv:2304.13361.
- [404] G.-J. Ding, F. Feruglio, and X.-G. Liu, Automorphic Forms and Fermion Masses, JHEP 01 (2021) 037, [arXiv:2010.07952].
- [405] M. Abbas and S. Khalil, Modular A<sub>4</sub> Symmetry With Three-Moduli and Flavor Problem, arXiv: 2212.10666.
- [406] Y. Gunji, K. Ishiwata, and T. Yoshida, Subcritical regime of hybrid inflation with modular A<sub>4</sub> symmetry, JHEP 11 (2022) 002, [arXiv:2208.10086].
- [407] Y. Abe, T. Higaki, F. Kaneko, T. Kobayashi, and H. Otsuka, Moduli inflation from modular flavor symmetries, JHEP 06 (2023) 187, [arXiv:2303.02947].
- [408] Y. Kariyazono, T. Kobayashi, S. Takada, S. Tamba, and H. Uchida, Modular symmetry anomaly in magnetic flux compactification, Phys. Rev. D 100 (2019), no. 4 045014, [arXiv:1904.07546].
- [409] A. Baur, H. P. Nilles, A. Trautner, and P. K. S. Vaudrevange, A String Theory of Flavor and &P, Nucl. Phys. B 947 (2019) 114737, [arXiv:1908.00805].
- [410] T. Kobayashi and H. Otsuka, Classification of discrete modular symmetries in Type IIB flux vacua, Phys. Rev. D 101 (2020), no. 10 106017, [arXiv:2001.07972].

- [411] H. Abe, T. Kobayashi, S. Uemura, and J. Yamamoto, Loop Fayet-Iliopoulos terms in T<sup>2</sup>/Z<sub>2</sub> models: Instability and moduli stabilization, Phys. Rev. D 102 (2020), no. 4 045005, [arXiv:2003.03512].
- [412] T. Kobayashi and H. Otsuka, Challenge for spontaneous CP violation in Type IIB orientifolds with fluxes, Phys. Rev. D 102 (2020), no. 2 026004, [arXiv:2004.04518].
- [413] S. Kikuchi, T. Kobayashi, S. Takada, T. H. Tatsuishi, and H. Uchida, Revisiting modular symmetry in magnetized torus and orbifold compactifications, Phys. Rev. D 102 (2020), no. 10 105010, [arXiv:2005.12642].
- [414] S. Kikuchi, T. Kobayashi, H. Otsuka, S. Takada, and H. Uchida, Modular symmetry by orbifolding magnetized  $T^2 \times T^2$ : realization of double cover of  $\Gamma_N$ , JHEP 11 (2020) 101, [arXiv:2007.06188].
- [415] A. Baur, M. Kade, H. P. Nilles, S. Ramos-Sanchez, and P. K. S. Vaudrevange, *The eclectic flavor symmetry of the*  $\mathbb{Z}_2$  *orbifold, JHEP* **02** (2021) 018, [arXiv:2008.07534].
- [416] K. Ishiguro, T. Kobayashi, and H. Otsuka, Spontaneous CP violation and symplectic modular symmetry in Calabi-Yau compactifications, Nucl. Phys. B 973 (2021) 115598, [arXiv:2010.10782].
- [417] H. P. Nilles, S. Ramos-Sánchez, and P. K. S. Vaudrevange, Eclectic flavor scheme from ten-dimensional string theory - II detailed technical analysis, Nucl. Phys. B 966 (2021) 115367, [arXiv:2010.13798].
- [418] K. Ishiguro, T. Kobayashi, and H. Otsuka, Landscape of Modular Symmetric Flavor Models, JHEP 03 (2021) 161, [arXiv:2011.09154].
- [419] K. Hoshiya, S. Kikuchi, T. Kobayashi, Y. Ogawa, and H. Uchida, Classification of three-generation models by orbifolding magnetized  $T^2 \times T^2$ , PTEP **2021** (2021), no. 3 033B05, [arXiv:2012.00751].
- [420] A. Baur, M. Kade, H. P. Nilles, S. Ramos-Sanchez, and P. K. S. Vaudrevange, Siegel modular flavor group and CP from string theory, Phys. Lett. B 816 (2021) 136176, [arXiv:2012.09586].
- [421] S. Kikuchi, T. Kobayashi, and H. Uchida, Modular flavor symmetries of three-generation modes on magnetized toroidal orbifolds, Phys. Rev. D 104 (2021), no. 6 065008, [arXiv:2101.00826].
- [422] Y. Tatsuta, Modular symmetry and zeros in magnetic compactifications, JHEP 10 (2021) 054, [arXiv:2104.03855].
- [423] H. P. Nilles, S. Ramos-Sanchez, A. Trautner, and P. K. S. Vaudrevange, *Orbifolds from Sp(4,Z)* and their modular symmetries, Nucl. Phys. B **971** (2021) 115534, [arXiv:2105.08078].
- [424] K. Ishiguro, T. Kobayashi, and H. Otsuka, Symplectic modular symmetry in heterotic string vacua: flavor, CP, and R-symmetries, JHEP 01 (2022) 020, [arXiv:2107.00487].

- [425] S. Kikuchi, T. Kobayashi, H. Otsuka, M. Tanimoto, H. Uchida, and K. Yamamoto, 4D modular flavor symmetric models inspired by a higher-dimensional theory, Phys. Rev. D 106 (2022), no. 3 035001, [arXiv:2201.04505].
- [426] K. Ishiguro, H. Okada, and H. Otsuka, Residual flavor symmetry breaking in the landscape of modular flavor models, JHEP 09 (2022) 072, [arXiv:2206.04313].
- [427] S. Kikuchi, T. Kobayashi, M. Tanimoto, and H. Uchida, Mass matrices with CP phase in modular flavor symmetry, PTEP 2022 (2022), no. 11 113B07, [arXiv:2206.08538].
- [428] S. Kikuchi, T. Kobayashi, K. Nasu, H. Otsuka, S. Takada, and H. Uchida, Remark on modular weights in low-energy effective field theory from type II string theory, JHEP 04 (2023) 003, [arXiv:2301.10356].
- [429] S. Kikuchi, T. Kobayashi, K. Nasu, S. Takada, and H. Uchida, Zero-modes in magnetized T6/ZN orbifold models through Sp(6,Z) modular symmetry, Phys. Rev. D 108 (2023), no. 3 036005, [arXiv:2305.16709].
- [430] K. Ishiguro, T. Kai, H. Okada, and H. Otsuka, Flavor, CP and metaplectic modular symmetries in Type IIB chiral flux vacua, JHEP 12 (2023) 136, [arXiv:2305.19155].
- [431] S. Kikuchi, T. Kobayashi, K. Nasu, and Y. Yamada, Moduli trapping mechanism in modular flavor symmetric models, JHEP 08 (2023) 081, [arXiv:2307.13230].
- [432] R. Barbieri and G. F. Giudice, Upper Bounds on Supersymmetric Particle Masses, Nucl. Phys. B 306 (1988) 63–76.
- [433] O. Deschamps, S. Descotes-Genon, S. Monteil, V. Niess, S. T'Jampens, and V. Tisserand, The Two Higgs Doublet of Type II facing flavour physics data, Phys. Rev. D 82 (2010) 073012, [arXiv:0907.5135].
- [434] D. Das, Implications Of The Higgs Discovery On Physics Beyond The Standard Model. PhD thesis, Calcutta U., 2015. arXiv:1511.02195.
- [435] P. Gambino and M. Misiak, Quark mass effects in anti-B —> X(s gamma), Nucl. Phys. B 611 (2001) 338–366, [hep-ph/0104034].
- [436] M. Misiak, A. Rehman, and M. Steinhauser, Towards  $\overline{B} \to X_s \gamma$  at the NNLO in QCD without interpolation in  $m_c$ , JHEP 06 (2020) 175, [arXiv:2002.01548].
- [437] Flavour Lattice Averaging Group Collaboration, S. Aoki et al., FLAG Review 2019: Flavour Lattice Averaging Group (FLAG), Eur. Phys. J. C 80 (2020), no. 2 113, [arXiv:1902.08191].
- [438] The GAP Group, GAP Groups, Algorithms, and Programming, . Version 4.10.2, 2019, https://www.gap-system.org.
- [439] H. U. Besche, B. Eick, and E. O'Brien, SmallGrp a GAP package, . Version 1.3, 2018, https://gap-packages.github.io/smallgrp.